ISSN 1007-9327 (print)
ISSN 2219-2840 (online)

World Journal of *Gastroenterology*

World J Gastroenterol 2017 June 21; 23(23): 4135-4316

Published by Baishideng Publishing Group Inc

World Journal of Gastroenterology

A peer-reviewed, online, open-access journal of gastroenterology and hepatology

Editorial Board

2014-2017

The *World Journal of Gastroenterology* Editorial Board consists of 1375 members, representing a team of worldwide experts in gastroenterology and hepatology. They are from 68 countries, including Algeria (2), Argentina (7), Australia (31), Austria (9), Belgium (11), Brazil (20), Brunei Darussalam (1), Bulgaria (2), Cambodia (1), Canada (25), Chile (4), China (165), Croatia (2), Cuba (1), Czech (6), Denmark (2), Egypt (9), Estonia (2), Finland (6), France (20), Germany (58), Greece (31), Guatemala (1), Hungary (14), Iceland (1), India (33), Indonesia (2), Iran (10), Ireland (9), Israel (18), Italy (194), Japan (149), Jordan (1), Kuwait (1), Lebanon (7), Lithuania (1), Malaysia (1), Mexico (11), Morocco (1), Netherlands (5), New Zealand (4), Nigeria (3), Norway (6), Pakistan (6), Poland (12), Portugal (8), Puerto Rico (1), Qatar (1), Romania (10), Russia (3), Saudi Arabia (2), Singapore (7), Slovenia (2), South Africa (1), South Korea (69), Spain (51), Sri Lanka (1), Sudan (1), Sweden (12), Switzerland (5), Thailand (7), Trinidad and Tobago (1), Tunisia (2), Turkey (55), United Kingdom (49), United States (180), Venezuela (1), and Vietnam (1).

Gordon Stanley Howarth, *Roseworthy*
Seungha Kang, *Brisbane*
Alfred King Lam, *Gold Coast*
Ian C Lawrance, *PerthFremantle*
Barbara Anne Leggett, *Brisbane*
Daniel A Lemberg, *Sydney*
Rupert W Leong, *Sydney*
Finlay A Macrae, *Victoria*
Vance Matthews, *Melbourne*
David L Morris, *Sydney*
Reme Mountifield, *Bedford Park*
Hans J Netter, *Melbourne*
Nam Q Nguyen, *Adelaide*
Liang Qiao, *Westmead*
Rajvinder Singh, *Adelaide*
Ross Cyril Smith, *StLeonards*
Kevin J Spring, *Sydney*
Debbie Trinder, *Fremantle*
Daniel R van Langenberg, *Box Hill*
David Ian Watson, *Adelaide*
Desmond Yip, *Garran*
Li Zhang, *Sydney*

Austria

Felix Aigner, *Innsbruck*
Gabriela A Berlakovich, *Vienna*
Herwig R Cerwenka, *Graz*
Peter Ferenci, *Wien*
Alfred Gangl, *Vienna*
Kurt Lenz, *Linz*
Markus Peck-Radosavljevic, *Vienna*
Markus Raderer, *Vienna*
Stefan Riss, *Vienna*

Belgium

Michael George Adler, *Brussels*
Benedicte Y De Winter, *Antwerp*
Mark De Ridder, *Jette*
Olivier Detry, *Liege*
Denis Dufrane Dufrane, *Brussels*
Sven M Francque, *Edegem*
Nikos Kotzampassakis, *Liège*
Geert KMM Robaeys, *Genk*
Xavier Sagaert, *Leuven*
Peter Starkel, *Brussels*
Eddie Wisse, *Keerbergen*

Brazil

SMP Balzan, *Santa Cruz do Sul*
JLF Caboclo, *Sao jose do rio preto*
Fábio Guilherme Campos, *Sao Paulo*
Claudia RL Cardoso, *Rio de Janeiro*
Roberto J Carvalho-Filho, *Sao Paulo*
Carla Daltro, *Salvador*
José Sebastiao dos Santos, *Ribeirao Preto*
Eduardo LR Mello, *Rio de Janeiro*
Sthela Maria Murad-Regadas, *Fortaleza*
Claudia PMS Oliveira, *Sao Paulo*
Júlio C Pereira-Lima, *Porto Alegre*
Marcos V Perini, *Sao Paulo*
Vietla Satyanarayana Rao, *Fortaleza*
Raquel Rocha, *Salvador*
AC Simoes e Silva, *Belo Horizonte*
Mauricio F Silva, *Porto Alefre*
Aytan Miranda Sipahi, *Sao Paulo*
Rosa Leonôra Salerno Soares, *Niterói*
Cristiane Valle Tovo, *Porto Alegre*
Eduardo Garcia Vilela, *Belo Horizonte*

Brunei Darussalam

Vui Heng Chong, *Bandar Seri Begawan*

Bulgaria

Tanya Kirilova Kadiyska, *Sofia*
Mihaela Petrova, *Sofia*

Cambodia

Francois Rouet, *Phnom Penh*

Canada

Brian Bressler, *Vancouver*
Frank J Burczynski, *Winnipeg*
Wangxue Chen, *Ottawa*
Francesco Crea, *Vancouver*
Jane A Foster, *Hamilton*
Hugh J Freeman, *Vancouver*
Shahrokh M Ghobadloo, *Ottawa*
Yuewen Gong, *Winnipeg*
Philip H Gordon, *Quebec*
Rakesh Kumar, *Edmonton*
Wolfgang A Kunze, *Hamilton*
Patrick Labonte, *Laval*
Zhikang Peng, *Winnipeg*
Jayadev Raju, *Ottawa*
Maitreyi Raman, *Calgary*
Giada Sebastiani, *Montreal*
Maida J Sewitch, *Montreal*
Eldon A Shaffer, *Alberta*
Christopher W Teshima, *Edmonton*
Jean Sévigny, *Québec*
Pingchang Yang, *Hamilton*
Pingchang Yang, *Hamilton*
Eric M Yoshida, *Vancouver*
Bin Zheng, *Edmonton*

Chile

Marcelo A Beltran, *La Serena*
Flavio Nervi, *Santiago*
Adolfo Parra-Blanco, *Santiago*
Alejandro Soza, *Santiago*

China

Zhao-Xiang Bian, *Hong Kong*
San-Jun Cai, *Shanghai*
Guang-Wen Cao, *Shanghai*
Long Chen, *Nanjing*
Ru-Fu Chen, *Guangzhou*
George G Chen, *Hong Kong*
Li-Bo Chen, *Wuhan*
Jia-Xu Chen, *Beijing*
Hong-Song Chen, *Beijing*
Lin Chen, *Beijing*
Yang-Chao Chen, *Hong Kong*
Zhen Chen, *Shanghai*
Ying-Sheng Cheng, *Shanghai*
Kent-Man Chu, *Hong Kong*
Zhi-Jun Dai, *Xi'an*
Jing-Yu Deng, *Tianjin*
Yi-Qi Du, *Shanghai*
Zhi Du, *Tianjin*
Hani El-Nezami, *Hong Kong*
Bao-Ying Fei, *Hangzhou*
Chang-Ming Gao, *Nanjing*
Jian-Ping Gong, *Chongqing*
Zuo-Jiong Gong, *Wuhan*
Jing-Shan Gong, *Shenzhen*
Guo-Li Gu, *Beijing*
Yong-Song Guan, *Chengdu*
Mao-Lin Guo, *Luoyang*
Jun-Ming Guo, *Ningbo*
Yan-Mei Guo, *Shanghai*
Xiao-Zhong Guo, *Shenyang*
Guo-Hong Han, *Xi'an*
Ming-Liang He, *Hong Kong*
Peng Hou, *Xi'an*
Zhao-Hui Huang, *Wuxi*
Feng Ji, *Hangzhou*
Simon Law, *Hong Kong*
Yan-Chang Lei, *Hangzhou*
Yu-Yuan Li, *Guangzhou*
Meng-Sen Li, *Haikou*
Shu-De Li, *Shanghai*
Zong-Fang Li, *Xi'an*
Qing-Quan Li, *Shanghai*
Kang Li, *Lasa*
Han Liang, *Tianjin*
Xing'e Liu, *Hangzhou*
Zheng-Wen Liu, *Xi'an*
Xiao-Fang Liu, *Yantai*
Bin Liu, *Tianjin*
Quan-Da Liu, *Beijing*
Hai-Feng Liu, *Beijing*
Fei Liu, *Shanghai*
Ai-Guo Lu, *Shanghai*
He-Sheng Luo, *Wuhan*
Xiao-Peng Ma, *Shanghai*
Yong Meng, *Shantou*
Ke-Jun Nan, *Xi'an*
Siew Chien Ng, *Hong Kong*
Simon SM Ng, *Hong Kong*
Zhao-Shan Niu, *Qingdao*
Di Qu, *Shanghai*
Ju-Wei Mu, *Beijing*
Rui-Hua Shi, *Nanjing*
Bao-Min Shi, *Shanghai*
Xiao-Dong Sun, *Hangzhou*
Si-Yu Sun, *Shenyang*
Guang-Hong Tan, *Haikou*
Wen-Fu Tang, *Chengdu*
Anthony YB Teoh, *Hong Kong*
Wei-Dong Tong, *Chongqing*
Eric Tse, *Hong Kong*
Hong Tu, *Shanghai*

Stavros Gourgiotis, *Athens*
Leontios J Hadjileontiadis, *Thessaloniki*
Thomas Hyphantis, *Ioannina*
Ioannis Kanellos, *Thessaloniki*
Stylianos Karatapanis, *Rhodes*
Michael Koutsilieris, *Athens*
Spiros D Ladas, *Athens*
Theodoros K Liakakos, *Athens*
Emanuel K Manesis, *Athens*
Spilios Manolakopoulos, *Athens*
Gerassimos John Mantzaris, *Athens*
Athanasios D Marinis, *Piraeus*
Nikolaos Ioannis Nikiteas, *Athens*
Konstantinos X Papamichael, *Athens*
George Sgourakis, *Athens*
Konstantinos C Thomopoulos, *Patras*
Konstantinos Triantafyllou, *Athens*
Christos Triantos, *Patras*
Georgios Zacharakis, *Athens*
Petros Zezos, *Alexandroupolis*
Demosthenes E Ziogas, *Ioannina*

Guatemala

Carlos Maria Parellada, *Guatemala*

Hungary

Mihaly Boros, *Szeged*
Tamás Decsi, *Pécs*
Gyula Farkas, *Szeged*
Andrea Furka, *Debrecen*
Y vette Mandi, *Szeged*
Peter L Lakatos, *Budapest*
Pal Miheller, *Budapest*
Tamás Molnar, *Szeged*
Attila Olah, *Gyor*
Maria Papp, *Debrecen*
Ferenc Sipos, *Budapest*
Miklós Tanyi, *Debrecen*
Tibor Wittmann, *Szeged*

Iceland

Tryggvi Bjorn Stefánsson, *Reykjavík*

Indiad

Brij B Agarwal, *New Delhi*
Deepak N Amarapurkar, *Mumbai*
Shams ul Bari, *Srinagar*
Sriparna Basu, *Varanasi*
Runu Chakravarty, *Kolkata*
Devendra C Desai, *Mumbai*
Nutan D Desai, *Mumbai*
Suneela Sunil Dhaneshwar, *Pune*
Radha K Dhiman, *Chandigarh*
Pankaj Garg, *Mohali*
Uday C Ghoshal, *Lucknow*
Kalpesh Jani, *Vadodara*
Premashis Kar, *New Delhi*
Jyotdeep Kaur, *Chandigarh*
Rakesh Kochhar, *Chandigarh*
Pradyumna K Mishra, *Mumbai*
Asish K Mukhopadhyay, *Kolkata*
Imtiyaz Murtaza, *Srinagar*
P Nagarajan, *New Delhi*
Samiran Nundy, *Delhi*
Gopal Pande, *Hyderabad*
Benjamin Perakath, *Vellore*
Arun Prasad, *New Delhi*
D Nageshwar Reddy, *Hyderabad*
Lekha Saha, *Chandigarh*
Sundeep Singh Saluja, *New Delhi*
Mahesh Prakash Sharma, *New Delhi*
Sadiq Saleem Sikora, *Bangalore*
Sarman Singh, *New Delhi*
Rajeev Sinha, *Jhansi*
Rupjyoti Talukdar, *Hyderabad*
Rakesh Kumar Tandon, *New Delhi*
Narayanan Thirumoorthy, *Coimbatore*

Indonesia

David Handojo Muljono, *Jakarta*
Andi Utama, *Jakarta*

Iran

Arezoo Aghakhani, *Tehran*
Seyed Mohsen Dehghani, *Shiraz*
Ahad Eshraghian, *Shiraz*
Hossein Khedmat, *Tehran*
Sadegh Massarrat, *Tehran*
Marjan Mohammadi, *Tehran*
Roja Rahimi, *Tehran*
Farzaneh Sabahi, *Tehran*
Majid Sadeghizadeh, *Tehran*
Farideh Siavoshi, *Tehran*

Ireland

Gary Alan Bass, *Dublin*
David J Brayden, *Dublin*
Ronan A Cahill, *Dublin*
Glen A Doherty, *Dublin*
Liam J Fanning, *Cork*
Barry Philip McMahon, *Dublin*
RossMcManus, *Dublin*
Dervla O'Malley, *Cork*
Sinead M Smith, *Dublin*

Israel

Dan Carter, *Ramat Gan*
Jorge-Shmuel Delgado, *Metar*
Eli Magen, *Ashdod*
Nitsan Maharshak, *Tel Aviv*
Shaul Mordechai, *Beer Sheva*
Menachem Moshkowitz, *Tel Aviv*
William Bahij Nseir, *Nazareth*
Shimon Reif, *Jerusalem*
Ram Reifen, *Rehovot*
Ariella Bar-Gil Shitrit, *Jerusalem*
Noam Shussman, *Jerusalem*
Igor Sukhotnik, *Haifa*
Nir Wasserberg, *Petach Tiqwa*
Jacob Yahav, *Rehovot*
Doron Levi Zamir, *Gedera*
Shira Zelber-Sagi, *Haifa*
Romy Zemel, *Petach-Tikva*

Italy

Ludovico Abenavoli, *Catanzaro*
Luigi Elio Adinolfi, *Naples*
Carlo Virginio Agostoni, *Milan*
Anna Alisi, *Rome*
Piero Luigi Almasio, *Palermo*
Donato Francesco Altomare, *Bari*
Amedeo Amedei, *Florence*
Pietro Andreone, *Bologna*
Imerio Angriman, *Padova*
Vito Annese, *Florence*
Paolo Aurello, *Rome*
Salavtore Auricchio, *Naples*
Gian Luca Baiocchi, *Brescia*
Gianpaolo Balzano, *Milan*
Antonio Basoli, *Rome*
Gabrio Bassotti, *San Sisto*
Mauro Bernardi, *Bologna*
Alberto Biondi, *Rome*
Ennio Biscaldi, *Genova*
Massimo Bolognesi, *Padua*
Luigi Bonavina, *Milano*
Aldo Bove, *Chieti*
Raffaele Bruno, *Pavia*
Luigi Brusciano, *Napoli*
Giuseppe Cabibbo, *Palermo*
Carlo Calabrese, *Bologna*
Daniele Calistri, *Meldola*
Vincenza Calvaruso, *Palermo*
Lorenzo Camellini, *Reggio Emilia*
Marco Candela, *Bologna*
Raffaele Capasso, *Naples*
Lucia Carulli, *Modena*
Renato David Caviglia, *Rome*
Luigina Cellini, *Chieti*
Giuseppe Chiarioni, *Verona*
Claudio Chiesa, *Rome*
Michele Cicala, *Roma*
Rachele Ciccocioppo, *Pavia*
Sandro Contini, *Parma*
Gaetano Corso, *Foggia*
Renato Costi, *Parma*
Alessandro Cucchetti, *Bologna*
Rosario Cuomo, *Napoli*
Giuseppe Currò, *Messina*
Paola De Nardi, *Milano*
Giovanni D De Palma, *Naples*
Raffaele De Palma, *Napoli*
Giuseppina De Petro, *Brescia*
Valli De Re, *Aviano*
Paolo De Simone, *Pisa*
Giuliana Decorti, *Trieste*
Emanuele Miraglia del Giudice, *Napoli*
Isidoro Di Carlo, *Catania*
Matteo Nicola Dario Di Minno, *Naples*
Massimo Donadelli, *Verona*
Mirko D'Onofrio, *Verona*
Maria Pina Dore, *Sassari*
Luca Elli, *Milano*
Massimiliano Fabozzi, *Aosta*
Massimo Falconi, *Ancona*

Ezio Falletto, *Turin*
Silvia Fargion, *Milan*
Matteo Fassan, *Verona*
Gianfranco Delle Fave, *Roma*
Alessandro Federico, *Naples*
Francesco Feo, *Sassari*
Davide Festi, *Bologna*
Natale Figura, *Siena*
Vincenzo Formica, *Rome*
Mirella Fraquelli, *Milan*
Marzio Frazzoni, *Modena*
Walter Fries, *Messina*
Gennaro Galizia, *Naples*
Andrea Galli, *Florence*
Matteo Garcovich, *Rome*
Eugenio Gaudio, *Rome*
Paola Ghiorzo, *Genoa*
Edoardo G Giannini, *Genova*
Luca Gianotti, *Monza*
Maria Cecilia Giron, *Padova*
Alberto Grassi, *Rimini*
Gabriele Grassi, *Trieste*
Francesco Greco, *Bergamo*
Luigi Greco, *Naples*
Antonio Grieco, *Rome*
Fabio Grizzi, *Rozzano*
Laurino Grossi, *Pescara*
Simone Guglielmetti, *Milan*
Tiberiu Hershcovici, *Jerusalem*
Calogero Iacono, *Verona*
Enzo Ierardi, *Bari*
Amedeo Indriolo, *Bergamo*
Raffaele Iorio, *Naples*
Paola Iovino, *Salerno*
Angelo A Izzo, *Naples*
Loreta Kondili, *Rome*
Filippo La Torre, *Rome*
Giuseppe La Torre, *Rome*
Giovanni Latella, *L'Aquila*
Salvatore Leonardi, *Catania*
Massimo Libra, *Catania*
Anna Licata, *Palermo*
C armela Loguercio, *Naples*
Amedeo Lonardo, *Modena*
Carmelo Luigiano, *Catania*
Francesco Luzza, *Catanzaro*
Giovanni Maconi, *Milano*
Antonio Macrì, *Messina*
Mariano Malaguarnera, *Catania*
Francesco Manguso, *Napoli*
Tommaso Maria Manzia, *Rome*
Daniele Marrelli, *Siena*
Gabriele Masselli, *Rome*
Sara Massironi, *Milan*
Giuseppe Mazzarella, *Avellino*
Michele Milella, *Rome*
Giovanni Milito, *Rome*
Antonella d'Arminio Monforte, *Milan*
Fabrizio Montecucco, *Genoa*
Giovanni Monteleone, *Rome*
Mario Morino, *Torino*
Vincenzo La Mura, *Milan*
Gerardo Nardone, *Naples*
Riccardo Nascimbeni, *Brescia*
Gabriella Nesi, *Florence*
Giuseppe Nigri, *Rome*
Erica Novo, *Turin*
Veronica Ojetti, *Rome*
Michele Orditura, *Naples*
Fabio Pace, *Seriate*
Lucia Pacifico, *Rome*
Omero Alessandro Paoluzi, *Rome*
Valerio Pazienza, *San Giovanni Rotondo*
Rinaldo Pellicano, *Turin*
Adriano M Pellicelli, *Rome*
Nadia Peparini, *Ciampino*
Mario Pescatori, *Rome*
Antonio Picardi, *Rome*
Alberto Pilotto, *Padova*
Alberto Piperno, *Monza*
Anna Chiara Piscaglia, *Rome*
Maurizio Pompili, *Rome*
Francesca Romana Ponziani, *Rome*
Cosimo Prantera, *Rome*
Girolamo Ranieri, *Bari*
Carlo Ratto, *Tome*
Barbara Renga, *Perugia*
Alessandro Repici, *Rozzano*
Maria Elena Riccioni, *Rome*
Lucia Ricci-Vitiani, *Rome*
Luciana Rigoli, *Messina*
Mario Rizzetto, *Torino*
Ballarin Roberto, *Modena*
Roberto G Romanelli, *Florence*
Claudio Romano, *Messina*
Luca Roncucci, *Modena*
Cesare Ruffolo, *Treviso*
L ucia Sacchetti, *Napoli*
Rodolfo Sacco, *Pisa*
Lapo Sali, *Florence*
Romina Salpini, *Rome*
Giulio Aniello, *Santoro Treviso*
Armando Santoro, *Rozzano*
Edoardo Savarino, *Padua*
Marco Senzolo, *Padua*
Annalucia Serafino, *Rome*
Giuseppe S Sica, *Rome*
Pierpaolo Sileri, *Rome*
Cosimo Sperti, *Padua*
Vincenzo Stanghellini, *Bologna*
Cristina Stasi, *Florence*
Gabriele Stocco, *Trieste*
Roberto Tarquini, *Florence*
Mario Testini, *Bari*
Guido Torzilli, *Milan*
Guido Alberto Massimo, *Tiberio Brescia*
Giuseppe Toffoli, *Aviano*
Alberto Tommasini, *Trieste*
Francesco Tonelli, *Florence*
Cesare Tosetti Porretta, *Terme*
Lucio Trevisani, *Cona*
Guglielmo M Trovato, *Catania*
Mariapia Vairetti, *Pavia*
Luca Vittorio Valenti, *Milano*
Mariateresa T Ventura, *Bari*
Giuseppe Verlato, *Verona*
Marco Vivarelli, *Ancona*
Giovanni Li Volti, *Catania*
Giuseppe Zanotti, *Padua*
Vincenzo Zara, *Lecce*
Gianguglielmo Zehender, *Milan*
Anna Linda Zignego, *Florence*
Rocco Antonio Zoccali, *Messina*
Angelo Zullo, *Rome*

Japan

Yasushi Adachi, *Sapporo*
Takafumi Ando, *Nagoya*
Masahiro Arai, *Tokyo*
Makoto Arai, *Chiba*
Takaaki Arigami, *Kagoshima*
Itaru Endo,*Yokohama*
Munechika Enjoji, *Fukuoka*
Shunji Fujimori, *Tokyo*
Yasuhiro Fujino, *Akashi*
Toshiyoshi Fujiwara, *Okayama*
Yosuke Fukunaga, *Tokyo*
Toshio Fukusato, *Tokyo*
Takahisa Furuta, *Hamamatsu*
Osamu Handa, *Kyoto*
Naoki Hashimoto, *Osaka*
Yoichi Hiasa, *Toon*
Masatsugu Hiraki, *Saga*
Satoshi Hirano, *Sapporo*
Keiji Hirata, *Fukuoka*
Toru Hiyama, *Higashihiroshima*
Akira Hokama, *Nishihara*
Shu Hoteya, *Tokyo*
Masao Ichinose, *Wakayama*
Tatsuya Ide, *Kurume*
Masahiro Iizuka, *Akita*
Toshiro Iizuka, *Tokyo*
Kenichi Ikejima, *Tokyo*
Tetsuya Ikemoto, *Tokushima*
Hiroyuki Imaeda, *Saitama*
Atsushi Imagawa, *Kan-onji*
Hiroo Imazu, *Tokyo*
Shuji Isaji, *Tsu*
Toru Ishikawa, *Niigata*
Toshiyuki Ishiwata, *Tokyo*
Soichi Itaba, *Kitakyushu*
Yoshiaki Iwasaki, *Okayama*
Tatehiro Kagawa, *Isehara*
Satoru Kakizaki, *Maebashi*
Naomi Kakushima, *Shizuoka*
Terumi Kamisawa, *Tokyo*
Akihide Kamiya, *Isehara*
Osamu Kanauchi, *Tokyo*
Tatsuo Kanda, *Chiba*
Shin Kariya, *Okayama*
Shigeyuki Kawa, *Matsumoto*
Takumi Kawaguchi, *Kurume*
Takashi Kawai, *Tokyo*
Soo Ryang Kim, *Kobe*
Shinsuke Kiriyama, *Gunma*
Tsuneo Kitamura, *Urayasu*
Masayuki Kitano, *Osakasayama*
Hirotoshi Kobayashi, *Tokyo*
Hironori Koga, *Kurume*
Takashi Kojima, *Sapporo*
Satoshi Kokura, *Kyoto*
Shuhei Komatsu, *Kyoto*
Tadashi Kondo, *Tokyo*
Yasuteru Kondo, *Sendai*
Yasuhiro Kuramitsu, *Yamaguchi*
Yukinori Kurokawa, *Osaka*
Shin Maeda, *Yokohama*
Koutarou Maeda, *Toyoake*

Hitoshi Maruyama, *Chiba*
Atsushi Masamune, *Sendai*
Hiroyuki Matsubayashi, *Suntogun*
Akihisa Matsuda, *Inzai*
Hirofumi Matsui, *Tsukuba*
Akira Matsumori, *Kyoto*
Yoichi Matsuo, *Nagoya*
Y Matsuzaki, *Ami*
Toshihiro Mitaka, *Sapporo*
Kouichi Miura, *Akita*
Shinichi Miyagawa, *Matumoto*
Eiji Miyoshi, *Suita*
Toru Mizuguchi, *Sapporo*
Nobumasa Mizuno, *Nagoya*
Zenichi Morise, *Nagoya*
Tomohiko Moriyama, *Fukuoka*
Kunihiko Murase, *Tusima*
Michihiro Mutoh, *Tsukiji*
Akihito Nagahara, *Tokyo*
Hikaru Nagahara, *Tokyo*
Hidenari Nagai, *Tokyo*
Koichi Nagata, *Shimotsuke-shi*
Masaki Nagaya, *Kawasaki*
Hisato Nakajima, *Nishi-Shinbashi*
Toshifusa Nakajima, *Tokyo*
Hiroshi Nakano, *Kawasaki*
Hiroshi Nakase, *Kyoto*
Toshiyuki Nakayama, *Nagasaki*
Takahiro Nakazawa, *Nagoya*
Shoji Natsugoe, *Kagoshima City*
Tsutomu Nishida, *Suita*
Shuji Nomoto, *Naogya*
Sachiyo Nomura, *Tokyo*
Takeshi Ogura, *Takatsukishi*
Nobuhiro Ohkohchi, *Tsukuba*
Toshifumi Ohkusa, *Kashiwa*
Hirohide Ohnishi, *Akita*
Teruo Okano, *Tokyo*
Satoshi Osawa, *Hamamatsu*
Motoyuki Otsuka, *Tokyo*
Michitaka Ozaki, *Sapporo*
Satoru Saito, *Yokohama*
Naoaki Sakata, *Sendai*
Ken Sato, *Maebashi*
Toshiro Sato, *Tokyo*
Tomoyuki Shibata, *Toyoake*
Tomohiko Shimatani, *Kure*
Yukihiro Shimizu, *Nanto*
Tadashi Shimoyama, *Hirosaki*
Masayuki Sho, *Nara*
Ikuo Shoji, *Kobe*
Atsushi Sofuni, *Tokyo*
Takeshi Suda, *Niigata*
M Sugimoto, *Hamamatsu*
Ken Sugimoto, *Hamamatsu*
Haruhiko Sugimura, *Hamamatsu*
Shoichiro Sumi, *Kyoto*
Hidekazu Suzuki, *Tokyo*
Masahiro Tajika, *Nagoya*
Hitoshi Takagi, *Takasaki*
Toru Takahashi, *Niigata*
Yoshihisa Takahashi, *Tokyo*
Shinsuke Takeno, *Fukuoka*
Akihiro Tamori, *Osaka*
Kyosuke Tanaka, *Tsu*
Shinji Tanaka, *Hiroshima*
Atsushi Tanaka, *Tokyo*
Yasuhito Tanaka, *Nagoya*
Shinji Tanaka, *Tokyo*
Minoru Tomizawa, *Yotsukaido City*
Kyoko Tsukiyama-Kohara, *Kagoshima*
Takuya Watanabe, *Niigata*
Kazuhiro Watanabe, *Sendai*
Satoshi Yamagiwa, *Niigata*
Takayuki Yamamoto, *Yokkaichi*
Hiroshi Yamamoto, *Otsu*
Kosho Yamanouchi, *Nagasaki*
Ichiro Yasuda, *Gifu*
Yutaka Yata, *Maebashi-city*
Shin-ichi Yokota, *Sapporo*
Norimasa Yoshida, *Kyoto*
Hiroshi Yoshida, *Tama-City*
Hitoshi Yoshiji, *Kashihara*
Kazuhiko Yoshimatsu, *Tokyo*
Kentaro Yoshioka, *Toyoake*
Nobuhiro Zaima, *Nara*

Jordan
Khaled Ali Jadallah, *Irbid*

Kuwait
Islam Khan, *Kuwait*

Lebanon
Bassam N Abboud, *Beirut*
Kassem A Barada, *Beirut*
Marwan Ghosn, *Beirut*
Iyad A Issa, *Beirut*
Fadi H Mourad, *Beirut*
AIa Sharara, *Beirut*
Rita Slim, *Beirut*

Lithuania
Antanas Mickevicius, *Kaunas*

Malaysia
Huck Joo Tan, *Petaling Jaya*

Mexico
Richard A Awad, *Mexico City*
Carlos R Camara-Lemarroy, *Monterrey*
Norberto C Chavez-Tapia, *Mexico City*
Wolfgang Gaertner, *Mexico City*
Diego Garcia-Compean, *Monterrey*
Arturo Panduro, *Guadalajara*
OT Teramoto-Matsubara, *Mexico City*
Felix Tellez-Avila, *Mexico City*
Omar Vergara-Fernandez, *Mexico City*
Saúl Villa-Trevino, *Cuidad de México*

Morocco
Samir Ahboucha, *Khouribga*

Netherlands
Robert J de Knegt, *Rotterdam*
Tom Johannes Gerardus Gevers, *Nijmegen*
Menno Hoekstra, *Leiden*
BW Marcel Spanier, *Arnhem*
Karel van Erpecum, *Utrecht*

New Zealand
Leo K Cheng, *Auckland*
Andrew Stewart Day, *Christchurch*
Jonathan Barnes Koea, *Auckland*
Max Petrov, *Auckland*

Nigeria
Olufunmilayo Adenike Lesi, *Lagos*
Jesse Abiodun Otegbayo, *Ibadan*
Stella Ifeanyi Smith, *Lagos*

Norway
Trond Berg, *Oslo*
Trond Arnulf Buanes, *Krokkleiva*
Thomas de Lange, *Rud*
Magdy El-Salhy, *Stord*
Rasmus Goll, *Tromso*
Dag Arne Lihaug Hoff, *Aalesund*

Pakistan
Zaigham Abbas, *Karachi*
Usman A Ashfaq, *Faisalabad*
Muhammad Adnan Bawany, *Hyderabad*
Muhammad Idrees, *Lahore*
Saeed Sadiq Hamid, *Karachi*
Yasir Waheed, *Islamabad*

Poland
Thomas Brzozowski, *Cracow*
Magdalena Chmiela, *Lodz*
Krzysztof Jonderko, *Sosnowiec*
Anna Kasicka-Jonderko, *Sosnowiec*
Michal Kukla, *Katowice*
Tomasz Hubert Mach, *Krakow*
Agata Mulak, *Wroclaw*
Danuta Owczarek, *Kraków*
Piotr Socha, *Warsaw*
Piotr Stalke, *Gdansk*
Julian Teodor Swierczynski, *Gdansk*
Anna M Zawilak-Pawlik, *Wroclaw*

Portugal
Marie Isabelle Cremers, *Setubal*
Ceu Figueiredo, *Porto*
Ana Isabel Lopes, *LIsbon*
M Paula Macedo, *Lisboa*
Ricardo Marcos, *Porto*
Rui T Marinho, *Lisboa*
Guida Portela-Gomes, *Estoril*

Filipa F Vale, *Lisbon*

Puerto Rico

Caroline B Appleyard, *Ponce*

Qatar

Abdulbari Bener, *Doha*

Romania

Mihai Ciocirlan, *Bucharest*
Dan LucianDumitrascu, *Cluj-Napoca*
Carmen Fierbinteanu-Braticevici, *Bucharest*
Romeo G Mihaila, *Sibiu*
Lucian Negreanu, *Bucharest*
Adrian Saftoiu, *Craiova*
Andrada Seicean, *Cluj-Napoca*
Ioan Sporea, *Timisoara*
Letiţia Adela Maria Streba, *Craiova*
Anca Trifan, *Iasi*

Russia

Victor Pasechnikov, *Stavropol*
Vasiliy Ivanovich Reshetnyak, *Moscow*
Vitaly Skoropad, *Obninsk*

Saudi Arabia

Abdul-Wahed N Meshikhes, *Dammam*
M Ezzedien Rabie, *Khamis Mushait*

Singapore

Brian KP Goh, *Singapore*
Richie Soong, *Singapore*
Ker-Kan Tan, *Singapore*
Kok-Yang Tan, *Singapore*
Yee-Joo Tan, *Singapore*
Mark Wong, *Singapore*
Hong Ping Xia, *Singapore*

Slovenia

Matjaz Homan, *Ljubljana*
Martina Perse, *Ljubljana*

South Korea

Sang Hoon Ahn, *Seoul*
Seung Hyuk Baik, *Seoul*
Soon Koo Baik, *Wonju*
Soo-Cheon Chae, *Iksan*
Byung-Ho Choe, *Daegu*
Suck Chei Choi, *Iksan*
Hoon Jai Chun, *Seoul*
Yeun-Jun Chung, *Seoul*
Young-Hwa Chung, *Seoul*
Ki-Baik Hahm, *Seongnam*
Sang Young Han, *Busan*
Seok Joo Han, *Seoul*
Seung-Heon Hong, *Iksan*
Jin-Hyeok Hwang, *Seoungnam*
Jeong Won Jang, *Seoul*
Jin-Young Jang, *Seoul*
Dae-Won Jun, *Seoul*
Young Do Jung, *Kwangju*
Gyeong Hoon Kang, *Seoul*
Sung-Bum Kang, *Seoul*
Koo Jeong Kang, *Daegu*
Ki Mun Kang, *Jinju*
Chang Moo Kang, *Seodaemun-gu*
Gwang Ha Kim, *Busan*
Sang Soo Kim, *Goyang-si*
Jin Cheon Kim, *Seoul*
Tae Il Kim, *Seoul*
Jin Hong Kim, *Suwon*
Kyung Mo Kim, *Seoul*
Kyongmin Kim, *Suwon*
Hyung-Ho Kim, *Seongnam*
Seoung Hoon Kim, *Goyang*
Sang Il Kim, *Seoul*
Hyun-Soo Kim, *Wonju*
Jung Mogg Kim, *Seoul*
Dong Yi Kim, *Gwangju*
Kyun-Hwan Kim, *Seoul*
Jong-Han Kim, *Ansan*
Sang Wun Kim, *Seoul*
Ja-Lok Ku, *Seoul*
Kyu Taek Lee, *Seoul*
Hae-Wan Lee, *Chuncheon*
Inchul Lee, *Seoul*
Jung Eun Lee, *Seoul*
Sang Chul Lee, *Daejeon*
Song Woo Lee, *Ansan-si*
Hyuk-Joon Lee, *Seoul*
Seong-Wook Lee, *Yongin*
Kil Yeon Lee, *Seoul*
Jong-Inn Lee, *Seoul*
Kyung A Lee, *Seoul*
Jong-Baeck Lim, *Seoul*
Eun-Yi Moon, *Seoul*
SH Noh, *Seoul*
Seung Woon Paik, *Seoul*
Won Sang Park, *Seoul*
Sung-Joo Park, *Iksan*
Kyung Sik Park, *Daegu*
Se Hoon Park, *Seoul*
Yoonkyung Park, *Gwangju*
Seung-Wan Ryu, *Daegu*
Il Han Song, *Cheonan*
Myeong Jun Song, *Daejeon*
Yun Kyoung Yim, *Daejeon*
Dae-Yeul Yu *Daejeon*

Spain

Mariam Aguas, *Valencia*
Raul J Andrade, *Málaga*
Antonio Arroyo, *Elche*
Josep M Bordas, *Barcelona*
Lisardo Boscá, *Madrid*
Ricardo Robles Campos, *Murcia*
Jordi Camps, *Reus*
Carlos Cervera *Barcelona*
Alfonso Clemente, *Granada*
Pilar Codoner-Franch, *Valencia*
Fernando J Corrales, *Pamplona*
Fermin Sánchez de Medina, *Granada*
Alberto Herreros de Tejada, *Majadahonda*
Enrique de-Madaria, *Alicante*
JE Dominguez-Munoz, *Santiago de Compostela*
Vicente Felipo, *Valencia*
CM Fernandez-Rodriguez, *Madrid*
Carmen Frontela-Saseta, *Murcia*
Julio Galvez, *Granada*
Maria Teresa García, *Vigo*
MI Garcia-Fernandez, *Málaga*
Emilio Gonzalez-Reimers, *La Laguna*
Marcel Jimenez, *Bellaterra*
Angel Lanas, *Zaragoza*
Juan Ramón Larrubia, *Guadalajara*
Antonio Lopez-Sanroman, *Madrid*
Vicente Lorenzo-Zuniga, *Badalona*
Alfredo J Lucendo, *Tomelloso*
Vicenta Soledad Martinez-Zorzano, *Vigo*
José Manuel Martin-Villa, *Madrid*
Julio Mayol, *Madrid*
Manuel Morales-Ruiz, *Barcelona*
Alfredo Moreno-Egea, *Murcia*
Albert Pares, *Barcelona*
Maria Pellise, *Barcelona*
José Perea, *Madrid*
Miguel Angel Plaza, *Zaragoza*
María J Pozo, *Cáceres*
Enrique Quintero, *La Laguna*
Jose M Ramia, *Madrid*
Francisco Rodriguez-Frias, *Barcelona*
Silvia Ruiz-Gaspa, *Barcelona*
Xavier Serra-Aracil, *Barcelona*
Vincent Soriano, *Madrid*
Javier Suarez, *Pamplona*
Carlos Taxonera, *Madrid*
M Isabel Torres, *Jaén*
Manuel Vazquez-Carrera, *Barcelona*
Benito Velayos, *Valladolid*
Silvia Vidal, *Barcelona*

Sri Lanka

Arjuna Priyadarsin De Silva, *Colombo*

Sudan

Ishag Adam, *Khartoum*

Sweden

Roland G Andersson, *Lund*
Bergthor Björnsson, *Linkoping*
Johan Christopher Bohr, *Örebro*
Mauro D'Amato, *Stockholm*
Thomas Franzen, *Norrkoping*
Evangelos Kalaitzakis, *Lund*
Riadh Sadik, *Gothenburg*
Per Anders Sandstrom, *Linkoping*
Ervin Toth, *Malmö*
Konstantinos Tsimogiannis, *Vasteras*
Apostolos V Tsolakis, *Uppsala*

Switzerland

Gieri Cathomas, *Liestal*
Jean Louis Frossard, *Geneve*
Christian Toso, *Geneva*
Stephan Robert Vavricka, *Zurich*
Dominique Velin, *Lausanne*

Thailand

Thawatchai Akaraviputh, *Bangkok*
P Yoysungnoen Chintana, *Pathumthani*
Veerapol Kukongviriyapan, *Muang*
Vijittra Leardkamolkarn, *Bangkok*
Varut Lohsiriwat, *Bangkok*
Somchai Pinlaor, *Khaon Kaen*
D Wattanasirichaigoon, *Bangkok*

Trinidad and Tobago

B Shivananda Nayak, *Mount Hope*

Tunisia

Ibtissem Ghedira, *Sousse*
Lilia Zouiten-Mekki, *Tunis*

Turkey

Inci Alican, *Istanbul*
Mustafa Altindis, *Sakarya*
Mutay Aslan, *Antalya*
Oktar Asoglu, *Istanbul*
Yasemin Hatice Balaban, *Istanbul*
Metin Basaranoglu, *Ankara*
Yusuf Bayraktar, *Ankara*
Süleyman Bayram, *Adiyaman*
Ahmet Bilici, *Istanbul*
Ahmet Sedat Boyacioglu, *Ankara*
Züleyha Akkan Cetinkaya, *Kocaeli*
Cavit Col, *Bolu*
Yasar Colak, *Istanbul*
Cagatay Erden Daphan, *Kirikkale*
Mehmet Demir, *Hatay*
Ahmet Merih Dobrucali, *Istanbul*
Gülsüm Ozlem Elpek, *Antalya*
Ayse Basak Engin, *Ankara*
Eren Ersoy, *Ankara*
Osman Ersoy, *Ankara*
Yusuf Ziya Erzin, *Istanbul*
Mukaddes Esrefoglu, *Istanbul*
Levent Filik, *Ankara*
Ozgur Harmanci, *Ankara*
Koray Hekimoglu, *Ankara*
Abdurrahman Kadayifci, *Gaziantep*
Cem Kalayci, *Istanbul*
Selin Kapan, *Istanbul*
Huseyin Kayadibi, *Adana*
Sabahattin Kaymakoglu, *Istanbul*
Metin Kement, *Istanbul*
Mevlut Kurt, *Bolu*
Resat Ozaras, *Istanbul*
Elvan Ozbek, *Adapazari*
Cengiz Ozcan, *Mersin*
Hasan Ozen, *Ankara*
Halil Ozguc, *Bursa*
Mehmet Ozturk, *Izmir*
Orhan V Ozkan, *Sakarya*
Semra Paydas, *Adana*
Ozlem Durmaz Suoglu, *Istanbul*
Ilker Tasci, *Ankara*
Müge Tecder-ünal, *Ankara*
Mesut Tez, *Ankara*
Serdar Topaloglu, *Trabzon*
Murat Toruner, *Ankara*
Gokhan Tumgor, *Adana*
Oguz Uskudar, *Adana*
Mehmet Yalniz, *Elazig*
Mehmet Yaman, *Elazig*
Veli Yazisiz, *Antalya*
Yusuf Yilmaz, *Istanbul*
Ozlem Yilmaz, *Izmir*
Oya Yucel, *Istanbul*
Ilhami Yuksel, *Ankara*

United Kingdom

Nadeem Ahmad Afzal, *Southampton*
Navneet K Ahluwalia, *Stockport*
Yeng S Ang, *Lancashire*
Ramesh P Arasaradnam, *Coventry*
Ian Leonard Phillip Beales, *Norwich*
John Beynon, *Swansea*
Barbara Braden, *Oxford*
Simon Bramhall, *Birmingham*
Geoffrey Burnstock, *London*
Ian Chau, *Sutton*
Thean Soon Chew, *London*
Helen G Coleman, *Belfast*
Anil Dhawan, *London*
Sunil Dolwani, *Cardiff*
Piers Gatenby, *London*
Anil T George, *London*
Pasquale Giordano, *London*
Paul Henderson, *Edinburgh*
Georgina Louise Hold, *Aberdeen*
Stefan Hubscher, *Birmingham*
Robin D Hughes, *London*
Nusrat Husain, *Manchester*
Matt W Johnson, *Luton*
Konrad Koss, *Macclesfield*
Anastasios Koulaouzidis, *Edinburgh*
Simon Lal, *Salford*
John S Leeds, *Aberdeen*
JK K Limdi, *Manchester*
Hongxiang Liu, *Cambridge*
Michael Joseph McGarvey, *London*
Michael Anthony Mendall, *London*
Alexander H Mirnezami, *Southampton*
J Bernadette Moore, *Guildford*
Claudio Nicoletti, *Norwich*
Savvas Papagrigoriadis, *London*
Sylvia LF Pender, *Southampton*
David Mark Pritchard, *Liverpool*
James A Ross, *Edinburgh*
Kamran Rostami, *Worcester*
Xiong Z Ruan, *London*
Frank I Tovey, *London*
Dhiraj Tripathi, *Birmingham*
Vamsi R Velchuru, *Great Yarmouth*
Nicholas T Ventham, *Edinburgh*
Diego Vergani, *London*
Jack Westwood Winter, *Glasgow*
Terence Wong, *London*
Ling Yang, *Oxford*

United States

Daniel E Abbott, *Cincinnati*
Ghassan K Abou-Alfa, *New York*
Julian Abrams, *New York*
David William Adelson, *Los Angeles*
Jonathan Steven Alexander, *Shreveport*
Tauseef Ali, *Oklahoma City*
Mohamed R Ali, *Sacramento*
Rajagopal N Aravalli, *Minneapolis*
Hassan Ashktorab, *Washington*
Shashi Bala, *Worcester*
Charles F Barish, *Raleigh*
P Patrick Basu, *New York*
Robert L Bell, *Berkeley Heights*
David Bentrem, *Chicago*
Henry J Binder, *New Haven*
Joshua Bleier, *Philadelphia*
Wojciech Blonski, *Johnson City*
Kenneth Boorom, *Corvallis*
Brian Boulay, *Chicago*
Carla W Brady, *Durham*
Kyle E Brown, *Iowa City*
Adeel A Butt, *Pittsburgh*
Weibiao Cao, *Providence*
Andrea Castillo, *Cheney*
Fernando J Castro, *Weston*
Adam S Cheifetz, *Boston*
Xiaoxin Luke Chen, *Durham*
Ramsey Cheung, *Palo Alto*
Parimal Chowdhury, *Little Rock*
Edward John Ciaccio, *New York*
Dahn L Clemens, *Omaha*
Yingzi Cong, *Galveston*
Laura Iris Cosen-Binker, *Boston*
Joseph John Cullen, *Lowa*
Mark J Czaja, *Bronx*
Mariana D Dabeva, *Bronx*
Christopher James Damman, *Seattle*
Isabelle G De Plaen, *Chicago*
Punita Dhawan, *Nashville*
Hui Dong, *La Jolla*
Wael El-Rifai, *Nashville*
Sukru H Emre, *New Haven*
Paul Feuerstadt, *Hamden*
Josef E Fischer, *Boston*
Laurie N Fishman, *Boston*
Joseph Che Forbi, *Atlanta*
Temitope Foster, *Atlanta*
Amy E Foxx-Orenstein, *Scottsdale*
Daniel E Freedberg, *New York*
Shai Friedland, *Palo Alto*
Virgilio George, *Indianapolis*
Ajay Goel, *Dallas*
Oliver Grundmann, *Gainesville*
Stefano Guandalini, *Chicago*
Chakshu Gupta, *St. Joseph*
Grigoriy E Gurvits, *New York*

World Journal of Gastroenterology

Contents

Weekly Volume 23 Number 23 June 21, 2017

CASE REPORT

World Journal of Gastroenterology
Volume 23 Number 23 June 21, 2017

Contents

EDITORS FOR THIS ISSUE

Responsible Assistant Editor: *Xiang Li*
Responsible Science Editor: *Ze-Mao Gong*
Responsible Electronic Editor: *Fen-Fen Zhang*
Proofing Editorial Office Director: *Jin-Lei Wang*
Proofing Editor-in-Chief: *Lian-Sheng Ma*

NAME OF JOURNAL
World Journal of Gastroenterology

ISSN
ISSN 1007-9327 (print)
ISSN 2219-2840 (online)

LAUNCH DATE
October 1, 1995

FREQUENCY
Weekly

EDITORIAL OFFICE
Jin-Lei Wang, Director
Yuan Qi, Vice Director
Ze-Mao Gong, Vice Director
World Journal of Gastroenterology
Baishideng Publishing Group Inc
7901 Stoneridge Drive, Suite 501,
Pleasanton, CA 94588, USA
Telephone: +1-925-2238242
Fax: +1-925-2238243
E-mail: editorialoffice@wjgnet.com
Help Desk: http://www.f6publishing.com/helpdesk
http://www.wjgnet.com

PUBLISHER
Baishideng Publishing Group Inc
7901 Stoneridge Drive, Suite 501,
Pleasanton, CA 94588, USA
Telephone: +1-925-2238242
Fax: +1-925-2238243
E-mail: bpgoffice@wjgnet.com
Help Desk: http://www.f6publishing.com/helpdesk
http://www.wjgnet.com

PUBLICATION DATE
June 21, 2017

INSTRUCTIONS TO AUTHORS
Full instructions are available online at http://www.wjgnet.com/bpg/gerinfo/204

ONLINE SUBMISSION
http://www.f6publishing.com

World Journal of Gastroenterology

Submit a Manuscript: http://www.f6publishing.com

World J Gastroenterol 2017 June 21; 23(23): 4135-4139

DOI: 10.3748/wjg.v23.i23.4135

ISSN 1007-9327 (print) ISSN 2219-2840 (online)

EDITORIAL

Attenuated adenomatous polyposis of the large bowel: Present and future

Luca Roncucci, Monica Pedroni, Francesco Mariani

Luca Roncucci, Monica Pedroni, Francesco Mariani, Department of Diagnostic and Clinical Medicine, and Public Health, University of Modena and Reggio Emilia, I-41125 Modena, Italy

Author contributions: Roncucci L, Pedroni M and Mariani F conceived the issues that formed the content of the manuscript; Roncucci L wrote the manuscript; Pedroni M and Mariani F discussed and edited the manuscript.

Conflict-of-interest statement: The authors have no conflict of interest to disclose.

Manuscript source: Invited manuscript

Correspondence to: Luca Roncucci, MD, PhD, Department of Diagnostic and Clinical Medicine, and Public Health, University of Modena and Reggio Emilia, Policlinico, Via Del Pozzo 71, I-41125 Modena, Italy. luca.roncucci@unimore.it
Telephone: +39-59-4224052
Fax: +39-59-4222958

Received: January 27, 2017
Peer-review started: February 6, 2017
First decision: March 16, 2017
Revised: April 3, 2017
Accepted: May 9, 2017
Article in press: May 9, 2017
Published online: June 21, 2017

Abstract

Attenuated adenomatous polyposis (AAP) is a poorly understood syndrome, that can be defined as the presence of 10-99 synchronous adenomas in the large bowel, and it is considered a phenotypic variant of familial adenomatous polyposis (FAP). This definition has the advantage of simplicity, but it may include sporadic multiple adenomas of the large bowel at an extreme, or FAP cases on the other side. AAP shows a milder phenotype than FAP, with an older age of onset of adenomas and cancer, and less frequent extracolonic manifestations. AAP may be diagnosed as a single case in a family or, less frequently, it may be present in other family members, and it shows distinct pattern of inheritance. In less than 50% of cases, it may be caused by adenomatous polyposis coli (*APC*) or *MUTYH* mutations, referred to as *APC*-associated polyposis, inherited as an autosomal dominant trait, or *MUTYH*-associated polyposis, which shows an autosomal recessive mechanism of inheritance, respectively. Surveillance should rely on colonoscopy at regular intervals, with removal of adenomas and careful histological examination. When removal of polyps is not possible or advanced lesions are observed, the surgical approach is mandatory, being subtotal colectomy with ileo-rectal anastomosis the treatment of choice. Studies on this syndrome are lacking, and controversies are still present on many issues, thus, other clinical and genetic studies are requested.

Key words: Attenuated adenomatous polyposis; Genetic testing; Surveillance; Attenuated familial adenomatous polyposis; Adenomatous polyposis coli; *MUTYH*

Core tip: Attenuated adenomatous polyposis is a poorly understood syndrome, which may be defined as the presence of 10-99 synchronous adenomas in the large bowel, when at least 50% of the polyps removed are adenomatous. It is a variant of Familial Adenomatous Polyposis with a milder phenotype. In less than 50%

of cases, it is caused by adenomatous polyposis coli (*APC*) or *MUTYH* mutations, and less frequently by other genes. Surveillance should rely on colonoscopy at regular intervals, with removal of adenomas and careful histological examination. If removal of all polyps is not possible or advanced lesions are observed, the surgical treatment is mandatory.

Roncucci L, Pedroni M, Mariani F. Attenuated adenomatous polyposis of the large bowel: Present and future. *World J Gastroenterol* 2017; 23(23): 4135-4139 Available from: URL: http://www.wjgnet.com/1007-9327/full/v23/i23/4135.htm DOI: http://dx.doi.org/10.3748/wjg.v23.i23.4135

INTRODUCTION

Familial adenomatous polyposis (FAP) is a disease characterized by the presence of at least 100 adenomas of the large bowel, several extracolonic manifestations, and it is inherited as an autosomal dominant trait[1]. It is caused by constitutional mutations in the adenomatous polyposis coli (*APC*) gene[2,3], and, less frequently, by mutations in the *MUTYH* gene[4]. Attenuated familial adenomatous polyposis (AFAP) is considered a phenotypic variant of FAP, whose main feature is the presence in the large bowel of less than 100 synchronous adenomas[5]. "Attenuated" also means that the disease has a milder phenotype than the classical FAP. Indeed, patients with AFAP develop adenomas and cancer at an older age, and extracolonic manifestations are less frequent than in FAP[5,6]. Moreover, only one individual is affected in most families[7]. Nowadays AFAP may be included in the broad category of adenomatous polyposis syndromes[8].

The first approach to an attenuated adenomatous polyposis (AAP) should be clinical, and it is extremely important for the further management of the disease. The first step for a correct evaluation of patients with an intestinal polyposis must be a careful collection of the family history of cancers and premalignant lesions of the gastrointestinal tract, in order to get an estimate of the risk of an inherited predisposition to cancer. Particular attention should be paid to vertical transmission of the disease (from a generation to the next), sibling aggregation, and age at diagnosis of cancers in the family, especially for first- and second-degree relatives, although very often we are dealing with single cases in a family. Another milestone in the management is the particular attention that should be put on the histology of polyps removed in the large bowel. Polyps are usually adenomas, but it is not infrequent to find other histological variants (hyperplastic, serrated, hamartomatous, juvenile, or mixed), sometimes associated with adenomas. It is conceivable to define an adenomatous polyposis when more than 50% of polyps are adenomas, otherwise other polyposis syndromes should be taken into account[9]. Then, relying on the familial pedigree and on the characteristics of the individual phenotype of the proband, genetic testing for a germline mutation should be proposed to the proband, or to the most informative family members, when appropriate. In the case of attenuated adenomatous polyposis, firstly *APC* and *MUTYH* mutations should be searched for[8].

Indeed, constitutional mutations in *APC* or *MUTYH* genes were found in a large fraction of patients with AFAP[9-11]. Accordingly, now the term *APC*-associated polyposis (AFAP) can be more appropriately used when the *APC* gene is mutated, as in the classical FAP, whereas *MUTYH*-associated polyposis (MAP) is preferred when *MUTYH* mutations are found. However, many patients with AAP remains "genetic orphans", because at present, no constitutional mutation can be demonstrated[12,13]. Moreover, mutations in other genes can cause rare forms of attenuated polyposis[14].

As mentioned above, there is still controversy also on the morphology of polyps that should be included in the definition of attenuated polyposis. In fact, according to some authors, hyperplastic or serrated polyposis should be included in this category[15,16], considering the risk of developing colorectal cancer in these forms of intestinal polyposis[17]. Other polyposis have peculiar morphologic characteristics that allow to classify them as Hamartomatous polyposis syndromes (Peutz-Jeghers syndrome, Juvenile polyposis, and Cowden syndrome).

Thus, the picture is far to be completely elucidated, and, despite attempts to refine diagnostic accuracy, AFAP still remains poorly understood and defined. We think that, before proceeding toward the genetic diagnosis, it is mandatory to try to reach a useful definition of the syndrome that we prefer to refer to as AAP. Probably one possible definition is to consider as AAP any patient with synchronous adenomas of the large bowel ranging between 10 and 99, not considering age of onset, other clinical features, or formal and molecular genetics. Of course this definition is totally clinical, and, as all definitions, it reflects only part of the truth. For example, near the upper and lower limits of 10 and 99 adenomas it is impossible to sharply cut off sporadic multiple adenomas for the lower limit, and classical FAP for the upper. Moreover, we do not know whether the development of further metachronous adenomas during surveillance of patients may change the definition and the management of the syndrome. Another controversial issue is the presence in the family of other patients with adenomas or cancer[10]. However this definition has the advantage of simplicity, and it allows to have a solid ground on which rely for the genetic and clinical management of affected patients and family members. Another issue is the fraction of adenomas on the total number of polyps necessary to define an adenomatous polyposis. We think that at least 50% histologically confirmed adenomas are necessary for the definition of AAP[9].

Since the definition is unclear and there is no real consensus, incidence and frequency of AAP are difficult to establish. Frequency may be estimated to be less than 15% of all adenomatous polyposis, but a systematic search for AAP has never been carried out. As mentioned above, the age of onset of AAP is delayed as compared with FAP[5,9], adenomas seem more prevalent in the proximal colon[18,19], to spare the rectum[20], and they tend to be flat[21,22], and sometimes also hyperplastic polyps and flat serrated adenomas are present[23]. The risk of developing cancer is not 100% as in classical FAP. Extracolonic manifestations [duodenal adenomas, periampullary carcinoma, desmoid tumors, osteomas, epidermoid cysts, congenital hypertrophy of the retinal pigmented epithelium (CHRPE), supernumerary teeth, thyroid carcinoma, and hepatoblastoma] seem less frequent than in FAP, though studies are very few on this topic[23,24].

As mentioned, genetic testing should be offered to patients with AAP. *APC* and *MUTYH* are the two genes most frequently involved in the pathogenesis of AAP. However, constitutional mutations of other known and unknown genes contribute to the AAP phenotype.

APC is a tumor-suppressor gene, located on the long arm of chromosome 5[25]. In classical FAP a mutated allele is inherited, the other allele is damaged or lost by a somatic event, and this allows the growth of adenomas. Then, other mutational events in other genes are required to push ahead the malignant transformation. Some correlations between the site of the mutations within the open reading frame of the gene and the clinical manifestations of the disease have been reported so far (the so-called genotype-phenotype correlations)[26]. As far as AAP is concerned, the overall frequency of *APC* mutations is difficult to establish, however it can be estimated around 10%-20% of patients with less than 100 adenomas[9]. In these cases, AAP (namely AFAP) is inherited as an autosomal dominant disease, as it happens for classical FAP. In AAP, we know that *APC* mutations are found mostly near the 5' and 3' ends of the gene, and sometimes on exon 9[7,26], but other regions of the gene can be mutated.

MUTYH is a base excision repair gene whose protein repairs oxidative damage to DNA[4]. Biallelic mutations of that gene cause CG-AT transversions in several other genes, including *APC* and *RAS*. The two most frequent mutations found in patients with AAP are Y179C and G396D, both missense[27]. Thus, *MUTYH*-associated polyposis (MAP) has a recessive pattern of inheritance, and it is particularly frequent in patients with less than 100 adenomas[28,29], though *MUTYH* mutations may be found also in a small fraction of patients with classical FAP and no *APC* mutation[28]. It can be estimated that *MUTYH* is mutated in 20%-40% of patients with AAP[12,29]. Mean age at diagnosis seems delayed, when compared with patients with *APC* mutations[30]. Mutations in one allele only of the *MUTYH* gene seem not to confer a higher risk of developing intestinal adenomatous polyposis.

Recently, other genes that may be constitutionally mutated in intestinal polyposis syndromes, were found associated with the AAP phenotype. These genes, involved in DNA synthesis are polymerase D1 (*POLD1*) and polymerase E gene (*POLE*). Mutations in one of these genes cause the rare Polymerase Proofreading-Associated Polyposis (PPAP)[14], which is inherited as an autosomal dominant trait. Mutations in these genes have been reported so far also for Lynch syndrome, and probably cause an excess also of brain tumors[31].

Constitutional mutations in other genes may explain a certain fraction of AAP: *NTHL1*[32], *MSH3*[33], *FOCAD*[34], *POLD3* or other polymerase genes[35]. In the near future, other genes will be discovered in the germline of patients with AAP.

No established guidelines exist for the management of AAP. When a mutation is found in *APC* or *MUTYH* (biallelic), a colonoscopy should be carried out, beginning at puberty, along with esophago-gastroduodenoscopy, and repeated over time every 2-3 years, and then regularly. However, since the genetic test is often negative for constitutional mutation, management is empirical and based on clinical findings in most cases. The choice of following a patient endoscopically or with a surgical approach is a matter of debate. The more convenient program is to continue an endoscopic follow-up when all polyps can be removed during colonoscopy, and to counsel surgery when the number of polyps is high or with multiple diminutive polyps, or in case of low compliance, or when a severe dysplasia or cancer is found at histological examination in one or more polyps[8,36]. When surgery is necessary, and the rectum is spared by polyps, a subtotal colectomy with ileo-rectal anastomosis is the treatment of choice[37]. Sometimes, when a severe phenotype (profuse polyposis) is present, due to mutations in particular zones of the genes, the surgical resection should be enlarged[38,39]. At variance with FAP, no valuable information is available for chemoprevention with non-steroidal anti-inflammatory or other drugs in AAP, though the smaller number of polyps might be an advantage. Surveillance for upper gastrointestinal lesions (gastric polyps and duodenal/jejunal adenomas) with gastroduodenoscopy may be recommended at lapses of time guided by the Spigelman' stage of duodenal polyposis, as in FAP, but no data are available at the moment[8].

CONCLUSION

AAP is a poorly defined syndrome which deserves further research. It may be defined as the presence of 10-99 synchronous adenomas in the large bowel, when at least 50% of the polyps removed are adenomatous (otherwise other polyposis syndromes should be suspected). This definition has the advantage of simplicity, but it may include sporadic multiple

adenomas of the large bowel at an extreme, or FAP cases at the upper limit. AAP shows a milder phenotype than FAP, with an older age of onset of adenomas and cancer, and less frequent extracolonic manifestations. AAP may be diagnosed as a single case in a family or, less frequently, it may be present in other family members. In less than 50% of cases, it may be caused by *APC* or *MUTYH* mutations, referred to as *APC*-associated polyposis (AFAP), or *MUTYH*-associated polyposis (MAP), respectively. Surveillance should rely on colonoscopy at regular intervals, with removal of adenomas and careful histological examination. If removal of all polyps is not possible or advanced lesions are observed, the surgical treatment is mandatory. With no doubt, we need further insights into the undefined and poorly understood issue of AAP.

ACKNOWLEDGMENTS

The authors recognize the continuous support of the Associazione per lo Ricerca Sui Tumori Intestinali (ARTI).

REFERENCES

1 **Half E**, Bercovich D, Rozen P. Familial adenomatous polyposis. *Orphanet J Rare Dis* 2009; **4**: 22 [PMID: 19822006 DOI: 10.1186/1750-1172-4-22]
2 **Kinzler KW**, Nilbert MC, Su LK, Vogelstein B, Bryan TM, Levy DB, Smith KJ, Preisinger AC, Hedge P, McKechnie D. Identification of FAP locus genes from chromosome 5q21. *Science* 1991; **253**: 661-665 [PMID: 1651562 DOI: 10.1126/science.1651562.]
3 **Groden J**, Thliveris A, Samowitz W, Carlson M, Gelbert L, Albertsen H, Joslyn G, Stevens J, Spirio L, Robertson M. Identification and characterization of the familial adenomatous polyposis coli gene. *Cell* 1991; **66**: 589-600 [PMID: 1651174 DOI: 10.1016/0092-8674(81)90021-0]
4 **Al-Tassan N**, Chmiel NH, Maynard J, Fleming N, Livingston AL, Williams GT, Hodges AK, Davies DR, David SS, Sampson JR, Cheadle JP. Inherited variants of MYH associated with somatic G:C--& gt; T: A mutations in colorectal tumors. *Nat Genet* 2002; **30**: 227-232 [PMID: 11818965 DOI: 10.1038/ng828]
5 **Hernegger GS**, Moore HG, Guillem JG. Attenuated familial adenomatous polyposis: an evolving and poorly understood entity. *Dis Colon Rectum* 2002; **45**: 127-134; discussion 134-136 [PMID: 11786778 DOI: 10.1007/s10350-004-6127-y]
6 **Knudsen AL**, Bisgaard ML, Bülow S. Attenuated familial adenomatous polyposis (AFAP). A review of the literature. *Fam Cancer* 2003; **2**: 43-55 [PMID: 14574166]
7 **Burt RW**, Leppert MF, Slattery ML, Samowitz WS, Spirio LN, Kerber RA, Kuwada SK, Neklason DW, Disario JA, Lyon E, Hughes JP, Chey WY, White RL. Genetic testing and phenotype in a large kindred with attenuated familial adenomatous polyposis. *Gastroenterology* 2004; **127**: 444-451 [PMID: 15300576 DOI: 10.1053/j.gastro.2004.05.003]
8 **Syngal S**, Brand RE, Church JM, Giardiello FM, Hampel HL, Burt RW. ACG clinical guideline: Genetic testing and management of hereditary gastrointestinal cancer syndromes. *Am J Gastroenterol* 2015; **110**: 223-262; quiz 263 [PMID: 25645574 DOI: 10.1038/ajg.2014.435]
9 **de Leon MP**, Pedroni M, Roncucci L, Domati F, Rossi G, Magnani G, Pezzi A, Fante R, Bonetti LR. Attenuated polyposis of the large bowel: a morphologic and molecular approach. *Fam Cancer* 2017; **16**: 211-220 [PMID: 27783336 DOI: 10.1007/s10689-016-9938-9]
10 **Nielsen M**, Hes FJ, Nagengast FM, Weiss MM, Mathus-Vliegen EM, Morreau H, Breuning MH, Wijnen JT, Tops CM, Vasen HF. Germline mutations in APC and MUTYH are responsible for the majority of families with attenuated familial adenomatous polyposis. *Clin Genet* 2007; **71**: 427-433 [PMID: 17489848 DOI: 10.1111/j.1399-0004.2007.00766.x]
11 **Filipe B**, Baltazar C, Albuquerque C, Fragoso S, Lage P, Vitoriano I, Mão de Ferro S, Claro I, Rodrigues P, Fidalgo P, Chaves P, Cravo M, Nobre Leitão C. APC or MUTYH mutations account for the majority of clinically well-characterized families with FAP and AFAP phenotype and patients with more than 30 adenomas. *Clin Genet* 2009; **76**: 242-255 [PMID: 19793053 DOI: 10.1111/j.1399-0004.2009.01241.x]
12 **Wang L**, Baudhuin LM, Boardman LA, Steenblock KJ, Petersen GM, Halling KC, French AJ, Johnson RA, Burgart LJ, Rabe K, Lindor NM, Thibodeau SN. MYH mutations in patients with attenuated and classic polyposis and with young-onset colorectal cancer without polyps. *Gastroenterology* 2004; **127**: 9-16 [PMID: 15236166 DOI: 10.1053/j.gastro.2004.03.070]
13 **de Leon MP**, Urso ED, Pucciarelli S, Agostini M, Nitti D, Roncucci L, Benatti P, Pedroni M, Kaleci S, Balsamo A, Laudi C, Di Gregorio C, Viel A, Rossi G, Venesio T. Clinical and molecular features of attenuated adenomatous polyposis in northern Italy. *Tech Coloproctol* 2013; **17**: 79-87 [PMID: 22976915 DOI: 10.1007/s10151-012-0887-5]
14 **Palles C**, Cazier JB, Howarth KM, Domingo E, Jones AM, Broderick P, Kemp Z, Spain SL, Guarino E, Salguero I, Sherborne A, Chubb D, Carvajal-Carmona LG, Ma Y, Kaur K, Dobbins S, Barclay E, Gorman M, Martin L, Kovac MB, Humphray S, Lucassen A, Holmes CC, Bentley D, Donnelly P, Taylor J, Petridis C, Roylance R, Sawyer EJ, Kerr DJ, Clark S, Grimes J, Kearsey SE, Thomas HJ, McVean G, Houlston RS, Tomlinson I. Germline mutations affecting the proofreading domains of POLE and POLD1 predispose to colorectal adenomas and carcinomas. *Nat Genet* 2013; **45**: 136-144 [PMID: 23263490 DOI: 10.1038/ng.2503]
15 **Gill P**, Wang LM, Bailey A, East JE, Leedham S, Chetty R. Reporting trends of right-sided hyperplastic and sessile serrated polyps in a large teaching hospital over a 4-year period (2009-2012). *J Clin Pathol* 2013; **66**: 655-658 [PMID: 23576460 DOI: 10.1136/jclinpath-2013-201608]
16 **Hazewinkel Y**, Tytgat KM, van Eeden S, Bastiaansen B, Tanis PJ, Boparai KS, Fockens P, Dekker E. Incidence of colonic neoplasia in patients with serrated polyposis syndrome who undergo annual endoscopic surveillance. *Gastroenterology* 2014; **147**: 88-95 [PMID: 24657624 DOI: 10.1053/j.gastro.2014.03.015]
17 **Boparai KS**, van den Broek FJ, van Eeden S, Fockens P, Dekker E. Increased polyp detection using narrow band imaging compared with high resolution endoscopy in patients with hyperplastic polyposis syndrome. *Endoscopy* 2011; **43**: 676-682 [PMID: 21811939 DOI: 10.1055/s-0030-1256447]
18 **Lynch HT**, Smyrk TC. Classification of familial adenomatous polyposis: a diagnostic nightmare. *Am J Hum Genet* 1998; **62**: 1288-1289 [PMID: 9585618 DOI: 10.1086/301890]
19 **Moisio AL**, Järvinen H, Peltomäki P. Genetic and clinical characterisation of familial adenomatous polyposis: a population based study. *Gut* 2002; **50**: 845-850 [PMID: 12010888 DOI: 10.1136/gut.50.6.845]
20 **Rozen P**, Samuel Z, Shomrat R, Legum C. Notable intrafamilial phenotypic variability in a kindred with familial adenomatous polyposis and an APC mutation in exon 9. *Gut* 1999; **45**: 829-833 [PMID: 10562580 DOI: 10.1136/gut.45.6.829]
21 **Matsubara N**, Isozaki H, Tanaka N. The farthest 3' distal end APC mutation identified in attenuated adenomatous polyposis coli with extracolonic manifestations. *Dis Colon Rectum* 2000; **43**: 720-721 [PMID: 10826438 DOI: 10.1007/BF02235596]
22 **O'Shea AM**, Cleary SP, Croitoru MA, Kim H, Berk T, Monga N, Riddell RH, Pollett A, Gallinger S. Pathological features of colorectal carcinomas in MYH-associated polyposis. *Histopathology* 2008; **53**: 184-194 [PMID: 18564191 DOI:

10.1111/j.1365-2559.2008.03071.x]
23 **Boparai KS**, Dekker E, Van Eeden S, Polak MM, Bartelsman JF, Mathus-Vliegen EM, Keller JJ, van Noesel CJ. Hyperplastic polyps and sessile serrated adenomas as a phenotypic expression of MYH-associated polyposis. *Gastroenterology* 2008; **135**: 2014-2018 [PMID: 19013464 DOI: 10.1053/j.gastro.2008.09.020]
24 **Su LK**, Barnes CJ, Yao W, Qi Y, Lynch PM, Steinbach G. Inactivation of germline mutant APC alleles by attenuated somatic mutations: a molecular genetic mechanism for attenuated familial adenomatous polyposis. *Am J Hum Genet* 2000; **67**: 582-590 [PMID: 10924409 DOI: 10.1086/303058]
25 **Bodmer WF**, Bailey CJ, Bodmer J, Bussey HJ, Ellis A, Gorman P, Lucibello FC, Murday VA, Rider SH, Scambler P. Localization of the gene for familial adenomatous polyposis on chromosome 5. *Nature* 1987; **328**: 614-616 [PMID: 3039373 DOI: 10.1038/328614a0]
26 **Nieuwenhuis MH**, Vasen HF. Correlations between mutation site in APC and phenotype of familial adenomatous polyposis (FAP): a review of the literature. *Crit Rev Oncol Hematol* 2007; **61**: 153-161 [PMID: 17064931 DOI: 10.1016/j.critrevonc.2006.07.004]
27 **Sieber OM**, Lipton L, Crabtree M, Heinimann K, Fidalgo P, Phillips RK, Bisgaard ML, Orntoft TF, Aaltonen LA, Hodgson SV, Thomas HJ, Tomlinson IP. Multiple colorectal adenomas, classic adenomatous polyposis, and germ-line mutations in MYH. *N Engl J Med* 2003; **348**: 791-799 [PMID: 12606733 DOI: 10.1056/NEJMoa025283]
28 **Sampson JR**, Dolwani S, Jones S, Eccles D, Ellis A, Evans DG, Frayling I, Jordan S, Maher ER, Mak T, Maynard J, Pigatto F, Shaw J, Cheadle JP. Autosomal recessive colorectal adenomatous polyposis due to inherited mutations of MYH. *Lancet* 2003; **362**: 39-41 [PMID: 12853198 DOI: 10.1016/S0140-6736(03)13805-6]
29 **Venesio T**, Molatore S, Cattaneo F, Arrigoni A, Risio M, Ranzani GN. High frequency of MYH gene mutations in a subset of patients with familial adenomatous polyposis. *Gastroenterology* 2004; **126**: 1681-1685 [PMID: 15188161 DOI: 10.1053/j.gastro.2004.02.022]
30 **Marabelli M**, Molinaro V, Khouzam RA, Berrino E, Panero M, Balsamo A, Venesio T, Ranzani GN. Colorectal Adenomatous Polyposis: Heterogeneity of Susceptibility Gene Mutations and Phenotypes in a Cohort of Italian Patients. *Genet Test Mol Biomarkers* 2016; **20**: 777-785 [PMID: 27705013 DOI: 10.1089/gtmb.2016.0198]
31 **Bellido F**, Pineda M, Aiza G, Valdés-Mas R, Navarro M, Puente DA, Pons T, González S, Iglesias S, Darder E, Piñol V, Soto JL, Valencia A, Blanco I, Urioste M, Brunet J, Lázaro C, Capellá G, Puente XS, Valle L. POLE and POLD1 mutations in 529 kindred with familial colorectal cancer and/or polyposis: review of reported cases and recommendations for genetic testing and surveillance. *Genet Med* 2016; **18**: 325-332 [PMID: 26133394 DOI: 10.1038/gim.2015.75]
32 **Weren RD**, Ligtenberg MJ, Kets CM, de Voer RM, Verwiel ET, Spruijt L, van Zelst-Stams WA, Jongmans MC, Gilissen C, Hehir-Kwa JY, Hoischen A, Shendure J, Boyle EA, Kamping EJ, Nagtegaal ID, Tops BB, Nagengast FM, Geurts van Kessel A, van Krieken JH, Kuiper RP, Hoogerbrugge N. A germline homozygous mutation in the base-excision repair gene NTHL1 causes adenomatous polyposis and colorectal cancer. *Nat Genet* 2015; **47**: 668-671 [PMID: 25938944 DOI: 10.1038/ng.3287]
33 **Adam R**, Spier I, Zhao B, Kloth M, Marquez J, Hinrichsen I, Kirfel J, Tafazzoli A, Horpaopan S, Uhlhaas S, Stienen D, Friedrichs N, Altmüller J, Laner A, Holzapfel S, Peters S, Kayser K, Thiele H, Holinski-Feder E, Marra G, Kristiansen G, Nöthen MM, Büttner R, Möslein G, Betz RC, Brieger A, Lifton RP, Aretz S. Exome Sequencing Identifies Biallelic MSH3 Germline Mutations as a Recessive Subtype of Colorectal Adenomatous Polyposis. *Am J Hum Genet* 2016; **99**: 337-351 [PMID: 27476653 DOI: 10.1016/j.ajhg.2016.06.015]
34 **Weren RD**, Venkatachalam R, Cazier JB, Farin HF, Kets CM, de Voer RM, Vreede L, Verwiel ET, van Asseldonk M, Kamping EJ, Kiemeney LA, Neveling K, Aben KK, Carvajal-Carmona L, Nagtegaal ID, Schackert HK, Clevers H, van de Wetering M, Tomlinson IP, Ligtenberg MJ, Hoogerbrugge N, Geurts van Kessel A, Kuiper RP. Germline deletions in the tumour suppressor gene FOCAD are associated with polyposis and colorectal cancer development. *J Pathol* 2015; **236**: 155-164 [PMID: 25712196 DOI: 10.1002/path.4520]
35 **Spier I**, Holzapfel S, Altmüller J, Zhao B, Horpaopan S, Vogt S, Chen S, Morak M, Raeder S, Kayser K, Stienen D, Adam R, Nürnberg P, Plotz G, Holinski-Feder E, Lifton RP, Thiele H, Hoffmann P, Steinke V, Aretz S. Frequency and phenotypic spectrum of germline mutations in POLE and seven other polymerase genes in 266 patients with colorectal adenomas and carcinomas. *Int J Cancer* 2015; **137**: 320-331 [PMID: 25529843 DOI: 10.1002/ijc.29396]
36 **Fornasarig M**, Minisini AM, Viel A, Quaia M, Canzonieri V, Veronesi A. Twelve years of endoscopic surveillance in a family carrying biallelic Y165C MYH defect: report of a case. *Dis Colon Rectum* 2006; **49**: 272-275 [PMID: 16416081 DOI: 10.1007/s10350-005-0257-8]
37 **Bülow C**, Vasen H, Järvinen H, Björk J, Bisgaard ML, Bülow S. Ileorectal anastomosis is appropriate for a subset of patients with familial adenomatous polyposis. *Gastroenterology* 2000; **119**: 1454-1460 [PMID: 11113066 DOI: 10.1053/gast.2000.20180]
38 **Rozen P**, Macrae F. Familial adenomatous polyposis: The practical applications of clinical and molecular screening. *Fam Cancer* 2006; **5**: 227-235 [PMID: 16998668 DOI: 10.1007/s10689-005-5674-2]
39 **Nielsen M**, Joerink-van de Beld MC, Jones N, Vogt S, Tops CM, Vasen HF, Sampson JR, Aretz S, Hes FJ. Analysis of MUTYH genotypes and colorectal phenotypes in patients With MUTYH-associated polyposis. *Gastroenterology* 2009; **136**: 471-476 [PMID: 19032956 DOI: 10.1053/j.gastro.2008.10.056]

P- Reviewer: Garcia-Olmo D, Topaloglu S **S- Editor**: Qi Y
L- Editor: A **E- Editor**: Zhang FF

World Journal of Gastroenterology

Submit a Manuscript: http://www.f6publishing.com

World J Gastroenterol 2017 June 21; 23(23): 4140-4145

DOI: 10.3748/wjg.v23.i23.4140

ISSN 1007-9327 (print) ISSN 2219-2840 (online)

EDITORIAL

Evolution of associating liver partition and portal vein ligation for staged hepatectomy: Simpler, safer and equally effective methods

Shu-You Peng, Xu-An Wang, Cong-Yun Huang, You-Yong Zhang, Jiang-Tao Li, De-Fei Hong, Xiu-Jun Cai

Shu-You Peng, Jiang-Tao Li, Department of Hepatobiliary and Pancreatic Surgery, The Second Affiliated Hospital of Zhejiang University School of Medicine, Hangzhou 310009, Zhejiang Province, China

Xu-An Wang, Department of General Surgery, Xinhua Hospital Affiliated to Shanghai Jiaotong University School of Medicine, Shanghai 200092, China

Cong-Yun Huang, Department of General Surgery, Yuebei People's Hospital Affiliated to Shantou University School of Medicine, Shantou 515063, Guangdong Province, China

You-Yong Zhang, Department of Radiology, Yuebei People's Hospital Affiliated to Shantou University School of Medicine, Shantou 515063, Guangdong Province, China

De-Fei Hong, Department of Hepatobiliary and Pancreatic Surgery, Zhejiang Provincial People's Hospital, Hangzhou 310009, Zhejiang Province, China

Xiu-Jun Cai, Department of Hepatobiliary and Pancreatic Surgery, Sir Run Run Shaw Hospital, Zhejiang University, Hangzhou 310016, Zhejiang Province, China

Author contributions: Peng SY and Wang XA contributed equally to this work; Peng SY and Wang XA wrote and revised the manuscript; Peng SY designed the TBPVE and TELPP approaches; Huang CY and Zhang YY performed the TBPVE and TACE and prepared the figures; all the authors participated in the TELPP operations except Zhang YY.

Supported by the National Natural Science Foundation of China, No. 81570559 and No. 81272673.

Conflict-of-interest statement: All the authors deny any form of conflict of interest.

Manuscript source: Invited manuscript

Correspondence to: Shu-You Peng, MD, FACS(Hon), Department of Hepatobiliary and Pancreatic Surgery, The Second Affiliated Hospital of Zhejiang University School of Medicine, 88 Jiefang Road, Hangzhou 310009, Zhejiang Province, China. zrwkpsy@zju.edu.cn
Telephone: +86-571-87783766

Received: January 28, 2017
Peer-review started: February 8, 2017
First decision: March 16, 2017
Revised: April 3, 2017
Accepted: May 4, 2017
Article in press: May 4, 2017
Published online: June 21, 2017

Abstract

Associating liver partition and portal vein ligation for staged hepatectomy (ALPPS) has been recently demonstrated as a method to induce rapid and extensive hypertrophy within a short time and has been employed for a variety of primary and metastatic liver tumors. However, controversies remain due to its high morbidity and mortality. To enable safer surgery, liver surgeons have searched for better technical modifications, such as partial ALPPS, mini-ALPPS, minimally invasive ALPPS, and Terminal branches portal vein Embolization Liver Partition for Planned hepatectomy (TELPP). It seems that TELPP is very promising, because it has the main advantage of ALPPS - the rapid increase of future liver remnant volume, but the morbidity and mortality are much lower because only one surgical operation is required.

Key words: Associating liver partition and portal vein ligation for staged hepatectomy; Terminal branches portal vein embolization; Terminal branches portal vein embolization liver partition for planned hepatectomy; Transarterial chemoembolization

Core tip: Many technical modifications have been proposed for associating liver partition and portal vein ligation for staged hepatectomy (ALPPS) due to its high morbidity and mortality. We described a new one, named Terminal branches portal vein Embolization Liver Partition for Planned hepatectomy, which uses a different method to interrupt the communicating portal vein branches, not by manipulation of the liver parenchyma but by the implementation of the embolization of terminal portal vein branches between both sides of the liver. It has the main advantage of ALPPS - the rapid increase of future liver remnant volume, but the morbidity and mortality are much lower.

Peng SY, Wang XA, Huang CY, Zhang YY, Li JT, Hong DF, Cai XJ. Evolution of associating liver partition and portal vein ligation for staged hepatectomy: Simpler, safer and equally effective methods. *World J Gastroenterol* 2017; 23(23): 4140-4145 Available from: URL: http://www.wjgnet.com/1007-9327/full/v23/i23/4140.htm DOI: http://dx.doi.org/10.3748/wjg.v23.i23.4140

INTRODUCTION

Associating liver partition and portal vein ligation (PVL) for staged hepatectomy (ALPPS) is a novel two-stage strategy for oncological liver surgery that was developed to induce future liver remnant (FLR) hypertrophy in patients with previously considered nonresectable liver tumors[1,2]. This great new approach was invented by chance by Schlitt in 2007 for a patient with hilar cholangiocarcinoma who was about to undergo right trisegmentectomy. Intraoperatively, it was found that the FLR would be insufficient. Then, he split the liver parenchyma along the falciform ligament to facilitate the left hepaticojejunostomy for palliation together with PVL to induce hypertrophy of the left lateral lobe. Finally, he performed the second stage operation to resect the diseased liver because the computed tomography (CT) scan showed enormous hypertrophy of the FLR on postoperative day 8. The patient recovered from the operation[2].

This technique was first reported by Baumgart *et al*[3] on a poster. In 2012, Schnitzbauer *et al*[1] published their experience with 25 cases performed in 5 German centers with a median FLR hypertrophy of 74% after a median time interval of 9 d. This value was markedly higher than that for portal vein occlusion (PVE or PVL), which increases the FLR between 10% to 46% within 2 to 8 wk[4-6]. The article attracted significant interest from liver surgeons worldwide, and de Santibañes and Clavien[2] proposed the term "ALPPS" for this novel approach. In that article, the authors also revealed a hospital lethality of 12% and a 24% rate of biliary leakage requiring radiologic or endoscopic intervention. Then, an international registry was initiated to collect information from multiple centers worldwide from 2012 to monitor the feasibility and safety of ALPPS. The first analysis of 202 patients by Schadde *et al*[7] in January 2014 reported a perioperative 90-d mortality of 9% and an impressive hypertrophy of 80% within a median of 7 d. The high mortality rate has elicited an intense discussion and debate about the safety of ALPPS[8,9].

EVOLUTION OF ALPPS

Even though ALPPS is significantly characterized by increasing the insufficient remnant liver volume within a shorter interval for two-stage resection, much controversy has surrounded it due to its safety; for example, the reported remarkable morbidity was 16%-64% and the mortality rate was 12%-23%[10-13]. Barroso considered ALPPS as the last option, or the ultimate possibility to cure some patients; he thought that it was not ethical to propose this kind of operation to a patient without first proposing a PVE[14]. Thus, to reduce the perioperative mortality and morbidity rates, to achieve a long-term disease-free survival and to enable safer surgery, liver surgeons have searched for better technical modifications.

General modifications of ALPPS

Based on their experimental model, Petrowsky *et al*[15] developed a technical modification, named p-ALPPS (partial ALPPS), to switch from full liver partition to partial transection (50%-80% of the transection surface). They compared 18 patients who underwent full transection with 6 patients who underwent 50% to 80% partition, and the results displayed a comparable degree of liver hypertrophy on postoperative day 11 with fewer severe complications (Dindo-Clavien grade $\geqslant$ 3b) and zero in-hospital mortality. Alvarez *et al*[16] confirmed the value of p-ALPPS by a prospectively multivariate analysis that included 21 patients who underwent partial partition. In addition, they defined partial partition as the level of the middle hepatic vein, whereas total partition as the vena cava. However, a partial partition during the first stage will challenge the second stage, as it requires longer liver parenchymal transection.

Hernandez-Alejandro *et al*[17] have cautioned that extensive dissection of the hepatoduodenal ligament increases the likelihood of segment 4 ischemia and potentially increases the risk of bile leakage and resulting septic complications. Consistent with this,

Tanaka *et al*[18] considered that sepsis originating from the ischemic area produced by parenchymal division increases mortality, accounting for one-third of postoperative deaths. They described a modified ALPPS procedure that preserves the portal pedicles during parenchymal division to avoid producing an ischemic area. Five patients received this modification without mortality. Mean hypertrophy of the FLR was 1.638 ± 0.384 a week after the first stage procedure.

de Santibañes *et al*[19] proposed mini-ALPPS, which combined partial transection and intraoperative PVE without hilum dissection or liver mobilization during the first stage. They applied this technique in four patients with a result of 62.6% (range, 49%-79%) FLR hypertrophy in a median of 11 d (range, 6-15 d), and no one developed liver failure or major complications.

SPECIAL MODIFICATIONS OF ALPPS

Avoidance of liver parenchymal division

The prominent advantage of ALPPS is the rapid and extensive hypertrophy of FLR within a short time period; however, the morbidity rate and the in-hospital mortality rate are incredibly high, which constitutes a major concern. Of note, septic complications and bile leakage were observed in 20%-25% of patients. Obviously, bile leakage stems from the two raw surfaces of the split liver that are left behind in the abdominal cavity after the first stage operation. The bile leakage may result in septic complications. Therefore, the avoidance of liver parenchymal division is important. According to Alvarez *et al*[12], the mechanisms for rapid FLR hypertrophy might be because: (1) PVL creates a redistribution of hepatotrophic factors to the FLR, and this produces the active and necessary phenomenon of FLR hypertrophy; (2) liver partition causes local surgical trauma that per se might represent an important regeneration stimulus; (3) the impairment of bilateral cross-portal circulation allows a more dramatic increase in portal flow to the FLR; and (4) unlike one-stage major hepatectomies, in which the liver remnant has to address hyper flow and portal hypertension, in this technique the diseased arterialized hemiliver allows the FLR to tolerate this hemodynamic stress, modulating the double hepatic vascular inflow.

Based on the third mechanism, liver parenchyma division can be avoided, so long as bilateral cross-portal circulation can be blocked by other methods. These methods are described below.

Using a liver tourniquet: In a 2013 case report, Robles Campos *et al*[20] described a modification termed ALTPS (associating liver tourniquet and portal ligation for staged hepatectomy) with a hypertrophy of 150% of the FLR. Instead of an *in situ* split, a tourniquet was positioned around the liver following either Cantlie's line or to the right of the umbilical fissure for the first stage of ALPPS. This tourniquet was then tied tightly enough to occlude all collateral vessels between the two lobes, which was confirmed by intraoperative ultrasound (IOUS). This modified approach might potentially decrease morbidity by decreasing technical complexity and shortening the operative time for the first stage of the operation.

Cai *et al*[21] adopted the execution of round-the-liver ligation to replace the *in situ* splitting of the liver, which could avoid postoperative bile leakage and might simplify the operation. The FLR volume increased by 37.9% according to the CT scan performed on day 10 after the first stage operation. The replacement of liver splitting by round-the-liver ligation could avoid biliary leakage, simplify the first stage operation and finally lead to a decrease in perioperative morbidity and mortality. Both the first and second stage operations were performed laparoscopically.

Using microwave liver ablation: Another new technique to avoid liver parenchymal division was presented by Gall *et al*[22]. After right PVL, an inline radiofrequency ablation (RFA) probe was applied to the parenchyma instead of the *in situ* liver partition. The hypertrophy of the FLR was 62.3% at a mean interval of 21.8 d. In 2015, Gringeri *et al*[23] described laparoscopic microwave ablation and PVL for staged hepatectomy (LAPS) on the future transection plane with a satisfactory hypertrophy of FLR and an easier second step in hepatocellular cancer (HCC) 10 d later. Compared with the traditional ALPPS, this technique may offer some advantages, such as an easier second operation due to the lack of adhesions and safer liver resection along the avascular groove.

Hong *et al*[24] presented a novel minimally invasive approach implementing percutaneous microwave ablation liver partition and portal vein embolization (PALPP) instead of the first step of ALPPS for rapid liver regeneration. The authors applied percutaneous microwave ablation (PMA) every 3 cm along the transection plane under ultrasonographic guidance until the formation of a necrotic groove from the inferior liver to the suprahepatic veins. The PMA line was positioned on the right side of the transection plane at a power of 60 W set as a 3-min ablation cycle. PVE was performed 3 d after PMA. Fourteen days later, a well-planned right trisectionectomy was performed. Three cases of HCC and 1 case of hilar cholangiocarcinoma were performed using this approach with a hypertrophic rate of 41.2%, which was similar to the results for HCC[25]. Hong's approach may have additional benefits. Tumor spread caused by ALPPS could be mitigated and intraoperative and postoperative bleeding along with bile leakage could be reduced as a result of microscopically coagulative necrosis.

Avoidance of two staged operations

Original PVE only requires one operation, but the proliferative speed is too slow. However, the ALPPS

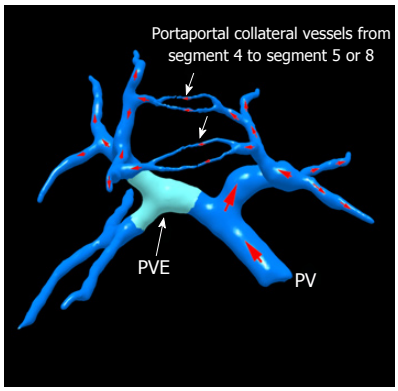

Figure 1 Bilateral cross-portal circulation after portal vein embolization. Red arrows indicate blood flow to the S8 or S5 from the collateral vessels. PV: Portal vein; PVE: Portal vein embolization.

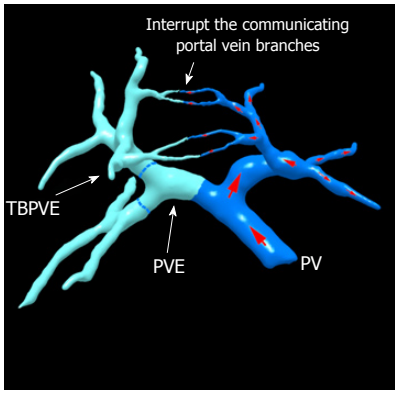

Figure 2 Terminal branches portal vein embolization of S8 and S5. The communicating portal vein branches were interrupted without liver parenchyma division (red arrows indicate that blood flow to the S8 or S5 was interrupted, and blue dotted lines indicate the boundary between PVE and TBPVE). PV: Portal vein; PVE: Portal vein embolization; TBPVE: Terminal branches portal vein embolization.

and all modifications require two-stage operations with high morbidity and mortality rates. Is it possible to merge the concepts of ALPPS and PVE for designing a simpler and safer technique? It would be preferred to perform a single surgical operation rather than two to achieve the same therapeutic effect.

TELPP: The aforementioned special modifications of ALPPS to avoid liver parenchymal division have proven that the blockage of bilateral cross-portal circulation can promote FLR hypertrophy. Trying to search for a better way, we proposed terminal branches portal vein embolization (TBPVE) by applying an additional embolization agent on the endings of the portal vein system of S5, S8 or S4 (Figures 1 and 2).

TBPVE uses a different method to interrupt the communicating portal vein branches, not by manipulation of the liver parenchyma but rather by the implementation of the embolization of terminal portal vein branches between both sides of the liver. The mechanism of TBPVE is to separate the left and right sides of the liver by blocking communicating branches.

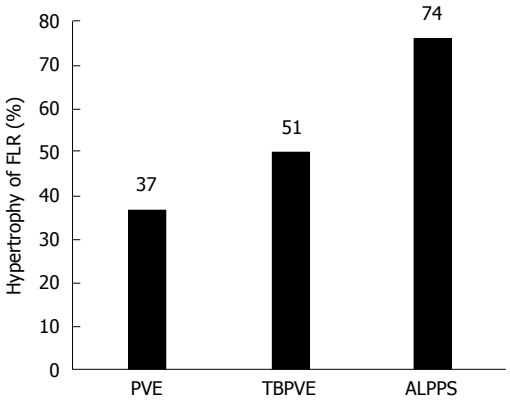

Figure 3 Mean future liver remnant hypertrophy with portal vein embolization, terminal branches portal vein embolization, and associating liver partition and portal vein ligation for staged hepatectomy. FLR: Future liver remnant; PVE: Portal vein embolization; TBPVE: Terminal branches portal vein embolization; ALPPS: Associating liver partition and portal vein ligation for staged hepatectomy.

All blood in the portal vein on one side is diverted to the other side, and consequently the remnant liver proliferates at a speed comparable to that after ALPPS. There is no need to manipulate the liver parenchyma, such as the division of liver parenchyma, placing a liver tourniquet, or executing liver ablation. Thus, only a single surgical operation is needed. In the initial report, four patients who underwent this procedure followed by right hemi-hepatectomy two weeks later did not have mortality and severe morbidity. The mean hypertrophy was 52.2% (68.4%, 33.1%, 54.2% and 53.1%, respectively), which was similar to that with ALPPS[26,27]. Currently, TBPVE has been performed for 20 cases, and the mean rate of volume increase was 51% (Figure 3, unpublished data).

Based on these preliminary practices, TBPVE can effectively increase FLR similarly to ALPPS, but much less invasively. This indicates that TBPVE is simple, safe and effective and is able to avoid some disadvantages of ALPPS. It only needs one interventional manipulation and a single surgical operation to achieve a similar therapeutic effect to ALPPS. We propose naming it "Terminal branches portal vein Embolization Liver Partition for Planned hepatectomy (TELPP)". The efficacy and safety of this new technique is expected to be verified by a large-scale, multi-center study.

TBPVE combined with TACE: There is concern about tumor growth during the lag between PVE and surgical operations, as hepatic arterial flow might increase to promote the tumor growth. Kokudo *et al*[28] described an increase of the tumor Ki-67 labeling index in intrahepatic metastases in the embolized liver after PVE. The same phenomenon was also noted with ALPPS. Fukami *et al*[29] reported an increase in the Ki-67 labeling index from 60% at the first stage to 80% at the second stage by tumor biopsy results of the same liver lesion at both stages. TBPVE also raises the same concern, but not as strongly as PVE. This

problem was solved by performing TBPVE combined with TACE. When we used this method in four cases, the average rate of FLR volume increase was 68.6%, while the tumor mass shrank.

Recently, Chao *et al*[30] found that lactic acidosis could effectively protect cancer cells against glucose starvation or deprivation and recruited 20 patients for a randomized trial to compare embolization alone with embolization plus bicarbonate treatment (TILA-TACE). The results showed that the tumors died more and patients survived longer if they received the bicarbonate. These data indicate that bicarbonate markedly enhances the anticancer activity of TACE. This therapy may be effective for patients with large tumors that are not amenable to surgery. Next, we would like to combine TBPVE with TILA-TACE to determine whether it could provide more benefit for patients with liver tumors previously considered nonresectable.

CONCLUSION

ALPPS is a revolutionary two-stage surgical procedure for the resection of hepatic malignancies, which has attracted the attention of many hepato-biliary surgeons around the world. Many modifications have been proposed to reduce its high morbidity and mortality rates. So far, we found that TELPP, which applies and merges the concepts of ALPPS and PVE to perform TBPVE, may be a promising procedure. TBPVE combined with TILA-TACE is even better in view of the tumor growth problem during the lag before hepatectomy. Their technical feasibility, safety and oncological outcomes need to be verified further in a larger-scale and multi-center study.

REFERENCES

1 **Schnitzbauer AA**, Lang SA, Goessmann H, Nadalin S, Baumgart J, Farkas SA, Fichtner-Feigl S, Lorf T, Goralcyk A, Hörbelt R, Kroemer A, Loss M, Rümmele P, Scherer MN, Padberg W, Königsrainer A, Lang H, Obed A, Schlitt HJ. Right portal vein ligation combined with in situ splitting induces rapid left lateral liver lobe hypertrophy enabling 2-staged extended right hepatic resection in small-for-size settings. *Ann Surg* 2012; **255**: 405-414 [PMID: 22330038 DOI: 10.1097/SLA.0b013e31824856f5]

2 **de Santibañes E**, Clavien PA. Playing Play-Doh to prevent postoperative liver failure: the "ALPPS" approach. *Ann Surg* 2012; **255**: 415-417 [PMID: 22330039]

3 **Baumgart J**, Lang S, Lang H. A new method for induction of liver hyper- trophy prior to right trisectionectomy: a report of three cases. *HPB* (Oxford) 2011; **13** (suppl 2): 1-145

4 **Abulkhir A**, Limongelli P, Healey AJ, Damrah O, Tait P, Jackson J, Habib N, Jiao LR. Preoperative portal vein embolization for major liver resection: a meta-analysis. *Ann Surg* 2008; **247**: 49-57 [PMID: 18156923 DOI: 10.1097/SLA.0b013e31815f6e5b]

5 **Liu H**, Zhu S. Present status and future perspectives of preoperative portal vein embolization. *Am J Surg* 2009; **197**: 686-690 [PMID: 19249737 DOI: 10.1016/j.amjsurg]

6 **Wicherts DA**, de Haas RJ, Andreani P, Sotirov D, Salloum C, Castaing D, Adam R, Azoulay D. Impact of portal vein embolization on long-term survival of patients with primarily unresectable colorectal liver metastases. *Br J Surg* 2010; **97**: 240-250 [PMID: 20087967 DOI: 10.1002/bjs.6756]

7 **Schadde E**, Ardiles V, Robles-Campos R, Malago M, Machado M, Hernandez-Alejandro R, Soubrane O, Schnitzbauer AA, Raptis D, Tschuor C, Petrowsky H, De Santibanes E, Clavien PA. Early survival and safety of ALPPS: first report of the International ALPPS Registry. *Ann Surg* 2014; **260**: 829-836; discussion 836-838 [PMID: 25379854 DOI: 10.1097/SLA.0000000000000947]

8 **Dokmak S**, Belghiti J. Which limits to the "ALPPS" approach? *Ann Surg* 2012; **256**: e6; author reply e16-e17 [PMID: 22895355 DOI: 10.1097/SLA.0b013e318265fd64]

9 **Aloia TA**, Vauthey JN. Associating liver partition and portal vein ligation for staged hepatectomy (ALPPS): what is gained and what is lost? *Ann Surg* 2012; **256**: e9; author reply e16-e19 [PMID: 22868369 DOI: 10.1097/SLA.0b013e318265fd3e]

10 **Sala S**, Ardiles V, Ulla M, Alvarez F, Pekolj J, de Santibañes E. Our initial experience with ALPPS technique: encouraging results. *Updates Surg* 2012; **64**: 167-172 [PMID: 22903531 DOI: 10.1007/s13304-012-0175-y]

11 **Li J**, Girotti P, Königsrainer I, Ladurner R, Königsrainer A, Nadalin S. ALPPS in right trisectionectomy: a safe procedure to avoid postoperative liver failure? *J Gastrointest Surg* 2013; **17**: 956-961 [PMID: 23288719 DOI: 10.1007/s11605-012-2132-y]

12 **Alvarez FA**, Ardiles V, Sanchez Claria R, Pekolj J, de Santibañes E. Associating liver partition and portal vein ligation for staged hepatectomy (ALPPS): tips and tricks. *J Gastrointest Surg* 2013; **17**: 814-821 [PMID: 23188224]

13 **Torres OJ**, Fernandes Ede S, Oliveira CV, Lima CX, Waechter FL, Moraes-Junior JM, Linhares MM, Pinto RD, Herman P, Machado MA. Associating liver partition and portal vein ligation for staged hepatectomy (ALPPS): the Brazilian experience. *Arq Bras Cir Dig* 2013; **26**: 40-43 [PMID: 23702869 DOI: 10.1590/S0102-67202013000100009]

14 **Conrad C**, Shivathirthan N, Camerlo A, Strauss C, Gayet B. Laparoscopic portal vein ligation with in situ liver split for failed portal vein embolization. *Ann Surg* 2012; **256**: e14-e15; author reply e16-e17 [PMID: 22895353 DOI: 10.1097/SLA.0b013e318265ff44]

15 **Petrowsky H**, Györi G, de Oliveira M, Lesurtel M, Clavien PA. Is partial-ALPPS safer than ALPPS? A single-center experience. *Ann Surg* 2015; **261**: e90-e92 [PMID: 25706390 DOI: 10.1097/SLA.0000000000001087]

16 **Alvarez FA**, Ardiles V, de Santibañes M, Pekolj J, de Santibañes E. Associating liver partition and portal vein ligation for staged hepatectomy offers high oncological feasibility with adequate patient safety: a prospective study at a single center. *Ann Surg* 2015; **261**: 723-732 [PMID: 25493362 DOI: 10.1097/SLA.000000000000]

17 **Hernandez-Alejandro R**, Bertens KA, Pineda-Solis K, Croome KP. Can we improve the morbidity and mortality associated with the associating liver partition with portal vein ligation for staged hepatectomy (ALPPS) procedure in the management of colorectal liver metastases? *Surgery* 2015; **157**: 194-201 [PMID: 25282528 DOI: 10.1016/j.surg.2014.08.041]

18 **Tanaka K**, Kikuchi Y, Kawaguchi D, Murakami T, Hiroshima Y, Matsuo K. Modified ALPPS Procedures Avoiding Division of Portal Pedicles. *Ann Surg* 2017; **265**: e14-e20 [PMID: 27611614 DOI: 10.1097/SLA.0000000000001967]

19 **de Santibañes E**, Alvarez FA, Ardiles V, Pekolj J, de Santibañes M. Inverting the ALPPS paradigm by minimizing first stage impact: the Mini-ALPPS technique. *Langenbecks Arch Surg* 2016; **401**: 557-563 [PMID: 27084508 DOI: 10.1007/s00423-016-1424-1]

20 **Robles Campos R**, Parrilla Paricio P, López Conesa A, Brusadín R, López López V, Jimeno Griñó P, Fuster Quiñonero M, García López JA, de la Peña Moral J. A new surgical technique for extended right hepatectomy: tourniquet in the umbilical fissure and right portal vein occlusion (ALTPS). Clinical case. *Cir Esp* 2013; **91**: 633-637 [PMID: 24246509 DOI: 10.1016/j.ciresp.2013.09.004]

21 **Cai X**, Peng S, Duan L, Wang Y, Yu H, Li Z. Completely laparoscopic ALPPS using round-the-liver ligation to replace

parenchymal transection for a patient with multiple right liver cancers complicated with liver cirrhosis. *J Laparoendosc Adv Surg Tech A* 2014; **24**: 883-886 [PMID: 25387325 DOI: 10.1089/lap.2014.0455]

22 **Gall TM**, Sodergren MH, Frampton AE, Fan R, Spalding DR, Habib NA, Pai M, Jackson JE, Tait P, Jiao LR. Radio-frequency-assisted Liver Partition with Portal vein ligation (RALPP) for liver regeneration. *Ann Surg* 2015; **261**: e45-e46 [PMID: 24670841 DOI: 10.1097/SLA.0000000000000607]

23 **Gringeri E**, Boetto R, D'Amico FE, Bassi D, Cillo U. Laparoscopic microwave ablation and portal vein ligation for staged hepatectomy (LAPS): a minimally invasive first-step approach. *Ann Surg* 2015; **261**: e42-e43 [PMID: 24651131 DOI: 10.1097/SLA.0000000000000606]

24 **Hong DF**, Zhang YB, Peng SY, Huang DS. Percutaneous Microwave Ablation Liver Partition and Portal Vein Embolization for Rapid Liver Regeneration: A Minimally Invasive First Step of ALPPS for Hepatocellular Carcinoma. *Ann Surg* 2016; **264**: e1-e2 [PMID: 26967629 DOI: 10.1097/SLA.0000000000001707]

25 **Chan AC**, Poon RT, Chan C, Lo CM. Safety of ALPPS Procedure by the Anterior Approach for Hepatocellular Carcinoma. *Ann Surg* 2016; **263**: e14-e16 [PMID: 26079914 DOI: 10.1097/SLA.0000000000001272]

26 **Peng SY**, Huang CY, Li JT, Zhang YY, He XW, Wang YF, Hong DF, Cai XJ. Terminal branches portal vein embolization for planed hepatectomy. *Zhonghua Waike Zazhi* 2016; **54**: 664-668 [PMID: 27587208 DOI: 10.3760/cma.j.issn.0529-5815.2016.09.004]

27 **Hasselgren K**, Sandström P, Björnsson B. Role of associating liver partition and portal vein ligation for staged hepatectomy in colorectal liver metastases: a review. *World J Gastroenterol* 2015; **21**: 4491-4498 [PMID: 25914457 DOI: 10.3748/wjg.v21.i15.4491]

28 **Kokudo N**, Tada K, Seki M, Ohta H, Azekura K, Ueno M, Ohta K, Yamaguchi T, Matsubara T, Takahashi T, Nakajima T, Muto T, Ikari T, Yanagisawa A, Kato Y. Proliferative activity of intrahepatic colorectal metastases after preoperative hemihepatic portal vein embolization. *Hepatology* 2001; **34**: 267-272 [PMID: 11481611 DOI: 10.1053/jhep.2001.26513]

29 **Fukami Y**, Kurumiya Y, Kobayashi S. Associating liver partition and portal vein ligation for staged hepatectomy (ALPPS): an analysis of tumor activity. *Updates Surg* 2014; **66**: 223-225 [PMID: 24864037 DOI: 10.1007/s13304-014-0256-1]

30 **Chao M**, Wu H, Jin K, Li B, Wu J, Zhang G, Yang G, Hu X. A nonrandomized cohort and a randomized study of local control of large hepatocarcinoma by targeting intratumoral lactic acidosis. *Elife* 2016; **5**: e15691 [PMID: 27481188 DOI: 10.7554/eLife.15691]

P- Reviewer: Chen CY **S- Editor**: Qi Y **L- Editor**: Wang TQ
E- Editor: Wang CH

World Journal of Gastroenterology

Submit a Manuscript: http://www.f6publishing.com

World J Gastroenterol 2017 June 21; 23(23): 4146-4157

DOI: 10.3748/wjg.v23.i23.4146

ISSN 1007-9327 (print) ISSN 2219-2840 (online)

REVIEW

Antioxidant dietary approach in treatment of fatty liver: New insights and updates

Alessandra Ferramosca, Mariangela Di Giacomo, Vincenzo Zara

Alessandra Ferramosca, Mariangela Di Giacomo, Vincenzo Zara, Dipartimento di Scienze e Tecnologie Biologiche ed Ambientali, Università del Salento, Via Provinciale Lecce-Monteroni, I-73100 Lecce, Italy

Author contributions: Ferramosca A designed the review and wrote the article; Di Giacomo M wrote the article; Zara V designed the review, wrote the article and made critical revisions.

Conflict-of-interest statement: The authors declare no conflict of interests for this article.

Manuscript source: Invited manuscript

Correspondence to: Dr. Alessandra Ferramosca, Dipartimento di Scienze e Tecnologie Biologiche ed Ambientali, Università del Salento, Via Provinciale Lecce-Monteroni, I-73100 Lecce, Italy. alessandra.ferramosca@unisalento.it
Telephone: +39-0832-298698
Fax: +39-0832-298626

Received: January 20, 2017
Peer-review started: January 22, 2017
First decision: February 9, 2017
Revised: February 22, 2017
Accepted: June 1, 2017
Article in press: June 1, 2017
Published online: June 21, 2017

Abstract

Non-alcoholic fatty liver disease (NAFLD) is a common clinicopathological condition, encompassing a range of conditions caused by lipid deposition within liver cells. To date, no approved drugs are available for the treatment of NAFLD, despite the fact that it represents a serious and growing clinical problem in the Western world. Identification of the molecular mechanisms leading to NAFLD-related fat accumulation, mitochondrial dysfunction and oxidative balance impairment facilitates the development of specific interventions aimed at preventing the progression of hepatic steatosis. In this review, we focus our attention on the role of dysfunctions in mitochondrial bioenergetics in the pathogenesis of fatty liver. Major data from the literature about the mitochondrial targeting of some antioxidant molecules as a potential treatment for hepatic steatosis are described and critically analysed. There is ample evidence of the positive effects of several classes of antioxidants, such as polyphenols (*i.e.*, resveratrol, quercetin, coumestrol, anthocyanins, epigallocatechin gallate and curcumin), carotenoids (*i.e.*, lycopene, astaxanthin and fucoxanthin) and glucosinolates (*i.e.*, glucoraphanin, sulforaphane, sinigrin and allyl-isothiocyanate), on the reversion of fatty liver. Although the mechanism of action is not yet fully elucidated, in some cases an indirect interaction with mitochondrial metabolism is expected. We believe that such knowledge will eventually translate into the development of novel therapeutic approaches for fatty liver.

Key words: Hepatic steatosis; Fatty liver; Lipogenesis; Mitochondria; Oxidative stress

Core tip: So far, there are no approved drugs for the treatment or the prevention of fatty liver and strategies mainly rely on dietary, physical activity and lifestyle modifications, as well as correction of hepatic steatosis-associated metabolic disturbances. This review mainly covers the biochemical mechanisms responsible for the

dysfunctions in mitochondrial bioenergetics observed in fatty liver and analyses the most recent data evidencing the effects of new bioactive compounds on the preservation of mitochondrial function. New insight into biochemical details underlying fat accumulation in the liver could lead to more targeted and effective therapeutics for fatty liver.

Ferramosca A, Di Giacomo M, Zara V. Antioxidant dietary approach in treatment of fatty liver: New insights and updates. *World J Gastroenterol* 2017; 23(23): 4146-4157 Available from: URL: http://www.wjgnet.com/1007-9327/full/v23/i23/4146.htm DOI: http://dx.doi.org/10.3748/wjg.v23.i23.4146

INTRODUCTION

Non-alcoholic fatty liver disease (NAFLD) is now considered the most prevalent form of chronic liver disease in the world, representing a serious and growing clinical problem in Western countries[1,2]. NAFLD is a clinicopathological condition, associated with a significant lipid deposition in hepatocytes and characterized by persistent defects in hepatic enzymes. Although NAFLD presents histological features of alcohol-induced liver injury, it affects patients who drink little to no alcohol. NAFLD is a histological disease which may progress from simple steatosis to nonalcoholic steatohepatitis (NASH), liver fibrosis, cirrhosis and eventually hepatocellular carcinoma[3-6].

To date, there are no approved drugs to treat patients with fatty liver disease and clinical management strategies mainly rely on modifications of diet, physical activity and lifestyle, as well as correction of hyperglycemia, insulin resistance and hyperlipidemia, which are metabolic disturbances associated with NAFLD[7-9].

The understanding of the molecular mechanisms responsible for lipid accumulation, oxidative balance impairment and fibrosis in the liver could improve the therapeutic approach to lower the risk of fatty liver development. Antioxidant compounds, which modulate lipogenesis, lipid oxidation and peroxidation, and inflammation, represent a new attractive therapeutic approach for patients suffering from hepatic steatosis.

In this review, we focus our attention on the biochemical mechanisms by which selected antioxidant molecules exert their beneficial effect by targeting mitochondria function. Such knowledge may translate into novel treatment strategies for fatty liver.

BIOCHEMICAL EVENTS ASSOCIATED WITH HEPATIC STEATOSIS

Steatosis is the biochemical result of an imbalance between the rates of fatty acid input (uptake and synthesis with subsequent esterification to triglycerides, TGs) and output (oxidation and secretion)[10]. Therefore, TGs levels in hepatocytes derives from a complex interaction between hepatic fatty acid uptake, *de novo* synthesis, oxidation and export within very low density lipoprotein (VLDL)-TG[11].

Hepatic fatty acid uptake is the result of plasma free fatty acids (FFAs) released from hydrolysis of adipose tissue TGs, FFAs deriving from hydrolysis of lipoproteins, and dietary FFAs.

De novo fatty acid synthesis occurs *via* a complex series of reactions that take place in the mitochondrial matrix and in the cytosol of hepatocytes[12]. The rate of *de novo* lipogenesis is dependent on the transport activity of the mitochondrial citrate carrier (CIC)[13] and on enzymatic activities of acetyl-CoA carboxylase (ACC), fatty acid synthase, (FAS)[12], diacylglycerol acyltransferase (DGAT) 1 and 2, and stearoyl-CoA desaturase 1 (SCD1). Induction of lipogenic genes occurs in response to the combined actions of several nuclear transcription factors: sterol regulatory element binding proteins (SREBPs), carbohydrate responsive element binding protein (ChREBP), liver X receptor α (LXRα), farnesoid X receptor (FXR) and peroxisome proliferator-activated receptors (PPARs)[14].

Liver fatty acid oxidation occurs primarily within the mitochondria, and a little part in peroxisomes and microsomes. Fatty acids are transported into the mitochondrial matrix by a carnitine-dependent enzyme shuttle. Mitochondrial β-oxidation implies a series of dehydrogenation, hydration and cleavage reactions catalyzed by membrane-bound and soluble enzymes transcriptionally regulated by PPARα[15]. Each cycle of β-oxidation shortens the acyl-CoA molecule by two carbon units. The released acetyl-CoA then enters the Krebs cycle if the supply of oxaloacetate is sufficient; alternatively, it can be utilized for the production of ketone bodies. Reducing equivalents ($FADH_2$ and NADH), that derived from the β-oxidation reactions then transfer their electrons to oxygen through the respiratory chain. Liver fatty acids may also be esterified to TGs and then stored as within hepatocytes or secreted into the blood as VLDL.

Metabolism of fatty acids plays a key role in the development of hepatic steatosis. Liver lipid accumulation is, therefore, the result of prolonged positive energy balance (*de novo* lipogenesis is the preferred mechanism to stock excess energy), adipose tissue dysfunction and insulin resistance, defects in fatty acid oxidation and mitochondrial metabolism, or imbalances in lipoprotein trafficking.

Hepatic TG accumulation (*i.e.*, steatosis) is the "first hit" and the basis for hepatocyte damage that leads to a variety of "second hits", such as cytokines, adipokines, bacterial endotoxins, mitochondrial dysfunction and/or endoplasmic reticulum stress. In fact, the traditional "two-hit" pathophysiological theory[16] is now being replaced by the "multiple parallel hits" hypothesis, which comprises lots of different parallel hits, represented by insulin resistance,

oxidative stress, genetic and epigenetic mechanisms, cytokines and microbiota modifications, along with environmental elements[17].

DYSFUNCTIONAL MITOCHONDRIAL BIOENERGETICS IN THE FATTY LIVER

Several lines of evidence indicate that structural and functional alterations in mitochondria are crucial to the development of NAFLD[18-20]. The structural alterations include depletion of mitochondrial DNA (mtDNA), as well as morphological and ultrastructural changes, whereas the functional alterations include defects in mitochondrial β-oxidation and respiration[21]. The functional alterations lead to a decrease in ATP levels, leakage of deleterious reactive oxygen species (ROS) and excessive depots of fat[22]. A study describing the pathogenesis of NAFLD[23] proposed that the overflow of FFAs to hepatocytes leads to an increase in mitochondrial energetic metabolism, to support energy demand for TG storage and droplet growth. Later, it was hypothesized that accumulation of intermediate lipids could lead to mitochondrial stress and cell apoptosis.

Defects in the activities of key mitochondrial enzymes have been investigated using animal models[24,25], in which a diet rich in fat (high-fat diet, HF diet) has been shown to induce hyperglycemia, hyperinsulinemia and the onset of obesity and fatty liver. Carnitine palmitoyl-CoA transferase (CPT) activity, which is involved in fatty acid oxidation, was inhibited in animals fed the HF diet and showing NAFLD. The observed reduction in CPT activity was associated with the concomitant modulation of the activity of citrate synthase, a Krebs cycle enzyme that catalyses the reaction between acetyl-CoA and oxaloacetate to form citrate.

Reducing equivalents (NADH and $FADH_2$) produced in the reactions of oxidation of fatty acids and Krebs cycle are used by the respiratory chain complexes to generate ATP. In fatty liver, mitochondrial respiration efficiency was decreased and this effect could be due to a possible uncoupling effect between ATP synthesis and transport through respiratory complexes. Expression of respiratory proteins are significantly increased to compensate the reduced activity of the respiratory complexes. Uncoupling between mitochondrial respiration and ATP synthesis could be the result of a different expression profile of the mitochondrial carriers responsible for proton conductance[25]. In accordance with this hypothesis, an increase in expression of the uncoupling protein (UCP) 2 isoform was found in rats with NAFLD[25,26]. In those animals, the expression of ATP/ATP carrier (AAC), another mitochondrial carrier which plays an important role in the mitochondrial permeability transition pore, was also found to be up-regulated[25]. Therefore, in uncoupled mitochondria, where proton gradient is dissipated by the entry of protons into the matrix *via* UCP2, an overexpression of AAC could compensate the reduced flux of ATP from mitochondria when membrane potential is reduced.

Alteration in mitochondrial function (Figure 1) leads to increased ROS production. The accumulation of lipid peroxidation and inactivation of key enzymatic activities leads to ROS-induced oxidative damage to cardiolipin. This phospholipid, which is almost exclusively present in the inner mitochondrial membrane, plays an important role in mitochondrial bioenergetics, as well as in the apoptosis[27,28].

As cytosolic fatty acids accumulate as a consequence of an impairment of the oxidative capacity of the mitochondria, alternative pathways are activated in the peroxisomes (β-oxidation) and microsomes (ω-oxidation) and additional ROS are produced[29]. In fact, in the initial step of peroxisomal β-oxidation, acyl-CoA oxidase donates electrons directly to molecular oxygen, producing hydrogen peroxide; ROS are also formed during the microsomal ω-oxidation of fatty acids *via* flavoprotein-mediated donation of electrons to molecular oxygen. In addition, during fatty acids ω-oxidation, the corresponding dicarboxylic acids of the metabolized fatty acids can uncouple oxidative phosphorylation. Therefore, extramitochondrial fatty acid oxidation leads to a further increase in oxidative stress, contributing to mitochondrial dysfunction.

CONTRIBUTION OF OXIDATIVE STRESS TO STEATOSIS PATHOGENESIS

Oxidative stress is one of the key mediators of hepatic damage and is a major contributor to the progression from simple steatosis to steatohepatitis[30]. The oxidative stress condition encompasses the various deleterious processes that result from an imbalance between the excessive formation of pro-oxidants (*i.e.*, ROS and/or reactive nitrogen species, RNS) and the counteracting antioxidant mechanisms. In mitochondria, increased ROS production can cause mtDNA depletion, attack biomolecules (*i.e.*, proteins, carbohydrates and lipids), and damage the mitochondrial membrane. It is worth noting that mitochondria have a substantial concentration of phospholipids containing polyunsaturated fatty acids (PUFAs). The PUFAs are more prone to oxidative damage, because of the double bonds in their chemical structure, which lead to lipid peroxidation. In turn, peroxidation of these mitochondrial membrane components, especially docosahexaenoic acid which is necessary for a functional assembly of the mitochondrial complexes[31], could lead to further impairment of the activity of the respiratory chain, with consequent decreased ATP synthesis and overproduction of ROS. PUFA peroxidation seems to be able to enhance post-endoplasmic reticulum presecretory proteolysis of ApoB, thereby reducing

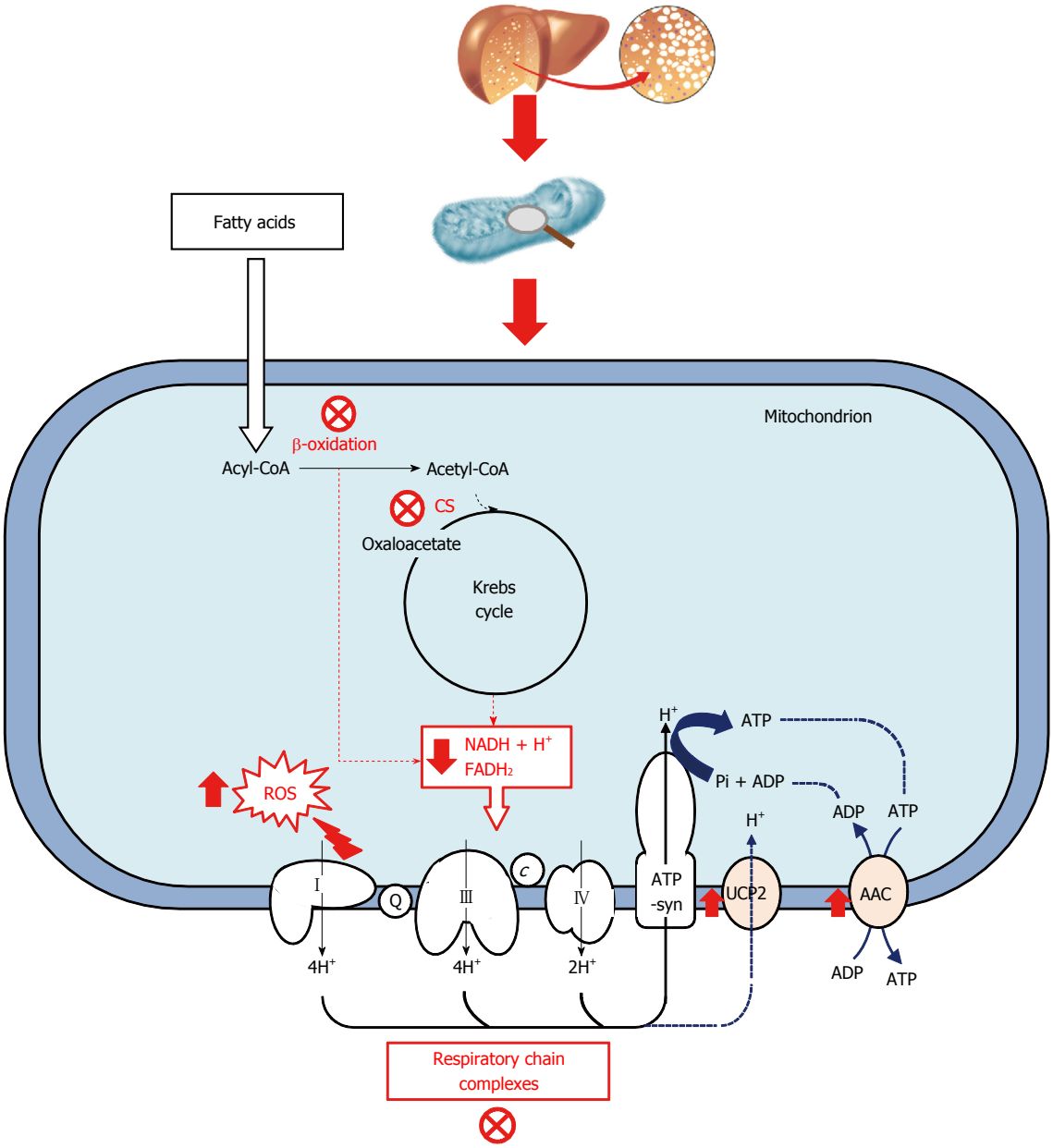

Figure 1 Dysfunctional mitochondrial bioenergetics in the fatty liver. In fatty liver, inhibition of β-oxidation and the reduction in citrate synthase (CS) activity implies a reduction in the flux of reducing equivalents to mitochondria. Mitochondrial respiration efficiency was decreased and this effect could be due to a possible uncoupling effect between ATP synthesis and transport through respiratory complexes. Alteration in mitochondrial function leads to increased ROS production. *c*: Cytochrome *c*; Q: Ubiquinone.

VLDL secretion[32]; this may further contribute to TG accumulation in the liver.

Moreover, aldehydes formed through PUFA peroxidation impair cellular homeostasis[33], because these molecules affect nucleotide and protein synthesis, reduce hepatic glutathione content and increase production of the proinflammatory cytokine TNF-α. These effects lead to hepatocyte death and necrosis, inflammation, and liver fibrosis.

NUTRITIONAL MANAGEMENT OF HEPATIC STEATOSIS

Elucidation of the molecular mechanisms leading to fat accumulation, mitochondrial dysfunction and oxidative balance impairment facilitates the development of specific interventions aimed at preventing the progression of hepatic steatosis. Food bioactive compounds, which modulate the activation of genes and the function of proteins involved in steatosis pathogenesis, represent a new attractive therapeutic approach for this condition[34].

General recommendations include reducing intakes of total fat, saturated and trans fatty acids and fructose[35,36]. Conversely, increasing intakes of PUFAs, especially of the long-chain n-3 fatty acids, and monounsaturated fatty acids is advised[12,37,38].

Many dietary natural compounds isolated from

fruits, vegetables and edible plants may be suggested as promising agents for treatment of fatty liver, since they are able to target mitochondria and to restore their function. Other molecules have not yet been tested for their potential effects on liver mitochondria, but they show potential for improving or restoring defective mitochondrial function in cells from different tissues. Since mitochondrial function is compromised in hepatic steatosis, in the following paragraphs we summarize the most recent data evidencing the mitochondrial targeting capabilities of new bioactive compounds.

POLYPHENOLS

Polyphenols are secondary metabolites of plants that have been studied primarily for their potential roles to combat oxidative stress and inflammatory processes. They contain at least one aromatic ring in their structure that is/are linked to different chemical groups, including phenolic, hydroxyl or carbon groups. Polyphenols can be broadly divided into flavonoids and nonflavonoids, based on their chemical structure. The flavonoids include flavonols (*i.e.*, quercetin), flavones (*i.e.*, luteolin), flavanols (*i.e.*, catechins), flavanones (*i.e.*, hesperetin, hesperidin naringenin and naringin), isoflavones (*i.e.*, genistein and daidzein), anthocyanidins (*i.e.*, cyanidin, malvidin, pelargonidin and delphinidin) and proanthocyanidins (*i.e.*, condensed tannins), while the nonflavonoids include stilbenes, phenolic acids and hydroxycinnamates[39].

Flavonoids are the most abundant natural antioxidants present in the human diet, and their antioxidant activity is due to the presence of hydroxyl groups in the phenolic structure of flavonoids[40]. These compounds exert their numerous beneficial and antioxidative effects through several mechanisms; indeed, they are able to target different pathways that are possibly involved in the pathogenesis of liver diseases. Flavonoids are able to control *de novo* lipogenesis, inhibiting lipogenic proteins (*i.e.*, ACC, SREBP-1, FAS and LXRα) and increasing lipolytic proteins (*i.e.*, AMPK, PPARα and CPT-1). They are also effective scavengers of ROS and RNS (*i.e.*, superoxide, hydrogen peroxide, hydroxyl radicals and peroxynitrite) that are elevated in pathological states and metabolic disorders such as NAFLD[41].

As mitochondria are an important source of ROS, redox-active compounds can be targeted to these organelles to counteract ROS production and its associated oxidative damage. However, as antioxidants, polyphenolic compounds may act directly by scavenging reactive species; alternatively may act indirectly by controlling the redox environment. In particular, findings from studies in several cellular models have indicated the abilities of polyphenols to modulate mitochondrial biogenesis and to control the mitochondrial membrane potential and oxidative phosphorylation[42].

Resveratrol

Resveratrol (trans-3,4′,5-trihydroxystilbene) is a stilbene naturally found in various food stuffs, such as grapes, berries, red wine and nuts. This molecule has been shown to control energetic metabolism in obese mice, improving the glucose homeostasis, increasing the fatty acid oxidation and inducing the expression of genes associated with the regulation of mitochondrial biogenesis[43,44]. The effects of high resveratrol doses (10-100 μmol/L) on mitochondrial metabolism have been evaluated in different models where it has been shown that resveratrol is able to increase the number of mitochondria in the tissues studied, and that this occurs *via* a sirtuin-dependent mechanism.

The sirtuins are a family of proteins that act as NAD-dependent deacetylases; three sirtuins are exclusively located in the mitochondrial compartment: SIRT3, -4 and -5[45]. However, the main target of resveratrol appears to be SIRT1. Although not found in the mitochondria, SIRT1 plays an important role in the regulation of metabolism, since it is able to stimulate both mitochondrial biogenesis and energetic metabolic fluxes *via* allosteric post-translational modifications of key enzymes[43]. A possible link between activation of SIRT1 and mitochondria could be the modulation of NAD^+ concentration[46,47], because a significant portion of the cellular NAD^+ pool is concentrated in the mitochondria[48]. In accordance with that hypothesis, a recent study[49] demonstrated that resveratrol can induce a mitochondrial complex I-dependent increase in NADH oxidation resulting in sirtuin activation in hepatocytes; moreover, this finding was obtained in different experimental models, including *in vitro* studies of isolated enzymes and HepG2 cells treated with resveratrol, as well as *in vivo* study of an aging model of mice fed with resveratrol. In particular, in the HepG2 cells (resveratrol administration at 1-5 μmol/L) and in the liver mitochondria from resveratrol-fed animals (administration of 50 mg/kg per day), complex I activation increased the mitochondrial NAD^+/NADH ratio and, in turn, the higher NAD^+ concentration initiated a SIRT3-dependent stimulation of the mitochondrial substrate supply pathways (*i.e.*, the Krebs cycle and β-oxidation of fatty acids)[49]. We can therefore hypothesize - as already has been suggested for the aging process[50] - that mitochondrial complex I activity may be involved in fatty liver through at least two mechanisms: a ROS-dependent mechanism, which is related to the control of complex I activity, and a ROS-independent mechanism *via* the regulation of the ratio NAD^+/NADH.

Quercetin

Quercetin is a type of flavonoid antioxidant that is found in plant foods, including leafy greens, tomatoes, berries and broccoli. Recent studies have shown that the beneficial effects of quercetin include the activation of mitochondrial biogenesis[42,51] through PGC-1α, which

is a transcriptional coactivator of genes associated with oxidative phosphorylation and mtDNA replication. In HepG2 cells, the observed increase in mitochondrial biogenesis is associated with cytochrome oxidase subunit IV (COXIV) overexpression[52]. Interestingly, an increase in cytochrome *c* concentration is typically associated with similar increases in other mitochondrial proteins involved in the respiratory chain, Krebs cycle and fatty acid oxidation pathway. The result is an overall increase in mitochondrial capacity[52,53].

Results obtained in animal models have suggested that 50 mg/kg and 100 mg/kg doses of quercetin significantly affect the mitochondrial biogenesis; moreover, mice treated with up to 3000 mg/kg quercetin did not show any toxic effects[53]. However, the effect of oral administration of quercetin on liver mitochondria has not been tested. This is an intriguing aspect, because there are several reports indicating that quercetin exhibits both antioxidant and pro-oxidant activity, in a concentration dependent manner[54,55]. Therefore, further studies are needed to determine the therapeutic efficacy of oral quercetin administration.

Coumestrol

Coumestrol is the most commonly studied coumestan, and is a natural organic compound present in some plants, including alfalfa, legumes, Brussels sprouts, spinach, clover and soybeans. Recent data[56] have suggested that coumestrol induces an increase in mitochondria number and function, by activating SIRT1. By promoting mitochondrial content, coumestrol appears to be able to increase cellular ATP levels and glucose uptake, thereby improving energy metabolism at the same time. Moreover, coumestrol stimulation has been shown to augment the protein expression of respiratory chain components, such as NADH dehydrogenase 1α subcomplex 9 (NDUFA9), succinate dehydrogenase complex subunit A (SDHA), ubiquinol cytochrome *c* reductase core protein 2 (UQCRC2), cytochrome oxidase subunit 1 (COX1) and ATP synthase mitochondria F_1 complex α subunit 1 (ATP5a), and of the transcriptional regulators that are responsible for mitochondrial biogenesis[56].

Coumestrol has also been shown to decrease the mRNA expression of lipogenic genes in adipocytes and hepatocytes and to increase fatty acid oxidation in myocytes. It has been proposed that SIRT1 and AMPK might reciprocally activate each other. AMPK enhances SIRT1 activity by increasing cellular NAD^+ levels[57], whereas SIRT1 mediates the deacetylation of liver kinase B1[58] (an upstream regulator of AMPK), thereby assembling a positive feedback loop that serves to enhance energy catabolism. It might, therefore, be possible for coumestrol to activate AMPK, itself a regulator of SIRT1; further studies are needed to determine which one - SIRT1 or AMPK - is the upstream regulator of the other[56].

Anthocyanins

Anthocyanidins are water-soluble pigments of coloured berries, fruits and vegetables. They can protect hepatocytes against injury caused by high glucose-induced oxidative damage, by improving antioxidant status and inhibiting the mitochondria pathways of apoptosis. The proposed mechanism has been shown to involve the prevention of hyperglycemia-induced mitochondrial depolarization, which helps mitochondria to maintain their function[59].

In addition, other studies have suggested that treatment with anthocyanins increases mitochondrial fatty acid oxidation *via* activation of genes participating in this metabolic pathway (*i.e.*, PPARα, PPARδ, UCP-2, UCP-3 and mitochondrial transcription factor A)[60].

Recent studies have suggested that these molecules can attenuate mitochondrial defects caused by inhibition of complex I in human and rat tissues[61,62]. In isolated mitochondria from ischemic hearts, anthocyanins were found to recover complex I activity, thereby enhancing the rate of ATP synthesis[63]. A normal functioning of respiratory complex I is necessary to ensuring mitochondrial ATP synthesis and its supply to cells. In fact, it is widely accepted that inhibition of complex I results in a decrease of oxidative phosphorylation[64]. The suggested mechanism of action of anthocyanins has been associated with their redox potential, since these molecules can act as electron acceptors in a similar way as endogenous coenzyme Q.

Epigallocatechin gallate

Epigallocatechin gallate is the ester of epigallocatechin and gallic acid. It is a flavonoid belonging to the chemical class of flavan-3-ols (catechins) and it is the most abundant catechin in green tea (*Camellia sinensis L.*), accounting for about 50% of its total polyphenols.

Some studies have suggested that epigallocatechin gallate can promote fat oxidation and energy expenditure[65]. At a cellular level, reduced energy uptake could activate the AMPK signalling pathway, which may further affect energy metabolism, inducing chronic alterations in mitochondrial architecture (morphology and mass). This may represent a crucial step for the generation of oxidative damage[66]. Such modifications also include increase in the levels of porin and mitochondrial respiratory proteins, and in mtDNA content. Therefore, epigallocatechin gallate is able to modulate systemic energy use by inducing mitochondrial changes[67]. On the other hand, this bioactive molecule has been reported to induce fatty acid β-oxidation through an increase in mRNA levels of CPT-1 and UCP2[68].

Curcumin

Curcumin [1,7-bis(4-hydroxy-3-methoxyphenyl)-1,6-heptadiene-3,5-dione] is a yellow polyphenol isolated from the rhizome of *Curcuma longa*, a characteristic

plant of tropical and subtropical regions, which has been used as a spice and traditional medicine in Asia for centuries due to its antioxidant, antiinflammatory, antimutagenic, antimicrobial and anticancer properties.

The antioxidant properties of curcumin have been shown to protect against mitochondrial dysfunction in several experimental models[69]. In particular, curcumin has been reported to increase oxygen consumption and respiratory chain complexes' activities, to prevent oxidative stress and to restore ATP content. Such an improvement in mitochondrial function was also shown to be associated with prevention against the decrease in the activity of aconitase[70], an oxidative stress marker. In addition, curcumin facilitated β-oxidation in *in vitro* experiments (by up-regulation of CPT-1), reducing lipogenesis at the same time[64].

CAROTENOIDS

Carotenoids are lipophilic pigments responsible for the yellow, orange or red colours of flowers and fruits. Their scavenging activity of ROS is well known, as well as the ability of β-carotenes to be the primary dietary source of provitamin A. The most prevalent carotenoids in the diet are α- and β-carotene, lutein, lycopene, zeaxanthin and cryptoxanthin.

Carotenoids accumulate mainly in the liver where they are incorporated into lipoproteins and released into the circulation in the form of lipoproteins. Dietary carotenoids may physiologically scavenge free radical species in the liver, thus inhibiting the development of hepatic dysfunction[71].

They are considered potent antioxidants and antiinflammatory micronutrients, and have been used in the prevention and treatment of NAFLD. Carotenoids are also critical regulators of macrophage polarization and thereby inhibit the development and the progression of NASH[72]. The molecular mechanism by which carotenoids exert their effects in NAFLD is not well defined, but it has been proposed that they may act through multiple mechanisms.

Lycopene

Lycopene is a carotenoid that lacks provitamin A activity and is responsible for the red to pink colours seen in tomatoes, red grapefruit, watermelon and apricots.

Epidemiological and experimental studies have suggested that lycopene may have chemopreventive properties against certain types of cancers, including NASH-promoted hepatocarcinogenesis, mainly as a consequence of oxidative stress decrease, which could be imparted through different mechanisms[73]. Moreover, lycopene also reduces the development of hepatic steatosis induced by an HF diet[74]. The key role of this carotenoid in protection against fatty liver was confirmed by the reduced plasma lycopene levels in subjects affected by NASH, suggesting a possible link between low lycopene levels and the development of liver diseases[75].

A possible effect of lycopene on mitochondrial function has been proposed in cardiomyocytes, where the protective effects of this molecule have been attributed to its roles in improving mitochondrial function[76]. An important factor associated with mitochondrial dysfunction is activation of the mitochondrial permeability transition pore (mPTP). Activation of mPTP leads to functional breakdown, and subsequently morphological disintegration of the mitochondria progresses to cell death. Lycopene was shown to suppress the activation of mPTP by reducing intracellular ROS levels and inhibiting oxidative damage[76]. In this way, the impairment of mitochondrial membrane potential and decrease in ATP levels were alleviated, suggesting that the cell protection is, in part, due to the prevention of mitochondrial dysfunction.

In accordance with this hypothesis, some studies have shown the ability of lycopene to enhance the mitochondrial activity in HepG2 cells that were exposed to aflatoxin B1[77] and to improve the mitochondrial function in nervous system of rats that were exposed to 3-nitropropionic acid[78]. Therefore, the antioxidative potential of lycopene should account for its ability to preserve the activity of endogenous free radical scavengers and of respiratory chain complexes directly, thus preventing ROS production and secondary oxidative damage.

Astaxanthin

Astaxanthin is a xanthophyll carotenoid found in various marine organisms, such as yeast, salmon, shrimp, crayfish and green microalga *Haematococcus pluvialis*. It is well demonstrated that this carotenoid has strong antioxidant properties[79], since it is 100-fold to 500-fold more effective than vitamin E in preventing lipid peroxidation and in reducing lipid accumulation in liver[80]. In mice models it has also been reported that astaxanthin can down-regulate genes involved in lipogenesis and lipid-uptake, without influencing fatty acid oxidation-related genes in the liver[80]. Moreover, it has also been shown to reduce hepatic levels of TGs and cholesterol in mice[81].

A role has been suggested for astaxantin in improvement of mitochondrial function. This molecule appears to be able to increase mitochondrial membrane potential and respiratory control[82], which are important measures of mitochondrial health when investigating isolated mitochondria. We can hypothesize that the increase in mitochondrial respiration efficiency observed in astaxanthin-treated cells is due to the increase in mitochondrial membrane potential.

Interestingly, astaxanthin is also present in krill oil, a dietary source of n-3 long-chain PUFAs, the effects of which in reducing liver lipids were more pronounced than that found with fish oil-fed rats[83]. Moreover, astaxanthin induces fatty acid catabolism. Acyl-CoA

oxidase (ACOX1) is a target gene of PPARα, a regulator of mitochondrial and peroxisomal β-oxidation, which can be activated by this carotenoid[84].

Fucoxanthin

Fucoxanthin is one of the most abundant marine carotenoids, accounting for more than 10% of the estimated total carotenoids in nature. It is a xanthophyll, the distinct structure of which includes an unusual allenic bond and some oxygenic functional groups in a polyene chain.

The hypolipidemic effects of fucoxanthin might be mediated by down-regulation of various lipogenic enzyme activities and up-regulation of fatty acid β-oxidation activity in fat tissues[85,86].

Recent literature[86] suggests that this carotenoid has also anti-obesity properties, mainly by stimulating UCP-1 expression in white adipose tissue. This mitochondrial protein is usually found in brown adipose tissue and is not expressed in white adipose tissue in the absence of any stimulation. The role of UCP-1 is the dissipation of the proton gradient created by respiration and this leads to heat generation (thermogenesis).

GLUCOSINOLATES

Glucosinolates are a family of sulphur-containing plant secondary metabolites usually found in cruciferous plants. They have a common structure containing a thioketal-linked glucose molecule and are hydrolysed by specific enzymes (*i.e.*, myrosinases) to produce biologically active sulfureted aglycones, the isothiocyanates. Glucosinolates and their respective enzymatic hydrolysis scavange harmful radicals and modulate enzymes involved in detoxification processes, thus preventing oxidative damage.

Preliminary studies have suggested that these molecules can suppress the activation of hepatic macrophages and also contribute to decrease liver damage and to protect against the development of liver tumorigenesis[87].

Glucoraphanin and sulforaphane

Glucoraphanin (4-methylsulfinylbutyl glucosinolate) is the major glucosinolate found within broccoli and is the precursor of sulforaphane. Indeed, the biologically active sulforaphane is not present as such in *Brassicaceae*, but is produced by enzymatic hydrolysis upon tissue disruption, such as the chewing of raw vegetables, which brings the endogenous enzyme β-thioglucoside glucohydrolase (a myrosinase) into contact with the glucosinolate. Several factors determine the degree of conversion from glucoraphanin to sulforaphane and, therefore, its cellular activity and protective effects[88].

Studies on *in vitro* and animal models have demonstrated that broccoli sulforaphane can mitigate some of the effects produced by inducers of inflammation and cell damage, such as carcinogens, toxins and ROS. The proposed molecular mechanism involves the inhibition of enzymes responsible for reactions related to oxidation, reduction and hydrolysis (*i.e.*, cytochrome P450 enzymes), and the induction of antioxidant and detoxification enzymes (*i.e.*, quinone reductase, thioredoxin reductase 1, and heme oxygenase 1)[89,90]. These last enzymes, known as phase II antioxidant enzymes, plays an important protective role in the maintenance of redox state in mammalian cells by providing a precise balance between the level of ROS and endogenous thiol buffers, which protect cells from oxidative stress-induced damage. They also play a critical role in maintaining the NAD^+/NADH and $NADP^+$/NADPH ratios[91]. As a consequence, dietary supplementation with the sulforaphane precursor glucoraphanin represents a potent method for improving liver function and for maintaining good liver condition[92,93].

Recently, a role has been suggested for glucoraphanin in the modulation of mitochondrial function. Metabolomic studies have supported the proposal that such a modulation may be mediated by control of FAD levels[94]. FAD, a redox cofactor, takes part in several important reactions in energetic metabolism (*i.e.*, fatty acid oxidation and Krebs cycle). Moreover, FAD acts as cofactor of lysine-specific demethylase-1, which, through epigenetic regulation, modulates the expression of genes involved in mitochondrial metabolism and energy expenditure[95]. Thus, when FAD levels are relatively high, expression of genes associated with mitochondrial respiration is down-regulated and export of citrate from the Krebs cycle is enhanced; this modulation results in elevated concentrations of fatty acids, lipids and steroids.

Sinigrin and allyl-isothiocyanate

Sinigrin is a major component of commonly consumed cruciferous vegetables, such as horseradish and wasabi. Its degradation product allyl-isothiocyanate is responsible for the characteristic pungent taste[96].

The potential of sinigrin to inhibit the growth of several types of cancer cells has been well investigated. In particular, sinigrin was shown to significantly prevent the proliferation of liver tumour cells, inducing apoptosis and gradually restoring liver functions[97].

A recent study suggested that allyl-isothiocyanate can improve mitochondrial respiration efficiency, reducing, at the same time, metabolic dysfunctions[98]. The effects of this molecule have been evaluated in muscle cells, which showed a higher mitochondrial activity after allyl-isothiocyanate treatment. In particular, increases in mitochondrial membrane potential, in mtDNA content and in respiratory capacity were observed.

CONCLUSION

Hepatic steatosis has become a very common cause of liver diseases in Western word. So far, there are

Table 1 Described effects of bioactive compounds on mitochondria

Compound	Effect
Polyphenols	
Resveratrol	↑Mitochondrial biogenesis
	↑Complex I activity
Quercetin	↑mtDNA
	↑Respiratory chain proteins
Coumestrol	↑Mitochondria number
	↑Respiratory chain proteins
	↑Mitochondrial function
Anthocyanins	↑Fatty acid oxidation
	↑Compex I activity
Epigallocatechin gallate	↑Fatty acid oxidation
	↑Energy expenditure
Curcumin	↑Fatty acid oxidation
	↑Respiratory complexes activity
Carotenoids	
Lycopene	↓Activation of mPTP
Astaxanthin	↑Fatty acid oxidation
	↑Mitochondrial membrane potential
	↑Respiration efficiency
Fucoxanthin	↑Fatty acid oxidation
Glucosinolates	
Glucoraphanin	↓FAD levels
Sinigrin	↑Mitochondrial membrane potential
	↑Respiration efficiency
	↑DNA content

mtDNA: Mitochondrial DNA; mPTP: Mitochondrial permeability transition pore.

no approved drugs for the treatment of this disease. Therefore, identification of the molecular mechanisms leading to the fat accumulation in liver may provide new avenues for the development of new diagnostic and therapeutic approaches.

Food bioactive compounds, which are important regulators of expression and activity of proteins associated with lipid homeostasis and metabolism, represent a novel therapeutic approach for fatty liver disease. In fact, there is evidence that several classes of antioxidants (*i.e.,* polyphenols, carotenoids and glucosinolates) are able to reverse hepatic steatosis. Although the mechanism of action remains understood, an indirect effect of bioactive molecules on mitochondrial function is expected (Table 1).

We believe that gaining a more complete understanding of the biochemical mechanisms underlying the hepatoprotective roles of the bioactive compounds such as those ones included in this review will lead to more targeted and effective therapeutics for hepatic steatosis.

REFERENCES

1 **Mikolasevic I**, Milic S, Turk Wensveen T, Grgic I, Jakopcic I, Stimac D, Wensveen F, Orlic L. Nonalcoholic fatty liver disease - A multisystem disease? *World J Gastroenterol* 2016; **22**: 9488-9505 [PMID: 27920470 DOI: 10.3748/wjg.v22.i43.9488]

2 **Azzam H**, Malnick S. Non-alcoholic fatty liver disease - the heart of the matter. *World J Hepatol* 2015; **7**: 1369-1376 [PMID: 26052382 DOI: 10.4254/wjh.v7.i10.1369]

3 **McCullough AJ**. Update on nonalcoholic fatty liver disease. *J Clin Gastroenterol* 2002; **34**: 255-262 [PMID: 11873108 DOI: 10.1097/00004836-200203000-00013]

4 **Bugianesi E**, Leone N, Vanni E, Marchesini G, Brunello F, Carucci P, Musso A, De Paolis P, Capussotti L, Salizzoni M, Rizzetto M. Expanding the natural history of nonalcoholic steatohepatitis: from cryptogenic cirrhosis to hepatocellular carcinoma. *Gastroenterology* 2002; **123**: 134-140 [PMID: 12105842 DOI: 10.1053/gast.2002.34168]

5 **Sass DA**, Chang P, Chopra KB. Nonalcoholic fatty liver disease: a clinical review. *Dig Dis Sci* 2005; **50**: 171-180 [PMID: 15712657 DOI: 10.1007/s10620-005-1267-z]

6 **Day CP**. From fat to inflammation. *Gastroenterology* 2006; **130**: 207-210 [PMID: 16401483 DOI: 10.1053/j.gastro.2005.11.017]

7 **Baran B**, Akyüz F. Non-alcoholic fatty liver disease: what has changed in the treatment since the beginning? *World J Gastroenterol* 2014; **20**: 14219-14229 [PMID: 25339808 DOI: 10.3748/wjg.v20.i39.14219]

8 **Dyson J**, Day C. Treatment of non-alcoholic fatty liver disease. *Dig Dis* 2014; **32**: 597-604 [PMID: 25034293 DOI: 10.1159/000360511]

9 **Hossain N**, Kanwar P, Mohanty SR. A Comprehensive Updated Review of Pharmaceutical and Nonpharmaceutical Treatment for NAFLD. *Gastroenterol Res Pract* 2016; **2016**: 7109270 [PMID: 27006654 DOI: 10.1155/2016/7109270]

10 **Donnelly KL**, Smith CI, Schwarzenberg SJ, Jessurun J, Boldt MD, Parks EJ. Sources of fatty acids stored in liver and secreted via lipoproteins in patients with nonalcoholic fatty liver disease. *J Clin Invest* 2005; **115**: 1343-1351 [PMID: 15864352 DOI: 10.1172/JCI200523621]

11 **Fabbrini E**, Sullivan S, Klein S. Obesity and nonalcoholic fatty liver disease: biochemical, metabolic, and clinical implications. *Hepatology* 2010; **51**: 679-689 [PMID: 20041406 DOI: 10.1002/hep.23280]

12 **Ferramosca A**, Zara V. Modulation of hepatic steatosis by dietary fatty acids. *World J Gastroenterol* 2014; **20**: 1746-1755 [PMID: 24587652 DOI: 10.3748/wjg.v20.i7.1746]

13 **Ferramosca A**, Zara V. Dietary fat and hepatic lipogenesis: mitochondrial citrate carrier as a sensor of metabolic changes. *Adv Nutr* 2014; **5**: 217-225 [PMID: 24829468 DOI: 10.3945/an.113.004762]

14 **Musso G**, Gambino R, Cassader M. Recent insights into hepatic lipid metabolism in non-alcoholic fatty liver disease (NAFLD). *Prog Lipid Res* 2009; **48**: 1-26 [PMID: 18824034 DOI: 10.1016/j.plipres.2008.08.001]

15 **Stefanovic-Racic M**, Perdomo G, Mantell BS, Sipula IJ, Brown NF, O'Doherty RM. A moderate increase in carnitine palmitoyltransferase 1a activity is sufficient to substantially reduce hepatic triglyceride levels. *Am J Physiol Endocrinol Metab* 2008; **294**: E969-E977 [PMID: 18349115 DOI: 10.1152/ajpendo.00497.2007]

16 **Day CP**, James OF. Steatohepatitis: a tale of two "hits"? *Gastroenterology* 1998; **114**: 842-845 [PMID: 9547102 DOI: 10.1016/S0016-5085(98)70599-2]

17 **Buzzetti E**, Pinzani M, Tsochatzis EA. The multiple-hit pathogenesis of non-alcoholic fatty liver disease (NAFLD). *Metabolism* 2016; **65**: 1038-1048 [PMID: 26823198 DOI: 10.1016/j.metabol.2015.12.012]

18 **Wei Y**, Rector RS, Thyfault JP, Ibdah JA. Nonalcoholic fatty liver disease and mitochondrial dysfunction. *World J Gastroenterol* 2008; **14**: 193-199 [PMID: 18186554 DOI: 10.3748/wjg.14.193]

19 **García-Ruiz C**, Baulies A, Mari M, García-Rovés PM, Fernandez-Checa JC. Mitochondrial dysfunction in non-alcoholic fatty liver disease and insulin resistance: cause or consequence? *Free Radic Res* 2013; **47**: 854-868 [PMID: 23915028 DOI: 10.3109/10715762.2013.830717]

20 **Ferramosca A**, Conte A, Damiano F, Siculella L, Zara V. Differential effects of high-carbohydrate and high-fat diets on hepatic lipogenesis in rats. *Eur J Nutr* 2014; **53**: 1103-1114 [PMID: 24197180 DOI: 10.1007/s00394-013-0613-8]

21 **Pessayre D**, Fromenty B. NASH: a mitochondrial disease. *J Hepatol* 2005; **42**: 928-940 [PMID: 15885365 DOI: 10.1016/

j.jhep.2005.03.004]
22 **Auger C**, Alhasawi A, Contavadoo M, Appanna VD. Dysfunctional mitochondrial bioenergetics and the pathogenesis of hepatic disorders. *Front Cell Dev Biol* 2015; **3**: 40 [PMID: 26161384 DOI: 10.3389/fcell.2015.00040]
23 **Flamment M**, Rieusset J, Vidal H, Simard G, Malthièry Y, Fromenty B, Ducluzeau PH. Regulation of hepatic mitochondrial metabolism in response to a high fat diet: a longitudinal study in rats. *J Physiol Biochem* 2012; **68**: 335-344 [PMID: 22278845 DOI: 10.1007/s13105-012-0145-3]
24 **Ferramosca A**, Conte A, Burri L, Berge K, De Nuccio F, Giudetti AM, Zara V. A krill oil supplemented diet suppresses hepatic steatosis in high-fat fed rats. *PLoS One* 2012; **7**: e38797 [PMID: 22685607 DOI: 10.1371/journal.pone.0038797]
25 **Ferramosca A**, Conte A, Zara V. Krill Oil Ameliorates Mitochondrial Dysfunctions in Rats Treated with High-Fat Diet. *Biomed Res Int* 2015; **2015**: 645984 [PMID: 26301251 DOI: 10.1155/2015/645984]
26 **Jiang Y**, Zhang H, Dong LY, Wang D, An W. Increased hepatic UCP2 expression in rats with nonalcoholic steatohepatitis is associated with upregulation of Sp1 binding to its motif within the proximal promoter region. *J Cell Biochem* 2008; **105**: 277-289 [PMID: 18543254 DOI: 10.1002/jcb.21827]
27 **Paradies G**, Petrosillo G, Pistolese M, Ruggiero FM. Reactive oxygen species affect mitochondrial electron transport complex I activity through oxidative cardiolipin damage. *Gene* 2002; **286**: 135-141 [PMID: 11943469 DOI: 10.1016/S0378-1119(01)00814-9]
28 **Paradies G**, Paradies V, Ruggiero FM, Petrosillo G. Oxidative stress, cardiolipin and mitochondrial dysfunction in nonalcoholic fatty liver disease. *World J Gastroenterol* 2014; **20**: 14205-14218 [PMID: 25339807 DOI: 10.3748/wjg.v20.i39.14205]
29 **Browning JD**, Horton JD. Molecular mediators of hepatic steatosis and liver injury. *J Clin Invest* 2004; **114**: 147-152 [PMID: 15254578 DOI: 10.1172/JCI22422]
30 **Sumida Y**, Niki E, Naito Y, Yoshikawa T. Involvement of free radicals and oxidative stress in NAFLD/NASH. *Free Radic Res* 2013; **47**: 869-880 [PMID: 24004441 DOI: 10.3109/10715762.2013.837577]
31 **Infante JP**, Huszagh VA. Secondary carnitine deficiency and impaired docosahexaenoic (22: 6n-3) acid synthesis: a common denominator in the pathophysiology of diseases of oxidative phosphorylation and beta-oxidation. *FEBS Lett* 2000; **468**: 1-5 [PMID: 10683429 DOI: 10.1016/S0014-5793(00)01083-8]
32 **Pan M**, Cederbaum AI, Zhang YL, Ginsberg HN, Williams KJ, Fisher EA. Lipid peroxidation and oxidant stress regulate hepatic apolipoprotein B degradation and VLDL production. *J Clin Invest* 2004; **113**: 1277-1287 [PMID: 15124019 DOI: 10.1172/JCI19197]
33 **Esterbauer H**, Schaur RJ, Zollner H. Chemistry and biochemistry of 4-hydroxynonenal, malonaldehyde and related aldehydes. *Free Radic Biol Med* 1991; **11**: 81-128 [PMID: 1937131 DOI: 10.1016/0891-5849(91)90192-6]
34 **Dongiovanni P**, Lanti C, Riso P, Valenti L. Nutritional therapy for nonalcoholic fatty liver disease. *J Nutr Biochem* 2016; **29**: 1-11 [PMID: 26895659 DOI: 10.1016/j.jnutbio.2015.08.024]
35 **Musso G**, Gambino R, De Michieli F, Cassader M, Rizzetto M, Durazzo M, Fagà E, Silli B, Pagano G. Dietary habits and their relations to insulin resistance and postprandial lipemia in nonalcoholic steatohepatitis. *Hepatology* 2003; **37**: 909-916 [PMID: 12668986 DOI: 10.1053/jhep.2003.50132]
36 **Chiu S**, Sievenpiper JL, de Souza RJ, Cozma AI, Mirrahimi A, Carleton AJ, Ha V, Di Buono M, Jenkins AL, Leiter LA, Wolever TM, Don-Wauchope AC, Beyene J, Kendall CW, Jenkins DJ. Effect of fructose on markers of non-alcoholic fatty liver disease (NAFLD): a systematic review and meta-analysis of controlled feeding trials. *Eur J Clin Nutr* 2014; **68**: 416-423 [PMID: 24569542 DOI: 10.1038/ejcn.2014.8]
37 **Ferramosca A**, Savy V, Conte L, Zara V. Dietary combination of conjugated linoleic acid (CLA) and pine nut oil prevents CLA-induced fatty liver in mice. *J Agric Food Chem* 2008; **56**: 8148-8158 [PMID: 18702470 DOI: 10.1021/jf8010728]
38 **Ferramosca A**, Savy V, Zara V. Olive oil increases the hepatic triacylglycerol content in mice by a distinct influence on the synthesis and oxidation of fatty acids. *Biosci Biotechnol Biochem* 2008; **72**: 62-69 [PMID: 18175925 DOI: 10.1271/bbb.70369]
39 **Del Rio D**, Rodriguez-Mateos A, Spencer JP, Tognolini M, Borges G, Crozier A. Dietary (poly)phenolics in human health: structures, bioavailability, and evidence of protective effects against chronic diseases. *Antioxid Redox Signal* 2013; **18**: 1818-1892 [PMID: 22794138 DOI: 10.1089/ars.2012.4581]
40 **Xie Y**, Chen X. Structures required of polyphenols for inhibiting advanced glycation end products formation. *Curr Drug Metab* 2013; **14**: 414-431 [PMID: 23330933 DOI: 10.2174/13892002113140040005]
41 **Van De Wier B**, Koek GH, Bast A, Haenen GR. The potential of flavonoids in the treatment of non-alcoholic fatty liver disease. *Crit Rev Food Sci Nutr* 2017; **57**: 834-855 [PMID: 25897647 DOI: 10.1080/10408398.2014.952399]
42 **Serrano JC**, Cassanye A, Martín-Gari M, Granado-Serrano AB, Portero-Otín M. Effect of dietary bioactive compounds on mitochondrial and metabolic flexibility. *Diseases* 2016; **4**: 14 [DOI: 10.3390/diseases4010014]
43 **Lagouge M**, Argmann C, Gerhart-Hines Z, Meziane H, Lerin C, Daussin F, Messadeq N, Milne J, Lambert P, Elliott P, Geny B, Laakso M, Puigserver P, Auwerx J. Resveratrol improves mitochondrial function and protects against metabolic disease by activating SIRT1 and PGC-1alpha. *Cell* 2006; **127**: 1109-1122 [PMID: 17112576 DOI: 10.1016/j.cell.2006.11.013]
44 **Mercader J**, Palou A, Bonet ML. Resveratrol enhances fatty acid oxidation capacity and reduces resistin and Retinol-Binding Protein 4 expression in white adipocytes. *J Nutr Biochem* 2011; **22**: 828-834 [PMID: 21109418 DOI: 10.1016/j.jnutbio.2010.07.007]
45 **Li X**, Kazgan N. Mammalian sirtuins and energy metabolism. *Int J Biol Sci* 2011; **7**: 575-587 [PMID: 21614150 DOI: 10.7150/ijbs.7.575]
46 **Park SJ**, Ahmad F, Philp A, Baar K, Williams T, Luo H, Ke H, Rehmann H, Taussig R, Brown AL, Kim MK, Beaven MA, Burgin AB, Manganiello V, Chung JH. Resveratrol ameliorates aging-related metabolic phenotypes by inhibiting cAMP phosphodiesterases. *Cell* 2012; **148**: 421-433 [PMID: 22304913 DOI: 10.1016/j.cell.2012.01.017]
47 **Price NL**, Gomes AP, Ling AJ, Duarte FV, Martin-Montalvo A, North BJ, Agarwal B, Ye L, Ramadori G, Teodoro JS, Hubbard BP, Varela AT, Davis JG, Varamini B, Hafner A, Moaddel R, Rolo AP, Coppari R, Palmeira CM, de Cabo R, Baur JA, Sinclair DA. SIRT1 is required for AMPK activation and the beneficial effects of resveratrol on mitochondrial function. *Cell Metab* 2012; **15**: 675-690 [PMID: 22560220 DOI: 10.1016/j.cmet.2012.04.003]
48 **Di Lisa F**, Ziegler M. Pathophysiological relevance of mitochondria in NAD(+) metabolism. *FEBS Lett* 2001; **492**: 4-8 [PMID: 11248227 DOI: 10.1016/S0014-5793(01)02198-6]
49 **Desquiret-Dumas V**, Gueguen N, Leman G, Baron S, Nivet-Antoine V, Chupin S, Chevrollier A, Vessières E, Ayer A, Ferré M, Bonneau D, Henrion D, Reynier P, Procaccio V. Resveratrol induces a mitochondrial complex I-dependent increase in NADH oxidation responsible for sirtuin activation in liver cells. *J Biol Chem* 2013; **288**: 36662-36675 [PMID: 24178296 DOI: 10.1074/jbc.M113.466490]
50 **Stefanatos R**, Sanz A. Mitochondrial complex I: a central regulator of the aging process. *Cell Cycle* 2011; **10**: 1528-1532 [PMID: 21471732 DOI: 10.4161/cc.10.10.15496]
51 **Davis JM**, Murphy EA, Carmichael MD, Davis B. Quercetin increases brain and muscle mitochondrial biogenesis and exercise tolerance. *Am J Physiol Regul Integr Comp Physiol* 2009; **296**: R1071-R1077 [PMID: 19211721 DOI: 10.1152/ajpregu.90925.2008]
52 **Rayamajhi N**, Kim SK, Go H, Joe Y, Callaway Z, Kang JG, Ryter SW, Chung HT. Quercetin induces mitochondrial biogenesis through activation of HO-1 in HepG2 cells. *Oxid Med Cell Longev* 2013; **2013**: 154279 [PMID: 24288584 DOI: 10.1155/2013/154279]

53 **Ruiz MJ**, Fernández M, Picó Y, Mañes J, Asensi M, Carda C, Asensio G, Estrela JM. Dietary administration of high doses of pterostilbene and quercetin to mice is not toxic. *J Agric Food Chem* 2009; **57**: 3180-3186 [PMID: 19292443 DOI: 10.1021/jf803579e]

54 **Wätjen W**, Michels G, Steffan B, Niering P, Chovolou Y, Kampkötter A, Tran-Thi QH, Proksch P, Kahl R. Low concentrations of flavonoids are protective in rat H4IIE cells whereas high concentrations cause DNA damage and apoptosis. *J Nutr* 2005; **135**: 525-531 [PMID: 15735088]

55 **Robaszkiewicz A**, Balcerczyk A, Bartosz G. Antioxidative and prooxidative effects of quercetin on A549 cells. *Cell Biol Int* 2007; **31**: 1245-1250 [PMID: 17583542 DOI: 10.1016/j.cellbi.2007.04.009]

56 **Seo DB**, Jeong HW, Lee SJ, Lee SJ. Coumestrol induces mitochondrial biogenesis by activating Sirt1 in cultured skeletal muscle cells. *J Agric Food Chem* 2014; **62**: 4298-4305 [PMID: 24712520 DOI: 10.1021/jf404882w]

57 **Cantó C**, Gerhart-Hines Z, Feige JN, Lagouge M, Noriega L, Milne JC, Elliott PJ, Puigserver P, Auwerx J. AMPK regulates energy expenditure by modulating NAD+ metabolism and SIRT1 activity. *Nature* 2009; **458**: 1056-1060 [PMID: 19262508 DOI: 10.1038/nature07813]

58 **Lan F**, Cacicedo JM, Ruderman N, Ido Y. SIRT1 modulation of the acetylation status, cytosolic localization, and activity of LKB1. Possible role in AMP-activated protein kinase activation. *J Biol Chem* 2008; **283**: 27628-27635 [PMID: 18687677 DOI: 10.1074/jbc.M805711200]

59 **Jiang X**, Tang X, Zhang P, Liu G, Guo H. Cyanidin-3-O-β-glucoside protects primary mouse hepatocytes against high glucose-induced apoptosis by modulating mitochondrial dysfunction and the PI3K/Akt pathway. *Biochem Pharmacol* 2014; **90**: 135-144 [PMID: 24821109 DOI: 10.1016/j.bcp.2014.04.018]

60 **Rupasinghe HP**, Sekhon-Loodu S, Mantso T, Panayiotidis MI. Phytochemicals in regulating fatty acid β-oxidation: Potential underlying mechanisms and their involvement in obesity and weight loss. *Pharmacol Ther* 2016; **165**: 153-163 [PMID: 27288729 DOI: 10.1016/j.pharmthera.2016.06.005]

61 **Lagoa R**, Graziani I, Lopez-Sanchez C, Garcia-Martinez V, Gutierrez-Merino C. Complex I and cytochrome c are molecular targets of flavonoids that inhibit hydrogen peroxide production by mitochondria. *Biochim Biophys Acta* 2011; **1807**: 1562-1572 [PMID: 22015496 DOI: 10.1016/j.bbabio.2011.09.022]

62 **Pajuelo D**, Quesada H, Díaz S, Fernández-Iglesias A, Arola-Arnal A, Bladé C, Salvadó J, Arola L. Chronic dietary supplementation of proanthocyanidins corrects the mitochondrial dysfunction of brown adipose tissue caused by diet-induced obesity in Wistar rats. *Br J Nutr* 2012; **107**: 170-178 [PMID: 21733324 DOI: 10.1017/S0007114511002728]

63 **Skemiene K**, Liobikas J, Borutaite V. Anthocyanins as substrates for mitochondrial complex I - protective effect against heart ischemic injury. *FEBS J* 2015; **282**: 963-971 [PMID: 25586661 DOI: 10.1111/febs.13195]

64 **Schapira AH**. Complex I: inhibitors, inhibition and neurodegeneration. *Exp Neurol* 2010; **224**: 331-335 [PMID: 20362572 DOI: 10.1016/j.expneurol.2010.03.028]

65 **Rains TM**, Agarwal S, Maki KC. Antiobesity effects of green tea catechins: a mechanistic review. *J Nutr Biochem* 2011; **22**: 1-7 [PMID: 21115335 DOI: 10.1016/j.jnutbio.2010.06.006]

66 **Serrano JC**, Gonzalo-Benito H, Jové M, Fourcade S, Cassanyé A, Boada J, Delgado MA, Espinel AE, Pamplona R, Portero-Otín M. Dietary intake of green tea polyphenols regulates insulin sensitivity with an increase in AMP-activated protein kinase α content and changes in mitochondrial respiratory complexes. *Mol Nutr Food Res* 2013; **57**: 459-470 [PMID: 23281062 DOI: 10.1002/mnfr.201200513]

67 **Oliveira MR**, Nabavi SF, Daglia M, Rastrelli L, Nabavi SM. Epigallocatechin gallate and mitochondria-A story of life and death. *Pharmacol Res* 2016; **104**: 70-85 [PMID: 26731017 DOI: 10.1016/j.phrs.2015.12.027]

68 **Lee MS**, Kim CT, Kim Y. Green tea (-)-epigallocatechin-3-gallate reduces body weight with regulation of multiple genes expression in adipose tissue of diet-induced obese mice. *Ann Nutr Metab* 2009; **54**: 151-157 [PMID: 19390166 DOI: 10.1159/000214834]

69 **Trujillo J**, Granados-Castro LF, Zazueta C, Andérica-Romero AC, Chirino YI, Pedraza-Chaverrí J. Mitochondria as a target in the therapeutic properties of curcumin. *Arch Pharm* (Weinheim) 2014; **347**: 873-884 [PMID: 25243820 DOI: 10.1002/ardp.201400266]

70 **Granados-Castro LF**, Rodríguez-Rangel DS, Fernández-Rojas B, León-Contreras JC, Hernández-Pando R, Medina-Campos ON, Eugenio-Pérez D, Pinzón E, Pedraza-Chaverri J. Curcumin prevents paracetamol-induced liver mitochondrial alterations. *J Pharm Pharmacol* 2016; **68**: 245-256 [PMID: 26773315 DOI: 10.1111/jphp.12501]

71 **Yilmaz B**, Sahin K, Bilen H, Bahcecioglu IH, Bilir B, Ashraf S, Halazun KJ, Kucuk O. Carotenoids and non-alcoholic fatty liver disease. *Hepatobiliary Surg Nutr* 2015; **4**: 161-171 [PMID: 26151056 DOI: 10.3978/j.issn.2304-3881.2015.01.11]

72 **Ni Y**, Zhuge F, Nagashimada M, Ota T. Novel Action of Carotenoids on Non-Alcoholic Fatty Liver Disease: Macrophage Polarization and Liver Homeostasis. *Nutrients* 2016; **8**: pii: E391 [PMID: 27347998 DOI: 10.3390/nu8070391]

73 **Wang Y**, Ausman LM, Greenberg AS, Russell RM, Wang XD. Dietary lycopene and tomato extract supplementations inhibit nonalcoholic steatohepatitis-promoted hepatocarcinogenesis in rats. *Int J Cancer* 2010; **126**: 1788-1796 [PMID: 19551842 DOI: 10.1002/ijc.24689]

74 **Bahcecioglu IH**, Kuzu N, Metin K, Ozercan IH, Ustündag B, Sahin K, Kucuk O. Lycopene prevents development of steatohepatitis in experimental nonalcoholic steatohepatitis model induced by high-fat diet. *Vet Med Int* 2010; **2010**: pii: 262179 [PMID: 20953409 DOI: 10.4061/2010/262179]

75 **Erhardt A**, Stahl W, Sies H, Lirussi F, Donner A, Häussinger D. Plasma levels of vitamin E and carotenoids are decreased in patients with Nonalcoholic Steatohepatitis (NASH). *Eur J Med Res* 2011; **16**: 76-78 [PMID: 21463986 DOI: 10.1186/2047-783X-16-2-76]

76 **Yue R**, Hu H, Yiu KH, Luo T, Zhou Z, Xu L, Zhang S, Li K, Yu Z. Lycopene protects against hypoxia/reoxygenation-induced apoptosis by preventing mitochondrial dysfunction in primary neonatal mouse cardiomyocytes. *PLoS One* 2012; **7**: e50778 [PMID: 23226382 DOI: 10.1371/journal.pone.0050778]

77 **Reddy L**, Odhav B, Bhoola K. Aflatoxin B1-induced toxicity in HepG2 cells inhibited by carotenoids: morphology, apoptosis and DNA damage. *Biol Chem* 2006; **387**: 87-93 [PMID: 16497168 DOI: 10.1515/BC.2006.012]

78 **Kumar P**, Kalonia H, Kumar A. Lycopene modulates nitric oxide pathways against 3-nitropropionic acid-induced neurotoxicity. *Life Sci* 2009; **85**: 711-718 [PMID: 19822156 DOI: 10.1016/j.lfs.2009.10.001]

79 **Guerin M**, Huntley ME, Olaizola M. Haematococcus astaxanthin: applications for human health and nutrition. *Trends Biotechnol* 2003; **21**: 210-216 [PMID: 12727382 DOI: 10.1016/S0167-7799(03)00078-7]

80 **Ni Y**, Nagashimada M, Zhuge F, Zhan L, Nagata N, Tsutsui A, Nakanuma Y, Kaneko S, Ota T. Astaxanthin prevents and reverses diet-induced insulin resistance and steatohepatitis in mice: A comparison with vitamin E. *Sci Rep* 2015; **5**: 17192 [PMID: 26603489 DOI: 10.1038/srep17192]

81 **Ikeuchi M**, Koyama T, Takahashi J, Yazawa K. Effects of astaxanthin in obese mice fed a high-fat diet. *Biosci Biotechnol Biochem* 2007; **71**: 893-899 [PMID: 17420580 DOI: 10.1271/bbb.60521]

82 **Wolf AM**, Asoh S, Hiranuma H, Ohsawa I, Iio K, Satou A, Ishikura M, Ohta S. Astaxanthin protects mitochondrial redox state and functional integrity against oxidative stress. *J Nutr Biochem* 2010; **21**: 381-389 [PMID: 19423317 DOI: 10.1016/j.jnutbio.2009.01.011]

83 **Ferramosca A**, Conte L, Zara V. A krill oil supplemented diet reduces the activities of the mitochondrial tricarboxylate carrier and of the cytosolic lipogenic enzymes in rats. *J Anim Physiol Anim Nutr* (Berl) 2012; **96**: 295-306 [PMID: 21429045 DOI:

10.1111/j.1439-0396.2011.01135.x]
84 **Jia Y**, Wu C, Kim J, Kim B, Lee SJ. Astaxanthin reduces hepatic lipid accumulations in high-fat-fed C57BL/6J mice via activation of peroxisome proliferator-activated receptor (PPAR) alpha and inhibition of PPAR gamma and Akt. *J Nutr Biochem* 2016; **28**: 9-18 [PMID: 26878778 DOI: 10.1016/j.jnutbio.2015.09.015]
85 **Ha AW**, Kim WK. The effect of fucoxanthin rich power on the lipid metabolism in rats with a high fat diet. *Nutr Res Pract* 2013; **7**: 287-293 [PMID: 23964316 DOI: 10.4162/nrp.2013.7.4.287]
86 **Gammone MA**, D'Orazio N. Anti-obesity activity of the marine carotenoid fucoxanthin. *Mar Drugs* 2015; **13**: 2196-2214 [PMID: 25871295 DOI: 10.3390/md13042196]
87 **Chen YJ**, Wallig MA, Jeffery EH. Dietary Broccoli Lessens Development of Fatty Liver and Liver Cancer in Mice Given Diethylnitrosamine and Fed a Western or Control Diet. *J Nutr* 2016; **146**: 542-550 [PMID: 26865652 DOI: 10.3945/jn.115.228148]
88 **James D**, Devaraj S, Bellur P, Lakkanna S, Vicini J, Boddupalli S. Novel concepts of broccoli sulforaphanes and disease: induction of phase II antioxidant and detoxification enzymes by enhanced-glucoraphanin broccoli. *Nutr Rev* 2012; **70**: 654-665 [PMID: 23110644 DOI: 10.1111/j.1753-4887.2012.00532.x]
89 **Juge N**, Mithen RF, Traka M. Molecular basis for chemoprevention by sulforaphane: a comprehensive review. *Cell Mol Life Sci* 2007; **64**: 1105-1127 [PMID: 17396224 DOI: 10.1007/s00018-007-6484-5]
90 **Zhang Y**, Tang L. Discovery and development of sulforaphane as a cancer chemopreventive phytochemical. *Acta Pharmacol Sin* 2007; **28**: 1343-1354 [PMID: 17723168 DOI: 10.1111/j.1745-7254.2007.00679.x]
91 **Dinkova-Kostova AT**, Talalay P. Direct and indirect antioxidant properties of inducers of cytoprotective proteins. *Mol Nutr Food Res* 2008; **52** Suppl 1: S128-S138 [PMID: 18327872 DOI: 10.1002/mnfr.200700195]
92 **Kikuchi M**, Ushida Y, Shiozawa H, Umeda R, Tsuruya K, Aoki Y, Suganuma H, Nishizaki Y. Sulforaphane-rich broccoli sprout extract improves hepatic abnormalities in male subjects. *World J Gastroenterol* 2015; **21**: 12457-12467 [PMID: 26604653 DOI: 10.3748/wjg.v21.i43.12457]
93 **Yoshida K**, Ushida Y, Ishijima T, Suganuma H, Inakuma T, Yajima N, Abe K, Nakai Y. Broccoli sprout extract induces detoxification-related gene expression and attenuates acute liver injury. *World J Gastroenterol* 2015; **21**: 10091-10103 [PMID: 26401074 DOI: 10.3748/wjg.v21.i35.10091]
94 **Armah CN**, Traka MH, Dainty JR, Defernez M, Janssens A, Leung W, Doleman JF, Potter JF, Mithen RF. A diet rich in high-glucoraphanin broccoli interacts with genotype to reduce discordance in plasma metabolite profiles by modulating mitochondrial function. *Am J Clin Nutr* 2013; **98**: 712-722 [PMID: 23964055 DOI: 10.3945/ajcn.113.065235]
95 **Hino S**, Sakamoto A, Nagaoka K, Anan K, Wang Y, Mimasu S, Umehara T, Yokoyama S, Kosai K, Nakao M. FAD-dependent lysine-specific demethylase-1 regulates cellular energy expenditure. *Nat Commun* 2012; **3**: 758 [PMID: 22453831 DOI: 10.1038/ncomms1755]
96 **Kushad MM**, Brown AF, Kurilich AC, Juvik JA, Klein BP, Wallig MA, Jeffery EH. Variation of glucosinolates in vegetable crops of Brassica oleracea. *J Agric Food Chem* 1999; **47**: 1541-1548 [PMID: 10564014 DOI: 10.1021/jf980985s]
97 **Jie M**, Cheung WM, Yu V, Zhou Y, Tong PH, Ho JW. Anti-proliferative activities of sinigrin on carcinogen-induced hepatotoxicity in rats. *PLoS One* 2014; **9**: e110145 [PMID: 25329483 DOI: 10.1371/journal.pone.0110145]
98 **Ahn J**, Lee H, Im SW, Jung CH, Ha TY. Allyl isothiocyanate ameliorates insulin resistance through the regulation of mitochondrial function. *J Nutr Biochem* 2014; **25**: 1026-1034 [PMID: 25034503 DOI: 10.1016/j.jnutbio.2014.05.006]

P- Reviewer: Gorrell MD, Kayadibi H, Lee HC **S- Editor**: Gong ZM
L- Editor: A **E- Editor**: Wang CH

World Journal of Gastroenterology

Submit a Manuscript: http://www.f6publishing.com

World J Gastroenterol 2017 June 21; 23(23): 4158-4169

DOI: 10.3748/wjg.v23.i23.4158

ISSN 1007-9327 (print) ISSN 2219-2840 (online)

REVIEW

Helicobacter pylori BabA in adaptation for gastric colonization

Shamshul Ansari, Yoshio Yamaoka

Shamshul Ansari, Yoshio Yamaoka, Department of Environmental and Preventive Medicine, Oita University Faculty of Medicine, Yufu-City, Oita 879-5593, Japan

Yoshio Yamaoka, Department of Medicine-Gastroenterology, Baylor College of Medicine, Houston, TX 77030, United States

Author contributions: Yamaoka Y conceived the design of the manuscript; Ansari S searched the published articles, extracted the core information and prepared the initial draft of the manuscript; Yamaoka Y revised the draft of the manuscript.

Supported by (in part) grants from the National Institutes of Health, No. DK62813; the Grants-in-Aid for Scientific Research from the Ministry of Education, Culture, Sports, Science, and Technology (MEXT) of Japan, No. 25293104, No. 26640114, No. 15H02657 and No. 16H05191 to Yamaoka Y; Japan Society for the Promotion of Science Institutional Program for Young Researcher Overseas Visits to Yamaoka Y; the Strategic Funds for the Promotion of Science and Technology from Japan Science and Technology Agency to Yamaoka Y; and the Japanese Government (Monbukagakusho: MEXT) Scholarship Program to Ansari S.

Conflict-of-interest statement: The authors declare that they have no any conflict of interests.

Manuscript source: Invited manuscript

Correspondence to: Yoshio Yamaoka MD, PhD, Department of Environmental and Preventive Medicine, Oita University Faculty of Medicine, 1-1 Idaigaoka, Hasama-machi, Yufu-City, Oita 879-5593, Japan. yyamaoka@oita-u.ac.jp
Telephone: +81-97-5865740
Fax: +81-97-5865749

Received: January 28, 2017
Peer-review started: February 7, 2017
First decision: March 16, 2017
Revised: April 12, 2017
Accepted: June 1, 2017
Article in press: June 1, 2017
Published online: June 21, 2017

Abstract

Helicobacter pylori (*H. pylori*) as a causative agent of gastric complications, is well adapted for the colonization of gastric mucosa. Although the infectious process depends on several factors, the adhesion to the gastric mucosa is the first and important step. Among several outer membrane proteins, BabA is one of the significant protein involving in many inflammatory processes in addition to its role in the attachment for the persistent colonization. We performed a PubMed search using the key words: "*babA*", "pylori", "gastric complications", "homologous recombination", "slipped strand mispairing"; a total of 249 articles were displayed. Of these we mainly focused on articles with the full text in English and published between 2005 and 2016. *H. pylori* BabA is involved in binding with receptors; however, its synthesis is regulated by phase variation. In this review we confirm that *H. pylori babA* can be modulated at the molecular and functional levels to adapt to the stress within the gastro-intestinal tract.

Key words: BabA; Gastric complications; *Helicobacter pylori*; Homologous recombination; Slipped strand mispairing

Core tip: *Helicobacter pylori* are well adapted to colonize the gastric mucosa. Although the infectious process depends on several factors, adhesion to the gastric mucosa is the first and critical step. Among outer membrane proteins, BabA is an important protein involved in many inflammatory processes in addition to playing a role in the aforementioned attachment process. In this review, we have summarized the current, published knowledge regarding its functional and molecular aspects by which the pathogen can attach to the host cell receptors.

Ansari S, Yamaoka Y. *Helicobacter pylori* BabA in adaptation for gastric colonization. *World J Gastroenterol* 2017; 23(23): 4158-4169 Available from: URL: http://www.wjgnet.com/1007-9327/full/v23/i23/4158.htm DOI: http://dx.doi.org/10.3748/wjg.v23.i23.4158

INTRODUCTION

The *Helicobacter pylori* (*H. pylori*) is a helical, Gram-negative bacterium that chronically infects the stomach of half of the world's population[1]. Since this bacterium is strongly associated with the development of duodenal ulcer and gastric cancer, International Agency for Research on Cancer categorized this bacterium under strong carcinogen (group I carcinogen) in 1994[2,3]. The global burden of gastric cancer is high which accounts for 6.2% of cancer burden worldwide[4]. However, the appearance of new cases of gastric cancer has been found variable in developing (8.4%) and developed countries (4.5%)[5]. Mortality rate due to the gastric cancer is the third most common cause among all cancer related deaths[6,7].

Although the exact means of transmission of this bacterium is not understood clearly the evidences suggest that this bacterium is transmitted from person to person contact between family members *via* fecal-oral or oral-oral route and mostly the infections are acquired in childhood[8-10]. The data from epidemiological studies conducted support the transmission of infection by exposure to contaminated water or food as well[11,12]. The socio-economic status of family highly reflects the infection rate among peoples as the infection rate tends to be higher in peoples belonging to family with low socio-economic status[13]. This contribution highly suggests the higher prevalence rate of *H. pylori* infection in developing countries than the developed countries. The infection rate ranging from 70%-90% and 25%-50% in developing and developed countries respectively[14].

H. pylori related clinical outcomes also depend on the ancestral relation between human and bacterium as suggested recently. The individuals infected with non-ancestral strains that are not evolutionarily adapted to their host develop severe histo-pathological damage and clinical outcomes than infected with co-evolutionarily developed strains[15]. However, being a truly opportunistic pathogen, the *H. pylori* utilizes the various virulence factors such as CagA and VacA as the effector protein for the development of gastric diseases[16] and the outer membrane proteins (OMPs) such as blood group antigen binding adhesion (BabA), sialic acid binding adhesin (SabA), and outer inflammatory protein (OipA) found on the surface (adhesins) of bacterial cell envelop for the attachment to the mucus layer of the gastric epithelium playing an important and initial step for the colonization and development of persistent infection for decades or for entire life time[17-19].

LITERATURE SEARCH

We conducted a PubMed search using the key terms "*babA*", "pylori", "gastric complications", "homologous recombination", "slipped strand mispairing"; 249 articles were found during the search. We focused on, but did not limit ourselves to, articles with the full text in English and published between 2005 and December 2016. For greater clarity and insight we considered few articles published between 1989 and 2005. We retrieved a total of 98 articles that studied BabA and its paralogs, presence, function, production, and role in the development of gastric complications, attachment to host cells, and adaptation. Abstract only publications, case reports, editorials, and review articles were excluded. While performing the search, irrelevant articles with authors' family names as 'Baba' were also excluded. We also performed a literature search in Google using the terms: "pylori", "gastric cancer", and "slipped strand mispairing". Through this, we selected three reports that were not indexed in PubMed.

bab paralogous genes and their chromosomal location

H. pylori colonization elicits humoral and cellular immune responses although, ineffective in the bacterial clearance. However, despite of the peristaltic movement of the intestinal tract and movement of the chyme, the bacterium establishes the strong interaction with the epithelial surfaces. The bacterial attachment on the epithelial surface is the interaction between the receptor molecules on the host cell surface and adhesin molecules found on the bacterial cell envelope and this interaction is the first and important step of the *H. pylori* related pathogenicity. The Gram-negative bacterial cell envelope consists of two concentric lipid bilayers, the inner membrane (cytoplasmic membrane) and the outer membrane. More than 50% of the outer membrane mass consists of OMPs. *H. pylori* genome encodes a large number of OMPs and most of them are surface exposed and consists of transport channels (porins), and adhesins. The closely related (at least partially redundant)

Table 1 Chromosomal location of *babA*, *babB* and *babC* genes in different strains

Strain	Locus A	Locus B	Locus C
26695	*babB*	*babA*	*babC*
J99	*babA*	*babB*	No corresponding gene
HPAG1	*babA*	*babC*	*babB*
G27	*babC*	No corresponding gene	*babA*
51	*babA*	*babB*	No corresponding gene
Shi470	*babA*	*babB*	No corresponding gene
P12	*babA*	*babB*	*babB* homolog[1]
52	*babA*	*babB*	No corresponding gene
B38	*babA*	No corresponding gene	No corresponding gene
v225d	*babA*	*babB*	No corresponding gene
SJM180	*babB*	*babC*	*babA*
PeCan4	*babA*	*babB*	No corresponding gene
Sat464	*babA*	*babB*	No corresponding gene
35A	*babA*	*babB*	No corresponding gene
India7	*babA*	*babB*	No corresponding gene
Gambia94/24	*babA*	*babB*	No corresponding gene
SouthAfrica7	*babA*	*babA*	No corresponding gene
Oki112	*babA*	*babA*	No corresponding gene
Oki154	*babA*	*babB*	No corresponding gene
Oki828	*babA*	*babA*	No corresponding gene
J166	*babA*	*babB*	No corresponding gene
SNT49	*babA*	*babB*	No corresponding gene
Puno120	*babA*	*babB*	No corresponding gene
Puno135	*babA*	*babB*	No corresponding gene
B8	*babA*	*babA*	No corresponding gene
83	*babA*	*babB*	No corresponding gene
ELS37	*babB*	*babA*	No corresponding gene
HUP-B14	*babA*	*babC*	No corresponding gene
F16	*babA*	*babB*	No corresponding gene
F30	*babA*	*babB*	No corresponding gene
Hp238	*babA*	*babB*	No corresponding gene
BM013A	*babB*	*babB*	No corresponding gene
29CaP	*babA*	*babA*	No corresponding gene

[1]Although the gene is homologous to babB but due to the insertion of adenine (A) caused the formation of stop codon and premature termination.

proteins are grouped into paralogous families[20].

Among the large group of adhesins identified BabA, SabA, adherence associated lipoprotein A and B (AlpA/B), OipA, and HopZ[17,18,21-24], BabA (or HopS or OMP28) is around 75-80 kDa major OMP which was the first identified member of adhesin family[25]. Two other closely related paralogs to BabA has been found, the BabB (HopT or OMP19) and BabC (HopU or OMP9)[26]. The function of BabB and BabC is not known yet and needs to be determined. The *bab* gene sequence analysis revealed that there is extensive 5' and 3' region homology particularly between *babA* and *babB* but the variability in middle region of sequence suggests that the middle divergent region of *babA* likely mediates the binding function[26,27].

The *babA, babB* and *babC* genes can be located in at least 3 different chromosomal loci. The three marker genes *hypD, s18* and heme oxygenase gene *hp0318* represent the chromosomal location of *bab* genes. The *bab* gene found downstream of *hypD*, *s18* and *hp0318* is said to be located at locus A, locus B and locus C respectively[28]. For example; in strain J99 (where *babC* is absent), *babA* (*jhp0833*) and *babB* (*jhp1164*) are located downstream of *hypD* and *s18* (locus A and locus B) respectively whereas in strain 26695, the locations for *babA* and *babB* are reversed; *babA* (*hp1243*), *babB* (*hp0896*) and *babC* (*hp0317*) are located downstream of *s18, hypD* and *hp0318* (locus B, locus A and locus C) respectively. Similarly, in strain HPAG1, the *babA, babB* and *babC* are located downstream of *hypD*, *hp0318* and *s18* (locus A, locus C and locus B) respectively whereas in strain G27 (where *babB* is absent), *babA* and *babC* are located downstream of *hp0318* and *hypD* (locus C and locus A) respectively and in strain 51 (where *babC* is absent), the *babA* and *babB* are located downstream of *hypD* and *s18* (locus A and locus B) respectively[29-31] as shown in Table 1. We made an attempt to find the *bab* genes in respective to their genomic locus in different strains deposited in gene bank. Among *H. pylori* deposited in gene bank by 30 November 2016, we randomly selected the 33 strains for the characterization of chromosomal locations of *bab* genes *(babA, babB and babC)* (Table 1). Although, the chromosomal locations of *babA, babB* and *babC* in few strains such as J99, 26695, HPAG1, G27 and 51 already have been described yet in other strains we made an effort to document the chromosomal location of these genes. In strain P12 there is a *babB* homologous gene at locus C but due to the insertion of one adenine (A) at position 679 resulted the shift in the nucleotide frame and the stop codon at position 230 and premature termination of the amino acid sequence. The reports of several studies from various parts of the world depicts that in majority of the strains *babA* and *babB* prefers to be located at locus A and locus B respectively[28-30,32]. Despite of the three identified loci there can be an unidentified locus. In a study, Hennig *et al*[29] found *babA* sequences from 2 strains not located at locus A, B or C and they hypothesized that there may be a yet not identified chromosomal locus for *babA*.

Production of BabA

As discussed in previous section, the *babA* can be located in at least three different identified loci. The BabA production has been claimed to be influenced by its genomic location. In strain J99, *babA* located at locus A is expressed and binds with Lewis blood group (Leb) antigen whereas in strain 26695; *babA* located at locus B is not expressed and does not bind to Leb antigen[33,34]. The detailed mechanisms involved in the expression of *babA* have not been depicted in detail. However, we have summarized the possible mechanisms published in several literatures.

The strain CCUG17875 was reported to possess two alleles of *babA* denoted as *babA1* found at locus B and *babA2* found at locus A[34]. The allelic form *babA1*

does not contain the translation initiation codon ATG because of the deletion of 10 bp including start codon in its signal sequence and is not expressed whereas the *babA2* containing the translation initiation codon ATG is expressed and involved in the Leb binding activity[34]. The expression of *babA* can be influenced on transcriptional as well as translational level. The absence of translation initiation codon ATG in *babA1* influence the translation, but this phenomenon is quite uncommon. Nonetheless, unfortunately, several epidemiological studies still use the methods to characterize *babA2* as the functional status of *babA* by using primers specific for the signal region to differentiate *babA1* and *babA2*. The presence of variable number of cytosine-thiamidine (CT) dinucleotide in the 5'-region of the *babA* sequence due to the intra-genomic recombination with *babB* leads to the phase variation and affects the expression of *babA* (discussed in latter section). The characteristics of the promoter sequence also play a critical role in the expression of *babA*. During protein expression all mRNAs are not synthesized in the same amount because of the promoter characteristics which controls the expression on transcriptional level. In a study, the presence of additional 4 adenines between the -10 and -35 motif in *babA* located at locus B could diminished the strength of the promoter of *babA*[34]. The nucleotide structure of -10 and -35 motifs sequence and the characteristics of nucleotides present between the -10 and -35 motifs tend to make the promoter strong or weak. For example, the promoter region of one of the OMP gene *sabA* contains a thymidine (T) nucleotide repeat tract adjacent to the -35 motif and the length of this T-tract varies between strain to strain and this variation have been suggested to affect the expression of *sabA*[35-37]. Recently it has been also suggested that the T-tract modulates the binding of RNA polymerase σ-factor and α-factor resulting in the alteration of SabA expression[38]. The nucleotide repeat motifs located between the -35 and -10 promoter motifs influence the docking of RNA polymerase σ-factor and the nucleotide repeat motif located upstream of -35 motif alters the binding of regulatory factors of RNA polymerase[38]. However, the detailed studies are needed to evaluate the characteristics of promoter regions responsible for the variation in expression of *babA* in loci A/B/C.

H. pylori babA is highly polymorphic being susceptible for the changes in their regulatory and coding sequence that leads to the loss of BabA expression in multiple animal models including mice, gerbils and macaques; therefore, it is difficult to study the role of BabA contribution in the development of gastric damages[39]. However, it has been shown that in *H. pylori* isolated from the chronically infected persons, the BabA expression was maintained in three quarter of the isolates surveyed over time and it suggests that there is selective advantage for BabA expression in human host[40].

Occurrences of babA containing H. pylori

Most epidemiological studies have reported the *babA* functional status using the *babA2* specific primers designed to detect the 10-bp deletion in the signal region of the *babA1* allele and its association with increased risk for gastric inflammation[41]. The reported prevalence of *H. pylori* containing *babA* shows great variation across different parts of the world[28,32,42-55] as shown in Table 2. However, we previously reported the BabA expression level by immunoblotting and Leb binding in diverse collection of *H. pylori* strains and divided in to high, low, and non BabA expressing strains[52]. The strains expressing low level of BabA were associated with higher incidence of gastrointestinal damages as compared to BabA with high expression and BabA negative strains. It was concluded that although, the *babA*2 detection provides an indication of functional *babA* status, it may not reliably reflect the complete information of genetic variants for *babA* expression.

BabA and its binding receptors

Adherence of *H. pylori* to the host cell receptor provides several benefits to the bacteria such as protection from the washing out during mucus shedding, provides nutrient access from damaged host epithelial cells, promotes delivery of the bacterial toxins and other effector molecules to the host cells for development of pathogenicity and facilitates the development of persistent infections[56-58]. The attachment of bacteria to the host cells also elicits immune response; however, no longer protective in *H. pylori* infection. Several functional molecules serving as a receptor for the binding of *H. pylori* through BabA has been reported (Table 3).

Since the postulated transmission for the *H. pylori* infection takes place through oral route, the possible initial attachment could be occurred with the salivary proteins. The BabA mediates the attachment by binding with difucosylated glycans found on Leb antigens of the salivary mucin MUC5B serving as a receptor for BabA[59,60]. The surface immobilized salivary agglutinin; glycoproteins-340 (gp-340) also provides the platform for the attachment of BabA[61]. Salivary prolin rich glycoprotein (PRG) is the major component of parotid and submandibular saliva containing several repeats of short prolin rich sequence. Salivary PRG containing Fucα1-2Galβ motif also provides the access for the attachment of BabA[59]. The secretory immunoglobulin A (s-IgA) is the major immunoglobulin found in the mucus secretions which protects the mucus membrane from invading organisms. However, the fucose-containing oligosaccharide motifs on s-IgA could play a role in the binding phenomena of BabA[17]. However, in a study this phenomenon was not confirmed suggesting that the variation in the glycosylation and sialylation between the salivary and gastric s-IgA or the proportions of s-IgA1 and s-IgA2 subclasses

Table 2 Prevalence of *babA* in different Asian and other countries

Ref.	Countries	Criteria for *babA* positive	Prevalence	Year
	Asia			
Abdullah *et al*[43]	Iraq	Positive with *babA2* specific primers	33.7% in NUD and 58.8% in PUD	2012
Karabiber *et al*[44]	Turkey	Positive with *babA2* specific primers	49% in gastritis	2014
Abadi *et al*[45]	Iran	Positive with *babA2* specific primers	Overall-40.6% 95%-GC, 18.1-DU, 26.1-NUD	2013
Yadegar *et al*[46]	Iran	Positive with *babA2* specific primers	Overall-96.7% 94.4%-NUD, 100%-PUD, 100%-GE, 100%-GC	2014
Saberi *et al*[42]	Iran	BabA expression	Overall-62%	2016
Osman *et al*[47]	Malaysia	Positive with *babA2* specific primers	41%-NUD	2015
Boonyanugomol *et al*[48]	Thailand	Positive with *babA2* specific primers	Overall-66.2%, 70.7%-CCA, 54.5%-Cholelithiasis	2012
Chomvarin *et al*[49]	Thailand	Positive with *babA2* specific primers	Overall-92% 92%-NUD, 85%-GU, 100%-DU, 94%-GC	2008
Ghosh *et al*[50]	India	Positive with *babA2* specific primers	Overall-67.5% 65.6%-NUD, 70%-DU	2016
Con *et al*[51]	Japan	Positive with *babA2* specific primers	Overall-96.8%	2010
Fujimoto *et al*[52]	Japan	Leb binding activity	Over all-88.0%	2007
Kim *et al*[32]	South Korea	Positive with *babA* specific primers	Overall-47.5%	2015
	Other countries			
Kim *et al*[32]	United States	Positive with *babA* specific primers	Overall-90%	2015
Biernat *et al*[53]	Poland	Positive with *babA2* specific primers	Overall-23.1% 18%-NUD, 30%-PUD, 31.8%-GERD	2014
Homan *et al*[54]	Slovenia	Positive with *babA2* specific primers	Overall-47.9%	2014
Boyanova *et al*[55]	Bulgaria	Positive with *babA2* specific primers	Overall-48.8% 59.3%-PUD, 43.5%-NUD	2010
Matteo *et al*[28]	Argentina	Positive with *babA* specific primers	Overall-67%	2011
Con *et al*[51]	Costa-Rica	Positive with *babA2* specific primers	Overall-73.7%	2010
Fujimoto *et al*[52]	Colombia	Leb binding activity	Overall-83.0%	2007

NUD: Non-ulcer disease; PUD: Peptic ulcer disease; GC: Gastric cancer; DU: Duodenal ulcer; GE: Gastric erosion; CCA: Cholangiocarcinoma; GERD: Gastroesophageal reflux disease; GU: Gastric ulcer.

Table 3 BabA receptors found on oral cavity and in stomach

Receptors identified	Localization	Ref.
Mucin MUC5B	Saliva	Walz *et al*[59] and Prakobphol *et al*[60]
Agglutinin glycoprotein-340 (gp-340)	Saliva	Prakobphol *et al*[61]
Prolin rich glycoprotein containing Fucα1-2Galβ motif	Saliva	Walz *et al*[59]
Secretory immunoglobulin A containing fucose-oligosaccharide motifs	Saliva	Borén *et al*[17] and Royle *et al*[62]
Salivary agglutinin DMBT1	Saliva	Issa *et al*[63]
Lewis b blood group antigen (Leb) and terminal fucose, H1-antigen, A-antigen and B-antigen	Gastric epithelia	Borén *et al*[17] and McGuckin *et al*[64]
Mucin MUC5AC with N-acetylgalactosamine-β-1,4-N-acetylglucosamine	Gastric mucus	Lindén *et al*[68] and Kenny *et al*[69]
Mucin MUC1	Gastric mucus	Lindén *et al*[71]
Mucin MUC2	Gastric mucus	Cohen *et al*[72]

which are known to be differently glycosylated may play this role[62]. Similarly, a salivary agglutinin called the deleted in malignant brain tumors 1 (DMBT1) is expressed in saliva and composed of highly fucosylated oligosaccharide. The salivary DMBT1 was found to act as the receptor to interact with BabA[63].

After transit to the stomach, the bacterium localizes to the specific locations and mediates adaptation through several ways. The gastrointestinal epithelium is covered by a semi-permeable mucus layer primarily consists of secreted mucins that protects the gastric epithelial surface by trapping the invading materials[64]. However, the attachment of bacteria to the epithelial surface mediates the survival adaptation and persistent infections. The di-fucosylated glycan found on Leb and mono-fucosylated glycans found on H1-antigen, A-antigen and B-antigen of blood group O, A and B respectively binds with BabA[17,33,65]. However, the binding affinity of BabA with H1 antigen is low because it lacks the Leb Fuc4 residue that forms a hydrogen bond with amino acid asparagine (N) at 206 position of BabA[66] as described below in next section. These antigens are expressed on the mucus surface and gastric epithelial surface of which the Leb antigen is the dominant antigen found on the surface of gastric epithelial cells and it is also the most studied receptor

Table 4 Oligosaccharides found in Leb involving in binding with amino acid of BabA

Oligosaccharide in Leb	Amino acid in BabA	Position of amino acid in BabA
Fuc1	Cysteine (C)	189
Fuc1	Glycine (G)	191
Fuc1	Asparagine (N)	194
Fuc4	Asparagine (N)	206
GlcNAc3 or Gal5	Aspartic acid (D)	233
Gal5	Serine (S)	234
GlcNAc3 or Gal5	Serine (S)	244
Fuc1	Threonine (T)	246

for BabA attachment[67].

Similarly, other molecules have also been reported to play a crucial role in the binding of BabA. The gastric mucin MUC5AC with N-acetylgalactosamine-β-1,4-N-acetylglucosamine residues on O-linked oligosaccharides from gastric MUC5AC has also been reported to act as receptor for BabA[68,69]. Most recent immunohistochemistry laden tissue profiling assay using mice model showed that the expression of Leb structure is a mucin α 1,2-fucosyltransferase (FUT2) enzyme dependent and consequently identified MUC5AC as the carrier molecule of the Leb structure[70].

The MUC1 is also notable to discuss. In case when bacteria do not bind to MUC1, an extracellular mucin domain of 200-500 nm long appears that physically distances the bacteria from the host cell surface and in case when it does bind MUC1, the extracellular mucin domain is released from the epithelial surface[71]. In another study by Cohen *et al*[72] conducted in children, the gastric mucin MUC2 was reported to be expressed in few foleolar cells and it was shown to participate in binding with BabA but only in 11.11% of children. Therefore, fucosylated glycans found on several glycoprotein molecules serve as the receptor.

Insight into BabA binding with receptors

The detailed molecular determination of BabA binding with its receptor Leb was studied recently by Hage *et al*[66]. They depicted that the Leb oligosaccharide molecules involving in the binding with BabA consists of two fucose residues (Fuc1 and Fuc4), two galactose residues (Gal2 and Gal5), an N-acetylglucosamine residue (GlcNAc3), and a glucose residue (Glc6). Using strain J99 as an experimental model they found that 8 highly conserved amino-acids of BabA involved in the interaction with Leb by hydrogen bond formation. The bond formation occurs between amino acid cysteine (C) at position 189 and Fuc1 (C189:Fuc1), glycine (G) at position 191 and Fuc1 (G191:Fuc1), asparagine (N) at position 194 and Fuc1 (N194:Fuc1), asparagine (N) at position 206 and Fuc4 (N206:Fuc4), aspartic acid (D) at position 233 and GlcNAc3 (D233:GlcNAc3), aspartic acid (D) at position 233 and Gal5 (D233:Gal5), serine (S) at position 234 and Gal5 (S234:Gal5), serine (S) at position 244 and GlcNAc3 (S244:GlcNAc3, Gal5), serine (S) at position 244 and Gal5 (S244:Gal5) and threonine (T) at position 246 and Fuc1 (T246:Fuc1) (Table 4). They also elaborated that the binding of N at position 206 with Fuc4 determines the binding affinity and substitution of N with alanine (A) at position 206 resulted in the reduction of binding affinity by about 2.3-fold and the binding of BabA with H-1 which lacks Fuc4 residue of Leb showed about 2.4 fold reduction in binding affinity[66]. Despite of the role of Leb for providing the binding receptor and enhancing the colonization, the several reports indicate the antagonistic effect of Leb. In a study led by Lindén *et al*[73] found that the individuals with Leb-negative showed significantly higher *H. pylori* density than Leb-positive, which is in accordance with the result obtained in a study using Rhesus monkey[74]. Therefore, it can be said that although, the attachment of bacterium *via* BabA-Leb is important but not elusive.

Based on their ABO blood group antigen binding preferences, BabA bearing *H. pylori* strains can be classified as "specialists" and "generalists". The specialist strains prefer to bind only on blood group O specific glycans whereas generalist strains bind blood group O as well as blood group A and B specific glycans[65]. Till recently the detailed insight concept about the binding of specialists and generalists with the mono-fucosylated glycan on A, B and O blood group was unknown. However, recently the X-ray structures of the BabA specialist and generalist adhesins have been revealed according to the O and ABO blood group preferences[75]. The preference shifting was found to be due to the single amino acid substitution in its carbohydrate binding domain. The carbohydrate binding domain contains one conserved loop (CL2) and two diversity loop (DL1 and DL2). The loop DL1 is responsible for making the BabA to be either specialist or generalist. Binding of specialists with blood group O antigen involves only CL2 and DL2 loops while the binding of generalists involve CL2, DL2 as well as DL1 loops. In specialists BabA, the domain DL1 contains the amino acid leucin (L) at 198 position which makes the DL1 to be inaccessible for binding with larger glycans present on blood group A and B. The replacement of L to serine (S) in generalists makes the DL1 to be accessible for the glycans found on blood group A and B as well as O (Figure 1). In this way the generalists can bind with glycans found on blood group A, B as well as O antigen whereas the specialists can bind the glycan found on blood group O antigen only[75]. Therefore, this capability of binding explains why the peoples of blood group O are more prone to develop duodenal ulcers[65]. The fucosylated oligosaccharide residue found on the H1 antigen is abundantly expressed by the healthy gastric mucosa of most Western peoples which makes them more susceptible to colonize by generalists as well as specialists and for the development of peptic ulcer[17,76].

The binding of BabA to the Leb receptor is severely affected by the level of BabA production which is

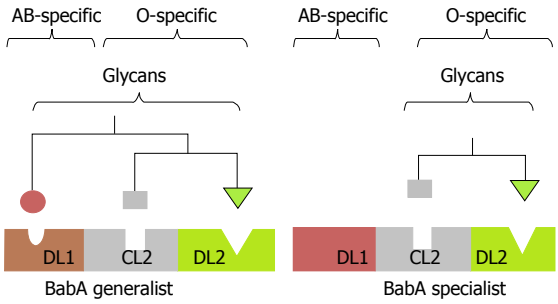

Figure 1 In BabA generalists the serine (S) at position 198 makes the DL1 domain to be accessible for the glycan found on blood group A, B as well as O antigen whereas in BabA specialists the replacement of S to leucine (L) makes DL1 to be inaccessible for binding with larger glycans present on blood group A and B antigen.

mediated on transcriptional and translational level. We detected that the strains expressing low levels (less than 10% to that of J99) of BabA protein did not mediate the enough Leb binding activity whereas, the strains expressing high level (more than 20% to that of J99) of BabA did enough Leb binding[52]. However, Saberi *et al*[42] categorized the *H. pylori* strains in four types depending on the BabA expression and Leb-binding, strains expressing high level BabA showed high Leb-binding, strains expressing low level BabA showed low Leb-binding whereas strains with no BabA expression showed no Leb-binding (8%) as well as low Leb-binding (30%) activity.

Homologous recombination and bab chimera formation

Recombination between similar sequences is called the homologous recombination. Homologous recombination takes part in the double strand DNA repair caused by environmental stress and it aids adaptation advantage for the development of persistent colonization to *H. pylori* to the changing gastric environment within a single host or to the new host[77-79]. *H. pylori* exhibits the highest genetic recombination rate than any other known bacterial species[80] and it suggests that the bacteria has a selective advantage of genetic recombination for long term survival and colonization in human stomach[81].

The allelic diversity in *H. pylori* is remarkable and it exhibits high transformation mediated homologous recombination[77]. Recent analyses of sequential sampling of *H. pylori* from the same individual elaborated the OMPs *futB, babA* and *hopZ* to be the genes with high recombination events whereas the *hopQ* with low recombination[82,83]. Although the function of the most closely related *babA* paralogs; the *babB* and *babC*, is unknown yet but extensive sequence similarity shows the intra-genomic recombination between these genes and the evolution of *bab* chimera[35]. The RecA-dependent intragenomic recombination between homologous genes causing fusion of portions of two or more coding regions results in the formation of chimeric genes. In *H. pylori* the recombinational gene conversion occurs in homologous genes *babA, babB* and *babC*. The formation of chimeric *babB/A* can lead to a non Leb binding strains regain Leb binding activity or it can abolish *babA*-dependent adhesion[35,84]. Varying proportions of chimeras have been reported from different studies across the world. In a study by Matteo *et al*[28], the chimeric *babA/B* gene was observed in 20% whereas chimeric *babB/A* gene was observed in 15%. Similarly, in another study among American and Korean strains, the *babA/B* chimera, *babB/A* chimera and *babB/C* chimera was identified in 28.7%, 2.5% and 1.25% respectively among American strains whereas *babA/B* chimera and *babB/A* chimera was identified from 6.25% and 1.25% respectively from Korean strains. The *babA/B* was most prevalent type of *bab* chimera among all types of chimera reported[32].

Slipped strand mispairing and phase variation

Slipped strand mispairing (SSM) is a phenomenon of either deletion or insertion of nucleotides during DNA replication because of the short, contiguous homogenous or heterogeneous repetitive DNA sequence of 6 base pairs or less. This repetitive sequence, susceptible for mispairing is designated as short sequence repeats (SSR), microsatellites or variable number of tandem repeats (VNTR)[85,86]. SSM is one of the mechanisms resulting in the phase variation that produces nucleotide mispairing between the mother and daughter strand during the DNA replication[87,88]. The OMP genes such as *babB, hopZ, oipA* that possess the dinucleotide CT-repeats in the 5'-coding region, likely undergo SSM to regulate their expression by phase variation[18,89,90]. Nucleotide slippage can be occurred in replicating or template strand. If slippage occurs in replicating strand, there is insertion of one CT-dinuleotide and if slippage occurs in template strand, there is deletion of one CT-dinucleotide (Figure 2)[91]. This phenomenon leading to the variation in the number of CT-dinucleotides over time may provide certain advantages for adaptation to different niches and stomach micro-environments *via* immune evasion or adhesion. In *H. pylori*, the fragments of *babB* containing CT repeats may recombine with *babA* or *babC* resulting in the formation of chimeric genes. According to the Bäckström *et al*[34] the strains with in-frame protein expression (ON) status contain 8-CT repeats whereas out of frame protein expression (OFF) phenotypes contained 7 or 9 CT repeats. The gain or loss of one CT-dinucleotide creates frame shifts and loss of expression of *babA*.

The number of CT-repeats in the 5'coding region of nucleotide sequence decides whether the protein expression is ON or OFF. The protein expression becomes in-frame if the number of CT-repeats is 5, 8, 11 and 14 whereas if the number of CT-repeats is 6, 7, 9, 10, 12, 13 it makes protein expression out of frame[30,34,84]. Out of frame status of protein

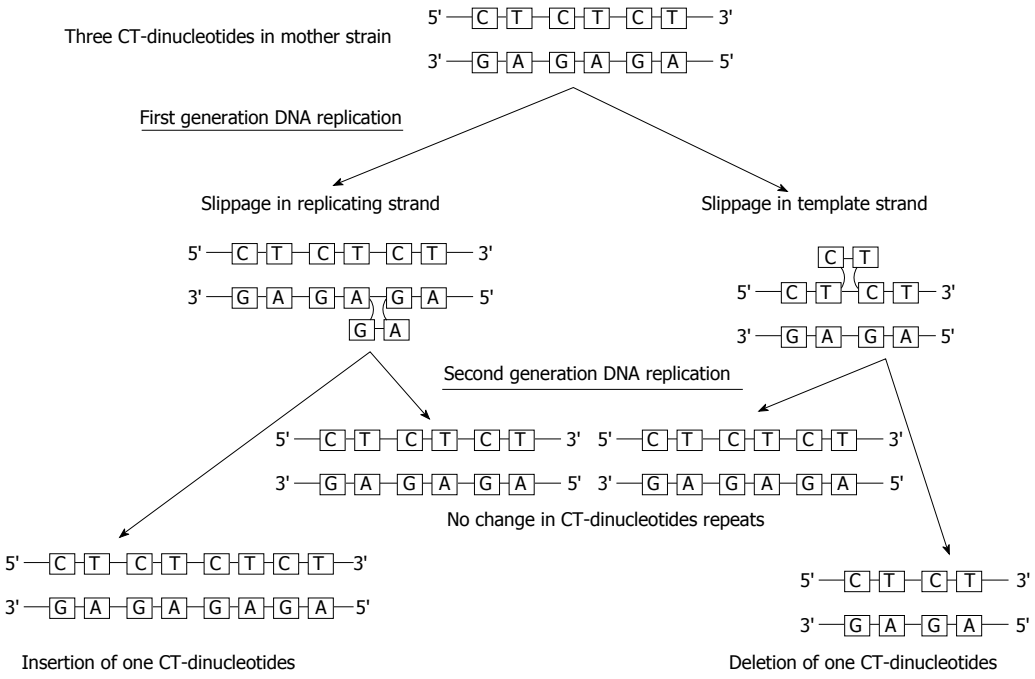

Figure 2 Cytosine-thiamidine-dinucleotide repeats and slipped strand mis-pairing. Both replicating and template strands are prone to undergo for slippage mis-pairing. Slippage occurring in replicating strand during first generation of replication causes insertion of one CT-dinucleotide in replicating strand whereas the template strand contains original number of CT-dinucleotide. If slippage occurs in template strand during first generation replication, one CT-dinucleotide is deleted in replicating strand to make base paring. During second generation of DNA replication, out of two progeny generating from slippage in replicating strand, one progeny contains DNA with one CT-dinucleotide more than the mother strain while the other progeny contains same number of CT-dinucleotide as mother strain. During second generation of DNA replication, out of two progeny generating from slippage in template strand, one progeny contains DNA with one CT-dinucleotide less than the mother strain while other progeny contains DNA with same number of CT-dinucleotide as do mother strain. CT: Cytosine-thiamidine.

expression evolved due to the insertion or deletion of one nucleotide resulting in the truncated (immature) proteins whereas if the status is in-frame it results in the full-length protein expression[92].

The genes containing variable number of nucleotide repeats may go to the phase variation. Phase variation is an adaptation mechanism that provides advantages for colonization[93]. In a study, the BabA expression was lost during the experimental infection in rhesus macaques by phase variation or allele replacement with BabB and in subsequent follow up study in mouse, the BabA expression was found to be lost due to phase variation in 5'-CT repeat regions of *H. pylori* strain J166[39]. The Leb binding clones from OFF to ON phase conversion express BabA adhesin that are functionally equivalent to the wild type but the quantity of BabA adhesin less abundant than the wild type[34].

Other clinical significance of BabA mediated attachment

The attachment of *H. pylori via* BabA mediates several outcomes. *H. pylori* BabA binds with Leb and induces the double strand breaks in the host cells, which is thought to be independent of VacA, γ-glutamyl transpeptidase and the *cag* PAI[94]. However, it has been also confirmed that BabA-positive status of infecting strains is associated with CagA-positive, OipA-positive (*oipA* "on") and *vacA* s1 genotype for the development of intestinal metaplasia[95]. The infection with BabA-positive strains has been associated with the increased risk for development of peptic ulcer diseases in Western countries[41,96]. However, the association of BabA with peptic ulcer diseases has not been confirmed in patients from East Asian or some other Western countries[97-99]. It has been claimed that the BabA-mediated attachment to gastric epithelial cells might enhance CagA translocation and the enhancement of inflammation[100]. Furthermore, the triple-positive (BabA, CagA and *vacA* s1-positive) strains of *H. pylori* shows greater colonization densities, elevated levels of gastric inflammation and a higher incidence of intestinal metaplasia in patients in contrast with the only CagA and *vacA*s1 positive strains[101,41]. Despite of the association of high level BabA with severe clinical outcomes, surprisingly, it has been also found that low level BabA expressing strains could more likely be associated with increased mucosal inflammation and severe clinical outcomes compared to that of high level BabA-positive and Leb binding strains[42,52]. Although, the underlying mechanisms remains unclear, it has been hypothesized that during adulthood, the induced hyperacidity may enhance the development of gastric metaplastic patches in the duodenum and the *H. pylori* expressing low levels of BabA and Leb attachment are able to detach from the gastric niche and reattached to the gastric metaplastic patches in the duodenum and develop the ulcers at the gastric-duodenal tissue border[42]. The BabA adhesin expression also seems tightly associated

with the onset of type 4 secretory system (T4SS)-related host response *in vivo*[100]. In an *in vivo* study, using the Mongolian gerbils, the BabA-mediated adherence of *H. pylori* to the epithelial cells has been shown to augment the *cag* PAI dependent *H. pylori* pathogenicity. The BabA-Leb interaction can trigger the production of pro-inflammatory cytokines and some factors that can enhance the cancer development[101].

CONCLUSION

H. pylori infection is a major cause of gastric complications including gastric cancer which is the third leading cause for mortality among all cancer related deaths. *H. pylori* being a Gram-negative organism, the OMP present in the cell envelope provides the initial step binding with the Leb antigen for the persistent colonization. BabA is capable of binding with receptors found on the oral mucosa and gastric mucus layer. The closer insight of *bab* genes revealed the presence of dinucleotide (CT) repeats in 5'-region which causes SSM leading to the phase variation. The formation of chimera with the homologous genes *babB* and *babC* causes the regulation of protein expression on transcriptional level. In addition to the high level BabA expression associated with the severe clinical outcomes many reports have also suggested the low level expression with severe outcomes where the underlying mechanism is not clear yet. Even though many roles of BabA in disease process have been evaluated, the role of BabB and BabC has not been assessed yet. Further study is under demand for the assessment of the role of BabB and BabC as well as to elaborate the underlying mechanism of low expression BabA and severe clinical outcomes.

REFERENCES

1 **Kusters JG**, van Vliet AH, Kuipers EJ. Pathogenesis of Helicobacter pylori infection. *Clin Microbiol Rev* 2006; **19**: 449-490 [PMID: 16847081 DOI: 10.1128/CMR.00054-05]

2 Schistosomes, liver flukes and Helicobacter pylori. IARC Working Group on the Evaluation of Carcinogenic Risks to Humans. Lyon, 7-14 June 1994. *IARC Monogr Eval Carcinog Risks Hum* 1994; **61**: 1-241 [PMID: 7715068]

3 **IARC Helicobacter pylori Working Group**. Helicobacter pylori Eradication as a Strategy for Preventing Gastric Cancer. Lyon, France 2014: International Agency for Research on Cancer (IARC Working Group Reports, No. 8). Available from: URL: http://www.iarc.fr/en/publications/pdfsonline/wrk/wrk8/index.php

4 **Plummer M**, Franceschi S, Vignat J, Forman D, de Martel C. Global burden of gastric cancer attributable to Helicobacter pylori. *Int J Cancer* 2015; **136**: 487-490 [PMID: 24889903 DOI: 10.1002/ijc.28999]

5 **Ferlay J**, Soerjomataram I, Dikshit R, Eser S, Mathers C, Rebelo M, Parkin DM, Forman D, Bray F. Cancer incidence and mortality worldwide: sources, methods and major patterns in GLOBOCAN 2012. *Int J Cancer* 2015; **136**: E359-E386 [PMID: 25220842 DOI: 10.1002/ijc.29210]

6 GLOBOCON 2012: Estimated cancer incidence, mortality and prevalence worldwide in 2012. Available from: URL: http://globocan.iarc.fr/Pages/fact_sheets_cancer.aspx

7 **Wroblewski LE**, Peek RM, Wilson KT. Helicobacter pylori and gastric cancer: factors that modulate disease risk. *Clin Microbiol Rev* 2010; **23**: 713-739 [PMID: 20930071 DOI: 10.1128/CMR.00011-10]

8 **Mamishi S**, Eshaghi H, Mahmoudi S, Bahador A, Hosseinpour Sadeghi R, Najafi M, Farahmand F, Khodadad A, Pourakbari B. Intrafamilial transmission of Helicobacter pylori: genotyping of faecal samples. *Br J Biomed Sci* 2016; **73**: 38-43 [PMID: 27182676 DOI: 10.1080/09674845.2016.1150666]

9 **Goh KL**, Chan WK, Shiota S, Yamaoka Y. Epidemiology of Helicobacter pylori infection and public health implications. *Helicobacter* 2011; **16** Suppl 1: 1-9 [PMID: 21896079 DOI: 10.1111/j.1523-5378.2011.00874.x]

10 **Bui D**, Brown HE, Harris RB, Oren E. Serologic Evidence for Fecal-Oral Transmission of Helicobacter pylori. *Am J Trop Med Hyg* 2016; **94**: 82-88 [PMID: 26598563 DOI: 10.4269/ajtmh.15-0297]

11 **Ranjbar R**, Khamesipour F, Jonaidi-Jafari N, Rahimi E. Helicobacter pylori isolated from Iranian drinking water: vacA, cagA, iceA, oipA and babA2 genotype status and antimicrobial resistance properties. *FEBS Open Bio* 2016; **6**: 433-441 [PMID: 27419049 DOI: 10.1002/2211-5463.12054]

12 **Talaei R**, Souod N, Momtaz H, Dabiri H. Milk of livestock as a possible transmission route of Helicobacter pylori infection. *Gastroenterol Hepatol Bed Bench* 2015; **8**: S30-S36 [PMID: 26171135]

13 **Graham DY**, Malaty HM, Evans DG, Evans DJ, Klein PD, Adam E. Epidemiology of Helicobacter pylori in an asymptomatic population in the United States. Effect of age, race, and socioeconomic status. *Gastroenterology* 1991; **100**: 1495-1501 [PMID: 2019355]

14 **Rowland M**, Daly L, Vaughan M, Higgins A, Bourke B, Drumm B. Age-specific incidence of Helicobacter pylori. *Gastroenterology* 2006; **130**: 65-72; quiz 211 [PMID: 16401469 DOI: 10.1016/S0016-5107(99)70352-4]

15 **Kodaman N**, Pazos A, Schneider BG, Piazuelo MB, Mera R, Sobota RS, Sicinschi LA, Shaffer CL, Romero-Gallo J, de Sablet T, Harder RH, Bravo LE, Peek RM, Wilson KT, Cover TL, Williams SM, Correa P. Human and Helicobacter pylori coevolution shapes the risk of gastric disease. *Proc Natl Acad Sci USA* 2014; **111**: 1455-1460 [PMID: 24474772 DOI: 10.1073/pnas.1318093111]

16 **Yamaoka Y**. Mechanisms of disease: Helicobacter pylori virulence factors. *Nat Rev Gastroenterol Hepatol* 2010; **7**: 629-641 [PMID: 20938460 DOI: 10.1038/nrgastro.2010.154]

17 **Borén T**, Falk P, Roth KA, Larson G, Normark S. Attachment of Helicobacter pylori to human gastric epithelium mediated by blood group antigens. *Science* 1993; **262**: 1892-1895 [PMID: 8018146 DOI: 10.1126/science.8018146]

18 **Mahdavi J**, Sondén B, Hurtig M, Olfat FO, Forsberg L, Roche N, Angstrom J, Larsson T, Teneberg S, Karlsson KA, Altraja S, Wadström T, Kersulyte D, Berg DE, Dubois A, Petersson C, Magnusson KE, Norberg T, Lindh F, Lundskog BB, Arnqvist A, Hammarström L, Borén T. Helicobacter pylori SabA adhesin in persistent infection and chronic inflammation. *Science* 2002; **297**: 573-578 [PMID: 12142529 DOI: 10.1126/science.1069076]

19 **Yamaoka Y**, Kwon DH, Graham DY. A M(r) 34,000 proinflammatory outer membrane protein (oipA) of Helicobacter pylori. *Proc Natl Acad Sci USA* 2000; **97**: 7533-7538 [PMID: 10852959 DOI: 10.1073/pnas.130079797]

20 **Alm RA**, Bina J, Andrews BM, Doig P, Hancock RE, Trust TJ. Comparative genomics of Helicobacter pylori: analysis of the outer membrane protein families. *Infect Immun* 2000; **68**: 4155-4168 [PMID: 10858232 DOI: 10.1128/IAI.68.7.4155-4168.2000]

21 **Yamaoka Y**. Roles of Helicobacter pylori BabA in gastroduodenal pathogenesis. *World J Gastroenterol* 2008; **14**: 4265-4272 [PMID: 18666312 DOI: 10.3748/wjg.14.4265]

22 **Moore ME**, Borén T, Solnick JV. Life at the margins: modulation of attachment proteins in Helicobacter pylori. *Gut Microbes* 2011; **2**: 42-46 [PMID: 21637017 DOI: 10.4161/gmic.2.1.14626]

23 **Odenbreit S**, Till M, Hofreuter D, Faller G, Haas R. Genetic and functional characterization of the alpAB gene locus essential for

the adhesion of Helicobacter pylori to human gastric tissue. *Mol Microbiol* 1999; **31**: 1537-1548 [PMID: 10200971 DOI: 10.1046/j.1365-2958.1999.01300.x]
24 **Peck B**, Ortkamp M, Diehl KD, Hundt E, Knapp B. Conservation, localization and expression of HopZ, a protein involved in adhesion of Helicobacter pylori. *Nucleic Acids Res* 1999; **27**: 3325-3333 [PMID: 10454640]
25 **Ilver D**, Arnqvist A, Ogren J, Frick IM, Kersulyte D, Incecik ET, Berg DE, Covacci A, Engstrand L, Borén T. Helicobacter pylori adhesin binding fucosylated histo-blood group antigens revealed by retagging. *Science* 1998; **279**: 373-377 [PMID: 9430586 DOI: 10.1126/science.279.5349.373]
26 **Pride DT**, Blaser MJ. Concerted evolution between duplicated genetic elements in Helicobacter pylori. *J Mol Biol* 2002; **316**: 629-642 [PMID: 11866522 DOI: 10.1006/jmbi.2001.5311]
27 **Pride DT**, Meinersmann RJ, Blaser MJ. Allelic Variation within Helicobacter pylori babA and babB. *Infect Immun* 2001; **69**: 1160-1171 [PMID: 11160014 DOI: 10.1128/IAI.69.2.1160-1171.2001]
28 **Matteo MJ**, Armitano RI, Romeo M, Wonaga A, Olmos M, Catalano M. Helicobacter pylori bab genes during chronic colonization. *Int J Mol Epidemiol Genet* 2011; **2**: 286-291 [PMID: 21915366]
29 **Hennig EE**, Allen JM, Cover TL. Multiple chromosomal loci for the babA gene in Helicobacter pylori. *Infect Immun* 2006; **74**: 3046-3051 [PMID: 16622249 DOI: 10.1128/IAI.74.5.3046-3051.2006]
30 **Colbeck JC**, Hansen LM, Fong JM, Solnick JV. Genotypic profile of the outer membrane proteins BabA and BabB in clinical isolates of Helicobacter pylori. *Infect Immun* 2006; **74**: 4375-4378 [PMID: 16790815 DOI: 10.1128/IAI.00485-06]
31 National Center for Biotechnology Information (NCBI): Helicobacter pylori. Available from: URL: https://www.ncbi.nlm.nih.gov/genome/genomes/169
32 **Kim A**, Servetas SL, Kang J, Kim J, Jang S, Cha HJ, Lee WJ, Kim J, Romero-Gallo J, Peek RM, Merrell DS, Cha JH. Helicobacter pylori bab Paralog Distribution and Association with cagA, vacA, and homA/B Genotypes in American and South Korean Clinical Isolates. *PLoS One* 2015; **10**: e0137078 [PMID: 26317221 DOI: 10.1371/journal.pone.0137078]
33 **Hennig EE**, Mernaugh R, Edl J, Cao P, Cover TL. Heterogeneity among Helicobacter pylori strains in expression of the outer membrane protein BabA. *Infect Immun* 2004; **72**: 3429-3435 [PMID: 15155649 DOI: 10.1128/IAI.72.6.3429-3435.2004]
34 **Bäckström A**, Lundberg C, Kersulyte D, Berg DE, Borén T, Arnqvist A. Metastability of Helicobacter pylori bab adhesin genes and dynamics in Lewis b antigen binding. *Proc Natl Acad Sci USA* 2004; **101**: 16923-16928 [PMID: 15557006 DOI: 10.1073/pnas.0404817101]
35 **Goodwin AC**, Weinberger DM, Ford CB, Nelson JC, Snider JD, Hall JD, Paules CI, Peek RM, Forsyth MH. Expression of the Helicobacter pylori adhesin SabA is controlled via phase variation and the ArsRS signal transduction system. *Microbiology* 2008; **154**: 2231-2240 [PMID: 18667556 DOI: 10.1099/mic.0.2007/016055-0]
36 **Kao CY**, Sheu SM, Sheu BS, Wu JJ. Length of thymidine homopolymeric repeats modulates promoter activity of sabA in Helicobacter pylori. *Helicobacter* 2012; **17**: 203-209 [PMID: 22515358 DOI: 10.1111/j.1523-5378.2012.00936.x]
37 **Åberg A**, Gideonsson P, Vallström A, Olofsson A, Öhman C, Rakhimova L, Borén T, Engstrand L, Brännström K, Arnqvist A. A repetitive DNA element regulates expression of the Helicobacter pylori sialic acid binding adhesin by a rheostat-like mechanism. *PLoS Pathog* 2014; **10**: e1004234 [PMID: 24991812 DOI: 10.1371/journal.ppat.1004234]
38 **Zhou K**, Aertsen A, Michiels CW. The role of variable DNA tandem repeats in bacterial adaptation. *FEMS Microbiol Rev* 2014; **38**: 119-141 [PMID: 23927439 DOI: 10.1111/1574-6976.12036]
39 **Styer CM**, Hansen LM, Cooke CL, Gundersen AM, Choi SS, Berg DE, Benghezal M, Marshall BJ, Peek RM, Borén T, Solnick JV. Expression of the BabA adhesin during experimental infection with Helicobacter pylori. *Infect Immun* 2010; **78**: 1593-1600 [PMID: 20123715 DOI: 10.1128/IAI.01297-09]
40 **Nell S**, Kennemann L, Schwarz S, Josenhans C, Suerbaum S. Dynamics of Lewis b binding and sequence variation of the babA adhesin gene during chronic Helicobacter pylori infection in humans. *MBio* 2014; **5**: pii: e02281-14 [PMID: 25516619 DOI: 10.1128/mBio.02281-14]
41 **Gerhard M**, Lehn N, Neumayer N, Borén T, Rad R, Schepp W, Miehlke S, Classen M, Prinz C. Clinical relevance of the Helicobacter pylori gene for blood-group antigen-binding adhesin. *Proc Natl Acad Sci USA* 1999; **96**: 12778-12783 [PMID: 10535999 DOI: 10.1073/pnas.96.22.12778]
42 **Saberi S**, Schmidt A, Eybpoosh S, Esmaili M, Talebkhan Y, Mohajerani N, Oghalaie A, Eshagh Hosseini M, Mohagheghi MA, Bugaytova J, Borén T, Mohammadi M. Helicobacter pylori Strains from Duodenal Ulcer Patients Exhibit Mixed babA/B Genotypes with Low Levels of BabA Adhesin and Lewis b Binding. *Dig Dis Sci* 2016; **61**: 2868-2877 [PMID: 27318698 DOI: 10.1007/s10620-016-4217-z]
43 **Abdullah SM**, Hussein NR, Salih AM, Merza MA, Goreal AA, Odeesh OY, Majed HS, Assafi MA, Hawrami K. Infection with Helicobacter pylori strains carrying babA2 and cagA is associated with an increased risk of peptic ulcer disease development in Iraq. *Arab J Gastroenterol* 2012; **13**: 166-169 [PMID: 23432983 DOI: 10.1016/j.ajg.2012.12.001]
44 **Karabiber H**, Selimoglu MA, Otlu B, Yildirim O, Ozer A. Virulence factors and antibiotic resistance in children with Helicobacter pylori gastritis. *J Pediatr Gastroenterol Nutr* 2014; **58**: 608-612 [PMID: 24792628 DOI: 10.1097/MPG.0000000000000273]
45 **Talebi Bezmin Abadi A**, Taghvaei T, Mohabbati Mobarez A, Vaira G, Vaira D. High correlation of babA 2-positive strains of Helicobacter pylori with the presence of gastric cancer. *Intern Emerg Med* 2013; **8**: 497-501 [PMID: 21604199 DOI: 10.1007/s11739-011-0631-6]
46 **Yadegar A**, Mobarez AM, Alebouyeh M, Mirzaei T, Kwok T, Zali MR. Clinical relevance of cagL gene and virulence genotypes with disease outcomes in a Helicobacter pylori infected population from Iran. *World J Microbiol Biotechnol* 2014; **30**: 2481-2490 [PMID: 24854336 DOI: 10.1007/s11274-014-1673-5]
47 **Osman HA**, Hasan H, Suppian R, Hassan S, Andee DZ, Abdul Majid N, Zilfalil BA. Prevalence of Helicobacter pylori cagA, babA2, and dupA genotypes and correlation with clinical outcome in Malaysian patients with dyspepsia. *Turk J Med Sci* 2015; **45**: 940-946 [PMID: 26422871 DOI: 10.3906/sag-1409-77]
48 **Boonyanugomol W**, Chomvarin C, Sripa B, Chau-In S, Pugkhem A, Namwat W, Wongboot W, Khampoosa B. Molecular analysis of Helicobacter pylori virulent-associated genes in hepatobiliary patients. *HPB* (Oxford) 2012; **14**: 754-763 [PMID: 23043664 DOI: 10.1111/j.1477-2574.2012.00533.x]
49 **Chomvarin C**, Namwat W, Chaicumpar K, Mairiang P, Sangchan A, Sripa B, Tor-Udom S, Vilaichone RK. Prevalence of Helicobacter pylori vacA, cagA, cagE, iceA and babA2 genotypes in Thai dyspeptic patients. *Int J Infect Dis* 2008; **12**: 30-36 [PMID: 17548220 DOI: 10.1016/j.ijid.2007.03.012]
50 **Ghosh P**, Sarkar A, Ganguly M, Raghwan J, De R, Mukhopadhyay AK. Helicobacter pylori strains harboring babA2 from Indian sub population are associated with increased virulence in ex vivo study. *Gut Pathog* 2016; **8**: 1 [PMID: 26759607 DOI: 10.1186/s13099-015-0083-z]
51 **Con SA**, Takeuchi H, Nishioka M, Morimoto N, Sugiura T, Yasuda N, Con-Wong R. Clinical relevance of Helicobacter pylori babA2 and babA2/B in Costa Rica and Japan. *World J Gastroenterol* 2010; **16**: 474-478 [PMID: 20101774 DOI: 10.3748/wjg.v16.i4.474]
52 **Fujimoto S**, Olaniyi Ojo O, Arnqvist A, Wu JY, Odenbreit S, Haas R, Graham DY, Yamaoka Y. Helicobacter pylori BabA expression, gastric mucosal injury, and clinical outcome. *Clin Gastroenterol Hepatol* 2007; **5**: 49-58 [PMID: 17157077 DOI: 10.1016/j.cgh.2006.09.015]
53 **Biernat MM**, Gościniak G, Iwańczak B. Prevalence of

Helicobacter pylori cagA, vacA, iceA, babA2 genotypes in Polish children and adolescents with gastroduodenal disease. *Postepy Hig Med Dosw* (Online) 2014; **68**: 1015-1021 [PMID: 25228509 DOI: 10.5604/17322693.1118211]

54 **Homan M**, Šterbenc A, Kocjan BJ, Luzar B, Zidar N, Orel R, Poljak M. Prevalence of the Helicobacter pylori babA2 gene and correlation with the degree of gastritis in infected Slovenian children. *Antonie Van Leeuwenhoek* 2014; **106**: 637-645 [PMID: 25055876 DOI: 10.1007/s10482-014-0234-0]

55 **Boyanova L**, Yordanov D, Gergova G, Markovska R, Mitov I. Association of iceA and babA genotypes in Helicobacter pylori strains with patient and strain characteristics. *Antonie Van Leeuwenhoek* 2010; **98**: 343-350 [PMID: 20454856 DOI: 10.1007/s10482-010-9448-y]

56 **Odenbreit S**. Adherence properties of Helicobacter pylori: impact on pathogenesis and adaptation to the host. *Int J Med Microbiol* 2005; **295**: 317-324 [PMID: 16173498 DOI: 10.1016/j.ijmm.2005.06.003]

57 **Rhen M**, Eriksson S, Clements M, Bergström S, Normark SJ. The basis of persistent bacterial infections. *Trends Microbiol* 2003; **11**: 80-86 [PMID: 12598130 DOI: 10.1016/S0966-842X(02)00038-0]

58 **Aspholm M**, Kalia A, Ruhl S, Schedin S, Arnqvist A, Lindén S, Sjöström R, Gerhard M, Semino-Mora C, Dubois A, Unemo M, Danielsson D, Teneberg S, Lee WK, Berg DE, Borén T. Helicobacter pylori adhesion to carbohydrates. *Methods Enzymol* 2006; **417**: 293-339 [PMID: 17132512 DOI: 10.1016/S0076-6879(06)17020-2]

59 **Walz A**, Odenbreit S, Stühler K, Wattenberg A, Meyer HE, Mahdavi J, Borén T, Ruhl S. Identification of glycoprotein receptors within the human salivary proteome for the lectin-like BabA and SabA adhesins of Helicobacter pylori by fluorescence-based 2-D bacterial overlay. *Proteomics* 2009; **9**: 1582-1592 [PMID: 19253298 DOI: 10.1002/pmic.200700808]

60 **Prakobphol A**, Borén T, Ma W, Zhixiang P, Fisher SJ. Highly glycosylated human salivary molecules present oligosaccharides that mediate adhesion of leukocytes and Helicobacter pylori. *Biochemistry* 2005; **44**: 2216-2224 [PMID: 15697247 DOI: 10.1021/bi0480180]

61 **Prakobphol A**, Xu F, Hoang VM, Larsson T, Bergstrom J, Johansson I, Frängsmyr L, Holmskov U, Leffler H, Nilsson C, Borén T, Wright JR, Strömberg N, Fisher SJ. Salivary agglutinin, which binds Streptococcus mutans and Helicobacter pylori, is the lung scavenger receptor cysteine-rich protein gp-340. *J Biol Chem* 2000; **275**: 39860-39866 [PMID: 11007786 DOI: 10.1074/jbc.M006928200]

62 **Royle L**, Roos A, Harvey DJ, Wormald MR, van Gijlswijk-Janssen D, Redwan el-RM, Wilson IA, Daha MR, Dwek RA, Rudd PM. Secretory IgA N- and O-glycans provide a link between the innate and adaptive immune systems. *J Biol Chem* 2003; **278**: 20140-20153 [PMID: 12637583 DOI: 10.1074/jbc.M301436200]

63 **Issa S**, Moran AP, Ustinov SN, Lin JH, Ligtenberg AJ, Karlsson NG. O-linked oligosaccharides from salivary agglutinin: Helicobacter pylori binding sialyl-Lewis x and Lewis b are terminating moieties on hyperfucosylated oligo-N-acetyllactosamine. *Glycobiology* 2010; **20**: 1046-1057 [PMID: 20466654 DOI: 10.1093/glycob/cwq066]

64 **McGuckin MA**, Lindén SK, Sutton P, Florin TH. Mucin dynamics and enteric pathogens. *Nat Rev Microbiol* 2011; **9**: 265-278 [PMID: 21407243 DOI: 10.1038/nrmicro2538]

65 **Aspholm-Hurtig M**, Dailide G, Lahmann M, Kalia A, Ilver D, Roche N, Vikström S, Sjöström R, Lindén S, Bäckström A, Lundberg C, Arnqvist A, Mahdavi J, Nilsson UJ, Velapatiño B, Gilman RH, Gerhard M, Alarcon T, López-Brea M, Nakazawa T, Fox JG, Correa P, Dominguez-Bello MG, Perez-Perez GI, Blaser MJ, Normark S, Carlstedt I, Oscarson S, Teneberg S, Berg DE, Borén T. Functional adaptation of BabA, the H. pylori ABO blood group antigen binding adhesin. *Science* 2004; **305**: 519-522 [PMID: 15273394 DOI: 10.1126/science.1098801]

66 **Hage N**, Howard T, Phillips C, Brassington C, Overman R, Debreczeni J, Gellert P, Stolnik S, Winkler GS, Falcone FH. Structural basis of Lewis(b) antigen binding by the Helicobacter pylori adhesin BabA. *Sci Adv* 2015; **1**: e1500315 [PMID: 26601230 DOI: 10.1126/sciadv.1500315]

67 **Sakamoto S**, Watanabe T, Tokumaru T, Takagi H, Nakazato H, Lloyd KO. Expression of Lewisa, Lewisb, Lewisx, Lewisy, siayl-Lewisa, and sialyl-Lewisx blood group antigens in human gastric carcinoma and in normal gastric tissue. *Cancer Res* 1989; **49**: 745-752 [PMID: 2910493]

68 **Lindén S**, Mahdavi J, Hedenbro J, Borén T, Carlstedt I. Effects of pH on Helicobacter pylori binding to human gastric mucins: identification of binding to non-MUC5AC mucins. *Biochem J* 2004; **384**: 263-270 [PMID: 15260802 DOI: 10.1042/BJ20040402]

69 **Kenny DT**, Skoog EC, Lindén SK, Struwe WB, Rudd PM, Karlsson NG. Presence of terminal N-acetylgalactosamineβ1-4N-acetylglucosamine residues on O-linked oligosaccharides from gastric MUC5AC: involvement in Helicobacter pylori colonization? *Glycobiology* 2012; **22**: 1077-1085 [PMID: 22543025 DOI: 10.1093/glycob/cws076]

70 **Magalhães A**, Rossez Y, Robbe-Masselot C, Maes E, Gomes J, Shevtsova A, Bugaytsova J, Borén T, Reis CA. Muc5ac gastric mucin glycosylation is shaped by FUT2 activity and functionally impacts Helicobacter pylori binding. *Sci Rep* 2016; **6**: 25575 [PMID: 27161092 DOI: 10.1038/srep25575]

71 **Lindén SK**, Sheng YH, Every AL, Miles KM, Skoog EC, Florin TH, Sutton P, McGuckin MA. MUC1 limits Helicobacter pylori infection both by steric hindrance and by acting as a releasable decoy. *PLoS Pathog* 2009; **5**: e1000617 [PMID: 19816567 DOI: 10.1371/journal.ppat.1000617]

72 **Cohen M**, Drut R, Cueto Rúa E. SIALYL-Tn antigen distribution in Helicobacter pylori chronic gastritis in children: an immunohistochemical study. *Pediatr Pathol Mol Med* 2003; **22**: 117-129 [PMID: 12556292 DOI: 10.1080/pdp.22.2.117.129]

73 **Lindén S**, Semino-Mora C, Liu H, Rick J, Dubois A. Role of mucin Lewis status in resistance to Helicobacter pylori infection in pediatric patients. *Helicobacter* 2010; **15**: 251-258 [PMID: 20633185 DOI: 10.1111/j.1523-5378.2010.00765.x]

74 **Lindén S**, Mahdavi J, Semino-Mora C, Olsen C, Carlstedt I, Borén T, Dubois A. Role of ABO secretor status in mucosal innate immunity and H. pylori infection. *PLoS Pathog* 2008; **4**: e2 [PMID: 18179282 DOI: 10.1371/journal.ppat.0040002]

75 **Moonens K**, Gideonsson P, Subedi S, Bugaytsova J, Romaõ E, Mendez M, Nordén J, Fallah M, Rakhimova L, Shevtsova A, Lahmann M, Castaldo G, Brännström K, Coppens F, Lo AW, Ny T, Solnick JV, Vandenbussche G, Oscarson S, Hammarström L, Arnqvist A, Berg DE, Muyldermans S, Borén T, Remaut H. Structural Insights into Polymorphic ABO Glycan Binding by Helicobacter pylori. *Cell Host Microbe* 2016; **19**: 55-66 [PMID: 26764597 DOI: 10.1016/j.chom.2015.12.004]

76 **Van de Bovenkamp JH**, Mahdavi J, Korteland-Van Male AM, Büller HA, Einerhand AW, Borén T, Dekker J. The MUC5AC glycoprotein is the primary receptor for Helicobacter pylori in the human stomach. *Helicobacter* 2003; **8**: 521-532 [PMID: 14535999 DOI: 10.1046/j.1523-5378.2003.00173.x]

77 **Suerbaum S**, Josenhans C. Helicobacter pylori evolution and phenotypic diversification in a changing host. *Nat Rev Microbiol* 2007; **5**: 441-452 [PMID: 17505524 DOI: 10.1038/nrmicro1658]

78 **Borst P**, Greaves DR. Programmed gene rearrangements altering gene expression. *Science* 1987; **235**: 658-667 [PMID: 3544215 DOI: 10.1126/science.3544215]

79 **Dworkin J**, Blaser MJ. Molecular mechanisms of Campylobacter fetus surface layer protein expression. *Mol Microbiol* 1997; **26**: 433-440 [PMID: 9402015 DOI: 10.1046/j.1365-2958.1997.6151958.x]

80 **Suerbaum S**, Smith JM, Bapumia K, Morelli G, Smith NH, Kunstmann E, Dyrek I, Achtman M. Free recombination within Helicobacter pylori. *Proc Natl Acad Sci USA* 1998; **95**: 12619-12624 [PMID: 9770535 DOI: 10.1073/pnas.95.21.12619]

81 **Loughlin MF**, Barnard FM, Jenkins D, Sharples GJ, Jenks PJ. Helicobacter pylori mutants defective in RuvC Holliday junction resolvase display reduced macrophage survival and

spontaneous clearance from the murine gastric mucosa. *Infect Immun* 2003; **71**: 2022-2031 [PMID: 12654822 DOI: 10.1128/IAI.71.4.2022-2031.2003]

82 **Kennemann L**, Didelot X, Aebischer T, Kuhn S, Drescher B, Droege M, Reinhardt R, Correa P, Meyer TF, Josenhans C, Falush D, Suerbaum S. Helicobacter pylori genome evolution during human infection. *Proc Natl Acad Sci USA* 2011; **108**: 5033-5038 [PMID: 21383187 DOI: 10.1073/pnas.1018444108]

83 **Yahara K**, Kawai M, Furuta Y, Takahashi N, Handa N, Tsuru T, Oshima K, Yoshida M, Azuma T, Hattori M, Uchiyama I, Kobayashi I. Genome-wide survey of mutual homologous recombination in a highly sexual bacterial species. *Genome Biol Evol* 2012; **4**: 628-640 [PMID: 22534164 DOI: 10.1093/gbe/evs043]

84 **Solnick JV**, Hansen LM, Salama NR, Boonjakuakul JK, Syvanen M. Modification of Helicobacter pylori outer membrane protein expression during experimental infection of rhesus macaques. *Proc Natl Acad Sci USA* 2004; **101**: 2106-2111 [PMID: 14762173 DOI: 10.1073/pnas.0308573100]

85 **Field D**, Wills C. Abundant microsatellite polymorphism in Saccharomyces cerevisiae, and the different distributions of microsatellites in eight prokaryotes and S. cerevisiae, result from strong mutation pressures and a variety of selective forces. *Proc Natl Acad Sci USA* 1998; **95**: 1647-1652 [PMID: 9465070]

86 **van Belkum A**, Scherer S, van Alphen L, Verbrugh H. Short-sequence DNA repeats in prokaryotic genomes. *Microbiol Mol Biol Rev* 1998; **62**: 275-293 [PMID: 9618442]

87 **Henderson IR**, Owen P, Nataro JP. Molecular switches--the ON and OFF of bacterial phase variation. *Mol Microbiol* 1999; **33**: 919-932 [PMID: 10476027 DOI: 10.1046/j.1365-2958.1999.01555.x]

88 **Levinson G**, Gutman GA. Slipped-strand mispairing: a major mechanism for DNA sequence evolution. *Mol Biol Evol* 1987; **4**: 203-221 [PMID: 3328815]

89 **Kennemann L**, Brenneke B, Andres S, Engstrand L, Meyer TF, Aebischer T, Josenhans C, Suerbaum S. In vivo sequence variation in HopZ, a phase-variable outer membrane protein of Helicobacter pylori. *Infect Immun* 2012; **80**: 4364-4373 [PMID: 23027539 DOI: 10.1128/IAI.00977-12]

90 **Zhang J**, Qian J, Zhang X, Zou Q. Outer membrane inflammatory protein A, a new virulence factor involved in the pathogenesis of Helicobacter pylori. *Mol Biol Rep* 2014; **41**: 7807-7814 [PMID: 25096514 DOI: 10.1007/s11033-014-3673-9]

91 **Myers P**. Tandem repeats and morphological variation. *Nature Education* 2007; **1**: 1 Available from URL: http://www.nature.com/scitable/topicpage/tandem-repeats-and-morphological-variation-40690

92 **de Vries N**, Duinsbergen D, Kuipers EJ, Pot RG, Wiesenekker P, Penn CW, van Vliet AH, Vandenbroucke-Grauls CM, Kusters JG. Transcriptional phase variation of a type III restriction-modification system in Helicobacter pylori. *J Bacteriol* 2002; **184**: 6615-6623 [PMID: 12426350 DOI: 10.1128/JB.184.23.6615-6624.2002]

93 **van der Woude MW**, Bäumler AJ. Phase and antigenic variation in bacteria. *Clin Microbiol Rev* 2004; **17**: 581-611, table of contents [PMID: 15258095 DOI: 10.1128/CMR.17.3.581-611.2004]

94 **Toller IM**, Neelsen KJ, Steger M, Hartung ML, Hottiger MO, Stucki M, Kalali B, Gerhard M, Sartori AA, Lopes M, Müller A. Carcinogenic bacterial pathogen Helicobacter pylori triggers DNA double-strand breaks and a DNA damage response in its host cells. *Proc Natl Acad Sci USA* 2011; **108**: 14944-14949 [PMID: 21896770 DOI: 10.1073/pnas.1100959108]

95 **Azevedo M**, Eriksson S, Mendes N, Serpa J, Figueiredo C, Resende LP, Ruvoën-Clouet N, Haas R, Borén T, Le Pendu J, David L. Infection by Helicobacter pylori expressing the BabA adhesin is influenced by the secretor phenotype. *J Pathol* 2008; **215**: 308-316 [PMID: 18498114 DOI: 10.1002/path.2363]

96 **Olfat FO**, Zheng Q, Oleastro M, Voland P, Borén T, Karttunen R, Engstrand L, Rad R, Prinz C, Gerhard M. Correlation of the Helicobacter pylori adherence factor BabA with duodenal ulcer disease in four European countries. *FEMS Immunol Med Microbiol* 2005; **44**: 151-156 [PMID: 15866209 DOI: 10.1016/j.femsim.2004.10.010]

97 **Sheu BS**, Sheu SM, Yang HB, Huang AH, Wu JJ. Host gastric Lewis expression determines the bacterial density of Helicobacter pylori in babA2 genopositive infection. *Gut* 2003; **52**: 927-932 [PMID: 12801945 DOI: 10.1136/gut.52.7.927]

98 **Mizushima T**, Sugiyama T, Komatsu Y, Ishizuka J, Kato M, Asaka M. Clinical relevance of the babA2 genotype of Helicobacter pylori in Japanese clinical isolates. *J Clin Microbiol* 2001; **39**: 2463-2465 [PMID: 11427555 DOI: 10.1128/JCM.39.7.2463-2465.2001]

99 **Oleastro M**, Cordeiro R, Yamaoka Y, Queiroz D, Mégraud F, Monteiro L, Ménard A. Disease association with two Helicobacter pylori duplicate outer membrane protein genes, homB and homA. *Gut Pathog* 2009; **1**: 12 [PMID: 19545429 DOI: 10.1186/1757-4749-1-12]

100 **Ishijima N**, Suzuki M, Ashida H, Ichikawa Y, Kanegae Y, Saito I, Borén T, Haas R, Sasakawa C, Mimuro H. BabA-mediated adherence is a potentiator of the Helicobacter pylori type IV secretion system activity. *J Biol Chem* 2011; **286**: 25256-25264 [PMID: 21596743 DOI: 10.1074/jbc.M111.233601]

101 **Rad R**, Gerhard M, Lang R, Schöniger M, Rösch T, Schepp W, Becker I, Wagner H, Prinz C. The Helicobacter pylori blood group antigen-binding adhesin facilitates bacterial colonization and augments a nonspecific immune response. *J Immunol* 2002; **168**: 3033-3041 [PMID: 11884476 DOI: 10.4049/jimmunol.168.6.3033]

P- Reviewer: Kuo FC, Safaei HG, Yamaoka Y **S- Editor**: Qi Y
L- Editor: A **E- Editor**: Zhang FF

World Journal of Gastroenterology

Submit a Manuscript: http://www.f6publishing.com

World J Gastroenterol 2017 June 21; 23(23): 4170-4180

DOI: 10.3748/wjg.v23.i23.4170

ISSN 1007-9327 (print) ISSN 2219-2840 (online)

MINIREVIEWS

Advances in surgical management for locally recurrent rectal cancer: How far have we come?

Daniel Jin-Keat Lee, Peter M Sagar, Gaitri Sadadcharam, Kok-Yang Tan

Daniel Jin-Keat Lee, Gaitri Sadadcharam, Kok-Yang Tan, Department of Surgery, Khoo Teck Puat Hospital, Singapore 768828, Singapore

Peter M Sagar, John Goligher Colorectal Surgery Unit, St James's University Hospital, Beckett Street, Leeds LS9 7TF, United Kingdom

Author contributions: Lee DJK performed the majority of the research around this topic, wrote the manuscript and obtained figures for the article; Sagar PM and Tan KY designed the article framework and contributed to the editing of the manuscript; Sadadcharam G contributed to the editing of the article as well as some of the writing.

Conflict-of-interest statement: Authors declare no conflict of interests for this article.

Manuscript source: Invited manuscript

Correspondence to: Dr. Kok-Yang Tan, Associate Professor, Head and Senior Consultant, Department of Surgery, Khoo Teck Puat Hospital, 90 Yishun Central, Singapore 768828, Singapore. tan.kok.yang@alexandrahealth.com.sg
Telephone: +65-6602-2207
Fax: +65-6602-3648

Received: January 27, 2017
Peer-review started: February 4, 2017
First decision: February 23, 2017
Revised: March 31, 2017
Accepted: May 9, 2017
Article in press: May 9, 2017
Published online: June 21, 2017

Abstract

Locally recurrent rectal cancer (LRRC) is a complex disease with far-reaching implications for the patient. Until recently, research was limited regarding surgical techniques that can increase the ability to perform an *en bloc* resection with negative margins. This has changed in recent years and therefore outcomes for these patients have improved. Novel radical techniques and adjuncts allow for more radical resections thereby improving the chance of negative resection margins and outcomes. In the past contraindications to surgery included anterior involvement of the pubic bone, sacral invasions above the level of S2/S3 and lateral pelvic wall involvement. However, current data suggests that previously unresectable cases may now be feasible with novel techniques, surgical approaches and reconstructive surgery. The publications to date have only reported small patient pools with the research conducted by highly specialised units. Moreover, the short and long-term oncological outcomes are currently under review. Therefore although surgical options for LRRC have expanded significantly, one should balance the treatment choices available against the morbidity associated with the procedure and select the right patient for it.

Key words: Recurrent rectal cancer; Sacrectomy; Pelvic exenteration; Pelvic sidewall; Radical resection

Core tip: This article provides an up-to-date review of the current international trends in surgical approaches for locally recurrent rectal cancer (LRRC), specifically highlighting the novel radical techniques that are now used in cases previously deemed unresectable. We have described these approaches according to anatomical locations of the recurrences and reviewed the respective oncological and functional outcomes. In

addition, laparoscopic surgeries for LRRC are discussed and their outcomes are outlined.

Lee DJK, Sagar PM, Sadadcharam G, Tan KY. Advances in surgical management for locally recurrent rectal cancer: How far have we come? *World J Gastroenterol* 2017; 23(23): 4170-4180 Available from: URL: http://www.wjgnet.com/1007-9327/full/v23/i23/4170.htm DOI: http://dx.doi.org/10.3748/wjg.v23.i23.4170

INTRODUCTION

The incidence of locally recurrent rectal cancer (LRRC) has undergone a dramatic decline since the application of total mesorectal excision and addition of preoperative radiotherapy[1-4]. Current studies have reported 5-year recurrence rates of between 5%-10% as compared to previously published figures of 20%-30%[5-7]. The majority of these recurrences occur within the first 2 years after surgery[8,9]. Without subsequent treatment these patients have an extremely poor prognosis. A recurrence has the capacity to significantly reduce a patient's quality of life by causing refractory pain as well as potentially resulting in a malodorous, fungating or fistulating mass. Non-operative approaches such as radiotherapy or chemoradiotherapy have been shown to offer little symptomatic relief, or survival benefit, and are often associated with significant side-effects[10-12]. Surgery offers the best hope in providing improved survival rates or as the best form of palliation.

In order to achieve clear resection margins radical surgery for pelvic recurrences often requires extended resection involving at least one organ that is adjacent to or involved by the tumour. Due to the morbidity associated with these procedures, LRRC cases previously received scant attention from the surgical world, except for a couple of notable exceptions[13,14]. Consequently, patients would often resort to palliative care either *via* systemic chemotherapy or a few boosts of radiotherapy. Since then, more specialised centres have taken the effort to provide and refine the provision of radical surgery for this condition. These together with improvements in perioperative intervention, extended resection or exenterative surgeries are now accepted management options in order to achieve a cure[15]. Results from several of these centres have demonstrated a 5-year survival rate of 35% to 50% after surgery for LRRC[16].

It should be noted that the surgical approach during resection of LRRC depends on the site of recurrence. There is significant variation in both techniques and outcomes. Although there is no standard classification system for recurrent rectal cancer, the general consensus amongst colorectal cancer surgeons generally describes a pattern of pelvic invasion based on the anatomic region of the pelvis involved with the disease (Figure 1). (1) Central: Tumour is localised to pelvic organ(s) and adjacent soft tissue structures without adherence to bone; (2) Sacral: Tumour presents in the presacral space and abuts or invades the sacrum or coccyx; and (3) Lateral pelvic sidewall: Tumour involves the soft tissue and structures of the pelvic sidewall (iliac vessels, lateral pelvic lymph nodes, pelvic ureters, pelvic nerves, sidewall musculature) and lateral bony pelvis.

Central recurrences have the most favourable prognosis as these recurrences have the highest chance of achieving clear margin resections[17,18]. If the recurrence has spread beyond the soft tissue structures and becomes adherent to or invades into the bony structures (sacrum, ischium, pubic ramus) or extends into the pelvic sidewall structures then en bloc resection becomes more challenging.

In recent times, there has been a steady increase in the number of centres worldwide having vested interest in LRRC. These centres are exploring new techniques in order to improve the likelihood of adequate oncological resection. Due to this peaked interest in LRRC, previously deemed contraindications[19] (Table 1) are now proven by certain specialized centres to be feasible and safe for so called "ultra-radical resection[15]". In addition, improved reconstructive techniques allow for better functional outcomes. Therefore the surgical approach to LRRC is currently limited by the surgeon's ability to achieve R0 resection margins with acceptable morbidity, and the patient's fitness for surgery. This review aims to present an update on the current international trends in surgical approaches as well as to assess the outcome and/or success of such radical procedure with emphasis on ultra-radical resections.

PREOPERATIVE IMAGING

Surgical planning includes preoperative review of imaging by a specialized multidisciplinary team. The roles of preoperative imaging are three-fold: (1) to exclude metastatic disease; (2) to determine resectability of the tumour; and (3) to guide in surgical planning particularly on the extent of margin resection. The metastatic work-up includes dedicated computed tomography (CT) scan of the chest, abdomen and pelvis, and more recently positron emission tomography (PET) scan. PET/CT can be used also to assess for uptake in areas of concern especially in cases of equivocal recurrence. Next, magnetic resonance (MR) imaging is used to assess resectability of the tumour, owing to its excellent delineation of soft tissue structures. It serves as a road map for the surgical procedure and increases the chances of margin clearance. The extent of resection is decided on the basis of organs, pelvic sidewall, and pelvic floor involvement, which MR imaging has been shown to accurately demonstrate[20,21]. The primary challenge

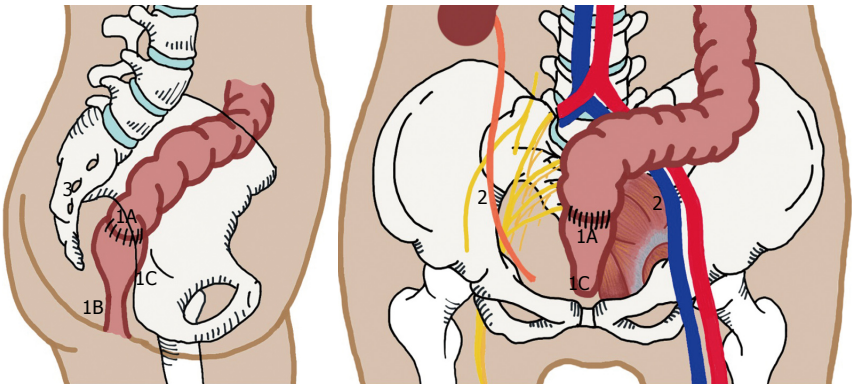

Figure 1 Patterns of pelvic recurrence. 1: Central; 1A: Anastomotic site; 1B: Perineal region, seen after abdominal perineal resection; 1C: Invasion to adjacent soft tissue involving genitourinary organs, or to pubic bone; 2: Lateral Pelvic Side Wall; 3: Posterior/Sacral Recurrence.

Table 1 Conditions previously deemed contraindication to surgery for recurrent rectal cancer

Distant metastases
Stage Ⅳ primary disease
Sacral invasion above S2-S3
Diffuse/circumferential pelvic sidewall involvement resulting in hydronephrosis
Encasement (> 180°)of external iliac vessels
Invasion to anterior pubic bone
Extension of tumour through the sciatic notch

would be to distinguish between fibrotic tissues from actual tumour invasion, particularly at the pelvic sidewalls. PET/MR hybrid, which is not widely available yet, is likely to be the modality of choice in future as it has been shown to improve interpretation of the radiologists in detecting bladder or pelvic sidewall invasion in gynaecologic malignancy[22].

MULTIMODALITY TREATMENT APPROACH

In general, cases of LRRC are discussed in a multi-disciplinary team (MDT) meeting which consists of surgeons, radiation oncologists, medical oncologists, pathologists, and radiologists. The important key aspects discussed are: the likelihood of obtaining R0 resection; the need for neoadjuvant therapies, and the appropriate approaches. In resectable, isolated local disease with previous history of pelvic radiotherapy, it is recommended to proceed straight to surgery. In radiotherapy naïve patients, one should consider preoperative chemoradiation and subsequently proceed with surgery 6-wk following completion of preoperative chemoradiation to allow maximum tumour response.

About 50% of patients with LRRC have synchronous distant disease[23], but this does not necessarily preclude surgical intervention. As experience has grown with the management of metastasectomy in primary disease, curative surgeries are increasingly being offered to recurrent cases. Hartley *et al*[24] reported on the outcome in a series of 42 patients with LRRC and synchronous resectable metastasis. Thirteen (13) patients had synchronous resection, and 9 patients had staged resection, resulting in a total of 22 patients rendered disease free (R0). When R0 is achieved (52% of patients), the median survival is 23 mo, compared to 7-mo in the non-RO group. One must take note that such benefits may be seen only in highly selected patients. The optimal sequence of surgery in the setting of resectable metastasis and LRRC remains to be clarified.

The use of preoperative chemoradiotherapy (CRT) for treatment of LRRC has been extrapolated from benefits seen in locally advanced primary rectal cancer. However, there is still a lack of good data in the literature, in particular there is a lack of prospective randomised trials, that justify the benefit of preoperative CRT. Yu *et al*[25] compared radiological response in patients with primary rectal cancer and recurrent rectal cancer after neoadjuvant CRT. Interestingly, their study showed that recurrent rectal cancer is 2.4 times less likely to show a > 50% reduction in tumour size following CRT. They concluded that recurrent rectal cancers appear to be relatively radioresistant compared with primary rectal cancer. The limited response may be due to the use of conventional dosages and methods of delivery *via* external beam radiotherapy. Recent advances in this aspect is seen in the development of more conformal radiotherapy techniques, such as intensity-modulated radiotherapy (IMRT) or intraoperative brachytherapy (IORT), which aims to deliver more targeted and higher dosage radiotherapy[26,27]. Whether such techniques, with a combination of chemosensitization, would achieve better tumour response in LRRC remains to be seen.

SURGERY FOR LRRC

The exact procedure performed is dictated by the anatomical location of the recurrence. The operating

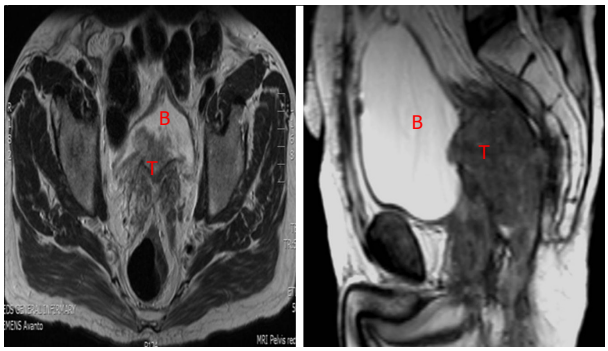

Figure 2 Central recurrence rectal cancer (T) involving the bladder (B).

surgeon must be experienced working in anatomic planes outside of those required for conventional resection in order to perform a complete resection in a safe manner. In addition, extended resection often requires expertise from other specialties such as urology, oncoplastic surgery, neurosurgery, vascular surgery, orthopaedic surgery and gynaecology. Aids such as ureteric stents, radiological tattooing of surface markings to identify the level of sacrectomy, and vascular bypass shunts are adjuncts for some of these surgeries. Special consideration should be given to patients with prior irradiation, especially if delivered in the distant past, as the dissection may be difficult due to fibrotic tissue. In cases of bulky tumour, tumours in close proximity to major vessels or when a difficult dissection was anticipated with no possibility of vascular control, preoperative arterial embolization of internal iliac artery can be considered.

In the next section, the different procedures are reviewed according to disease location and novel techniques are described.

SURGICAL APPROACH BASED ON LOCATION OF DISEASE

Central recurrences

The surgical principle for central recurrence is straightforward. It is to resect as wide as possible to avoid positive margins to avoid leaving residual cancer post-resection. If the recurrence is at the anastomosis or in a mesorectal region without involvement of genitourinary organs, the standard operation would be an abdominal perineal resection or a ultralow Hartmann's procedure[28]. During the pelvic phase, the plane of dissection is directed more laterally than the usual mesorectal plane to provide adequate margins from the centrally located anastomotic recurrence. A re-do anterior resection has been shown to be risky and has only been reported in selected patients with a high rate of recurrence[29-32]. It is usually difficult to accurately determine the extent of tumour spread due to the disruption of normal planes from previous operation(s) and from radiotherapy related fibrosis. Most specialised colorectal surgeons tend to prefer an augmented wide resection margin and will potentially sacrifice the possibility of restoring intestinal continuity in order to obtain a superior oncological resection margin.

If the genitourinary tract is involved, an en bloc resection is recommended[28]. Limited involvement of structures such as dome of bladder and posterior vagina can be treated adequately with partial resection provided negative margins are achieved. Tumours involving the bladder trigone or the prostate in men and cervix in women usually require a total pelvic exenteration (Figure 2). Posterior pelvic exenteration involves en bloc resection of the rectum (or tumour recurrence) and reproductive organs, sparing the bladder and distal ureters. Pelvic exenteration is still reported to have a 2%-14% operative mortality rate and a 33%-75% morbidity rate despite improved surgical techniques and perioperative care[33]. Hence, this procedure should only be attempted if the surgeon concerned is confident of achieving R0 resection margin.

A recent study by Bhangu *et al*[34] reviewed cases of pelvic exenteration performed for both locally advanced primary rectal cancer (LAPR) and LRRC done at a specialised colorectal centre with extensive experience in managing LRRC. In this study, R0 resections were achieved in 62% of LRRC cases, compared to 91% of primary rectal cancer cases. The ability to achieve a R0 resection margin status was found to be associated with improved disease-free-survival and local re-currence free survival on multivariate analysis. In the subgroup analysis of cases with R0 resection margin, the survival rate between LRRC and LAPR cases are comparable (79% *vs* 85%, respectively, $P = 0.766$). Although LRRC is at higher risk of positive resection margin, a good radical operation can still ensure a significant survival benefit provided negative resection margins are achieved.

To ensure a good functional outcome, after a radical resection, reconstructive measures of resected viscera and soft tissue are often required. Examples of reconstructive surgery after radical en bloc resection include bladder reconstruction, the formation of an ileal conduit and the reconstruction of perineal defects. Local rotation and pedicle myocutaneous flaps are particularly useful in reconstructing the perineum and filling the dead-space in the exenterated pelvis (Figure 3). A vertical rectum abdominis myocutaneous (VRAM) flap would be the more sensible option when patients have been subjected to radiotherapy or after sacrificing the gluteal vessels which significantly compromise the flap perfusion. However these procedures are complex and it is recommended that they are performed by an experienced team[35-37]. It is important to discuss with plastic surgeons preoperatively to decide on the side of the VRAM flap that is best utilised. Most plastic surgeons would prefer to harvest the flap

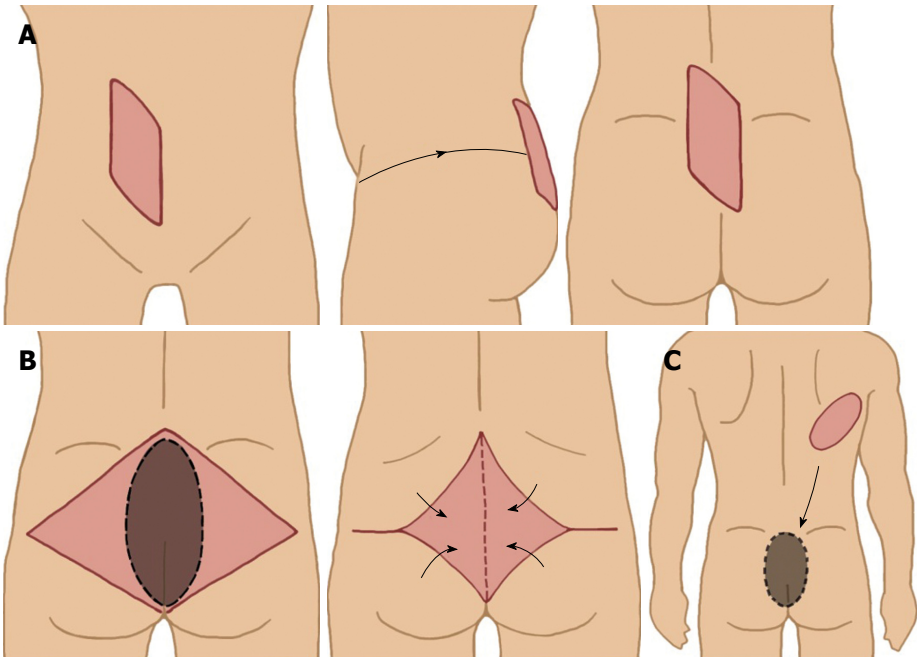

Figure 3 Various myocutaneous flaps used to cover perineal/sacral defect. A: Vertical rectus abdominis myocutaneous flap; B: Gluteal muscle flap; C: Latissimus dorsi free flap.

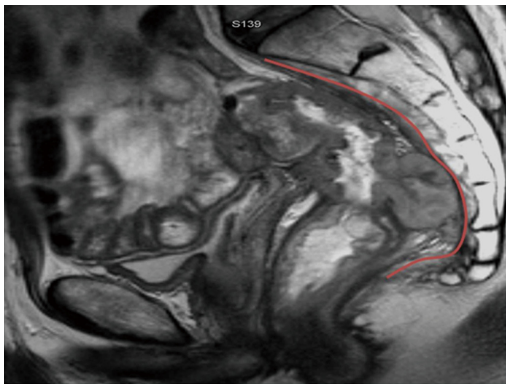

Figure 4 Posterior recurrence involving the presacral fascia (outlined in red).

from the right side (unless a prior ileostomy or ileal conduit has been performed) in anticipation of citing a colostomy of the left side. When a locoregional flap is not possible, either due to the presence of infection or an ileo-regional flap is being utilized in an index operation, free flaps such as a latissimus dorsi flap can be considered.

Anterior involvement of the pubic bone

Tumour recurrences infiltrating anteriorly into the pubic bone are surgically challenging, and in the past were considered inoperable[38,39]. However, Solomon *et al*[40] have described a surgical approach for composite resection of the anterior pubic bones as part of exenteration procedure. This surgical technique typically involves an abdominal and perineal phase. The key step during abdominal phase is to mobilize the bladder en bloc with the pubic bone and separate the anterior abdominal wall from the symphysis pubis. The level of pubic bone transection delineates the extent of resection inferiorly. The superior and inferior pubic rami are fully exposed during the perineal phase. They are then transected using either an oscillating or Gigli saw. The pelvis is structurally stable even after pubic bone resection and does not require reconstruction. The same group of surgeons have reported an acceptable quality of life after pelvic exenteration with or without en bloc pelvic bone excision[41]. While this technique has proven feasible, the short and long-term oncological outcomes are currently under review.

Sacral invasions

A number of possible treatment options are available when the tumour recurrence extends posteriorly. When sacral involvement is limited to the sacral fascia (Figure 4), an en bloc resection with periosteal elevation may achieve negative margins. However, this method carries an increased risk of intraoperative haemorrhage. A reasonable method to assess the haemorrhage risk is to attempt a trial dissection and to have a low threshold for sacrectomy. As an individual surgeon gains experience with sacrectomies, the intraoperative blood loss can be minimized by resecting the sacrum en bloc with the attached presacral venous plexus[19].

When bony invasion is present (Figure 5), sacrectomy is mandatory and is performed *via* a 2-stage composite abdomino-sacral approach. A number of series have reported the safety and feasibility for sacral resection, but sacrectomies were limited to

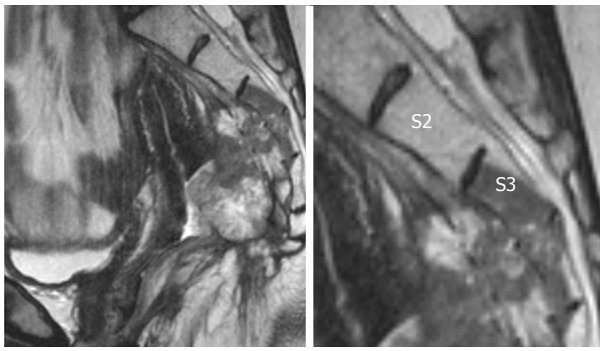

Figure 5 Posterior recurrence invading into distal sacrum.

Table 2 Results of previous studies of composite abdominal-sacral resection for recurrent rectal cancer

Studies	*n*	Morbidity	Mortality	R0	Survival
Sagar *et al*[42]	40	60%	2.5%	50%	56% (3-yr)
Ferenschild *et al*[43]	17	68%	0%	NA	46% (3-yr)
					30% (5-yr)
Melton *et al*[44]	29	58%	3.4%	62%	63% (2-yr)
					20% (5-yr)
Moriya *et al*[45]	57	58%	4%	84%	54% (3-yr)
Weber *et al*[46]	23	78%	0%	91%	51% (3-yr)

recurrence below the S2/S3 junction. These series reported promising oncological outcomes that translate to a survival benefit (Table 2). In these studies, wound-related complications are the most common and the majority were managed conservatively[42-46]. Postoperative morbidity is reduced by limiting the resection to no higher than the S2/S3 junction. This technique maintains the patient's urogenital function *via* preservation of the S2/S3 nerve roots as well as the motor function of S1 nerve roots. Sacral involvement at or above the level of S2 from LRRC was considered by many as a contraindication for resection[47].

Considering the oncological outcomes of low sacrectomy, there are now considerations made regarding the risk-benefit ratio of a high sacrectomy. This is in spite of the associated high morbidity, particularly neurologic injury and spinopelvic instability[48]. Several publications have demonstrated oncological benefit of high sacral resection for primary sacral tumours[49-51]. Wanebo *et al*[52] were the first to report on high sacral resection for LRRC. In their series of 53 patients, an R0 resection was achieved in 85% with a 5-year survival of 31%. Subsequently, Dozois *et al*[53] reported on a series of nine patients that underwent high sacral resection, in which all cases had a R0 resection with a 5-year survival rate of 30%. This represents a promising oncological outcome with regards to high sacrectomies.

More recently, Milne *et al*[54] compared both high and low sacrectomies. The study found that both have comparable rate of R0 resection (76% high sacrectomy *vs* 71% low sacrectomy). Interestingly, they found that the level of sacrectomy did not significantly increase the risk of neurological complications (P = 0.112). In addition, high sacrectomies are not associated with higher rate of major complications (43% for high sacrectomies *vs* 36% for low sacrectomies, P = 0.612)[54].

Sacrectomies are typically completed in the prone jack-knife position. There are few limitations to this approach which includes difficult access to the lateral compartments of the pelvis, inability to gain vascular control of major intra-pelvic vessels, and anaesthetic concerns when ventilating in the prone position. These risks are especially significant for high sacral resection. An abdominal-only approach, first described by Solomon *et al*[55] in 2014, is an alternative. This route offers the distinct advantage of allowing definitive vascular control and access to major arteries at all times throughout the procedure. However, exposure to the muscular and ligamentous attachments of the sacrum can be limited in this approach. To offset this, the authors suggested placing a rolled towel at the lower back of the patient during pre-operative positioning. This allows for elevation of the lumbar sacral curve towards the operative field and facilitates a safer and more measured dissection of the sacrum during the perineal phase.

One of the technical challenges of a high sacrectomy is that it requires reconstructive surgery to restore pelvic stability. The aim of reconstruction is to ensure a stable fixation between the lumbar spine and the pelvis. This can be achieved with either titanium rod fixation or occasionally *via* lumbopelvic bony fusion using bone allograft bone fusion[56,57]. Perineal and sacral defects can be quite extensive after en bloc sacral resection of the tumour recurrence. Primary closure may be achieved without tension and may be reinforced with a biological mesh[19,42,58,59]. Alternatively, there are various myocutaneous flaps that can be used for soft tissue reconstruction, as discussed above.

Lateral/pelvic sidewall involvement

Recurrences involving the lateral pelvic side wall often adhere to the bony pelvis or involve key structures such as the ureters, iliac vessels and the sciatic nerve (Figures 6 and 7). This makes it least likely to achieve negative surgical resection margins and therefore results in a poorer prognosis compared to central, anterior and posterior diseases[17-18,31]. Resection of the tumour would encompass en bloc resection of attached structures with subsequent reconstruction. These procedures are technically challenging and their roles are still debatable. Two recent Delphi studies[60,61], have confirmed the views of many world experts that extensive lateral side wall involvement still remains a relative contraindication to curative surgery.

Austin *et al*[62] from the Sydney group have described

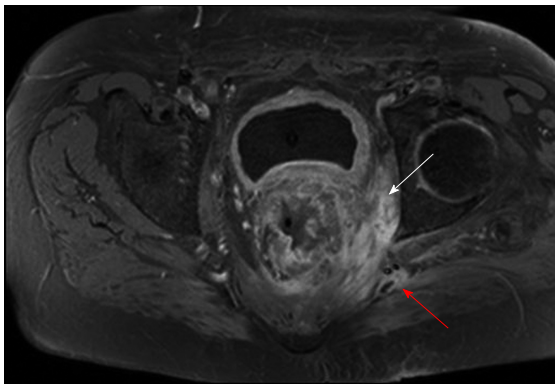

Figure 6 Recurrent rectal cancer in the lower left lateral compartment invading the obturator internus muscle (white arrow) and posteriorly involving the superior gluteal nerve (red arrow).

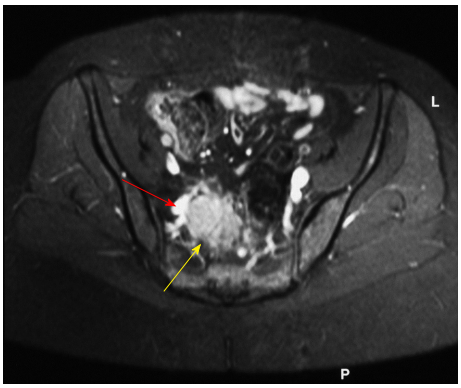

Figure 7 Recurrent rectal cancer at right lateral side wall (yellow arrow), with close proximity to iliac vessels (red arrow); this requires excision of involved vascular segment and reconstruction.

a promising approach to extensive lateral sidewall disease, with dissection in the plane between the bony pelvis and the sidewall musculature. The surgery begins with mobilization of the common and external iliac vessels from the main bifurcation of the aorta and vena cava. The ureter is identified and mobilized distally to the vesico-ureteric junction. If the ureter is involved with tumour, en bloc resection is required and the ureter is divided proximal to the level of tumour involvement. The internal iliac artery and vein are ligated and divided at their origins. This will mitigate the risk of heavy pelvic haemorrhage when dissection of the tumour is carried out. The external iliac vessels are mobilized down to the level of the inguinal ligaments.

When the external iliac vessels are involved with either adherence or encasement of the tumour, the involved segment is to be removed en bloc with the tumour to achieve a clear margin. Various vascular reconstruction methods have been described using autologous and synthetic grafts[63,64]. The key is immediate reconstruction to prevent compartment syndrome and thrombosis. Once the major vessels are reflected away, and with medial retraction of the tumour mass, a posterolateral plane of dissection will lead to the lumbar-sacral trunk and sacral nerve roots and then on to the piriformis and obturator muscles as appropriate. An energy device can be used to better achieve hemostasis. If required, lateral recurrence within the greater sciatic notch, the bony ischium, the sacrotuberous and sacrospinatus ligaments could be resected en bloc.

En bloc resection of the sciatic nerve is an established practice for pelvic and lower limb soft tissue sarcoma with acceptable postoperative functional outcomes[65,66]. In the 1990s, Kameyama *et al*[67] reported on three patients with LRRC involving the sciatic nerve that underwent pelvic exenteration with en bloc sciatic nerve resection. All showed improved quality of life and an ability to walk unassisted with the help of below-the-knee braces.

As expected, the literature is limited regarding the outcomes of patients undergoing surgery for LRRC involving the lateral pelvic side wall. One othe earlier reports from is from Japan. Yamada *et al*[17] showed no survivors at 5 years for 17 patients with lateral recurrent disease that underwent radical resection. Moore and colleague at Memorial Sloan-Kettering Cancer Centre[18] demonstrated that in cases where pelvic side wall recurrence was suggested preoperatively, there was a 19% rate of R0 resection rate and a similar poor oncological outcome as the study by Yamada. A more recent study, the largest series to date, has reported a hundred cases of pelvic exenteration with lateral pelvic wall excision for LRRC[68]. This was the same group that described the novel approach to lateral pelvic wall excision mentioned above. With the use of this radical technique, they could achieve R0 resection in 62% of patients with LRRC and this has translated to a median overall survival of 35 mo and overall 3-year survival rate of 45%. The authors have observed improved results following experience with this technique and progressive support from multidisciplinary experts.

An alternative approach has been recently described by the St Mark's group[69]. It involves an initial transgluteal approach to the sciatic notch which is performed with patient in prone position. Once the lateral recurrence has been fully excised, the patient is turned supine to complete the operation *via* laparotomy. The group successfully achieved R0 resection margin in all their 6 patients. In our opinion, this technique is feasible only in selected patients. It does not permit adequate vascular access and hence would not be suitable for patients with disease involving the iliac vessels.

LAPAROSCOPIC SURGERY FOR LRRC

Open surgery for laparoscopic surgery for LRRC is considered by many as technically challenging, let alone a laparoscopic approach. To date, there are only

Table 3 Studies on laparoscopic surgery for recurrent rectal cancer

Ref.	Year	Study design	No. of patients	Site of recurrence	Median blood loss, mL (range)	Median operative time, min (range)	R0 resection rate	Overall postoperative mortality/morbidity rate
Lu *et al*[70]	2006	Case series	7	Central recurrence: 6 Presacral: 1	200 (109-291)	211 (198–224)	100%	NR
Kim *et al*[71]	2008	Case report	1	Central/anastomotic recurrence	50	185	100%	NR
Park *et al*[72]	2011	Comparative study	Lap: 15 Open: 26	Anastomotic site, ovary and pelvic lateral LN	NR	Lap: 150 (48-460) Open: 259 (40-514) $P = 0.059$	Lap: 100% Open: 84.6% P = NS	Lap: 13.3% Open: 57.7% $P \leqslant 0.05$
Nagasaki *et al*[73]	2014	Comparative study	Lap: 13 Open: 17	Central and Lateral pelvic LN	Lap: 110 (60-800) Open: 450 (25-1600) $P = 0.075$	Lap: 381 (227-554) Open: 241 (125-694) $P = 0.024$	Lap: 100% Open: 94% $P = 0.99$	Lap: 30.8% Open: 23.5% $P = 0.69$
Akiyoshi *et al*[74]	2015	Case series	9	Lateral pelvic LN	130 (25-200)	381 (227-554)	100%	33.30%

a few reporting the safety and feasibility of laparoscopic surgery for LRRC (Table 3). The key factors for cases deemed suitable for laparoscopic surgery (all reported cases were non-exenterative surgeries) are (1) centrally located tumour or at most with lateral pelvic nodal recurrence; and (2) surgeons who are skilled in laparoscopic rectal surgery particularly in laparoscopic lateral pelvic node dissection. The authors of these studies[70-74] commented on the advantage of the high-definition magnified view obtained during laparoscopy that facilitates precise dissection in the deep pelvis with distorted anatomical plane. The laparoscopic approach also demonstrated reduced blood loss and earlier return of bowel function[72-74]. From the oncological point of view, all the laparoscopic cases have achieved R0 resection.

CONCLUSION

Management strategies for LRRC cases have evolved over time with more surgeons expanding the criteria in offering curative surgery. With the continuously evolving techniques in radical surgery, as evident in the literature, there has been significant improvement in achieving an R0 margin status. The prospect of survival for these patients has therefore improved significantly. However, due to the complexity of the disease, there is no "one-size-fits-all" surgical approach. LRRC is usually not confined to a single compartment within the pelvis. It is therefore of paramount importance to have a good understanding of the complex anatomy of the pelvis in order to formulate the most appropriate surgical approach. The extent of the radical resection should be tailored to the needs of the patient. A few novel techniques have been developed to encompass a "wider" and "higher" excision, including en bloc resections of the sciatic notch and composite high sacral (S1 and S2) resection. The preliminary data is promising, but the patient pool in each case series is small. In addition, the studies were conducted in highly specialised units. Understandably, there is a lack of substantial research and/or evidence in terms of long-term outcomes. Although surgical options for LRRC have expanded significantly, one should balance the treatment choices available against the morbidity associated with the procedure and select the right patient for it.

REFERENCES

1 **Phillips RK**, Hittinger R, Blesovsky L, Fry JS, Fielding LP. Local recurrence following 'curative' surgery for large bowel cancer: II. The rectum and rectosigmoid. *Br J Surg* 1984; **71**: 17-20 [PMID: 6689963]

2 **Bokey EL**, Ojerskog B, Chapuis PH, Dent OF, Newland RC, Sinclair G. Local recurrence after curative excision of the rectum for cancer without adjuvant therapy: role of total anatomical dissection. *Br J Surg* 1999; **86**: 1164-1170 [PMID: 10504371 DOI: 10.1046/j.1365-2168.1999.01216x]

3 **Cedermark B**, Dahlberg M, Glimelius B, Påhlman L, Rutqvist LE, Wilking N. Improved survival with preoperative radiotherapy in resectable rectal cancer. *N Engl J Med* 1997; **336**: 980-987 [PMID: 9091798 DOI: 10.1056/NEJM199704033361402]

4 **Hansen MH**, Kjaeve J, Revhaug A, Eriksen MT, Wibe A, Vonen B. Impact of radiotherapy on local recurrence of rectal cancer in Norway. *Br J Surg* 2007; **94**: 113-118 [PMID: 17083107 DOI: 10.1002/bjs.5576]

5 **Shoup M**, Guillem JG, Alektiar KM, Liau K, Paty PB, Cohen AM, Wong WD, Minsky BD. Predictors of survival in recurrent rectal cancer after resection and intraoperative radiotherapy. *Dis Colon Rectum* 2002; **45**: 585-592 [PMID: 12004205]

6 **Palmer G**, Martling A, Cedermark B, Holm T. A population-based study on the management and outcome in patients with locally recurrent rectal cancer. *Ann Surg Oncol* 2007; **14**: 447-454 [PMID: 17139457 DOI: 10.1245/s10434-006-9256-9]

7 **Silberfein EJ**, Kattepogu KM, Hu CY, Skibber JM, Rodriguez-Bigas MA, Feig B, Das P, Krishnan S, Crane C, Kopetz S, Eng C, Chang GJ. Long-term survival and recurrence outcomes following surgery for distal rectal cancer. *Ann Surg Oncol* 2010; **17**: 2863-2869 [PMID: 20552409 DOI: 10.1245/s10434-010-1119-8]

8 **Gunderson LL**, Sosin H. Areas of failure found at reoperation (second or symptomatic look) following "curative surgery" for adenocarcinoma of the rectum. Clinicopathologic correlation and implications for adjuvant therapy. *Cancer* 1974; **34**: 1278-1292 [PMID: 4424091 DOI: 10.1002/1097-0142]

9 **Wanebo HJ**, Koness RJ, Vezeridis MP, Cohen SI, Wrobleski DE. Pelvic resection of recurrent rectal cancer. *Ann Surg* 1994; **220**: 586-595; discussion 595-597 [PMID: 7524455]

10 **Wong CS**, Cummings BJ, Brierley JD, Catton CN, McLean M, Catton P, Hao Y. Treatment of locally recurrent rectal carcinoma--results and prognostic factors. *Int J Radiat Oncol Biol Phys* 1998; **40**: 427-435 [PMID: 9457832 DOI: 10.1016/S0360-3016(97)00737-2]

11 **Ito Y**, Ohtsu A, Ishikura S, Boku N, Nihei K, Ogino T, Ikeda H. Efficacy of chemoradiotherapy on pain relief in patients with intrapelvic recurrence of rectal cancer. *Jpn J Clin Oncol* 2003; **33**: 180-185 [PMID: 12810832 DOI: 10.1093/jjco/hyg036]]

12 **Danjoux CE**, Gelber RD, Catton GE, Klaassen DJ. Combination chemo-radiotherapy for residual, recurrent or inoperable carcinoma of the rectum: E.C.O.G. study (EST 3276). *Int J Radiat Oncol Biol Phys* 1985; **11**: 765-771 [PMID: 3980272 DOI: 10.1016/0360-3016(85)90309-8]

13 **Wanebo HJ**, Gaker DL, Whitehill R, Morgan RF, Constable WC. Pelvic recurrence of rectal cancer. Options for curative resection. *Ann Surg* 1987; **205**: 482-495 [PMID: 2437869]

14 **Magrini S**, Nelson H, Gunderson LL, Sim FH. Sacropelvic resection and intraoperative electron irradiation in the management of recurrent anorectal cancer. *Dis Colon Rectum* 1996; **39**: 1-9 [PMID: 8601342 DOI: 10.1007/BF02048260]

15 **Sagar PM**. Ultraradical resection for locally recurrent rectal cancer. *Dis Colon Rectum* 2014; **57**: 1-2 [PMID: 24316939 DOI: 10.1097/DCR.0000000000000014]

16 **Harris CA**, Solomon MJ, Heriot AG, Sagar PM, Tekkis PP, Dixon L, Pascoe R, Dobbs BR, Frampton CM, Harji DP, Kontovounisios C, Austin KK, Koh CE, Lee PJ, Lynch AC, Warrier SK, Frizelle FA. The Outcomes and Patterns of Treatment Failure After Surgery for Locally Recurrent Rectal Cancer. *Ann Surg* 2016; **264**: 323-329 [PMID: 26692078 DOI: 10.1097/SLA.0000000000001524]

17 **Yamada K**, Ishizawa T, Niwa K, Chuman Y, Akiba S, Aikou T. Patterns of pelvic invasion are prognostic in the treatment of locally recurrent rectal cancer. *Br J Surg* 2001; **88**: 988-993 [PMID: 11442533 DOI: 10.1046/j007-1323.2001.01811.x]

18 **Moore HG**, Shoup M, Riedel E, Minsky BD, Alektiar KM, Ercolani M, Paty PB, Wong WD, Guillem JG. Colorectal cancer pelvic recurrences: determinants of resectability. *Dis Colon Rectum* 2004; **47**: 1599-1606 [PMID: 15540287 DOI: 10.1007/s10350-004-0677-x]

19 **Mirnezami AH**, Sagar PM. Surgery for recurrent rectal cancer: technical notes and management of complications. *Tech Coloproctol* 2010; **14**: 209-216 [PMID: 20461538 DOI: 10.1007/s10151-010-0585-0]

20 **Messiou C**, Chalmers A, Boyle K, Sagar P. Surgery for recurrent rectal carcinoma: The role of preoperative magnetic resonance imaging. *Clin Radiol* 2006; **61**: 250-258 [PMID: 16488206 DOI: 10.1016/j.crad.2005.11.008]

21 **Dresen RC**, Kusters M, Daniels-Gooszen AW, Cappendijk VC, Nieuwenhuijzen GA, Kessels AG, de Bruïne AP, Beets GL, Rutten HJ, Beets-Tan RG. Absence of tumor invasion into pelvic structures in locally recurrent rectal cancer: prediction with preoperative MR imaging. *Radiology* 2010; **256**: 143-150 [PMID: 20574091 DOI: 10.1148/radiol.10090725]

22 **Vargas HA**, Burger IA, Donati OF, Andikyan V, Lakhman Y, Goldman DA, Schöder H, Chi DS, Sala E, Hricak H. Magnetic resonance imaging/positron emission tomography provides a roadmap for surgical planning and serves as a predictive biomarker in patients with recurrent gynecological cancers undergoing pelvic exenteration. *Int J Gynecol Cancer* 2013; **23**: 1512-1519 [PMID: 24257566 DOI: 10.1097/IGC.0b013e3182a41e61]

23 **Gagliardi G**, Hawley PR, Hershman MJ, Arnott SJ. Prognostic factors in surgery for local recurrence of rectal cancer. *Br J Surg* 1995; **82**: 1401-1405 [PMID: 7489178]

24 **Hartley JE**, Lopez RA, Paty PB, Wong WD, Cohen AM, Guillem JG. Resection of locally recurrent colorectal cancer in the presence of distant metastases: can it be justified? *Ann Surg Oncol* 2003; **10**: 227-233 [PMID: 12679306]

25 **Yu SK**, Bhangu A, Tait DM, Tekkis P, Wotherspoon A, Brown G. Chemoradiotherapy response in recurrent rectal cancer. *Cancer Med* 2014; **3**: 111-117 [PMID: 24403010 DOI: 10.1002/cam4.169]

26 **Glimelius B**. Recurrent rectal cancer. The pre-irradiated primary tumour: can more radiotherapy be given? *Colorectal Dis* 2003; **5**: 501-503 [PMID: 12925089]

27 **Guo S**, Reddy CA, Kolar M, Woody N, Mahadevan A, Deibel FC, Dietz DW, Remzi FH, Suh JH. Intraoperative radiation therapy with the photon radiosurgery system in locally advanced and recurrent rectal cancer: retrospective review of the Cleveland clinic experience. *Radiat Oncol* 2012; **7**: 110 [PMID: 22817880 DOI: 10.1186/1748-717X-7-110]

28 **Mirnezami AH**, Sagar PM, Kavanagh D, Witherspoon P, Lee P, Winter D. Clinical algorithms for the surgical management of locally recurrent rectal cancer. *Dis Colon Rectum* 2010; **53**: 1248-1257 [PMID: 20706067 DOI: 10.1007/DCR.0b013e3181e10b0e]

29 **Salo JC**, Paty PB, Guillem J, Minsky BD, Harrison LB, Cohen AM. Surgical salvage of recurrent rectal carcinoma after curative resection: a 10-year experience. *Ann Surg Oncol* 1999; **6**: 171-177 [PMID: 10082043 DOI: 10.1007/s10434-999-0171-8]

30 **Boyle KM**, Sagar PM, Chalmers AG, Sebag-Montefiore D, Cairns A, Eardley I. Surgery for locally recurrent rectal cancer. *Dis Colon Rectum* 2005; **48**: 929-937 [PMID: 15785880 DOI: 10.1007/s10350-004-0909-0]

31 **Heriot AG**, Byrne CM, Lee P, Dobbs B, Tilney H, Solomon MJ, Mackay J, Frizelle F. Extended radical resection: the choice for locally recurrent rectal cancer. *Dis Colon Rectum* 2008; **51**: 284-291 [PMID: 18204879 DOI: 10.1007/s10350-007-9152-9]

32 **Yun JA**, Huh JW, Kim HC, Park YA, Cho YB, Yun SH, Lee WY, Chun HK. Local recurrence after curative resection for rectal carcinoma: The role of surgical resection. *Medicine* (Baltimore) 2016; **95**: e3942 [PMID: 27399067 DOI: 10.1097/MD.0000000000003942]

33 **Yang TX**, Morris DL, Chua TC. Pelvic exenteration for rectal cancer: a systematic review. *Dis Colon Rectum* 2013; **56**: 519-531 [PMID: 23478621 DOI: 10.1097/DCR.0b013e31827a7868]

34 **Bhangu A**, Ali SM, Brown G, Nicholls RJ, Tekkis P. Indications and outcome of pelvic exenteration for locally advanced primary and recurrent rectal cancer. *Ann Surg* 2014; **259**: 315-322 [PMID: 23478530 DOI: 10.1087/SLA.0b013e31828a0d22]

35 **Christensen HK**, Nerstrøm P, Tei T, Laurberg S. Perineal repair after extralevator abdominoperineal excision for low rectal cancer. *Dis Colon Rectum* 2011; **54**: 711-717 [PMID: 21552056 DOI: 10.1007/DCR.0b013e3182163c89]

36 **Hinojosa MW**, Parikh DA, Menon R, Wirth GA, Stamos MJ, Mills S. Recent experience with abdominal perineal resection with vertical rectus abdominis myocutaneous flap reconstruction after preoperative pelvic radiation. *Am Surg* 2009; **75**: 995-999 [PMID: 19886152]

37 **Anderin C**, Martling A, Lagergren J, Ljung A, Holm T. Short-term outcome after gluteus maximus myocutaneous flap reconstruction of the pelvic floor following extra-levator abdominoperineal excision of the rectum. *Colorectal Dis* 2012; **14**: 1060-1064 [PMID: 21981319 DOI: 10.1111/j.1463-1318.2011.02848.x]

38 **Yu HH**, Leong CH, Ong GB. Pelvic exenteration for advanced pelvic malignancies. *Aust N Z J Surg* 1976; **46**: 197-201 [PMID: 1070292]

39 **Hahnloser D**, Nelson H, Gunderson LL, Hassan I, Haddock MG, O'Connell MJ, Cha S, Sargent DJ, Horgan A. Curative potential of multimodality therapy for locally recurrent rectal cancer. *Ann Surg* 2003; **237**: 502-508 [PMID: 12677146 DOI: 10.1097/01.SLA.0000059972.90598.5F]

40 **Solomon MJ**, Austin KK, Masya L, Lee P. Pubic Bone Excision and Perineal Urethrectomy for Radical Anterior Compartment Excision During Pelvic Exenteration. *Dis Colon Rectum* 2015; **58**: 1114-1119 [PMID: 26445189 DOI: 10.1097/DCR.0000000000000479]

41 **Austin KK**, Young JM, Solomon MJ. Quality of life of survivors after pelvic exenteration for rectal cancer. *Dis Colon*

Rectum 2010; **53**: 1121-1126 [PMID: 20628274 DOI: 10.1007/DCR.0b013e318e10c46]
42 **Sagar PM**, Gonsalves S, Heath RM, Phillips N, Chalmers AG. Composite abdominosacral resection for recurrent rectal cancer. *Br J Surg* 2009; **96**: 191-196 [PMID: 19160364 DOI: 10.1002/bjs.6464]
43 **Ferenschild FT**, Vermaas M, Verhoef C, Dwarkasing RS, Eggermont AM, de Wilt JH. Abdominosacral resection for locally advanced and recurrent rectal cancer. *Br J Surg* 2009; **96**: 1341-1347 [PMID: 19847877 DOI: 10.1002/bjs.6695]
44 **Melton GB**, Paty PB, Boland PJ, Healey JH, Savatta SG, Casas-Ganem JE, Guillem JG, Weiser MR, Cohen AM, Minsky BD, Wong WD, Temple LK. Sacral resection for recurrent rectal cancer: analysis of morbidity and treatment results. *Dis Colon Rectum* 2006; **49**: 1099-1107 [PMID: 16779712 DOI: 10.1007/s10350-006-0563-9]
45 **Moriya Y**, Akasu T, Fujita S, Yamamoto S. Total pelvic exenteration with distal sacrectomy for fixed recurrent rectal cancer in the pelvis. *Dis Colon Rectum* 2004; **47**: 2047-2053; discussion 2053-2054 [PMID: 15657653 DOI: 10.1007/s10350-004-0714-9]
46 **Weber KL**, Nelson H, Gunderson LL, Sim FH. Sacropelvic resection for recurrent anorectal cancer. A multidisciplinary approach. *Clin Orthop Relat Res* 2000; (**372**): 231-240 [PMID: 10738432]
47 **Hansen PJ**. Effects of coat colour on physiological responses to solar radiation in Holsteins. *Vet Rec* 1990; **127**: 333-334 [PMID: 2256242 DOI: 10.1111/j.1463-1318.2012.03076.x]
48 **Wanebo HJ**, Marcove RC. Abdominal sacral resection of locally recurrent rectal cancer. *Ann Surg* 1981; **194**: 458-471 [PMID: 7283507]
49 **Sahakitrungruang C**, Chantra K, Dusitanond N, Atittharnsakul P, Rojanasakul A. Sacrectomy for primary sacral tumors. *Dis Colon Rectum* 2009; **52**: 913-918 [PMID: 19502856 DOI: 10.1007/DCR.0b013e3181a0d932]
50 **Huth JF**, Dawson EG, Eilber FR. Abdominosacral resection for malignant tumors of the sacrum. *Am J Surg* 1984; **148**: 157-161 [PMID: 6588768 DOI: 10.1016/0002-9610(84)90304-0]
51 **Fourney DR**, Rhines LD, Hentschel SJ, Skibber JM, Wolinsky JP, Weber KL, Suki D, Gallia GL, Garonzik I, Gokaslan ZL. En bloc resection of primary sacral tumors: classification of surgical approaches and outcome. *J Neurosurg Spine* 2005; **3**: 111-122 [PMID: 16370300 DOI: 10.3171/spi.2005.3.2.0111]
52 **Wanebo HJ**, Antoniuk P, Koness RJ, Levy A, Vezeridis M, Cohen SI, Wrobleski DE. Pelvic resection of recurrent rectal cancer: technical considerations and outcomes. *Dis Colon Rectum* 1999; **42**: 1438-1448 [PMID: 10566532 DOI: 10.1007/BF02235044]
53 **Dozois EJ**, Privitera A, Holubar SD, Aldrete JF, Sim FH, Rose PS, Walsh MF, Bower TC, Leibovich BC, Nelson H, Larson DW. High sacrectomy for locally recurrent rectal cancer: Can long-term survival be achieved? *J Surg Oncol* 2011; **103**: 105-109 [PMID: 21259242 DOI: 10.1002/jso.21774]
54 **Milne T**, Solomon MJ, Lee P, Young JM, Stalley P, Harrison JD. Assessing the impact of a sacral resection on morbidity and survival after extended radical surgery for locally recurrent rectal cancer. *Ann Surg* 2013; **258**: 1007-1013 [PMID: 23364701 DOI: 10.1097/SLA.0b013e318283a5b6]
55 **Solomon MJ**, Tan KK, Bromilow RG, Al-mozany N, Lee PJ. Sacrectomy via the abdominal approach during pelvic exenteration. *Dis Colon Rectum* 2014; **57**: 272-277 [PMID: 24401892 DOI: 10.1097/DCR.0000000000000039]
56 **Bederman SS**, Shah KN, Hassan JM, Hoang BH, Kiester PD, Bhatia NN. Surgical techniques for spinopelvic reconstruction following total sacrectomy: a systematic review. *Eur Spine J* 2014; **23**: 305-319 [PMID: 24150036 DOI: 10.1007/s00586-013-3075-z]
57 **Kawahara N**, Murakami H, Yoshida A, Sakamoto J, Oda J, Tomita K. Reconstruction after total sacrectomy using a new instrumentation technique: a biomechanical comparison. *Spine* (Phila Pa 1976) 2003; **28**: 1567-1572 [PMID: 12865846]
58 **Butler CE**, Rodriguez-Bigas MA. Pelvic reconstruction after abdominoperineal resection: is it worthwhile? *Ann Surg Oncol* 2005; **12**: 91-94 [PMID: 15827784 DOI: 10.1245/ASO.2005.11.923]
59 **Jacombs AS**, Rome P, Harrison JD, Solomon MJ. Assessment of the selection process for myocutaneous flap repair and surgical complications in pelvic exenteration surgery. *Br J Surg* 2013; **100**: 561-567 [PMID: 23188415 DOI: 10.1002/bjs.9002]
60 **Chew MH**, Brown WE, Masya L, Harrison JD, Myers E, Solomon MJ. Clinical, MRI, and PET-CT criteria used by surgeons to determine suitability for pelvic exenteration surgery for recurrent rectal cancers: a Delphi study. *Dis Colon Rectum* 2013; **56**: 717-725 [PMID: 23652745 DOI: 10.1097/DCR.0b013e31812bec]
61 **Beyond TME Collaborative**. Consensus statement on the multidisciplinary management of patients with recurrent and primary rectal cancer beyond total mesorectal excision planes. *Br J Surg* 2013; **100**: 1009-1014 [PMID: 23754654 DOI: 10.1002/bjs.9192]
62 **Austin KK**, Solomon MJ. Pelvic exenteration with en bloc iliac vessel resection for lateral pelvic wall involvement. *Dis Colon Rectum* 2009; **52**: 1223-1233 [PMID: 19571697 DOI: 10.1007/DCR.0b013e3181a73f48]
63 **Brown KG**, Koh CE, Solomon MJ, Choy IC, Dubenec S. Spiral saphenous vein graft for major pelvic vessel reconstruction during exenteration surgery. *Ann Vasc Surg* 2015; **29**: 1323-1326 [PMID: 25770390 DOI: 10.1016/j.avsg.2015.01.028]
64 **Abdelsattar ZM**, Mathis KL, Colibaseanu DT, Merchea A, Bower TC, Larson DW, Dozois EJ. Surgery for locally advanced recurrent colorectal cancer involving the aortoiliac axis: can we achieve R0 resection and long-term survival? *Dis Colon Rectum* 2013; **56**: 711-716 [PMID: 23652744 DOI: 10.1097/DCR.0b013e31827dbcb0]
65 **Brooks AD**, Gold JS, Graham D, Boland P, Lewis JJ, Brennan MF, Healey JH. Resection of the sciatic, peroneal, or tibial nerves: assessment of functional status. *Ann Surg Oncol* 2002; **9**: 41-47 [PMID: 11829429 DOI: 10.1245/aso.2002.9.1.41]
66 **Fuchs B**, Davis AM, Wunder JS, Bell RS, Masri BA, Isler M, Turcotte R, Rock MG. Sciatic nerve resection in the thigh: a functional evaluation. *Clin Orthop Relat Resp* 2001; **382**: 34-41 [PMID: 11154002]
67 **Kameyama M**, Nakamori S, Imaoka S, Hinakawa M, Sasaki Y, Ishikawa O, Kabuto T, Furukawa H, Iwanaga T, Ueda T. [Composite resection of sciatic nerve for local recurrence of rectal cancer]. *Gan To Kagaku Ryoho* 1993; **20**: 1689-1691 [PMID: 8373250]
68 **Solomon MJ**, Brown KG, Koh CE, Lee P, Austin KK, Masya L. Lateral pelvic compartment excision during pelvic exenteration. *Br J Surg* 2015; **102**: 1710-1717 [PMID: 26694992 DOI: 10.1002/bjs.9915]
69 **Shaikh I**, Aston W, Hellawell G, Ross D, Littler S, Burling D, Marshall M, Northover JM, Antoniou A, Jenkins JT. Extended lateral pelvic sidewall excision (ELSiE): an approach to optimize complete resection rates in locally advanced or recurrent anorectal cancer involving the pelvic sidewall. *Tech Coloproctol* 2014; **18**: 1161-1168 [PMID: 25380742 DOI: 10.1007/s10151-014-1234-9]
70 **Lu AG**, Wang ML, Hu WG, Li JW, Zang L, Mao ZH, Dong F, Feng B, Ma JJ, Zong YP, Zheng MH. [Experience of laparoscopic salvage surgery for locally recurrent rectal cancer]. *Zhonghua Waike Zazhi* 2006; **44**: 597-599 [PMID: 16784651]
71 **Kim SH**, Neve RS, Joh YG. Multimedia article. Relaparoscopy for salvage surgery in anastomotic recurrence of rectal cancer: feasible and safe. *Dis Colon Rectum* 2008; **51**: 1712-1713 [PMID: 18670818 DOI: 10.1007/s10350-008-9296-2]
72 **Park SY**, Choi GS, Jun SH, Park JS, Kim HJ. Laparoscopic salvage surgery for recurrent and metachronous colorectal cancer: 15 years' experience in a single center. *Surg Endosc* 2011; **25**: 3551-3558 [PMID: 21638182 DOI: 10.1007/s00464-011-1756-4]
73 **Nagasaki T**, Akiyoshi T, Ueno M, Fukunaga Y, Nagayama S, Fujimoto Y, Konishi T, Yamaguchi T. Laparoscopic salvage surgery for locally recurrent rectal cancer. *J Gastrointest Surg* 2014; **18**:

1319-1326 [PMID: 24838997 DOI: 10.1007/s11605-014-2537-x]
74 **Akiyoshi T**, Nagata J, Nagasaki T, Konishi T, Fujimoto Y, Nagayama S, Fukunaga Y, Ueno M. Laparoscopic salvage lateral pelvic lymph node dissection for locally recurrent rectal cancer. *Colorectal Dis* 2015; **17**: O213-O216 [PMID: 26277783 DOI: 10.1111/codi.13088]

P- Reviewer: Augustin G, Lakatos PL, Piso P, Seow-Choen F
S- Editor: Qi Y **L- Editor**: A **E- Editor**: Zhang FF

World Journal of Gastroenterology

Submit a Manuscript: http://www.f6publishing.com

World J Gastroenterol 2017 June 21; 23(23): 4181-4190

DOI: 10.3748/wjg.v23.i23.4181

ISSN 1007-9327 (print) ISSN 2219-2840 (online)

ORIGINAL ARTICLE

Basic Study

Anti-steatotic and anti-fibrotic effects of the KCa3.1 channel inhibitor, Senicapoc, in non-alcoholic liver disease

Latha Paka, David E Smith, Dawoon Jung, Siobhan McCormack, Ping Zhou, Bin Duan, Jing-Song Li, Jiaqi Shi, Yong-Jie Hao, Kai Jiang, Michael Yamin, Itzhak D Goldberg, Prakash Narayan

Latha Paka, David E Smith, Dawoon Jung, Siobhan McCormack, Ping Zhou, Bin Duan, Jing-Song Li, Jiaqi Shi, Yong-Jie Hao, Kai Jiang, Michael Yamin, Itzhak D Goldberg, Prakash Narayan, Department of Research and Development, Angion Biomedica Corp., Uniondale, NY 11553, United States

Author contributions: Paka L, Yamin M, Goldberg ID and Narayan P substantially contributed to the conception and design of the study, acquisition, analysis and interpretation of data; Narayan P drafted the article related to the intellectual content of the manuscript; and Paka L made revisions for the final version of the article to be published; Jung D performed image analysis using Image J Program. All other authors contributed for performing all the technical aspects of *in vitro* and *in-vivo* work; McCormack S and Zhou P performed *in vitro* work; Smith DE, Duan B, Li JS, Shi J, Hao YJ and Jiang K performed animal care, experimental dosing, pre and post-surgical procedures in animal models.

Institutional animal care and use committee statement: Angion's Animal Welfare Assurance # A4532-01. All the study protocols were designed to minimize pain and distress to the animals and were reviewed approved by our Angion's animal care and use committee.

Conflict-of-interest statement: To the best of our knowledge, no conflict of interest exists.

Data sharing statement: Angion Biomedica is a for-profit small business engaged in developing therapeutics for unmet medical needs. In keeping with corporate policy, data and research resources generated by the company are proprietary. Once all intellectual property that results from the generation of the data and research resources is protected *via* filing of patents, data and research resources generated will be made available.

Manuscript source: Unsolicited manuscript

Correspondence to: Latha Paka, PhD, Senior Research Scientist, Department of Research and Development, Angion Biomedica Corp., 51 Charles Lindbergh Blvd, Uniondale, NY 11553, United States. spaka@angion.com
Telephone: +1-516-3261200
Fax: +1-516-3071659

Received: November 18, 2016
Peer-review started: November 21, 2016
First decision: January 19, 2017
Revised: February 4, 2017
Accepted: April 13, 2017
Article in press: April 13, 2017
Published online: June 21, 2017

Abstract

AIM

To evaluate a calcium activated potassium channel (KCa3.1) inhibitor attenuates liver disease in models of non-alcoholic fatty liver disease (NAFLD).

METHODS

We have performed a series of *in vitro* and *in vivo* studies using the KCa3.1 channel inhibitor, Senicapoc. Efficacy studies of Senicapoc were conducted in toxin-, thioacetamide (TAA) and high fat diet (HFD)-induced models of liver fibrosis in rats. Efficacy and pharmacodynamic effects of Senicapoc was determined through biomarkers of apoptosis, inflammation, steatosis and fibrosis.

RESULTS

Upregulation of KCa3.1 expression was recorded in

TAA-induced and high fat diet-induced liver disease. Treatment with Senicapoc decreased palmitic acid-driven HepG2 cell death. (P < 0.05 *vs* control) supporting the finding that Senicapoc reduces lipid-driven apoptosis in HepG2 cell cultures. In animals fed a HFD for 6 wk, co-treatment with Senicapoc, (1) reduced non-alcoholic fatty liver disease (NAFLD) activity score (NAS) (0-8 scale), (2) decreased steatosis and (3) decreased hepatic lipid content (Oil Red O, P < 0.05 *vs* vehicle). Randomization of TAA animals and HFD fed animals to Senicapoc was associated with a decrease in liver fibrosis as evidenced by hydroxyproline and Masson's trichrome staining (P < 0.05 *vs* vehicle). These results demonstrated that Senicapoc mitigates both steatosis and fibrosis in liver fibrosis models.

CONCLUSION

These data suggest that Senicapoc interrupts more than one node in progressive fatty liver disease by its anti-steatotic and anti-fibrotic activities, serving as a double-edged therapeutic sword.

Key words: High fat diet; Liver; Steatosis; Fibrosis; KCa3.1 channel; Senicapoc; Inflammation

Core tip: Given the large numbers of people with fatty livers and even relatively indolent steatosis can result in a significant population progressing to non-alcoholic steatohepatitis (NASH), NASH with fibrosis and cirrhosis. We report for the first time that a KCa3.1 channel inhibitor exerts an anti-steatotic effect in the setting of fatty liver disease which can be harnessed for the treatment of liver fibrosis. Second, we are the first to report that Senicapoc, a drug that has been through Phase Ⅲ clinical trials, can be repurposed for the treatment of fatty liver disease and potentially for the treatment of other lipid disorders.

Paka L, Smith DE, Jung D, McCormack S, Zhou P, Duan B, Li JS, Shi J, Hao YJ, Jiang K, Yamin M, Goldberg ID, Narayan P. Anti-steatotic and anti-fibrotic effects of the KCa3.1 channel inhibitor, Senicapoc, in non-alcoholic liver disease. *World J Gastroenterol* 2017; 23(23): 4181-4190 Available from: URL: http://www.wjgnet.com/1007-9327/full/v23/i23/4181.htm DOI: http://dx.doi.org/10.3748/wjg.v23.i23.4181

INTRODUCTION

Obesity, diabetes and metabolic syndrome drive non-alcoholic fatty liver disease (NAFLD), the accumulation of fat in hepatocytes not caused by excessive consumption of alcohol. Twenty-five percent of the adult United States population is thought to suffer from NAFLD, which can progress to nonalcoholic steatohepatitis (NASH) or accumulation of fat within the liver accompanied by inflammation[1]. Left untreated, NASH, which affects several million persons in the United States alone, can progress to liver fibrosis, the precursor to cirrhosis and decompensated organ failure[2]. The development of new therapies that prevent the transition from steatosis and inflammation to fibrosis would have substantial clinical value.

The intermediate-conductance Ca^{2+}-activated K^+ channel $K_{Ca}3.1$/KCNN4 is expressed in non-excitable tissues affecting proliferation, migration and vascular resistance and plays an important role in the modulation of Ca^{2+} signaling and cell function[3]. Modulators of this channel have been reported to confer therapeutic benefit in models of inflammatory bowel disease and chronic kidney disease[4-6]. In activated hepatic stellate cells (HSC) and fibrotic livers, KCa3.1 channel expression is upregulated and in liver disease the KCa3.1 channel inhibitor TRAM-34 downregulated fibrosis-associated gene expression and reduced portal perfusion pressure[7]. These results suggest that the KCa3.1 channel might represent a novel target for the treatment of hepatic fibrosis. Interestingly, long-term KCa3.1 blockade therapy with clotrimazole or TRAM-34 reduced atherosclerosis in the murine aorta and carotid arteries[8]. These data suggest that inhibition of KCa3.1 might impact events upstream of and leading to extracellular matrix accumulation.

Senicapoc ($C_{20}H_{15}F_2NO$; 323.34 Da) is an orally bioavailable, potent and selective blocker of the KCa3.1 channel[9]. A clinical stage compound, Senicapoc was deemed safe and generally well-tolerated in Phase Ⅰ, Ⅱ and Ⅲ clinical trials[9-13]. We herein test the hypothesis that in NASH with fibrosis, the KCa3.1 inhibitor Senicapoc mitigates interstitial collagen accumulation *via* a reduction in steatosis.

MATERIALS AND METHODS

Lipid uptake and cell death

HepG2 cells (ATCC) were maintained in DMEM/10% FCS supplemented with L-glutamine. For the experiment, cells were seeded onto a 96 well plate using 10K cells/well. Cells were allowed to attach overnight. On the day of the study, cells were incubated with DMEM/0.2%FCS/L-glutamine. Senicapoc (OX-CHEM Corp., CA, United States) was added to final concentrations of 0, 0.1, 1.0 or 10 μmol/L and incubated for 30 min following which palmitic acid (hexadecanoic acid; $C_{16}H_{32}O_2$; Sigma) coupled to fatty acid-free BSA (Sigma) was added to a final concentration of 0, 75 or 150 μmol/L[14,15]. Cells were incubated overnight and apoptosis measured using the Caspase Glo 3/7 reagent (Promega).

Animal studies

All studies relating to animals were approved by our institutional animal use and care committee. Animals had access to drinking water *ad libitum* throughout the

experimental protocols.

Hepatic KCa3.1 channel expression

Biliary obstruction: Adult male Wistar rats (175-200 g; *n* = 3) were submitted to biliary occlusion using a previously reported method[16]. Briefly, after general anaesthesia (25/5 m/kg ketamine/xylazine, ip), laparotomy was performed by using midline abdominal skin and muscle incisions. The common bile duct was exposed and ligated with 6-0 silk sutures, the abdominal wall sutured closed and the animal returned to its cage. Twenty-eight days after surgery, animals were anesthetized and the livers removed. Sham-operated rats (*n* = 3) were used as control.

Thioacetamide administration: Adult male Wistar-Furth rats (225-250 g) were administered thioacetamide (TAA) (150 mg/kg; *n* = 3) twice a week for 8 wk[17] after which some animals were sacrificed and the livers removed. Sham (saline-administered; *n* = 3) rats were used as control.

Senicapoc efficacy studies

Intervention with senicapoc in TAA model: Adult male Wistar-Furth rats (225-250 g) were administered TAA (150 mg/kg, IP) or saline (0.5 mL, IP) twice a week for 8 wk after which some animals (*n* = 6/group) were sacrificed and the livers retrieved to confirm disease. TAA-administered animals were then randomized to vehicle (Cremaphor 10% and PEG400 10% in water; *n* = 12) or Senicapoc (50 mg/kg, PO, BID; *n* = 12) for 8 wk. Animals were sacrificed 16 wk into TAA administration following which livers were retrieved for analysis.

Diet-induced liver disease: Adult male C57BL/6 mice (18-22 g) were randomized to standard laboratory rodent diet (5001 LabDiet, MO; sham group) or a modified HFD - an L-amino acid diet with 60 kcal% fat with 0.1% methionine and no added choline (CDAHFD; Research Diets, NJ, United States)[18] - for 8 wk after which animals (*n* = 3/group) were sacrificed and livers retrieved for analysis.

Intervention with Senicapoc in CDAHFD model: Adult male C57BL/6 mice (18-22 g) were randomized to standard laboratory rodent diet (sham group) or CDAHFD. After 4 wk on these diets, animals (*n* = 6/group) were sacrificed and the livers retrieved for confirmation of disease. Animals on the special diet were randomized immediately to vehicle (*n* = 12) or Senicapoc (10 mg/kg, PO, BID; *n* = 12) for 4 wk following which they were sacrificed and their livers harvested.

Pretreatment with Senicapoc in CDAHFD model: Adult male C57BL/6 mice (18-22 g) were randomized to standard laboratory rodent diet (sham group; *n* = 8) or CDAHFD (*n* = 16) for 7 d after which animals were sacrificed and livers retrieved for analysis. Treatment with vehicle (*n* = 8) or Seniapoc (10 mg/kg, PO, BID; *n* = 8) was started on day 1 of CDAHFD and continued until sacrifice.

Pretreatment with Senicapoc in HFD model: Adult male C57BL/6 mice were randomized to standard laboratory rodent diet or a high fat diet fat (HFD) containing 10% lard, 5% corn oil and 2% cholesterol (Research Diets, NJ, United States)[19]. Animals on the special diet were randomized immediately to vehicle or Senicapoc (10 mg/kg, PO, BID). After 6 wk days on this diet, animals were sacrificed and livers retrieved for analysis.

KCa3.1 channel expression

As described by Freise *et al*[7] KCa3.1 protein expression (normalized to GAPDH) was determined in liver homogenates using anti-K_{Ca}3.1 (12 hr incubation, K4, $IK_{Ca}1$, #APC-06, Alomone Labs) antibody followed by incubation with anti-rabbit secondary antibody (Santa Cruz Biotechnology, Santa Cruz, CA, United States). The signal was detected by enhanced chemiluminescence (Amersham Pharmacia Biotech, Piscataway, NJ, United States) and densitometry was performed using Bioquant. Immunohistochemical staining of liver sections were performed with the same antibody as described previously.

Liver hydroxyproline: Liver tissues (approximately 200 mg) were prepared and analyzed for hydroxyproline as described by Zhang *et al*[20]. The total hydroxyproline within each liver tissue was determined by total wet liver mass.

Liver fibrosis

Fibrosis was detected histologically by Masson's trichrome and picrosirius red staining of collagen by using digital slide scanning and associated image analysis software as described previously[21].

NAFLD activity score, steatosis and inflammation

An observed blinded to the treatment groups assigned NAFLD activity score (NAS) (0-8 scale), steatosis (0-3 scale) and inflammation (0-3 scale) values to H&E-stained liver sections as described previously[22].

Liver triglycerides: Triglyceride content in liver homogenates was measured using a commercial enzyme-linked immunosorbent assay kit (ELI Tech, Seoul, South Korea).

Liver histopathology: For hematoxylin and eosin (H&E) staining, formalin-fixed liver was embedded into paraffin and cut into 4 μm sections. For Oil Red-O staining, liver tissue was dehydrated before embedded into OCT compound (Sakura, Tokyo, Japan), and cut into 4 μm frozen sections. Commercially available kits (Beyotime, Shanghai, China) were used to stain

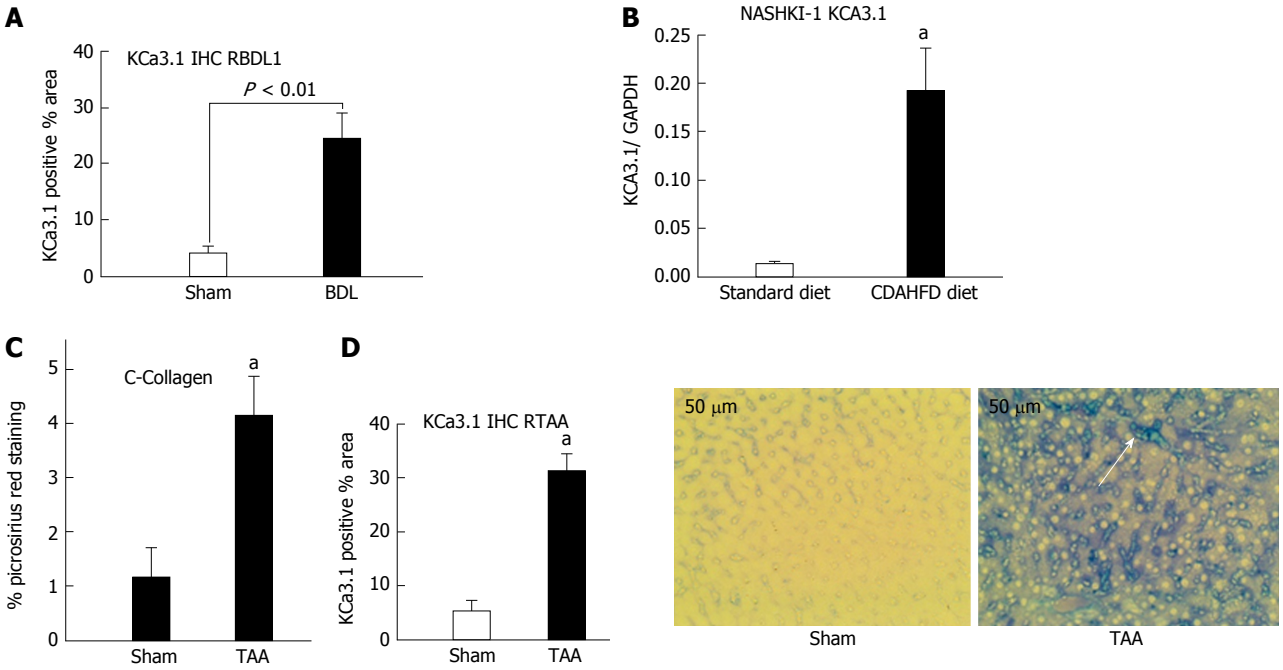

Figure 1 Upregulation of KCa3.1 expression in diseased livers. A: In rats subjected to biliary occlusion, hepatic KCa3.1 expression, probed with anti-KCa3.1 (SK4, IKCa1) antibody, was several-fold that in of sham operated rats. B: Densitometric analysis was made of Western blots for KCa3.1 expression in liver lysates from mice fed a standard diet or CDAHFD for 8 wk. Compared to its expression in livers from animals on a standard diet, KCa3.1 expression is increased several-fold in livers from the CDAHFD cohort ($^{a}P < 0.05$ *vs* standard diet). C: Left: Livers from rats administered TAA for 8 wk exhibited increased fibrosis evidenced by increased picrosirius red staining ($^{a}P < 0.05$ *vs* sham). D: Increased KCa3.1 expression significantly ($^{a}P < 0.05$ *vs* Sham) (middle). (20 ×), intense blue membranous staining (white arrow and right bottom) was noted in these fibrotic livers.

sections. Analysis was performed by an observer blinded to the treatment groups. Lipid vacuoles in H&E sections and lipid content in Oil Red O sections were semi-quantified using Bioquant Image analysis software program (Nashville, TN, United States).

Hepatic inflammation (F4/80) and lipid peroxidation (4-hydroxynonenal): Five-μm-thick paraffin sections of liver tissue were prepared from the center of each hepatic lobe. Sections were subsequently stained with antibodies against F4/80 (anti-F4/80; sc-59171, Santa Cruz, CA, United States) and 4-hydroxynonenal (4-HNE) (anti-4HNE antibody; JaICA, Shizuoka, Japan). Staining was quantified (Bioquant) by an observer blinded to the treatment groups.

Statistical analysis

Data are expressed as mean ± SEM. Differences between groups were measured by one-way ANOVA with Tukey's posthoc test for multiple comparisons. *P* values less than 0.05 were considered significant.

RESULTS

KCa3.1 channel expression in liver disease

Upregulation of KCa3.1 has been reported in fibrotic liver[18]. We evaluated hepatic KCa3.1 expression in 3 distinct rodent models of liver fibrosis. As seen in Figure 1, hepatic KCa3.1 expression was elevated in livers from animals submitted to biliary occlusion for 4 wk (Figure 1A), in livers from animals fed CDAHFD for 8 wk (Figure 1B) and in fibrotic livers from animals administered TAA for 8 wk (Figure 1C and D).

Anti-fibrotic effect of Senicapoc

Consistent with published literature[3,7] and having confirmed a potential role for KCa3.1 channels in liver disease we evaluated whether intervention with Senicapoc decreases hepatic collagen accumulation. Drug effects were evaluated in 2 etiologically distinct models of liver fibrosis. Rats administered TAA for 8 wk exhibited significant increase in liver collagen (hydroxyproline, Figure 2A) at which time they were randomized to Senicapoc or vehicle. As seen in Figure 2A and B, treatment with Senicapoc with continued administration of TAA, blocked the increase in liver collagen from weeks 8 through 16.

Animals fed CDAHFD for 4 wk exhibited hepatomegaly evidenced by increased liver to body mass ratio (7.5% ± 0.2% *vs* 4.8% ± 0.1%, standard diet; $P < 0.05$). Furthermore, animals on this diet exhibited a NAS (0 to 8 scale) of 5.1 ± 0.9 *vs* 1 ± 0.2, standard diet; $P < 0.05$. Randomization of animals on CDAHFD to Senicapoc for 4 wk was associated with a decrease in liver fibrosis as evidenced by hydroxyproline (Figure 3A) and Masson's trichrome staining (Figure 3B).

Anti-Steatotic effect of Senicapoc

We sought to evaluate whether the anti-fibrotic effects of Senicapoc in diet-induced liver disease, is mediated,

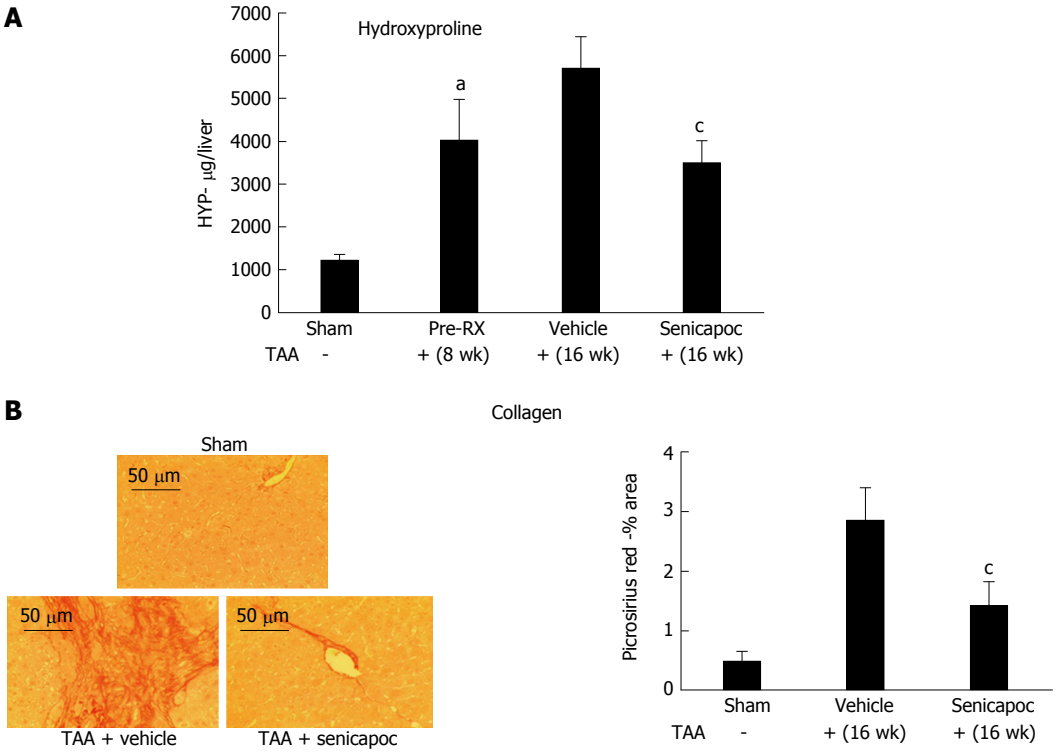

Figure 2 Senicapoc is anti-fibrotic in toxin-induced liver disease. A: Eight weeks after administration of TAA, livers exhibited increased hydroxyproline (collagen) content ($^{a}P < 0.05$ *vs* sham). Animals randomized to Senicapoc between weeks 8 and 16, exhibited reduced liver fibrosis at week 16 ($^{c}P < 0.05$ *vs* TAA + vehicle). B: Picosirus red stained livers (20 ×) from representative sham, TAA + vehicle or TAA + Senicapoc-treated animals (16 wk TAA; 8 wk drug) are shown. Intervention with Senicapoc reduced hepatic collagen accumulation ($^{c}P < 0.05$ *vs* TAA + vehicle).

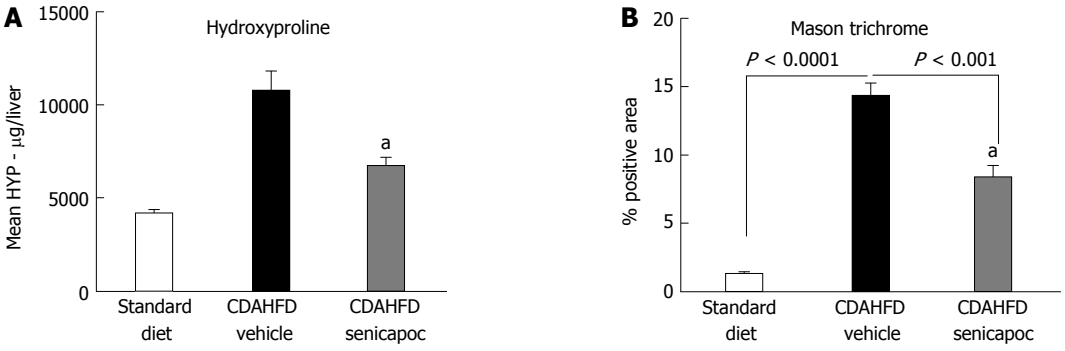

Figure 3 Senicapoc is anti-fibrotic in diet-induced liver disease. In animals randomized to Senicapoc for 4 wk after 4 wk on CDAHFD (total 8 wk on diet), A: measurement of liver hydroxyproline, a readout of tissue collagen; and B: analysis of Masson's trichrome showed that Senicapoc decreases liver fibrosis. $^{a}P < 0.05$ *vs* vehicle.

at least, in part, *via* a reduction in liver lipid levels. To this end, we first compared NAS and steatosis (0 to 3 scale) in CDAHFD (8 wk) animals randomized to vehicle or Senicapoc (weeks 4 through 8). Intervention with Senicapoc, reduced both NAS (Figure 4A) and steatosis (Figure 4B). Next, we evaluated the effect of Senicapoc on liver triglycerides, the main form of fat stored in the liver. Intervention with Senicapoc reduced hepatic triglyceride content (Figure 4C) in the CDAHFD model.

Lipid accumulation occurring in NAFLD can trigger a cascade including hepatocyte apoptosis, hepatic inflammation and extracellular matrix deposition. The effect of Senicapoc on steatosis was further investigated in models of diet-induced liver disease. In animals fed CDAHFD for 7 d and concomitantly treated with Senicapoc, a reduction in NAS was observed in comparison to the CDAHFD+vehicle cohort (Figure 5A). Again, Senicapoc reduced steatosis (Figure 5B). To further verify this effect of Senicapoc on hepatic lipid homeostasis, we analyzed the lipid vacuole area in hepatic sections stained with H&E from vehicle and drug-treated animals. As seen in Figure 5C, treatment with Senicapoc was associated with decreased hepatic lipid vacuole area. Furthermore, Senicapoc reduced hepatic lipid peroxidation, a measure of macrophage

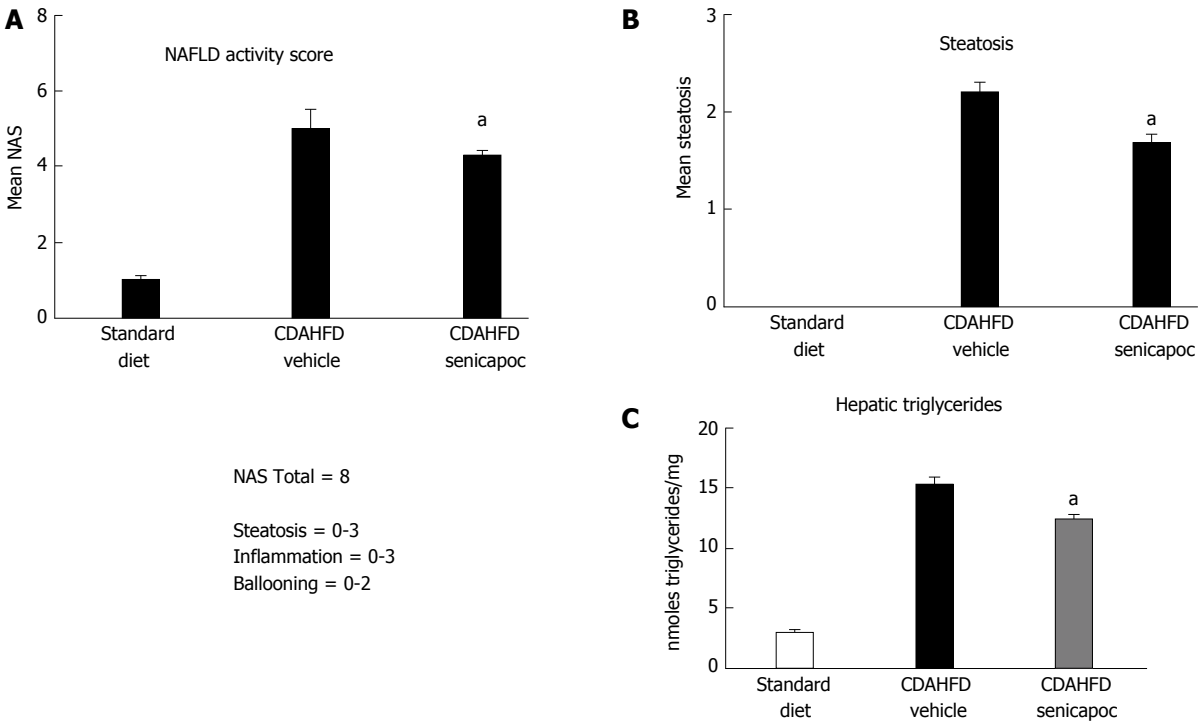

Figure 4 Intervention with Senicapoc is anti-steatotic in the CDAHFD Model. In animals randomized to Senicapoc for 4 wk after 4 wk on CDAHFD (total 8 wk on diet), A: Reduced NAS (0-8 scale); B: Reduced steatosis (0-3 scale); and (C) reduced accumulation of hepatic triglycerides was observed. $^{a}P < 0.05$ *vs* CDAHFD + vehicle.

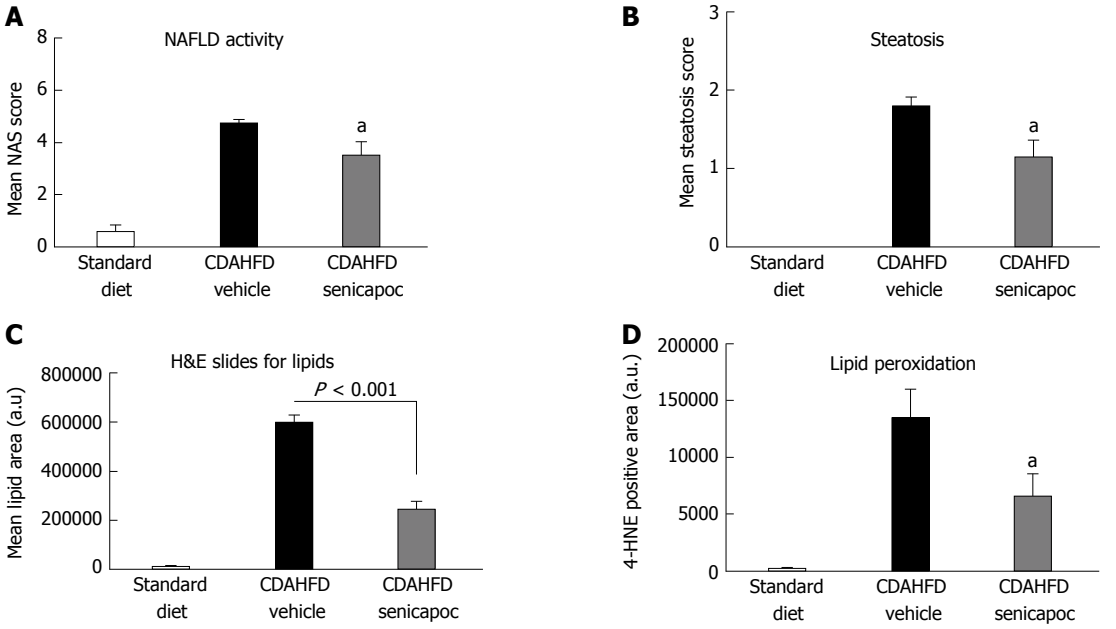

Figure 5 Senicapoc prevents steatosis in the CDAHFD Model. In animals fed CDAHFD for a week, co-treatment with Senicapoc, A: Decreased NAS (0-8 scale); B: Decreased steatosis (0-3 scale); C: Decreased the lipid vacuole area measured by planimetry in H&E-stained sections; and D: Treatment with Senicapoc reduced hepatic lipid peroxidation (4-HNE) observed in the CDAHFD + vehicle cohort. $^{a}P < 0.05$ *vs* vehicle.

oxidative burst and early inflammation as evidenced by 4-HNE staining (Figure 5D).

To confirm that the anti-steatotic effect of Senicapoc was not unique to the CDAHFD model, we evaluated use of this drug in the HFD model of NAFLD-NASH[18,19]. As seen in Figure 6A, treatment with Senicapoc reduced NAS observed in this model of metabolic insult. Senicapoc reduced steatosis (Figure 6B) which was also evident in the extent of Oil Red O staining of the liver (Figure 6C). Since 6 wk on this diet is sufficient to trigger an inflammatory response in the liver, we investigated whether the anti-steatotic

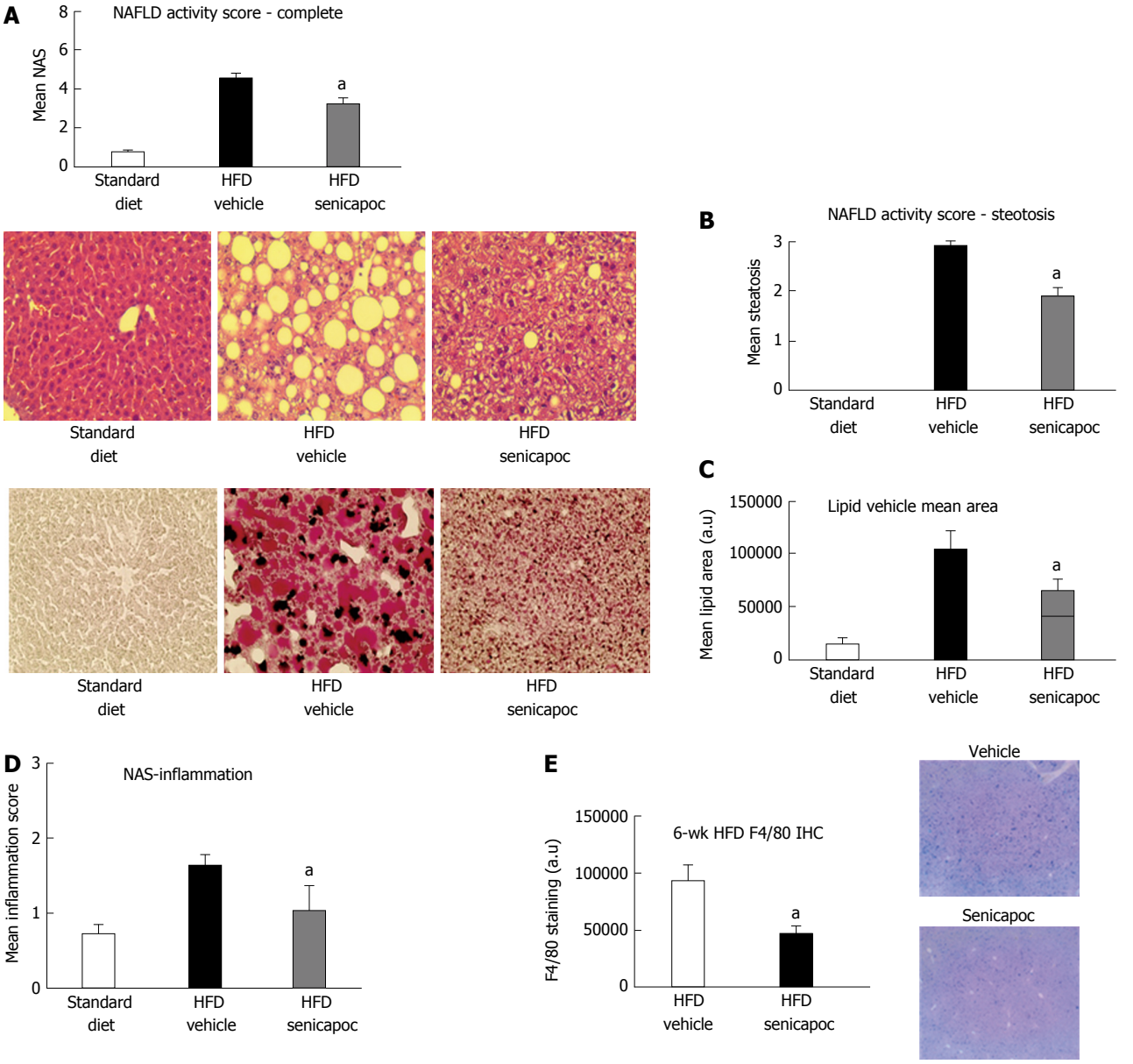

Figure 6 Senicapoc prevents steatosis in the high fat diet Model. In animals fed a HFD for 6 wk, co-treatment with Senicapoc, A: Reduced NAS (0-8 scale); B: Decreased steatosis [H&E-stained section (40 ×) on left, steatosis score on right]; C: Decreased hepatic lipid content (Oil Red O- stained section (40 ×) on left; lipid vesicular area right); D: Six weeks on HFD is associated with inflammation (0-3 scale) which is mitigated with Senicapoc; and E: Senicapoc reduces F4/80 staining, a marker of macrophage activity, in the liver. $^{a}P < 0.05$ *vs* vehicle. HFD: High fat diet.

effect of Senicapoc translates to a reduction in hepatic inflammation. Senicapoc reduced inflammation (Figure 6D, 0-3 scale) which was also evident by decreased hepatic F4/80 staining (Figure 6E), a marker of active macrophage population.

While lipid accumulation in hepatocytes is a critical event in the genesis and progression of fatty liver disease, hepatocytes overloaded with saturated free fatty acids such as palmitic acid undergo apoptosis[14,15]. Cell death is therefore a surrogate marker of hepatocyte lipid accumulation. We determined whether the anti-steatotic effect of Senicapoc translates to reduced apoptosis in eHpG2 cells challenged with increasing concentrations of palmitic acid. Senicapoc was without effect on cells alone (without palmitic acid; data not shown). As seen in Figure 7, at each concentration of palmitic acid tested, Senicapoc dose-dependently decreased HepG2 apoptosis.

DISCUSSION

Left untreated, NAFLD can progress to NASH, fibrosis, cirrhosis and decompensated liver failure. The continuum between steatosis, hepatitis and fibrosis lends itself to therapeutic intervention at any one of these nodes. This study is the first to demonstrate that Senicapoc, a KCa3.1 channel inhibitor, exerts an anti-fibrotic effect in the liver and that in diet-induced liver disease this anti-fibrotic effect is mediated *via* a reduction in steatosis.

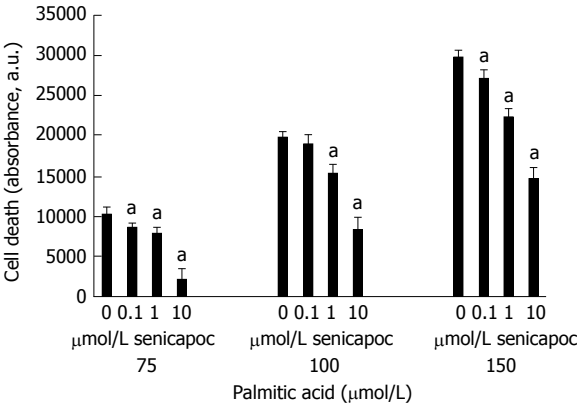

Figure 7 Senicapoc prevents lipid-induced apoptosis. HepG2 cells were treated with Senicapoc (0-10 μmol/L) and then loaded with palimitic acid (75-150 μmol/L). Following overnight incubation, apoptosis was measured using the Caspase Glo assay. Treatment with Senicapoc decreased palmitic acid-driven HepG2 cell death [$^{a}P < 0.05$ *vs* corresponding control (0 μmol/L Senicapoc) at each concentration of palmitic acid].

Given the obesity, diabetes and metabolic syndrome epidemics, in the United States alone approximately 81 million people are suspected to have some underlying steatosis; approximately 16 million people are suspected to have NASH of which approximately 5 million are suspected to have NASH with fibrosis[1]. Left untreated, the disease can progress to cirrhosis and decompensated liver failure. Non-clinical and clinical reports[2,3] indicate that in this form of liver disease there is continuum from steatosis to inflammation to fibrosis. In an elegant proof-of-concept study[22], mice fed a fatty diet for 49 wk, presented with steatosis but not inflammation at 8 wk, progressed to steatohepatitis and early fibrosis at 27 wk and then to steatohepatitis, fibrosis and hepatocellular carcinoma by week 49. The investigators hypothesized that the gradual progression to fibrosis associated with prolonged metabolic insult results from "multiple hits" including steatosis and activation of pathways involving inflammatory cytokines and inflammatory cells. In a clinical sample set, Leandro *et al*[23] reported that the association between steatosis and fibrosis invariably was dependent on a simultaneous association between steatosis and hepatic inflammation. Together, these findings suggest that the fibrotic program secondary to metabolic insult can be interrupted at a number of nodes including steatosis.

There is increasing recognition of the role ion channels play in both health and disease (channelopathies) and in the modulation of these channels to therapeutic benefit[2,3,24]. Freise *et al*[7] was the first to report that the KCa3.1 channel is upregulated in activated HSCs and the fibrotic liver and that the KCa3.1 inhibitor TRAM-34 blocks proliferation and TGF-β1-induced activation of HSCs and reduces portal hypertension in cholestatic liver disease. This group of investigators argued that KCa3.1 inhibition may provide a novel therapeutic rationale for treatment of progressive hepatic fibrosis and recommended further study of the therapeutic potential of this target in other models of hepatic fibrosis. Consistent with these findings, we found that KCa3.1 channel expression is indeed upregulated in liver disease. In fact, this phenomenon is independent of disease etiology as channel upregulation was observed in 3 distinct models of liver disease viz. diet-, cholestasis- and toxin-induced. To the best of our knowledge, this study is the first to report hepatic KCa3.1 channel expression in metabolic insult-induced liver disease.

Unlike clotrimazole or TRAM-34 that are accompanied by severe cytochrome P450 liability[1], Senicapoc is a clinical trial ready, potent (IC_{50} 6-20 nmol/L) and selective (IC_{50} > 1 μmol/L for Kv1.5, hERG, Na (tetrodotoxin-sensitive), IKs, KvLQT and h-H1) blocker of the KCa3.1 channel[24]. Senicapoc was safe and generally well tolerated in multiple clinical trials involving healthy volunteers or patients with sickle cell anemia or asthma over a dosing period of up to 1 year[10-13]. It has a half-life of approximately 13 d in human. Clinical development of this compound for sickle cell anemia was discontinued for lack of efficacy and not safety[9].

Based on the afore-referenced findings of KCa3.1 channel upregulation in liver disease and successful intervention with a KCa3.1 inhibitor, the objective of the present study was to evaluate the effects of Senicapoc on the progression of fatty liver disease. Specifically, we sought to determine whether Senicapoc mitigates liver disease, at least, in part, *via* reducing steatosis. Our findings from both the cell culture studies and the *in vivo* studies support this notion. Palmitic acid is a major form of fatty acid stored in the body. Multiple studies have shown a direct relation between uptake of palmitic acid and hepatocyte and HeG2 cell death[14,25]. While we did not measure lipid accumulation in HepG2 cells, their protection from palmitic acid-induced death by.

Senicapoc is a surrogate for the anti-steatotic activity of this drug. Our results from diet-induced, but mechanistically distinct, models of fatty liver disease suggest that Senicapoc decreases lipid accumulation within the liver. The aggressive CDAHFD model has been demonstrated to mimic human NASH in rodents by sequentially producing steatohepatitis and liver fibrosis[22]. Steatosis in this model is more than likely a defect in the export of triglycerides from the liver to peripheral tissue[22]. The HFD model by contrast is associated primarily with a more gradual accumulation of lipid within the hepatocytes followed by inflammation. Liver fibrosis in this model takes months to appear and is manifest with picrosirius red staining as a fine filigree network rather than a bridging phenotype[19]. Senicapoc's effect on lipid accumulation in both models appears to be very consistent as evinced by multiple different readouts including cell apoptosis, NAS, lipid vacuole measurement (H&E), lipid

content measurement (Oil Red O) and liver triglycerides across the diet-induced models studied. In fact, these anti-steatotic effects are consistent with similar effects of TRAM-34 on the development of lipid-rich lesions within the vascular bed of atherosclerosis-prone mice[8]. Furthermore, associated with this reduction in hepatic steatosis by Senicapoc was a reduction in markers of hepatic inflammation - the inflammatory component of NAS, 4-HNE and F4/80. While the present study did not seek to determine whether this anti-inflammatory effect derived from the upstream anti-steatotic effect or was a direct effect of KCa3.1 inhibition on Kupffer cells as reported previously, our results with Senicapoc are in line with that of TRAM-34 in a model of murine airway inflammation and remodeling[26]. In that study, TRAM-34 inhibited the generation and maintenance of inflammation and subepithelial extracellular matrix deposition.

The other major finding in this study was that Senicapoc mitigates hepatic collagen accumulation evidenced in two etiologically distinct models of liver fibrosis viz. diet- and toxin-induced. Importantly, these effects of Senicapoc were interventional since animals on the CDAHFD for 4 wk exhibited significant liver pathology prior to initiation of therapy and livers from TAA-treated animals exhibited fibrosis prior to randomization. This anti-fibrotic effect of Senicapoc appears to derive from both its anti-steatotic effect, evidenced in the CDAHFD model as well as a direct anti-fibrotic effect, evidenced in the TAA study. While association between steatosis, inflammation and fibrosis has been documented and observed in the present study, the direct anti-fibrotic effects of Senicapoc might relate to an effect of KCa3.1 channel inhibitors on hepatic stellate cells (HSCs). Freise *et al*[25] reported that KCa3.1 inhibition with TRAM-34 reduced HSC proliferation by induction of cell cycle arrest and reduced TGF-β1- induced gene expression of collagen Ⅰ, α-SMA and TGF-β1 itself. Furthermore, TRAM-34 blocked TGF-β1-induced activation of TGF-β1 signaling in HSCs.

In conclusion, together, our study and data suggests that Senicapoc interrupts more than one node in progressive fatty liver disease, perhaps serving as a double-edged therapeutic sword.

COMMENTS

Background

Nonalcoholic steatohepatitis (NASH), a potentially serious form of the disease due to liver inflammation, which may progress to scarring and irreversible damage. This damage is similar to the damage caused by heavy alcohol use. In severe cases NASH can progress to cirrhosis and liver failure risk factors being obesity, diabetes and aging. Nonalcoholic fatty liver disease (NAFLD) is increasingly common around the world, especially in Western nations. In the United States, it is the most common form of chronic liver disease, affecting an estimated 80 to 100 million people.

Research frontiers

Given the large numbers of people with fatty livers and the generally increased life expectancy even relatively indolent steatosis can result in a significant population progressing to NASH, NASH with fibrosis and finally cirrhosis. The development of new therapies that prevent the transition from steatosis and inflammation to fibrosis would have substantial clinical value.

Innovations and breakthroughs

The authors report for the first time that a KCa3.1 channel inhibitor exerts an anti-steatotic effect in the setting of fatty liver disease which can be harnessed for the treatment of liver fibrosis. Second, we are the first to report that Senicapoc, a drug that has been through Phase III clinical trials, can be repurposed for the treatment of fatty liver disease and potentially for the treatment of other lipid disorders.

Applications

Based on its selectivity for the KCa3.1 channel, its half-life in humans, it's highly favorable safety profile and its activity against steatosis, Senicapoc is an ideal candidate to be repurposed for NASH or other lipid-related disorders.

Terminology

The continuum between steatosis, hepatitis, fibrosis and cirrhosis lends itself to therapeutic intervention at any one of these nodes. This study is the first to demonstrate that Senicapoc, a KCa3.1 channel inhibitor, exerts an anti-fibrotic effect in the liver and that in diet-induced liver disease this anti-fibrotic effect is mediated *via* a reduction in steatosis.

Peer-review

The authors aimed to determine the anti-fibrotic effects of Senicapoc (a KCa3.1 channel inhibitor) in different animal models. Senicapoc therapeutic effect seems to be mediated by a reduction in steatosis suggesting that fat accumulation in the hepatocytes might be directly related to the development of inflammation and in turn of fibrosis. The authors conclude that Senicapoc could be a good candidate for the treatment of NASH for the improvement of both steastosis and fibrosis.

REFERENCES

1 **Sanyal AJ**, Friedman SL, McCullough AJ, Dimick-Santos L; American Association for the Study of Liver Diseases; United States Food and Drug Administration. Challenges and opportunities in drug and biomarker development for nonalcoholic steatohepatitis: findings and recommendations from an American Association for the Study of Liver Diseases-U.S. Food and Drug Administration Joint Workshop. *Hepatology* 2015; **61**: 1392-1405 [PMID: 25557690 DOI: 10.1002/hep.27678]

2 **Spengler EK**, Loomba R. Recommendations for Diagnosis, Referral for Liver Biopsy, and Treatment of Nonalcoholic Fatty Liver Disease and Nonalcoholic Steatohepatitis. *Mayo Clin Proc* 2015; **90**: 1233-1246 [PMID: 26219858 DOI: 10.1016/j.mayocp.2015.06.013]

3 **Wulff H**, Castle NA. Therapeutic potential of KCa3.1 blockers: recent advances and promising trends. *Expert Rev Clin Pharmacol* 2010; **3**: 385-396 [PMID: 22111618 DOI: 10.1586/ecp.10.11]

4 **Wulff H**, Kolski-Andreaco A, Sankaranarayanan A, Sabatier JM, Shakkottai V. Modulators of small- and intermediate-conductance calcium-activated potassium channels and their therapeutic indications. *Curr Med Chem* 2007; **14**: 1437-1457 [PMID: 17584055]

5 **Di L**, Srivastava S, Zhdanova O, Ding Y, Li Z, Wulff H, Lafaille M, Skolnik EY. Inhibition of the K+ channel KCa3.1 ameliorates T cell-mediated colitis. *Proc Natl Acad Sci USA* 2010; **107**: 1541-1546 [PMID: 20080610 DOI: 10.1073/pnas.0910133107]

6 **Huang C**, Shen S, Ma Q, Chen J, Gill A, Pollock CA, Chen XM. Blockade of KCa3.1 ameliorates renal fibrosis through the TGF-β1/Smad pathway in diabetic mice. *Diabetes* 2013; **62**: 2923-2934 [PMID: 23656889 DOI: 10.2337/db13-0135]

7 **Freise C**, Heldwein S, Erben U, Hoyer J, Köhler R, Jöhrens K, Patsenker E, Ruehl M, Seehofer D, Stickel F, Somasundaram R.

K^+ -channel inhibition reduces portal perfusion pressure in fibrotic rats and fibrosis associated characteristics of hepatic stellate cells. *Liver Int* 2015; **35**: 1244-1252 [PMID: 25212242 DOI: 10.1111/liv.12681]

8 **Toyama K**, Wulff H, Chandy KG, Azam P, Raman G, Saito T, Fujiwara Y, Mattson DL, Das S, Melvin JE, Pratt PF, Hatoum OA, Gutterman DD, Harder DR, Miura H. The intermediate-conductance calcium-activated potassium channel KCa3.1 contributes to atherogenesis in mice and humans. *J Clin Invest* 2008; **118**: 3025-3037 [PMID: 18688283 DOI: 10.1172/JCI30836]

9 PF-05416266 (senicapoc; ICA-17043). Available from: URL: https://ncats.nih.gov/files/PF-05416266.pdf

10 **Ataga KI**, Reid M, Ballas SK, Yasin Z, Bigelow C, James LS, Smith WR, Galacteros F, Kutlar A, Hull JH, Stocker JW; ICA-17043-10 Study Investigators. Improvements in haemolysis and indicators of erythrocyte survival do not correlate with acute vaso-occlusive crises in patients with sickle cell disease: a phase III randomized, placebo-controlled, double-blind study of the Gardos channel blocker senicapoc (ICA-17043). *Br J Haematol* 2011; **153**: 92-104 [PMID: 21323872 DOI: 10.1111/j.1365-2141.2010.08520.x]

11 **Ataga KI**, Smith WR, De Castro LM, Swerdlow P, Saunthararajah Y, Castro O, Vichinsky E, Kutlar A, Orringer EP, Rigdon GC, Stocker JW; ICA-17043-10 Study Investigators. Efficacy and safety of the Gardos channel blocker, senicapoc (ICA-17043), in patients with sickle cell anemia. *Blood* 2008; **111**: 3991-3997 [PMID: 18192510 DOI: 10.1182/blood-2007-08-110098]

12 **Ataga KI**, Stocker J. Senicapoc (ICA-17043): a potential therapy for the prevention and treatment of hemolysis-associated complications in sickle cell anemia. *Expert Opin Investig Drugs* 2009; **18**: 231-239 [PMID: 19236269 DOI: 10.1517/13543780802708011]

13 **Minniti CP**, Wilson J, Mendelsohn L, Rigdon GC, Stocker JW, Remaley AT, Kato GJ. Anti-haemolytic effect of senicapoc and decrease in NT-proBNP in adults with sickle cell anaemia. *Br J Haematol* 2011; **155**: 634-636 [PMID: 21651507 DOI: 10.1111/j.1365-2141.2011.08757.x]

14 **Shan X**, Miao Y, Fan R, Song C, Wu G, Wan Z, Zhu J, Sun G, Zha W, Mu X, Zhou G, Chen Y. Suppression of Grb2 expression improved hepatic steatosis, oxidative stress, and apoptosis induced by palmitic acid in vitro partly through insulin signaling alteration. *In Vitro Cell Dev Biol Anim* 2013; **49**: 576-582 [PMID: 23771793 DOI: 10.1007/s11626-013-9646-9]

15 **Yao HR**, Liu J, Plumeri D, Cao YB, He T, Lin L, Li Y, Jiang YY, Li J, Shang J. Lipotoxicity in HepG2 cells triggered by free fatty acids. *Am J Transl Res* 2011; **3**: 284-291 [PMID: 21654881]

16 **Kawazoe Y**, Miyauchi M, Nagasaki A, Furusho H, Yanagisawa S, Chanbora C, Inubushi T, Hyogo H, Nakamoto T, Suzuki K, Moriwaki S, Tazuma S, Niida S, Takata T. Osteodystrophy in Cholestatic Liver Diseases Is Attenuated by Anti-γ-Glutamyl Transpeptidase Antibody. *PLoS One* 2015; **10**: e0139620 [PMID: 26418133 DOI: 10.1371/journal.pone.0139620]

17 **Traber PG**, Chou H, Zomer E, Hong F, Klyosov A, Fiel MI, Friedman SL. Regression of fibrosis and reversal of cirrhosis in rats by galectin inhibitors in thioacetamide-induced liver disease. *PLoS One* 2013; **8**: e75361 [PMID: 24130706 DOI: 10.1371/journal.pone.0075361]

18 **Ganz M**, Bukong TN, Csak T, Saha B, Park JK, Ambade A, Kodys K, Szabo G. Progression of non-alcoholic steatosis to steatohepatitis and fibrosis parallels cumulative accumulation of danger signals that promote inflammation and liver tumors in a high fat-cholesterol-sugar diet model in mice. *J Transl Med* 2015; **13**: 193 [PMID: 26077675 DOI: 10.1186/s12967-015-0552-7]

19 **Huang B**, Abbott NAE, Dacon L, McCormack ES, Zhou P, Zhang L, Duan B, Li J, Zhang B, Yamin M,Paka L, Goldberg ID, Narayan P. Acute Injury in Natural Diet-Induced Fatty Livers - A Model for Therapy Development. *Recent Patents on Biomarkers* 2015; **5**: 101-107

20 **Zhang GB**, Song YN, Chen QL, Dong S, Lu YY, Su MY, Liu P, Su SB. Actions of Huangqi decoction against rat liver fibrosis: a gene expression profiling analysis. *Chin Med* 2015; **10**: 39 [PMID: 26691002 DOI: 10.1186/s13020-015-0066-5]

21 **Ronis MJ**, Hennings L, Stewart B, Basnakian AG, Apostolov EO, Albano E, Badger TM, Petersen DR. Effects of long-term ethanol administration in a rat total enteral nutrition model of alcoholic liver disease. *Am J Physiol Gastrointest Liver Physiol* 2011; **300**: G109-G119 [PMID: 21051528 DOI: 10.1152/ajpgi.00145.2010]

22 **Matsumoto M**, Hada N, Sakamaki Y, Uno A, Shiga T, Tanaka C, Ito T, Katsume A, Sudoh M. An improved mouse model that rapidly develops fibrosis in non-alcoholic steatohepatitis. *Int J Exp Pathol* 2013; **94**: 93-103 [PMID: 23305254 DOI: 10.1111/iep.12008]

23 **Leandro G**, Mangia A, Hui J, Fabris P, Rubbia-Brandt L, Colloredo G, Adinolfi LE, Asselah T, Jonsson JR, Smedile A, Terrault N, Pazienza V, Giordani MT, Giostra E, Sonzogni A, Ruggiero G, Marcellin P, Powell EE, George J, Negro F; HCV Meta-Analysis (on) Individual Patients' Data Study Group. Relationship between steatosis, inflammation, and fibrosis in chronic hepatitis C: a meta-analysis of individual patient data. *Gastroenterology* 2006; **130**: 1636-1642 [PMID: 16697727 DOI: 10.1053/j.gastro.2006.03.014]

24 **Stocker JW**, De Franceschi L, McNaughton-Smith GA, Corrocher R, Beuzard Y, Brugnara C. ICA-17043, a novel Gardos channel blocker, prevents sickled red blood cell dehydration in vitro and in vivo in SAD mice. *Blood* 2003; **101**: 2412-2418 [PMID: 12433690 DOI: 10.1182/blood-2002-05-1433]

25 **Alkhouri N**, Dixon LJ, Feldstein AE. Lipotoxicity in nonalcoholic fatty liver disease: not all lipids are created equal. *Expert Rev Gastroenterol Hepatol* 2009; **3**: 445-451 [PMID: 19673631 DOI: 10.1586/egh.09.32]

26 **Yu ZH**, Xu JR, Wang YX, Xu GN, Xu ZP, Yang K, Wu DZ, Cui YY, Chen HZ. Targeted inhibition of KCa3.1 channel attenuates airway inflammation and remodeling in allergic asthma. *Am J Respir Cell Mol Biol* 2013; **48**: 685-693 [PMID: 23492185 DOI: 10.1165/rcmb.2012-0236OC]

P- Reviewer: Rosso C **S- Editor**: Gong ZM **L- Editor**: A
E- Editor: Zhang FF

World Journal of Gastroenterology

Submit a Manuscript: http://www.f6publishing.com

World J Gastroenterol 2017 June 21; 23(23): 4191-4199

DOI: 10.3748/wjg.v23.i23.4191

ISSN 1007-9327 (print) ISSN 2219-2840 (online)

ORIGINAL ARTICLE

Basic Study

Induction of chronic cholestasis without liver cirrhosis - Creation of an animal model

Felix Dondorf, René Fahrner, Michael Ardelt, Eleonora Patsenker, Felix Stickel, Uta Dahmen, Utz Settmacher, Falk Rauchfuß

Felix Dondorf, René Fahrner, Michael Ardelt, Uta Dahmen, Utz Settmacher, Falk Rauchfuß, Department of General, Visceral and Vascular Surgery, Jena University Hospital, 07747 Jena, Germany

Eleonora Patsenker, Felix Stickel, Division of Gastroenterology and Hepatology, University Hospital Zürich, 8091 Zürich, Switzerland

Author contributions: Dondorf F, Settmacher U and Rauchfuß F designed the study; Dondorf F, Fahrner R, Patsenker E, Stickel F, Dahmen U and Rauchfuß F performed the data acquisition; Dondorf F, Settmacher U and Rauchfuß F analyzed the data; Dondorf F and Rauchfuß F wrote the paper; Fahrner R, Ardelt M, Settmacher U and Rauchfuß F revised the paper.

Institutional review board statement: Since this study is an animal research project, an institutional review board statement is not needed in our institution.

Institutional animal care and use committee statement: All animal experiments were approved by the Thuringian State Office of Food Safety and Consumer Protection (Department Consumer Protection, Veterinary and Pharmacy, Bad Langensalza, Germany). Protocol number: 02-039/12.

Conflict-of-interest statement: All authors have no conflicts of interest or financial ties to disclose.

Data sharing statement: The technical appendix and dataset are available from the corresponding author at felix.dondorf@med.uni-jena.de.

Manuscript source: Invited manuscript

Correspondence to: Falk Rauchfuß, MD, MSc, Department of General, Visceral and Vascular Surgery, Jena University Hospital, Am Klinikum 1, 07747 Jena, Germany. falk.rauchfuss@med.uni-jena.de
Telephone: +49-3641-9322601
Fax: +49-3641-9322602

Received: December 27, 2016
Peer-review started: December 28, 2016
First decision: February 10, 2017
Revised: February 27, 2017
Accepted: May 9, 2017
Article in press: May 9, 2017
Published online: June 21, 2017

Abstract

AIM

To analyze time intervals of inflammation and regeneration in a cholestatic rat liver model.

METHODS

In 36 Lewis rats, divided into six groups of 6 animals (postoperative observation periods: 1, 2, 3, 4, 6, 8 wk), the main bile duct was ligated with two ligatures and observed for the periods mentioned above. For laboratory evaluation, cholestasis parameters (bilirubin, γ-GT), liver cell parameters (ASAT, ALAT) and liver synthesis parameters (quick, albumin) were determined. For histological analysis, HE, EvG, ASDCL and HMGB-1 stainings were performed. Furthermore, we used the mRNA of IL-33, GADD45a and p-21 for analyzing cellular stress and regeneration in cholestatic rats.

RESULTS

In chemical laboratory and histological evaluation, a distinction between acute and chronic cholestatic liver injury with identification of inflammation and regeneration could be demonstrated by an increase in cholestasis (bilirubin: 1-wk group, 156.83 ± 34.12 μmol/L, P = 0.004) and liver cell parameters (ASAT: 2-wk group, 2.1 ± 2.19 μmol/L.s, P = 0.03; ALAT: 2-wk group, 1.03 ± 0.38 μmol/L.s, P = 0.03) after bile duct ligation (BDL). Histological evaluation showed an increase of bile ducts per portal field (3-wk group, 48 ± 6.13, P = 0.004) during the first four weeks after bile duct ligation. In addition to inflammation, which is an expression of acute cholestasis, there was an increase of necrotic areas in the histological sections (2-wk group, 1.38% ± 2.28% per slide, P = 0.002). Furthermore, the inflammation could be verified by ASDCL (4-wk group, 22 ± 5.93 positive cells per portal field, P = 0.041) and HMGB-1 [2-wk group, 13 ± 8.18 positive cells per field of view (FoV), P = 0.065] staining. Therefore, in summary of the laboratory evaluation and histological studies, acute cholestasis could be found during the first four weeks after bile duct ligation. Subsequently, the described parameters declined so that chronic cholestasis could be assumed. For quantification of secondary biliary cirrhosis, eosin staining was performed, which did not reveal any signs of liver remodeling, thus precluding the development of a chronic cholestasis model. Additionally, to establish the chronic cholestasis model, we evaluated liver regeneration capacity through measurements of IL-33, p-21 and GADD45a mRNA.

CONCLUSION

We created a chronic cholestasis model. The point of inflammatory and regenerative balance was reached after four weeks. This finding should be used for experimental approaches dealing with chronic cholestatic liver damage.

Key words: Rats; Cholestasis; Chronic cholestasis; Rat liver model

Core tip: Animal research models mostly address either acute cholestasis or secondary biliary cirrhosis, neither of which reflect the clinical reality of central liver tumors with cholestatic liver damage without secondary liver cirrhosis. In this work, we present our data from a model simulating chronic cholestatic liver damage in an otherwise healthy liver.

Dondorf F, Fahrner R, Ardelt M, Patsenker E, Stickel F, Dahmen U, Settmacher U, Rauchfuß F. Induction of chronic cholestasis without liver cirrhosis - Creation of an animal model. *World J Gastroenterol* 2017; 23(23): 4191-4199 Available from: URL: http://www.wjgnet.com/1007-9327/full/v23/i23/4191.htm DOI: http://dx.doi.org/10.3748/wjg.v23.i23.4191

INTRODUCTION

Liver resection is performed as a first-line treatment for certain types of benign and malignant liver tumors, especially hepatocellular carcinoma (HCC), cholangiocellular carcinoma (CCC) and colorectal liver metastases. In most patients, this procedure can be performed safely with low morbidity and mortality. However, in a subgroup of patients with impaired regenerative capacity or in those undergoing extended resection, the risk of post-resection liver failure is significant[1,2].

Obstructive cholestasis is a well-known risk factor for complications after liver surgery. Thus, patients with cholestasis, for example, those with cancer of the extrahepatic bile ducts, are at greater risk for postoperative liver failure, sepsis, and death[3]. Cholestasis, which is often a symptom of central bile duct carcinoma, considerably disturbs liver function and regenerative ability and contributes to perioperative morbidity and mortality[4]. The clinical situation is usually characterized by subacute or chronic cholestasis. Condensed cholestasis increases the risk of postoperative hepatic insufficiency[5]. In 2007, Yokoyama *et al*[4] presented various theses on the pathophysiological background of attenuated regenerative response established by cholestasis, including decreased portal venous inflow, decreased production of proliferation associated factors, decreased or absent enterohepatic circulation, and an increased rate of apoptosis.

Rodent models have been established especially for hepatobiliary surgery experiments focusing on extended liver resections, additionally, rat models are often used for other experimental procedures, such as examination of liver regeneration after BDL (bile duct ligation)[6]. For larger animals, logistical, financial, and ethical conditions are particularly limiting. Therefore, these approaches play a minor role in the experimental setting of advanced liver resections[7]. Therefore, most of our knowledge about liver regeneration originates from studies of rats after 2/3 hepatectomy[7,8].

In experimental liver surgery, induction of cholestasis with subsequent treatment of liver regeneration is often used[9]. It is especially remarkable that models with induction of acute cholestasis are used in literature. There are no rat models of chronic cholestasis without induced secondary biliary cirrhosis found in the current literature.

To consider the acute phase of cholestatic liver damage and the transition to chronic hepatic parenchymal damage (fibrosis/cirrhosis), the establishment of a rat model is essential to approach clinical reality as closely as possible.

MATERIALS AND METHODS

Animals

Male Lewis rats (Charles River, Sulzfeld, Germany)

aged 11 ± 1.18 wk, with body weights of 310 ± 27 g, were kept under standard animal care conditions and were fed with rat chow and water ad libitum. Six animals were in each group (observation time 1, 2, 3, 4, 6 and 8 wk).

Surgery

For the implementation of anesthesia, isoflurane (3.0%-4.0%) in combination with oxygen (0.5 L/min) was used. After laparotomy, the main bile duct was separated and double ligated (Prolene 6-0, Ethicon, Norderstedt, Germany) at the liver hilum with secure protection of the pancreatic duct.

After the observation period (1, 2, 3, 4, 6 and 8 wk), the animals were harvested through blood collection (inferior caval vein), hepatectomy and subsequent exsanguination under anesthesia.

Body and liver weights

Animal body weights were measured before the operation, during the observation period (daily during the first post-operative week, and every second day afterwards) and before harvesting. The wet liver weight was measured after hepatectomy.

Laboratory measurements

The collected blood was analyzed to obtain the following parameters: bilirubin, ASAT, ALAT, γ-GT, quick, albumin. Collected blood samples were analyzed using ARCHITECT ci16200 (Abbott, Wiesbaden, Deutschland) and a Scil Vet ABC Hematology Analyzer (Scil Animal Care Company Inc., Viernheim, Germany).

Histologic examination

3-4 μm paraffin-embedded liver sections were stained using several methods: H&E (hematoxylin and eosin), EvG (van Gieson stain), ASDCL (Naphtol AS-D chloroacetate esterase) and HMGB-1 (high-mobility group box 1).

The images were scanned by the Digital Slide Scanner Nano Zoomer 2.0-HT (Hamamatsu Photonics, Herrsching am Ammersee, Germany) and were analyzed using the Histologic viewer NDP.view. 2.3.1 (Hamamatsu Photonics, Herrsching am Ammersee, Germany).

Furthermore, the histology examination program Histocad Virtual liver (Fraunhofer MEVIS, Bremen, Germany) was used[10].

mRNA analysis (p-21, GADD45a, IL-33)

Total RNA was isolated from 30 mg of snap frozen liver tissues using the RNeasy kit (Qiagen, Basel, Switzerland) according to the manufacturer's instructions. cDNA was transcribed from 1 μg of RNA using M-MLV reverse transcriptase (Invitrogen, Basel, Switzerland) with a random hexanucleotide mix (Roche). Quantitative real-time PCR was performed using an ABI 7700 sequence detector (Applied Biosystems, Rotkreuz, Switzerland). Primers and probe sequences for all genes measured came from ready-to-use kits produced by Applied Biosystems (Rotkreuz, Switzerland), for which the sequences were not provided. For normalization, the housekeeping gene glycerinaldehyd-3-phosphat-dehydrogenase (GAPDH) was amplified in a parallel reaction (5'-ACTGGCATGGCCTTCCG; 3'-CAGGCGGCACGTCAGATC; Probe - TTCCTACCCCCAATGTGTCCGTCGT).

Ethical consideration

Since this study is an animal research project, an institutional review board statement is not needed in our institution.

Animal care and use statement

The animal handling protocol was designed to minimize pain or discomfort to the animals. The animals were acclimatized to laboratory conditions for two weeks before experimentation. The animals were kept under defined conventional conditions (temperature: 19-21 ℃, humidity: 30%-70%, day-night cycle of 12 h with light changes at 6:00 am and 6:00 pm) with up to three animals per cage. The conditions were recorded hourly by sensor and were personally controlled daily.

The animals had access to food (1324 TPF - totally pathogen-free, Altromin) and water ad libitum. For the implementation of anesthesia, isoflurane (3.0%-4.0%) was used in combination with oxygen (0.5 L/min). All animals were euthanized by exsanguination under general anesthesia.

Statistical analysis

Data were presented as the mean ± SD. The results were analyzed using the non-parametric Mann-Whitney-*U*-Test. Differences between two groups with P values < 0.05 were considered statistically significant. For analysis, SPSS (IBM; Version 23.0.0.0) was used.

RESULTS

Body weight

The average preoperative body weight was 310 ± 27 g. Body weight loss was measured during the immediate postoperative course. The minimum body weight was 286 ± 21 g. Based on the preoperative body weight; a body weight loss percentage of 7.62% ± 2.46% was calculated. After four days, an increase in weight was recorded. Preoperative body weights were reached after 15 ± 2.55 d.

Laboratory measurements

Laboratory measurements are displayed in Table 1.

Necrosis

No extensive necrosis was detected in any animals. Nevertheless, a dynamic pattern was identified during

Table 1 Group-wise description of mean laboratory measurements + standard deviations (bilirubin, γ-GT, ASAT, ALAT, albumin, quick), laboratory measurements + standard deviation of IL-33, p-21 and GADD45a mRNA, mean measurements + standard deviation of histology

	Control	7 d	14 d	21 d	28 d	42 d	56 d
Bilirubin (μmol/L)	2 ± 0	156.83 ± 34.12	37.34 ± 54.39	43.6 ± 61.49	20.5 ± 38.02	20 ± 40.25	2 ± 0
		P = 0.004	*P* = 0.004	*P* = 0.008	*P* = 0.429	*P* = 0.690	*P* = 1.000
Albumin (g/L)	8.4 ± 0.89	5.83 ± 0.41	7 ± 1.09	7.6 ± 1.34	8 ± 1.22	9.25 ± 0.96	9.2 ± 0.84
		P = 0.004	*P* = 0.052	*P* = 0.421	*P* = 0.329	*P* = 0.690	*P* = 0.222
Quick (%)	127 ± 3.13	137 ± 10.33	126 ± 5.02	126 ± 8.94	128 ± 4.49	96 ± 30.89	107 ± 4.79
		P = 0.052	*P* = 1.000	*P* = 0.548	*P* = 0.429	*P* = 0.095	*P* = 0.016
ASAT (μmol/L.s)	0.91 ± 0.06	5.9 ± 0.66	2.1 ± 2.19	4.05 ± 2.55	1.9 ± 1.94	2.06 ± 1.82	1.07 ± 0.23
		P = 0.004	*P* = 0.030	*P* = 0.008	*P* = 0.009	*P* = 0.151	*P* = 0.095
ALAT (μmol/L.s)	0.74 ± 0.09	2.11 ± 0.29	1.03 ± 0.38	1.95 ± 0.48	1.09 ± 0.18	0.93 ± 0.24	0.96 ± 0.15
		P = 0.004	*P* = 0.030	*P* = 0.008	*P* = 0.004	*P* = 0.310	*P* = 0.032
γ-GT (μmol/L.s)	0.07 ± 0	0.4 ± 0.09	0.22 ± 0.36	0.35 ± 0.31	0.12 ± 0.11	0.12 ± 0.12	0.07 ± 0
		P = 0.004	*P* = 0.662	*P* = 0.151	*P* = 0.662	*P* = 0.690	*P* = 1.000
GADD45a (GADD45a/GAPDH mRNA)	1 ± 0.58	0.84 ± 0.15	0.91 ± 0.35	3.25 ± 0.36	2.37 ± 1	0.99 ± 0.38	0.9 ± 0.43
		P = 0.841	*P* = 0.931	*P* = 0.008	*P* = 0.030	*P* = 1.000	*P* = 0.393
p-21 (p21/GAPDH mRNA)	1 ± 0.64	7.06 ± 1.8	7.1 ± 2.55	1.93 ± 1.19	3.04 ± 1.33	1.52 ± 1.44	3.07 ± 1.24
		P = 0.008	*P* = 0.004	*P* = 0.151	*P* = 0.009	*P* = 0.841	*P* = 0.036
IL-33 (IL33/GAPDH mRNA)	1 ± 0.21	0.91 ± 0.2	1.33 ± 0.44	4.14 ± 1.93	2.41 ± 0.82	2.58 ± 0.17	1.23 ± 0.26
		P = 0.841	*P* = 0.329	*P* = 0.008	*P* = 0.004	*P* = 0.008	*P* = 0.036
Bile ducts (bile ducts per PF)		8 ± 0.65	17 ± 3.47	48 ± 6.13	14 ± 2.76	4 ± 0.24	5 ± 0.46
			P = 0.002	*P* = 0.004	*P* = 0.015	*P* = 0.126	*P* = 0.004
Necrosis (% per slide)		0.29 ± 0.14	1.38 ± 2.28	1.31 ± 1.03	0.47 ± 0.21	0.09 ± 0.07	0.21 ± 0.2
			P = 0.002	*P* = 0.004	*P* = 0.065	*P* = 0.004	*P* = 0.662
Fibrosis (% per slide)		1.09 ± 0.61	1.3 ± 0.9	1.22 ± 1.33	2.32 ± 1.67	1.76 ± 0.61	1.53 ± 0.83
			P = 1.000	*P* = 1.000	*P* = 0.132	*P* = 0.247	*P* = 1.000
ASDCL (PF) (positive cells per PF)		36 ± 5.38	43 ± 13	34 ± 2.15	22 ± 5.93	11 ± 1.74	6 ± 1.01
			P = 0.394	*P* = 0.931	*P* = 0.041	*P* = 0.004	*P* = 0.004
HMGB-1 (PF) (positive cells per PF)		17 ± 7.07	18 ± 7.67	12 ± 5.91	13 ± 5.2	8 ± 4.39	6 ± 3.78
			P = 0.394	*P* = 0.329	*P* = 0.310	*P* = 0.009	*P* = 0.004
HMGB-1 (SF) (positive cells per FoV)		25 ± 13.1	13 ± 8.18	10 ± 4.17	9 ± 8.43	5.4 ± 3.42	4 ± 3.09
			P = 0.065	*P* = 0.052	*P* = 0.002	*P* = 0.009	*P* = 0.004

P values of Mann-Whitney-*U*-Test ($P < 0.05$).

the period of observation. Specifically, during the first three weeks, an increase in the percentage of necrosis per section was seen. Subsequently, a decline of necrosis at week three was recorded (Table 1 and Figure 1).

Bile ducts

Quantifying the bile ducts, an increase in the number of bile ducts per portal field was seen during the first four weeks. Thereafter, from week 4, a decrease in recorded bile ducts per portal field was observed (Table 1, Figures 1 and 2).

Connective tissue/fibrosis/cirrhosis

To evaluate the formation of biliary cirrhosis, EvG staining was performed. During the entire observation period, an increase of connective tissue was shown with a maximum increase during the 4th wk after BDL. Subsequently, during the 6th to 8th wk groups, a slight reduction of connective tissue was seen in the liver (Table 1 and Figure 1).

ASDCL

Regarding neutrophil infiltration in the portal fields, an increase during the first week with maximal increase until the second postoperative week could be measured. Afterwards, a decrease in neutrophil infiltration was shown (Table 1 and Figure 1).

HMGB-1

Regarding evaluation of the portal fields, an increase of HMGB-1 positive cells could be seen during the first two weeks. Thereafter, counting revealed a transition period until the fourth postoperative week, after which a decrease of HMGB-1 positive cells was shown. In contrast to the results described above, the HMGB1-positive cells in liver tissue but not directly located near a portal field reached maximum levels seven days after BDL with a subsequent continuous decrease observed (Table 1 and Figure 1).

IL-33, p-21, GADD45a

Regarding p-21 mRNA in liver tissue, an increase could

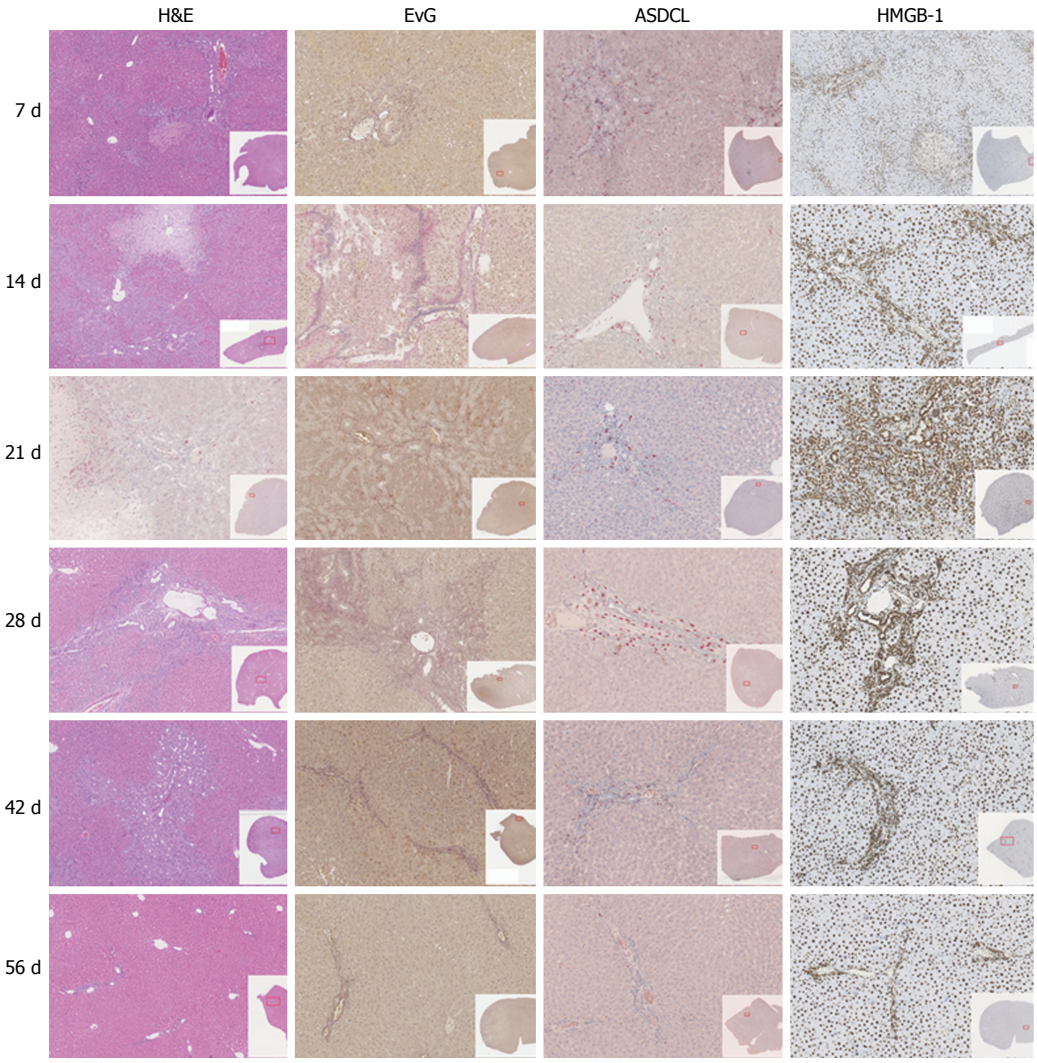

Figure 1 Graphics of histologic sections (H&E, EvG, ASDCL, HMGB-1), divided by group.

be measured seven days after BDL with a decline in p-21 values after four weeks, as seen in Table 1 and Figure 3. In contrast to p-21, the levels of GADD45a and IL-33 mRNA increased, reaching a peak 21 d after BDL (Table 1 and Figure 3).

DISCUSSION

This experimental study aimed to induce chronic cholestasis without the development of liver cirrhosis in a rodent model. We showed a balance between hepatic inflammation and liver regeneration four weeks after BDL. Thus, our work provides an important contribution to further experimental studies of chronic cholestatic liver damage.

Animals were followed up for 1-8 wk. These observation time points were chosen on the basis of the current literature. As described by Georgiev *et al*[11], the best time point to evaluate acute cholestatic liver injury after BDL in mice should be after one week. To evaluate chronic cholestatic injury after BDL, follow-up periods greater than 2 wk were selected. In a review by Marques *et al*[12], BDL was seen as a safer method for induction of cirrhosis in the rat compared to the use of carbon tetrachloride (CCl_4), which induces cirrhosis after 4-6 wk. Therefore, to exclude the possible transition to secondary biliary cirrhosis (which should be avoided in our setting), an observation period of up to eight weeks was selected.

It must be mentioned that there is a difference between the results of BDL and BDL + transection of the main bile duct. In 1957, Symeonidis *et al*[13] reported that there is a reconstitution of laboratory measurements and histologic findings after BDL in rats in contrast to the results after BDL with simultaneous transection between two ligatures. Wright *et al*[14] also found that there is a reconstitution of biliary flow after BDL in the rat.

Overall, with regard to this methodology, it can be stated that bile duct ligation or double bile duct ligation with subsequent separation of the bile duct between the ligatures would produce more clear results. However, there is no clinical relevance because in clinical practice, central liver tumors rarely lead to

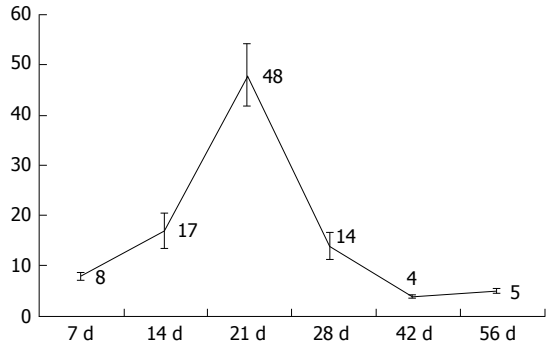

Figure 2 Bile duct quantification, mean bile ducts per portal field + standard deviations, divided by group.

rapid and complete occlusion of the extrahepatic bile ducts. In contrast, severe stenosis of the bile duct with residual flow is seen in clinical practice. Therefore, double ligature was performed without transecting the bile duct to establish potential relevance to clinical practice. In a subsequent study it could be interesting to compare both approaches (double ligation *vs* transection) but the direct comparison was not aim of the present work.

Measurements and monitoring of body weight after BDL showed a regain of body weight 2-4 d after BDL and a return to preoperative body weight after 15 d. Comparing this with the results of other research groups, similar time periods can be seen in rats after BDL[15-17]. Regarding liver weight, Geerts *et al*[18] observed an increase one week after BDL in a murine model, which was best achieved through ductal proliferation. Our data also showed an increase after one week with a peak after three weeks. This correlated with the bile duct measurements; therefore, the hypothesis of ductal proliferation is representative.

Additionally, Kountouras *et al*[15] noted an increase in bilirubin after BDL, which stabilized around the 15th postoperative day with subsequent decline. Symeonidis *et al*[13] assessed the same findings in 1957. In addition to these reports, Abdel-Aziz *et al*[19] detected the same changes in bilirubin after BDL. They noticed an acute cholestasis during the first week and a significant decline after two weeks of observation.

Regarding the development of cholestasis, it can be stated that cholestasis arises acutely during the first week after BDL and then changes into a chronic state. This was also described in a review by Marques *et al*[12] in 2012. During the development of acute cholestasis, transaminases also rose during the observation period. Laboratory measurements showed an increase of transaminase levels during the first week after BDL, and acute liver cell damage was clearly visible by way of cholestasis. Similar findings were also generated by Woolbright *et al*[20]. In a study by Lessa *et al*[21] an additional increase of transaminases during the third week after BDL was visible (but not significant), which was also detectable in our data. This phenomenon might be explained by the small number of animals in each group. Furthermore, a second process of cell injury or regeneration might lead to a release of transaminases, as at this time, markers of cellular stress and inflammation increased in tissue mRNA levels, and histological changes from caused by necrotic and regenerative processes were detected.

In addition to the liver cell damage, hepatic synthesis was restricted after BDL due to acute cholestasis, as represented by the serum albumin levels. Therefore, the results regarding these values displayed a reduction in albumin levels seven days after BDL, reflecting impaired synthesis due to acute cholestasis, with a subsequent increase in values over time. Additionally, Krähenbühl *et al*[17] described hypoalbuminemia after BDL in rat with a subsequent increase during the observation period. Contrary to the impaired albumin synthesis, the values of the hepatically metabolized clotting factors, measured by the quick value, remained stable throughout the entire observation period.

Histologic analysis, in correlation with the laboratory measurements, revealed inflammation during the first four weeks. During this time, levels of the proinflammatory cytokine IL-33 increased further, with a peak after day 21, followed by decline during subsequent weeks.

No significant rate of necrosis could be detected; however, a dynamic variation over time could be observed, with an increase during the first two weeks after BDL. This increase of necrotic areas in the stained sections can be seen as an expression of acute liver cell damage due to cholestasis. After three weeks, the reduction of necrosis can be interpreted as a reduction in acute injury caused by cholestasis. Additionally, Johnstone *et al*[22] were able to determine the formation of necrosis immediately after biliary obstruction, which reversed during follow up. Furthermore, the formation of necrosis was demonstrated by Prado *et al*[23] after BDL in mice. In the process of biliary obstruction, necrosis is the expression of dead liver cells resulting from an acute metabolic disorder, which depletes ATP[24].

The results of bile duct quantification with the described increase until the first four weeks of observation can be seen as a histologic manifestation of cholestasis, but the subsequent drop after four weeks must be discussed as a reconstitution of biliary flow despite BDL. Therefore, according to Steiner *et al*[25] and Cameron *et al*[26], an insufficient ligature must be considered in this discussion. Furthermore, the formation of new bile ducts in the area of ligature must also be discussed in this context.

The radiological cholangiography to examine this hypothesis was not performed in this study because the primary focus was placed on hepatic regeneration ability. Accordingly, radiological cholangiography by opening the bile ducts would have brought a possible change of data.

Wright *et al*[14] observed the formation of new bile

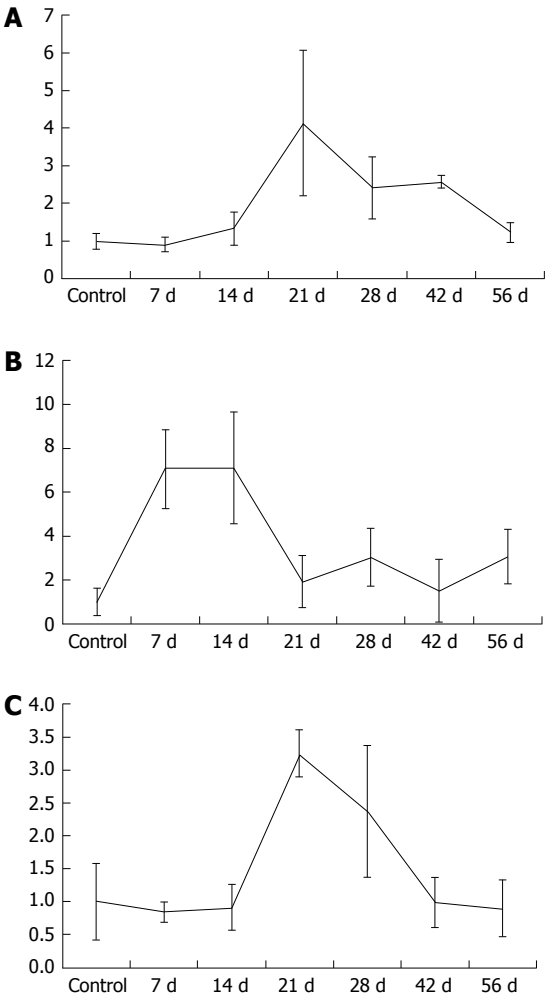

Figure 3 Mean laboratory, mean + SD of IL-33 (A), p-21 (B) and GADD45a (C) mRNA, divided by group.

ducts by using contrast agents, both proximal and distal to the ligature, and noticed the formation of new bile ducts around a sufficient ligature. According to the results of the research group, new bile ducts formed between the 14th and 20th d postoperatively with reconstruction of biliary flow from day 28, which is comparable to the findings reported in this work.

In their review from 2012, Marques *et al*[12] determined that cholestasis occurs two weeks after BDL in the rat, and after 4-6 wk, the transition to a secondary biliary cirrhosis could be seen. In contrast to that, Johnstone *et al*[22] could not find secondary biliary cirrhosis after double ligation of the bile duct after an observation period of 40 d.

The results of this study showed an increase in connective tissue during the period of observation with an increase in the fourth week, followed by a recorded decline in the six and eight-week groups. Overall, our findings indicate the incipient reconstruction of hepatic tissue after induction of cholestasis without the development of fibrosis.

There was a peak in the number of neutrophil granulocytes in the area of the portal fields after 14 d of observation period using ASDCL staining. This supports the hypothesis of an acute inflammatory reaction within the first two weeks after BDL, which regresses subsequently.

High mobility group box 1 acts as a mediator of early organ damage and inflammation[27]. Thus, HMGB-1 will be released from ischemic liver cells to mediate inflammation and damage[28]. In this context, a translocation of nuclear HMGB-1 can be seen in the cytoplasm as an important first step in response to damage[27]. Direct injury in the liver parenchyma was measured by an increase of HMGB-1 positive cells after seven days.

Comparable to our results, Woolbright *et al*[20]. also detected an increase of HMGB-1 immediately after BDL in mice and declared their results as an expression of the acute inflammatory response to cholestatic liver injury. In the present work, a decline of HMGB-1 positive cells was recorded during the subsequent observation period. This fact reveals that the HMGB-1 cytokine is one of the early responses to injury. Following the course of acute inflammation as mentioned above, these results clearly show that liver regeneration occurs after 2-3 wk during the observation period.

The role of p-21 in the regulation of liver regeneration is complex and not completely understood[29]. Several studies have shown that overexpression of p-21 can inhibit liver regeneration[29]. Furthermore, several genetic studies in mice confirmed the importance of p-21 for the regulation of liver regeneration as well as its ability to delay tumor development in the liver[30]. We detected an increase of p-21 immediately after BDL. We explain this up-regulation as a result of the acute cholestatic liver injury. Hui *et al*[29] demonstrated in 2002 that impaired liver regeneration is associated with up-regulation of the cyclin dependent kinase inhibitor p-21. Additionally, Lehmann *et al*[31] found that p-21 mediates a transient physiological barrier to the progression and completion of the cell cycle, thus inhibiting liver regeneration. We demonstrated that p-21 is a marker for impaired liver regeneration with up-regulation immediately after BDL. The decrease of p-21 after 14 d could be viewed as the reduction of inflammation and a shift to chronic cholestatic liver injury with liver regenerative capacity.

The results of the IL-33 and GADD45a mRNA in liver tissue after two weeks provide evidence of incipient chronic liver tissue damage. In correlation with the other recorded parameters, this hypothesis can be supported. According to the literature, up-regulated IL-33 can be seen in acute as well as in chronic liver injury. The first step of IL-33 up-regulation can be seen in acute liver injury, such that IL-33 has a function as an alarm protein[32]. The second up-regulation of IL-33 is described in chronic liver injury, and its positive correlation with liver fibrosis is revealed by the up-regulation of collagen expression[32-34]. We

could confirm these findings: IL-33 increases during chronic cholestasis, in correlation with the number of bile ducts and the increase of connective tissue observed in histological analysis.

Concerning the acute IL-33 up-regulation during the 24-48 h period[34], it must be critically noted that this was not addressed due to the study design, in which the first time point of measurement occurred seven days after BDL.

The growth arrest and DNA damage 45 (*GADD45*) family genes regulate DNA repair, the cell cycle, cell survival, apoptosis, senescence, and DNA demethylation within cells under various stress stimuli. The *GADD45* gene family encodes three proteins: GADD45A, GADD45B, and GADD45G[35]. The GADD45 genes are located on different chromosomes, and their cognate proteins are small, highly homologous, and localized to both the cell nucleus and cytoplasm[35]. The cellular senescence process involves several steps, including promotion of DNA damage, generating a DNA repair signal, eliciting permanent cell cycle arrest, and the final entry into senescence[35]. Therefore, according to literature, we conclude that GADD45a is part of the cellular senescence pathway. Accordingly, the up-regulation of GADD45a in chronic cholestatic rats can be seen as a kind of cellular senescence with a junction to an early sign of liver fibrosis.

Summarizing the present study in the overall context of experimental hepatobiliary surgery, it can be held that the work illuminates a significant aspect of liver parenchymal remodeling in the cholestatic liver. However, there are limitations to the work because the considered animal group is not compared with a group of BDL + transection. In our opinion, this limitation of the experimental setup is not essential toward achievement of the primary goal, as the model should be representative of chronic cholestasis. In clinical practice, chronic cholestasis plays a relevant role in a subgroup of patients undergoing liver resection. This issue has not yet been investigated in experimental designs. This investigation in a rat BDL model has revealed the first insights into this problem.

COMMENTS

Background

The aim of the present work was to develop an animal model with chronic cholestasis without inducing secondary biliary cirrhosis, in order to investigate liver conditioning with the following liver regeneration in this model (similar to the clinical situation).

Research frontiers

For the evaluation of new therapeutic approaches, in case of conditioning of the liver parenchyma, rodent models are offered. However, there are no defined approaches in rat models that represent a chronic cholestatic damage in a standardized way without the formation of a secondary biliary cirrhosis. In order to take account of the acute phase of cholestatic damage and a transition to chronic hepatic parenchyma damage, the establishment of a rat model is useful in order to approach the clinical reality as closely as possible.

Innovations and breakthroughs

In summary of all the parameters and histological results obtained in this work, an acute cholestasis with the following regeneration could be determined. An acute cholestasis was observed after 7 d. The inflammation parameters recorded during the first four weeks show an inflammation in the first 3 wk after cholestasis induction. Subsequently, a decrease in inflammation and tissue damage was observed, so that a regeneration of the cholestatic parenchyma can be assumed. Thus, a chronic cholestasis from the 3-4 wk after cholestasis induction was detected. This time is thus to be regarded as a transition from an acute to a chronic cholestasis, which was the primary question of the present work.

Applications

Overall, the authors were able to establish a chronic cholestastic rat model without inducing secondary biliary cirrhosis with this present study. It must be noted that the experimental work in the cholestatic liver is of great relevance for clinical practice in the establishment of new therapeutic concepts.

Terminology

Cholestasis refers to an accumulation of bile acid due to an obstruction of bile ducts or bile formation disorder. A distinction is made between acute and chronic cholestasis due to intra- and extrahepatic causes, with functional or mechanical genesis. Liver regeneration is significantly impaired by chronic cholestasis. Often patients with a central liver tumor have to be operated in the situation of cholestasis, with impaired liver regeneration capacity after liver resection, which results in increased morbidity as well as mortality due to postoperative hepatic failure.

Peer-review

The authors described an animal model of cholestasis and they evaluated parameters of parenchymal a biliary tree damage and regeneration. The text is brief and well-arranged.

REFERENCES

1 **Hammond JS**, Guha IN, Beckingham IJ, Lobo DN. Prediction, prevention and management of postresection liver failure. *Br J Surg* 2011; **98**: 1188-1200 [PMID: 21725970 DOI: 10.1002/bjs.7630]

2 **Rauchfuss F**, Scheuerlein H, Götz M, Dittmar Y, Voigt R, Heise M, Settmacher U. [Hepatocellular carcinoma and cholangiocarcinoma]. *Chirurg* 2010; **81**: 941-952; quiz 953 [PMID: 20827454 DOI: 10.1007/s00104-009-1864-z]

3 **Heinrich S**, Georgiev P, Weber A, Vergopoulos A, Graf R, Clavien PA. Partial bile duct ligation in mice: a novel model of acute cholestasis. *Surgery* 2011; **149**: 445-451 [PMID: 20817234 DOI: 10.1016/j.surg.2010.07.046]

4 **Yokoyama Y**, Nagino M, Nimura Y. Mechanism of impaired hepatic regeneration in cholestatic liver. *J Hepatobiliary Pancreat Surg* 2007; **14**: 159-166 [PMID: 17384907 DOI: 10.1007/s00534-006-1125-1]

5 **Heinrich S**, Lang H. [Primary liver tumors. Preoperative conditioning of the liver and perioperative management in extended liver resection]. *Chirurg* 2015; **86**: 125-131 [PMID: 25673223 DOI: 10.1007/s00104-014-2881-0]

6 **Rodríguez-Garay EA**. Cholestasis: human disease and experimental animal models. *Ann Hepatol* 2003; **2**: 150-158 [PMID: 15115953]

7 **Palmes D**, Spiegel HU. Animal models of liver regeneration. *Biomaterials* 2004; **25**: 1601-1611 [PMID: 14697862]

8 **Mao SA**, Glorioso JM, Nyberg SL. Liver regeneration. *Transl Res* 2014; **163**: 352-362 [PMID: 24495569 DOI: 10.1016/j.trsl.2014.01.005]

9 **Lin SY**, Wang YY, Chen WY, Chuang YH, Pan PH, Chen CJ. Beneficial effect of quercetin on cholestatic liver injury. *J Nutr Biochem* 2014; **25**: 1183-1195 [PMID: 25108658 DOI: 10.1016/j.jnutbio.2014.06.003]

10 **Homeyer A**, Schenk A, Arlt J, Dahmen U, Dirsch O, Hahn HK. Practical quantification of necrosis in histological whole-slide images. *Comput Med Imaging Graph* 2013; **37**: 313-322 [PMID: 23796718 DOI: 10.1016/j.compmedimag.2013.05.002]

11 **Georgiev P**, Jochum W, Heinrich S, Jang JH, Nocito A, Dahm F, Clavien PA. Characterization of time-related changes after experimental bile duct ligation. *Br J Surg* 2008; **95**: 646-656 [PMID: 18196571 DOI: 10.1002/bjs.6050]

12 **Marques TG**, Chaib E, da Fonseca JH, Lourenço AC, Silva FD, Ribeiro MA, Galvão FH, D'Albuquerque LA. Review of experimental models for inducing hepatic cirrhosis by bile duct ligation and carbon tetrachloride injection. *Acta Cir Bras* 2012; **27**: 589-594 [PMID: 22850713]

13 **Symeonidis A**, Trams EG. Morphologic and functional changes in the livers of rats after ligation or excision of the common bile duct. *Am J Pathol* 1957; **33**: 13-27 [PMID: 13394688]

14 **Wright JE**, Braithwaite JL. The effects of ligation of the common bile duct in the rat. *J Anat* 1964; **98**: 227-233 [PMID: 14154425]

15 **Kountouras J**, Billing BH, Scheuer PJ. Prolonged bile duct obstruction: a new experimental model for cirrhosis in the rat. *Br J Exp Pathol* 1984; **65**: 305-311 [PMID: 6743531]

16 **Vasconcellos Lde S**, Alberti LR, Romeiro JR, Petroianu A. Influence of cholestatic jaundice on the weight variance in an experimental model. *Rev Col Bras Cir* 2012; **39**: 502-508 [PMID: 23348647]

17 **Krähenbühl S**, Marti U, Grant I, Garlick PJ, Ballmer PE. Characterization of mechanisms causing hypoalbuminemia in rats with long-term bile duct ligation. *J Hepatol* 1995; **23**: 79-86 [PMID: 8530813]

18 **Geerts AM**, Vanheule E, Praet M, Van Vlierberghe H, De Vos M, Colle I. Comparison of three research models of portal hypertension in mice: macroscopic, histological and portal pressure evaluation. *Int J Exp Pathol* 2008; **89**: 251-263 [PMID: 18715470 DOI: 10.1111/j.1365-2613.2008.00597.x]

19 **Abdel-Aziz G**, Lebeau G, Rescan PY, Clément B, Rissel M, Deugnier Y, Campion JP, Guillouzo A. Reversibility of hepatic fibrosis in experimentally induced cholestasis in rat. *Am J Pathol* 1990; **137**: 1333-1342 [PMID: 2260623]

20 **Woolbright BL**, Antoine DJ, Jenkins RE, Bajt ML, Park BK, Jaeschke H. Plasma biomarkers of liver injury and inflammation demonstrate a lack of apoptosis during obstructive cholestasis in mice. *Toxicol Appl Pharmacol* 2013; **273**: 524-531 [PMID: 24096036 DOI: 10.1016/j.taap.2013.09.023]

21 **Lessa JF**, Rangel LS, Costa NJ, Castro e Silva O, Cruz CA, Sousa JB. Effects of albumin administration in serum liver enzymes of rats in the presence of extrahepatic biliary obstruction. *Acta Cir Bras* 2011; **26** Suppl 2: 70-73 [PMID: 22030818]

22 **Johnstone JM**, Lee EG. A quantitative assessment of the structural changes the rat's liver following obstruction of the common bile duct. *Br J Exp Pathol* 1976; **57**: 85-94 [PMID: 1268043]

23 **Prado IB**, dos Santos MH, Lopasso FP, Iriya K, Laudanna AA. Cholestasis in a murine experimental model: lesions include hepatocyte ischemic necrosis. *Rev Hosp Clin Fac Med Sao Paulo* 2003; **58**: 27-32 [PMID: 12754587]

24 **Malhi H**, Gores GJ, Lemasters JJ. Apoptosis and necrosis in the liver: a tale of two deaths? *Hepatology* 2006; **43**: S31-S44 [PMID: 16447272 DOI: 10.1002/hep.21062]

25 **Steiner PE**, Martinez JB. Effects on the Rat Liver of Bile Duct, Portal Vein and Hepatic Artery Ligations. *Am J Pathol* 1961; **39**: 257-289 [PMID: 19971005]

26 **Cameron GR**, Prasad LB. Recovery from biliary obstruction after spontaneous restoration of the obstructed common bile-duct. *J Pathol Bacteriol* 1960; **80**: 127-136 [PMID: 13807153]

27 **Liu A**, Dirsch O, Fang H, Sun J, Jin H, Dong W, Dahmen U. HMGB1 in ischemic and non-ischemic liver after selective warm ischemia/reperfusion in rat. *Histochem Cell Biol* 2011; **135**: 443-452 [PMID: 21431875 DOI: 10.1007/s00418-011-0802-6]

28 **Tsung A**, Sahai R, Tanaka H, Nakao A, Fink MP, Lotze MT, Yang H, Li J, Tracey KJ, Geller DA, Billiar TR. The nuclear factor HMGB1 mediates hepatic injury after murine liver ischemia-reperfusion. *J Exp Med* 2005; **201**: 1135-1143 [PMID: 15795240 DOI: 10.1084/jem.20042614]

29 **Hui TT**, Mizuguchi T, Sugiyama N, Avital I, Rozga J, Demetriou AA. Immediate early genes and p21 regulation in liver of rats with acute hepatic failure. *Am J Surg* 2002; **183**: 457-463 [PMID: 11975936]

30 **Buitrago-Molina LE**, Marhenke S, Longerich T, Sharma AD, Boukouris AE, Geffers R, Guigas B, Manns MP, Vogel A. The degree of liver injury determines the role of p21 in liver regeneration and hepatocarcinogenesis in mice. *Hepatology* 2013; **58**: 1143-1152 [PMID: 23526443 DOI: 10.1002/hep.26412]

31 **Lehmann K**, Tschuor C, Rickenbacher A, Jang JH, Oberkofler CE, Tschopp O, Schultze SM, Raptis DA, Weber A, Graf R, Humar B, Clavien PA. Liver failure after extended hepatectomy in mice is mediated by a p21-dependent barrier to liver regeneration. *Gastroenterology* 2012; **143**: 1609-1619.e4 [PMID: 22960658 DOI: 10.1053/j.gastro.2012.08.043]

32 **Arshad MI**, Piquet-Pellorce C, Samson M. IL-33 and HMGB1 alarmins: sensors of cellular death and their involvement in liver pathology. *Liver Int* 2012; **32**: 1200-1210 [PMID: 22530772 DOI: 10.1111/j.1478-3231.2012.02802.x]

33 **Hammerich L**, Tacke F. Interleukins in chronic liver disease: lessons learned from experimental mouse models. *Clin Exp Gastroenterol* 2014; **7**: 297-306 [PMID: 25214799 DOI: 10.2147/CEG.S43737]

34 **Marvie P**, Lisbonne M, L'helgoualc'h A, Rauch M, Turlin B, Preisser L, Bourd-Boittin K, Théret N, Gascan H, Piquet-Pellorce C, Samson M. Interleukin-33 overexpression is associated with liver fibrosis in mice and humans. *J Cell Mol Med* 2010; **14**: 1726-1739 [PMID: 19508382 DOI: 10.1111/j.1582-4934.2009.00801.x]

35 **Zhang L**, Yang Z, Liu Y. GADD45 proteins: roles in cellular senescence and tumor development. *Exp Biol Med* (Maywood) 2014; **239**: 773-778 [PMID: 24872428 DOI: 10.1177/1535370214531879]

P- Reviewer: Sticova E **S- Editor**: Qi Y **L- Editor**: A
E- Editor: Zhang FF

World Journal of Gastroenterology

Submit a Manuscript: http://www.f6publishing.com

World J Gastroenterol 2017 June 21; 23(23): 4200-4210

DOI: 10.3748/wjg.v23.i23.4200

ISSN 1007-9327 (print) ISSN 2219-2840 (online)

ORIGINAL ARTICLE

Basic Study

Solid lipid nanoparticles delivering anti-inflammatory drugs to treat inflammatory bowel disease: Effects in an *in vivo* model

Chiara Dianzani, Federica Foglietta, Benedetta Ferrara, Arianna Carolina Rosa, Elisabetta Muntoni, Paolo Gasco, Carlo Della Pepa, Roberto Canaparo, Loredana Serpe

Chiara Dianzani, Federica Foglietta, Benedetta Ferrara, Arianna Carolina Rosa, Elisabetta Muntoni, Carlo Della Pepa, Roberto Canaparo, Loredana Serpe, Department of Drug Science and Technology, University of Torino, 10125 Torino, Italy

Paolo Gasco, Nanovector s.r.l, 10144 Torino, Italy

Author contributions: Dianzani C, Foglietta F, Ferrara B and Rosa AC performed the *in vitro* and *in vivo* experiments; Muntoni E was responsible for animal handling and performed the *in vivo* disease activity evaluation; Gasco P synthesized and characterized the anti-inflammatory drug nanoformulation; Della Pepa C analyzed the data and contributed to the discussion; Canaparo R analyzed the data, contributed to the discussion and reviewed the manuscript; Serpe L designed the study, analyzed the data and wrote the manuscript. All the authors have read and approved the final manuscript.

Supported by Regione Piemonte (grant "Converging Technologies", NanoIGT) and University of Torino (grant "Ricerca Locale", Linea A).

Institutional review board statement: The study was reviewed and approved by the Institutional Review Board of the University of Torino (Torino, Italy).

Conflict-of-interest statement: The authors declare that they have no competing interests.

Data sharing statement: The technical appendix, statistical code, and dataset are available from the corresponding author at email address loredana.serpe@unito.it.

Manuscript source: Invited manuscript

Correspondence to: Loredana Serpe, MD, PhD, Department of Drug Science and Technology, University of Torino, Via Pietro Giuria 13, 10125 Torino, Italy. loredana.serpe@unito.it
Telephone: +39-11-6706235
Fax: +39-11-6706230

Received: February 7, 2017
Peer-review started: February 10, 2017
First decision: March 21, 2017
Revised: April 3, 2017
Accepted: May 4, 2017
Article in press: May 4, 2017
Published online: June 21, 2017

Abstract

AIM

To improve anti-inflammatory activity while reducing drug doses, we developed a nanoformulation carrying dexamethasone and butyrate.

METHODS

Dexamethasone cholesteryl butyrate-solid lipid nanoparticles (DxCb-SLN) were obtained with the warm microemulsion method. The anti-inflammatory activity of this novel nanoformulation has been investigated *in vitro* (cell adhesion to human vascular endothelial cells and pro-inflammatory cytokine release by lipopolysaccharide-induced polymorphonuclear cells) and *in vivo* (disease activity index and cytokine plasma concentrations in a dextran sulfate sodium-induced mouse colitis) models. Each drug was also administered separately to compare its effects with those induced by their co-administration in SLN at the same concentrations.

RESULTS

DxCb-SLN at the lowest concentration tested (Dx 2.5 nmol/L and Cb 0.1 μmol/L) were able to exert a more than additive effect compared to the sum of the individual effects of each drug, inducing a significant *in vitro* inhibition of cell adhesion and a significant decrease of pro-inflammatory cytokine (IL-1β and TNF-α) in both *in vitro* and *in vivo* models. Notably, only the DxCb nanoformulation administration was able to achieve a significant cytokine decrease compared to the cytokine plasma concentration of the untreated mice with dextran sulfate sodium-induced colitis. Specifically, DxCb-SLN induced a IL-1β plasma concentration of 61.77% ± 3.19%, whereas Dx or Cb used separately induced a concentration of 90.0% ± 2.8% and 91.40% ± 7.5%, respectively; DxCb-SLN induced a TNF-α plasma concentration of 30.8% ± 8.9%, whereas Dx or Cb used separately induced ones of 99.5% ± 4.9% and 71.1% ± 10.9%, respectively.

CONCLUSION

Our results indicate that the co-administration of dexamethasone and butyrate by nanoparticles may be beneficial for inflammatory bowel disease treatment.

Key words: Nanoparticles; Dexamethasone; Butyrate; Inflammatory bowel disease; Drug delivery systems

Core tip: The oral treatment with dexamethasone and butyrate co-loaded into nanoparticles was effective in achieving strong anti-inflammatory effects at doses significantly lower than those required for each single drug. This nanoformulation may open a new window on the treatment of chronic inflammatory conditions such as inflammatory bowel disease, where dose- and time-dependent side effects can limit the drug's therapeutic usefulness. Notably, dexamethasone cholesteryl butyrate-solid lipid nanoparticles significantly relieved and repaired colon inflammation in a colitis mouse model thanks to the nanoformulation, which displayed an additive synergism among the corticosteroid, dexamethasone, and the short-chain fatty acid, butyrate.

Dianzani C, Foglietta F, Ferrara B, Rosa AC, Muntoni E, Gasco P, Della Pepa C, Canaparo R, Serpe L. Solid lipid nanoparticles delivering anti-inflammatory drugs to treat inflammatory bowel disease: Effects in an *in vivo* model. *World J Gastroenterol* 2017; 23(23): 4200-4210 Available from: URL: http://www.wjgnet.com/1007-9327/full/v23/i23/4200.htm DOI: http://dx.doi.org/10.3748/wjg.v23.i23.4200

INTRODUCTION

Inflammation is a physiological process that involves different cells, such as leukocytes and endothelial cells that establish adhesive interactions in order to transverse the vascular wall and migrate to the damaged tissue. Inflammatory bowel diseases (IBDs), including ulcerative colitis and Crohn's disease, are comprised of chronic and deregulated inflammation of the intestinal mucosa characterized by active inflammation, tissue destruction and repeated attempts at tissue repair that lead to a waxing-waning course. This persistent inflammation is triggered by neutrophil and macrophage infiltration, with activated macrophages producing a potent mixture of broadly active inflammatory cytokines, including interleukin (IL)-1β and tumor necrosis factor (TNF)-α[1,2]. In response to such pro-inflammatory cytokines, endothelial cells undergo inflammatory activation, resulting in an increased surface expression of cell adhesion molecules (CAMs), such as ICAM-1, VCAM-1 and E-selectin[3]. These endothelial CAMs play a fundamental role in leukocyte recruitment from the blood for tissue infiltration. Chronic induction of these CAMs leads to abnormal leukocyte recruitment, like that observed in chronic inflammatory diseases characterized by profound tissue remodeling and loss of function[4].

Recently, the traditional therapeutic approach of IBD, with the introduction of biologic agents, has moved away from non-specific immunomodulators, including corticosteroids, thiopurines, and methotrexate toward a pathway-based anti-inflammatory approach. Even though the introduction of TNF inhibitors such as infliximab, as well as anti-integrins, has initiated a new therapeutic era, these biologics are clinically effective only in a subgroup of IBD patients[5,6]. Therefore, IBD treatment is still a difficult challenge, and efforts to facilitate effective drug treatment are still necessary. Corticosteroids exert their anti-inflammatory and immunosuppressive effects by reducing the expression of cytokines and adhesion molecules, inhibiting leukocyte traffic and access to the inflammation site. In particular, dexamethasone (Dx) has been used for decades in the treatment of IBD flares, even if a such life-long treatment might produce several adverse reactions that are mostly time- and dose-dependent, limiting its clinical usefulness[1,7,8]. Hence, attempts to maintain the IBD therapeutic effects of corticosteroids while minimizing their systemic side effects might provide a major therapeutic improvement.

With regard to corticosteroids and pharmaceutical technology, to date only the novel oral formulation of budesonide using multi-matrix (MMX) drug delivery technology has been introduced as a treatment option for patients with ulcerative colitis, allowing a wider colonic targeting with low systemic bioavailability. The MMX strategy is an extension of the pH-responsive polymer technique that allows the sustained release of a drug enclosed within a gastro-resistant, pH-dependent coating[9]. However, it seems likely that all such systems relying on pH-responsive polymers will not be truly colon site-specific[10].

Recent advances in nanotechnology have enabled the development of new corticosteroid formulations with a nanometric approach to ameliorate

pharmacological properties, resulting in increased efficacy and reduction of side effects[11]. Different from the MMX strategy, the nanoparticle drug delivery strategy relies on the nanosize as the cardinal property for interaction with biological systems. Indeed, the nanosize determines the ability to penetrate cell membranes, thus facilitating the passage across biological barriers, interaction with the immune system, uptake, absorption and distribution[12]. For instance, the size of orally assumed nanoparticles may somehow determine their fate, addressing the kind of cell with which to interact (*i.e.*, epithelial or phagocytic cells), or the depth level in the intestinal mucosa. Moreover, nanoparticles can directly enter into phagocytic cells populating the inflamed tissue, thus providing a wider distribution and an additional mechanism for drug targeting[13].

Furthermore, the potential inhibitory effect of nanoparticle formulations of Dx on cyclooxygenase-2 (COX-2) expression is interesting. Although the physiological activity of COX-2 may provide a benefit to the organism, its aberrant expression has been implicated in the pathogenesis of many diseases, such as chronic inflammation and carcinogenesis[14]. Moreover, the effective inhibitory activity displayed by nanoparticle formulations of Dx on CAM expression by "inflamed" endothelial cells may be beneficial in blunting detrimental inflammatory reactions[15,16]. In particular, the incorporation of Dx into solid lipid nanoparticles (SLN) showed a significant improvement of its anti-inflammatory activity in a human IBD whole-blood model. SLN loaded with Dx exerted earlier anti-inflammatory effects and at lower doses than free Dx, highlighting how this nanoparticle formulation may be of therapeutic interest[17]. It is well-known that nanoparticles are efficiently taken up by immunocompetent cells, so that nanoparticulate drug carriers may be useful in targeting the inflamed regions. Indeed, in the presence of IBD there is a strong cellular immunoresponse from the inflamed regions, and the nanoparticle passive targeting may allow for the accumulation of the drug loaded into the nanoparticulate carrier in the inflamed area[11].

Furthermore, our group investigated whether the association between Dx and another anti-inflammatory agent such as butyrate might be of therapeutic interest in IBD. Butyrate is a short-chain fatty acid (SCFA) normally released by intestinal epithelial cells, which exhibit several physiological and immunological functions[18]. Like other SCFA, such as acetate and propionate, butyrate has regulatory effects on the proliferation, differentiation, gene expression and immune regulation of colon epithelial and immune cells. In particular, in experimental models, butyrate has been demonstrated to stimulate mucus production by colon epithelial cells, to inhibit colon inflammation and oxidative stress, and to improve the colon defense barriers, inhibiting colon carcinogenesis as well[19-21]. Butyrate has emerged as a modulator of adaptive responses, owing to its multiple biofunctions, *i.e.*, restoring transforming growth factor-β (TGF-β) and IL-10 production in the colonic mucosa, inducing T cell apoptosis and dampening interferon-γ (IFN-γ) secretion[22,23]. Clinical trials have shown the effectiveness of butyrate monotherapy and/or in combination with conventional treatment in patients with diversion colitis, acute radiation proctitis, as well as ulcerative colitis[24-27]. In this regard, in the 1990s non-controlled pilot clinical trials using oral administration or enemas of butyrate yielded promising results in ulcerative colitis patients[28]. However, extended confirmatory studies have not yet been performed. On the other hand, in a randomized, double-blind, placebo-controlled study on ulcerative colitis patients, the combined treatment of oral sodium butyrate tablets in combination with mesalazine significantly decreased the disease activity index score and improved disease outcomes with respect to mesalazine alone[26].

Therefore, owing to partial patient compliance or restricted indications, these treatments were not established as a standard of care. Recent studies have renewed the expectations in regard to strategies related to intestinal SCFA. The administration of probiotic bacteria with the capacity to produce butyrate has been shown to improve the symptoms in IBD models *in vivo*[29]. Moreover, the treatment with butyrate has been shown to increase apoptosis and differentiation, and to inhibit proliferation in colon, breast, gastric, lung, brain and pancreas cancer cells[30,31]. Butyrate is characterized by a short half-life, due to its rapid metabolism and excretion through the liver. Therefore, continuous administration of the drug is required in order to maintain therapeutic concentrations[32]. In addition, the use of butyrate in therapy is limited by its dose-dependent side effects, such as anemia, headache, nausea, diarrhea and abdominal cramps.

In order to overcome these limitations, SLN have been proposed for improving butyrate therapy, in that they constitute a drug delivery system able to ensure high drug loading, enhanced drug pharmacokinetic profile, good biocompatibility and scale-up feasibility[33-35]. The use of SLN has been under investigation in various preclinical and clinical trials, especially in cancer therapy, and their employment has been approved for clinical use in some cases[36]. Cholesteryl butyrate (Cb) as a butyrate SLN formulation has been evaluated in several *in vitro* and *in vivo* studies as an anticancer agent[37-41] and only in *in vitro* studies as anti-inflammatory agent[17,42].

Thus, our group sought to develop a new SLN formulation carrying dexamethasone and cholesteryl butyrate (DxCb) and investigated the efficacy of this strategy in strengthening the effect of each single drug in the treatment of inflammation. Specifically, investigations of this new anti-inflammatory SLN formulation were carried out in the following IBD models: (1) *in vitro,* evaluating the effects on cell adhesion to human vascular endothelial cells and on pro-inflammatory cytokine release by lipopolysaccharide

Table 1 Composition of warm microemulsion for cholesteryl butyrate and dexamethasone cholesteryl butyrate-solid lipid nanoparticles formulations

Molar composition of warm microemulsion	Cb, mmol/L	DxCb-SLN, mmol/L
Dexamethasone 21-acetate	-	8.1
Cholesteryl butyrate	273.7	273.7
Epikuron™ 200 (purified phosphatidylcholine 92%)	335.5	335.5
Sodium glycocholate	194.8	194.8

Cb: Cholesteryl butyrate; DxCb-SLN: Dexamethasone cholesteryl butyrate-solid lipid nanoparticles.

Table 2 Concentration of main components of water dispersion of cholesteryl butyrate and dexamethasone cholesteryl butyrate-solid lipid nanoparticles formulations after 4 washing steps (HPLC method determination)

Molar composition of final dispersion after washing	Cb, mmol/L	DxCb-SLN, mmol/L
Dexamethasone 21-acetate	-	1.1
Cholesteryl butyrate	36.0	38.5
Phosphatidylcholine	48.4	49.2
Sodium glycocholate	12.5	11.2

Cb: Cholesteryl butyrate; DxCb-SLN: Dexamethasone cholesteryl butyrate-solid lipid nanoparticles.

Table 3 Average value of hydrodynamic diameter (Zave) and polidispersity index of cholesteryl butyrate and dexamethasone cholesteryl butyrate-solid lipid nanoparticles formulations

Physical characterization DLS analysis	Cb	DxCb-SLN
Zave in nm	79.6	72.9
Polydispersity index	0.25	0.28

Cb: Cholesteryl butyrate; DxCb-SLN: Dexamethasone cholesteryl butyrate-solid lipid nanoparticles.

(LPS)-induced polymorphonuclear cells; and (2) *in vivo,* evaluating the effects in dextran sulfate sodium-induced mouse colitis.

MATERIALS AND METHODS

Preparation and characterization of DxCb-SLN

Cb and DxCb-SLN were obtained with the warm microemulsion method (patent WO0030620). This process is based on mixing, in precise ratio, the melted lipid matrix loaded with hydrophobic drug with water phase (maintained at the same melting temperature as the lipid matrix) which contains surfactants, mainly phospholipids, and other co-surfactants, like SCFA, bile salts or short-chain fatty alcohols. When a clear warm microemulsion is obtained, it is dispersed in cold water (2 ℃) to generate nanoparticles by solidifying the lipid matrix. The SLN dispersion obtained is then washed by tangential flow filtration (cut-off 30-100 kDa) to remove components and drug not incorporated into SLN, and the final product can then be filtered at 0.2 μm for sterility or can be subjected to freeze drying.

The Cb was prepared from cholesteryl butyrate (Asia Talent Chemical, Shenzen China), Epikuron 200 (Cargill, Milano, Italy) and sodium glycocholate (PCA, Basaluzzo, Italy). In this formulation, cholesteryl butyrate lipid matrix acts as a prodrug of butyrate. For preparation of the DxCb-SLN, Dx 21-acetate (hereafter referred to as Dx; Sigma-Aldrich, Milano, Italy) was previously added and dissolved into melted cholesteryl butyrate matrix before adding other excipients as by the preparation protocol of Cb. The full compositions of warm microemulsions used to prepare Cb and DxCb-SLN are reported in Table 1. The temperature of these warm microemulsions was 85 ℃ for both. After clear microemulsions had been obtained, they were dispersed in cold water (2 ℃) under stirring, at a 1:5 volume ratio. The dispersions obtained were then washed by tangential flow filtration (Vivaflow50 membrane with cut-off of 100 kDa; Sartorius Stedim Biotech GmbH, Goettingen, Germany) by adding and removing the same volume of water 4 times (4 washings); the final concentrations of the main components are reported in Table 2. In both formulations, 2-phenylethanol was added to aid in microemulsion formation. In particular, it works mainly to reduce viscosity and further helps in the formation of an interface between the oil phase and the lipid phase. Due to the multiple washings applied to purify the final products - four washings in this case - the concentration of 2-phenylethanol was strongly reduced in the final dispersion, where it finally acted as a preservative. Dx (water:ethanol 9:1, 1 mmol/L) was also prepared as a free drug reference.

Physical characterization was performed by dynamic light scattering (DLS) (Malvern Zetasizer - Nano ZS; Malvern Instruments, Malvern, United Kingdom). The data are reported in Table 3. Finally, electron microscopy analysis by ZEISS Supra 40 Field Emission Scanning Electron Microscopy confirmed the regular shape and nanosize of the particles (Figure 1) (courtesy of Prof. Pirri, Laboratory FESEM Microscopy, DISAT, Politecnico of Torino).

Cell lines

Leukemic human T cells (Jurkat, clone E6-1) were obtained from American Type Culture Collection (ATCC) (Manassas, VA, United States), and were cultured in RPMI 1640 medium supplemented with 10% fetal calf serum (FCS) (v/v), 2 mmol/L L-glutamine and antibiotics (100 U/mL streptomycin and 200 U/mL penicillin) (Sigma-Aldrich).

Human vascular endothelial cells (HUVECs) were isolated from human umbilical veins from healthy parturients aged between 18-35 years undergoing a natural birth (informed consent was obtained from all donors). The umbilical cord was collected at birth

and stored at 4 ℃ until the isolation procedure by trypsin treatment (1%). HUVECs were cultured in M199 medium with the addition of 20% FCS (v/v) and 100 U/mL penicillin, 100 mg/mL streptomycin, 5 UI/mL heparin, 12 mg/mL bovine brain extract and 200 mmol/L glutamine (Sigma-Aldrich). HUVECs were grown to confluence in flasks and used between the second and fifth passages; HUVEC viability was not affected by the drug treatment.

Peripheral blood mononuclear cells (PBMCs) were isolated from heparinized peripheral rat blood samples by density-gradient centrifugation over Ficoll-Paque (Pharmacia Biotech, Uppsala, Sweden) according to the method of Liu *et al*[43] (the study was approved by the Ethics Committee of the University of Torino). PBMCs were cultured in RPMI 1640 medium supplemented with 10% FCS (v/v), 2 mmol/L L-glutamine and antibiotics (100 U/mL streptomycin and 200 U/mL penicillin). All the cell lines were cultured at 37 ℃ in a humidified 5% CO_2-95% air incubator.

In vitro cell adhesion assay

HUVECs were grown to confluence in 24-well culture plates, washed and rested for 1 d in M199 medium plus 10% FCS (v/v). Cells were pre-activated with IL-1β (0.01 μmol/L) for 1 h and then exposed or not exposed to increasing concentrations of Dx (2.5, 25 and 250 nmol/L), Cb (0.1, 1 and 10 μmol/L) and DxCb-SLN (2.5 nmol/L:0.1 μmol/L, 25 nmol/L:1 μmol/L and 250 nmol/L:10 μmol/L) for 24 h, washed with fresh medium twice and incubated for 1 h with Jurkat cells (1×10^5 per well). The 1 h incubation time was chosen to allow full sedimentation of the adhering cells, but similar results were obtained with shorter incubation times (10 and 20 min). After incubation, non-adherent cells were removed by being washed three times with M199 medium. The center of each well was analyzed by fluorescence imaging[42]. Adherent cells were counted by the ImagePro Plus Software for micro-imaging (version 5.0; Media Cybernetics, Bethesda, MD, United States). Single experimental points were assayed in triplicate, and the standard error of three replicates was always below 10%. Data are shown as the percentage of inhibition of treated cells *vs* the control adhesion measured on untreated cells (control adhesion was 65 ± 5 cells per microscope field; $n = 5$).

In vitro PBMC assay

PBMC viability was assayed by trypan blue dye exclusion, and 5×10^5/mL viable cells were cultured in 24-well culture plates with culture medium containing 1 μg/mL LPS (Sigma-Aldrich) for 24 h. PBMCs were then incubated with increasing concentration of Dx (2.5, 25 and 250 nmol/L), Cb (0.1, 1 and 10 μmol/L) and DxCb-SLN (2.5 nmol/L:0.1 μmol/L, 25 nmol/L:1 μmol/L and 250 nmol/L:10 μmol/L) for 24 h. In order to exclude the possibility that the drugs might affect cell viability, 24 h after drug incubation a trypan blue dye exclusion assay was performed for each condition.

The IL-1β and TNF-α protein concentrations in culture supernatants of PBMCs were determined at 24 h incubation by specific enzyme-linked immunosorbent assay (ELISA) (eBioscience, Thermo Fisher Scientific, Milano, Italy) according to the manufacturer's instructions. Data are shown as the percentage of the cytokine secretion of LPS-treated PBMCs after each drug treatment *vs* the cytokine secretion of control cells, *i.e.*, LPS-stimulated PBMCs.

Animals

Male, 8 wk-old BALB/c mice, with an average weight of 18 g, were obtained from Charles River (Milano, Italy). The mice were housed in a specific pathogen-free environment, and a 12 h light/dark cycle was maintained. The mice had access to water and rodent laboratory chow *ad libitum*; the weights of the mice as well as diarrhea were recorded daily. The procedures for the care and handling of the animals used in the study were approved by the local "Animal Use and Care Committee" (protocol number 12201), and they were in accordance with the European Directive 2010/63/EU on the protection of animals used for scientific purposes.

In vivo model of colitis

Colitis was induced in mice by adding 4% (w/v) dextran sulfate sodium salt (DSS, molecular weight 40000) (Sigma-Aldrich) to the drinking water and allowing *ad libitum* access, starting from day 0 for 5 d. Groups of mice (at least 5 mice per group) were then orally treated (by gavage) daily with Dx (0.0001 mg/g bw), Cb (0.004 mg/g bw) or DxCb-SLN (0.0001 mg/g bw:0.004 mg/g bw) starting from day 6 for 3 d. Moreover, in a group in which colitis was induced, as a sham treatment mice were administered orally with sterile phosphate-buffered saline solution (150 μL/mouse per day) starting from day 6 for 3 d (DSS group), whereas in another group colitis was not induced (control group). All groups were sacrificed on day 10. There were at least 5 mice per group, and two separate experiments were carried out. There was no significant difference in the water consumption and food intake of each group during all experimental periods.

Assessment of in vivo inflammation

The mice were weighed and inspected for diarrhea and rectal bleeding every day. The disease activity index (DAI) (*i.e.*, the combined score of weight loss and bleeding) was determined according to a standard scoring system, as previously described by Rachmilewitz *et al*[44]. Specifically, the scores were defined as follows: (1) bodyweight (bw) loss (0: no bw loss; 1: 5%-10% bw loss; 2: 10%-15% bw loss; 3: 15%-20% bw loss; 4: > 20% bw loss); (2) fecal occult blood (0: no blood; 2: positive; 4: gross blood); and (3) diarrhea (0: no diarrhea; 1: mild diarrhea, 2: severe diarrhea). All groups were sacrificed on day 10.

The IL-1β and TNF-α plasma concentrations were determined on day 9, *i.e.*, 24 h after the different

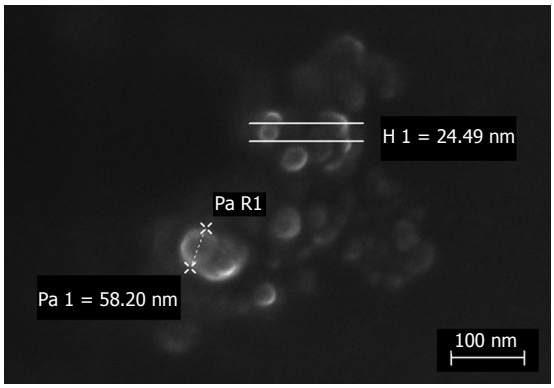

Figure 1 FeSEM micrograph of dexamethasone cholesteryl butyrate-solid lipid nanoparticles. Electron microscopy analysis showed regular shape and nanosize of particles by height (H) or radius (R) measurements.

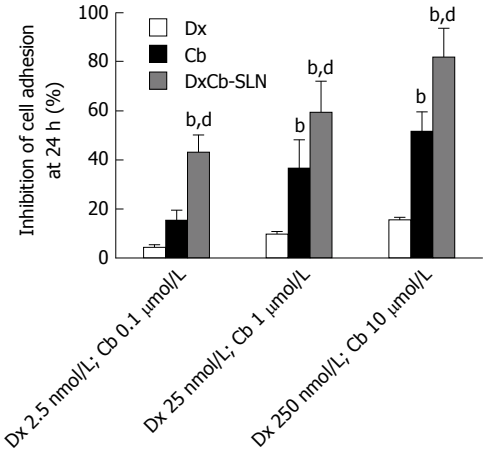

Figure 2 Effect of dexamethasone, cholesteryl butyrate and dexamethasone cholesteryl butyrate-solid lipid nanoparticles on human vascular endothelial cell adhesiveness to Jurkat cells. Human vascular endothelial cells were pre-activated with IL-1β (0.01 μmol/L) for 1 h and then exposed or not exposed to increasing concentrations of Dx (2.5, 25 and 250 nmol/L), Cb (0.1, 1 and 10 μmol/L) and DxCb-SLN (2.5 nmol/L:0.1 μmol/L, 25 nmol/L:1 μmol/L and 250 nmol/L:10 μmol/L) for 24 h and then incubated with Jurkat for 1 h. $^{b}P < 0.01$, *vs* Dx; $^{d}P < 0.01$, *vs* Cb. Dx: Dexamethasone; Cb: Cholesteryl butyrate; DxCb-SLN: Dexamethasone cholesteryl butyrate-solid lipid nanoparticles.

treatments by specific sandwich enzyme immunoassay (eBioscience, Thermo Fisher Scientific) according to the manufacturer's instructions. Data are shown as the percentage of the cytokine secretion of DSS-treated mice after each drug treatment *vs* the cytokine secretion of DSS-treated mice.

Statistical analysis

Results are expressed throughout as mean ± SD of three independent experiments for *in vitro* studies and of two independent experiments for *in vivo* studies. Statistical analyses were performed on GraphPad Prism 6.0 software (La Jolla, CA, United States). The two-way or one-way analysis of variance and Bonferroni's test were used to determine statistical significance in the different treatment groups. The statistical significance threshold was set at $P < 0.05$.

RESULTS

Effects of DxCb-SLN on in vitro cell adhesion

First, we analyzed the effect of DxCb-SLN on the adhesion of Jurkat cells, a widely used continuous model of human T lymphocytes, to HUVECs comparing it with the effect of the drug separately, *i.e.*, Dx and Cb. In order to reproduce an inflammatory environment, we pre-activated HUVECs with 0.01 μmol/L IL-1β for 1 h. The treatment with IL-1β increased Jurkat adhesion by 180%, and this value was used as control. The concentration used for each drug had been found not to be toxic for HUVECs.

HUVECs were treated with increasing concentrations of each single drug, *i.e.*, Dx (2.5, 25 and 250 nmol/L) and Cb (0.1, 1 and 10 μmol/L), and of the DxCb nanoformulation (DxCb-SLN with a Dx:Cb concentration of 2.5 nmol/L:0.1 μmol/L, 25 nmol/L:1 μmol/L and 250 nmol/L:10 μmol/L) for 24 h, washed and used in the adhesion assay with Jurkat cells. Figure 2 shows that DxCb SLN inhibited cell adhesion to HUVEC in a concentration-dependent manner. A significant 43.1% ± 7.3% inhibition of cell adhesion was already determined at the lowest concentration tested of the DxCb nanoformulation (DxCb-SLN with a Dx:Cb concentration of 2.5 nmol/L M:0.1 μmol/L), reaching an 81.8% ± 11.7% inhibition of cell adhesion at the highest concentration tested (DxCb-SLN with a Dx:Cb concentration of 250 nmol/L:10 μmol/L). Considering the inhibition of cell adhesion determined by the single drugs, Dx produced a 4.2% ± 0.8% inhibition at the lowest concentration tested (2.5 nmol/L), reaching a 15.4% ± 0.9% inhibition at the highest concentration tested (250 nmol/L) and Cb determined a 14.9% ± 4.3% inhibition at the lowest concentration tested (0.1 μmol/L), reaching a 51.6% ± 7.8% inhibition at the highest concentration tested (10 μmol/L). Therefore, taking all the data together, the nanoformulation containing Dx 2.5 nmol/L and Cb 0.1 μmol/L was able to exert an inhibition of cell adhesion in a more than additive manner with respect to the sum of the individual effects of each drug if they had been used separately (Figure 2).

Effects of DxCb-SLN on in vitro cytokine production

With respect to the effects on IL-1β production in PBMC culture supernatant, 24 h after the incubation a statistically significant ($P < 0.05$) higher decrease of IL-1β compared to the effect induced by each single drug was observed only with the nanoformulation containing the lowest concentrations tested (DxCb-SLN with a Dx:Cb concentration of 2.5 nmol/L:0.1 μmol/L; Figure 3A). Assuming as 100% the IL-1β production of untreated PBMCs, an IL-1β production of 74.3% ± 8.7% was observed with the nanoformulation, in contrast to a 98.7% ± 9.8% and a 89.1% ± 8.2% production with Dx (2.5 nmol/L) and with Cb (0.1 μmol/L), respectively. On increasing the concentrations, no significant differences on the IL-1β production were

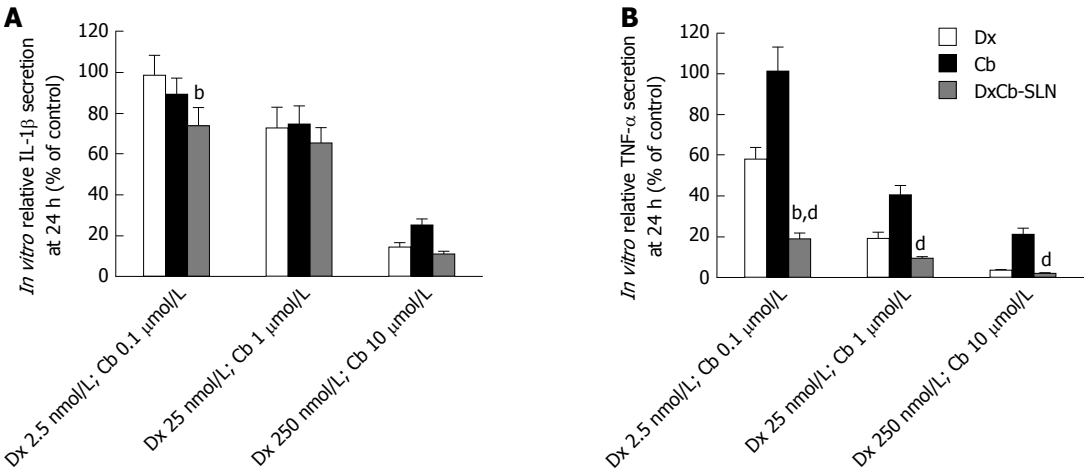

Figure 3 *In vitro* effect of dexamethasone, cholesteryl butyrate and dexamethasone cholesteryl butyrate-solid lipid nanoparticles on interleukin-1β and tumor necrosis factor-α secretion. Cells were treated with increasing concentrations of Dx (2.5, 25 and 250 nmol/L), Cb (0.1, 1 and 10 μmol/L) and DxCb-SLN (2.5 nmol/L:0.1 μmol/L, 25 nmol/L:1 μmol/L and 250 nmol/L:10 μmol/L) for 24 h. IL-1β (A) and TNF-α (B) secretion in culture supernatant of PBMCs stimulated with lipopolysaccharide (LPS; 1 μg/mL for 24 h) were analyzed by ELISA. $^{b}P < 0.01$, *vs* Dx; $^{d}P < 0.01$, *vs* Cb. Dx: Dexamethasone; Cb: Cholesteryl butyrate; DxCb-SLN: Dexamethasone cholesteryl butyrate-solid lipid nanoparticles; IL: Interleukin; TNF: Tumor necrosis factor.

observed using either the DxCb nanoformulation or each single drug (Figure 3A).

Regarding the effects on TNF-α production in the PBMC culture supernatant, 24 h after incubation a statistically significant ($P < 0.001$) higher decrease of TNF-α compared to the effect induced by single Dx was observed only with the nanoformulation at the lowest concentrations tested (DxCb-SLN with a Dx:Cb concentration of 2.5 nmol/L:0.1 μmol/L; Figure 3B). Assuming as 100% the TNF-α production of untreated PBMCs, a TNF-α production of 19.2% ± 2.8% was observed with the nanoformulation, compared to a 58.4% ± 5.3% and a 101.3% ± 11.3% production with Dx (2.5 nmol/L) and with Cb (0.1 μmol/L), respectively. On increasing the concentrations, no significant differences on TNF-α production were observed using either the DxCb nanoformulation or Dx single drug (Figure 3B). Therefore, in regard to all the data, the nanoformulation containing Dx 2.5 nmol/L and Cb 0.1 μmol/L was able to exert a strong decrease of TNF-α production in a more than additive manner with respect to the sum of the individual effects of each drug if they had been used separately (Figure 3B).

Effects of DxCb-SLN on in vivo mice colitis

In order to evaluate the effect of the DxCb nanoformulation on a mouse colitis model, the mice were divided into groups, and each was given drugs separately or as DxCb-SLN at the same concentrations. Specifically, doses of Dx (0.0001 mg/g bw), Cb (0.004 mg/g bw) or DxCb-SLN (0.0001 mg/g bw:0.004 mg/g bw) per day were administered orally from day 6 to day 8 after the colitis induction from day 0 to day 5. In addition, another group was composed of untreated mice (DSS group), and another of mice in which colitis was not induced (control group). Changes in mice bw were significantly different between the control group and the DSS group starting from day 7 and between groups treated with Dx or Cb and the control group starting from day 9 (Figure 4A). Instead, a slight but significant change in mice bw between DxCb-SLN treated-group and control group was recorded only at the last day of observation, *i.e.*, day 10 ($P < 0.05$; Figure 4A). According to the DAI score determined for each treatment group, we observed that Dx alone was able to induce a significant decrease of the score compared to untreated mice (DSS group), with a 25% reduction of the disease symptoms (*i.e.*, 6.0 *vs* 4.5, $P < 0.05$; Figure 4B). Notably, DxCb-SLN was able to induce a higher significant decrease of the disease score compared to untreated mice, with a 42% reduction of the disease symptoms (*i.e.*, 6.0 *vs* 3.5, $P < 0.01$; Figure 4B).

Considering the cytokine plasma concentration on day 9, *i.e.*, 24 h after drug treatment, only the DxCb nanoformulation administration was able to achieve a significant cytokine decrease compared to the cytokine plasma concentration of the DSS group. Assuming as 100% the IL-1β or TNF-α production of mice with DSS-induced colitis on day 9, 24 h after the 3 d of oral treatments, only DxCb-SLN (0.0001 mg/g bw:0.004 mg/g bw) were able to induce a significant decrease (Figure 5). Specifically, DxCb-SLN induced a IL-1β plasma concentration of 61.77% ± 3.19%, whereas Dx or Cb used separately induced a concentration of 90.0% ± 2.8% and 91.40% ± 7.5%, respectively (Figure 5A); DxCb-SLN induced a TNF-α plasma concentration of 30.8% ± 8.9%, whereas Dx or Cb used separately induced ones of 99.5% ± 4.9% and 71.1% ± 10.9%, respectively (Figure 5B). Thus, DxCb-SLN significantly ameliorated DSS-induced colitis in the mice compared to the treatments with each drug separately, given that the observed anti-inflammatory effect was higher than what would be expected from a

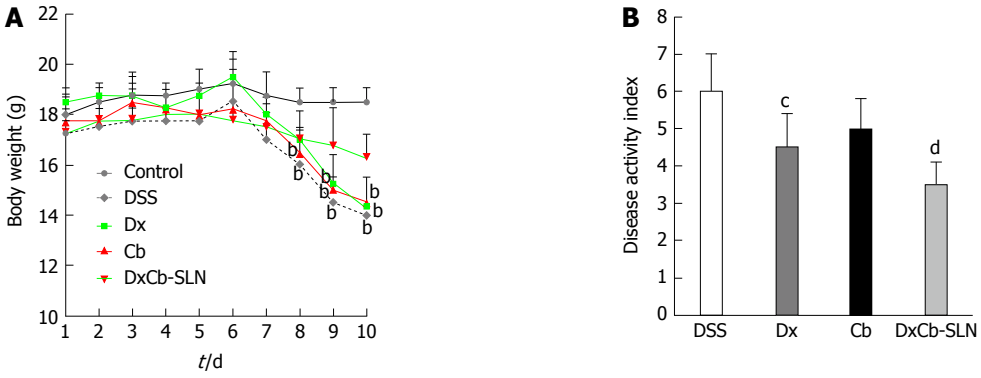

Figure 4 ***In vivo*** **effect of dexamethasone, cholesteryl butyrate and dexamethasone cholesteryl butyrate-solid lipid nanoparticles on bodyweight and disease activity index.** Animals received no treatment (control), DSS alone (DSS), or a combination of DSS and Dx (Dx, 0.0001 mg/g bw for 3 d), DSS and Cb (Cb, 0.004 mg/g bw for 3 d) and DSS and DxCb-SLN (DxCb-SLN, 0.0001 mg/g bw:0.004 mg/g bw for 3 d). After 7 d, DSS was replaced with a water cycle (*ad libitum*) for another 7 d. Body weight of the mice was recorded daily (A) and the disease activity rate at day 9 (B). $^{b}P < 0.01$, *vs* control; $^{c}P < 0.05$; $^{d}P < 0.01$, *vs* DSS. Dx: Dexamethasone; Cb: Cholesteryl butyrate; DxCb-SLN: Dexamethasone cholesteryl butyrate-solid lipid nanoparticles; DSS: Dextran sulfate sodium.

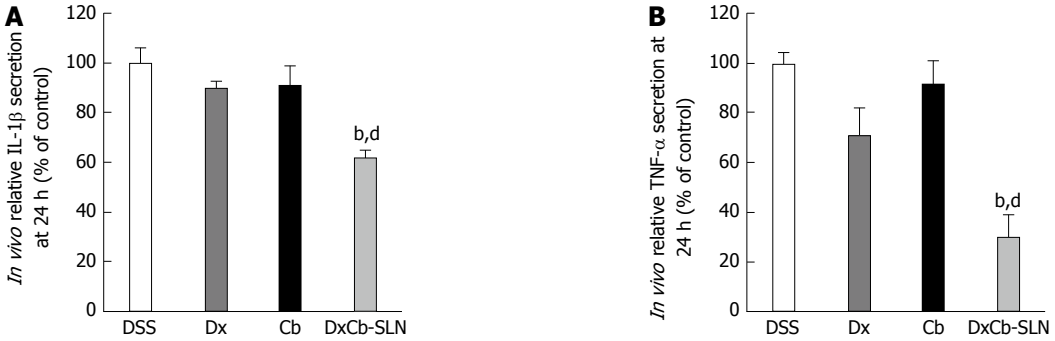

Figure 5 ***In vivo*** **effect of dexamethasone, cholesteryl butyrate and dexamethasone cholesteryl butyrate-solid lipid nanoparticles on interleukin-1β and tumor necrosis factor-α secretion.** Animals were treated with DSS alone (DSS), or a combination of DSS and Dx (Dx, 0.0001 mg/g bw for 3 d), DSS and Cb (Cb, 0.004 mg/g bw for 3 d) and DSS and DxCb-SLN (DxCb-SLN, 0.0001 mg/g bw:0.004 mg/g bw for 3 d). IL-1β and TNF-α secretion in mice plasma were analyzed by ELISA at day 9, 24 h after drug treatment. $^{b}P < 0.01$, *vs* Dx; $^{d}P < 0.01$, *vs* Cb. Dx: Dexamethasone; Cb: Cholesteryl butyrate; DxCb-SLN: Dexamethasone cholesteryl butyrate-solid lipid nanoparticles; DSS: Dextran sulfate sodium; IL: Interleukin; TNF: Tumor necrosis factor.

simple additive effect (Figures 4 and 5).

DISCUSSION

In a previous work, we observed that the incorporation of butyrate and Dx separately into SLN was effective in enhancing the anti-inflammatory activity of the drugs on PBMCs of IBD patients[17]. In the research presented herein, we observed that the combination therapy of Dx and butyrate co-loaded into an oral nanoformulation, namely DxCb-SLN, was effective in reducing the disease activity in a mouse model of DSS-induced colitis, as verified by its effect on macroscopic and biochemical parameters.

Before moving to an *in vivo* IBD model, we first tested DxCb-SLN on *in vitro* inflammation models. In a IL-1β-stimulated leukocyte-endothelial cell adhesion model, where the use of the cytokine allowed us to reproduce the initiation phase of IBD, the combination treatment with DxCb-SLN was able to significantly inhibit cell adhesion already at the lowest concentration tested, showing a significant inhibition at doses 10-fold lower than the dose required to achieve the same effects with each single drug. In a LPS-stimulated PBMC model, DxCb-SLN demonstrated a significant decrease of cytokine release that was higher for TNF-α rather than IL-1β secretion. Once again, the combination treatment was more effective at doses 10-fold lower than the dose required to achieve the same effects with the single drug treatment, *i.e.*, 2.5 nmol/L:0.1 μmol/L Cb for DxCb-SLN with respect to 25 nmol/L for Dx and 1 μmol/L for Cb. We did not observe significant further decreases of both cytokine release at the highest concentration tested of DxCb-SLN because the free drugs, especially Dx, had a strong anti-inflammatory activity by themselves.

We then investigated this novel oral nanoformulation on a DSS-induced colitis *in vivo* model, which is one of the experimental models most frequently used in investigation of novel treatments for IBD[45]. Confirming the data observed *in vitro*, the *in vivo* pro-inflammatory cytokine release was significantly decreased by the DxCb-SLN oral administration, the decrease for TNF-α being more pronounced than IL-1β plasma concentration, 24 h after a daily treatment for 3 d. It is interesting that, on comparing the *in vitro* cytokine release at the lowest concentration of DxCb-SLN, we observed the same more pronounced decrease for

TNF-α than IL-1β secretion.

This anti-inflammatory activity was consistent with the decreased DAI determined by the oral treatment with DxCb-SLN compared to the effects induced by the treatment with each drug separately. Notably, the bw loss induced by DSS was recovered significantly only after the oral treatment with DxCb-SLN. Therefore, thanks to this novel oral nanoformulation, the combination therapy of Dx and butyrate had better effects than any other single treatment, as specifically revealed by the significant decrease of plasma pro-inflammatory cytokines, *i.e.*, IL-1β and TNF-α, and of the DAI. The efficacy of DxCb-SLN demonstrated in these *in vitro* and *in vivo* models may be explained by various mechanisms, such as particular abilities of nanoparticulate drug delivery systems and positive interaction mechanisms between Dx and butyrate.

However, further research is necessary to examine in depth the mechanism underpinning the enhanced anti-inflammatory effect determined by the simultaneous oral administration of Dx and butyrate as SLN formulation rather than as free drugs. For instance, a pharmacokinetic study comparing the simultaneous administration of the two drugs as free or loaded into the same SLN will be necessary to evaluate if the drug delivery system is effective in improving the bioavailability and inflamed tissue targeting. Also, molecular investigations will be necessary to evaluate differences in modulating inflammatory pathways by administering, at the same time, the two drugs as free or SLN formulation.

Thanks to pharmaceutical technology, we had the opportunity to develop an efficient drug delivery system able to improve the treatment of such a disease mediated by inflammation[11,46]. The use of a nanoparticulate drug carrier is useful to prevent early drug biological environmental degradation, to modulate drug pharmacokinetics, but also to enhance the treatment selectivity by targeting. Indeed, nanoparticles depending on their physico-chemical properties can preferentially accumulate in areas of intestinal inflammation when delivered orally[11,12]. They are particularly well-suited to the treatment of IBD through the local delivery of drugs to areas of inflammation, allowing site-specific delivery and minimizing side effects in other organs.

Targeting IBD sites is a challenging task to ensure the release of an intact and quantitatively clear amount of the administered drugs. Since drugs encounter a harmful environment after oral administration, high doses and/or frequent administration are usual to counter the degradation by stomach acidic pH or small intestine digestive enzymes; on the other hand, the occurrence of side effects are more likely[11,47]. In particular, SLN have been one of most studied carriers worldwide for drug delivery, since this nanosystem is mainly composed of solid lipid core and lecithin, has very low toxicity profile, good affinity for biological membrane, ability to facilitate up-taking/overcoming, and capacity to improve drug pharmacokinetics[48,49].

Therefore, the therapeutic potential of this novel anti-inflammatory drug nanoformulation in IBD is due to: (1) time protection of the loaded drug, especially for butyrate; (2) controlled release of the loaded drug, allowing a prolonged drug exposure; and (3) passive targeting of IBD sites, as a result of the abnormal permeability of inflamed colonic mucosa and the nanoparticle preferential uptake by immunocompetent cells.

Moreover, because some studies have reported the ability of butyrate to enhance the anti-inflammatory activity of corticosteroids or non-steroidal drugs[50,51], we decided to evaluate the effect of a combination therapy of Dx and butyrate. It is well-known that butyrate may play an important role in regulating intestinal inflammation[52,53]. As reported by Place *et al*[22], butyrate influences NF-κB activity by preventing the proteasome-dependent degradation of IκBα. This inhibition appears to arise from butyrate's ability to inhibit histone deacetylase (HDAC)[54]. Specifically, the selective changes in gene expression induced by HDAC inhibitors, such as butyrate, arise from the enhanced acetylation of histone proteins and gene-regulatory transcription factors (*e.g.,* p53, Sp1 and Sp3)[22].

NF-κB is a central mediator of the immune and inflammatory response and, upon activation, it rapidly enhances the expression of pro-inflammatory genes such as those encoding cytokines and cell adhesion molecules[55]. Dx effect on cytokine modulation in IBD is achieved through the translocation and activation of the glucocorticoid-receptor complex that can both bind to, and inactivate, key pro-inflammatory transcription factors, such as NF-κB[56]. Therefore, the greater effect observed in both *in vitro* and *in vivo* inflammation models by DxCb-SLN on TNF-α rather than IL-1β secretion might be modulated by a gene transcriptional regulation of NF-κB. Thus, according to our data we can speculate that an additive synergistic effect on NF-κB modulation due to the co-administration of Dx and butyrate might be responsible for the higher anti-inflammatory effect observed compared to the use of each drug separately, even if further molecular investigations are needed to confirm this hypothesis.

DxCb-SLN may provide a novel approach to treating IBD by taking advantage of a combination treatment achieved by co-loading Dx and butyrate into the same nanoparticle, which is able to exert a more than additive anti-inflammatory effect. Moreover, the pronounced anti-inflammatory activity of the DxCb-SLN oral treatment may be also due to passive targeting of the inflamed IBD sites, with the potential to reduce systemic side effects of each single drug in addition to the reduced amount of each drug required to achieve such an important anti-inflammatory activity.

ACKNOWLEDGMENTS

We are grateful to the Obstetrics and Gynecology Unit, Martini Hospital, Torino, Italy, for providing human umbilical cords.

COMMENTS

Background

Dexamethasone has been used for decades in the treatment of inflammatory bowel disease (IBD) flares, even if such a life-long treatment might produce several adverse reactions that are mostly time- and dose-dependent, limiting its clinical usefulness. Hence, attempts to maintain the IBD therapeutic effects of corticosteroids while minimizing their systemic side effects might provide a major therapeutic improvement.

Research frontiers

Nanotechnology can be used to improve the pharmacokinetic and pharmacodynamic properties of such a powerful drug. The authors have developed a nanoformulation carrying dexamethasone and the short-chain fatty acid, butyrate, to improve anti-inflammatory activity while reducing drug doses.

Innovations and breakthroughs

The authors developed a new solid lipid nanoparticle formulation carrying dexamethasone and butyrate highlighting the efficacy of this strategy in strengthening the effect of each single drug in the treatment of inflammation.

Applications

This nanoformulation may open a new window on the treatment of chronic inflammatory conditions such as inflammatory bowel disease, where dose- and time-dependent side effects can limit the drug's therapeutic usefulness. Notably, dexamethasone cholesteryl butyrate-solid lipid nanoparticles significantly relieved and repaired colon inflammation in a colitis mouse model thanks to the nanoformulation, which displayed an additive synergism among the corticosteroid, dexamethasone, and the short-chain fatty acid, butyrate.

Terminology

Solid lipid nanoparticles are mainly composed of solid lipid core and lecithin, have very low toxicity profile, good affinity for biological membrane, ability to facilitate up-taking, and capacity to improve drug pharmacokinetics.

Peer-review

This is a very interesting article discussing a novel drug delivery using dexamethasone cholesteryl butyrate-solid lipid nanoparticles in *in vitro* and *in vivo* models.

REFERENCES

1 **Beattie RM**, Croft NM, Fell JM, Afzal NA, Heuschkel RB. Inflammatory bowel disease. *Arch Dis Child* 2006; **91**: 426-432 [PMID: 16632672 DOI: 10.1136/adc.2005.080481]
2 **Gabay C**, Kushner I. Acute-phase proteins and other systemic responses to inflammation. *N Engl J Med* 1999; **340**: 448-454 [PMID: 9971870 DOI: 10.1056/NEJM199902113400607]
3 **Sans M**, Panés J, Ardite E, Elizalde JI, Arce Y, Elena M, Palacín A, Fernández-Checa JC, Anderson DC, Lobb R, Piqué JM. VCAM-1 and ICAM-1 mediate leukocyte-endothelial cell adhesion in rat experimental colitis. *Gastroenterology* 1999; **116**: 874-883 [PMID: 10092309]
4 **Szmitko PE**, Wang CH, Weisel RD, de Almeida JR, Anderson TJ, Verma S. New markers of inflammation and endothelial cell activation: Part I. *Circulation* 2003; **108**: 1917-1923 [PMID: 14568885 DOI: 10.1161/01.CIR.0000089190.95415.9F]
5 **Coskun M**, Vermeire S, Nielsen OH. Novel Targeted Therapies for Inflammatory Bowel Disease. *Trends Pharmacol Sci* 2017; **38**: 127-142 [PMID: 27916280 DOI: 10.1016/j.tips.2016.10.014]
6 **van Deventer SJ**. The future of inflammatory bowel disease therapy. *Inflamm Bowel Dis* 2002; **8**: 301-305; discussion 306 [PMID: 12131615]
7 **Barnes PJ**, Adcock I. Anti-inflammatory actions of steroids: molecular mechanisms. *Trends Pharmacol Sci* 1993; **14**: 436-441 [PMID: 7510080]
8 **Sands BE**. Therapy of inflammatory bowel disease. *Gastroenterology* 2000; **118**: S68-S82 [PMID: 10868899]
9 **Hoy SM**. Budesonide MMX(®): a review of its use in patients with mild to moderate ulcerative colitis. *Drugs* 2015; **75**: 879-886 [PMID: 25920500 DOI: 10.1007/s40265-015-0396-8]
10 **Amidon S**, Brown JE, Dave VS. Colon-targeted oral drug delivery systems: design trends and approaches. *AAPS PharmSciTech* 2015; **16**: 731-741 [PMID: 26070545 DOI: 10.1208/s12249-015-0350-9]
11 **Serpe L**, Canaparo R, Foglietta F, Zara GP. Innovative formulations for the controlled and site-specific delivery of antiinflammatory drugs. *Curr Pharm Des* 2013; **19**: 7219-7236 [PMID: 23489201]
12 **Viscido A**, Capannolo A, Latella G, Caprilli R, Frieri G. Nanotechnology in the treatment of inflammatory bowel diseases. *J Crohns Colitis* 2014; **8**: 903-918 [PMID: 24686095]
13 **Collnot EM**, Ali H, Lehr CM. Nano- and microparticulate drug carriers for targeting of the inflamed intestinal mucosa. *J Control Release* 2012; **161**: 235-246 [PMID: 22306429 DOI: 10.1016/j.jconrel.2012.01.028]
14 **Takahashi M**, Mutoh M, Kawamori T, Sugimura T, Wakabayashi K. Altered expression of beta-catenin, inducible nitric oxide synthase and cyclooxygenase-2 in azoxymethane-induced rat colon carcinogenesis. *Carcinogenesis* 2000; **21**: 1319-1327 [PMID: 10874009]
15 **d'Alessio P**. Endothelium as a pharmacological target. *Curr Opin Investig Drugs* 2001; **2**: 1720-1724 [PMID: 11892934]
16 **Meager A**. Cytokine regulation of cellular adhesion molecule expression in inflammation. *Cytokine Growth Factor Rev* 1999; **10**: 27-39 [PMID: 10379910]
17 **Serpe L**, Canaparo R, Daperno M, Sostegni R, Martinasso G, Muntoni E, Ippolito L, Vivenza N, Pera A, Eandi M, Gasco MR, Zara GP. Solid lipid nanoparticles as anti-inflammatory drug delivery system in a human inflammatory bowel disease whole-blood model. *Eur J Pharm Sci* 2010; **39**: 428-436 [PMID: 20138213 DOI: 10.1016/j.ejps.2010.01.013]
18 **Scheppach W**, Weiler F. The butyrate story: old wine in new bottles? *Curr Opin Clin Nutr Metab Care* 2004; **7**: 563-567 [PMID: 15295277]
19 **Vinolo MA**, Rodrigues HG, Nachbar RT, Curi R. Regulation of inflammation by short chain fatty acids. *Nutrients* 2011; **3**: 858-876 [PMID: 22254083 DOI: 10.3390/nu3100858]
20 **Liu Q**, Shimoyama T, Suzuki K, Umeda T, Nakaji S, Sugawara K. Effect of sodium butyrate on reactive oxygen species generation by human neutrophils. *Scand J Gastroenterol* 2001; **36**: 744-750 [PMID: 11444474]
21 **Hamer HM**, Jonkers D, Venema K, Vanhoutvin S, Troost FJ, Brummer RJ. Review article: the role of butyrate on colonic function. *Aliment Pharmacol Ther* 2008; **27**: 104-119 [PMID: 17973645 DOI: 10.1111/j.1365-2036.2007.03562.x]
22 **Place RF**, Noonan EJ, Giardina C. HDAC inhibition prevents NF-kappa B activation by suppressing proteasome activity: down-regulation of proteasome subunit expression stabilizes I kappa B alpha. *Biochem Pharmacol* 2005; **70**: 394-406 [PMID: 15950952 DOI: 10.1016/j.bcp.2005.04.030]
23 **Vinolo MA**, Rodrigues HG, Hatanaka E, Sato FT, Sampaio SC, Curi R. Suppressive effect of short-chain fatty acids on production of proinflammatory mediators by neutrophils. *J Nutr Biochem* 2011; **22**: 849-855 [PMID: 21167700]
24 **Breuer RI**, Soergel KH, Lashner BA, Christ ML, Hanauer SB, Vanagunas A, Harig JM, Keshavarzian A, Robinson M, Sellin JH, Weinberg D, Vidican DE, Flemal KL, Rademaker AW. Short chain fatty acid rectal irrigation for left-sided ulcerative colitis: a randomised, placebo controlled trial. *Gut* 1997; **40**: 485-491 [PMID: 9176076]
25 **Scheppach W**. Treatment of distal ulcerative colitis with short-chain fatty acid enemas. A placebo-controlled trial. German-Austrian SCFA Study Group. *Dig Dis Sci* 1996; **41**: 2254-2259 [PMID: 8943981]
26 **Vernia P**, Marcheggiano A, Caprilli R, Frieri G, Corrao G, Valpiani D, Di Paolo MC, Paoluzi P, Torsoli A. Short-chain fatty acid topical treatment in distal ulcerative colitis. *Aliment Pharmacol Ther* 1995; **9**: 309-313 [PMID: 7654893]
27 **Hamer HM**, Jonkers DM, Vanhoutvin SA, Troost FJ, Rijkers G, de Bruïne A, Bast A, Venema K, Brummer RJ. Effect of butyrate

enemas on inflammation and antioxidant status in the colonic mucosa of patients with ulcerative colitis in remission. *Clin Nutr* 2010; **29**: 738-744 [PMID: 20471725]
28 **Wan P**, Chen H, Guo Y, Bai AP. Advances in treatment of ulcerative colitis with herbs: from bench to bedside. *World J Gastroenterol* 2014; **20**: 14099-14104 [PMID: 25339799 DOI: 10.3748/wjg.v20.i39.14099]
29 **Eeckhaut V**, Ducatelle R, Sas B, Vermeire S, Van Immerseel F. Progress towards butyrate-producing pharmabiotics: Butyricicoccus pullicaecorum capsule and efficacy in TNBS models in comparison with therapeutics. *Gut* 2014; **63**: 367 [PMID: 23766442 DOI: 10.1136/gutjnl-2013-305293]
30 **Mariadason JM**. HDACs and HDAC inhibitors in colon cancer. *Epigenetics* 2008; **3**: 28-37 [PMID: 18326939]
31 **Pajak B**, Orzechowski A, Gajkowska B. Molecular basis of sodium butyrate-dependent proapoptotic activity in cancer cells. *Adv Med Sci* 2007; **52**: 83-88 [PMID: 18217395]
32 **Daniel P**, Brazier M, Cerutti I, Pieri F, Tardivel I, Desmet G, Baillet J, Chany C. Pharmacokinetic study of butyric acid administered in vivo as sodium and arginine butyrate salts. *Clin Chim Acta* 1989; **181**: 255-263 [PMID: 2667816]
33 **Brioschi A**, Zara GP, Calderoni S, Gasco MR, Mauro A. Cholesterylbutyrate solid lipid nanoparticles as a butyric acid prodrug. *Molecules* 2008; **13**: 230-254 [PMID: 18305415]
34 **Pellizzaro C**, Coradini D, Morel S, Ugazio E, Gasco MR, Daidone MG. Cholesteryl butyrate in solid lipid nanospheres as an alternative approach for butyric acid delivery. *Anticancer Res* 1999; **19**: 3921-3925 [PMID: 10628332]
35 **Ugazio E**, Marengo E, Pellizzaro C, Coradini D, Peira E, Daidone MG, Gasco MR. The effect of formulation and concentration of cholesteryl butyrate solid lipid nanospheres (SLN) on NIH-H460 cell proliferation. *Eur J Pharm Biopharm* 2001; **52**: 197-202 [PMID: 11522486]
36 **Manjunath K**, Reddy JS, Venkateswarlu V. Solid lipid nanoparticles as drug delivery systems. *Methods Find Exp Clin Pharmacol* 2005; **27**: 127-144 [PMID: 15834465 DOI: 10.1358/mf.2005.27.2.876286]
37 **Foglietta F**, Serpe L, Canaparo R, Vivenza N, Riccio G, Imbalzano E, Gasco P, Zara GP. Modulation of butyrate anticancer activity by solid lipid nanoparticle delivery: an in vitro investigation on human breast cancer and leukemia cell lines. *J Pharm Pharm Sci* 2014; **17**: 231-247 [PMID: 24934552]
38 **Minelli R**, Occhipinti S, Gigliotti CL, Barrera G, Gasco P, Conti L, Chiocchetti A, Zara GP, Fantozzi R, Giovarelli M, Dianzani U, Dianzani C. Solid lipid nanoparticles of cholesteryl butyrate inhibit the proliferation of cancer cells in vitro and in vivo models. *Br J Pharmacol* 2013; **170**: 233-244 [PMID: 23713413]
39 **Minelli R**, Serpe L, Pettazzoni P, Minero V, Barrera G, Gigliotti C, Mesturini R, Rosa AC, Gasco P, Vivenza N, Muntoni E, Fantozzi R, Dianzani U, Zara GP, Dianzani C. Cholesteryl butyrate solid lipid nanoparticles inhibit the adhesion and migration of colon cancer cells. *Br J Pharmacol* 2012; **166**: 587-601 [PMID: 22049973 DOI: 10.1111/j.1476-5381.2011.01768.x]
40 **Serpe L**, Catalano MG, Cavalli R, Ugazio E, Bosco O, Canaparo R, Muntoni E, Frairia R, Gasco MR, Eandi M, Zara GP. Cytotoxicity of anticancer drugs incorporated in solid lipid nanoparticles on HT-29 colorectal cancer cell line. *Eur J Pharm Biopharm* 2004; **58**: 673-680 [PMID: 15451544 DOI: 10.1016/j.ejpb.2004.03.026]
41 **Serpe L**, Laurora S, Pizzimenti S, Ugazio E, Ponti R, Canaparo R, Briatore F, Barrera G, Gasco MR, Bernengo MG, Eandi M, Zara GP. Cholesteryl butyrate solid lipid nanoparticles as a butyric acid pro-drug: effects on cell proliferation, cell-cycle distribution and c-myc expression in human leukemic cells. *Anticancer Drugs* 2004; **15**: 525-536 [PMID: 15166628]
42 **Dianzani C**, Cavalli R, Zara GP, Gallicchio M, Lombardi G, Gasco MR, Panzanelli P, Fantozzi R. Cholesteryl butyrate solid lipid nanoparticles inhibit adhesion of human neutrophils to endothelial cells. *Br J Pharmacol* 2006; **148**: 648-656 [PMID: 16702992 DOI: 10.1038/sj.bjp.0706761]
43 **Liu FC**, Hoyt DB, Coimbra R, Junger WG. Proliferation assays with human, rabbit, rat, and mouse lymphocytes. *In Vitro Cell Dev Biol Anim* 1996; **32**: 520-523 [PMID: 8946221]
44 **Rachmilewitz D**, Karmeli F, Takabayashi K, Hayashi T, Leider-Trejo L, Lee J, Leoni LM, Raz E. Immunostimulatory DNA ameliorates experimental and spontaneous murine colitis. *Gastroenterology* 2002; **122**: 1428-1441 [PMID: 11984528]
45 **Yan Y**, Kolachala V, Dalmasso G, Nguyen H, Laroui H, Sitaraman SV, Merlin D. Temporal and spatial analysis of clinical and molecular parameters in dextran sodium sulfate induced colitis. *PLoS One* 2009; **4**: e6073 [PMID: 19562033 DOI: 10.1371/journal.pone.0006073]
46 **Takedatsu H**, Mitsuyama K, Torimura T. Nanomedicine and drug delivery strategies for treatment of inflammatory bowel disease. *World J Gastroenterol* 2015; **21**: 11343-11352 [PMID: 26525603 DOI: 10.3748/wjg.v21.i40.11343]
47 **Nakase H**, Okazaki K, Tabata Y, Uose S, Ohana M, Uchida K, Matsushima Y, Kawanami C, Oshima C, Ikada Y, Chiba T. Development of an oral drug delivery system targeting immune-regulating cells in experimental inflammatory bowel disease: a new therapeutic strategy. *J Pharmacol Exp Ther* 2000; **292**: 15-21 [PMID: 10604927]
48 **Geszke-Moritz M**, Moritz M. Solid lipid nanoparticles as attractive drug vehicles: Composition, properties and therapeutic strategies. *Mater Sci Eng C Mater Biol Appl* 2016; **68**: 982-994 [PMID: 27524099 DOI: 10.1016/j.msec.2016.05.119]
49 **Suchaoin W**, Bernkop-Schnürch A. Nanocarriers protecting toward an intestinal pre-uptake metabolism. *Nanomedicine* (Lond) 2017; **12**: 255-269 [PMID: 28093952 DOI: 10.2217/nnm-2016-0331]
50 **Song M**, Xia B, Li J. Effects of topical treatment of sodium butyrate and 5-aminosalicylic acid on expression of trefoil factor 3, interleukin 1beta, and nuclear factor kappaB in trinitrobenzene sulphonic acid induced colitis in rats. *Postgrad Med J* 2006; **82**: 130-135 [PMID: 16461476 DOI: 10.1136/pgmj.2005.037945]
51 **Guerron AD**, Rawat R, Sali A, Spurney CF, Pistilli E, Cha HJ, Pandey GS, Gernapudi R, Francia D, Farajian V, Escolar DM, Bossi L, Becker M, Zerr P, de la Porte S, Gordish-Dressman H, Partridge T, Hoffman EP, Nagaraju K. Functional and molecular effects of arginine butyrate and prednisone on muscle and heart in the mdx mouse model of Duchenne Muscular Dystrophy. *PLoS One* 2010; **5**: e11220 [PMID: 20574530]
52 **Berni Canani R**, Di Costanzo M, Leone L. The epigenetic effects of butyrate: potential therapeutic implications for clinical practice. *Clin Epigenetics* 2012; **4**: 4 [PMID: 22414433 DOI: 10.1186/1868-7083-4-4]
53 **Rieder F**, Karrasch T, Ben-Horin S, Schirbel A, Ehehalt R, Wehkamp J, de Haar C, Velin D, Latella G, Scaldaferri F, Rogler G, Higgins P, Sans M. Results of the 2nd scientific workshop of the ECCO (III): basic mechanisms of intestinal healing. *J Crohns Colitis* 2012; **6**: 373-385 [PMID: 22405177]
54 **Felice C**, Lewis A, Armuzzi A, Lindsay JO, Silver A. Review article: selective histone deacetylase isoforms as potential therapeutic targets in inflammatory bowel diseases. *Aliment Pharmacol Ther* 2015; **41**: 26-38 [PMID: 25367825]
55 **Tak PP**, Firestein GS. NF-kappaB: a key role in inflammatory diseases. *J Clin Invest* 2001; **107**: 7-11 [PMID: 11134171]
56 **Auphan N**, DiDonato JA, Rosette C, Helmberg A, Karin M. Immunosuppression by glucocorticoids: inhibition of NF-kappa B activity through induction of I kappa B synthesis. *Science* 1995; **270**: 286-290 [PMID: 7569976]

P- Reviewer: Battat R, Ozturk E, Vidal S **S- Editor**: Ma YJ
L- Editor: Filipodia **E- Editor**: Zhang FF

World Journal of Gastroenterology

Submit a Manuscript: http://www.f6publishing.com

World J Gastroenterol 2017 June 21; 23(23): 4211-4221

DOI: 10.3748/wjg.v23.i23.4211

ISSN 1007-9327 (print) ISSN 2219-2840 (online)

ORIGINAL ARTICLE

Basic Study

Relevance of proteolysis and proteasome activation in fatty liver graft preservation: An Institut Georges Lopez-1 *vs* University of Wisconsin appraisal

Mohamed Amine Zaouali, Arnau Panisello-Roselló, Alexandre Lopez, Carlos Castro Benítez, Emma Folch-Puy, Agustín García-Gil, Teresa Carbonell, René Adam, Joan Roselló-Catafau

Mohamed Amine Zaouali, Arnau Panisello-Roselló, Emma Folch-Puy, Joan Roselló-Catafau, Experimental Hepatic Ischemia-Reperfusion Unit, Institut d'Investigacions Biomèdiques de Barcelona, Spanish National Research Council, 08036 Barcelona, Spain

Mohamed Amine Zaouali, Research Unit of Biology and molecular anthropology applied to development and Health (UR12ES11), Faculty of Pharmacy, University of Monastir, Monastir 5000, Tunisia

Mohamed Amine Zaouali, Tunisia and Institute of Biotechnology of Monastir, University of Monastir, Monastir 5000, Tunisia

Alexandre Lopez, Carlos Castro Benítez, René Adam, Centre Hépatobiliaire, AP-PH, Hôpital Paul Brousse, 94804 Paris, France

Agustín García-Gil, Hospital Clínico de Zaragoza, 50009 Zaragoza, Spain

Teresa Carbonell, Facultat Biologia, Universitat de Barcelona, 08028 Barcelona, Catalonia, Spain

Author contributions: Zaouali MA and Panisello-Roselló A contributed equally to this study and carried out the experimental work; Lopez A, Folch-Puy E and Castro Benítez C provided protocols and analyzed data; Panisello-Roselló A, García-Gil A, Carbonell T and Adam R established the animal experimental model used in this study and contributed to the critical analyses of the data; Zaouali MA, Panisello-Roselló A and Roselló-Catafau J designed the study, coordinated the experiments and wrote the paper.

Supported by Instituto de Salud Carlos III (ISCIII) through the FIS project PI12/0056, co-funded by FEDER from Regional Development European Funds (European Union).

Conflict-of-interest statement: None of the authors have any conflict of interest to declare related to this paper.

Data sharing statement: Technical data are available from the corresponding author at jrcbam@iibb.csic.es. Participants gave informed consent for data sharing.

Manuscript source: Invited manuscript

Correspondence to: Dr. Joan Roselló-Catafau, Experimental Hepatic Ischemia-Reperfusion Unit, Institut d'Investigacions Biomèdiques de Barcelona, Spanish National Research Council, C/Rosselló 161, 7th floor, 08036 Barcelona, Spain. joan.rosello@iibb.csic.es
Telephone: +34-93-3638333
Fax: +34-93-3638301

Received: January 25, 2017
Peer-review started: February 1, 2017
First decision: March 16, 2017
Revised: April 8, 2017
Accepted: June 1, 2017
Article in press: June 1, 2017
Published online: June 21, 2017

Abstract

AIM

To compare liver proteolysis and proteasome activation in steatotic liver grafts conserved in University of Wisconsin (UW) and Institut Georges Lopez-1 (IGL-1)

solutions.

METHODS

Fatty liver grafts from male obese Zücker rats were conserved in UW and IGL-1 solutions for 24 h at 4 ℃ and subjected to "*ex vivo*" normo-thermic perfusion (2 h; 37 ℃). Liver proteolysis in tissue specimens and perfusate was measured by reverse-phase high performance liquid chromatography. Total free amino acid release was correlated with the activation of the ubiquitin proteasome system (UPS: measured as chymotryptic-like activity and 20S and 19S proteasome), the prevention of liver injury (transaminases), mitochondrial injury (confocal microscopy) and inflammation markers (TNF 1 alpha, high mobility group box-1 (HGMB-1) and PPAR gamma), and liver apoptosis (TUNEL assay, cytochrome c and caspase 3).

RESULTS

Profiles of free AA (alanine, proline, leucine, isoleucine, methionine, lysine, ornithine, and threonine, among others) were similar for tissue and reperfusion effluent. In all cases, the IGL-1 solution showed a significantly higher prevention of proteolysis than UW ($P < 0.05$) after cold ischemia reperfusion. Livers conserved in IGL-1 presented more effective prevention of ATP-breakdown and more inhibition of UPS activity (measured as chymotryptic-like activity). In addition, the prevention of liver proteolysis and UPS activation correlated with the prevention of liver injury (AST/ALT) and mitochondrial damage (revealed by confocal microscopy findings) as well as with the prevention of inflammatory markers (TNF1alpha and HMGB) after reperfusion. In addition, the liver grafts preserved in IGL-1 showed a significant decrease in liver apoptosis, as shown by TUNEL assay and the reduction of cytochrome c, caspase 3 and P62 levels.

CONCLUSION

Our comparison of these two preservation solutions suggests that IGL-1 helps to prevent ATP breakdown more effectively than UW and subsequently achieves a higher UPS inhibition and reduced liver proteolysis.

Key words: Liver proteolysis; Proteasome activation; Fatty liver preservation; Institut Georges Lopez-1; University of Wisconsin; High mobility group box 1; Cold ischemia reperfusion injury

Core tip: Although several reports have confirmed that proteolytic activity during cold storage determines graft outcome after transplantation, the effect of preservation solution on steatotic liver graft proteolysis and on the activation of ATP-dependent proteasome during cold ischemia injury has not been fully investigated. Here, we compared the effect of two preservation solutions Institut Georges Lopez-1(IGL-1) and University of Wisconsin on liver proteolysis and ubiquitin-proteasome activation when steatotic liver grafts were subjected to cold storage. We provide evidence for a protective role of proteasome and proteolysis inhibition using IGL-1 during steatotic liver graft preservation.

Zaouali MA, Panisello-Roselló A, Lopez A, Castro Benítez C, Folch-Puy E, García-Gil A, Carbonell T, Adam R, Roselló-Catafau J. Relevance of proteolysis and proteasome activation in fatty liver graft preservation: An Institut Georges Lopez-1 *vs* University of Wisconsin appraisal. *World J Gastroenterol* 2017; 23(23): 4211-4221 Available from: URL: http://www.wjgnet.com/1007-9327/full/v23/i23/4211.htm DOI: http://dx.doi.org/10.3748/wjg.v23.i23.4211

INTRODUCTION

Functional graft recovery remains one of the major complications after liver surgery. Cold static preservation is an inherent feature of liver transplantation (LT) and is strongly associated with graft outcome after transplantation[1]. Despite continued attempts to improve preservation solutions, success in liver transplantation is always hampered by the complexity of ischemia reperfusion (I/R) injury[2,3]. In addition, exacerbated I/R injury is due, to a large extent, to the quality of the graft and to its conservation in preservation solutions[4,5]. In the liver, the presence of steatosis makes the graft more vulnerable to cold I/R injury[6] and thus aggravates the detrimental effects of cold I/R injury in fatty liver grafts preserved in commercial solutions.

University of Wisconsin (UW) solution is considered to be the standard solution for liver graft preservation. However, alternative preservation solutions have been used in clinical liver transplantation, such as Institut Georges Lopez-1 (IGL-1), histidine-tryptophan-ketoglutarate (HTK) and Celsior solutions. Briefly, IGL-1 is a new preservation solution whose differences vis-à-vis UW are the oncotic agent used (PEG35, instead of HES) and its lower potassium and lower viscosity. HTK and Celsior solutions have no oncotic agent[2,7].

The ubiquitin-proteasome system (UPS) is the principal non-lysosomal proteolytic system and is thought to contribute to a large variety of pathologies, including I/R injury associated with LT[8-10]. Recently, we showed that UPS modulation is a pharmacological target for improving graft preservation and for reducing I/R injury in the liver[10].

Moreover, it is has been well established that proteolysis is necessary to control protein concentration and to prevent its abnormal accumulation[8]. Proteasomes also perform multiple intracellular functions, such as the degradation of damaged proteins and the modulation of many regulatory proteins that are involved in inflammatory processes including the cell cycle, metabolism, growth and differentiation[8]. In

fact, proteolytic activity is necessary for amino acid (AA) recycling of proteins that are no longer needed, thus preventing their accumulation in the cytoplasm[11,12].

The first evidence that proteolysis has a detrimental effect on liver graft out-come after transplantation was provided by Calmus *et al*[13] who showed that the degree of proteolytic activity detected by the free amino acids in the effluent of human liver grafts is a good predictive marker for postoperative graft function when using UW solution. Later, Upadhya *et al*[14] proved that the composition of the preservation solution may be relevant for the prevention of liver proteolysis. These authors demonstrated that lactobionate, a component of the UW solution, is a key factor for preventing the release of matrix metalloproteinases, particularly gelatinases, during cold preservation[15]. More recently, other solutions such as IGL-1 have also been considered as potential alternatives to UW[1,16]. Despite the proven efficiency of IGL-1, especially in steatotic liver preservation, its effects on graft proteolysis have not been investigated to date.

It is well known that energy breakdown following oxygen deprivation in liver graft is the main event during cold storage, and that its effects are concomitant with a significant decrease in ATP content which leads to severe graft damage[2]. It was recently reported that this ATP decline may activate a subset of 26S proteasomes, a cell-destructive protease that contributes to myocardial injury during cold ischemia[17,18]. Moreover, this proteasome inhibition contributes to prolonging myocardial viability in hypothermic preservation[19]. Recently, we demonstrated that proteasome inhibitors such as MG132 and bortezomib protected fatty liver grafts when they were used as additives to UW and IGL-1 solutions[10,20]. However, the role of the UPS system and liver proteolysis in fatty liver graft preservation has not been fully investigated.

The aim of this study is to assess the potential relationship between proteolysis, energy breakdown and liver injury using UW and IGL-1 solutions, in order to shed new light on the molecular and cellular mechanisms involved in liver cold I/R injury.

MATERIALS AND METHODS

Animals

Homozygous (obese [Ob]) Zücker rats aged 16-18 wk were purchased from Iffa-Credo (L'Abresle, France). An "*ex vivo*" perfused rat liver model was used, as previously described. All procedures were performed under isofluorane inhalation anesthesia according to the European Union regulations (Directive 86/609 EEC) for animal experiments[21].

Preservation solutions

We used UW (gold standard) and IGL-1 solutions. IGL-1 solution is a modification of UW solution in which hydroxyethyl starch (HES) is substituted by polyethylene glycol 35 (PEG 35) and the ionic K/Na ratio is also reversed.

Experimental groups and isolated perfused liver model

Briefly, 24 rats were randomly divided into three groups. The abdomen was opened by midline incision, following cannulation of the common bile duct, and the portal vein, the splenic and gastroduodenal veins were ligated. After organ recovery the livers were flushed with UW (UW group) and IGL-1 (IGL-1 group) preservation solutions respectively, and then stored in each solution for 24 h at 4 ℃. Next, the preserved livers were flushed with a perfusion liquid consisting of a cell culture medium (William's medium E, Bio Whitaker, Barcelona, Spain), with a Krebs-Henseleit-like electrolyte composition enriched with 5% albumin as osmotic support. For the reperfusion, livers were connected *via* the portal vein to a recirculating perfusion system for 2 h at 37 ℃. The third study group was a Control group (Cont) in which livers were flushed and immediately perfused *ex vivo* without ischemic preservation. Time 0 was the point at which the portal catheter was satisfactorily connected to the circuit. During an initial equilibration period of 15 min of perfusion, the flow was progressively increased in order to stabilize the portal pressure at 12 mmHg (Pression Monitor BP-1, Instruments, Inc., Sarasota, FL, United States). In order to maintain the portal pressure at 12 mmHg, the flow rate was modified using a peristaltic pump (Minipuls 3, Gilson, France). The buffer was continuously ventilated with a 95% O_2 and 5% CO_2 gas mixture. It was subsequently passed through a heat exchanger (37 ℃) and a bubble trap prior to entering the liver[21,22].

Protocol I Proteasome activity and ATP levels after 24 h cold storage: In order to evaluate the proteasome activity and ATP breakdown in steatotic liver grafts following 24 h-cold storage in UW or IGL-1, aliquots of the flush effluents and liver tissue samples were collected and stored at -80 ℃ for subsequent measurement. Control livers (Cont 1 group) were flushed with Ringer's lactate solution *via* the portal vein without ischemic preservation.

Protocol II Evaluation of proteasome activity and liver viability after 2 h reperfusion: To examine the role of UW and IGL-1 solutions in proteasome activation and their subsequent effect on proteolysis, liver function and also liver damage, fatty livers were subjected to two hours of normoxic reperfusion. Then, the perfusate effluent and the liver tissue sample were collected and stored at -80 ℃ for later measurement. In control group (Cont 2) livers were flushed with Ringer's lactate and immediately perfused *ex vivo* without ischemic preservation.

Biochemical determinations

Nucleotide analysis and ATP content: Livers were homogenized in perchloric acid solution, and

the adenine nucleotide pool was measured by high-performance liquid chromatography (HPLC) as previously reported[23,24].

Assessment of liver proteolysis[7]: Free amino acid content in *ex vivo* eluates and tissue specimens was measured by HPLC techniques, as previously described[25]. Briefly, effluent and tissue homogenization samples were first deproteinized by ultrafiltration and then derivatized with phenylisothiocyanate (PITC) to produce phenylthiocarbamyl (PTC) amino acids. Amino acids were determined by automated gradient reverse phase HPLC and ultraviolet detection at 254 nm. Quantitative analysis of total free amino acids was performed using the PICO.TAG Amino Acid Analysis System[25].

Transaminase assay: Hepatic injury was evaluated according to transaminase levels using a commercial kit from Boehringer Mannheim (Munich, Germany)[10].

Proteasome chymotryptic-like activity assay[9,10]: ATP-dependent chymotryptic activity of the proteasome was measured using the substrate N-Suc-Leu-Leu-Val-Tyr-aminomethylcoumarin (ENZO Life Sciences). The cleavage products AMC were analyzed in a fluorimeter (excitation/emission 380/460 nm). Product formation was linear with time (at least for 60 min). Background activity (caused by nonproteasomal degradation) was determined by the addition of the proteasome inhibitor epoxomicin at a final concentration of 20 μmol/L (ENZO Life Sciences).

Glutamate dehydrogenase activity[10]: Liver mitochondrial damage was measured by GLDH activity levels at the end of reperfusion, as previously reported.

Inflammatory mediators: TNF alpha and IL-1/IL10

TNF alpha levels were measured using a commercial immunoassay kit for rat TNF alpha from Biosource (Caramillo)[10,26]. IL-1 beta and IL10 were measured by enzyme-linked immunosorbent assay as previously reported[10,27]. Commercial kits from Amersham LifeScience (Amersham, United Kingdom) were used.

Confocal microscopy for mitochondrial damage

During 2 h of normothermic preservation, fatty livers were perfused with Krebs supplemented with rhodamine 123 (0.11 mg/L, Sigma, R8004) for mitochondrial membrane potential staining and 1% Evans blue dye used as a viability assay on the basis of its penetration into non-viable cells. Fatty livers were then carefully sectioned (0.5 cm^3 fragments) and the internal side of the liver was exposed on the glass coverslip mounted on the stage of a Leica TCS SP5 resonant scan multiphoton confocal microscope (Leica Microsystems Heidelberg GmbH) equipped with a HCX IR APO L 25 × water immersion objective (Numerical Aperture 0.95), scanner at 400 lines/s, and a near infrared Titanium:Saphire laser (MaiTai, SpectraPhysics) for two-photon excitation running at 800 nm. Images were acquired with resonant scan at 8000 lines/s. Two-photon excitation was performed at 800 nm and emission of the different fluorescent dyes was captured at the following wavelength ranges: Evans blue dye (515-560 nm), and rhodamine 123 (500-550 nm)[28,29].

Western blotting analysis of PPARγ, HMGB-1, Caspase3, cytochrome C, 20S5beta and 19S proteasome subunit and β-Actin

Liver tissue was homogenized as described elsewhere[30], and proteins were separated by sodium dodecyl sulfate polyacrylamide gel electrophoresis and transferred to polyvinylidene fluoride membranes. Membranes were immunoblotted with antibodies against 20S5beta and 19S proteasome subunits (BML-PW 8895,and BML-PW8825 respectively, ENZO Life Sciences, Madrid, Spain), PPAR-γ and HMGB-1 (Abcam, United Kingdom), cleaved caspase 3 and cytochrome C (Cell Signaling, Beverly, MA, United States), and β-Actin (Sigma Chemical, St. Louis, MO, United States). Signals were detected by enhanced chemiluminescence and quantified by scanning densitometry[10].

Terminal deoxynucleotidyl transferase-mediated dUTP nick end-labeling method[31]

To detect apoptotic cells, 16-μm-thick frozen sections from livers were collected on poly-L-lysine-coated glass slides, and the nuclear DNA fragmentation of apoptotic cells was labeled *in situ* by the TUNEL method using an ApopTag Peroxidase In Situ Apoptosis Detection Kit (Intergen Co. Purchase, NY, United States). Briefly, the sections were fixed in 1% paraformaldehyde in PBS, pH 7.4 for 10 min at room temperature and, after washing in PBS, they were post-fixed in precooled ethanol:acetic acid 2:1 for 5 min at -20 ℃. After rinsing in distilled water, the sections were treated with 3% hydrogen peroxide in 10% methanol for 5 min, washed with distilled water and incubated in the equilibration buffer provided for 10 min. Then, the sections were incubated with terminal deoxynucleotide transferase (TdT) in the reaction buffer provided with digoxigenin-dUTP, in a humidifier chamber at 37 ℃ for 1 h. The incorporated digoxigenin-dUTP was detected by peroxidase-conjugated antidigoxigenin antibody and the signal developed by incubation with 3,3-diamino-benzidine (DAB) in the presence of H_2O_2. The slides were counterstained with Harris hematoxylin. Negative controls were prepared by replacing the antidigoxigenin antibody with phosphate saline buffer, and a case of breast carcinoma was included as positive control.

Statistical analysis

Data are expressed as means ± SD and were compared statistically by variance analysis, followed by the

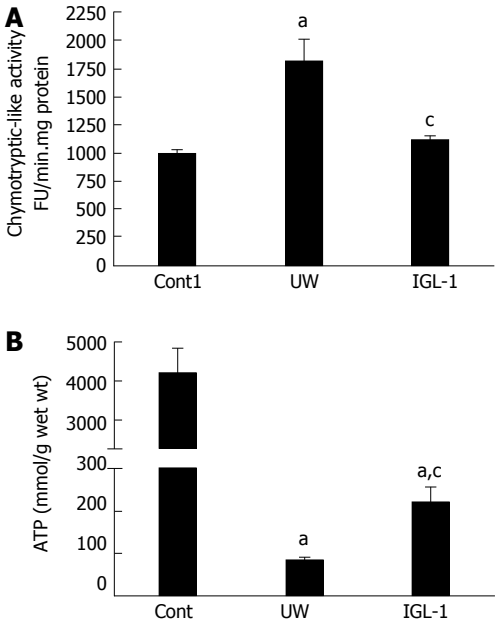

Figure 1 Chymotryptic-like proteasome activity (A) and ATP content (B) in steatotic livers after cold preservation. $^{a}P < 0.05$ *vs* Cont1, $^{c}P < 0.05$ *vs* UW. Cont1: Liver flushed without cold preservation; UW: Liver preserved in UW solution; IGL-1: Liver preserved in IGL-1 solution; UW: University of Wisconsin; IGL-1: Institut Georges Lopez-1.

Student-Newman-Keuls test. $P < 0.05$ was considered significant.

RESULTS

We evaluated the relevance of proteasome activity and proteolysis in fatty livers preserved in IGL-1 and UW solutions when subjected to normothermic reperfusion. As Figure 1A shows, chymotryptic-like proteasome activity increased in steatotic liver grafts during cold preservation in UW solution compared with control non-preserved livers. However, steatotic livers preserved in IGL-1 solution showed lower chymotryptic-like proteasome activity than those preserved in UW solution.

Given the close relationship between proteasome activity and the ATP contents during cold preservation[18], we next evaluated the ATP concentration during liver preservation. Lower ATP levels during cold storage were observed in steatotic livers preserved in UW solution than in non-preserved livers. ATP breakdown was more effectively prevented by the use of IGL-1 solution (Figure 1B).

With these results in mind, we also evaluated the chymotryptic-like proteasome activity and the 19S and 20S proteasome protein levels after reperfusion. As indicated in Figure 2A, the chymotryptic-like proteasome activity after reperfusion follows the same pattern profile as those observed for cold storage. The 20S proteasome protein levels were reduced only when IGL-1 preservation solution was used. In contrast, the 19S subset protein levels remained unchanged

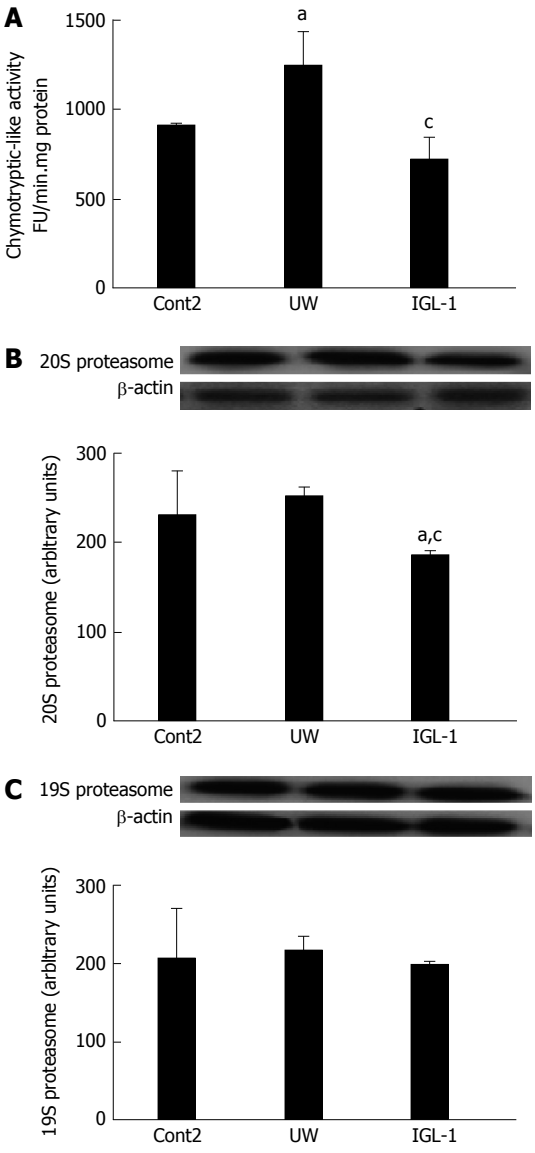

Figure 2 Chymotryptic-like activity (A) and 20S (B) and 19S (C) protein levels after reperfusion. Representative Western blot at the top and densitometric analysis at the bottom of 20S (B) and 19S (C). $^{a}P < 0.05$ *vs* Cont1, $^{c}P < 0.05$ *vs* UW. Cont2: Liver flushed and perfused ex vivo without cold preservation; UW: Liver preserved in UW solution; IGL-1: Liver preserved in IGL-1 solution; UW: University of Wisconsin; IGL-1: Institut Georges Lopez-1.

across all experimental groups (Figure 2B and C).

Also, the AA profiling studies confirmed that IGL-1 offered more efficient prevention of AA release in tissue graft specimens and effluents after 2 h-reperfusion at 37 ℃. The AA profiles obtained in liver tissue (Figure 3B) and eluate samples (Figure 3A) were similar but were seen more in tissue samples than in *ex vivo* eluates, thus confirming the relevance of proteolysis (measured as free AA release) after cold I/R injury. The better prevention of liver proteolysis in grafts preserved in IGL-1 solution than in UW was consistent with significant reductions in other parameters associated with the pathophysiology of liver I/R injury, such as transaminases (ALT and AST) and GLDH release as sensitive and specific markers of

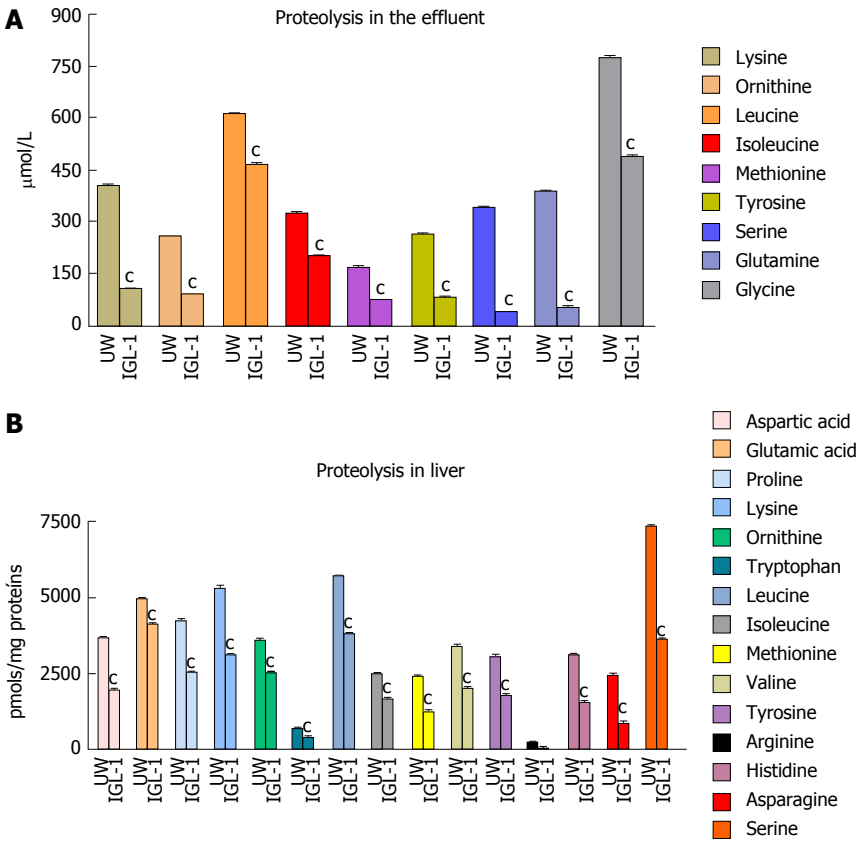

Figure 3 Proteolysis in effluent and liver grafts after reperfusion. Amino acid levels in the effluent and tissue after reperfusion. $^{c}P < 0.05$ *vs* UW. UW: Liver preserved in UW solution; IGL-1: Liver preserved in IGL-1 solution; UW: University of Wisconsin; IGL-1: Institut Georges Lopez-1.

Table 1 ALT and AST (Liver injury) and GLDH (mitochondrial damage) in steatotic liver grafts preserved in University of Wisconsin and Institut Georges Lopez-1 solutions and then subjected to two hours of normothermic reperfusion

Liver injury	Cont2	UW	IGL-1
ALT, U/L	26.76 ± 4.095	172.1 ± 10.81[a]	92.99 ± 8.64[a,c]
AST, U/L	24.92 ± 2.42	280.93 ± 14.14[a]	202.24 ± 24.71[a,c]
GLDH, U/L	26.13 ± 6.83	425.22 ± 156.92[a]	143 ± 31.16[a,c]

$^{a}P < 0.05$ *vs* Cont, $^{c}P < 0.05$ *vs* UW. UW: University of Wisconsin; IGL-1: Institut Georges Lopez-1.

mitochondrial damage (Table 1).

Given that proteasome activity plays a crucial role in the modulation of many of the regulatory proteins involved in inflammatory processes in fatty liver grafts[8], we evaluated the involvement of other inflammatory markers in fatty liver, such as PPARγ, in the proteasome changes and proteolysis inhibition in steatotic liver grafts subjected to cold I/R injury. As shown in Figure 4A, PPARγ protein levels in steatotic liver grafts preserved in UW solution remained unchanged compared with control non preserved grafts, but increased significantly in grafts preserved in IGL-1 preservation solution. We also measured the effect of preservation solution on other cytokines such as high mobility group box 1 (HMGB1) which was recently shown to be involved in fatty liver preservation and transplantation[32]. IGL-1 showed lower levels of HMGB-1 than UW (Figure 4B) concomitant with a significant reduction in the release of other inflammatory cytokines such as TNFα but not for IL1. IGL-1 also increased the concomitant release of anti-inflammatory IL-10 in fatty livers after reperfusion (Table 2).

Next, we evaluated the effect of proteasome activity and proteolysis modulation on apoptosis and autophagy induction. Figure 5 shows a significant increase in cytochrome C and cleaved caspase 3 protein levels in steatotic livers preserved in UW solution compared with non-preserved ones. However, preservation in IGL-1 solution significantly reduced both apoptotic markers. In addition, the autophagy-related ubiquitin-binding protein SQSTM1/p62, which is involved in aggresome formation and degradation through autophagy, is increased in steatotic livers preserved in UW solution compared with those preserved in IGL-1 solution (Figure 5C).

This effect on liver apoptosis in both IGL-1 and UW solutions was also corroborated by the percentage of TUNEL-positive hepatocytes (Figure 6). Only a few sinusoidal lining cells were positive to TUNEL staining in control non-preserved steatotic livers (Figure 6B). After preservation with UW and reperfusion, the number of positive cells significantly increased (Figure 6B). Preservation with IGL-1 reduced apoptotic

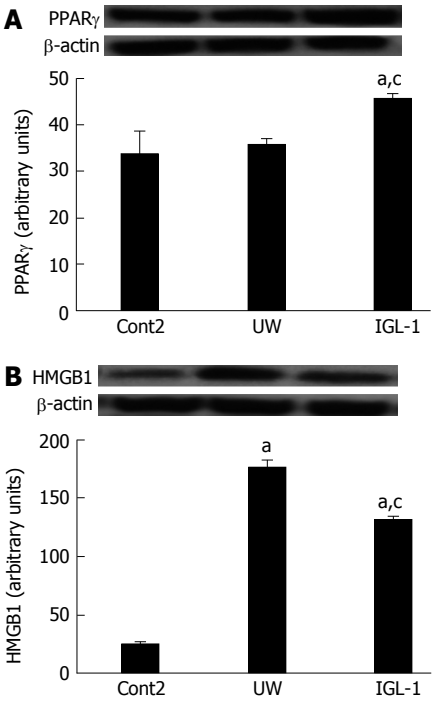

Figure 4 PPARγ and HMGB-1 protein levels after reperfusion. Representative Western blot at the top and densitometric analysis at the bottom of protein levels of PPARγ (A) and HMGB-1 (B) in steatotic liver grafts. $^{a}P < 0.05$ *vs* Cont2, $^{c}P < 0.05$ *vs* UW. Cont2: Liver flushed and perfused ex vivo without cold preservation; UW: Liver preserved in UW solution; IGL-1: Liver preserved in IGL-1 solution; UW: University of Wisconsin; IGL-1: Institut Georges Lopez-1.

Table 2 TNFα, IL-1 and IL-10 levels (inflammation) in steatotic liver grafts preserved in University of Wisconsin and Institut Georges Lopez-1 solutions and then subjected to two hours of normothermic reperfusion

Inflammation	Cont2	UW	IGL-1
TNFα (pg/mL)	26.17 ± 5.85	1285.89 ± 231.32[a]	1005.83 ± 101.94[a,c]
IL-1β (pg/mL)	4.29 ± 1.66	89.01 ± 10.53[a]	84.69 ± 7.79[a]
IL-10 (pg/mL)	134.89 ± 14.84	109.33 ± 17.3[a]	192.13 ± 7.73[a,c]

$^{a}P < 0.05$ *vs* Cont, $^{c}P < 0.05$ *vs* UW. UW: University of Wisconsin; IGL-1: Institut Georges Lopez-1.

cell death (Figure 6B). In all cases, single (but not clustered) TUNEL-stained cells were observed more extensively in periportal and mid-zonal areas. Finally, the confocal microscopic study confirmed that steatotic livers preserved in IGL-1 solution conserved the membrane potential of liver mitochondria more efficiently, as shown by an increase in the rhodamine 123 cell viability marker (in green) and a decrease in Evans blue labeling (in red), indicating the albumin content and the disrupted mitochondrial membranes (Figure 6A).

DISCUSSION

At present, a considerable number of fatty donor livers have to be discarded, a situation that accentuates even further the critical shortage of human donor livers.

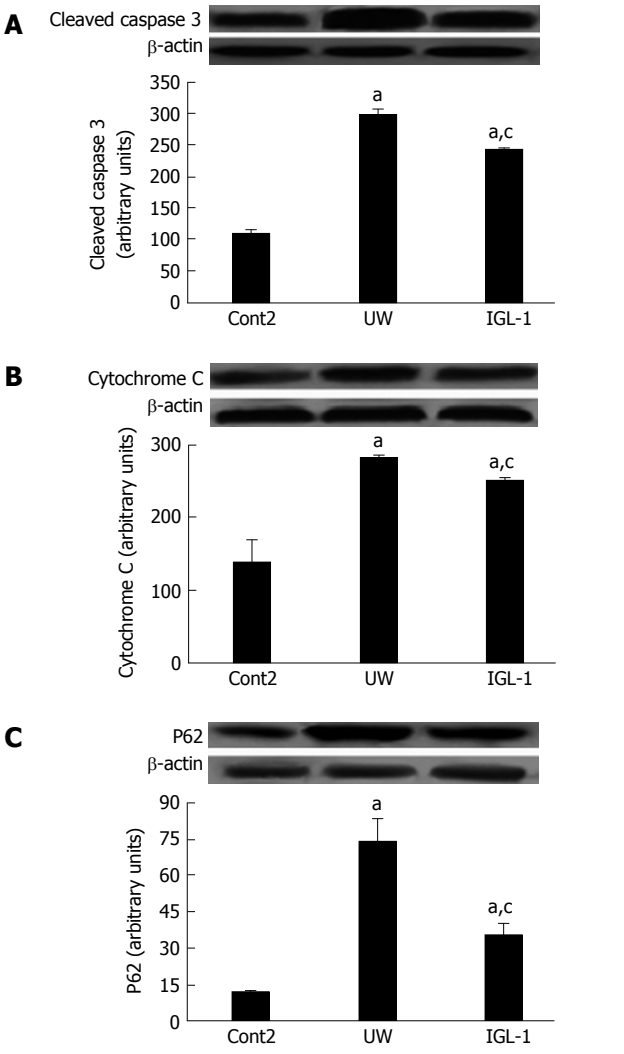

Figure 5 Liver graft apoptosis and autophagy after reperfusion. Representative Western blot at the top and densitometric analysis at the bottom of protein levels of cleaved caspase 3 (A), cytochrome C (B) and P62 (C) in steatotic liver grafts. $^{a}P < 0.05$ *vs* Cont2, $^{c}P < 0.05$ *vs* UW. Cont2: Liver flushed and perfused ex vivo without cold preservation; UW: Liver preserved in UW solution; IGL-1: Liver preserved in IGL-1 solution; UW: University of Wisconsin; IGL-1: Institut Georges Lopez-1.

A better knowledge of the preservation mechanisms of steatotic liver grafts is urgently needed to reduce their high vulnerability to cold I/R injury, and thus to improve their viability after transplantation[33,34].

In this study, we investigated the involvement of UPS activation and liver proteolysis and their relationship with the breakdown energy metabolism in steatotic liver grafts preserved in different commercial preservation solutions such as IGL-1 and UW. We also associated the changes in UPS activation during cold I/R injury with the inflammatory events and liver apoptosis. Our data demonstrate that IGL-1 prevented liver proteolysis more effectively than UW. In all cases, free AA levels determined in tissue specimens and eluates were lower in IGL-1 than in UW after cold I/R. This improved prevention of liver proteolysis with IGL-1 is consistent with its more effective protection against I/R injury. This could be explained, in part,

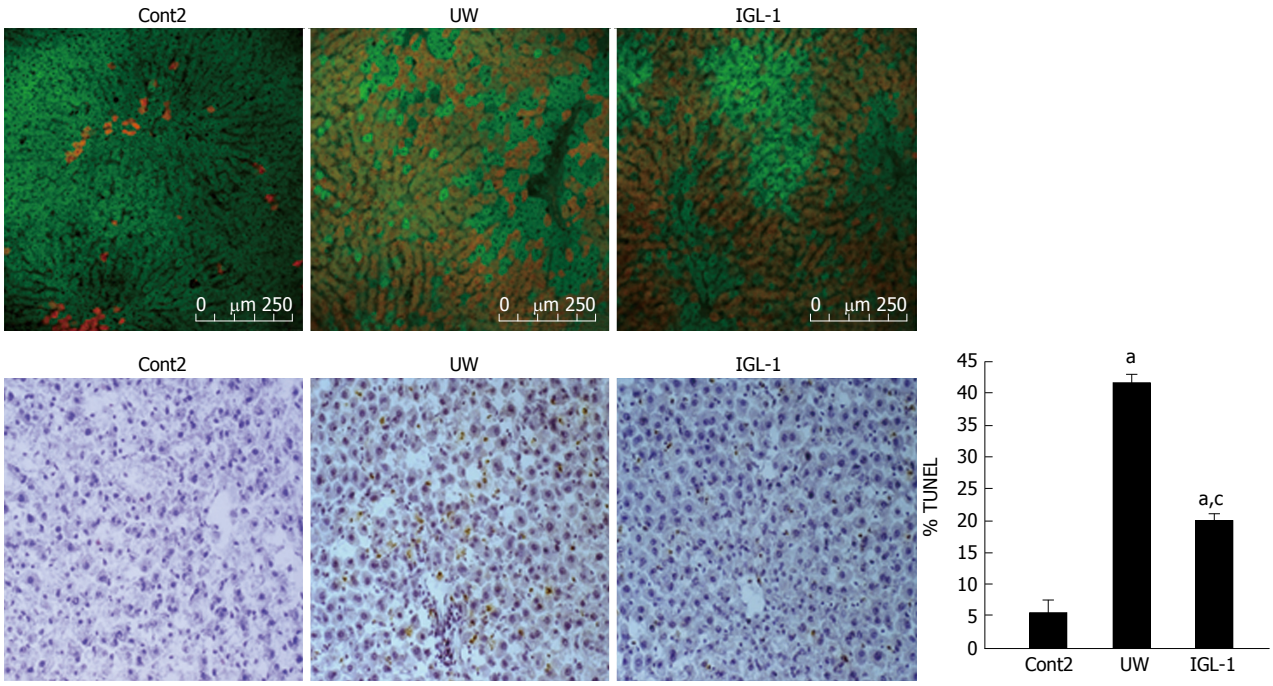

Figure 6 Confocal microscopy findings and Tunel assay after reperfusion. Confocal microscopy images showing green fluorescence of rhodamine 123 cell viability marker and Evans blue dye (in red) used as a viability assay on the basis of its penetration into non-viable cells. Representative light photomicrographs of TUNEL-stained sections. Steatotic livers submitted to cold storage preservation with UW showed numerous positive cells (both hepatocytes and sinusoidal lining cells) compared with control non-preserved livers. The positivity decreased when the livers were submitted to cold storage preservation with IGL-1 solution. $^{a}P < 0.05$ *vs* Cont2, $^{c}P < 0.05$ *vs* UW. Scale bar 50 μm. Cont2: Liver flushed and perfused ex vivo without cold preservation; UW: Liver preserved in UW solution; IGL-1: Liver preserved in IGL-1 solution; UW: University of Wisconsin; IGL-1: Institut Georges Lopez-1.

by the presence of different oncotic agents: PEG35 in IGL-1, and HES in UW. In fact, we have recently demonstrated that the addition of PEG35 to washout solution protects the liver against I/R injury by the inhibition of metalloproteinases MMP9 and MMP2, a finding that may explain its role in preventing liver proteolysis[21]. The presence of lactobionate (a common ingredient of the UW and IGL-1 solutions) may also help to prevent liver proteolysis due its strong inhibitory effect on gelatinases, presumably *via* calcium or zinc chelation[13,14]. This effective prevention of proteolysis is also consistent with the significant reduction in proteasome activity reflected by decreases in chymotryptic-like proteasome activity and 20S proteasome protein levels and the better prevention of energy metabolism breakdown with IGL-1 solution. In fact, a recent report established a functional link between 26S proteasome activity and ATP depletion in tissue during cold I/R injury[18]. Those authors advanced that ATP depletion during ischemic insult appears to activate the 26S proteasome which is formed from a multimeric proteasome core particle (20S proteasome) which is singly or doubly capped at its ends by a 19S regulator complex[17]. Taking this into account, we suggest that the reduced 20S proteasome protein levels in steatotic livers preserved in IGL-1 solution are to do some extent the consequence of the better preservation of ATP content in this group, which thus affects 26S assembly and activity. Furthermore, our results are in accordance with previous studies which have demonstrated the relevance of proteasome inhibition in protecting steatotic liver grafts against I/R injury when preservation solutions were supplemented with proteasome inhibitors MG132 and bortezomib[10,20].

In order to explain the mechanisms by which proteasome modulation and proteolysis inhibition protect steatotic livers against cold I/R injury, we also assessed levels of PPARγ and HMGB-1 proteins, which are both involved in the modulation of the inflammatory response after I/R injury[35-37]. It is clear that PPARγ belongs to the hormone nuclear receptor superfamily of ligand-activated transcription factors which are major regulators of post-ischemic liver injury[35]. Its protective effect is mediated by its anti-inflammatory properties *via* the inhibition of pro-inflammatory gene expression[35] in which the UPS has recently been implicated; the UPS is responsible for PPAR turnover and is also involved in the modulation of the ligand-dependent activity of these nuclear receptors[38].

The fact that the UPS is the major system for selective degradation of short-lived proteins in eukaryotic cells such as PPARγ[38] suggests that proteasome inhibition after steatotic liver graft preservation in IGL-1 solution may be responsible for the PPARγ accumulation induced, thus leading to a reduction in the expression of pro-inflammatory proteins[39]. These findings were also confirmed by the lower HMGB-1 protein levels in livers preserved in IGL-1 solution than in livers preserved in UW. HMGB-1 is a well-known extracellular signaling pro-inflammatory mediator which, when released from cells,

leads to cell death in several pathologies including liver I/R[32]. Our results corroborate those of a previous study which demonstrated that PPARγ-mediated upregulation of miR-142-3p inhibits HMGB-1 expression, which, in turn, is a novel anti-inflammatory mechanism of PPARγ and plays an important role in the treatment of inflammatory diseases[40]. Moreover, HMGB-1 is associated with apoptotic cell death[41] and autophagy modulation[42,43].

Next we evaluated both parameters after cold I/R injury in steatotic livers preserved in UW and IGL-1 solutions. Our results demonstrated that the use of IGL-1 reduced apoptotic cell death, as reflected by decreases in cleaved caspase3 and cytochrome C protein levels when compared with UW solution. The relevance of cytochrome c as a reliable biomarker of mitochondrial damage in fatty liver disease was also reported by another study[44]. These results were correlated with a better prevention of liver mitochondrial damage and were also consistent with the finding that IGL-1 solution efficiently prevented liver apoptosis in rat liver transplantation[45].

Finally, in order to explore the effect of proteasome modulation on autophagy, we determined the levels of autophagy-related ubiquitin-binding protein SQSTM1/p62. This protein is involved in aggresome formation and degradation through autophagy which is associated with the liver graft self-response to cold I/R injury (the SQSTM/p62 substrate that accumulates in autophagy-deficient cells)[46,47]. Our results demonstrated that UW solution increased SQSTM1/p62 protein levels, which are inversely correlated to autophagy, while the use of IGL-1 solution reduced SQSTM1/p62 protein levels, thus showing autophagic activation, as a response to better preservation mechanisms. These results corroborate our previous finding that impaired autophagic clearance after steatotic liver preservation is correlated with increased liver injury[31].

In conclusion, we show that liver graft proteolysis and proteasome activation are dependent on the organ preservation solutions used for liver transplantation such as UW and IGL-1. Our results confirm the relevance of both markers for evaluating the graft damage caused by cold I/R injury in fatty liver preservation.

ACKNOWLEDGMENTS

The authors would like to thank Michael Maudsley at the Language Advisory Service of the University of Barcelona for revising the English text.

COMMENTS

Background

Cold ischemia reperfusion (I/R) injury is a multifactorial process that can interfere with graft function after liver transplantation (LT). A better understanding of the pathophysiology of this injury is fundamental for the development of protective strategies able to improve the outcome of LT. The ischemic graft damage that occurs during cold storage of fatty liver grafts depends in part on the ATP-energy breakdown. It is well known that the prevention of ATP-breakdown during cold static preservation is associated with inhibition of ubiquitin-proteasome system (UPS) activity, which helps to protect the liver graft against reperfusion. In this context the selection of commercial organ solution seems crucial for modulating the UPS, as well as the graft proteolysis against cold I/R injury. We demonstrate that Institut Georges Lopez-1 (IGL-1) solution reduces cold I/R injury more efficiently by helping to prevent ATP- breakdown and subsequently achieving a higher UPS inhibition than University of Wisconsin (UW). Both these factors are modulated by the organ preservation solution and determine the degree of proteolysis in the liver graft.

Research frontiers

The authors focused on strategies for interfering with the mechanisms responsible for hepatic I/R injury associated with LT, and on strategies for enhancing the endogenous mechanisms that protect against cold ischemic damage. UW and IGL-1 solutions are widely used in LT. They demonstrate that the nature of the oncotic agent present in UW and IGL-1 solutions is responsible, in part, for the modulation of energy breakdown and its subsequent inhibitory action on the UPS, which are key factors in graft protection against I/R insult. In the present study IGL-1 showed more hepato-protective effects than UW, due, in part, to the presence of the oncotic agent PEG-35.

Innovations and breakthroughs

This study demonstrates for the first time that UPS inhibition is a key factor in fatty liver preservation using different commercial organ preservation solutions such as UW and IGL-1. UPS inhibition may explain the better prevention of the proteolysis observed in IGL-1 than in UW, thus favoring the use of IGL-1 in fatty liver graft preservation.

Applications

UPS inhibition and the degree of proteolysis can be used to predict the viability of steatotic liver grafts after prolonged static preservation.

Terminology

The UPS system and proteolysis are involved in the complex pathophysiology of hepatic cold I/R injury. Both are helpful for evaluating the fatty liver preservation using either static or dynamic preservation (with machine perfusion) strategies.

Peer-review

The manuscript is about Relevance of proteolysis and proteasome activation in fatty liver graft preservation. There must be possible prospective achievement in this basic studies. The authors try to solve the problem of preservation of fatty donor liver from ischemic injury in liver transplantation, and the study design was reasonable. The results were also good and provided some scientific hints.

REFERENCES

1 **Adam R**, Delvart V, Karam V, Ducerf C, Navarro F, Letoublon C, Belghiti J, Pezet D, Castaing D, Le Treut YP, Gugenheim J, Bachellier P, Pirenne J, Muiesan P. Compared efficacy of preservation solutions in liver transplantation: a long-term graft outcome study from the European Liver Transplant Registry. *Am J Transplant* 2015; **15**: 395-406 [PMID: 25612492 DOI: 10.1111/ajt.13060]

2 **Zaouali MA**, Ben Abdennebi H, Padrissa-Altés S, Mahfoudh-Boussaid A, Roselló-Catafau J. Pharmacological strategies against cold ischemia reperfusion injury. *Expert Opin Pharmacother* 2010; **11**: 537-555 [PMID: 20163266 DOI: 10.1517/14656560903547836]

3 **Salahudeen AK**. Cold ischemic injury of transplanted organs: some new strategies against an old problem. *Am J Transplant* 2004; **4**: 1 [PMID: 14678026 DOI: 10.1046/j.1600-6143.2003.00323.x]

4 **McLaren AJ**, Friend PJ. Trends in organ preservation. *Transpl Int* 2003; **16**: 701-708 [PMID: 14530855 DOI: 10.1007/s00147-003-0659-2]

5 **Jamieson RW**, Friend PJ. Organ reperfusion and preservation. *Front Biosci* 2008; **13**: 221-235 [PMID: 17981540 DOI: 10.2741/2672]

6 **Busuttil RW**, Tanaka K. The utility of marginal donors in liver transplantation. *Liver Transpl* 2003; **9**: 651-663 [PMID: 12827549 DOI: 10.1053/jlts.2003.50105]

7 **Bejaoui M**, Pantazi E, Folch-Puy E, Baptista PM, García-Gil A, Adam R, Roselló-Catafau J. Emerging concepts in liver graft preservation. *World J Gastroenterol* 2015; **21**: 396-407 [PMID: 25593455 DOI: 10.3748/wjg.v21.i2.396]

8 **Padrissa-Altés S**, Zaouali MA, Bartrons R, Roselló-Catafau J. Ubiquitin-proteasome system inhibitors and AMPK regulation in hepatic cold ischaemia and reperfusion injury: possible mechanisms. *Clin Sci* (Lond) 2012; **123**: 93-98 [PMID: 22455352 DOI: 10.1042/CS20110093]

9 **Padrissa-Altés S**, Zaouali MA, Boncompagni E, Bonaccorsi-Riani E, Carbonell T, Bardag-Gorce F, Oliva J, French SW, Bartrons R, Roselló-Catafau J. The use of a reversible proteasome inhibitor in a model of Reduced-Size Orthotopic Liver transplantation in rats. *Exp Mol Pathol* 2012; **93**: 99-110 [PMID: 22475623 DOI: 10.1016/j.yexmp.2012.03.011]

10 **Zaouali MA**, Bardag-Gorce F, Carbonell T, Oliva J, Pantazi E, Bejaoui M, Ben Abdennebi H, Rimola A, Roselló-Catafau J. Proteasome inhibitors protect the steatotic and non-steatotic liver graft against cold ischemia reperfusion injury. *Exp Mol Pathol* 2013; **94**: 352-359 [PMID: 23305864 DOI: 10.1016/j.yexmp.2012.12.005]

11 **Hochstrasser M**. Ubiquitin-dependent protein degradation. *Annu Rev Genet* 1996; **30**: 405-439 [PMID: 8982460 DOI: 10.1146/annurev.genet.30.1.405]

12 **Goldberg AL**. Protein degradation and protection against misfolded or damaged proteins. *Nature* 2003; **426**: 895-899 [PMID: 14685250 DOI: 10.1038/nature02263]

13 **Calmus Y**, Cynober L, Dousset B, Lim SK, Soubrane O, Conti F, Houssin D, Giboudeau J. Evidence for the detrimental role of proteolysis during liver preservation in humans. *Gastroenterology* 1995; **108**: 1510-1516 [PMID: 7729644 DOI: 10.1016/0016-5085(95)90701-7]

14 **Upadhya GA**, Strasberg SM. Glutathione, lactobionate, and histidine: cryptic inhibitors of matrix metalloproteinases contained in University of Wisconsin and histidine/tryptophan/ketoglutarate liver preservation solutions. *Hepatology* 2000; **31**: 1115-1122 [PMID: 10796887 DOI: 10.1053/he.2000.6780]

15 **Upadhya AG**, Harvey RP, Howard TK, Lowell JA, Shenoy S, Strasberg SM. Evidence of a role for matrix metalloproteinases in cold preservation injury of the liver in humans and in the rat. *Hepatology* 1997; **26**: 922-928 [PMID: 9328314 DOI: 10.1002/hep.510260418]

16 **Ben Mosbah I**, Roselló-Catafau J, Franco-Gou R, Abdennebi HB, Saidane D, Ramella-Virieux S, Boillot O, Peralta C. Preservation of steatotic livers in IGL-1 solution. *Liver Transpl* 2006; **12**: 1215-1223 [PMID: 16724331 DOI: 10.1002/lt.20788]

17 **Majetschak M**. Regulation of the proteasome by ATP: implications for ischemic myocardial injury and donor heart preservation. *Am J Physiol Heart Circ Physiol* 2013; **305**: H267-H278 [PMID: 23709597 DOI: 10.1152/ajpheart.00206.2012]

18 **Geng Q**, Romero J, Saini V, Baker TA, Picken MM, Gamelli RL, Majetschak M. A subset of 26S proteasomes is activated at critically low ATP concentrations and contributes to myocardial injury during cold ischemia. *Biochem Biophys Res Commun* 2009; **390**: 1136-1141 [PMID: 19944202 DOI: 10.1016/j.bbrc.2009.10.067]

19 **Baker TA**, Geng Q, Romero J, Picken MM, Gamelli RL, Majetschak M. Prolongation of myocardial viability by proteasome inhibition during hypothermic organ preservation. *Biochem Biophys Res Commun* 2010; **401**: 548-553 [PMID: 20875792 DOI: 10.1016/j.bbrc.2010.09.093]

20 **Bejaoui M**, Zaouali MA, Folch-Puy E, Pantazi E, Bardag-Gorce F, Carbonell T, Oliva J, Rimola A, Abdennebi HB, Roselló-Catafau J. Bortezomib enhances fatty liver preservation in Institut George Lopez-1 solution through adenosine monophosphate activated protein kinase and Akt/mTOR pathways. *J Pharm Pharmacol* 2014; **66**: 62-72 [PMID: 24127984 DOI: 10.1111/jphp.12154]

21 **Zaouali MA**, Bejaoui M, Calvo M, Folch-Puy E, Pantazi E, Pasut G, Rimola A, Ben Abdennebi H, Adam R, Roselló-Catafau J. Polyethylene glycol rinse solution: an effective way to prevent ischemia-reperfusion injury. *World J Gastroenterol* 2014; **20**: 16203-16214 [PMID: 25473175 DOI: 10.3748/wjg.v20.i43.16203]

22 **Zaouali MA**, Ben Mosbah I, Boncompagni E, Ben Abdennebi H, Mitjavila MT, Bartrons R, Freitas I, Rimola A, Roselló-Catafau J. Hypoxia inducible factor-1alpha accumulation in steatotic liver preservation: role of nitric oxide. *World J Gastroenterol* 2010; **16**: 3499-3509 [PMID: 20653058 DOI: 10.3748/wjg.v16.i28.3499]

23 **Peralta C**, Bartrons R, Serafín A, Blázquez C, Guzmán M, Prats N, Xaus C, Cutillas B, Gelpí E, Roselló-Catafau J. Adenosine monophosphate-activated protein kinase mediates the protective effects of ischemic preconditioning on hepatic ischemia-reperfusion injury in the rat. *Hepatology* 2001; **34**: 1164-1173 [PMID: 11732006 DOI: 10.1053/jhep.2001.29197]

24 **Ben Mosbah I**, Casillas-Ramírez A, Xaus C, Serafín A, Roselló-Catafau J, Peralta C. Trimetazidine: is it a promising drug for use in steatotic grafts? *World J Gastroenterol* 2006; **12**: 908-914 [PMID: 16521219 DOI: 10.3748/wjg.v12.i6.908]

25 **v Frankenberg M**, Stachlewitz RF, Forman DT, Frey W, Bunzendahl H, Lemasters JJ, Thurman RG. Amino acids in rinse effluents as a predictor of graft function after transplantation of fatty livers in rats. *Transpl Int* 1999; **12**: 168-175 [PMID: 10429953 DOI: 10.1111/j.1432-2277.1999.tb00602.x]

26 **Zaouali MA**, Padrissa-Altés S, Ben Mosbah I, Ben Abdennebi H, Boillot O, Rimola A, Saidane-Mosbahi D, Roselló-Catafau J. Insulin like growth factor-1 increases fatty liver preservation in IGL-1 solution. *World J Gastroenterol* 2010; **16**: 5693-5700 [PMID: 21128318 DOI: 10.3748/wjg.v16.i45.5693]

27 **Zaouali MA**, Ben Mosbah I, Padrissa-Altés S, Calvo M, Ben Abdennebi H, Saidane-Mosbahi D, Bjaoui M, Garcia-Gil FA, Panisello A, Roselló-Catafau J. Relevance of epidermal growth factor to improve steatotic liver preservation in IGL-1 solution. *Transplant Proc* 2010; **42**: 3070-3075 [PMID: 20970612 DOI: 10.1016/j.transproceed.2010.07.071]

28 **Bejaoui M**, Pantazi E, Calvo M, Folch-Puy E, Serafín A, Pasut G, Panisello A, Adam R, Roselló-Catafau J. Polyethylene Glycol Preconditioning: An Effective Strategy to Prevent Liver Ischemia Reperfusion Injury. *Oxid Med Cell Longev* 2016; **2016**: 9096549 [PMID: 26981166 DOI: 10.1155/2016/9096549]

29 **Hamer PW**, McGeachie JM, Davies MJ, Grounds MD. Evans Blue Dye as an in vivo marker of myofibre damage: optimising parameters for detecting initial myofibre membrane permeability. *J Anat* 2002; **200**: 69-79 [PMID: 11837252 DOI: 10.1046/j.0021-8782.2001.00008.x]

30 **Massip-Salcedo M**, Zaouali MA, Padrissa-Altés S, Casillas-Ramirez A, Rodés J, Roselló-Catafau J, Peralta C. Activation of peroxisome proliferator-activated receptor-alpha inhibits the injurious effects of adiponectin in rat steatotic liver undergoing ischemia-reperfusion. *Hepatology* 2008; **47**: 461-472 [PMID: 18098300 DOI: 10.1002/hep.21935]

31 **Zaouali MA**, Boncompagni E, Reiter RJ, Bejaoui M, Freitas I, Pantazi E, Folch-Puy E, Abdennebi HB, Garcia-Gil FA, Roselló-Catafau J. AMPK involvement in endoplasmic reticulum stress and autophagy modulation after fatty liver graft preservation: a role for melatonin and trimetazidine cocktail. *J Pineal Res* 2013; **55**: 65-78 [PMID: 23551302 DOI: 10.1111/jpi.12051]

32 **Ilmakunnas M**, Tukiainen EM, Rouhiainen A, Rauvala H, Arola J, Nordin A, Mäkisalo H, Höckerstedt K, Isoniemi H. High mobility group box 1 protein as a marker of hepatocellular injury in human liver transplantation. *Liver Transpl* 2008; **14**: 1517-1525 [PMID: 18825712 DOI: 10.1002/lt.21573]

33 **Fukumori T**, Ohkohchi N, Tsukamoto S, Satomi S. The mechanism of injury in a steatotic liver graft during cold preservation. *Transplantation* 1999; **67**: 195-200 [PMID: 10075580 DOI: 10.1097/00007890-199901270-00002]

34 **Xu C**, Yu C, Li Y. Current studies on therapeutic approaches for ischemia/reperfusion injury in steatotic livers. *Hepatol Res* 2008; **38**: 851-859 [PMID: 18507690 DOI: 10.1111/j.1872-034X.2008.00354.x]

35 **Elias-Miró M**, Jiménez-Castro MB, Mendes-Braz M, Casillas-Ramírez A, Peralta C. The Current Knowledge of the Role of PPAR in Hepatic Ischemia-Reperfusion Injury. *PPAR Res* 2012; **2012**: 802384 [PMID: 22675337 DOI: 10.1155/2012/802384]

36 **Liu A**, Dirsch O, Fang H, Dong W, Jin H, Huang H, Sun J, Dahmen U. HMGB1 translocation and expression is caused by warm ischemia reperfusion injury, but not by partial hepatectomy in rats. *Exp Mol Pathol* 2011; **91**: 502-508 [PMID: 21640719 DOI: 10.1016/j.yexmp.2011.05.005]

37 **Liu A**, Dirsch O, Fang H, Sun J, Jin H, Dong W, Dahmen U. HMGB1 in ischemic and non-ischemic liver after selective warm ischemia/reperfusion in rat. *Histochem Cell Biol* 2011; **135**: 443-452 [PMID: 21431875 DOI: 10.1007/s00418-011-0802-6]

38 **Genini D**, Catapano CV. Control of peroxisome proliferator-activated receptor fate by the ubiquitinproteasome system. *J Recept Signal Transduct Res* 2006; **26**: 679-692 [PMID: 17118805 DOI: 10.1080/10799890600928202]

39 **Yuan ZY**, Liu Y, Liu Y, Zhang JJ, Kishimoto C, Wang YN, Ma AQ, Liu ZQ. PPAR-gamma ligands inhibit the expression of inflammatory cytokines and attenuate autoimmune myocarditis. *Chin Med J* (Engl) 2004; **117**: 1253-1255 [PMID: 15361304]

40 **Yuan Z**, Luo G, Li X, Chen J, Wu J, Peng Y. PPARγ inhibits HMGB1 expression through upregulation of miR-142-3p in vitro and in vivo. *Cell Signal* 2016; **28**: 158-164 [PMID: 26721185 DOI: 10.1016/j.cellsig.2015.12.013]

41 **Liu A**, Jin H, Dirsch O, Deng M, Huang H, Bröcker-Preuss M, Dahmen U. Release of danger signals during ischemic storage of the liver: a potential marker of organ damage? *Mediators Inflamm* 2010; **2010**: 436145 [PMID: 21197406]

42 **Tang D**, Kang R, Livesey KM, Cheh CW, Farkas A, Loughran P, Hoppe G, Bianchi ME, Tracey KJ, Zeh HJ, Lotze MT. Endogenous HMGB1 regulates autophagy. *J Cell Biol* 2010; **190**: 881-892 [PMID: 20819940 DOI: 10.1083/jcb.200911078]

43 **Kang R**, Zeh HJ, Lotze MT, Tang D. The Beclin 1 network regulates autophagy and apoptosis. *Cell Death Differ* 2011; **18**: 571-580 [PMID: 21311563 DOI: 10.1038/cdd.2010.191]

44 **Tarantino G**, Colao A, Capone D, Conca P, Tarantino M, Grimaldi E, Chianese D, Finelli C, Contaldo F, Scopacasa F, Savastano S. Circulating levels of cytochrome C, gamma-glutamyl transferase, triglycerides and unconjugated bilirubin in overweight/obese patients with non-alcoholic fatty liver disease. *J Biol Regul Homeost Agents* 2011; **25**: 47-56 [PMID: 21382273]

45 **Mosbah IB**, Zaouali MA, Martel C, Bjaoui M, Abdennebi HB, Hotter G, Brenner C, Roselló-Catafau J. IGL-1 solution reduces endoplasmic reticulum stress and apoptosis in rat liver transplantation. *Cell Death Dis* 2012; **3**: e279 [PMID: 22402603 DOI: 10.1038/cddis.2012.12]

46 **Gustafsson AB**, Gottlieb RA. Eat your heart out: Role of autophagy in myocardial ischemia/reperfusion. *Autophagy* 2008; **4**: 416-421 [PMID: 18253087 DOI: 10.4161/auto.5655]

47 **Korolchuk VI**, Menzies FM, Rubinsztein DC. A novel link between autophagy and the ubiquitin-proteasome system. *Autophagy* 2009; **5**: 862-863 [PMID: 19458478 DOI: 10.4161/auto.8840]

P- Reviewer: Chow WK, Tarantino G **S- Editor**: Gong ZM
L- Editor: A **E- Editor**: Zhang FF

World Journal of Gastroenterology

Submit a Manuscript: http://www.f6publishing.com

World J Gastroenterol 2017 June 21; 23(23): 4222-4232

DOI: 10.3748/wjg.v23.i23.4222

ISSN 1007-9327 (print) ISSN 2219-2840 (online)

ORIGINAL ARTICLE

Basic Study

Naturally occurring mutations in the reverse transcriptase region of hepatitis B virus polymerase from treatment-naïve Korean patients infected with genotype C2

Ji-Eun Kim, So-Young Lee, Hong Kim, Ki-Jeong Kim, Won-Hyeok Choe, Bum-Joon Kim

Ji-Eun Kim, So-Young Lee, Hong Kim, Bum-Joon Kim, Department of Biomedical Sciences, Microbiology and Immunology, and Liver Research Institute, Seoul National University College of Medicine, Seoul 110-799, South Korea

Ki-Jeong Kim, Department of Microbiology, School of Medicine, Joong-Ang University, Seoul 110-799, South Korea

Won-Hyeok Choe, Department of Internal Medicine, Konkuk University School of Medicine, Seoul 110-799, South Korea

Author contributions: Kim BJ conceived this research and participated in its design and coordination; Kim JE, Lee SY and Kim H performed the experiments; Kim JE and Lee SY analyzed and interpreted the data; Kim BJ, Kim KJ and Choe WH contributed the reagents, materials, and analysis tools; Kim JE and Lee SY wrote and reviewed the manuscript; all authors approved the final manuscript; Kim JE and Lee SY are equally contributed to this work.

Supported by Basic Science Research Program through the National Research Foundation of Korea (NRF) funded by the Ministry of Education, Science and Technology No. NRF-2015R1C1A1A02037267; and Korea Health Technology R&D Project through the Korea Health Industry Development Institute, funded by the Ministry of Health and Welfare, South Korea, No. HI14C0955.

Institutional review board statement: All serum samples collected from patients at the Konkuk University Hospital and Seoul National University Hospital, South Korea. The ethical permission was obtained for participation in the study.

Conflict-of-interest statement: There was no conflict of interest exists.

Manuscript source: Unsolicited manuscript

Correspondence to: Dr. Bum-Joon Kim, Professor, Department of Biomedical Sciences, Microbiology and Immunology, and Liver Research Institute, Seoul National University College of Medicine, 103 Daehak-ro, Jongno-gu, Seoul 110-799, South Korea. kbumjoon@snu.ac.kr
Telephone: +82-2-7408316
Fax: +82-2-7430881

Received: January 13, 2017
Peer-review started: January 14, 2017
First decision: March 16, 2017
Revised: March 28, 2017
Accepted: May 9, 2017
Article in press: May 9, 2017
Published online: June 21, 2017

Abstract

AIM

To report naturally occurring mutations in the reverse transcriptase region (RT) of hepatitis B virus (HBV) polymerase from treatment naïve Korean chronic patients infected with genotype C2.

METHODS

Here, full-length HBV reverse transcriptase RT sequences were amplified and sequenced from 131 treatment naïve Korean patients chronically infected with hepatitis B genotype C2. The patients had two distinct clinical statuses: 59 patients with chronic hepatitis (CH) and 72 patients with hepatocellular carcinoma (HCC). The deduced amino acids (AAs) at

42 previously reported potential nucleos(t)ide analog resistance (NAr) mutation positions in the RT region were analyzed.

RESULTS

Potential NAr mutations involving 24 positions were found in 79 of the 131 patients (60.3%). Notably, AA substitutions at 2 positions (rt184 and rt204) involved in primary drug resistance and at 2 positions (rt80 and rt180) that functioned as secondary/compensatory mutations were detected in 10 patients (1 CH patient and 9 HCC patients) and 7 patients (1 CH and 6 HCC patients), respectively. The overall mutation frequencies in the HCC patients (3.17%, 96/3024 mutations) were significantly higher than the frequencies in the CH patients (2.09%, 52/2478 mutations) (P = 0.003). In addition, a total of 3 NAr positions, rt80, rt139 and rt204 were found to be significantly related to HCC from treatment naïve Korean patients.

CONCLUSION

Our data showed that naturally occurring NAr mutations in South Korea might contribute to liver disease progression (particularly HCC generation) in chronic patients with genotype C2 infections.

Key words: Hepatitis B virus; Polymerase; Reverse transcriptase; Potential nucleos(t)ide analog resistance; Chronic hepatitis; Hepatocellular carcinoma

Core tip: To date, naturally occurring mutations in hepatitis B virus (HBV) reverse transcriptase region (RT) in genotype C2-infected patients have rarely been introduced in terms of clinical severity. So, this study characterized the AA substitutions at the aforementioned 42 potential NAr mutation positions in HBV RT sequences from a cohort of 131 Korean treatment-naïve CHB patients with genotype C2 infections. Notably, AA substitutions at positions involved in primary (rt184 and rt204) or secondary drug resistance (rt80 and rt180) were detected in 10 patients [1 CH patient and 9 hepatocellular carcinoma (HCC) patients] and 7 patients (1 CH and 6 HCC patients), respectively. The overall mutation frequencies in the HCC patients (3.17%, 96/3024 mutations) were significantly higher than the frequencies in the CH patients (2.09%, 52/2478 mutations), suggesting that naturally occurring NAr mutations in South Korea might contribute to liver disease progression (particularly HCC generation) in chronic patients with genotype C2 infections. In addition, a total of 3 NAr positions, rt80, rt139 and rt204 were found to be significantly related to HCC from treatment naïve Korean patients.

Kim JE, Lee SY, Kim H, Kim KJ, Choe WH, Kim BJ. Naturally occurring mutations in the reverse transcriptase region of hepatitis B virus polymerase from treatment-naïve Korean patients infected with genotype C2. *World J Gastroenterol* 2017; 23(23): 4222-4232 Available from: URL: http://www.wjgnet.com/1007-9327/full/v23/i23/4222.htm DOI: http://dx.doi.org/10.3748/wjg.v23.i23.4222

INTRODUCTION

Despite the availability of an effective vaccine, more than 240 million people are chronic carriers of the virus[1]. The annual number of deaths caused by hepatitis B virus (HBV)-related diseases, including cirrhosis and hepatocellular carcinoma (HCC), is estimated to be approximately 786000 worldwide[2]. HBV infection is endemic in South Korea; based on the Korean National Health and Nutrition Survey of 2011, the prevalence of hepatitis B virus surface antigen (HBsAg) positivity was 3.4% among men and 2.6% among women[3]. There is increasing evidence that specific HBV genotypes may play significant roles in the development of different disease profiles during chronic hepatitis B (CH) infection[4,5]. Notably, an extraordinary prevalence of genotype C2, which is more virulent than genotype B[4], has been reported in South Korea[6-8]. Furthermore, the high prevalence of basal core promoter (BCP) double mutations and the presence of a distinct immune response against HBV proteins in the Korean population can lead to the generation of unique HBV variants that are rarely encountered in other areas, resulting in distinct clinical manifestations in Korean chronic patients[9]. Indeed, several unique types of HBV mutations related to the progression of liver disease (particularly HCC) that are rarely, if ever, encountered in other areas have been found in South Korea[10-27].

HBV has an incomplete double-stranded DNA genome that is approximately 3.2 kb in length and contains 4 overlapping open reading frames (ORFs) encoding the polymerase (P), core (C), surface antigen (S), and X protein[28]. The HBV reverse transcriptase (RT) lacks proofreading ability, which can lead to HBV mutations that occur at a 10-fold higher frequency compared to other DNA viruses[29]. The high rate of mutations in the HBV genome compromises antiviral therapy with nucleos(t)ide analogues (NAs), leading to the generation of drug-resistant viral strains and disease. Although antiviral therapy using NAs is an effective control measure[30], obstacles remain, including the limited types of NAs available and the inevitable emergence of antiviral resistance conferred by viral mutations during long-term treatment[31]. Thus, elucidating the mechanisms underlying the evolutionary basis of the drug resistance mutations is important for their prevention and control. Drug resistant mutations in RT have been extensively explored during antiviral therapy using NAs, including lamivudine (LMV)[32], adefovir (ADV)[33], entecavir (ETV)[34], telbivudine (LdT)[35] and tenofovir (TNF).

Recently, RT mutations from treatment-naïve Chinese patients has been reported *via* analysis of 42 RT positions that were previously reported to be NArs[36]. These mutations could be divided into 4 categories [*i.e.*, primary drug resistance mutation (Category 1), secondary/compensatory mutation (Category 2), putative NAr mutation (Category 3) and pretreatment mutation (Category 4)].

To date, naturally occurring mutations in HBV RT in genotype C2-infected patients have rarely been introduced in terms of clinical severity. Therefore, this study characterized the AA substitutions at the aforementioned 42 potential NAr mutation positions in HBV RT sequences from a cohort of 131 Korean treatment-naïve CHB patients with genotype C2 infections. The clinical characteristics and significance of these identified NAr mutations were also investigated in the present study.

MATERIALS AND METHODS

Patients

Serum samples were collected from 135 chronic hepatitis B patients who visited Konkuk University Hospital and met the inclusion criteria of hepatitis B surface antigen (HBsAg) positivity and HBV DNA positivity and were LMV, ADV, ETV, LdT and TNF treatment-naïve. All patients had negative tests for hepatitis C virus, human immunodeficiency virus and markers for coexisting autoimmune liver disease. Among 135 patients, the 131 patients proved to be infected with genotype C2, which showed two clinical statuses: chronic hepatitis (CH, 59 patients) and hepatocellular carcinoma (HCC, 72 patients), were used in the NAr mutation analysis. This study was approved by the Institutional Review Boards (IRB) of Seoul National University Hospital (IRB-1605-065-761) and Konkuk University Hospital (KUH-1010544). The experiments were primarily based on extracted virion DNA from isolates; hence, the study did not require informed consent and the waiver of informed consent was agreed upon by the IRBs.

HBV DNA extraction and PCR amplification

HBV DNA was extracted from the secured 200 μL of serum samples using the QIAamp DNA Blood Mini Kit (QIAGEN Inc, Hilden, Germany). To analyze the mutation patterns and the frequencies of mutations in the RT region, a nested PCR based sequencing protocol was used as previously described[37]. The first-round PCR was performed using the sense primer Pol-RT-F1 (5′-CAGCCTACTCCCATCTCTCCACCTCTAAG-3′) and the antisense primer Pol-RT-R1 (5′-GCTCCAGACCGGCT GCGAGC-3′) to yield a 1375-bp amplicon between positions 3157 nt and 1316 nt of the HBV genome. The second-round PCR was performed using the sense primer Pol-RT-F2 (5′-CCTCAGGCCATGCAGTGGAA-3′) and the antisense primer Pol-RT-R2 (5′-GTATGGA TCGGCAGAGGAGC-3′) to yield a 1291-bp amplicon between positions 3196 nt and 1271 nt of the HBV genome. The PCR was initiated in a 20 μL PCR mixture containing 1.5 mmol/L $MgCl_2$, 250 μmol/L dNTPs, and 1.0 U of the ProFi Taq DNA polymerase (Bioneer). For both rounds, the protocol was as follows: 95 ℃ for 10 min, followed by 15 cycles at 94 ℃ (15 s), 55 ℃ (15 s) and 68 ℃ (3 min). A final extension step was performed at 72 ℃ for 5 min. The second-round PCR protocol used 2 μL of the product from the first-round PCR and was identical to the conditions described above except that 30 cycles were performed. The PCR products were analyzed by electrophoresis on 1.0% agarose gels, stained with ethidium bromide, and visualized on a UV transilluminator.

HBV genotyping

For genotyping, a phylogenetic analysis based on entire sequences of the RT region (1032 bp) was performed for PCR-positive 135 HBV strains. The 1032-bp RT sequences of the 135 HBV strains were compared with the sequences of eight reference strains representing each of the genotypes (A-F including the C2 strains) obtained from GenBank [accession numbers M57663 (A), AB100695 (B), AB074755 (C1), AY247032 (C2), AY641559 (C2), X02496 (D), AB106564 (E), and X75663 (F)]. Phylogenetic trees were inferred using the neighbor-joining method in MEGA version 7.0.14[38]. A mutation was defined through comparisons with the consensus sequence of the HBV strains in our cohort and the eight reference strains. The RT sequences of 131 patients with HBV genotype C2 infections were registered at GenBank [CH patients (GenBank Nos: KX264864-KX264922) and HCC patients (GenBank Nos: KX264792-KX264863)]

Mutation analysis and definitions

Generally, the mutation definition and analysis were performed as previously described. Briefly, 42 potential NAr-relevant AA positions in RT were analyzed for AA mutations and concomitant HBsAg mutations. The AA mutations were identified by comparing HBV RT sequences with the genotype C-matched consensus sequence generated based on the HBV sequences obtained in this study and the reference sequences reported in previous studies[39]. A mutation type referred to the replacement of the consensus AA of genotype C with a novel AA.

Statistical analyses

The results were expressed as means ± SD, percentages. Differences between categorical variables were analyzed using Fisher's exact test or the χ^2 test. For continuous variables, Student's *t*-test was used when the data showed a normal distribution, and the Mann-Whitney *U* test was used when the data were not normally distributed. The level of significance of each test was adjusted for multiple tests *via* Bonferroni correction. The *P* value < 0.05 (two-tailed) was considered statistically significant. To adjust *P* values for

Table 1 Comparison of clinical data between chronic hepatitis and hepatocellular carcinoma patients

Clinical factors	CH (n = 59)	HCC (n = 72)	Total (n = 131)	P value
Age, yr, mean ± SD	38.9 ± 11.1	52.3 ± 9.7	45.7 ± 12.3	< 0.001
Gender, male	47.40%	79.10%	64.80%	< 0.001
HBeAg negative	35.50%	54.10%	45.80%	0.04%
ALT (IU/L), mean ± SD	94.5 ± 105.6	74.2 ± 85.1	106.8 ± 191.2	NS
AST (IU/L), mean ± SD	70.4 ± 92.0	127.1 ± 139.8	113.2 ± 141.0	< 0.001
HBV DNA	6.5 ± 2.0	5.3 ± 1.1	6.53 ± 1.7	< 0.001
HBsAg	3.7 ± 0.6	3.3 ± 0.7	3.43 ± 0.6	< 0.001

HbsAg: Hepatitis B virus surface antigen.

Table 2 Correlation between the frequency of potential nucleos(t)ide analog resistance mutation and clinical features

No. of mutations	CH/HCC	HBeAg (positive/negative)	ALT (IU/L)	AST (IU/L)	HBV DNA	HBsAg
0	27/25	29/23	108.51 ± 105.8	122.92 ± 106.8	6.50 ± 6.5	3.97 ± 3.8
1	18/16	21/13	101.61 ± 108.7	71.42 ± 126.1[a]	6.91 ± 6.4	3.95 ± 3.8
2	9/19	15/13	81.10 ± 113.8	113.75 ± 113.0	6.65 ± 6.1	3.65 ± 3.9[a]
3	4/7	3/8	211.45 ± 97.3	205.18 ± 104.8[a]	6.84 ± 6.5	3.84 ± 3.8
4	1/4	2/3	56.60 ± 108.8	72.00 ± 114.8	5.85 ± 6.5	3.68 ± 3.8
5	0/1	1/0	24.23	39.05	7.49	2.83
⩾ 1 (n = 79)	32/47	42/37	105.81 ± 216.19	106.86 ± 131.51	5.11 ± 1.55	3.37 ± 0.77
Total (n = 131)	59/72	71/60	107.21 ± 191.16	113.2 ± 141.06	4.98 ± 1.51	3.43 ± 0.73

The significant values were shown in boldface and marked with asterisk ([a]P < 0.05). HbsAg: Hepatitis B virus surface antigen; HCC: Hepatocellular carcinoma.

multiple testing and control the false discover rate for multiple testing was used[40]. We appreciate statistical consultation from the Medical Research Collaborating Center at the Seoul National University Hospital and the Seoul National University College of Medicine.

RESULTS

Genotype distribution and clinical features of treatment-naïve patients

The 131 patients were proved to be infected with genotype C2 by phylogenetic analysis based on 1032bp RT sequences and were used for the NAr mutation analysis. The clinical features of our cohort are summarized in Table 1. The patient cohort consisted of CH (45%, 59 patients) and HCC patients (55%, 72 patients) and included 85 males (64.8%) and 46 females (35.1%) with a median age of 45 years (range 22-73 years). The main characteristics of the CH and HCC patients were compared. The HCC patients were significantly older (P < 0.001), included a significantly higher number of male patients (P < 0.001), have a lower number of HBeAg-positive patients (P = 0.037) and had significantly lower HBV DNA (P < 0.001) and secreted HBsAg levels (P < 0.001) compared to the CH patients.

Correlation between the frequency of potential NAr mutation and clinical features

Using sequence analysis of the full-length HBV RT from 131 patients, we deduced the amino acids (AAs) at 42 previously reported potential NA resistance (NAr) mutation positions in the RT region[36]. The correlation between the frequency of potential NAr mutation in 131 patients and clinical features were summarized in Table 2. The analysis indicated that potential NAr mutations were present in 79 of the 131 patients (60.3 %). Of these, 32 (40.5%) and 47 patients (59.5%) belonged to the CH and HCC patient groups, respectively and 42 (53.2%) and 37 patients (46.8%) were HBeAg-positive and negative, respectively. Of the 79 patients with NAr mutations, 34 patients (43.03%) had a single mutation and 45 patients (56.96%) had multiple mutations, including 28 patients (35.44%) with double mutations, 11 patients (13.92%) with triple mutations, 5 patients (6.3%) with a quadruple mutation, and 1 patient (1.26%) with a quintuple mutation. No significant difference in clinical factors was observed between the patients with potential NAr mutations (79 patients) and those without mutations (52 patients) (Table 2).

Characterization of potential NAr mutation from treatment naïve patients

All AA substitutions detectable in the 79 patients with NAr mutations at the 42 positions previously reported to be potential NArs that could be grouped into 4 categories[36], and a total of 24 NAr mutation sites were detectable among the 79 patients. Two dominant mutation sites rt128 in Category 3 and rt224 in Category 4 were present in 16 patients (20.25%, CH: 11 and HCC: 5) and 16 patients (20.25%, CH: 4, HCC: 12), respectively (Table 3). The AA substitutions at 2 positions (rt184 and rt204) in Category 1 consisting of 8 primary NAr mutation positions (rt169, rt181, rt184,

Table 3 Characterization of potential 42 NAr mutation from treatment naive Korean patients of genotype C2 infections

Category	Mutation	Drug resistance	CH	HCC	*P* value
Primary drug resistance	T184A/C/F	ETV	1	-	0.021
	M204I/V	LMV, ETV, TNF	-	9	
Mutation number (%)/no. of patients number			1/472 (0.21%)	9/576 (1.56%)	
			1	9 patients	
Secondary mutation	L80I	LMV	-	5	NS
	L180M	LMV, ETV, LdT	1	2	
Mutation number (%)/no. of patients number			1/177 (0.56%)	7/216 (3.24%)	
			1	6	
Putative NAr mutation	S53N	LMV	1	1	N.S
	L82M/V	LMV	-	1	
	V84M/I	ADV	1	-	
	H126C/Y/Q	ADV	5	6	
	I128I/N/A	LMV	11	5	
	R/W153Q	LMV	2	-	
	V191I/D	LMV, ADV	2	3	
	V207I	LMV	-	1	
	S213T	ADV	-	3	
	Q215P/S/H	LMV, ADV	-	2	
	L217R	ADV	1	-	
	F221Y	ADV	3	9	
	L229G/V/W	LMV	-	2	
	P237H	ADV	-	2	
	N238D/S/T	ADV	3	6	
Mutation number (%)/no. of patients number			29/1475 (1.96%)	41/1800 (2.27%)	
			23	31	
Pre-treatment mutation	T38A		9	5	NS
	Y124H	Found	4	6	
	D134E/N/C	Before	4	8	
	N139K/H	Therapy	-	8	
	I224V		4	12	
Mutation number (%)/no. of patients number			21/351 (5.93%)	39/432 (9.02%)	
			17	31	
Total Mutation number (%)/no. of patients (%)			52/2478 (2.09)	96/3024 (3.17)	0.003
			32 patients (54.2)	47 patients (65.2)	
			148/5502 (2.68)		
			79 (60.3)		

ETV: Entecavir; LMV: Lamivudine; TNF: Tenofovir; ADV: Adefovir; CH: Chronic hepatitis; HCC: Hepatocellular carcinoma.

rt194, rt202, rt204, rt236 and rt250) were detected in 10 patients (1 CH patient and 9 HCC patients). The mutation frequency in primary drug resistance Category was significantly higher in the HCC patients than in the CH patients (P = 0.021). The AA substitutions at 2 positions (rt80 and rt180) in the second Category, which included 3 secondary/compensatory NAr mutation positions (rt80, rt173 and rt180), were detected in 7 patients (1 CH patient and 6 HCC patients), indicating that the mutation frequency in Category 2 tended to be higher in the HCC patients than in the CH patients (P = 0.109). Potential NAr mutations in Categories 3 and 4 were found in 54 patients (23 CH patients and 31 HCC patients) and 48 patients (17 CH patients and 31 HCC patients), respectively, but had no significant difference in the variant frequencies in Categories 3 and 4 were found between the CH and HCC patients (Table 3).

Mutation rates of potential NAr mutation in terms of clinical stages

Mutation rates of 79 patients with NAr mutations were compared in terms of clinical liver disease stages. The mean values of potential NAr mutation rates at the 42 positions of 131 our cohort was 2.68% (148/5502) (Table 3). Overall, mutation frequencies in the HCC patients (3.17%, 96/3024), were significantly higher than in those of CH patients (2.09%, 52/2478) (P = 0.003) (Table 3).

Mutation distribution and frequency in different RT sections

HBV RT region consists of 7 functional domains (G, F, A, B, C, D and E) and 6 interdomains (G-F, F-A, A-B, B-C, C-D and D-E) connecting domains (Figure 1)[41]. Our mutation distribution analyses revealed that of 11 domains, mutations within A-B interdomain were the most frequently found in our cohort (58.22%, 46/79 patients). The mutations in this region were detected in all 6 reported sites (6/6, 100%), rt124 (10 patients), rt126 (11 patients), rt128 (16 patients), rt134 (12 patients), rt139 (8 patients) and rt153 (2 patients) (Figure 1 and Table 4). The mutation frequency of A-B interdomain (7.50%, 59/786) was also higher than those of the domain (1.07%, P = 0.008) and non A-B interdomain (3.16%) (Table 4), in line with the previous report that potential NAr positions within this region

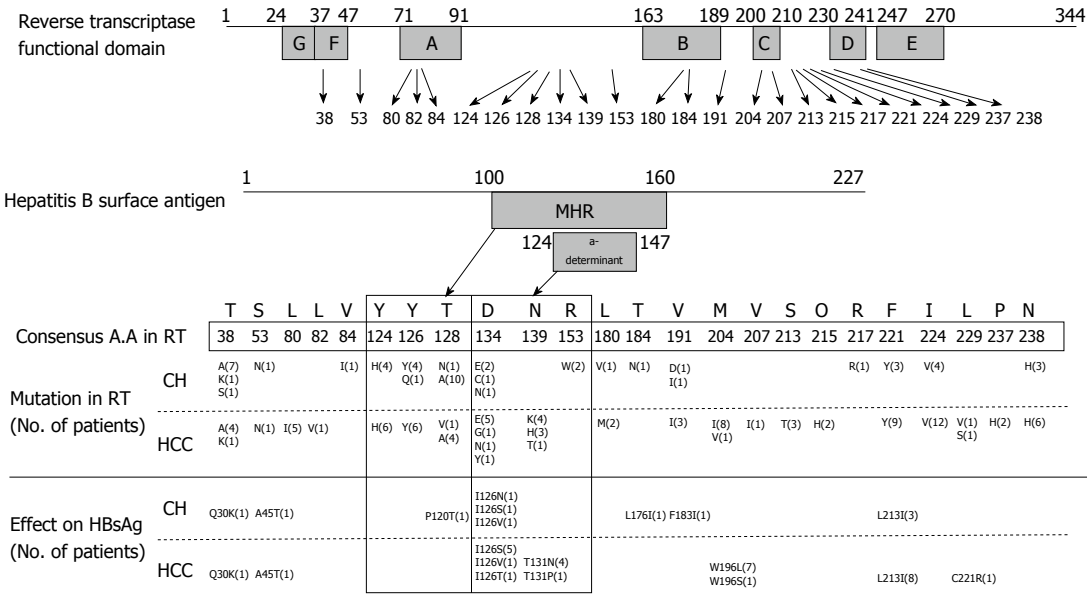

Figure 1 Mutations identified in reverse transcriptase region and the overlapped hepatitis B virus surface antigen. The identified NAr mutations in this study in the hepatitis B virus (HBV) reverse transcriptase (RT) sequence (1-344 aa) and overlapped HBsAg (1-227 aa) were shown. RT consists of 6 functional domains, G (24-36 aa), F (37-47 aa), A (71-91 aa), B (163-189 aa), C (200-210 aa), D (230-241 aa) and E (247-270 aa). HBsAg contains MHR region (100-160 aa) including "a" determinant region (124-147 aa). Lower box indicated 24 identified NAr mutations in this study and comparison of mutation types between CH and hepatocellular carcinoma patients. CH: Chronic hepatitis; HCC: Hepatocellular carcinoma.

Table 4 Mutation site distributions and mutation rate in different sections of hepatitis B virus RT and overlapped hepatitis B surface antigen regions

	Region (amino acid)	No. of mutation site	Mutation frequency	*P* value
Reverse transcriptase	Domain (22)	9 (40.9)	1.07%	0.008
	A-B interdomain (6)	6 (100)	7.50%	-
	Non A-B interdomain (14)	10 (71.4)	3.16%	NS
	Total (42)	25 (59.5)	2.68%	-
HBsAg	A-determinant (3)	2 (66.6)	3.81%	
	Non A-determinant (37)	8 (21.6)	0.55%	< 0.001
	Total (40)	10 (28.5)	0.80%	-

Statistics were calculated between Domain/Non A-B interdomain and A-B interdomain in reverse transcriptase region. In category 2, the statistical significant showed between A-determinant and Non-A-determinant in HBsAg region.

might be hotspots of naturally occurring mutation in this treatment-naïve population[36]. The RT include the complete HBsAg region[42]. In this study, 35 out of 42 mutated positions in RT were within the corresponding region of HBsAg positions (except mutations at rt236, rt237, rt238, rt242, rt245, rt256 and rt250). Our data showed that the AA mutations at 10 of 42 NAr positions were accompanied by 15 types of AA changes of HBsAg in 32.06% (42/131) patients. It should be noted that the 15 AA mutations at 3 NAr positions, rt134, rt139 and rt153 were found in the "a" determinant region of s126,s131 at HBsAg in 11.45% (15/131) patients (Figure 1) and these region had significantly higher mutation frequency, compared to non-"a" determinant (3.81%: 0.55%, $P < 0.001$, Table 4).

Identification of NAr and overlapped HBsAg mutations related to HCC

Of detected 24 mutated positions, a total of 3 NAr positions, rt80, rt139 and rt204 were found to be significantly related to HCC from treatment naïve Korean patients (Figure 2 and Table 5). Of these, two, rt139 and rt204 except rt80 led to simultaneous HCC related mutations in overlapped HBsAg, s131 and s196. In this study, 2 mutation type of M204I (8 patients) and M204V (1 patient) at rt204 in Category 1, leading to YMDD motif mutations were found from 9 HCC patients but not from CH patients ($P = 0.004$), which also led to the simultaneous W196L (7 patients) and W196S (1 patient) HBsAg mutations in 8 HCC patients. The only one type mutation, L80I at rt80 in Category 2 were also found only in HCC patients (5 patients), but not in CH patients ($P = 0.036$). The third mutation types, N139K (4 patients), N139H (3 patients) and N139T (1 patient) at the rt139 in the Category 4 mutations were found from 8 HCC patients, but not in CH patients ($P = 0.008$), which also led to the simultaneous T131N (4 patients) and T131P (1 patients) HBsAg mutations in 5

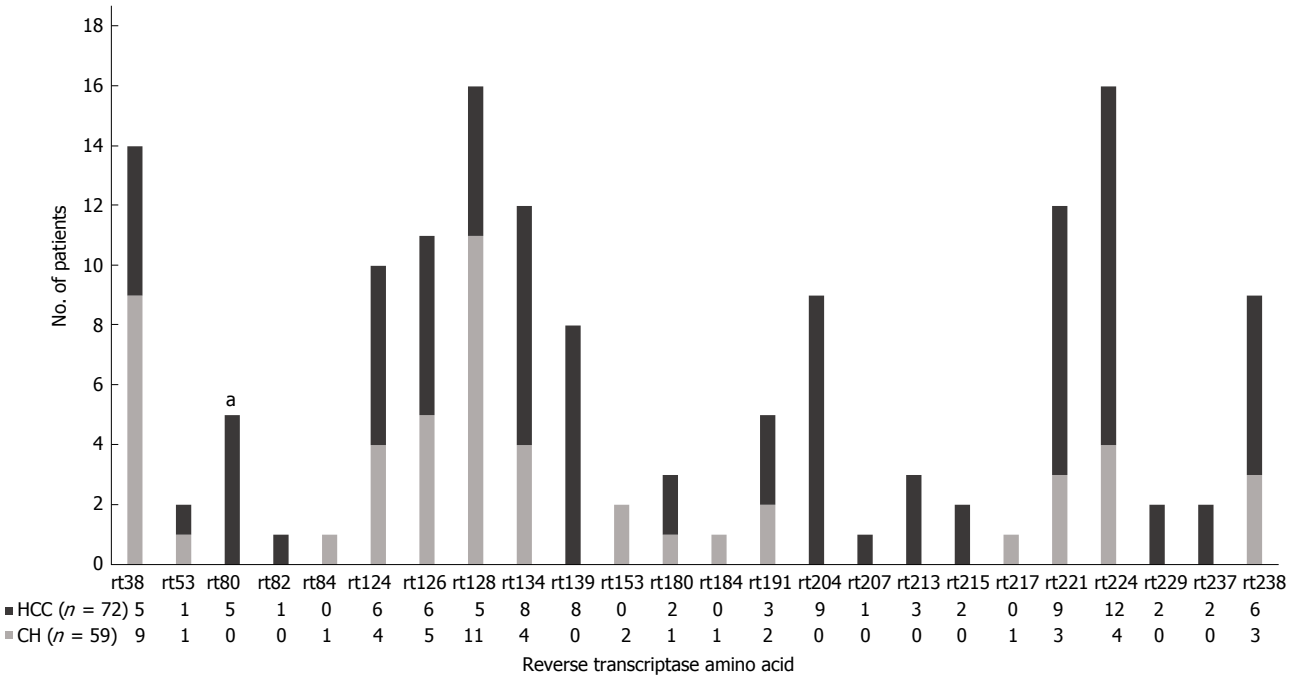

Figure 2 Comparison of nucleos(t)ide analog resistance variants frequency between chronic hepatitis and hepatocellular carcinoma patients. Of identified 24 mutations, mutation frequency at the 3 sites, rt80, rt139 and rt204 was significantly higher in hepatocellular carcinoma patients than in CH patients. $^{a}P < 0.05$. CH: Chronic hepatitis; HCC: Hepatocellular carcinoma.

Table 5 Frequency and patterns of 3 types of NAr Mutations related to hepatocellular carcinoma

Mutations	No. of patients		Nucleotide sequences	Codons in RT genes (patients)	Codons in HBsAg genes (patients)	*P* value
	CH	HCC				
rtL80I	0	5	GGCTAT→GGATAT	CTA(L)→ATA(I) (5)	TAT(Y)→TAT(Y) (5)	0.036
rtN139K/T/H	0	8	GGAACC→GGAAAC	AAC(N)→AAA(K) (4)	ACC(T)→AAC(N) (4)	
(sT131N/P)			→GGCACC	→CAC(H) (3)	→ACC(T) (3)	0.008
			→GGACCC	→ACC(T) (1)	→CCC(P) (1)	
rtM204I/V	0	9	ATATGG→ATATTG	ATG(M)→ATT(I) (7)	TGG(W)→TTG(L) (7)	
(sW196L/S/W)			→ATATCG	→ATC(I) (1)	→TCG(S) (1)	0.004
			→ATGTGG	→GTG(V) (1)	→TGG(W) (1)	

The point mutation bases of the three truncations are shown in bold and italic. H: Histidine; I: Isoleucine; K: Lysine; L: Leucine; M: Methionine; N: Asparagine; P: Proline; S: Serine; T: Threonine; V: Valine; W: Tryptophan; Y: Tyrosine; CH: Chronic hepatitis; HCC: Hepatocellular carcinoma.

HCC patients (Table 5).

DISCUSSION

Naturally occurring RT mutations associated with HBV drug resistance have been reported from treatment naïve chronic patients from several countries[43-46]. In South Korea, higher mutation rates and unique mutation patterns related to clinical implications in several HBV ORFs (the HBsAg, preS, X, and preC/C regions) compared to other countries have been reported to date[10-15]. Furthermore, higher relapse rates after antiviral therapy in Korean chronic patients have also been reported[47]. However, there have been no reports regarding potential NAr mutations from Korean treatment naïve patients to date. In this study, we analyzed potential NAr mutations from 131 Korean treatment naïve patients with genotype C2 infections using direct sequencing protocols.

There are three notable findings in our study. First, our data demonstrated that the prevalence of patients with potential NAr mutations was 60.3% (79/131) (Table 3), which was almost two times higher than the prevalence of these mutations [30.73% (59/192)] in a treatment naïve Chinese cohort[36] using the same direct sequencing protocols applied for the detection of potential NAr mutations in the treatment naive Korean cohort. The difference in the mutation rates between the 2 cohorts was more pronounced with the Korean and Chinese cohorts [2.68% (148/5502) (Table 3) and 0.94% (76/8064)[36], respectively]. In particular, we found primary NA mutations at Category 1 positions from 10 patients (7.8%) [rt184 related to ETV resistance (1 patient) and rt204 related to LMV resistance (9 patients)] and the so called YMDD mutation or secondary/compensatory mutations at Category 2 positions [rt80 and rt180 from 7 patients (5.3 %)] (Table 3). These findings were in contrast to

Table 6 Comparison of clinical features between patients with or without L80I

Clinical factors	Wild type (n = 126)	L80I (n = 5)	Total (n = 131)	P value
Age, yr, mean ± SD	45.8 ± 12.2	57.2 ± 8.1	45.7 ± 12.3	0.043
Gender, Male	63.50%	100%	64.80%	NS
HBeAg negative	45.20%	60.00%	45.80%	NS
ALT (IU/L), mean ± SD	84.0 ± 96.8	68.6 ± 19.7	100.8 ± 191.2	NS
AST (IU/L), mean ± SD	100.9 ± 125.3	118.6 ± 65.0	113.2 ± 141.0	NS
HBV DNA	5.8 ± 1.7	6.7 ± 0.2	6.5 ± 1.7	< 0.001
HBsAg	3.4 ± 0.65	3.5 ± 0.32	3.4 ± 0.6	NS
CH: HCC, HCC (%)	59/67 (53.9)	0/5 (100)	59/72 (54.9)	0.036

HBV: Hepatitis B virus; CH: Chronic hepatitis; HCC: Hepatocellular carcinoma.

the two previous reports of Chinese cohorts[36,46] which showed that any mutations were not found within both regions. This findings may partially provide a likely explanation for why relapse after antiviral therapy is so prevalent in Korean patients[48] and also suggest that these patients should be treated with newer NAs, such as tenofovir (TDF), which is very potent and has a high genetic barrier to antiviral resistance.

Second, potential NAr mutations in our cohort were distributed in a non-random manner, as was shown in other studies[36]. The potential NAr mutations were found more frequently in the A-B interdomain overlapped with the HBsAg MHR region than in domain regions (7.50% *vs* 1.07%, P = 0.008) (Table 4), which was in line with the previous report[36] that potential NAr positions within this region might be hotspots of naturally occurring mutations in this treatment naïve population. Notably, significantly higher mutation frequencies were found in 2 overlapped "a" determinant positions (3.81%, 15/393) compared to non-"a" determinant region (0.55%, 27/4847, P < 0.001) (Table 4). These findings suggest that host immune pressure against B cells could contribute to the generation of potential NAr mutations[36].

Third, our data showed there was significant difference in overall frequency of potential NAr mutations between CH patients (2.09%) and HCC patients (3.17%, P = 0.003, Table 3). In particular, mutations at the 3 NAr positions (rt80, rt139, and rt204) seemed to be the most pronounced contributors to hepatocarcinogenesis in the Korean Cohort [CH (0%, 0/59) *vs* HCC (30.6%, 22/72), P < 0.001]. Of these, the YMDD-motif mutation at rt204 was reported to naturally occur in chronic HBV patients without antiviral treatment, such as lamivudine therapy, by several studies[49,50]. The other HCC-related mutation (rtL80I) was first introduced as a mutation associated with LMV resistance[51]. These authors found that these mutants were associated with increased viral loads accompanied by an elevation in serum aminotransferase activity and exacerbation of liver disease in every case. In line with the previous report[51,52], our data indicated that L80I might have contributed to clinical deterioration[52]. Notably, our findings that L80I was combined with the rtM204I/V mutations in all 5 patients (data not shown) and L80I was also significantly related to increased HBV replication (Table 6) suggested that this mutation might play a role in compensating for the defective replication of rtM204I/V. Thus, our finding regarding relationships of exacerbation of liver disease with rtL80I and rtM204I/V in treatment naïve patients may be primarily attributed to the co-selection of these two mutation types. These results suggest that potential NAr mutations may contribute to hepatocarcinogenesis, possibly *via* increases in HBV replication fitness or evasion of B cell immune responses against HBsAg.

In conclusion, our data showed that potential NAr mutations, including the classical antiviral resistance mutations, were very prevalent in treatment naïve Korean patients compared to populations from other countries. Naturally occurring potential NAr mutations may contribute to liver disease progression (particularly HCC generation) in Korean chronic patients with genotype C2 infections and provide a likely explanation for why patients with advanced liver disease are difficult to treat with NAs. Additionally, we identified 3 HCC-related NAr mutations (L80I, N139K/T/H and M204I/V).

ACKNOWLEDGMENTS

We appreciate statistical consultation from the Medical Research Collaborating Center at the Seoul National University Hospital and the Seoul National University College of Medicine.

COMMENTS

Background

Naturally occurring reverse transcriptase mutations associated with hepatitis B virus (HBV) drug resistance have been reported from treatment naïve chronic patients from several countries. However, there have been no reports regarding potential nucleos(t)ide analog resistance (NAr) mutations from Korean treatment naïve patients to date.

Research frontiers

Here, they found naturally occurring potential NAr mutations may contribute to liver disease progression in Korean chronic patients with genotype C2 infections.

Hotspots or important area

Notably, the authors identified 3 hepatocellular carcinoma (HCC)-related NAr

mutations (L80I, N139K/T/H and M204I/V).

Applications

The three HCC-related NAr mutations (L80I, N139K/T/H and M204I/V) found in this study could be applied as markers of molecular detection method for the HCC of HBV infected chronic patients in the future.

Peer-review

The authors showed that potential NAr mutations, including the classical antiviral resistance mutations, were very prevalent in treatment naïve Korean patients and naturally occurring potential NAr mutations may contribute to liver disease progression in Korean chronic patients with genotype C2 infections. In addition, authors identified 3 HCC-related NAr mutations (L80I, N139K/T/H and M204I/V).

REFERENCES

1 **Lee WM**. Hepatitis B virus infection. *N Engl J Med* 1997; **337**: 1733-1745 [PMID: 9392700 DOI: 10.1056/nejm199712113372406]

2 **Lozano R**, Naghavi M, Foreman K, Lim S, Shibuya K, Aboyans V, Abraham J, Adair T, Aggarwal R, Ahn SY, Alvarado M, Anderson HR, Anderson LM, Andrews KG, Atkinson C, Baddour LM, Barker-Collo S, Bartels DH, Bell ML, Benjamin EJ, Bennett D, Bhalla K, Bikbov B, Bin Abdulhak A, Birbeck G, Blyth F, Bolliger I, Boufous S, Bucello C, Burch M, Burney P, Carapetis J, Chen H, Chou D, Chugh SS, Coffeng LE, Colan SD, Colquhoun S, Colson KE, Condon J, Connor MD, Cooper LT, Corriere M, Cortinovis M, de Vaccaro KC, Couser W, Cowie BC, Criqui MH, Cross M, Dabhadkar KC, Dahodwala N, De Leo D, Degenhardt L, Delossantos A, Denenberg J, Des Jarlais DC, Dharmaratne SD, Dorsey ER, Driscoll T, Duber H, Ebel B, Erwin PJ, Espindola P, Ezzati M, Feigin V, Flaxman AD, Forouzanfar MH, Fowkes FG, Franklin R, Fransen M, Freeman MK, Gabriel SE, Gakidou E, Gaspari F, Gillum RF, Gonzalez-Medina D, Halasa YA, Haring D, Harrison JE, Havmoeller R, Hay RJ, Hoen B, Hotez PJ, Hoy D, Jacobsen KH, James SL, Jasrasaria R, Jayaraman S, Johns N, Karthikeyan G, Kassebaum N, Keren A, Khoo JP, Knowlton LM, Kobusingye O, Koranteng A, Krishnamurthi R, Lipnick M, Lipshultz SE, Ohno SL, Mabweijano J, MacIntyre MF, Mallinger L, March L, Marks GB, Marks R, Matsumori A, Matzopoulos R, Mayosi BM, McAnulty JH, McDermott MM, McGrath J, Mensah GA, Merriman TR, Michaud C, Miller M, Miller TR, Mock C, Mocumbi AO, Mokdad AA, Moran A, Mulholland K, Nair MN, Naldi L, Narayan KM, Nasseri K, Norman P, O'Donnell M, Omer SB, Ortblad K, Osborne R, Ozgediz D, Pahari B, Pandian JD, Rivero AP, Padilla RP, Perez-Ruiz F, Perico N, Phillips D, Pierce K, Pope CA, 3rd, Porrini E, Pourmalek F, Raju M, Ranganathan D, Rehm JT, Rein DB, Remuzzi G, Rivara FP, Roberts T, De Leon FR, Rosenfeld LC, Rushton L, Sacco RL, Salomon JA, Sampson U, Sanman E, Schwebel DC, Segui-Gomez M, Shepard DS, Singh D, Singleton J, Sliwa K, Smith E, Steer A, Taylor JA, Thomas B, Tleyjeh IM, Towbin JA, Truelsen T, Undurraga EA, Venketasubramanian N, Vijayakumar L, Vos T, Wagner GR, Wang M, Wang W, Watt K, Weinstock MA, Weintraub R, Wilkinson JD, Woolf AD, Wulf S, Yeh PH, Yip P, Zabetian A, Zheng ZJ, Lopez AD, Murray CJ, AlMazroa MA, Memish ZA. Global and regional mortality from 235 causes of death for 20 age groups in 1990 and 2010: a systematic analysis for the Global Burden of Disease Study 2010. *Lancet* (London, England) 2012; **380**: 2095-2128 [PMID: 23245604 DOI: 10.1016/s0140-6736(12)61728-0]

3 **Kweon S**, Kim Y, Jang MJ, Kim Y, Kim K, Choi S, Chun C, Khang YH, Oh K. Data resource profile: the Korea National Health and Nutrition Examination Survey (KNHANES). *Int J Epidemiol* 2014; **43**: 69-77 [PMID: 24585853 DOI: 10.1093/ije/dyt228]

4 **Chan HL**, Wong ML, Hui AY, Hung LC, Chan FK, Sung JJ. Hepatitis B virus genotype C takes a more aggressive disease course than hepatitis B virus genotype B in hepatitis B e antigen-positive patients. *J Clin Microbiol* 2003; **41**: 1277-1279 [PMID: 12624067]

5 **Osiowy C**, Giles E, Trubnikov M, Choudhri Y, Andonov A. Characterization of Acute and Chronic Hepatitis B Virus Genotypes in Canada. *PLoS One* 2015; **10**: e0136074 [PMID: 26406309 DOI: 10.1371/journal.pone.0136074]

6 **Kim H**, Kim BJ. Association of preS/S Mutations with Occult Hepatitis B Virus (HBV) Infection in South Korea: Transmission Potential of Distinct Occult HBV Variants. *Int J Mol Sci* 2015; **16**: 13595-13609 [PMID: 26084041 DOI: 10.3390/ijms160613595]

7 **Kim H**, Jee YM, Song BC, Shin JW, Yang SH, Mun HS, Kim HJ, Oh EJ, Yoon JH, Kim YJ, Lee HS, Hwang ES, Cha CY, Kook YH, Kim BJ. Molecular epidemiology of hepatitis B virus (HBV) genotypes and serotypes in patients with chronic HBV infection in Korea. *Intervirology* 2007; **50**: 52-57 [PMID: 17164558 DOI: 10.1159/000096313]

8 **Kim H**, Jee YM, Song BC, Hyun JW, Mun HS, Kim HJ, Oh EJ, Yoon JH, Kim YJ, Lee HS, Hwang ES, Cha CY, Kook YH, Kim BJ. Analysis of hepatitis B virus quasispecies distribution in a Korean chronic patient based on the full genome sequences. *J Med Virol* 2007; **79**: 212-219 [PMID: 17245716 DOI: 10.1002/jmv.20789]

9 **Kim BJ**. Hepatitis B virus mutations related to liver disease progression of Korean patients. *World J Gastroenterol* 2014; **20**: 460-467 [PMID: 24574714 DOI: 10.3748/wjg.v20.i2.460]

10 **Kim DW**, Lee SA, Hwang ES, Kook YH, Kim BJ. Naturally occurring precore/core region mutations of hepatitis B virus genotype C related to hepatocellular carcinoma. *PLoS One* 2012; **7**: e47372 [PMID: 23071796 DOI: 10.1371/journal.pone.0047372]

11 **Kim H**, Lee SA, Kim DW, Lee SH, Kim BJ. Naturally occurring mutations in large surface genes related to occult infection of hepatitis B virus genotype C. *PLoS One* 2013; **8**: e54486 [PMID: 23349904 DOI: 10.1371/journal.pone.0054486]

12 **Lee SA**, Kim KJ, Kim DW, Kim BJ. Male-specific W4P/R mutation in the pre-S1 region of hepatitis B virus, increasing the risk of progression of liver diseases in chronic patients. *J Clin Microbiol* 2013; **51**: 3928-3936 [PMID: 24025913 DOI: 10.1128/jcm.01505-13]

13 **Kim H**, Gong JR, Lee SA, Kim BJ. Discovery of a Novel Mutation (X8Del) Resulting in an 8-bp Deletion in the Hepatitis B Virus X Gene Associated with Occult Infection in Korean Vaccinated Individuals. *PLoS One* 2015; **10**: e0139551 [PMID: 26437447 DOI: 10.1371/journal.pone.0139551]

14 **Lee SA**, Kim H, Won YS, Seok SH, Na Y, Shin HB, Inn KS, Kim BJ. Male-specific hepatitis B virus large surface protein variant W4P potentiates tumorigenicity and induces gender disparity. *Mol Cancer* 2015; **14**: 23 [PMID: 25645622 DOI: 10.1186/s12943-015-0303-7]

15 **Lee SA**, Kim KJ, Kim H, Choi WH, Won YS, Kim BJ. Hepatitis B virus preS1 deletion is related to viral replication increase and disease progression. *World J Gastroenterol* 2015; **21**: 5039-5048 [PMID: 25945020 DOI: 10.3748/wjg.v21.i16.5039]

16 **Song BC**, Kim SH, Kim H, Ying YH, Kim HJ, Kim YJ, Yoon JH, Lee HS, Cha CY, Kook YH, Kim BJ. Prevalence of naturally occurring surface antigen variants of hepatitis B virus in Korean patients infected chronically. *J Med Virol* 2005; **76**: 194-202 [PMID: 15834881 DOI: 10.1002/jmv.20354]

17 **Song BC**, Kim H, Kim SH, Cha CY, Kook YH, Kim BJ. Comparison of full length sequences of hepatitis B virus isolates in hepatocellular carcinoma patients and asymptomatic carriers of Korea. *J Med Virol* 2005; **75**: 13-19 [PMID: 15543574 DOI: 10.1002/jmv.20230]

18 **Kim H**, Jee Y, Mun HS, Park JH, Yoon JH, Kim YJ, Lee HS, Hyun JW, Hwang ES, Cha CY, Kook YH, Kim BJ. Characterization of two hepatitis B virus populations in a single Korean hepatocellular carcinoma patient with an HBeAg-negative serostatus: a novel X-Gene-deleted strain with inverted duplication sequences of upstream enhancer site II. *Intervirology* 2007; **50**: 273-280 [PMID: 17570929 DOI: 10.1159/000103915]

19 **Kim H**, Jee Y, Mun HS, Song BC, Park JH, Hyun JW, Hwang ES, Cha CY, Kook YH, Kim BJ. Comparison of full genome sequences between two hepatitis B virus strains with or without preC mutation (A1896) from a single Korean hepatocellular carcinoma patient. *J*

Microbiol Biotechn 2007; **17**: 701-704 [PMID: 18051288]
20 **Kim HJ**, Park JH, Jee Y, Lee SA, Kim H, Song BC, Yang S, Lee M, Yoon JH, Kim YJ, Lee HS, Hwang ES, Kook YH, Kim BJ. Hepatitis B virus X mutations occurring naturally associated with clinical severity of liver disease among Korean patients with chronic genotype C infection. *J Med Virol* 2008; **80**: 1337-1343 [PMID: 18551606 DOI: 10.1002/jmv.21219]
21 **Mun HS**, Lee SA, Jee Y, Kim H, Park JH, Song BC, Yoon JH, Kim YJ, Lee HS, Hyun JW, Hwang ES, Kook YH, Kim BJ. The prevalence of hepatitis B virus preS deletions occurring naturally in Korean patients infected chronically with genotype C. *J Med Virol* 2008; **80**: 1189-1194 [PMID: 18461612 DOI: 10.1002/jmv.21208]
22 **Lee SA**, Cho YK, Lee KH, Hwang ES, Kook YH, Kim BJ. Gender disparity in distribution of the major hydrophilic region variants of hepatitis B virus genotype C according to hepatitis B e antigen serostatus. *J Med Virol* 2011; **83**: 405-411 [PMID: 21264860 DOI: 10.1002/jmv.21988]
23 **Lee SA**, Mun HS, Kim H, Lee HK, Kim BJ, Hwang ES, Kook YH, Kim BJ. Naturally occurring hepatitis B virus X deletions and insertions among Korean chronic patients. *J Med Virol* 2011; **83**: 65-70 [PMID: 21108340 DOI: 10.1002/jmv.21938]
24 **Mun HS**, Lee SA, Kim H, Hwang ES, Kook YH, Kim BJ. Novel F141L pre-S2 mutation in hepatitis B virus increases the risk of hepatocellular carcinoma in patients with chronic genotype C infections. *J Virol* 2011; **85**: 123-132 [PMID: 20962085 DOI: 10.1128/JVI.01524-10]
25 **Kim DW**, Lee SA, Kim H, Won YS, Kim BJ. Naturally occurring mutations in the nonstructural region 5B of hepatitis C virus (HCV) from treatment-naïve Korean patients chronically infected with HCV genotype 1b. *PLoS One* 2014; **9**: e87773 [PMID: 24489961 DOI: 10.1371/journal.pone.0087773]
26 **Kim H**, Lee SA, Kim BJ. X region mutations of hepatitis B virus related to clinical severity. *World J Gastroenterol* 2016; **22**: 5467-5478 [PMID: 27350725 DOI: 10.3748/wjg.v22.i24.5467]
27 **Kim H**, Lee SA, Do SY, Kim BJ. Precore/core region mutations of hepatitis B virus related to clinical severity. *World J Gastroenterol* 2016; **22**: 4287-4296 [PMID: 27158197 DOI: 10.3748/wjg.v22.i17.4287]
28 **Liang TJ**. Hepatitis B: the virus and disease. *Hepatology* 2009; **49**: S13-S21 [PMID: 19399811 DOI: 10.1002/hep.22881]
29 **Nowak MA**, Bonhoeffer S, Hill AM, Boehme R, Thomas HC, McDade H. Viral dynamics in hepatitis B virus infection. *Proc Natl Acad Sci USA* 1996; **93**: 4398-4402 [PMID: 8633078]
30 **Marcellin P**, Chang TT, Lim SG, Tong MJ, Sievert W, Shiffman ML, Jeffers L, Goodman Z, Wulfsohn MS, Xiong S, Fry J, Brosgart CL. Adefovir dipivoxil for the treatment of hepatitis B e antigen-positive chronic hepatitis B. *N Engl J Med* 2003; **348**: 808-816 [PMID: 12606735 DOI: 10.1056/NEJMoa020681]
31 **Locarnini S**, Mason WS. Cellular and virological mechanisms of HBV drug resistance. *J Hepatol* 2006; **44**: 422-431 [PMID: 16364492 DOI: 10.1016/j.jhep.2005.11.036]
32 **Selabe SG**, Lukhwareni A, Song E, Leeuw YG, Burnett RJ, Mphahlele MJ. Mutations associated with lamivudine-resistance in therapy-naïve hepatitis B virus (HBV) infected patients with and without HIV co-infection: implications for antiretroviral therapy in HBV and HIV co-infected South African patients. *J Med Virol* 2007; **79**: 1650-1654 [PMID: 17854040 DOI: 10.1002/jmv.20974]
33 **Rodriguez C**, Chevaliez S, Bensadoun P, Pawlotsky JM. Characterization of the dynamics of hepatitis B virus resistance to adefovir by ultra-deep pyrosequencing. *Hepatology* 2013; **58**: 890-901 [PMID: 23505208 DOI: 10.1002/hep.26383]
34 **Tenney DJ**, Rose RE, Baldick CJ, Pokornowski KA, Eggers BJ, Fang J, Wichroski MJ, Xu D, Yang J, Wilber RB, Colonno RJ. Long-term monitoring shows hepatitis B virus resistance to entecavir in nucleoside-naïve patients is rare through 5 years of therapy. *Hepatology* 2009; **49**: 1503-1514 [PMID: 19280622 DOI: 10.1002/hep.22841]
35 **Zhang Y**, Lian JQ, Li Y, Wang JP, Huang CX, Bai XF, Wang JP. Telbivudine plus adefovir therapy for chronic hepatitis B patients with virological breakthrough or genotypic resistance to telbivudine. *Eur J Gastroenterol Hepatol* 2013; **25**: 814-819 [PMID: 23406845 DOI: 10.1097/MEG.0b013e32835ee516]
36 **Liu BM**, Li T, Xu J, Li XG, Dong JP, Yan P, Yang JX, Yan L, Gao ZY, Li WP, Sun XW, Wang YH, Jiao XJ, Hou CS, Zhuang H. Characterization of potential antiviral resistance mutations in hepatitis B virus reverse transcriptase sequences in treatment-naïve Chinese patients. *Antiviral Res* 2010; **85**: 512-519 [PMID: 20034521 DOI: 10.1016/j.antiviral.2009.12.006]
37 **Kramvis A**, Bukofzer S, Kew MC. Comparison of hepatitis B virus DNA extractions from serum by the QIAamp blood kit, GeneReleaser, and the phenol-chloroform method. *J Clin Microbiol* 1996; **34**: 2731-2733 [PMID: 8897174]
38 **Kumar S**, Tamura K, Jakobsen IB, Nei M. MEGA2: molecular evolutionary genetics analysis software. *Bioinformatics* 2001; **17**: 1244-1245 [PMID: 11751241]
39 **Rhee SY**, Margeridon-Thermet S, Nguyen MH, Liu TF, Kagan RM, Beggel B, Verheyen J, Kaiser R, Shafer RW. Hepatitis B virus reverse transcriptase sequence variant database for sequence analysis and mutation discovery. *Antiviral Res* 2010; **88**: 269-275 [PMID: 20875460 DOI: 10.1016/j.antiviral.2010.09.012]
40 **Benjamini Y**, Hochberg Y. Controlling the False Discovery Rate: A Practical and Powerful Approach to Multiple Testing. *J Roy Stat Soc B Met* 1995; **57**: 289-300
41 **Kwon H**, Lok AS. Hepatitis B therapy. *Nat Rev Gastroenterol Hepatol* 2011; **8**: 275-284 [PMID: 21423260 DOI: 10.1038/nrgastro.2011.33]
42 **Sheldon J**, Rodès B, Zoulim F, Bartholomeusz A, Soriano V. Mutations affecting the replication capacity of the hepatitis B virus. *J Viral Hepat* 2006; **13**: 427-434 [PMID: 16792535 DOI: 10.1111/j.1365-2893.2005.00713.x]
43 **Masaadeh HA**, Hayajneh WA, Alqudah EA. Hepatitis B virus genotypes and lamivudine resistance mutations in Jordan. *World J Gastroenterol* 2008; **14**: 7231-7234 [PMID: 19084939 DOI: 10.3748/wjg.14.7231]
44 **Vutien P**, Trinh HN, Garcia RT, Nguyen HA, Levitt BS, Nguyen K, da Silveira E, Daugherty T, Ahmed A, Garcia G, Lutchman GA, Nguyen MH. Mutations in HBV DNA polymerase associated with nucleos(t)ide resistance are rare in treatment-naive patients. *Clin Gastroenterol Hepatol* 2014; **12**: 1363-1370 [PMID: 24342744 DOI: 10.1016/j.cgh.2013.11.036]
45 **Zhang Q**, Liao Y, Cai B, Li Y, Li L, Zhang J, An Y, Wang L. Incidence of natural resistance mutations in naïve chronic hepatitis B patients: a systematic review and meta-analysis. *J Gastroenterol Hepatol* 2015; **30**: 252-261 [PMID: 25318660 DOI: 10.1111/jgh.12831]
46 **Xu J**, Wu B, Wang JH, Huang L, Wang DY, Zhao L, Zhao GP, Wang Y. Pre-existing mutations in reverse transcriptase of hepatitis B virus in treatment-naive Chinese patients with chronic hepatitis B. *PLoS One* 2015; **10**: e0117429 [PMID: 25821965 DOI: 10.1371/journal.pone.0117429]
47 **Song BC**, Suh DJ, Lee HC, Chung YH, Lee YS. Hepatitis B e antigen seroconversion after lamivudine therapy is not durable in patients with chronic hepatitis B in Korea. *Hepatology* 2000; **32**: 803-806 [PMID: 11003626 DOI: 10.1053/jhep.2000.16665]
48 **Chainuvati S**, Cheng J, Hou JL, Hsu CW, Jia JD, Komolmit P, Kwon SY, Lee CH, Li H, Li Y, Liu CJ, Neo BL, Peng CY, Tanwandee T, Wongcharatrawee S, Wu JC, Yu ML, Zhang XX. Patterns of managing chronic hepatitis B treatment-related drug resistance: a survey of physicians in Mainland China, South Korea, Taiwan, and Thailand. *Hepatol Int* 2009; **3**: 453-460 [PMID: 19669246 DOI: 10.1007/s12072-009-9139-9]
49 **Mahmoud Ali M**. Mutation Patterns at Codons RT204 And RT180 of the HBV Polymerase Gene Associated with Lamivudine Resistance in Treated and Untreated Chronic HBV Patients in Kuwait: A Case Series. *J Clin Case Rep* 2013; **3**: 276 [DOI: 10.4172/2165-7920.1000276]
50 **Lee SH**, Kim HS, Byun IS, Jeong SW, Kim SG, Jang JY, Kim YS, Kim BS. Pre-existing YMDD mutants in treatment-naïve patients with chronic hepatitis B are not selected during lamivudine therapy. *J Med Virol* 2012; **84**: 217-222 [PMID: 22170540 DOI: 10.1002/

jmv.23191]
51 **Ogata N**, Fujii K, Takigawa S, Nomoto M, Ichida T, Asakura H. Novel patterns of amino acid mutations in the hepatitis B virus polymerase in association with resistance to lamivudine therapy in japanese patients with chronic hepatitis B. *J Med Virol* 1999; **59**: 270-276 [PMID: 10502255]
52 **Warner N**, Locarnini S, Kuiper M, Bartholomeusz A, Ayres A, Yuen L, Shaw T. The L80I substitution in the reverse transcriptase domain of the hepatitis B virus polymerase is associated with lamivudine resistance and enhanced viral replication in vitro. *Antimicrob Agents Chemother* 2007; **51**: 2285-2292 [PMID: 17438047 DOI: 10.1128/AAC.01499-06]

P- Reviewer: Kato M, Sghaier I **S- Editor**: Qi Y **L- Editor**: A
E- Editor: Zhang FF

World Journal of Gastroenterology

Submit a Manuscript: http://www.f6publishing.com

World J Gastroenterol 2017 June 21; 23(23): 4233-4242

DOI: 10.3748/wjg.v23.i23.4233

ISSN 1007-9327 (print) ISSN 2219-2840 (online)

ORIGINAL ARTICLE

Basic Study

Inhibition of N-methyl-N-nitrosourea-induced gastric tumorigenesis by Liuwei Dihuang Pill in db/db mice

Shan Zhuang, Yong-Mei Jian, Yong-Ning Sun

Shan Zhuang, Yong-Mei Jian, Yong-Ning Sun, Department of Traditional Chinese Medicine, Shanghai Jiao Tong University Affiliated Sixth People's Hospital, Shanghai 200233, China

Author contributions: Sun YN contributed to the conception and design of the study; Zhuang S and Jian YM contributed to acquisition, analysis and interpretation of the data; all authors drafted the article and made critical revisions related to the intellectual content of the manuscript, and approved the final version of the article to be published.

Institutional review board statement: The study was reviewed and approved by the Institutional Review Board of Shanghai Sixth People's Hospital.

Institutional animal care and use committee statement: All procedures involving animals were reviewed and approved by the Institutional Animal Care and Use Committee of Shanghai Jiao Tong University Affiliated Sixth People's Hospital (IACUC Protocol No. 2017-0002).

Conflict-of-interest statement: All authors declare that there are no conflicts of interest.

Data sharing statement: All authors declare that no additional data are available.

Manuscript source: Unsolicited manuscript

Correspondence to: Yong-Ning Sun, PhD, Director, Department of Traditional Chinese Medicine, Shanghai Jiao Tong University Affiliated Sixth People's Hospital, 600 Yishan Road, Shanghai 200233, China. ynsun@sjtu.edu.cn
Telephone: +86-21-20953075
Fax: +86-21-20953075

Received: February 9, 2017
Peer-review started: February 9, 2017
First decision: March 16, 2017
Revised: March 30, 2017
Accepted: May 9, 2017
Article in press: May 9, 2017
Published online: June 21, 2017

Abstract

AIM

To investigate the inhibitory effect of Liuwei Dihuang Pill (LDP) on gastric tumorigenesis induced by N-methyl-N-nitrosourea (MNU) in diabetic mice.

METHODS

Four-week-old mice were divided into four groups: A, 12 db/m mice treated with MNU and saline, as the non-diabetic control; B, 12 db/db mice treated with MNU and saline, as the diabetic control; C, 12 db/db mice treated with MNU and metformin, as the positive control; and D, 12 db/db mice treated with MNU and LDP. MNU was administrated for 20 wk to induce gastric carcinogenesis. LDP was administrated for 10 wk for improvement of insulin resistance. Body weight and food intake were measured every week. Blood samples were collected for assays of fasting blood glucose, insulin, insulin-like growth factor (IGF)-1, adiponectin and leptin. Stomach tissues were collected for histopathological analysis, immunohistochemical staining of Ki67, quantitative reverse transcription-polymerase chain reaction and western blotting.

RESULTS

The incidence of MNU-induced gastric dysplasia was significantly elevated in diabetic (db/db) mice relative to the control (db/m) mice. The incidence of gastric

dysplasia was significantly reduced by LDP with suppression of cell proliferation, as demonstrated by a decrease in Ki67 staining. Hyperglycemia, hyperinsulinemia and serum IGF-1 were inhibited by LDP. Expression of IGF-1 and insulin receptor mRNAs was decreased, phosphorylation of IGF-1 receptor and AKT protein was reduced in the stomach tissues by LDP. In addition, adiponectin was increased and leptin was decreased in the serum by LDP.

CONCLUSION

LDP decreased risk of gastric dysplasia in type 2 diabetic mice by down-regulation of IGF and insulin activity and correction of adipokines disorders.

Key words: Diabetes; Gastric cancer; Liuwei Dihuang Pill; Insulin; Insulin-like growth factor

Core tip: Type 2 diabetes is reported to increase risk of gastric carcinogenesis, partly by hyperinsulinemia, hyperglycemia, excessive activation of insulin-like growth factor (IGF)-1, and disorders of adipokines. In this study, we demonstrated that Liuwei Dihuang Pill decreased the risk of gastric tumorigenesis in type 2 diabetic mice by alleviating insulin resistance and decreasing IGF-1 and insulin activity, followed by down-regulation of the IGF-1/AKT signaling pathway. The improvement in adiponectin and leptin may also contribute to the effects.

Zhuang S, Jian YM, Sun YN. Inhibition of N-methyl-N-nitrosourea-induced gastric tumorigenesis by Liuwei Dihuang Pill in db/db mice. *World J Gastroenterol* 2017; 23(23): 4233-4242 Available from: URL: http://www.wjgnet.com/1007-9327/full/v23/i23/4233.htm DOI: http://dx.doi.org/10.3748/wjg.v23.i23.4233

INTRODUCTION

Gastric cancer is one of the most common malignancies, particularly among populations of East Asia. The prevention and treatment of gastric cancer remain a challenge due to the absence of effective strategies. Multiple risk factors, such as *Helicobacter pylori* infection, high salt intake, smoking and obesity, contribute to the initiation of gastric cancer[1,2]. Recent studies in humans have demonstrated that type 2 diabetes may be a new risk factor for gastric cancer. The incidence of gastric cancer is affected by duration of diabetes and some anti-diabetic drugs. Given the high prevalence of type 2 diabetes and gastric cancer worldwide, control of gastric cancer in diabetic patients has become a new challenge.

The etiology of gastric cancer remains unknown in type 2 diabetic patients. However, hyperinsulinemia and insulin-like growth factor (IGF) may play a central role in the promotion of tumorigenesis. A large Japanese case-control study has demonstrated that hyperinsulinemia and serum C peptide are positively correlated with increased risk of gastric cancer[3]. A high level of insulin increases the bioavailability of serum IGF-1. Both insulin and IGF-1 activate the mitogenic signaling pathways, including the phosphoinositide 3-kinase/protein kinase B (PI3K/AKT) and mitogen-activated protein kinase pathways[4]. In addition, imbalance of adipokines in diabetes and obesity, such as the high level of leptin and low level of adiponectin, is associated with the risk of cancer[5].

Strategies targeting those factors may decrease the risk of cancer. Metformin is an effective drug in the control of insulin resistance in type 2 diabetes. Population studies have revealed that long-term use of metformin can decrease the risk of gastric cancer[6]. The antitumor effect of metformin may be mediated by activation of the AMP-activated protein kinase pathway or inhibition of the IGF-1 receptor signaling pathway[7,8]. In the present study, metformin was selected as a positive control in the control of gastric tumorigenesis.

The choice of effective and safe drugs remains limited for gastric cancer. Low-grade gastric dysplasia is a precancerous lesion in the early phase of gastric cancer. Inhibition of the dysplasia is able to block advancement of the precancerous lesion into gastric cancer[9]. We propose that this strategy may be used in the control of gastric cancer in diabetes and obesity. Traditional Chinese medicine (TCM) represents a rich resource in the treatment of diabetes and cancer[10,11], and Liuwei Dihuang Pill (LDP) is one of the examples.

LDP is made from a TCM formula that is often prescribed for treatment of diabetes. Studies in rodents have suggested that LDP reduces serum insulin as well as leptin *via* weight loss and fat reduction[12,13]. LDP also has beneficial effects against certain types of cancers. Several studies have demonstrated that LDP inhibits spontaneous tumorigenesis and suppresses liver tumors[14,15]. In clinical practice, long-term application of LDP prevents epithelial dysplasia of the esophagus[16]. These results suggest that LDP is an effective therapy for both type 2 diabetes and cancer. Despite this knowledge, there is no report on LDP activity in the risk control of gastric cancer in patients with type 2 diabetes.

In the present study, we addressed the issue in diabetic db/db mice, which have a high susceptibility to the carcinogen N-methyl-N-nitrosourea (MNU) for gastric cancer[17-19]. The mice were treated with MNU in drinking water to induce gastric dysplasia. LDP was tested for its ability to inhibit gastric tumorigenesis in the model.

MATERIALS AND METHODS

Animals

Thirty-six male db/db mice and 12 control (db/m) mice

Table 1 Compositions of Liuwei Dihuang Pill

Chinese name	Latin name	Parts used	Weight, g
Shu di huang	*Rehmannia glutinosa Libosch*	Root	160
Shan zhu yu	*Cornus officinalis Sieb*	Fruit	80
Shan yao	*Dioscorea opposite Thunb*	Rootstock	80
Ze xie	*Alisma orientale (G. Samuelsson) Juz*	Rootstock	60
Fu ling	*Poria cocos (Schw.) Wolf*	Sclerotium	60
Mu dan pi	*Paeonia suffruticosa Andrews*	Bark	60

Plant name as verified at http://www.theplantlist.org.

at age 4 wk were obtained from the Nanjing University Animal Laboratories, China (Certification No. SCXK 2015-0001). The animal protocol was designed to minimize pain or discomfort to the animals. The mice were maintained in specific pathogen-free conditions with a 12-h light-dark cycle, room temperature of 25 ℃ ± 1 ℃, and relative humidity of 60% ± 5% in the animal facility of Shanghai Jiao Tong University. The mice had free access to regular chow diet and water. All the experimental protocols were approved by the Institutional Animal Care and Use Committee of Shanghai Jiao Tong University.

LDP water extract and dosage

LDP was purchased from Tongrentang Group (Beijing, China). LDP is made of six raw medicinal materials (Table 1) and manufactured in accordance with the quality control standards in the Chinese Pharmacopoeia. The bioactive components of LDP were certified according to the high-performance liquid chromatography-fingerprints, which included loganin, paeoniflorin, paeonol, gallic acid, and morroniside[20,21]. The LDP was ground, extracted ultrasonically with distilled water for 30 min, and filtered through a screen with 90 μm aperture. LDP is taken orally at 0.15 g/kg per d of herbal materials in humans, and this dosage is equal to 1.8 g/kg per d in mice. LDP was administrated through the drinking water at a final concentration of 0.09 g/mL (about 9 g/kg per d) for 10 wk. Metformin (Sino-American Shanghai Squibb Co., Shanghai, China) was dissolved in distilled water at a concentration of 5 mg/mL, as described in a previous report[22].

Gastric tumor model

MNU (Sigma, St. Louis, MO, United States) was administered to the mice through drinking water 3 times weekly at a concentration of 120 ppm in light-shielded bottles. The administration was performed every other week for 20 wk as described previously[23].

Study design and samples collection

Following 1-wk acclimation, the mice were randomly divided into four groups. Group A, 12 control (db/m) mice were treated with MNU for 20 wk followed by saline treatment for 10 wk to serve as the non-diabetic control. Group B, 12 diabetic (db/db) mice were treated with MNU for 20 wk followed by saline treatment for 10 wk to serve as the diabetic control. Group C, 12 diabetic mice were treated with MNU for 20 wk followed by metformin treatment for 10 wk, as the positive control. Group D, 12 diabetic mice were treated with MNU for 20 wk followed by LDP treatment for 10 wk. At the end of treatment (30 wk), all mice were fasted for 12 h and blood samples were collected from the left ventricle for fasting blood glucose (FBG) measurement.

All animals were euthanized with 1% pentobarbital sodium. Serum was collected and stored at -80 ℃ for biochemical analysis after centrifugation of the blood at 1000 *g* for 10 min. The stomach was removed and divided into two parts along the greater curvature. One part was quickly frozen in liquid nitrogen and then stored at -80 ℃ for quantitative reverse transcription-polymerase chain reaction (qRT-PCR) and western blot analysis. The other part was fixed in neutral-buffered formalin (40 g/L) for 24 h for histological assessment.

Histological examination of gastric lesions

Fixed stomach tissue was cut longitudinally into three strips. After dehydration and rinsing in xylol, the strips were embedded in paraffin, sectioned at 4-μm thickness, and stained with hematoxylin and eosin. Gastric lesions were classified as chronic gastritis, gastric dysplasia and gastric carcinoma. These lesions were determined independently by two pathologists. The incidence of gastric lesions in each group was presented as percentage of mice with gastric lesions. If two gastric lesions were found in the same stomach, each lesion was counted.

Immunohistochemistry

Paraffin-embedded stomach sections were deparaffinized, rehydrated, and then immersed in 3% hydrogen peroxide to quench endogenous peroxidase. The sections were blocked with 10% goat serum for 20 min followed by incubation with a rabbit anti-Ki67 antibody (1:100; Proteintech, Rosemont, IL, United States) at 4 ℃ for 12 h. After washing, the tissue sections were incubated with a biotin-conjugated secondary antibody for 60 min and were visualized using diaminobenzidine. Ki67-positive cells were stained brown in the nucleus and were counted in ⩾ 10 fields in each slide to obtain the average value.

Biochemical analyses

FBG was measured using a OneTouch glucometer (ACCU-CHEK Performa; Roche, Shanghai, China). Serum IGF-1 and fasting insulin (FINS) were determined with enzyme-linked immunosorbent assay (ELISA) kits (Shibayagi Co. Ltd., Shibukawa, Japan). Serum adiponectin and leptin concentrations were determined with ELISA kits from Crystal Chem (Downers Grove, IL, United States). The homeostatic model assessment of insulin resistance (HOMA-IR) was used to determine insulin resistance by the formula:

Table 2 Sequences of primers for qRT-PCR

Gene	Forward primer (5′-3′)	Reverse primer (5′-3′)
IGF-1	CTGGACCAGAGACCCTTTGC	GGACGGGGACTTCTGAGTCTT
IGF-1R	CATGTGCTGGCAGTATAACCC	TCGGGAGGCTTGTTCTCCT
IGF-2	ACAACTTCGATTTGAACCACATTC	GAGAGCTCAAACCATGCAAACT
IGF-2R	TGAATGGTGATCCTTGCCCTC	CCGGTAGCTGTTGGTCTGTC
Insulin receptor	TCAAGACCAGACCCGAAGATT	TCTCGAAGATAACCAGGG
GAPDH	CCAATGTGTCCGTCGTGGATCT	GTTGAAGTCGCAGGAGACAACC

HOMA-IR = (FBG × FINS)/22.5. The liver function was examined with serum aspartate aminotransferase (AST) and alanine aminotransferase (ALT). The renal function was evaluated by measuring the levels of blood urea nitrogen (BUN) and creatinine (Cr) using commercial kits (Nanjing Jiancheng Bioengineering, China).

RNA extraction and qRT-PCR

Total RNA was extracted from the stomach tissues with TRIzol reagent (Invitrogen, Carlsbad, CA, United States) and subjected to treatment with DNase I (Takara, Tokyo, Japan) to avoid genomic DNA contamination. RNA (1 μg) was reverse transcribed into cDNA using the RevertAid First Strand cDNA Synthesis Kit (Takara). Real-time PCR was conducted with SYBR Green PCR Master Mix (Takara) using ABI 7500 Fast real-time PCR system (Applied Biosystems, Foster City, CA, United States). Primers sequences are shown in Table 2. Gene expression was normalized to the expression of GAPDH gene using the $2^{-\Delta\Delta Ct}$ method.

Western blotting

The stomach tissues were ground in liquid nitrogen, homogenized on ice using lysis buffer containing protease inhibitors, and centrifuged at 12000 rpm for 15 min to obtain the supernatant. The concentration of total protein was determined with a BCA protein assay kit (Beyotime Biotechnology Company, Beijing, China). Protein from each mouse was separated at 50 μg/sample using 8% SDS-PAGE and electrotransferred onto polyvinylidene difluoride membranes (Millipore, Billerica, MA, United States). The membrane was blocked in tris-buffered saline with 0.1% Tween-20 and 5% fat-free milk, incubated with anti-phospho-IGF-1R (Tyr1135/1136; Cell Signaling Technology, Danvers, MA, United States), anti-IGF-1R (Proteintech), anti-phospho-AKT (Ser473; Cell Signaling Technology), anti-AKT (Proteintech), and β-actin (Cell Signaling Technology) at 4 ℃ overnight. After being washed in tris-buffered saline with 0.1% Tween-20 3 times, the membranes were incubated with horseradish-peroxidase-conjugated anti-rabbit antibodies at room temperature for 1 h, and then visualized using an enhanced chemiluminescence kit (Millipore). The protein abundance was determined using the intensity of protein bands using Image-J 1.46r software (National Institutes of Health, Bethesda, MD, United States), and normalized to β-actin (loading control).

Statistical analysis

Data were expressed as mean ± SE and analyzed using SPSS version 19.0 software (IBM Corp., Armonk, NY, United States). Differences among the groups were evaluated with ANOVA, Bonferroni multiple comparisons test, and Fisher's exact test. Results were considered to be statistically significant at $P < 0.05$ and highly significant at $P < 0.01$. The statistical methods were reviewed by Xu-Hong Hou from the Clinical Epidemiology Center of Shanghai Diabetes Research Institution.

RESULTS

General observations

The diabetic mice had higher body weights than non-diabetic mice. There was no significant reduction in body weight in the diabetic mice treated with LDP compared to the untreated mice (Table 3). In the positive control, the body weight was significantly reduced by metformin. The diabetic mice had higher level of serum ALT relative to the non-diabetic mice. Moreover, both LDP and metformin significantly reduced serum ALT (Table 3). There was no significant difference in serum AST, BUN and Cr among the four groups, suggesting that LDP did not cause toxicity in the liver and kidney. LDP-treated mice had normal appearance without hair depilation, subcutaneous hematoma, and skin ulcers. There was no difference in mortality between LDP-treated and untreated groups (Table 4). All these data suggest that the mice had good tolerance to LDP without toxicity.

Reduction of gastric dysplasia by LDP

It is reported that diabetes increases and metformin decreases the incidence of gastric cancer[24]. The incidence of gastric dysplasia was significantly increased in the diabetic mice compared to the non-diabetic mice (67% *vs* 17%; Table 4, Figure 1A and 1B). The incidence was markedly reduced by LDP (10% *vs* 67%; Table 4 and Figure 1E) or metformin (10% *vs* 67%; Table 4 and Figure 1D). Metformin was used as the positive control for suppression of gastric tumorigenesis in the diabetic mice. Two diabetic mice had gastric tumors in the untreated group (Figure 1C), while tumors were not observed in the treated groups.

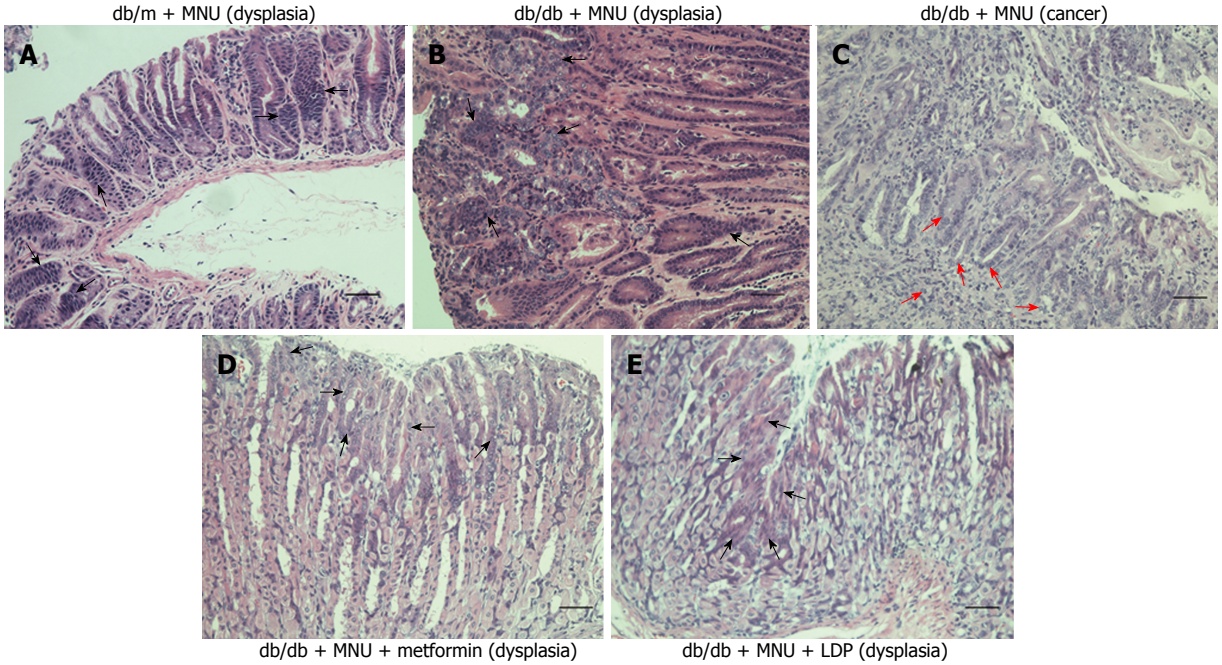

Figure 1 Hematoxylin and eosin staining of stomach tissue. A: Gastric dysplasia in non-diabetic control group (db/m); B: Gastric dysplasia in diabetic control group (db/db); C: Gastric cancer in diabetic control group (db/db); D: Gastric dysplasia in metformin-treated group (db/db); E: Gastric dysplasia in LDP-treated group (db/db). The black arrows indicate cell dysplasia with irregular and hyperchromatic cell nuclei. The red arrows show invasive gastric cancer cells in the submucosa. Bar represents 50 μm. LDP: Liuwei Dihuang Pill; MNU: N-methyl-N-nitrosourea.

Table 3 Effects of Liuwei Dihuang Pill on body weights and serum biochemical parameters

Group	Body weights at week 20, g	Body weights at week 30, g	ALT, U/L	AST, U/L	BUN, mmol/L	Cr, μmol/L
db/m + MNU + saline	24.80 ± 1.08	25.56 ± 1.78	8.98 ± 1.78[e]	8.91 ± 1.45	4.80 ± 0.26	13.94 ± 4.17
db/db + MNU + saline	59.22 ± 5.61	61.18 ± 2.10	53.31 ± 8.31	10.23 ± 0.90	4.65 ± 0.52	18.44 ± 6.28
db/db + MNU + metformin	59.44 ± 3.38	48.90 ± 4.99[b]	23.40 ± 2.37[b]	10.79 ± 1.52	4.64 ± 0.51	9.45 ± 3.07
db/db + MNU + LDP	62.79 ± 5.03	57.96 ± 3.34	38.08 ± 4.81[a]	11.30 ± 1.14	4.85 ± 0.45	9.00 ± 1.50

Data are presented as mean ± SE. [a]$P < 0.05$, [b]$P < 0.01$, [e]$P < 0.001$ *vs* db/db + MNU + saline group by one-way ANOVA. ALT: Alanine aminotransferase; AST: Aspartate aminotransferase; LDP: Liuwei Dihuang Pill; MNU: N-methyl-N-nitrosourea.

Table 4 Incidence of gastric dysplasia and carcinoma in the experimental mice

Group	Survival	Mortality	Histopathology findings (no. of mice)		
			Chronic gastritis	Gastric dysplasia	Gastric carcinoma
db/m + MNU + saline	12	0	5 (42)	2 (17)[a]	0
db/db + MNU + saline	9	3 (25)	6 (67)	6 (67)	2 (22)
db/db + MNU + metformin	10	2 (17)	6 (60)	1 (10)[a]	0
db/db + MNU + LDP	10	2 (17)	5 (50)	1 (10)[a]	0

Data are presented as *n* (%). [a]$P < 0.05$ *vs* incidence of gastric dysplasia in db/db + MNU + saline group. Fisher's exact test was used for comparison among groups. LDP: Liuwei Dihuang Pill; MNU: N-methyl-N-nitrosourea.

However, the difference was not significant among the four groups, which may have been related to the small number of mice in each group. The incidence of chronic gastritis did not differ among the four groups. These data suggest that the incidence of gastric dysplasia was markedly decreased by LDP in the diabetic mice.

Decreased expression of Ki67 by LDP

Ki67 is a well-known antigen located in the nucleus and a marker of cell proliferation. We examined the marker to measure dysplasia. The percentage of Ki67-positive cells was significantly increased by the carcinogen MNU. The induction was attenuated by LDP or metformin (Figure 2). These results suggest that diabetes promoted gastric mucosal proliferation in the MNU tumor model. The proliferative activity was inhibited by LDP and metformin.

Decrease in fasting insulin and IGF-1 by LDP

Hyperinsulinemia, hyperglycemia and IGF-1 elevation

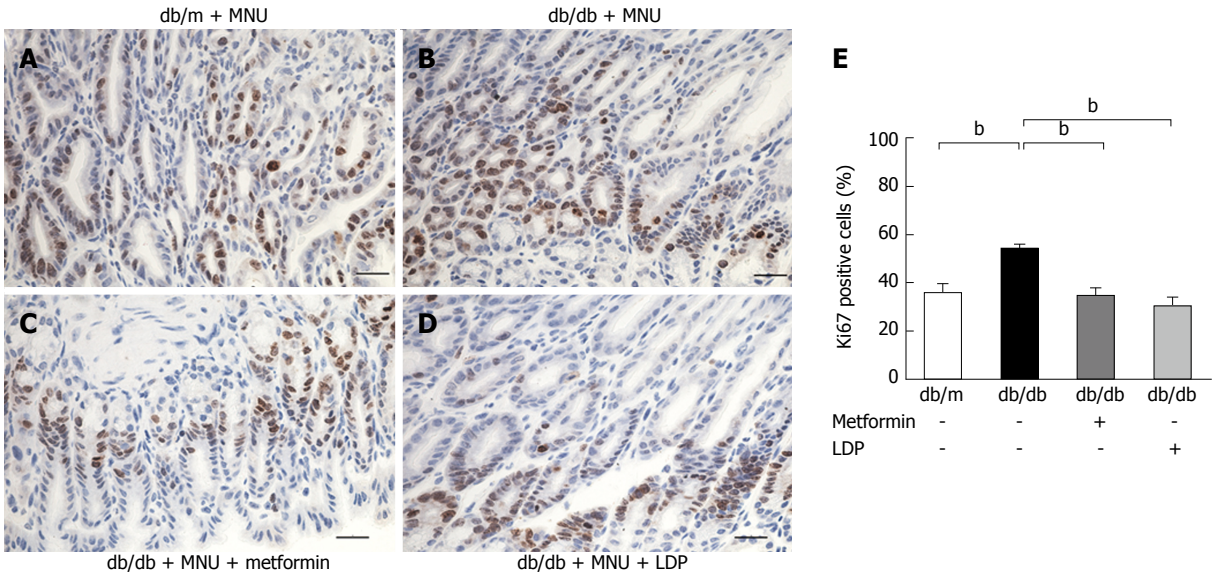

Figure 2 Cell proliferation assay with immunohistological staining of Ki67 in gastric dysplasia. A: Ki67 expression in non-diabetic control group (n = 2); B: Ki67 expression in diabetic control group (n = 6); C: Ki67 expression in metformin-treated group (n = 1); D: Ki67 expression in LDP-treated group (n = 1); E: Ki67-positive cells in each group. Results are presented as mean ± SE. $^{b}P < 0.01$ *vs* control. Bar represents 25 μm. LDP: Liuwei Dihuang Pill; MNU: N-methyl-N-nitrosourea.

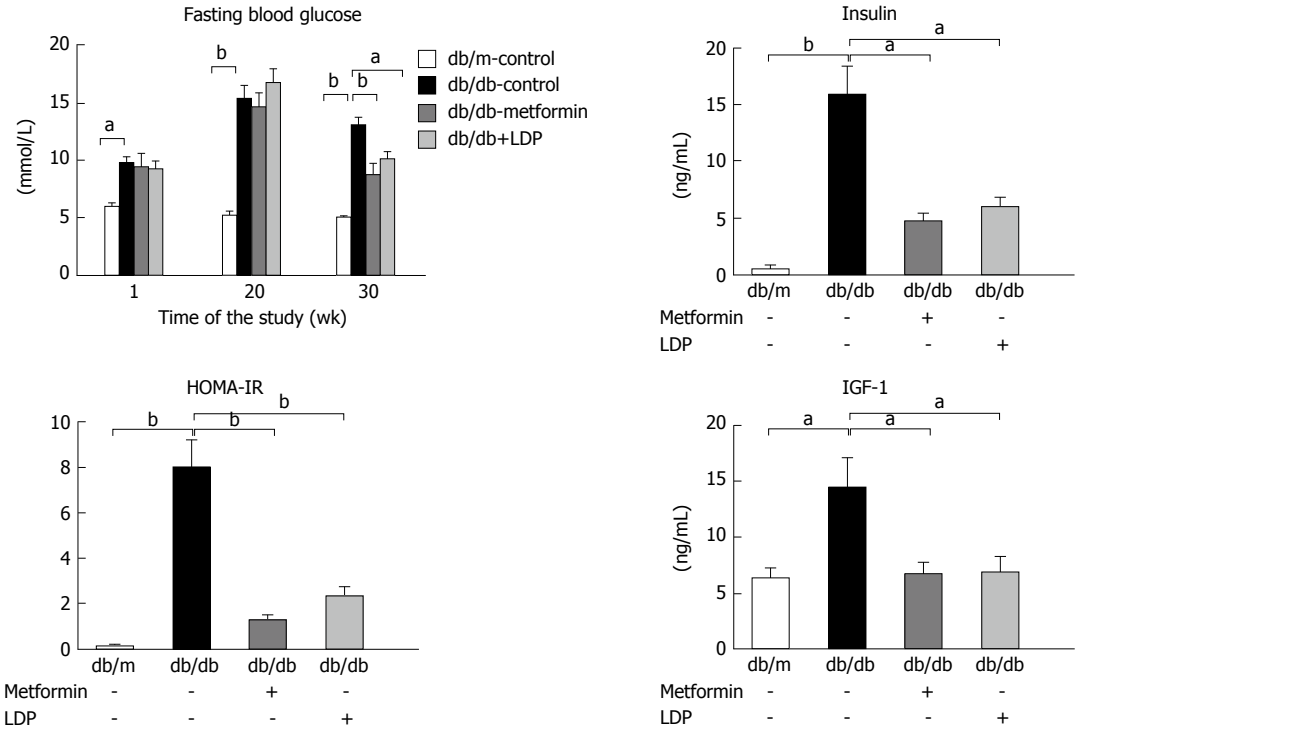

Figure 3 Effects of Liuwei Dihuang Pill on fasting blood glucose, insulin, insulin-like growth factor and insulin resistance. The fasting blood glucose at baseline (weeks 1 and 20) and week 30 was measured. The levels of insulin and IGF-1 were measured with ELISA kits. HOMA-IR was calculated for insulin resistance. Data represent the mean ± SE (n = 9). $^{a}P < 0.05$, $^{b}P < 0.01$ *vs* control. ELISA: Enzyme-linked immunosorbent assay; HOMA-IR: Homeostatic model assessment of insulin resistance; IGF-1: Insulin-like growth factor-1.

are important pathological characteristics of type 2 diabetes. These factors have potent activity in the promotion of tumor growth and their activity was significantly elevated in diabetic mice. The elevation was significantly inhibited by LDP or metformin (Figure 3). Insulin resistance was significantly improved by LDP or metformin, as suggested by a reduction in HOMA-IR (Figure 3), indicating that the LDP activity is related to improvement of insulin sensitivity.

Expression of IGF and insulin receptor

IGF-1 and insulin exert mitogenic effects on cancer cells through activation of their receptors. In this study, their receptor mRNAs were examined by qRT-PCR. The

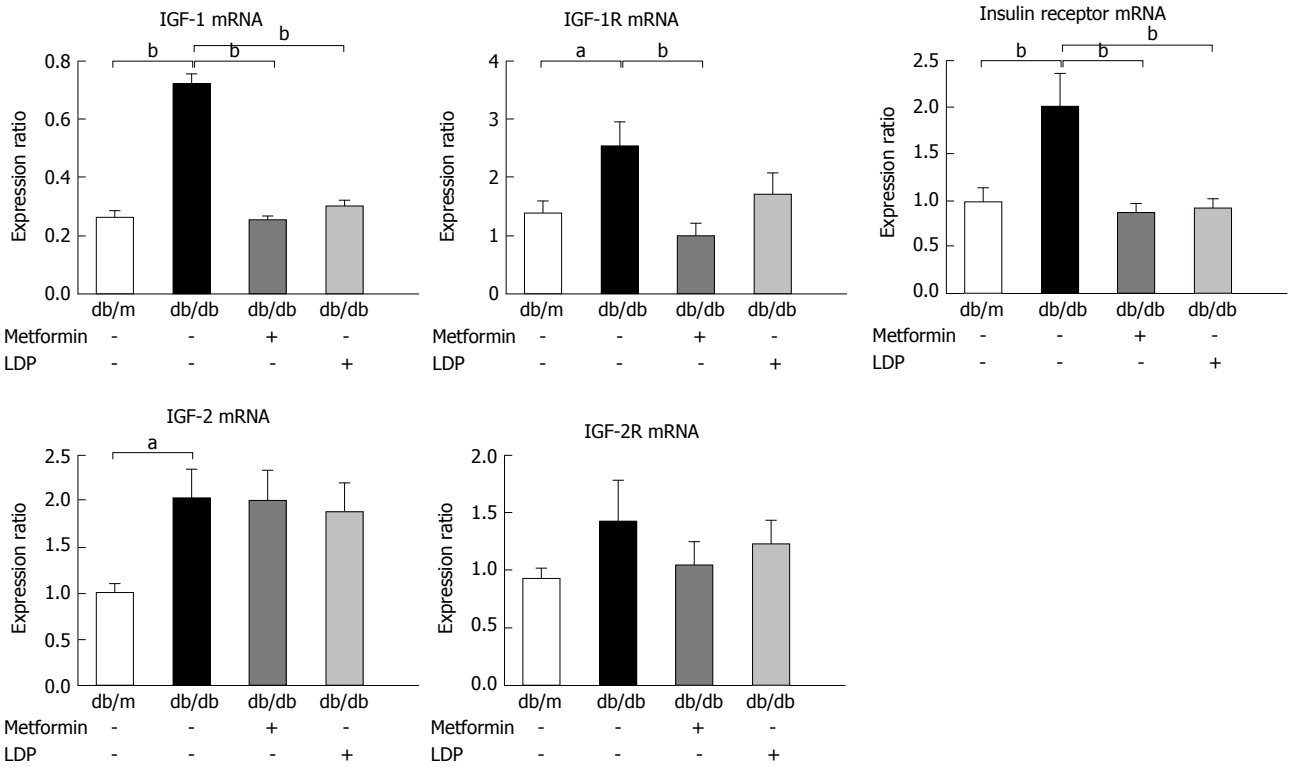

Figure 4 Effects of Liuwei Dihuang Pill on gene expression in gastric tissues. mRNA expression of IGF-1, IGF-1R, IGF-2, IGF-2R and insulin receptor was determined in stomach tissues by qRT-PCR. mRNA expression was normalized to that of GAPDH. Data represent the mean ± SE. $^{a}P < 0.05$, $^{b}P < 0.01$ *vs* control. IGF-1/2: Insulin-like growth factor-1 or 2; IGF-1/2R: Insulin-like growth factor-1 or 2 receptor; LDP: Liuwei Dihuang Pill; qRT-PCR: Quantitative reverse transcription-polymerase chain reaction.

diabetic mice exhibited an increase in the expression of IGF-1, IGF-1 receptor (IGF-1R), insulin receptor, and IGF-2 mRNAs (Figure 4). LDP inhibited the increases in IGF-1 and insulin receptor, but not in IGF-1R, IGF-2 and IGF-2R (Figure 4). A similar activity was observed for metformin in the regulation of gene expression (Figure 4).

Decreased activation of IGF-1R and AKT proteins in stomach

Insulin and IGF-1 activate their receptor signaling pathways during promotion of carcinogenesis. As a key signaling molecule, AKT plays a central role in cell growth, cell survival, cancer progression and metastasis. Phosphorylation of AKT and IGF-1R was examined along with total AKT and IGF-1R proteins. Phosphorylation was significantly higher in the diabetic mice than in the non-diabetic mice. The signals were significantly down-regulated by LDP or metformin (Figure 5). These data suggest that LDP inhibits activation of the IGF-1/IGF-1R/AKT signaling pathways in the gastric dysplasia tissue of diabetic mice.

Decreased serum leptin and increased serum adiponectin

Adipokine change in the context of type 2 diabetes may be associated with gastric carcinogenesis. Serum adiponectin and leptin were examined in this study to investigate adipokine activity. Adiponectin was decreased and leptin was increased in diabetic mice compared with non-diabetic mice (Figure 6). Metformin significantly reduced the level of leptin, but did not markedly increase serum adiponectin. LDP significantly increased adiponectin and decreased leptin in the serum of diabetic mice (Figure 6). These data imply that LDP may significantly improve imbalance of adipokines in the diabetic mice.

DISCUSSION

In this study, we established a model of gastric dysplasia in diabetic mice by administration of MNU. Gastric dysplasia was enhanced by type 2 diabetes, which was associated with hyperinsulinemia and IGF-1 elevation. The carcinogenic change was significantly inhibited by LDP in the diabetic mice, as indicated by the reduction in Ki67 signaling. The inhibition was associated with a reduction in serum insulin and IGF-1, suggesting improvement of insulin sensitivity by LDP. Insulin sensitivity was improved by LDP as indicated by the HOMA-IR and the pattern of adipokine change in LDP-treated diabetic mice. These data suggest that LDP may reduce the risk of gastric cancer by improvement of insulin sensitivity in diabetic mice.

Our results suggest that LDP may improve insulin sensitivity in the absence of weight loss. Hyperinsulinemia is the most prominent feature of type 2 diabetes, as a result of insulin resistance. The high

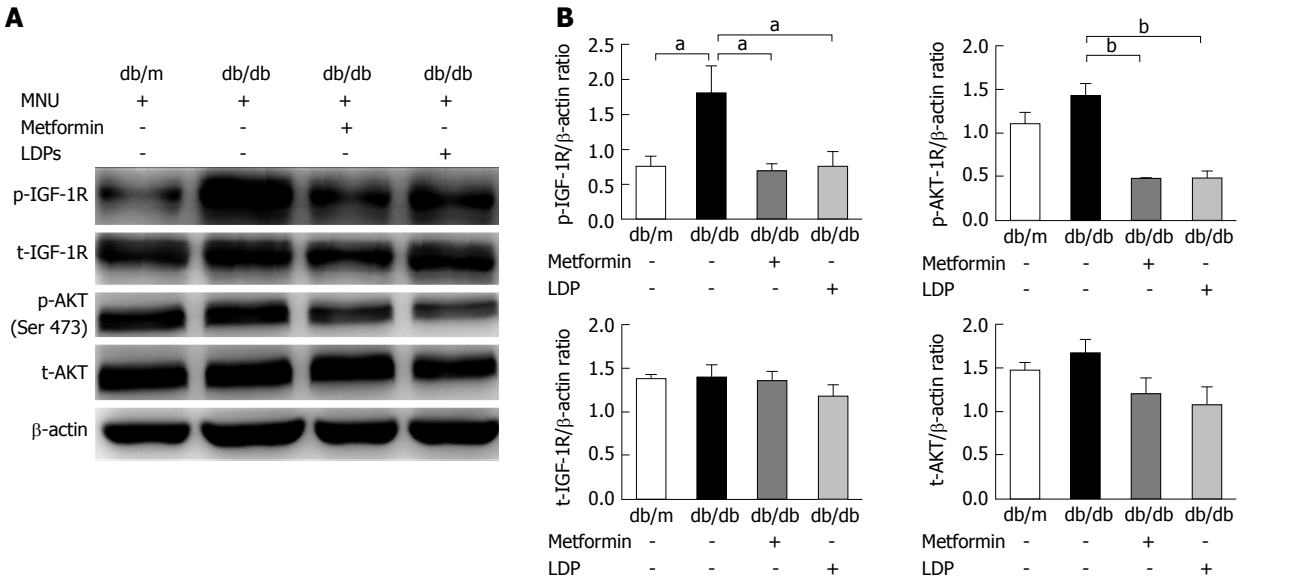

Figure 5 Effects of Liuwei Dihuang Pill on insulin and insulin-like growth factor signaling pathways. A: A representative blot is presented. IGF-1R, AKT and their phosphorylated status were determined by western blotting. β-actin served as a loading control; B: Intensity of protein bands was determined with Image-J 1.46r software. The expression ratios of target proteins relative to β-actin were calculated. Data represent the mean ± SE. $^{a}P < 0.05$, $^{b}P < 0.01$ *vs* control. IGF-1R: Insulin-like growth factor-1 receptor.

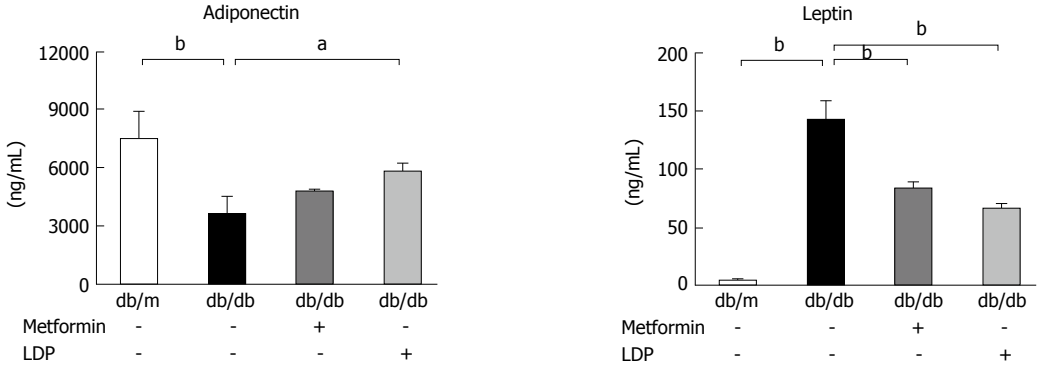

Figure 6 Effects of Liuwei Dihuang Pill on serum adiponectin and leptin. Serum levels of adiponectin and leptin were examined with ELISA kits. Values are the mean ± SE. $^{a}P < 0.05$, $^{b}P < 0.01$ *vs* control. ELISA: Enzyme-linked immunosorbent assay; IGF-1: Insulin-like growth factor; LDP: Liuwei Dihuang Pill.

level of insulin is a risk of gastric cancer for promotion of cell proliferation[3]. This possibility is supported by a study in mice, in which hyperinsulinemia promoted gastric tumor growth in diet-induced obesity[25]. LDP increased insulin sensitivity and reduced hyperinsulinemia through weight loss in one study[12]. However, weight loss was not observed in our study. The discrepancy might be a result of differences in LDP dosage and the animal models. Our data suggest that LDP improves insulin sensitivity without weight loss, although weight loss may contribute to the effect under certain conditions.

A reduction in IGF-1 may have contributed to the cancer preventive effect of LDP in diabetic mice. IGF-1 is a potent growth factor in tumor cells in addition to insulin. IGF-1 promotes cell proliferation and inhibits apoptosis through activation of IGF-1R. Both IGF-1 and IGF-1R are overexpressed in human gastric cancer in most conditions[26]. Inhibition of the signaling pathway is associated with suppression of gastric cancer growth and cancer metastasis[27]. IGF-1 level was elevated in the serum, expression of IGF-1 and its receptor was increased in the lesion tissue of db/db mice. Those alterations were attenuated by LDP in the gastric cancer model. The conclusion was supported by the decrease in phosphorylation of IGF-1R and AKT. IGF-2 and IGF-2R are members of the IGF family. IGF-2 can promote gastric cancer proliferation like IGF-1, while IGF-2R has a tumor-suppressive effect through clearance of IGF-2[28,29]. Our results suggest that expression of IGF-2 and IGF-2R was not changed by LDP, although IGF-2 expression was elevated in the diabetic mice. These results suggest that inhibition of IGF-1 activity contributes to the LDP effect in the suppression of gastric dysplasia.

AKT is activated by both insulin and IGF-1 in their signaling pathways. AKT promotes tumor formation by stimulation of cell proliferation and inhibition of

apoptosis. These activities are related to activation of cylin D1 and inhibition of caspase-9, respectively. In gastric cancer, abnormal activation of AKT is widely observed and AKT has become a key target of antitumor agents[30]. Inhibition of phospho-AKT may represent another antineoplastic mechanism of LDP.

In addition to the insulin/IGF signaling, alteration of adipokines may contribute to the chemopreventive effects of LDP in our model. Adiponectin and leptin are two important adipokines that link type 2 diabetes to cancer. Adiponectin has an anti-inflammatory activity in addition to regulation of cell metabolism, proliferation and apoptosis[31]. Contrary to adiponectin, leptin has proinflammatory activity[32], which may increase the cancer risk. Human studies have revealed that a low level of adiponectin and high level of leptin are associated with an increased risk of gastric cancer[33,34]. Correction of the adipokines' imbalance may contribute to the inhibition of gastric carcinogenesis by LDP. In this study, the effects of LDP on the adipokines are consistent with those reported by Perry *et al*[12] in obese rats[35]. These findings suggest that restoration of the balance of adiponectin and leptin may contribute to LDP activity.

In our study, LDP did not exhibit toxicity, as determined by body weight, mortality, appearance and physical activity of the mice. In addition, there was no significant increase in other parameters including AST, BUN and Cr in LDP-treated mice, suggesting that our dosage of LDP did not generate any adverse effect on liver and renal function. These results suggest that LDP is safe for treatment of type 2 diabetes and control of gastric tumorigenesis.

In summary, LDP exhibited excellent activity in the risk control of gastric tumorigenesis in diabetic mice. The activity was observed without any toxicity. Inhibition of gastric tumorigenesis was associated with reduction in hyperinsulinemia, serum IGF-1, and local IGF-1 signaling in the gastric tissue. Improvement of adiponectin and leptin imbalance may also contribute to the tumor control effect of LDP. The current study shed light on the potential of LDP in the management of both gastric dysplasia and type 2 diabetes.

ACKNOWLEDGMENTS

The authors thank Professor Jian-Ping Ye very much for providing language help and writing assistance.

COMMENTS

Background

Accumulating studies suggest that type 2 diabetes increases the risk of gastric cancer, and some antidiabetic drugs, such as metformin, reduce the incidence of gastric cancer in patients with type 2 diabetes. Traditional Chinese medicine Liuwei Dihuang Pill (LDP) has a history of thousands of years in treating diabetes, and modern pharmacological research shows that LDP also prevents gastrointestinal tumors. However, it remains unknown whether and how LDP inhibits incidence and progression of diabetes-related gastric cancer *in vivo*.

Research frontiers

The increased incidence of gastric cancer in type 2 diabetes may be associated with insulin resistance, hyperinsulinemia, excessive activity of insulin-like growth factor (IGF)-1, chronic inflammation, and abnormal alteration of adipokines. Therefore, targeting these abnormal metabolic alterations may be a promising strategy for reducing risk of gastric cancer in type 2 diabetes. Recent studies suggest that LDP reduces insulin resistance and hyperinsulinemia, and improves imbalance of adipokines. Investigation of the effects of LDP on the insulin/IGF-1 axis and adipokines will facilitate our understanding of the underlying mechanism of LDP in preventing gastric tumorigenesis in type 2 diabetes.

Innovations and breakthroughs

In the present study, LDP inhibited the early phase of gastric carcinogenesis in diabetic and obese mice, partly by alleviating insulin resistance, reducing insulin/IGF-1 activity and restoring adipokine abnormality. To the best of our knowledge, this is the first study to show the chemopreventive effect of LDP on diabetes-related gastric tumorigenesis and the underlying mechanism.

Applications

LDP may be a potential candidate for preventing gastric tumorigenesis in type 2 diabetic individuals and has value in clinical applications.

Terminology

IGF-1 is a peptide hormone with a similar structure to insulin. Both insulin and IGF-1 exert their mitogenic effects by binding to their receptors. The activated insulin receptor and IGF-1 receptor mediate two pivotal signaling transduction pathways, phosphoinositide 3-kinase/protein kinase B and mitogen-activated protein kinase. Both pathways are involved in cancer cell growth, proliferation, apoptosis and angiogenesis.

Peer-review

This paper describes mechanisms of LDP for prevention of development of gastric dysplasia. This paper has several points to be revised before accepted for publication.

REFERENCES

1 **Tseng CH**, Tseng FH. Diabetes and gastric cancer: the potential links. *World J Gastroenterol* 2014; **20**: 1701-1711 [PMID: 24587649 DOI: 10.3748/wjg.v20.i7.1701]

2 **Sekikawa A**, Fukui H, Maruo T, Tsumura T, Okabe Y, Osaki Y. Diabetes mellitus increases the risk of early gastric cancer development. *Eur J Cancer* 2014; **50**: 2065-2071 [PMID: 24934410 DOI: 10.1016/j.ejca.2014.05.020]

3 **Hidaka A**, Sasazuki S, Goto A, Sawada N, Shimazu T, Yamaji T, Iwasaki M, Inoue M, Noda M, Tajiri H, Tsugane S. Plasma insulin, C-peptide and blood glucose and the risk of gastric cancer: the Japan Public Health Center-based prospective study. *Int J Cancer* 2015; **136**: 1402-1410 [PMID: 25066446 DOI: 10.1002/ijc.29098]

4 **Gristina V**, Cupri MG, Torchio M, Mezzogori C, Cacciabue L, Danova M. Diabetes and cancer: A critical appraisal of the pathogenetic and therapeutic links. *Biomed Rep* 2015; **3**: 131-136 [PMID: 25798235 DOI: 10.3892/br.2014.399]

5 **Tahergorabi Z**, Khazaei M, Moodi M, Chamani E. From obesity to cancer: a review on proposed mechanisms. *Cell Biochem Funct* 2016; **34**: 533-545 [PMID: 27859423 DOI: 10.1002/cbf.3229]

6 **Chae YK**, Arya A, Malecek MK, Shin DS, Carneiro B, Chandra S, Kaplan J, Kalyan A, Altman JK, Platanias L, Giles F. Repurposing metformin for cancer treatment: current clinical studies. *Oncotarget* 2016; **7**: 40767-40780 [PMID: 27004404 DOI: 10.18632/oncotarget.8194]

7 **Han G**, Gong H, Wang Y, Guo S, Liu K. AMPK/mTOR-mediated inhibition of survivin partly contributes to metformin-induced apoptosis in human gastric cancer cell. *Cancer Biol Ther* 2015; **16**: 77-87 [PMID: 25456211 DOI: 10.4161/15384047.2014.987021]

8 **Quinn BJ**, Dallos M, Kitagawa H, Kunnumakkara AB, Memmott RM, Hollander MC, Gills JJ, Dennis PA. Inhibition of lung tumorigenesis by metformin is associated with decreased plasma IGF-I and diminished receptor tyrosine kinase signaling. *Cancer Prev Res* (Phila) 2013; **6**: 801-810 [PMID: 23771523 DOI: 10.1158/1940-6207.CAPR-13-0058-T]

9 **Kato M**. Diagnosis and therapies for gastric non-invasive neoplasia. *World J Gastroenterol* 2015; **21**: 12513-12518 [PMID: 26640329 DOI: 10.3748/wjg.v21.i44.12513]

10 **Zeng JH**, Pan HF, Liu YZ, Xu HB, Zhao ZM, Li HW, Ren JL, Chen LH, Hu X, Yan Y. Effects of Weipixiao (胃痞消) on Wnt pathway-associated proteins in gastric mucosal epithelial cells from rats with gastric precancerous lesions. *Chin J Integr Med* 2016; **22**: 267-275 [PMID: 25877463 DOI: 10.1007/s11655-015-2131-4]

11 **Deng X**, Liu ZW, Wu FS, Li LH, Liang J. A clinical study of weining granules in the treatment of gastric precancerous lesions. *J Tradit Chin Med* 2012; **32**: 164-172 [PMID: 22876438]

12 **Perry B**, Zhang J, Sun C, Saleh T, Wang Y. Liuwei dihuang lowers body weight and improves insulin and leptin sensitivity in obese rats. *Evid Based Complement Alternat Med* 2012; **2012**: 847167 [PMID: 21904565 DOI: 10.1155/2012/847167]

13 **Nair SV**, Zhang J, Wang Y. Ethanol extract of Liuwei Dihuang reduces weight gain and visceral fat in obese-prone CD rats fed a high-fat diet. *Exp Biol Med* (Maywood) 2014; **239**: 552-558 [PMID: 24603076 DOI: 10.1177/1535370214525313]

14 **Zhao L**, Yan S, Jiang T. [Inhibitory effect of liuwei dihuang decoction on induced mutation and spontaneous tumor]. *Zhongxiyi Jiehe Zazhi* 1990; **10**: 433-435, 390 [PMID: 2208427]

15 **Cai B**, Jiang T. Study on preventive and curative effects of liu wei di huang tang on tumors. *J Tradit Chin Med* 1994; **14**: 207-211 [PMID: 7799656]

16 **Jiang TL**, Yan SC, Zhao LF. Preventing effect of "liuwei dihuang decoction" on esophageal carcinoma. *Gan To Kagaku Ryoho* 1989; **16**: 1511-1518 [PMID: 2543308]

17 **Yoshizawa N**, Yamaguchi H, Yamamoto M, Shimizu N, Furihata C, Tatematsu M, Seto Y, Kaminishi M. Gastric carcinogenesis by N-Methyl-N-nitrosourea is enhanced in db/db diabetic mice. *Cancer Sci* 2009; **100**: 1180-1185 [PMID: 19432903 DOI: 10.1111/j.1349-7006.2009.01157.x]

18 **Kwon HJ**, Won YS, Nam KT, Yoon YD, Jee H, Yoon WK, Nam KH, Kang JS, Han SU, Choi IP, Kim DY, Kim HC. Vitamin D_3 upregulated protein 1 deficiency promotes N-methyl-N-nitrosourea and Helicobacter pylori-induced gastric carcinogenesis in mice. *Gut* 2012; **61**: 53-63 [PMID: 21917648 DOI: 10.1136/gutjnl-2011-300361]

19 **Hayakawa Y**, Hirata Y, Nakagawa H, Sakamoto K, Hikiba Y, Kinoshita H, Nakata W, Takahashi R, Tateishi K, Tada M, Akanuma M, Yoshida H, Takeda K, Ichijo H, Omata M, Maeda S, Koike K. Apoptosis signal-regulating kinase 1 and cyclin D1 compose a positive feedback loop contributing to tumor growth in gastric cancer. *Proc Natl Acad Sci USA* 2011; **108**: 780-785 [PMID: 21187402 DOI: 10.1073/pnas.1011418108]

20 **Liu JP**, Feng L, Zhang MH, Ma DY, Wang SY, Gu J, Fu Q, Qu R, Ma SP. Neuroprotective effect of Liuwei Dihuang decoction on cognition deficits of diabetic encephalopathy in streptozotocin-induced diabetic rat. *J Ethnopharmacol* 2013; **150**: 371-381 [PMID: 24041458 DOI: 10.1016/j.jep.2013.09.003]

21 **Xie B**, Gong T, Tang M, Mi D, Zhang X, Liu J, Zhang Z. An approach based on HPLC-fingerprint and chemometrics to quality consistency evaluation of Liuwei Dihuang Pills produced by different manufacturers. *J Pharm Biomed Anal* 2008; **48**: 1261-1266 [PMID: 18930621 DOI: 10.1016/j.jpba.2008.09.011]

22 **Quinn BJ**, Dallos M, Kitagawa H, Kunnumakkara AB, Memmott RM, Hollander MC, Gills JJ, Dennis PA. Inhibition of lung tumorigenesis by metformin is associated with decreased plasma IGF-I and diminished receptor tyrosine kinase signaling. *Cancer Prev Res* (Phila) 2013; **6**: 801-810 [PMID: 23771523 DOI: 10.1158/1940-6207.CAPR-13-0058-T]

23 **Yamachika T**, Nakanishi H, Inada K, Tsukamoto T, Shimizu N, Kobayashi K, Fukushima S, Tatematsu M. N-methyl-N-nitrosourea concentration-dependent, rather than total intake-dependent, induction of adenocarcinomas in the glandular stomach of BALB/c mice. *Jpn J Cancer Res* 1998; **89**: 385-391 [PMID: 9617343]

24 **Kim YI**, Kim SY, Cho SJ, Park JH, Choi IJ, Lee YJ, Lee EK, Kook MC, Kim CG, Ryu KW, Kim YW. Long-term metformin use reduces gastric cancer risk in type 2 diabetics without insulin treatment: a nationwide cohort study. *Aliment Pharmacol Ther* 2014; **39**: 854-863 [PMID: 24612291 DOI: 10.1111/apt.12660]

25 **Li HJ**, Che XM, Zhao W, He SC, Zhang ZL, Chen R, Fan L, Jia ZL. Diet-induced obesity promotes murine gastric cancer growth through a nampt/sirt1/c-myc positive feedback loop. *Oncol Rep* 2013; **30**: 2153-2160 [PMID: 23970286 DOI: 10.3892/or.2013.2678]

26 **Wang HB**, Zhou CJ, Song SZ, Chen P, Xu WH, Liu B, Zhu KX, Yu WH, Wu HL, Wang HJ, Lin S, Guo JQ, Qin CY. Evaluation of Nrf2 and IGF-1 expression in benign, premalignant and malignant gastric lesions. *Pathol Res Pract* 2011; **207**: 169-173 [PMID: 21367536 DOI: 10.1016/j.prp.2010.12.009]

27 **Li H**, Adachi Y, Yamamoto H, Min Y, Ohashi H, Ii M, Arimura Y, Endo T, Lee CT, Carbone DP, Imai K, Shinomura Y. Insulin-like growth factor-I receptor blockade reduces tumor angiogenesis and enhances the effects of bevacizumab for a human gastric cancer cell line, MKN45. *Cancer* 2011; **117**: 3135-3147 [PMID: 21264842 DOI: 10.1002/cncr.25893]

28 **Yi HK**, Hwang PH, Yang DH, Kang CW, Lee DY. Expression of the insulin-like growth factors (IGFs) and the IGF-binding proteins (IGFBPs) in human gastric cancer cells. *Eur J Cancer* 2001; **37**: 2257-2263 [PMID: 11677116]

29 **Pollak M**. Insulin and insulin-like growth factor signalling in neoplasia. *Nat Rev Cancer* 2008; **8**: 915-928 [PMID: 19029956 DOI: 10.1038/nrc2536]

30 **Sasaki T**, Kuniyasu H. Significance of AKT in gastric cancer (Review). *Int J Oncol* 2014; **45**: 2187-2192 [PMID: 25270272 DOI: 10.3892/ijo.2014.2678]

31 **Alemán JO**, Eusebi LH, Ricciardiello L, Patidar K, Sanyal AJ, Holt PR. Mechanisms of obesity-induced gastrointestinal neoplasia. *Gastroenterology* 2014; **146**: 357-373 [PMID: 24315827 DOI: 10.1053/j.gastro.2013.11.051]

32 **Wang H**, Ye J. Regulation of energy balance by inflammation: common theme in physiology and pathology. *Rev Endocr Metab Disord* 2015; **16**: 47-54 [PMID: 25526866 DOI: 10.1007/s11154-014-9306-8]

33 **Ishikawa M**, Kitayama J, Kazama S, Hiramatsu T, Hatano K, Nagawa H. Plasma adiponectin and gastric cancer. *Clin Cancer Res* 2005; **11**: 466-472 [PMID: 15701829]

34 **Capelle LG**, de Vries AC, Haringsma J, Steyerberg EW, Looman CW, Nagtzaam NM, van Dekken H, ter Borg F, de Vries RA, Kuipers EJ. Serum levels of leptin as marker for patients at high risk of gastric cancer. *Helicobacter* 2009; **14**: 596-604 [PMID: 19889078 DOI: 10.1111/j.1523-5378.2009.00728.x]

35 **Perry B**, Zhang J, Saleh T, Wang Y. Liuwei Dihuang, a traditional Chinese herbal formula, suppresses chronic inflammation and oxidative stress in obese rats. *J Integr Med* 2014; **12**: 447-454 [PMID: 25292344 DOI: 10.1016/S2095-4964(14)60044-3]

P- Reviewer: Shimoyama S **S- Editor**: Ma YJ **L- Editor**: Filipodia
E- Editor: Zhang FF

World Journal of Gastroenterology

Submit a Manuscript: http://www.f6publishing.com

World J Gastroenterol 2017 June 21; 23(23): 4243-4251

DOI: 10.3748/wjg.v23.i23.4243

ISSN 1007-9327 (print) ISSN 2219-2840 (online)

ORIGINAL ARTICLE

Basic Study

miR-382 functions as a tumor suppressor against esophageal squamous cell carcinoma

Jie Feng, Bo Qi, Ling Guo, Ling-Yun Chen, Xiu-Feng Wei, Yu-Zhen Liu, Bao-Sheng Zhao

Jie Feng, Bo Qi, Ling Guo, Xiu-Feng Wei, Yu-Zhen Liu, Bao-Sheng Zhao, Department of Thoracic Surgery, The First Affiliated Hospital of Xinxiang Medical University, Weihui 453100, Henan Province, China

Ling-Yun Chen, Department of Operating Room, The First Affiliated Hospital of Xinxiang Medical University, Weihui 453100, Henan Province, China

Author contributions: Feng J and Qi B contributed equally to this work; Liu YZ and Zhao BS contributed to conception and design; Feng J and Qi B designed methods and performed the majority of experiments; Guo L, Chen LY and Wei XF contributed to revision of the manuscript for intellectual content; Liu YZ interpreted the results and wrote the paper.

Supported by Key Technologies R&D Program of Science and Technology Commission of Henan Province, No. 152102310110 to Zhao BS; and Key Science and Technique Fund of Xinxiang, No. ZG15018 to Zhao BS.

Institutional review board statement: This study was reviewed and approved by the First Affiliated Hospital of Xinxiang Medical University Institutional Review Board.

Conflict-of-interest statement: The authors declared that no conflict of interest exists in this study.

Data sharing statement: No additional data are available.

Manuscript source: Unsolicited manuscript

Correspondence to: Bao-Sheng Zhao, MD, Professor of Surgery, Chief, Department of Thoracic Surgery, The First Affiliated Hospital of Xinxiang Medical University, 88 Jiankang Road, Weihui 453100, Henan Province, China. zhaobscn@126.com
Telephone: +86-373-4404718
Fax: +86-373-4402573

Received: January 1, 2017
Peer-review started: January 4, 2017
First decision: February 9, 2017
Revised: March 14, 2017
Accepted: March 31, 2017
Article in press: March 31, 2017
Published online: June 21, 2017

Abstract

AIM

To explore the effect of miR-382 on esophageal squamous cell carcinoma (ESCC) *in vitro* and its possible molecular mechanism.

METHODS

Eca109 cells derived from human ESCC and Het-1A cells derived from human normal esophageal epithelium were used. Lentivirus-mediated miR-382 was overexpressed in Eca109 cells. The effect of miR-382 on cell proliferation was evaluated by MTT and colony formation assay. For cell cycle analysis, cells were fixed and stained for 30 min with propidium iodide (PI) staining buffer containing 10 mg/mL PI and 100 mg/mL RNase A, and analyzed by BD FACSCalibur™ flow cytometer. For cell apoptosis assay, cells were stained with an Annexin V-FITC/PI Apoptosis Detection Kit according to the manufacturer's instructions and analyzed by a dual-laser flow cytometer. Cell invasion and migration abilities were determined through use of transwell chambers, non-coated or pre-coated with matrigel. Levels of proteins related to cell growth and migration were examined by western blotting.

RESULTS
Endogenous miR-382 was down-regulated in Eca109 cells compared with Het-1A. Introduction of miR-382 not only significantly inhibited proliferation and colony formation, but also arrested cell cycle at the G2/M phase, as well as promoted apoptosis and autophagy in Eca109 cells. Migration, invasion and epithelial-mesenchymal transition of Eca109 cells were suppressed by overexpressing miR-382. Western blotting results showed that miR-382 inhibited the phosphorylation of mTOR and 4E-BP1.

CONCLUSION
miR-382 functions as a tumor suppressor against ESCC development and metastasis, and could be considered as a potential drug source for the treatment of ESCC patients.

Key words: miR-382; Esophageal squamous cell carcinoma; Tumor suppressor; Proliferation; Migration; Invasion

Core tip: Our previous study revealed that miR-382 was significantly down-regulated in esophageal squamous cell carcinoma (ESCC) patients with short-term motility, implying that miR-382 may display antitumor function in ESCC development and metastasis. We present here that miR-382 functions as a tumor suppressor by inhibiting proliferation, migration, invasion and epithelial-mesenchymal transition, in addition to inducing cell cycle arrest, apoptosis and autophagy in Eca109 cells. Inhibitory influence on protein translation mediated by mTOR/4E-BP1 signaling might be involved in the antitumor activity of miR-382 against ESCC. Thus, manipulation of miR-382 level can be a potentially therapeutic intervention for ESCC.

Feng J, Qi B, Guo L, Chen LY, Wei XF, Liu YZ, Zhao BS. miR-382 functions as a tumor suppressor against esophageal squamous cell carcinoma. *World J Gastroenterol* 2017; 23(23): 4243-4251 Available from: URL: http://www.wjgnet.com/1007-9327/full/v23/i23/4243.htm DOI: http://dx.doi.org/10.3748/wjg.v23.i23.4243

INTRODUCTION

MicroRNAs (miRNAs) are classes of small non-coding, 17-25 nucleotides long, RNAs that bind to the 3'-untranslated region of target genes to induce post-transcription suppression or translational repression[1]. Evidence has demonstrated that miRNAs as either oncogenes or tumor suppressors are frequently dysregulated in many types of cancers and linked with its diagnosis and prognosis, implying that miRNAs play a substantial role in the pathogenesis of human cancers[2,3].

Esophageal cancer (EC) is one of the most common human malignancies[4] and can be pathologically classified into two major types, called esophageal squamous cell carcinoma (ESCC) and adenocarcinoma[5]. It is especially prevalent among Asian populations, with the most common type (90%) of EC in Asian countries being ESCC[6]. Despite improvement in diagnosis and treatment, ESCC has become one of the major diseases that negatively impact overall health and quality of life, as manifested by its rising incidence and poor 5-year survival rate (19%)[7]. ESCC is a complicated disease related to chromosomal instability, epigenetic variability, and expression abnormalities of genes, including both coding and noncoding genes[3].

miRNA as a noncoding gene has been demonstrated as having an expression signature associated with ESCC development and progression[8,9]. In our previous report, miRNA profiling results showed that 46 miRNAs were differentially expressed in ESCC tissues *vs* non-tumorous esophageal tissues, with further research demonstrating that four of these miRNAs affect the direction of patient outcomes[10]. These results imply that altered expression of these miRNAs may be potential predictive biomarkers for both prognosis and treatment of ESCC.

MicroRNA-382 (miR-382) is a member of the metastatic signature found in our previous study. Recent studies have demonstrated that miR-382 is dysregulated in multiple types of cancer, including breast, osteosarcoma, colorectal and ovarian cancers[11-14]. We found that miR-382 was significantly down-regulated in ESCC patients with short-term motility. Accordingly, in conjunction with relevant literature, our results indicate that low levels of miR-382 may contribute to the development and metastasis of ESCC[15]. However, the possible roles and mechanisms of miR-382 in human ESCC are still not well established.

In the present study, we found that miR-382 expression in the ESCC cell line was lower than that of the normal esophageal epithelial cell line. We determined a functional role of miR-382 in ESCC tumor progression using the *in vitro* cell model by lentivirus-mediated miR-382 overexpression. We found that overexpression of miR-382 inhibited ESCC cell proliferation by promoting cell cycle arrest at the G2/M phase as well as at apoptosis. Moreover, we observed that overexpression of miR-382 suppressed ESCC cell migration and invasion *via* the mechanism associated with blocking the *epithelial-mesenchymal transition* (EMT) process. The mammalian target of rapamycin (mTOR)/translation repressor 4E binding protein 1 (4E-BP1) signaling pathway and autophagy process might be involved in the antitumor activity of miR-382 on ESCC cells. Our study provides the evidence that miR-382 functions as a tumor suppressor against the development and metastasis of ESCC.

MATERIALS AND METHODS

Reagents and antibodies

3-(4,5-dimethylthiazol-2-yl)-2,5-diphenyl-tetrazolium bromide (MTT), the Propidium Iodide (PI) Cell Cycle Assay Kit and the Annexin V-FITC/PI Apoptosis Detection Kit were purchased from Beyotime (Jiangsu, China). The All-in-One™ First-Strand cDNA Synthesis Kit, the All-in-One™ miRNA qRT-PCR Detection Kit and miRNA primers were purchased from Genecopoeia (Rockville, MD, United States). DMEM and fetal bovine serum were obtained from Thermo Fisher Scientific (Waltham, MA, United States). All primary antibodies including p21Cip1/Waf1, E-cadherin, β-catenin, vimentin and snail, mTOR, p-mTOR (Ser2448), p-4E-BP1 (Thr37/46), LC3 and β-actin were purchased from Cell Signaling Technologies (Danvers, MA, United States). All other common chemicals and buffers were from Boster (Wuhan, China).

Cell culture and lentivirus infection

Eca109 and Het-1A were obtained from Cobioer Biosciences (Nanjing, China). Both cell lines were cultured in DMEM medium containing 10% fetal bovine serum in a humidified atmosphere under 5% CO_2 at 37 ℃. Lentiviral vectors LV10-(U6/RFP & Puro) expressing a scrambled control (LV-Con) and mature miR-382 (MIMAT0000737, 5'GAAGUUGUUCGUGGUGGAUUC G3', LV-miR-382) were generated by GenePharma (Shanghai, China). The virus infection was carried out according to GenePharma's recommendations. Expression of mature miR-382 was confirmed by real-time reverse transcription (RT)-PCR.

RT and quantitative (q)PCR

Total RNA was isolated using TRIzol reagent from Ambion (Austin, TX, United States) according to the manufacturer's protocol. The All-in-One™ First-Strand cDNA Synthesis Kit and the All-in-One™ miRNA qPCR Detection Kit were used for RT and qPCR respectively, and RT-qPCR was performed through Applied Biosystems QuantStudio™ 6 Flex Real-Time PCR System (Applied Biosystems, Foster City, CA, United States). Expression of U6 was used to normalize the miR-382 level.

Cell proliferation and colony formation assay

MTT was used to measure cell proliferation. Eca109 cells (4×10^3 cells /well) were seeded in 96-well culture plates and incubated overnight at 37 ℃ in a humidified 5% CO_2 incubator. At an indicated time, 10 μL of MTT dye was added to each well at a final concentration of 5 mg/mL. After 4 h incubation, the blue MTT formazan crystal was then dissolved in 100 μL/well of DMSO. The absorbance at 490 nm was measured on Multisken Spectrum (Thermo Fisher Scientific) microplate reader. The amount of viable cells after infection with LV-miR-382 and LV-Con was measured in triplicate. For the colony formation assay, cells were seeded into a 6-well plate with 1×10^3 cells/well. After 10 d of culturing, cells were washed twice with phosphate-buffered saline (PBS), then fixed with 4% paraformaldehyde for 15 min and stained with 0.5% crystal violet. The number of colonies was calculated by use of ImageJ software. The experiment was performed in triplicate.

Cell cycle and apoptosis analyses

Cells were seeded into a 35-mm dish with 1×10^5 cells/dish. After 72 h, harvested cells were washed with cold PBS for three times and fixed in 70% ethyl alcohol at 4 ℃ overnight. Cells were then treated with 10 μg/mL RNase and stained with 50 μg/mL PI for 30 min at room temperature in the dark. The cell cycle was then measured by BD FACSCalibur™ (BD Biosciences, San Jose, CA, United States) and the cell cycle distribution was analyzed by ModFit software (BD Biosciences). For the apoptosis analysis, cells were stained using the Annexin V-FITC/PI Apoptosis Detection Kit according to the manufacturer's instructions. The apoptotic cells were detected by BD FACSCalibur™.

Transwell migration and invasion assay

A 24-well plate was used as a "feeder tray". For the migration assay, 6.5-mm transwell chambers with 8 μm micro-pores (Corning Costar, Manassas, VA, United States) were used. For the invasion assay, the same filters were pre-coated with BD Matrigel (BD, Franklin Lakes, NJ, United States). A total of 60 μL of 1 mg/mL matrigel was briefly added on top of the filter into the upper chamber of each 24-well transwell and incubated at 37 ℃ for 8 h, followed by removal of the excess solution. In both migration and invasion tests, 200 μL of cell suspension (at 1×10^5 cells/mL) in serum-free medium was seeded on top of the filter, which was then immersed into the feeder tray and incubated at 37 ℃ in 600 μL of complete medium. After allowing the cells to migrate for 24 h, the non-migrated cells or non-invaded cells on the upper surface of each membrane were cleaned with a cotton swab. Cells adhering to the bottom surface of each membrane were fixed and stained with 0.1% crystal violet. Migrated or invaded cells in five different fields were counted through a phase contrast microscope. Both the migration assay and invasion assay were performed three times using triplicate wells.

Western blot analysis

Cell lysates were prepared with RIPA lysis buffer (50 mmol/L Tris-HCl, 150 mmol/L NaCl, 0.1% SDS, 1% NP40, 0.5% sodium deoxycholate, 1 mmol/L phenylmethylsulfonyl fluoride, 100 μmmol/L leupeptin, and 2 μg/mL aprotinin, pH 8.0). A total of 30 μg protein extract was subjected to sodium dodecyl sulfate-polyacrylamide gel and transferred onto nitrocellulose membranes (Amersham Biosciences, Piscataway, NJ, United States). After blocking with 5% nonfat dry milk, membranes were incubated at 4 ℃ overnight with each

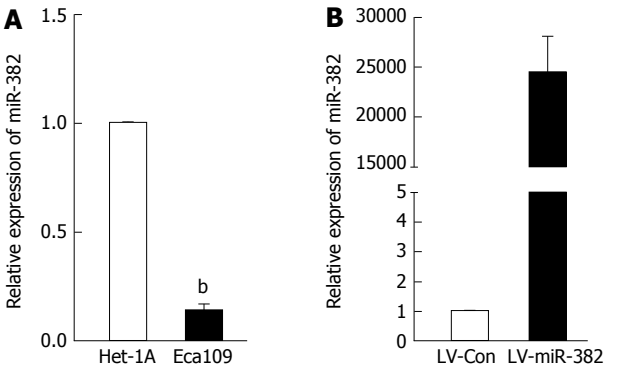

Figure 1 miR-382 was down-regulated in the esophageal squamous cell carcinoma cell line Eca109. A: The expression of miR-382 in Het-1A cells and Eca109 cells was examined by RT-qPCR; B: The relative expression level of miR-382 after introduction of either lentivirus-mediated miR-382 (LV-miR-382) or lentivirus-mediated scrambled control (LV-Con) into Eca109 cells was examined by RT-qPCR. The data in A and B is expressed as mean ± SD of three independent experiments. $^{b}P < 0.01$, *vs* control. ESCC: Esophageal squamous cell carcinoma.

of the following primary antibodies: p21Cip1/Waf1, E-cadherin, β-catenin, vimentin, snail, mTOR, p-mTOR (Ser2448), p-4E-BP1 (Thr37/46), LC3 (all 1:1000 dilution) and β-actin. Membranes were then washed with PBS-Tween and incubated with horseradish peroxidase-conjugated secondary antibodies. After incubation, the membranes were washed three times with Tris-buffered saline-Tween and processed with the SuperSignal West Pico Chemiluminescent Substrate Detection Kit (Thermo Fisher Scientific) in accordance with the manufacturer's instructions. Chemiluminescent detection of western blots was performed using the Amersham™ Imager 600 System (GE Healthcare Bio-Sciences, Pittsburgh, PA, United States).

Statistical analysis

Data was analyzed using Student's *t*-test, and all data was expressed as the mean ± SD. $P < 0.05$ was considered statistically significant.

RESULTS

Endogenous miR-382 was down-regulated in Eca109 cells

We have previously shown that miR382 level was explicitly down-regulated in ESCC patients with poor outcome compared to those with good outcome. However, the functional role of miR-382 in human ESCC remains elusive. In this study, we sought to confirm the miR-382 down-regulation in the Eca109 cell line derived from human ESCC tissue compared to the Het-1A cell line derived from human normal esophageal epithelium. As shown in Figure 1A, endogenous miR-382 in Eca109 was 7.69-fold lower than that in Het-1A cells ($P < 0.01$). This result is consistent with our previous clinical finding. In order to further explore the function of miR-382, Eca109 cells were infected with lentivirus-mediated miR-382 (LV-miR-382). As indicated in Figure 1B, miR-382 levels of LV-miR-382 infected Eca109 cells were 24153.06-fold higher than that of LV-Con control cells. Therefore, we utilized this *in vitro cell* model to investigate the functional role of miR-382 in ESCC progression in the following experiments.

miR-382 inhibited Eca109 cell proliferation and colony formation

As the expression of endogenous miR-382 in Eca109 cells was down-regulated, we speculated that miR-382 might affect the proliferation rate of ESCC cells. Thus, we examined the effect of overexpression of miR-382 on the proliferation of Eca109 cells. As shown in Figure 2A, the cell proliferation rate of miR-382 overexpressed Eca109 cells was significantly inhibited when compared with that of the control cells at the 72-h culture time point (LV-miR-382 *vs* LV-Con, 312.01 ± 27.53 *vs* 176.76 ± 18.49, $P < 0.01$). Moreover, colony formation assay shown in Figure 2B and C showed that enforced expression of miR-382 resulted in a more than 69% decrease in colony numbers in miR-382 overexpressed Eca109 cells compared with control cells (LV-miR-382 *vs* LV-Con, 421.00 ± 41.24 *vs* 127.33 ± 27.46, $P < 0.01$). These results indicated that miR-382 inhibited Eca109 proliferation *in vitro*.

miR-382 induced cell cycle arrest at G2/M phase and apoptosis

To elucidate the possible mechanisms by which miR-382 inhibited the proliferation of ESCC cells, we studied the impact of miR-382 on Eca109 cell cycle progression and apoptosis. The cell cycle distribution analyzed by flow cytometry showed that the cell number at G2/M phase was increased in LV-miR-382 infected cells compared with LV-Con cells (LV-miR-382 *vs* LV-Con, 100% ± 10.14% *vs* 215% ± 16.60%, $P < 0.05$; Figure 3A-C). Western blot analysis was performed to determine the expression of p21Cip1/Waf1, which is an important negative cell cycle regulator. The result in Figure 3D clearly indicated that the expression level of p21Cip1/Waf1 was augmented by miR-382 overexpression. These data suggested that the miR-382-induced cell cycle arrest at G2/M phase in Eca109 cells may be mediated through p21Cip1/Waf1 down-regulation.

To investigate whether the anti-proliferative activity of miR-382 was related to an apoptotic effect, apoptosis was determined by flow cytometry after double staining with Annexin-V FITC/PI. As shown in Figure 4, either early or late apoptotic cell number of LV-miR-382 infected cells was clearly increased when compared to control cells (early: LV-miR-382 *vs* LV-Con, 1.00 ± 0.09 *vs* 5.50 ± 0.00, $P < 0.05$; late: LV-miR-382 *vs* LV-Con, 1.00 ± 0.72 *vs* 14.57 ± 1.84, $P < 0.01$). These results suggested that the miR-382 inhibitory effect of miR-382 on Eca109 proliferation may be related to increased G2/M cell cycle arrest and active apoptosis.

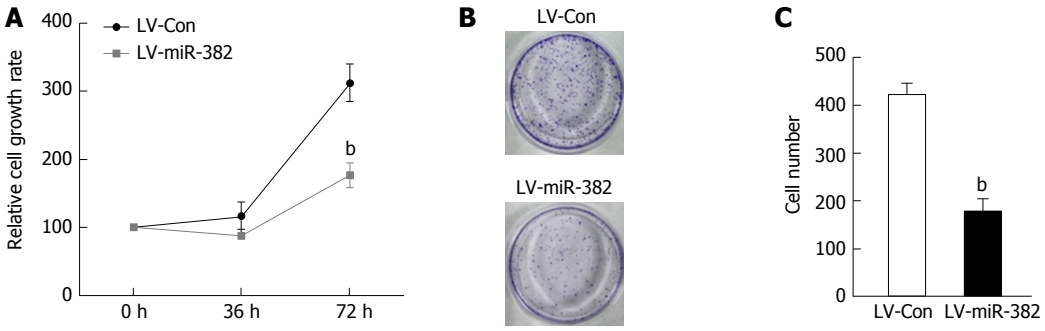

Figure 2 miR-382 inhibited Eca109 cell proliferation and colony formation. A: The proliferation of miR-382 overexpressed Eca109 cells and LV-Con control cells was measured by MTT. The Y-axis represents the relative number of viable cells presented as mean ± SD, $^{b}P < 0.01$; B: Representative photomicrographs show the colony formation in cultured LV-Con Eca109 cells and LV-miR-382 Eca109; C: Data is presented as mean ± SD, $^{b}P < 0.01$.

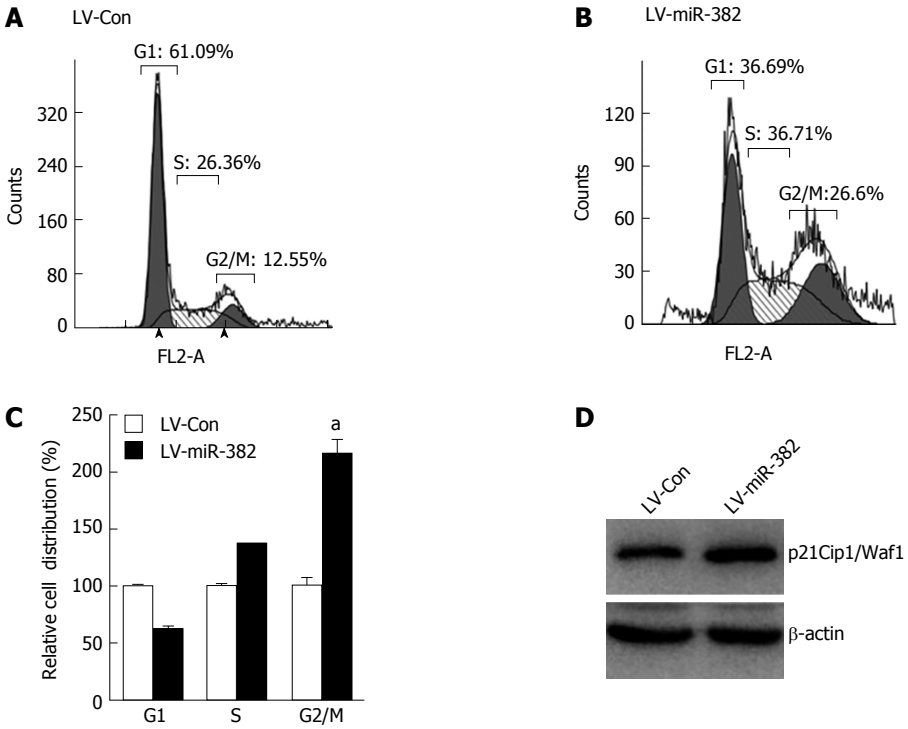

Figure 3 miR-382 induced cell cycle arrest at G2/M phase in Eca109 cells. A and B: Cell cycle distribution of miR-382 overexpressed Eca109 cells and control cells was analyzed by flow cytometry at post-culture 48 h; C: Relative cell distribution percentage of LV-miR-382 expressed Eca109 cells to LV-Con control cells in each cell cycle phase. The data presented is mean ± SD of three independent experiments. $^{a}P < 0.05$, *vs* control; D: Protein expression level of p21Cip1/Waf1 was examined in LV-Con Eca109 cells and LV-miR-382 Eca109 cells. β-actin was as a loading control.

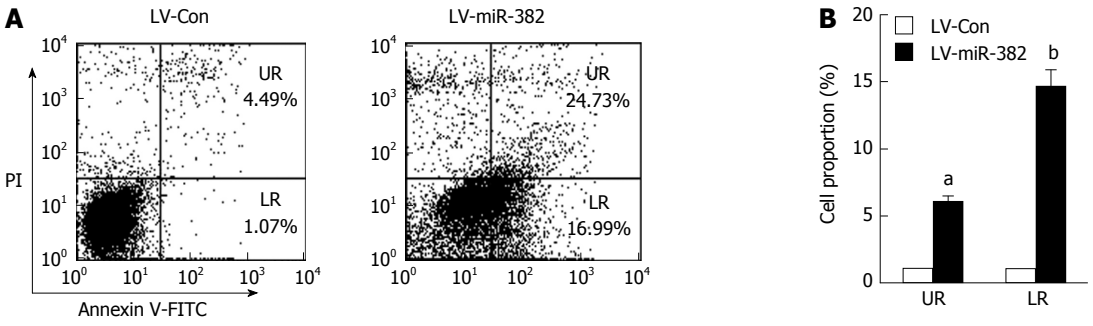

Figure 4 miR-382 promoted the apoptotic process in Eca109 cells. A: Apoptosis of LV-Con Eca109 cells and LV-miR-382 Eca109 cells was a negative cell cycle regulator, as measured using flow cytometry; B: Apoptotic cell values were expressed as mean ± SD of three experiments. $^{a}P < 0.05$ and $^{b}P < 0.01$, *vs* control.

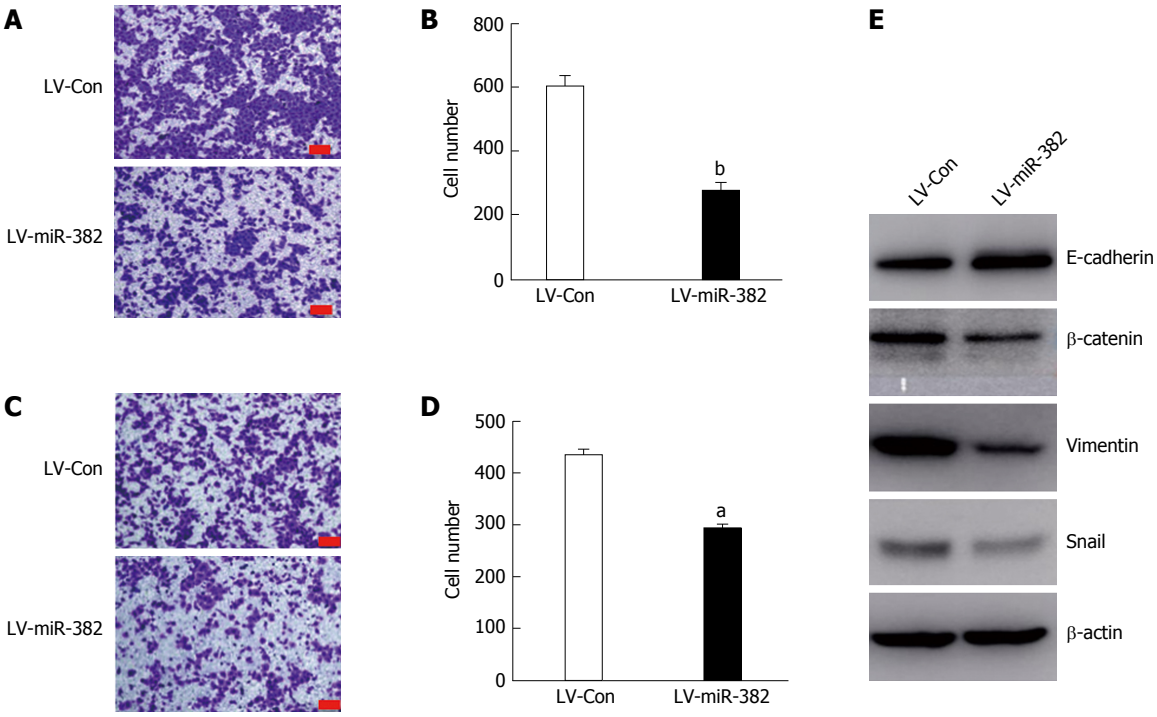

Figure 5 Overexpression miR-382 inhibited migration, invasion and epithelial-mesenchymal transition in Eca109 cells. A: Representative photomicrographs showed migrated cells stained with crystal violet after post-culture for 24 h in the transwell migration assay. The bars represent 200 μm; B: The migrated cells in five different fields were counted and the Y-axis represents the migrated cell number from three independent experiments. Data is presented as mean ± SD, $^{b}P < 0.01$; C: Representative photomicrographs showing invaded cells stained with crystal violet after post-culture for 24 h in the transwell invasion assay. The bars are 200 μm; D: The invaded cells in five different fields were counted and the Y-axis represents the invaded cell number from three independent experiments. Data are presented as mean ± SD, $^{a}P < 0.05$; E: Western blot analysis of the expression of epithelial marker E-cadherin, and mesenchymal markers β-catenin, vimentin and snail in Eca109 cells infected with LV-miR-382 or LV-Con(c). β-actin served as a loading control.

miR-382 inhibited Eca109 cell migration and invasion

Cancer metastasis is greatly associated with cancer cell migratory and invasive abilities. To further investigate the influence of miR-382 over the migration and invasion of ESCC cells, migration transwell assay was initially performed to determine the migratory ability of the cells. As shown in Figure 5A and B, in the group infected with LV-miR-382 the rate of cell migration into the bottom chamber was significantly reduced by 32% compared with that of the scrambled control cells (LV-Con *vs* LV-miR-382, 433.50 ± 20.72 *vs* 292.25 ± 18.02, $P < 0.05$). Subsequently, matrigel invasion assay, a three-dimensional model, was utilized to investigate the inhibitory effect of miR-382 on the invasive potency of the cells. The result shown in Figure 5C and D demonstrates that miR-382 significantly suppressed invasion of Eca109 cells by 54% (LV-Con *vs* LV-miR-382, 603.80 ± 64.46 *vs* 273.80 ± 54.99, $P < 0.01$). These data indicated that miR-382 exerted an inhibitory effect on the migration and invasion of ESCC cells.

The role of miR-382 in regulating EMT was further studied by investigation of the protein expression of several key EMT effectors, including E-cadherin, β-catenin, vimentin and snail. Interestingly, miR-382 attenuated expressions of three mesenchymal markers (β-catenin, vimentin and snail). Moreover, we also observed that the expression of E-cadherin, which is one of the epithelial markers, was significantly augmented in LV-miR-382 cells, as shown in Figure 5E. Taken together, these results suggested that the inhibitory effect of miR-382 on the migration and invasion of ESCC cells may be mediated through restraining EMT processes in ESCC.

miR-382 inhibited mTOR signaling pathway and activated autophagy process

mTOR plays a key role in cell growth and homeostasis and may be abnormally regulated in tumors. To address the functional activation of mTOR regulated by miR-382, western blot analyses were performed to examine the phosphorylation level of both mTOR and 4E-BP1, a target of mTOR known to bind to translation initiation factor eIF4E to inhibit cap-dependent translation. Overexpression of miR-382 noticeably inhibited the phosphorylation of both mTOR (Ser2448) and 4E-BP1 (Thr37/46) (Figure 6). Previous studies have indicated that autophagy has roles in various cellular functions, including cell proliferation and apoptosis. During autophagy, LC3-I is converted to LC3-II and recruited into the membrane of the phagophore, a double membrane required for the recycling of protein aggregates and organelles. To determine whether miR-382 might induce autophagy in Eca109, we examined the level of LC3 protein in LV-miR-382 infected Eca109 cells and control cells. As

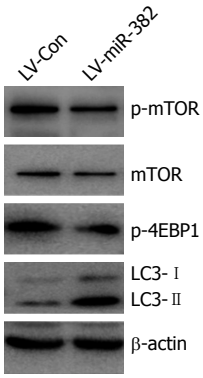

Figure 6 miR-382 inhibited mTOR and 4E-BP1 phosphorylation and activated autophagy. p-mTOR, mTOR, p-4E-BP1 and LC3 were evaluated by western blot. Experiments were performed in triplicate. Equal protein loading was confirmed by β-actin.

shown in Figure 6, increased levels of either LC3-I or LC3-II were detected in LV-miR-382 cells compared to control cells, indicating that miR-382 activated the autophagy process. These data suggested that inhibition of the mTOR/4E-BP1 signaling pathway together with activation of the autophagy process may be important targets of miR-382 actions.

DISCUSSION

Accumulating evidence has revealed that miRNAs participate in the initiation and progression of human cancers. Thus, exploration of cancer-specific miRNAs contributes to the identification of novel biomarkers and therapeutic targets for human cancers. To date, correlation analyses between miRNAs and ESCC have shown that a number of dysregulated miRNAs levels correlate with ESCC patients' outcomes.

Human miR-382 (has–mir-382, MIMAT0000737, 5'-GAAGUUGUUCGUGGUGGAUUCG-3') resides in a miRNA cluster in the imprinted DLK1-DIO3 region on the 14q32 locus, which hosts one of the largest miRNA clusters in the genome. Many of these miRNAs are differentially expressed in several pathologic processes and various cancers, with recent studies reporting that miR-382 is aberrantly regulated in several types of human malignancies. miR-382 levels were found to be decreased in ovarian cancer[13] and osteosarcoma, but increased in breast cancer[16] and acute myeloid leukemia tumor tissue[17]. Based off these findings, the role of miR-382 in tumor development and metastasis is heterogeneous and it functions in a cell-driven and tissue-driven manner.

Our earlier study discovered that decreased miR382 expression in tumor tissues from ESCC patients was clinically correlated with short-term motility, and significantly linked to poor patient outcome. This indicates that miR-382 may play antitumor functions in esophageal carcinogenesis, and could be a potential predictive biomarker for ESCC prognosis. On the other hand, the mechanism by which miR-382 functionally affects ESCC phenotype has not been elucidated; therefore, in this study, we began by evaluating the expression of endogenous levels of miR-382 in Eca109 tumor cell line and Het-1A normal esophageal epithelia cell line. Consistent with our previous clinical results, we found that miR-382 was reduced in Eca109 cells compared with Het-1A. Moreover, we found that lentivirus-mediated overexpression of miR-382 significantly inhibited Eca109 cell proliferation, colony formation, migration and invasion. These findings together with our previous result suggest that miR-382 functions as a tumor suppressor in ESCC.

Cell cycle arrest and apoptosis are closely linked to cell proliferation in mammalian cells. In the present study, we found that overexpression of miR-382 significantly increased initiation of cell cycle arrest at G2/M phase and promoted the apoptotic process of Eca109 cells. Therefore, the inhibitory influence of miR-382 on Eca109 proliferation seems to be related with increased G2/M cell cycle arrest and active apoptosis. In addition, it is known that cell cycle progression and apoptosis are regulated by numerous proteins, with one of these proteins being the cyclin-dependent kinase inhibitor p21Cip1/Waf1, which facilitates cell cycle arrest in response to a variety of stimuli[18]. Our results showed that miR-382 clearly increased p21Cip1/Waf1 expression, indicating that the miR-382-induced cell cycle arrest in G2/M phase may occur through regulation of p21Cip1/Waf1.

EMT comprises the process by which epithelial cells are transited into mesenchymal cells, and display reduced intracellular adhesion and increased motility[19]. Most evidence supports EMT playing the integral roles through which epithelial cancers invade and metastasize. The EMT process is related to a number of cellular and molecular events and is accompanied by the loss of epithelial markers (*e.g.*, E-cadherin) and the gain of mesenchymal markers (*e.g.*, vimentin, β-catenin and snail). Our study showed that miR-382 inhibited Eca109 cell migration, as well as invasion *in vitro*. Overexpression of miR-382 enhanced the level of E-cadherin and reduced levels of vimentin, β-catenin, and snail. Accordingly, these data indicated that miR-382 might suppress the EMT process, so that Eca109 cell invasion and metastasis may be restrained.

Autophagy is a catabolic process for proteolytic degradation of damaged intracellular proteins and organelles in lysosomes. Autophagy dysfunction is associated with multiple human diseases, such as cancer. It has been reported that autophagy deficiency promotes cell proliferation, migration and invasion. Our data revealed that overexpression of miR-382 was able to up-regulate the expression of two distinctive hallmarks of autophagy, LC3-I and LC3-II[20], in Eca109 cells, implying that miR-382 could induce autophagy in Eca109 cells.

Regulation of translation is critical for controlling

many major cellular processes, including cell proliferation, apoptosis and metastasis. The mTOR signaling pathway plays a pivotal role in regulation of the translation process, with one of the best-characterized downstream effectors of mTOR being 4E-BP1. mTOR phosphorylates 4E-BP1, which promotes the dissociation of eIF4E from 4E-BP1, consequently alleviating the inhibitory effect of 4E-BP1 on eIF4E-dependent translation initiation[21]. Therefore, overall translation levels are lowered when 4E-BP1 is active, which is thought to be regulated by mTOR-dependent phosphorylation. Our results showed that miR-382 dramatically inhibited the phosphorylation of mTOR as well as 4E-BP1. These results indicated that miR-382 might suppress the overall protein translation process through mTOR/4E-BP1, and could potentially function as a tumor suppressor against ESCC.

In conclusion, our results indicated that miR-382 was dramatically down-regulated in ESCC cells. Overexpression of miR-382 inhibited proliferation, migration and invasion of Eca109 cells. mTOR/4E-BP1 signaling mediated inhibitory influence on protein translation and may be involved in the antitumor activity of miR-382 against esophageal cancer. Our results could provide insights into a new therapeutic strategy for the treatment of ESCC through the up-regulation of miR-382 expression.

COMMENTS

Background

MicroRNAs (miRNAs) are classes of small non-coding RNAs involved in the process of silencing gene expression. Evidence has shown that miRNAs are frequently dysregulated in many types of cancers and play a substantial role in the pathogenesis of human cancers. They previously found that miRNA-382 (miR-382) was significantly down-regulated in esophageal squamous cell carcinoma (ESCC) patients with short-term motility, implying that miR-382 may contribute to the development and metastasis of ESCC. However, the possible roles and mechanisms of miR-382 in human ESCC are still not well established.

Innovations and breakthroughs

This study revealed that endogenous miR-382 was dramatically down-regulated in ESCC cells in comparison to normal esophageal epithelial cells. This is consistent with our previous clinical data. Overexpression of miR-382 inhibited cell proliferation, migration and invasion of Eca109 cells. The mTOR/4E-BP1 signaling-mediated inhibitory influence on protein translation might be involved in the antitumor activity of miR-382 against esophageal carcinoma.

Applications

This study suggests that the miR-382 is down-regulated in ESCC and plays an inhibitory role in the growth and invasion of ESCC. Because of this, miR-382 is considered a tumor suppressor of ESCC and provides new insights into a possible therapeutic strategy for ESCC through the up-regulation of miR-382 expression.

Terminology

Previous literature indicates that miR-382 was reduced and associated with poor survival in osteosarcoma patients. In contrast, increased miR-382 levels were found in acute myeloid leukemia tumor tissue. These findings illustrate the role of miR-382 in tumor development and metastasis as a heterogeneous one that is cell-driven and tissue-driven.

Peer-review

This is an interesting topic aiming to reveal more advanced and detailed functions of miR-382 on ESCC. The authors demonstrated that overexpression of miR-382 inhibited cell proliferation and invasion, and induced cell apoptosis and cell autophagy. The antitumor activity of miR-382 might be initiated by inhibition of an mTOR/4E-BP1-mediated protein translation process. Thus, manipulation of miR-382 level is a potential therapeutic strategy for ESCC.

REFERENCES

1 **Lagos-Quintana M**, Rauhut R, Lendeckel W, Tuschl T. Identification of novel genes coding for small expressed RNAs. *Science* 2001; **294**: 853-858 [PMID: 11679670 DOI: 10.1126/science.1064921]

2 **Bartel DP**. MicroRNAs: target recognition and regulatory functions. *Cell* 2009; **136**: 215-233 [PMID: 19167326 DOI: 10.1016/j.cell.2009.01.002]

3 **Croce CM**. Causes and consequences of microRNA dysregulation in cancer. *Nat Rev Genet* 2009; **10**: 704-714 [PMID: 19763153 DOI: 10.1038/nrg2634]

4 **Torre LA**, Bray F, Siegel RL, Ferlay J, Lortet-Tieulent J, Jemal A. Global cancer statistics, 2012. *CA Cancer J Clin* 2015; **65**: 87-108 [PMID: 25651787 DOI: 10.3322/caac.21262]

5 **Holmes RS**, Vaughan TL. Epidemiology and pathogenesis of esophageal cancer. *Semin Radiat Oncol* 2007; **17**: 2-9 [PMID: 17185192 DOI: 10.1016/j.semradonc.2006.09.003]

6 **Su M**, Liu M, Tian DP, Li XY, Zhang GH, Yang HL, Fan X, Huang HH, Gao YX. Temporal trends of esophageal cancer during 1995-2004 in Nanao Island, an extremely high-risk area in China. *Eur J Epidemiol* 2007; **22**: 43-48 [PMID: 17195051 DOI: 10.1007/s10654-006-9086-x]

7 **Chen W**, Zheng R, Baade PD, Zhang S, Zeng H, Bray F, Jemal A, Yu XQ, He J. Cancer statistics in China, 2015. *CA Cancer J Clin* 2016; **66**: 115-132 [PMID: 26808342 DOI: 10.3322/caac.21338]

8 **Yang M**, Liu R, Sheng J, Liao J, Wang Y, Pan E, Guo W, Pu Y, Yin L. Differential expression profiles of microRNAs as potential biomarkers for the early diagnosis of esophageal squamous cell carcinoma. *Oncol Rep* 2013; **29**: 169-176 [PMID: 23124769 DOI: 10.3892/or.2012.2105]

9 **Yi Y**, Lu X, Chen J, Jiao C, Zhong J, Song Z, Yu X, Lin B. Downregulated miR-486-5p acts as a tumor suppressor in esophageal squamous cell carcinoma. *Exp Ther Med* 2016; **12**: 3411-3416 [PMID: 27882172 DOI: 10.3892/etm.2016.3783]

10 **Zhao BS**, Liu SG, Wang TY, Ji YH, Qi B, Tao YP, Li HC, Wu XN. Screening of microRNA in patients with esophageal cancer at same tumor node metastasis stage with different prognoses. *Asian Pac J Cancer Prev* 2013; **14**: 139-143 [PMID: 23534712]

11 **Fu L**, Li Z, Zhu J, Wang P, Fan G, Dai Y, Zheng Z, Liu Y. Serum expression levels of microRNA-382-3p, -598-3p, -1246 and -184 in breast cancer patients. *Oncol Lett* 2016; **12**: 269-274 [PMID: 27347136 DOI: 10.3892/ol.2016.4582]

12 **Xu M**, Jin H, Xu CX, Sun B, Mao Z, Bi WZ, Wang Y. miR-382 inhibits tumor growth and enhance chemosensitivity in osteosarcoma. *Oncotarget* 2014; **5**: 9472-9483 [PMID: 25344865 DOI: 10.18632/oncotarget.2418]

13 **Zhou B**, Song J, Han T, Huang M, Jiang H, Qiao H, Shi J, Wang Y. MiR-382 inhibits cell growth and invasion by targeting NR2F2 in colorectal cancer. *Mol Carcinog* 2016; **55**: 2260-2267 [PMID: 26800338 DOI: 10.1002/mc.22466]

14 **Tan H**, He Q, Gong G, Wang Y, Li J, Wang J, Zhu D, Wu X. miR-382 inhibits migration and invasion by targeting ROR1 through regulating EMT in ovarian cancer. *Int J Oncol* 2016; **48**: 181-190 [PMID: 26575700 DOI: 10.3892/ijo.2015.3241]

15 **Qi B**, Lu JG, Yao WJ, Chang TM, Qin XG, Ji YH, Wang TY, Liu SG, Li HC, Liu YZ, Zhao BS. Downregulation of microRNA-382 is associated with poor outcome of esophageal squamous cell carcinoma. *World J Gastroenterol* 2015; **21**: 6884-6891 [PMID: 26078564 DOI: 10.3748/wjg.v21.i22.6884]

16 **Ho JY**, Hsu RJ, Liu JM, Chen SC, Liao GS, Gao HW, Yu CP. MicroRNA-382-5p aggravates breast cancer progression by regulating the RERG/Ras/ERK signaling axis. *Oncotarget* 2017; **8**: 22443-22459 [PMID: 27705918 DOI: 10.18632/oncotarget.12338]
17 **Li Z**, Lu J, Sun M, Mi S, Zhang H, Luo RT, Chen P, Wang Y, Yan M, Qian Z, Neilly MB, Jin J, Zhang Y, Bohlander SK, Zhang DE, Larson RA, Le Beau MM, Thirman MJ, Golub TR, Rowley JD, Chen J. Distinct microRNA expression profiles in acute myeloid leukemia with common translocations. *Proc Natl Acad Sci USA* 2008; **105**: 15535-15540 [PMID: 18832181 DOI: 10.1073/pnas.0808266105]
18 **Kang MR**, Park KH, Yang JO, Lee CW, Oh SJ, Yun J, Lee MY, Han SB, Kang JS. miR-6734 Up-Regulates p21 Gene Expression and Induces Cell Cycle Arrest and Apoptosis in Colon Cancer Cells. *PLoS One* 2016; **11**: e0160961 [PMID: 27509128 DOI: 10.1371/journal.pone.0160961]
19 **Yang G**, Yuan J, Li K. EMT transcription factors: implication in osteosarcoma. *Med Oncol* 2013; **30**: 697 [PMID: 23975634 DOI: 10.1007/s12032-013-0697-2]
20 **Li Y**, Jiang W, Hu Y, Da Z, Zeng C, Tu M, Deng Z, Xiao W. MicroRNA-199a-5p inhibits cisplatin-induced drug resistance via inhibition of autophagy in osteosarcoma cells. *Oncol Lett* 2016; **12**: 4203-4208 [PMID: 27895792 DOI: 10.3892/ol.2016.5172]
21 **Li W**, Chang J, Wang S, Liu X, Peng J, Huang D, Sun M, Chen Z, Zhang W, Guo W, Li J. miRNA-99b-5p suppresses liver metastasis of colorectal cancer by down-regulating mTOR. *Oncotarget* 2015; **6**: 24448-24462 [PMID: 26259252 DOI: 10.18632/oncotarget.4423]

P- Reviewer: Arigami T, Lin Q **S- Editor**: Yu J **L- Editor**: Filipodia
E- Editor: Zhang FF

World Journal of Gastroenterology

Submit a Manuscript: http://www.f6publishing.com

World J Gastroenterol 2017 June 21; 23(23): 4252-4261

DOI: 10.3748/wjg.v23.i23.4252

ISSN 1007-9327 (print) ISSN 2219-2840 (online)

ORIGINAL ARTICLE

Case Control Study

Pancreas preserving distal duodenectomy: A versatile operation for a range of infra-papillary pathologies

W Kyle Mitchell, Pradeep F Thomas, Abed M Zaitoun, Adam J Brooks, Dileep N Lobo

W Kyle Mitchell, Pradeep F Thomas, Adam J Brooks, Dileep N Lobo, Gastrointestinal Surgery, Nottingham Digestive Diseases Centre, National Institute for Health Research Nottingham Biomedical Research Centre, Nottingham University Hospitals and University of Nottingham, Queen's Medical Centre, Nottingham NG7 2UH, United Kingdom

Abed M Zaitoun, Cellular Pathology, Nottingham Digestive Diseases Centre, National Institute for Health Research Nottingham Biomedical Research Centre, Nottingham University Hospitals and University of Nottingham, Queen's Medical Centre, Nottingham NG7 2UH, United Kingdom

Author contributions: Mitchell WK designed this work, collected data, drafting of manuscript, final approval, accountability for the manuscript; Thomas PF designed of the work, collected data, drafting of manuscript, art work, final approval, and accountability for the manuscript; Zaitoun AM designed this work, collected and interpreted data, critical revision of manuscript, final approval, accountability for the manuscript; Brooks AJ designed this work, collected data and interpretation, critical revision of manuscript, final approval, accountability for the manuscript; Lobo DN conceived and designed this work, collected and interpreted data, critical revision of manuscript, final approval, accountability for the manuscript, overall supervision.

Institutional review board statement: The prospective maintenance of a database of operative procedures is considered part of routine clinical governance. This database has been used in line with local information governance policy.

Conflict-of-interest statement: No benefits in any form have been received or will be received from a commercial party related directly or indirectly to the subject of this article.

Data sharing statement: No additional data are available.

Manuscript source: Invited manuscript

Correspondence to: Dr. Dileep N Lobo, Professor, Gastrointestinal Surgery, Nottingham Digestive Diseases Centre, National Institute for Health Research Nottingham Biomedical Research Centre, Nottingham University Hospitals and University of Nottingham, Queen's Medical Centre, Derby Rd, Nottingham NG7 2UH, United Kingdom. dileep.lobo@nottingham.ac.uk
Telephone: +44-115-8231149
Fax: +44-115-8231160

Received: January 26, 2017
Peer-review started: February 3, 2017
First decision: February 23, 2017
Revised: April 1, 2017
Accepted: May 19, 2017
Article in press: May 19, 2017
Published online: June 21, 2017

Abstract

AIM

To investigate the range of pathologies treated by pancreas preserving distal duodenectomy (PPDD) and present the outcome of follow-up.

METHODS

Neoplastic lesions of the duodenum are treated conventionally by pancreaticoduodenectomy. Lesions distal to the major papilla may be suitable for a pancreas-preserving distal duodenectomy, potentially reducing morbidity and mortality. We present our experience with this procedure. Selective intraoperative duodenoscopy assessed the relationship of the papilla to the lesion. After duodenal mobilisation and confirmation of the site of the lesion, the duodenum

was transected distal to the papilla and beyond the duodenojejunal flexure and a side-to-side duodenojejunal anastomosis was formed. Patients were identified from a prospectively maintained database and outcomes determined from digital health records with a dataset including demographics, co-morbidities, mode of presentation, preoperative imaging and assessment, nutritional support needs, technical operative details, blood transfusion requirements, length of stay, pathology including lymph node yield and lymph node involvement, length of follow-up, complications and outcomes. Related published literature was also reviewed.

RESULTS

Twenty-four patients had surgery with the intent of performing PPDD from 2003 to 2016. Nineteen underwent PPDD successfully. Two patients planned for PPDD proceeded to formal pancreaticoduodenectomy (PD) while three had unresectable disease. Median post-operative follow-up was 32 mo. Pathologies resected included duodenal adenocarcinoma (n = 6), adenomas (n = 5), gastrointestinal stromal tumours (n = 4) and lipoma, bleeding duodenal diverticulum, locally advanced colonic adenocarcinoma and extrinsic compression (n = 1 each). Median postoperative length of stay (LOS) was 8 d and morbidity was low [pain and nausea/vomiting (n = 2), anastomotic stricture (n = 1), pneumonia (n = 1), and overwhelming post-splenectomy sepsis (n = 1, asplenic patient)]. PPDD was associated with a significantly shorter LOS than a contemporaneous PD series [PPDD 8 (6-14) d *vs* PD 11 (10-16) d, median (IQR), P = 0.026]. The 30-d mortality was zero and 16 of 19 patients are alive to date. One patient died of recurrent duodenal adenocarcinoma 18 mo postoperatively and two died of unrelated disease (at 2 mo and at 8 years respectively).

CONCLUSION

PPDD is a versatile operation that can provide definitive treatment for a range of duodenal pathologies including adenocarcinoma.

Key words: Pancreas preserving distal duodenectomy; Duodenojejunostomy; Duodenal disease; Surgical technique; Adults; Indications; Treatment; Outcome

Core tip: Pancreas preserving distal duodenectomy is a versatile operation that can provide definitive treatment for a range of duodenal pathologies including adenocarcinoma. It avoids the morbidity and mortality of a pancreaticoenteric anastomosis and can be undertaken safely with shorter postoperative length of stay than pancreaticoduodenectomy.

Mitchell WK, Thomas PF, Zaitoun AM, Brooks AJ, Lobo DN. Pancreas preserving distal duodenectomy: A versatile operation for a range of infra-papillary pathologies. *World J Gastroenterol* 2017; 23(23): 4252-4261 Available from: URL: http://www.wjgnet.com/1007-9327/full/v23/i23/4252.htm DOI: http://dx.doi.org/10.3748/wjg.v23.i23.4252

INTRODUCTION

The duodenum gives rise to more neoplasia, and possibly pathology in general, per unit length, than does any other part of the small bowel[1,2]. The retroperitoneal position of the duodenum, its shared blood supply with the pancreas, and its relationship with the ampulla of Vater and the superior mesenteric vessels ensure that any duodenal resection is potentially a major undertaking. Pancreaticoduodenectomy (PD) constitutes the mainstay of surgical treatment of duodenal lesions[3] and up to 10% of PDs are undertaken for lesions that actually arise in the duodenum[4]. However, PD is associated with significant morbidity and mortality, which is due in part to pancreatic resection and anastomosis. Moreover, it is likely that the actual risks associated with PD are widely underestimated[5].

Duodenal resection with pancreas preservation is possible and has been used in the treatment of a range of duodenal conditions. Pancreas preserving total duodenectomy is an option for the treatment of diffuse non-invasive mucosal disease such as FAP-associated polyposis[6,7] whilst pancreas preserving distal duodenectomy (PPDD) has been described in the treatment of a range of benign and malignant lesions arising distal to the papilla complex[8,9].

We describe how we perform a PPDD and present the long-term results of a series of 19 patients who underwent the procedure in a single centre for a variety of pathologies over a 14-year period and also review the relevant literature.

MATERIALS AND METHODS

Preoperative investigations and preparation

This procedure is usually undertaken in an elective or scheduled capacity for patients with infra-papillary conditions that, in the opinion of the multidisciplinary team, warrant surgical resection. Criteria include M_0 duodenal adenocarcinoma; large adenomata or those in positions that prevent effective endoscopic mucosal resection; and gastrointestinal stromal tumours. Patients routinely undergo multi-slice pancreas protocol computed tomography (CT) with occasional fluoroscopic investigations. Most have one or more modalities of endoscopic investigation. Poor nutritional status at presentation is considered an indication for nasojejunal feeding which is commenced 7-14 d preoperatively. Representative CT and endoscopic findings are shown in Figures 1-3. The relationship of the tumour or lesion to the ampulla of Vater on

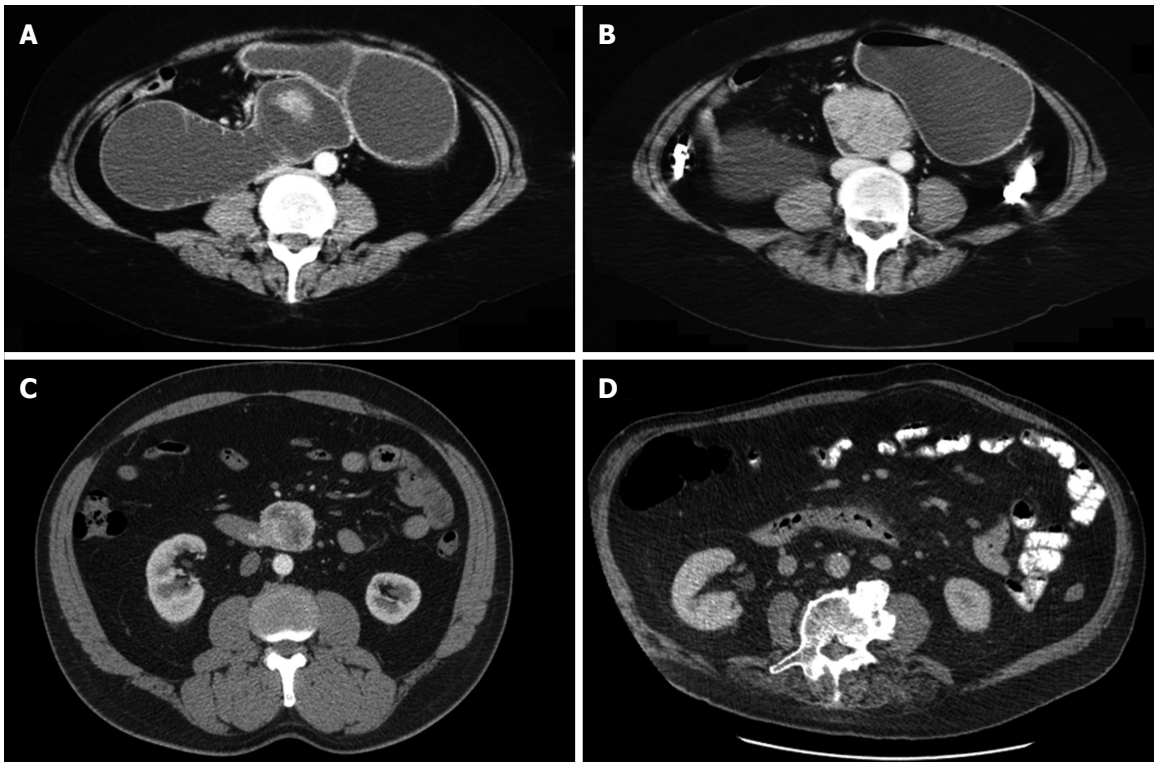

Figure 1 Representative axial computed tomography imaging of duodenal adenocarcinoma. A and B: obstruction due to a large duodenal mass (same patient); C: exophytic mass without obstruction; D: subtle thickening of duodenum and periduodenal fat stranding reported as duodenitis, but in fact was a malignant tumour on post resection histology.

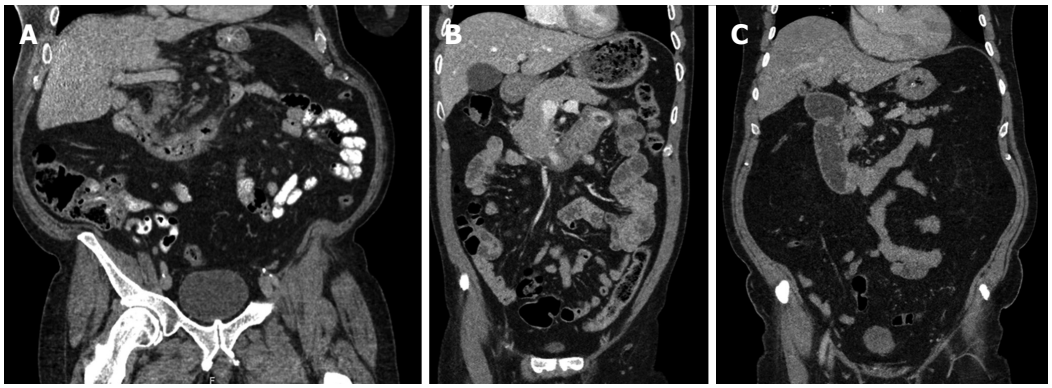

Figure 2 Representative coronal computed tomography imaging of duodenal adenocarcinoma. A: thickening of the duodenal wall with non-obstructive narrowing; B: mass in the distal duodenum, C: stricture of D2/3 junction with some obstructive features.

preoperative endoscopy or CT is vital in determining the feasibility of offering the patient a PPDD. Nevertheless, the procedure should only be undertaken in an institution with expertise and facilities to perform a PD, as a small number of patients will not be suitable for a PPDD on surgical exploration because of close proximity of a malignant pathology to the ampulla or involvement of the pancreas by the malignant process. This should be considered in the consent process and we usually obtain consent to perform a PPDD with a view to proceed to a PD or perform a bypass procedure in the event of unresectability.

Operative technique

Arterial, central venous, epidural and bladder catheterisations are performed for monitoring and pain relief. Flow-guided intraoperative fluid therapy is used. In cases where there is concern regarding the proximity of the lesion to the ampulla, their relationship is confirmed intraoperatively with side-viewing duodenoscopy. A transverse upper abdominal incision with appropriate fixed table retraction is used. The key operative steps are shown in Figure 4. Wide Kocherisation of the duodenum is undertaken, facilitated by a variable degree of right medial visceral

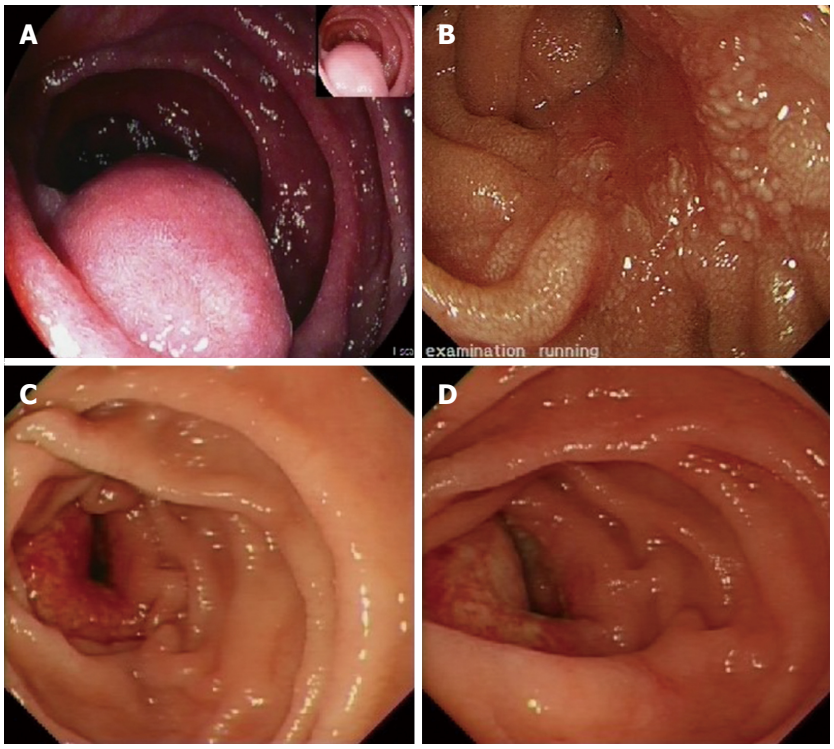

Figure 3 Endoscopic features. A: pedunculated lesion (gastrointestinal stromal tumour); B: sessile lesion (large adenoma with previous endoscopic mucosal resection); C and D: malignant ulceration of a duodenal adenocarcinoma.

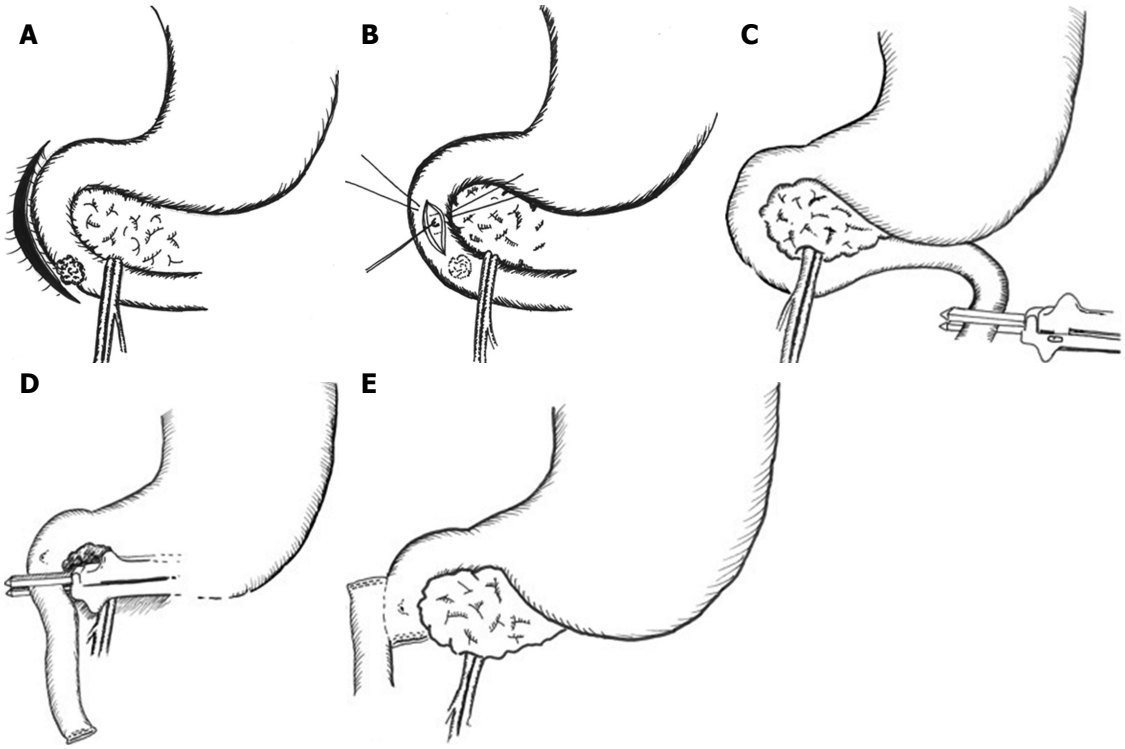

Figure 4 Operative technique. After wide Kocherisation (A) the papilla and lesion are palpated. For benign pathology close to the papilla, the ampullary complex can be further protected by cannulation (B). The proximal jejunum is transected (C), the distal duodenum taken off its short vessels and the resection is completed (D). Reconstruction is by a retrocolic isoperistaltic side-to-side duodenojejunostomy (E).

rotation (Cattell-Braasch manoeuver)[10]. Resectability is determined by excluding involvement of the pancreas and peripancreatic vessels and by confirming macroscopic proximal clearance of at least 10 mm with preservation of the major papilla complex. Macroscopic nodal and distant metastatic disease are also excluded. Frozen section biopsies are taken when necessary. After confirming resectability, the proximal jejunum is transected with a transverse linear cutting stapler and its mesentery, along with the ligament of Treitz and the peritoneal attachments of the duodenojejunal junction, are divided to permit delivery of the proximal jejunum behind the superior mesenteric vessels into the supracolic compartment. The third part of the duodenum (D3) and distal second part (D2) are then separated from the pancreatic head and uncinate process. The mobile, devascularised distal duodenum is then excised, again with linear stapler. For benign lesions close to the papilla, the latter is cannulated with a 4F infant feeding tube *via* a duodenotomy to facilitate proximal transection with preservation of the ampullary complex. PD is undertaken if the lesion involved to papilla. The proximal, blind end of jejunum is delivered through a window in the transverse mesocolon to permit a sutured side-to-side isoperistaltic duodenojejunostomy, which is performed with 3-0 or 4-0 polydioxanone (PDS®II, Ethicon, Edinburgh, United Kingdom) sutures in a single continuous layer. In cases assessed at risk of malnutrition or anticipated delayed gastric emptying, as in patients with preoperative gastric outlet obstruction, a fine bore nasojejunal feeding tube is placed across the anastomosis for postoperative feeding. A cholecystectomy is performed if the gallbladder is still *in situ*. A peritoneal drain is placed selectively if there is of a perceived risk of postoperative pancreatic fistulation following dissection on or close to the pancreas.

Postoperative management

Postoperative care is initially in a surgical high dependency unit and has, in recent years, proceeded according to enhanced recovery after surgery (ERAS) principles[11]. Somatostatin analogues are not used routinely. The peritoneal drain, if used, is removed on the third postoperative day provided fluid amylase does not exceed three times serum amylase and there is no evidence of enteric content.

RESULTS

All patients undergoing PPDD within a large teaching hospital were identified using a prospectively maintained database and crosschecked against a hospital database of pathology specimens. Electronic healthcare records were reviewed for relevant information.

Between 2003 and 2016, 24 patients were explored with the intention of performing PPDD. In 3 patients, malignant involvement of the superior mesenteric artery precluded resection and palliative gastroenterostomy was undertaken. Two patients had intraoperative findings that necessitated PD, as the malignant process was close to the papilla and adequate resection margins could not have been obtained without a PD. Thus, 19 patients proceeded to PPDD. Median Charlson co-morbidity index was 4 (range 0-6). Patient characteristics and modes of presentation and are shown in Table 1. Either of two surgeons (DNL, AJB) oversaw each operation.

All patients survived 30 d and to discharge home. Two of nineteen patients required blood products and median postoperative length of stay was 8 d (range 4-21) The Mann-Whitney test was employed to compare length of stay (LOS) following PPDD *vs* PD undertaken in the same centre, using a continuous series of PD, February to August 2015 (n = 26). PPDD was associated with a significantly shorter LOS than PD [8 (6-14) d *vs* 11 (10-16) d, median (IQR), P = 0.026] No procedure-related deaths were observed in this series and only 1 patient went on to die of related disease within the follow up period. This patient developed distant recurrence (transcoelomic spread to rectouterine pouch). Neoplastic conditions accounted for 17 (90%) of operations (Table 2). Median (IQR) follow-up was 36 (11-114) mo. Representative images of pathological specimens are shown in Figure 5.

DISCUSSION

In our experience, PPDD provides a valuable surgical treatment for a range of infra-papillary pathologies, which were in the most part neoplastic, including duodenal adenocarcinomas (n = 6, 32%), adenomas (n = 5, 26%) and gastrointestinal stromal tumours (n = 4, 21%).

PPDD avoids the potential complications associated with a pancreaticoenteric anastomosis. Although the infrequency of PPDD, along with differences in underlying disease, prevented meaningful comparison of morbidity and mortality between PD and PPDD, a significantly shorter median length of stay was observed following PPDD than PD.

Neither cross-sectional imaging nor forward-viewing endoscopies provide a detailed description of the relationship of the lesion to the papilla. For this reason, patients had consented to PD and selected cases underwent side-viewing on-table endoscopy and duodenotomy/papillary cannulation. The authors would advocate that PPDD should only be undertaken where expertise and facilities support progression to PD.

Eight of the nineteen PPDD undertaken in this 14-year period were performed in the last two years. It is likely that this reflects changes in referral patterns to the centre and an increase in the population catchment area, and better awareness of the option of pancreas preservation may have contributed to this increase.

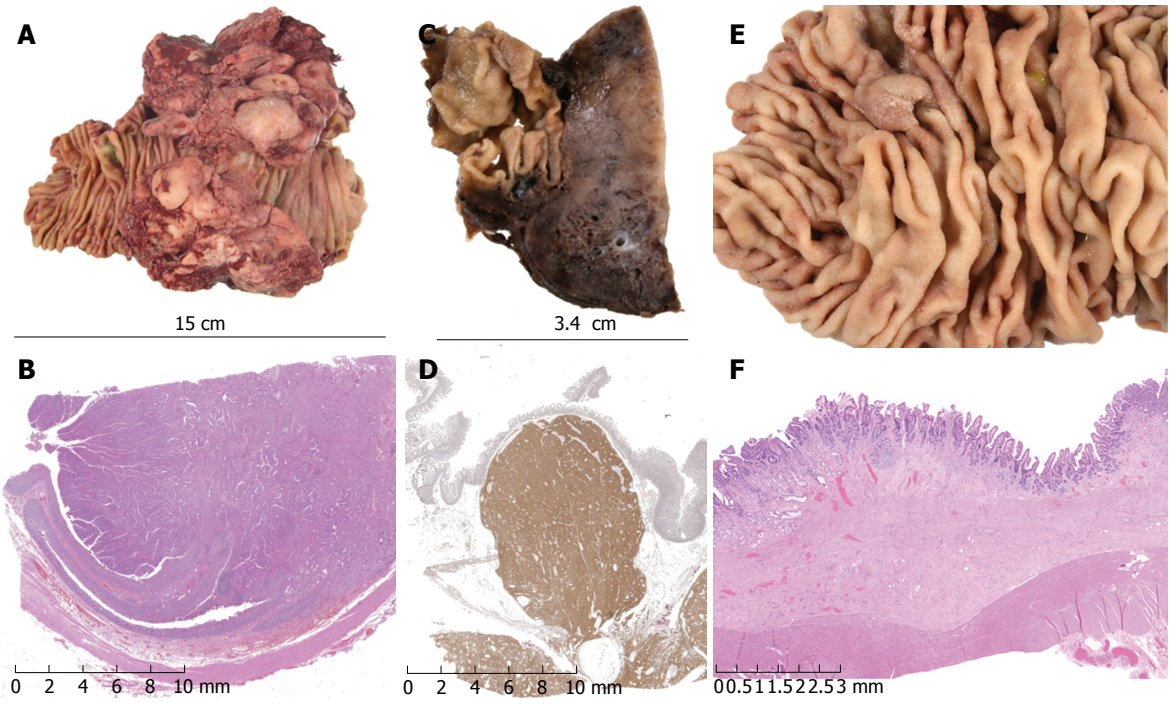

Figure 5 Pathological findings. A and B: exophytic lesion in the duodenum shown to be a moderately differentiated duodenal adenocarcinoma on histology (haematoxylin and eosin stain); C and D: gastrointestinal stromal tumour confirmed on immunohistochemistry with CD117 and DOG1 staining; E and F: tubulovillous adenoma of the duodenum with low-grade dysplasia on histology (haematoxylin and eosin stain).

Table 1 Patient characteristics

No.	Age	Sex	Presentation	Comorbidities	CCI	Radiological assessment	Endoscopic assessment	Nutritional support	Year
1	67	M	Asymptomatic (incidental on OGD)	Coeliac disease	4	CT	OGD, EUS		2011
2	56	F	Weight loss, anaemia, vomiting	Malnutrition	3	CT, Ba study	OGD	NJ	2004
3	66	F	Vomiting	Asthma, depression	4	CT	-		2015
4	51	M	Epigastric pain, weight loss, vomiting	Nil	3	CT	OGD		2016
5	68	M	Epigastric pain, vomiting	Hiatus hernia	4	CT	-		2015
6	77	M	Epigastric pain, weight loss, vomiting, anaemia	Bronchiectasis, GORD	6	CT	OGD, enteroscopy		2016
7	73	F	Anaemia	Metachronous colonic cancer	10	CT	-		2016
8	61	M	Asymptomatic (incidental on ultrasound)	GORD	4	CT	OGD, EUS		2013
9	48	F	Epigastric pain, weight loss, vomiting	Nil	2	CT	OGD, EUS		2014
10	65	M	Asymptomatic (incidental on aneurysm screening)	Nil	4	CT	OGD, EUS		2016
11	83	F	Epigastric pain, weight loss, vomiting	Glaucoma, hypothyroidism	6	CT	-		2016
12	76	F	Dyspepsia/reflux	NASH, cirrhosis, colectomy for cancer	4	CT	OGD		2008
13	76	M	Epigastric pain, back pain	Functional asplenia	3	CT	OGD, EUS		2006
14	76	M		HTN, Stroke, MI	5	-	OGD		2007
15	64	F	Dyspepsia/reflux	Hiatus hernia	2	CT	OGD, EUS		2004
16	68	F	Epigastric pain, vomiting, early satiety	Stricture post EMR	1	CT, Wat Sol St	OGD, EUS	NJ	2016
17	36	M	Recurrent pancreatitis	Nil	0	CT	OGD		2003
18	80	F	Melaena	Glaucoma	4	CT	OGD		2004
19	39	F	Epigastric pain, weight loss, vomiting	Nil	0	CT, Wat Sol St	OGD		2016

Ba: Barium; CCI: Charlson comorbidity index; CT: Computed tomography; EMR: Endoscopic submucosal resection; EUS: Endoscopic ultrasound; GORD: Gastroesophageal reflux disease; HTN: Hypertension; MI: Myocardial infarction; NASH: Non-alcoholic steatohepatosis; NJ: Nasojejunal; OGD: Oesophagogastroduodenoscopy; Wat Sol St: Water soluble contrast study.

Table 2 Pathology and outcome

No.	Diagnosis	Total lymph nodes	Nodes +ve	Proximal margin (mm)	Blood transfusion (units)	Length of stay (d)	FU (mo)	Complications	Outcome
1	Adenocarcinoma Mod diff pT4 Nx Mx G2 V0 R0	0	-	15	0	4	72	-	Alive, disease free[2]
2	Adenocarcinoma Mod diff pT3 N0 Mx G2 V1 R0	4	0	55	NR	14	155	-	Alive, disease free
3	Adenocarcinoma Mod diff T4 N1 Mx V0 G2 R0	11	1	30	0	13	18[1]	Recurrence	Died (distant metastases)[2]
4	Adenocarcinoma Poorly diff T4 N2 Mx V1 G3 R0	29	16	62	0	5	13	-	Alive, disease free[2]
5	Adenocarcinoma Mod diff pT3 N0 M0 V1 G2 R0	7	0	30	0	14	15	Incisional hernia at 1 yr	Alive, disease free
6	Adenocarcinoma Mod diff pT3 N0 Mx V1 G2 R0	19	0	25	0	6	7	-	Alive, disease free
7	Adenocarcinoma of colon	10	1		2	7	100	-	Alive, disease free[2]
8	GIST (low grade malignant potential)	0	0		0	4	48	-	Alive, disease free
9	GIST (low grade malignant potential)	0	0		0	10	36	Anast. stricture; GJ at 2 yr	Alive, disease free
10	GIST (low grade malignant potential)	1	0		0	8	10	-	Alive, disease free
11	GIST (low grade malignant potential)	6	0		0	6	5	-	Alive, disease free
12	Villous adenoma (high grade dysplasia)	NR	-		8	19	2[1]	Ascitic leak (cirrhotic)	Died of unrelated causes
13	Tubulovillous adenoma (high grade dysplasia)	NR	-		NR	21	126	OPSI	Alive, disease free
14	Tubular adenoma (high grade dysplasia)	NR	-		0	8	102[1]	-	Died of unrelated causes
15	Tubular adenoma (low grade dysplasia)	NR	-		0	18	146	Postoperative pneumonia	Alive, disease free
16	Multiple tubular adenomas (low grade dysplasia)	1	0		0	7	8	-	Alive, disease free
17	Lipoma	NR	-		NR	10	168	-	Alive, disease free
18	Bleeding duodenal diverticulum	NR	-		NR	13	144	-	Alive, disease free
19	Superior mesenteric artery syndrome	NR	-		0	5	12	Poor pain control, N&V	Alive, disease free

[1]Postoperative death; [2]Received adjuvant chemotherapy. Mod diff: Moderately differentiated; NR: Not relevant; GIST: Gastrointestinal stromal tumour; GJ: Gastrojejunostomy; OPSI: Overwhelming postsplenectomy infection; N&V: Nausea and vomiting.

This raises the possibility that the technique of PPDD is underused and improved surgical awareness may prevent some patients undergoing unnecessary pancreatic resection with an associated longer hospital stay and likely increased morbidity and mortality.

To the knowledge of the authors, this series brings to 83 the total number of patients undergoing PPDD that have been reported in published literature, which comprises 4 other series and 10 reports of individual cases[3,8,9,12-22]. These are summarized in Table 3. Represented pathologies include 27 adenocarcinomas of the duodenum (33%), 20 gastrointestinal stromal tumours (24%), 12 adenomas (14%) and 5 trauma (6%) as well as lipoma and liposarcoma, locally invading colon cancer, metastases from seminoma and lung cancer, Crohn's disease, plasmacytoma and lymphoma. Technical variation includes different longitudinal extent of resection and different anastomotic technique with end-to-end, end-to-side and side-to-side all represented. Three deaths within 30 d of PPDD have been reported; 2 due to cholecystitis and one due to anastomotic leak; giving a periprocedural mortality of 3.7%. Of the 27 patients undergoing PPDD for adenocarcinoma, 10 deaths were recorded and of the 17 patients alive at the time of publication of the individual reports, 7 had survived more than 36 mo. Procedural morbidity included cholangitis/ cholecystitis, anastomotic bleeding, delayed gastric emptying and, unexpectedly, pancreatic fistulae. Overall, morbidity was reported in 32 patients (39%).

Laparoscopic[3,16] and laparoscopic-assisted[23] approaches to distal duodenal resection have also been described and may offer patients the expected benefits of minimally invasive surgery. However, an open approach may be better to achieve adequate assessment and margins for lesions close to the papilla.

Table 3 Published reports of distal duodenectomy

First Author	Year	No. of cases	Histology	Anastomosis	Complications	Outcome
Kerremans *et al*[8]	1979	1	1 adenocarcinoma	-	Jejunocutaneous fistula	Death at 20 mo
Kawano *et al*[9]	1995	1	1 GIST	1 end-to-side	-	NR
Maher *et al*[12]	1996	24	11 adenocarcinomas 1 GIST 2 adenomas 1 lymphoma 1 liposarcoma 2 Crohn's disease 5 trauma 1 peptic ulceration	10 end-to-end 8 end-to-side 3 side-to-end 3 side-to-side	1 death (anastomotic leak) 2 pancreatic fistulae 2 DGE 2 anastomotic bleeds	Adenocarcinoma; Median survival 18.5 mo GIST; NR
Sohn *et al*[13]	1998	2	2 adenocarcinomas	NR	2 cholangitis	NR
Suzuki *et al*[14]	1999	1	1 GIST	1 end-to-side	DGE	Alive/ well 2 yr postop
Orda *et al*[15]	2000	1	1 GIST	end-to-end	-	Alive/ well 13 yr postop
Ammori[16]	2002	1	1 benign stricture	side-to-side	Intra-abdominal bleeding	NR
Eisenberger *et al*[17]	2004	1	1 GIST	NR	-	Alive/ well 1 yr postop
Spalding *et al*[18]	2007	14	5 adenocarcinomas 4 GIST 1 adenoma 1 lipoma 1 metastatic seminoma 1 ulcer 1 plasmacytoma	14 end-to-end	1 death (cholecystitis) 1 anastomotic stricture (reoperated) 1 DGE 1 anastomotic bleed (reoperated)	Adenocarcinoma; 1 death at 3 mo, Median survival 56 mo. GIST; 1 death at 3 mo, Median survival 120 mo
Cavaniglia *et al*[19]	2012	1	1 GIST	1 end-to-end	-	NR
Stauffer *et al*[3]	2013	1	5 adenomas 2 adenocarcinomas 1 lymphangiolipoma 1 GIST 1 NET	7 side-to-side 2 end-to-side gastrojejunostomy	1 DGE 1 pancreatic fistula	NR
Waisberg *et al*[20]	2013	1	1 carcinoid	NR	NR	Death at 6 mo
Shimizu *et al*[21]	2015	1	1 adenoma	1 end-to-side	NR	NR
García-Molina *et al*[22]	2015	8	1 adenocarcinoma 5 GIST 1 metastasis from lung 1 colon cancer		1 death	Adenocarcinoma; 1 death at 12 mo GIST; 5 Alive/ well at 4-6 yr
Current series	2017	19	6 adenocarcinomas 5 adenomas 4 GIST 1 lipoma 1 colon cancer 1 bleeding diverticulum 1 extrinsic compression	19 side-to-side	1 recurrent adenocarcinoma 1 anastomotic Stricture 1 incisional hernia	Adenocarcinoma: 1 death at 18 mo Alive/well 1 < 1 yr, 2 > 1 yr, 1 > 6 yr, 1 > 12 yr GIST: Alive/ well 2 < 1 yr, 2 > 3 yr

DGE: Delayed gastric emptying; GIST: Gastrointestinal stromal tumour; NET: Neuroendocrine tumor; NR: Not recorded.

Concern may exist regarding the oncological effectiveness of PPDD. We suggest that no evidence exists to show benefit of including a pancreatic resection in the treatment of a distal duodenal cancer. This study shows that an adequate lymphadenectomy may be achieved with PPDD (Table 2). Consistent R0 margin status and adequate histopathological proximal resection margins have been achieved by conversion to PD if intraoperative doubt exists regarding the macroscopic relationship of the disease to surrounding structures. The only pattern of recurrence observed in this series was distant spread to pelvic peritoneum (after resection of T4 lesion with serosal involvement) and the authors propose that there would have been no oncological benefit from the addition of pancreatic head resection. An algorithm describing pre- and intraoperative decision making is presented (Figure 6).

PPDD is a valuable technique for the treatment of a wide range of infra-papillary duodenal lesions and an expanding body of published literature exists to support its use. It should be undertaken where expertise and facilities permit conversion to PD if

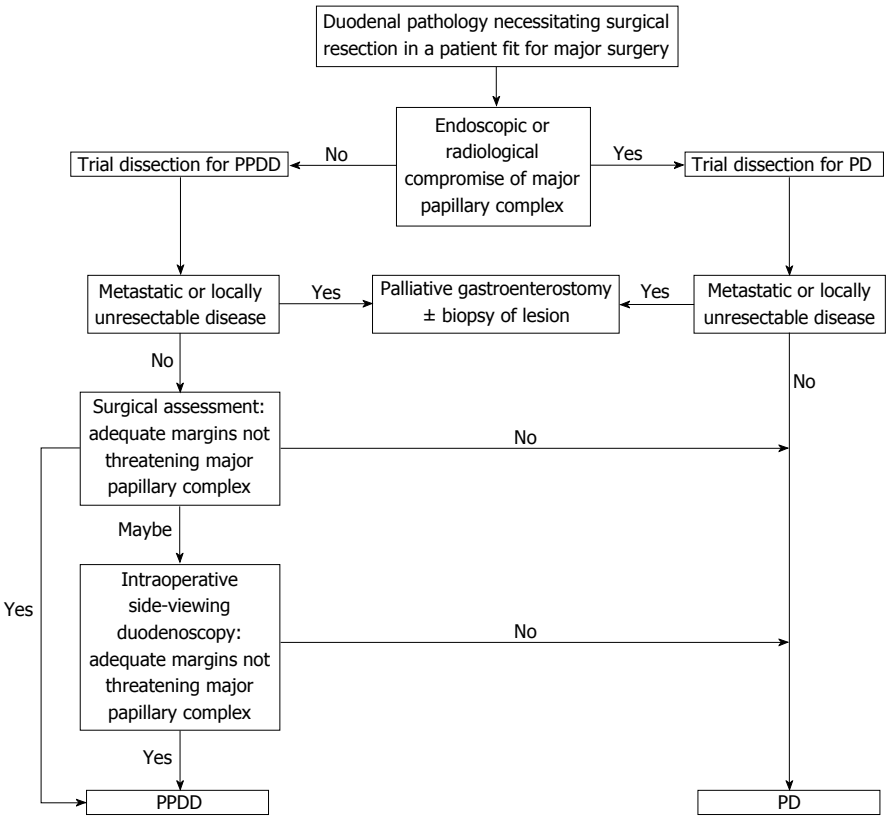

Figure 6 Flow chart summarising the local algorithm for the management of infrapapillary duodenal lesions. PD: Pancreaticoduodenectomy; PPDD: Pancreas preserving distal duodenectomy.

necessitated by intraoperative findings.

COMMENTS

Background

Neoplastic lesions of the duodenum are treated conventionally by pancreaticoduodenectomy. Lesions distal to the major papilla may be suitable for a pancreas-preserving distal duodenectomy (PPDD), potentially reducing morbidity and mortality. Limited awareness of this technique may deprive patients of the opportunity to avoid pancreas-specific complications following treatment for infrapapillary diseases.

Research frontiers

Early series suggested poor outcomes after PPDD for duodenal adenocarcinoma. Adenocarcinoma may thus be considered a contentious indication for PPDD.

Innovations and breakthroughs

The authors widen the range of conditions treated with this surgery, provide detail on lymph node harvests, demonstrate a shorter length of stay than after pancreaticoduodenectomy, and we present relatively good outcomes after PPDD for adenocarcinoma.

Applications

This work supports the consideration of PPDD in the resection of any infrapapillary lesion but demonstrates that, in a minority of patients, intraoperative findings may mandate proceeding to a formal pancreaticoduodenectomy.

Terminology

The authors consider a circumferential full thickness resection of an infrapapillary portion of the duodenal tube without macroscopic resection of pancreas to constitute a pancreas-preserving distal duodenectomy; this is typically after full Kocherisation and with a primary duodenojejunal anastomosis.

Peer-review

It's a well-written manuscript. The authors described surgical technique and its results of pancreas preserving distal duodenectomy.

REFERENCES

1 **Perey B**. Neoplasms of the duodenum. In: Scott H, Sawyers JL, editor Surgery of the Stomach, Duodenum and Small Intestine. Boston: Blackwell Scientific Publications, 1987: 571-584
2 **Jefferson G**. Carcinoma of suprapapillary duodenum casually associated with pre-existing simple ulcer. *Br J Surg* 1916; **4**: 209 [DOI: 10.1002/bjs.1800041402]
3 **Stauffer JA**, Raimondo M, Woodward TA, Goldberg RF, Bowers SP, Asbun HJ. Laparoscopic partial sleeve duodenectomy (PSD) for nonampullary duodenal neoplasms: avoiding a whipple by separating the duodenum from the pancreatic head. *Pancreas* 2013; **42**: 461-466 [PMID: 23462322 DOI: 10.1097/MPA.0b013e3182649956]
4 **Cameron JL**, Riall TS, Coleman J, Belcher KA. One thousand consecutive pancreaticoduodenectomies. *Ann Surg* 2006; **244**: 10-15 [PMID: 16794383 DOI: 10.1097/01.sla.0000217673.04165.ea]
5 **Nimptsch U**, Krautz C, Weber GF, Mansky T, Grützmann R. Nationwide in-hospital mortality following pancreatic surgery in Germany is higher than anticipated. *Ann Surg* 2016; **264**: 1082-1090 [PMID: 26978570 DOI: 10.1097/SLA.0000000000001693]
6 **Chung RS**, Church JM, vanStolk R. Pancreas-sparing duodenectomy: indications, surgical technique, and results. *Surgery* 1995; **117**: 254-259 [PMID: 7878529 DOI: 10.1016/S0039-6060(05)80198-9]

7 **Al-Sarireh B**, Ghaneh P, Gardner-Thorpe J, Raraty M, Hartley M, Sutton R, Neoptolemos JP. Complications and follow-up after pancreas-preserving total duodenectomy for duodenal polyps. *Br J Surg* 2008; **95**: 1506-1511 [PMID: 18991295 DOI: 10.1002/bjs.6412]

8 **Kerremans RP**, Lerut J, Penninckx FM. Primary malignant duodenal tumors. *Ann Surg* 1979; **190**: 179-182 [PMID: 464691 DOI: 10.1097/00000658-197908000-00010]

9 **Kawano N**, Ryu M, Kinoshita T, Konishi M, Iwasaki M, Furuse J, Yoshino M, Hasebe T. Segmental resection of the duodenum for treating leiomyosarcoma associated with von Recklinghausen's disease: a case report. *Jpn J Clin Oncol* 1995; **25**: 109-112 [PMID: 7596048]

10 **Cattell RB**, Braasch JW. A technique for the exposure of the third and fourth portions of the duodenum. *Surg Gynecol Obstet* 1960; **111**: 378-379 [PMID: 13808480]

11 **Lassen K**, Coolsen MM, Slim K, Carli F, de Aguilar-Nascimento JE, Schäfer M, Parks RW, Fearon KC, Lobo DN, Demartines N, Braga M, Ljungqvist O, Dejong CH. Guidelines for perioperative care for pancreaticoduodenectomy: Enhanced Recovery After Surgery (ERAS®) Society recommendations. *Clin Nutr* 2012; **31**: 817-830 [PMID: 23079762 DOI: 10.1016/j.clnu.2012.08.011]

12 **Maher MM**, Yeo CJ, Lillemoe KD, Roberts JR, Cameron JL. Pancreas-sparing duodenectomy for infra-ampullary duodenal pathology. *Am J Surg* 1996; **171**: 62-67 [PMID: 8554153 DOI: 10.1016/S0002-9610(99)80075-0]

13 **Sohn TA**, Lillemoe KD, Cameron JL, Pitt HA, Kaufman HS, Hruban RH, Yeo CJ. Adenocarcinoma of the duodenum: factors influencing long-term survival. *J Gastrointest Surg* 1998; **2**: 79-87 [PMID: 9841972 DOI: 10.1016/S1091-255X(98)80107-8]

14 **Suzuki H**, Yasui A. Pancreas-sparing duodenectomy for a huge leiomyosarcoma in the third portion of the duodenum. *J Hepatobiliary Pancreat Surg* 1999; **6**: 414-417 [PMID: 10664293 DOI: 10.1007/s005340050142]

15 **Orda R**, Sayfan J, Wasserman I. Surgical treatment of leiomyosarcoma of the distal duodenum. *Dig Surg* 2000; **17**: 410-412 [PMID: 11053954]

16 **Ammori BJ**. Laparoscopic pancreas-preserving distal duodenectomy for duodenal stricture related to nonsteroidal antiinflammatory drugs (NSAIDs). *Surg Endosc* 2002; **16**: 1362-1363 [PMID: 12072993 DOI: 10.1007/s00464-002-4201-x]

17 **Eisenberger CF**, Knoefel WT, Peiper M, Yekebas EF, Hosch SB, Busch C, Izbicki JR. Pancreas-sparing duodenectomy in duodenal pathology: indications and results. *Hepatogastroenterology* 2004; **51**: 727-731 [PMID: 15143902]

18 **Spalding DR**, Isla AM, Thompson JN, Williamson RC. Pancreas-sparing distal duodenectomy for infrapapillary neoplasms. *Ann R Coll Surg Engl* 2007; **89**: 130-135 [PMID: 17346405 DOI: 10.1308/003588407X155815]

19 **Cavaniglia D**, Petrucciani N, Lorenzon L, Caterino S, Cavallini M. Partial duodenectomy with end-to-end anastomosis for duodenal gastrointestinal stromal tumor. *Am Surg* 2012; **78**: E273-E275 [PMID: 22691326]

20 **Waisberg J**, Joppert-Netto G, Vasconcellos C, Sartini GH, Miranda LS, Franco MI. Carcinoid tumor of the duodenum: a rare tumor at an unusual site. Case series from a single institution. *Arq Gastroenterol* 2013; **50**: 3-9 [PMID: 23657299 DOI: 10.1590/S0004-28032013000100002]

21 **Shimizu K**, Hashimoto D, Abe S, Chikamoto A, Baba H. Pancreas-preserving partial duodenectomy of the distal region for large duodenal adenoma: report of a case. *Surg Today* 2015; **45**: 390-393 [PMID: 24549473 DOI: 10.1007/s00595-014-0868-6]

22 **García-Molina FJ**, Mateo-Vallejo F, Franco-Osorio Jde D, Esteban-Ramos JL, Rivero-Henández I. Surgical approach for tumours of the third and fourth part of the duodenum. Distal pancreas-sparing duodenectomy. *Int J Surg* 2015; **18**: 143-148 [PMID: 25917202 DOI: 10.1016/j.ijsu.2015.04.051]

23 **Abe N**, Hashimoto Y, Kawaguchi S, Shimoyama H, Kojima Y, Yoshimoto E, Kondo E, Ohki A, Takeuchi H, Nagao G, Suzuki Y, Masaki T, Mori T, Sugiyama M. Successful treatment of large adenoma extending close to the papilla in the duodenum by laparoscopy-assisted pancreas-sparing duodenectomy. *Asian J Endosc Surg* 2016; **9**: 52-56 [PMID: 26781527 DOI: 10.1111/ases.12246]

P- Reviewer: Andrianello S, Kawabata Y, Schafer M, Takahashi H
S- Editor: Qi Y **L- Editor**: A **E- Editor**: Zhang FF

World Journal of Gastroenterology

Submit a Manuscript: http://www.f6publishing.com

World J Gastroenterol 2017 June 21; 23(23): 4262-4269

DOI: 10.3748/wjg.v23.i23.4262

ISSN 1007-9327 (print) ISSN 2219-2840 (online)

ORIGINAL ARTICLE

Retrospective Study

Clinical importance of colonoscopy in patients with gastric neoplasm undergoing endoscopic submucosal dissection

Chieko Tsuchida, Naoto Yoshitake, Hitoshi Kino, Yoshihito Kaneko, Masakazu Nakano, Kohei Tsuchida, Keiichi Tominaga, Takako Sasai, Hironori Masuyama, Hidetsugu Yamagishi, Yasuo Imai, Hideyuki Hiraishi

Chieko Tsuchida, Naoto Yoshitake, Hitoshi Kino, Yoshihito Kaneko, Masakazu Nakano, Kohei Tsuchida, Keiichi Tominaga, Takako Sasai, Hironori Masuyama, Hideyuki Hiraishi, Department of Gastroenterology, Dokkyo Medical University, Shimotsuga, Tochigi 321-0293, Japan

Hidetsugu Yamagishi, Yasuo Imai, Department of Diagnostic Pathology, Dokkyo Medical University, 880, Kitakobayashi, Mibu, Shimotsuga, Tochigi 321-0293, Japan

Author contributions: Tsuchida C and Yoshitake N were involved in the design of this study; Tsuchida C, Yoshitake N, Kino H, Kaneko Y, Nakano M and Tsuchida K performed the endoscopic treatment; Tsuchida C, Yoshitake N, Kino H, Kaneko Y and Nakano M conducted data collection and statistical analysis; The manuscript was written by Tsuchida C and Yoshitake N, and Tominaga K, Sasai T, Masuyama H, Yamagishi H, Imai Y and Hiraishi H provided advice on the manuscript; all authors read and approved the final manuscript.

Institutional review board statement: This study was reviewed and approved by the ethics committee of Dokkyo Medical University.

Conflict-of-interest statement: The authors declare that they have no competing interests.

Data sharing statement: No additional data are available.

Manuscript source: Invited manuscript

Correspondence to: Naoto Yoshitake, MD, PhD, Department of Gastroenterology, Dokkyo Medical University, 880, Kitakobayashi, Mibu, Shimotsuga, Tochigi 321-0293, Japan. naoto-y@dokkyomed.ac.jp
Telephone: +81-282-872147
Fax: +81-282-867761

Received: December 17, 2016
Peer-review started: December 20, 2016
First decision: March 16, 2017
Revised: March 29, 2017
Accepted: May 19, 2017
Article in press: May 19, 2017
Published online: June 21, 2017

Abstract

AIM

To evaluate the usefulness of total colonoscopy (TCS) for patients undergoing gastric endoscopic submucosal dissection (ESD) and to assess risk factors for colorectal neoplasms.

METHODS

Of the 263 patients who underwent ESD at our department between May 2010 and December 2013, 172 patients undergoing TCS during a one-year period before and after ESD were targeted. After excluding patients with a history of surgery or endoscopic therapy for colorectal neoplasms, 158 patients were analyzed. Of the 868 asymptomatic patients who underwent TCS during the same period because of positive fecal immunochemical test (FIT) results, 158 patients with no history of either surgery or endoscopic therapy for colorectal neoplasms who were matched for age and sex served as the control group for comparison.

RESULTS

TCS revealed adenoma less than 10 mm in 53 patients (33.6%), advanced adenoma in 17 (10.8%), early colorectal cancer in 5 (3.2%), and advanced colorectal

cancer in 4 (2.5%). When the presence or absence of adenoma less than 10 mm, advanced adenoma, and colorectal cancer and the number of adenomas were compared between patients undergoing ESD and FIT-positive patients, there were no statistically significant differences in any of the parameters assessed. The patients undergoing ESD appeared to have the same risk of colorectal neoplasms as the FIT-positive patients. Colorectal neoplasms were clearly more common in men than in women (P = 0.031). Advanced adenoma and cancer were significantly more frequent in patients with at least two of the following conditions: hypertension, dyslipidemia, and diabetes mellitus (P = 0.019).

CONCLUSION

In patients undergoing gastric ESD, TCS appears to be important for detecting synchronous double neoplasms. Advanced adenoma and cancer were more common in patients with at least two of the following conditions: hypertension, dyslipidemia, and diabetes mellitus. Caution is therefore especially warranted in patients with these risk factors.

Key words: Colonoscopy; Colorectal neoplasm; Gastric neoplasm; Endoscopic submucosal dissection; Fecal immunochemical test

Core tip: This is a retrospective study to evaluate the usefulness of total colonoscopy (TCS) for patients undergoing gastric endoscopic submucosal dissection (ESD). The frequency of detecting colorectal lesions, especially advanced adenoma and carcinoma, was higher in patients with early gastric cancer or gastric adenoma. This observation suggests that such patients are at a risk equivalent to that of fecal immunochemical test positive patients, suggesting that screening TCS should be performed as extensively as possible in patients undergoing ESD.

Tsuchida C, Yoshitake N, Kino H, Kaneko Y, Nakano M, Tsuchida K, Tominaga K, Sasai T, Masuyama H, Yamagishi H, Imai Y, Hiraishi H. Clinical importance of colonoscopy in patients with gastric neoplasm undergoing endoscopic submucosal dissection. *World J Gastroenterol* 2017; 23(23): 4262-4269 Available from: URL: http://www.wjgnet.com/1007-9327/full/v23/i23/4262.htm DOI: http://dx.doi.org/10.3748/wjg.v23.i23.4262

INTRODUCTION

Gastric endoscopic submucosal dissection (ESD) has been established as a common curative resection procedure for gastric neoplasms including early gastric cancer and gastric adenoma[1,2]. ESD showed a superior efficacy with respect to endoscopic mucosal resection in a recent meta-analysis[3]. As adoption of this procedure becomes ever more widespread, the indications for endoscopic therapy are being expanded[4]. The curative resection rate with gastric ESD is approximately 85%[5,6], and the 5-year cancer-specific survival rate is reported to be approximately 99% in patients undergoing curative resection[7,8]. As these rates indicate, the gastric cancer mortality rate is very low after endoscopic resection of gastric neoplasms. To further improve outcomes, screening for neoplasms in other organs is assumed to be important.

Colorectal neoplasms are among the most common malignancies in Europe and North America. The incidence of these malignancies has markedly increased in the past 20 to 30 years in Asia, including Japan[9,10].

Colorectal neoplasms are the most commonly observed tumors outside of the stomach in patients with gastric cancer. Synchronous or metachronous colorectal cancer is reportedly detected in approximately 1% of patients with gastric cancer[11,12]. Therefore, screening colonoscopy before surgical interventions for the stomach is now well established. However, the usefulness of screening colonoscopy in patients undergoing gastric ESD for gastric adenoma or early gastric cancer has yet to be clarified, and there are many facilities that do not perform colonoscopy for such patients.

In the present study, we determined the prevalence of synchronous colorectal neoplasms in patients undergoing gastric ESD and compared this prevalence with the prevalence in patients with positive fecal occult blood test results to assess the usefulness of screening colonoscopy for patients undergoing gastric ESD. The risk factors for colorectal neoplasms in patients undergoing gastric ESD were also assessed.

MATERIALS AND METHODS

Enrollment of patients

Of the 263 patients who underwent ESD for gastric adenoma or early gastric cancer at the Department of Gastroenterology, Dokkyo Medical University, between May 2010 and December 2013, 172 patients receiving total colonoscopy (TCS) during a one-year period before and after ESD were targeted. None of these patients had familial adenomatous polyposis or inflammatory bowel disease. Seven patients who had undergone endoscopic resection of the large bowel in the past and 7 who had undergone colectomy were excluded. In total, 158 patients were included (ESD group) in this study. There were 130 men and 28 women. Of the 868 asymptomatic patients who underwent TCS during the same period because of positive fecal immunochemical test (FIT) results, we excluded those who had undergone endoscopic resection of the large bowel or colectomy in the past. Therefore, 158 randomly selected subjects who were matched for age and sex served as the control group

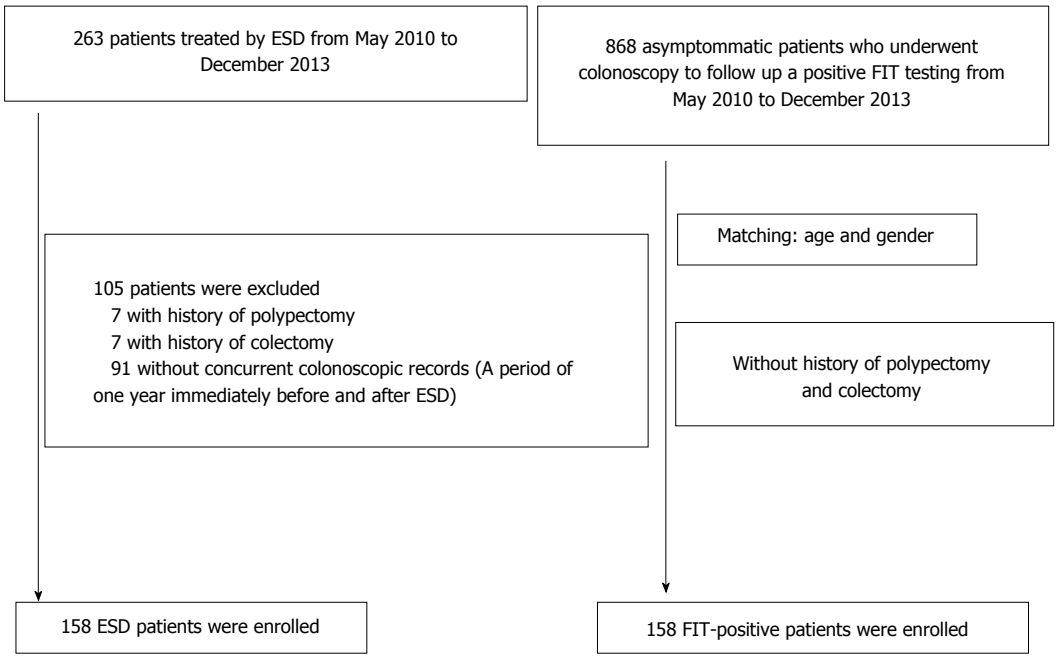

Figure 1 Design chart of this study. ESD: Endoscopic submucosal dissection; FIT: Fecal immunochemical test.

for comparison (FIT group) (Figure 1).

The study protocol was approved by the ethics committee of Dokkyo Medical University. Written informed consent was obtained from all participants before the procedures.

Definition of colorectal neoplasms

The number, size, and histology of colorectal neoplasms were examined. The number was assessed by dividing the patients into those with 1 to 3 neoplasms and those with 4 or more neoplasms. Sizes were determined employing biopsy forceps. Regarding histology, neoplasms measuring 6 mm or more were resected and pathologically assessed, in principle, whereas those measuring 5 mm or less were assessed by macroscopic evaluation including magnifying endoscopy. The pathological assessment was performed according to the Japanese classification of cancer of the colon and rectum[13], while magnifying endoscopy was performed according to the pit pattern and narrow band imaging classifications[14,15]. Non-neoplastic polyps, such as inflammatory and hyperplastic polyps, were excluded. Neoplasms were classified into low grade adenoma measuring less than 10 mm, advanced adenoma (adenoma measuring 10 mm or more, adenoma containing villous components, and adenoma with high-grade dysplasia), early cancer (cancer with infiltration limited to the mucosa or submucosa), advanced cancer (cancer with infiltration reaching the proper muscular layer), and neuroendocrine tumors.

Data collection

For each patient, electronic and paper medical records were reviewed in terms of history of treatment and surgery, endoscopic findings, images, and pathological findings. To identify risk factors for colorectal neoplasms, benign *vs* malignant neoplasms, neoplasm diameter, neoplasm site, sex, age, body mass index (BMI), history of cancer, underlying diseases (hypertension, diabetes mellitus, and dyslipidemia), and lifestyle history (smoking and drinking history) were assessed. Whether gastric lesions were benign or malignant was determined by differentiating between adenoma and cancer according to the histopathological results. The sites of gastric neoplasms were classified into 3 regions. The upper (U) region was defined as the cardia, fundus, and proximal third of the body of the stomach. The middle (M) region was defined as the distal two-thirds of the body and the angle of the stomach. The lower (L) region was defined as the vestibule and anterior part of the pylorus. BMI was calculated by dividing the weight by the square of the height. Levels of cholesterol, triglyceride, and fasting blood glucose were measured with autoanalyzers. Hypertension was defined as a systolic blood pressure of 140 mmHg or more and/or a diastolic blood pressure of 90 mmHg or more. Diabetes mellitus was defined as a fasting blood glucose level of 126 mg/dL or more, a 2-h level of 200 mg/dL or more on 75-g glucose tolerance test, or a casual blood glucose level of 200 mg/dL or more. Dyslipidemia was defined as a low-density lipoprotein (LDL) cholesterol level of more than 140, a high-density lipoprotein (HDL) cholesterol level of less than 45, and a triglyceride level of more than 150. For smoking history, patients currently or previously smoking 10 cigarettes or more per day for 5 years were regarded as having a smoking history, and all others were considered as having no smoking history. For alcohol consumption history, patients who were current or former non-drinkers or social drinkers

Table 1 Prevalence of colorectal neoplasm in the endoscopic submucosal dissection group *n* (%)

Colorectal neoplasm	ESD group (*n* = 158)
Non-lesion	78 (49.4)
Adenoma (< 1 cm)	53 (33.5)
Advanced adenoma	17 (10.8)
Large tubular adenoma (⩾ 1 cm)	
Tubulovillous/villous adenoma	
High grade dysplasia	
Early cancer (depth of mucosa/submucosa)	5 (3.2)
Advanced cancer	4 (2.5)
Neuroendocrine tumor	1 (0.6)

ESD: Endoscopic submucosal dissection.

Table 2 Comparison of characteristics between endoscopic submucosal dissection group and fecal immunochemical test group *n* (%)

	ESD group (*n* = 158)	FIT group (*n* = 158)	*P* value
Age (year, mean ± SD)	69.5 ± 8.9	69.5 ± 8.9	0.999
Gender, male/female	130 (82.3)/ 28 (17.7)	130 (82.3)/ 28 (17.7)	0.999
BMI (kg/m^2)	23.0 ± 3.1	22.8 ± 3.4	0.589
Smoking	100 (63.0)	86 (54.4)	0.137
Alcohol	74 (46.8)	66 (41.8)	0.428
Diabetes mellitus	20 (12.7)	27 (17.1)	0.343
Dyslipidemia	25 (15.8)	40 (25.3)	0.051
Hypertension	73 (46.2)	88 (55.7)	0.115
History of other organs' cancer	24 (15.2)	17 (10.8)	0.315

ESD: Endoscopic submucosal dissection; FIT: Fecal immunochemical test; BMI: Body mass index.

only were regarded as having no drinking history, and all others were considered as having a drinking history.

Statistical analysis

Univariate analyses were performed for each parameter. Student's *t*-test was used for age, neoplasm diameter, and BMI. For the other parameters, the χ^2 test was performed, except for those with an expected value of 5 or less, for which the Fisher exact test was used. Multivariate analyses for independent risk factors for overall colorectal neoplasms or for advanced adenoma and carcinoma were performed by logistic regression. Odds ratios (OR) and 95%CI were calculated for each variable. A statistically significant difference was defined as a *P* value of less than 0.05.

RESULTS

In the ESD group undergoing TCS, adenoma less than 10 mm was detected in 53 patients (33.6%), advanced adenoma in 17 (10.8%), early colorectal cancer in 5 (3.2%), advanced colorectal cancer in 4 (2.5%), and a rectal neuroendocrine tumor (NET) in 1 (0.6%) (Table 1).

Regarding clinicopathological characteristics, no difference was observed between the ESD and FIT groups (Table 2). These two groups were compared for the presence or absence of adenoma less than 10 mm, advanced adenoma, colorectal cancer or NET, and the number of adenomas. Adenoma less than 10 mm was observed in 33.5% of patients in the ESD group and in 41.8% of those in the FIT group. Patients with 1 to 3 adenomas accounted for 37.3% of the ESD group and 44.9% of the FIT group, whereas those with 4 adenomas or more accounted for 7.0% and 12.0%, respectively. Advanced adenoma was observed in 10.8% of patients in the ESD group and 15.2% of those in the FIT group, while colorectal cancer or NET was observed in 6.3% of patients in both groups. Because there were no statistically significant differences among the types of neoplasms, the ESD group was assumed to have a colorectal neoplasm risk equal to that of the FIT group (Table 3).

Table 3 Comparison of prevalence of colorectal neoplasm between endoscopic submucosal dissection group and fecal immunochemical test group *n* (%)

Colorectal neoplasm	ESD group (*n* = 158)	FIT group (*n* = 158)	*P* value
Adenoma (< 1 cm)	53 (33.5)	66 (41.8)	0.164
Advanced adenoma	17 (10.8)	24 (15.2)	0.315
Large tubular adenoma (⩾ 1 cm)			
Tubulovillous/villous adenoma			
High grade dysplasia			
Number of adenomas			0.507
1 to 3	59 (37.3)	71 (44.9)	
⩾ 4	11 (7.0)	19 (12.0)	
Cancer or NET	10 (6.3)	10 (6.3)	0.999

ESD: Endoscopic submucosal dissection; FIT: Fecal immunochemical test; NET: Neuroendocrine tumor.

When benign *vs* malignant neoplasms, neoplasm diameter, neoplasm site, sex, age, BMI, history of cancer, underlying disorders (hypertension, diabetes mellitus, and dyslipidemia), and tobacco and alcohol consumption were assessed to identify risk factors for colorectal neoplasms in the ESD group, it was evident that colorectal neoplasms were more common in men than in women ($P = 0.031$) (Table 4). Regarding the risk factors for advanced adenoma and carcinoma in the ESD group, the risk was significantly higher in patients with at least two of the following conditions: hypertension, dyslipidemia, and diabetes mellitus (life related disease, $P = 0.019$) (Table 5).

We also performed multivariate analyses correcting for gender and life related disease, which have significant differences in univariate analyses, age and BMI, which are well known as risk factors of colorectal carcinoma. These analyses showed that male sex was the independent risk factor for colorectal neoplasm (OR = 2.65, 95%CI: 1.11-6.36, $P = 0.029$) and that life related disease was the independent risk factor for

Table 4 Analysis of risk factors related to colorectal neoplasm in gastric endoscopic submucosal dissection patients *n* (%)

	CRN group (*n* = 80)	Non-CRN group (*n* = 78)	*P* value
Gender, male/female	71 (88.8)/ 9 (11.3)	59 (75.6)/ 19 (24.4)	0.031
Age (yr, mean ± SD)	70.8 ± 8.3	68.9 ± 10.4	0.215
Histopathology (adenoma/ carcinoma)	69 (86.3)/ 11 (13.8)	70 (89.7)/ 8 (10.3)	0.667
Tumor size (mm, mean ± SD)	19.3 ± 12.3	19.0 ± 17.2	0.926
Tumor location			
U	17 (21.3)	16 (20.5)	0.999
M	33 (41.3)	28 (35.9)	0.598
L	30 (37.5)	34 (43.6)	0.538
BMI	23.3 ± 3.3	22.7 ± 2.8	0.219
Lifestyle related disease[1]	16 (20.0)	13 (16.7)	0.737
Smoking	55 (68.8)	45 (57.7)	0.202
Alcohol	41 (51.3)	33 (42.3)	0.334
History of other organs' cancer	16 (20.0)	9 (11.5)	0.215

[1]The lifestyle related disease is one that is suffering from two or three of hypertension and dyslipidemia and diabetes mellitus. ESD: Endoscopic submucosal dissection; CRN: Colorectal neoplasm; BMI: body mass index.

Table 5 Analysis of risk factors related to advanced adenoma and carcinoma in gastric endoscopic submucosal dissection patients

	AAC group (*n* = 26)	Non-AAC group (*n* = 132)	*P* value
Gender, male/female	23 (88.5)/ 3 (11.5)	107 (81.1)/ 25 (18.9)	0.574
Age (yr, mean ± SD)	70.4 ± 8.5	69.7 ± 9.6	0.732
Histopathology (adenoma/ carcinoma)	6 (23.1)/ 20 (76.9)	13 (9.85/ 119 (90.2)	0.117
Tumor size (mm, mean ± SD)	21.9 ± 12.5	18.6 ± 12.7	0.305
Tumor location			
U	4 (15.4)	29 (22.0)	0.601
M	13 (50.0)	48 (36.4)	0.278
L	9 (34.6)	55 (41.7)	0.652
BMI	23.9 ± 3.8	22.8 ± 2.9	0.074
Lifestyle related disease[1]	9 (34.6)	20 (15.2)	0.019
Smoking	20 (76.9)	80 (60.6)	0.175
Alcohol	15 (57.7)	59 (44.7)	0.318
History of other organs' cancer	6 (23.1)	19 (14.4)	0.415

[1]The lifestyle related disease is one that is suffering from two or three of hypertension and dyslipidemia and diabetes mellitus. ESD: Endoscopic submucosal dissection; AAC: Advanced adenoma and carcinoma; BMI: Body mass index.

advanced adenoma and carcinoma in the ESD group (OR = 3.01, 95%CI: 1.16-7.86, *P* = 0.024) (Table 6).

Table 6 Multivariate logistic regression analyses for risk ratio of overall colorectal neoplasm, and advanced adenoma and carcinoma in gastric endoscopic submucosal dissection patients

	Overall colorectal neoplasm		AAC	
	OR (95%CI)	*P* value	OR (95%CI)	*P* value
Age (≥ 65 yr)	1.42 (0.68-3.00)	0.350	0.70 (0.27-1.82)	0.460
Gender (male)	2.65 (1.11-6.36)	0.029	1.85 (0.49-6.97)	0.362
BMI (≥ 25)	1.21 (0.57-2.56)	0.613	1.80 (0.71-4.58)	0.217
Lifestyle related disease[1]	1.24 (0.54-2.85)	0.608	3.01 (1.16-7.86)	0.024

[1]The lifestyle related disease is one that is suffering from two or three of hypertension and dyslipidemia and diabetes mellitus. ESD: Endoscopic submucosal dissection; AAC: Advanced adenoma and carcinoma; BMI: Body mass index.

DISCUSSION

In the present study, colorectal neoplastic lesions were observed in 50.6% of patients in the ESD group undergoing TCS, including advanced adenoma in 10.8% and colorectal cancer in 5.7%. It has been reported that in patients who underwent operations for gastric malignancies including advanced gastric cancer, preoperative TCS detects colorectal cancer in approximately 5% and colorectal adenoma in approximately 40%[16,17]. These rates are essentially consistent with the results of our present study targeting only early gastric cancer and gastric adenoma. Recently, a small number of studies have assessed the risk of colorectal neoplasms in patients undergoing gastric ESD. Kim *et al*[18], who examined 416 patients (123 with gastric adenoma and 293 with gastric cancer) undergoing gastric ESD, reported that colorectal lesions were observed in 50.2% of their patients including 9.4% with advanced adenoma and 1.4% with colorectal cancer. Lee *et al*[19], who examined 107 patients (54 with gastric adenoma and 53 with gastric cancer) undergoing gastric ESD, reported that colorectal lesions were observed in 56.1% of their patients, including 26.2% with high-risk colorectal neoplasms (advanced adenoma and adenocarcinoma). Moreover, Joo *et al*[20], in a study of 186 patients (81 with gastric adenoma and 105 with gastric cancer) undergoing gastric ESD, found that colorectal lesions were observed in 40.9%, including 15.6% with advanced adenoma and 4.3% with colorectal cancer. These results are consistent with ours, suggesting that the prevalence of colorectal neoplastic lesions including colorectal cancer is high even in patients undergoing gastric ESD for gastric lesions other than advanced cancer.

While the risk of colorectal neoplasms was assessed by comparison to healthy volunteers in past studies, we herein assessed the risk by comparison to FIT-positive patients who were matched for age and sex. The fecal occult blood test is a noninvasive method that is widely used for colorectal cancer screening. While this test could be performed employing chemical or immunological methods, the latter method is commonly used in Japan. The ESD and FIT groups, which did not differ in clinicopathological characteristics, showed no significant differences in detection rates of adenoma (33.5% *vs* 41.8%), advanced adenoma (10.8% *vs* 15.2%), and cancer (5.7% *vs* 6.3%), or

in the number of adenomas (1-3 adenomas, 37.3% *vs* 44.9%; ⩾ 4 adenomas, 7.0% *vs* 12.0%). We can reasonably assume that the ESD group has a risk of developing colorectal neoplasms equivalent to that of the FIT group. According to past reports, the detection rates of colorectal neoplasms in FIT-positive patients are approximately 30%, 10% and 1% for adenoma, advanced adenoma, and cancer[21,22], respectively, *i.e.*, slightly lower than the rates in the our FIT group. Because the FIT group was matched to the ESD group for age and sex in the present study, the mean age of the FIT group was approximately 70 years, and approximately 80% were men. On the other hand, in past reports, the mean age of FIT-positive patients was lower, at approximately 60 years, and the proportion of men was also smaller, at approximately 50%. A possible reason for the differences in the detection rates might be that our study included patients with a higher risk of colorectal cancer.

There are several possible explanations for the association between gastric and colorectal neoplasms. In patients with colorectal neoplasms, the rate of infection with *Helicobacter pylori* (*H. pylori*) is reportedly high[23]. It has been indicated that *H. pylori* infection may promote the development of colorectal cancer through increased secretion of gastrin[24]. Moreover, there might be effects of vacuolating cytotoxin A and cytotoxin-associated gene-A protein, which are frequently detected in patients with colorectal cancer[25]. There is a study in which the risk of colorectal neoplasms was assessed according to types of gastric neoplasms, which were classified into adenoma, intestinal-type cancer, and diffuse-type cancer. Although no difference was detected in the morbidity of colorectal lesions between adenoma and intestinal-type cancer, morbidity was found to be significantly lower in patients with diffuse-type cancer[18]. There is strong evidence for the association of *H. pylori* infection with gastric adenoma and intestinal-type cancer, and this result appears to support the association between colorectal neoplasms and *H. pylori* infection. Abnormalities in genes, such as P53, APC (adenomatous polyposis coli), DCC (deleted in colorectal carcinoma), and K-ras, are also known to be associated with development of gastrointestinal cancer of both the stomach and the large bowel[26-28]. In addition, microsatellite instability was reported to frequently be observed in synchronous multiple gastrointestinal cancers[29]. Although these genetic abnormalities could reasonably be speculated to affect the association between gastric and colorectal neoplasms, reports of studies on these abnormalities remain limited. This issue merits further investigation.

In the present analysis of risk factors for colorectal neoplasms, sex was the only significant risk factor in the ESD group. Colorectal neoplasms were significantly more common in men than in women. Schoenfeld *et al*[30], who examined more than 50000 participants in a colorectal cancer screening program using colonoscopy, reported that colorectal neoplasia was detected at a 73% higher frequency in men than in women. Moreover, male gender is also considered an important predictor of colorectal adenomatous polyps[31]. Because there are several reports similar to that of Schoenfeld *et al*[30], we are confident that our current results are valid[32,33]. Although the analysis of patients with advanced adenoma and carcinoma revealed no clearly significant difference according to sex, the prevalence of these conditions tended to be higher in men. It was assumed that the small number of patients might have accounted for the lack of a significant difference. Although no significant differences were detected when the hypertension, dyslipidemia, and diabetes mellitus parameters were examined separately, advanced adenoma and carcinoma were significantly more common in patients with at least two of these conditions. Jinjuvadia *et al*[34] conducted a systematic review and meta-analysis, showing the risk of colorectal neoplasia to be increased by 34% in patients with metabolic syndrome. Moreover, Park *et al*[35], who conducted a study of 492 patients with gastric neoplasm, reported that synchronous colorectal neoplasm was 1.96 times more frequent in patients with metabolic syndrome. These reports appear to provide support for the results of our present study. Our results suggest that abdominal circumference, which is a diagnostic criterion for metabolic syndrome, might not be a risk factor for advanced adenoma and carcinoma. In our view, the effects of abdominal circumference should be clarified by future studies. Meanwhile, our study revealed no significant difference in age, which is known to be a major risk factor for colorectal adenoma and cancer. A preceding report describing a systematic review and meta-analysis showed that the risk of colorectal neoplasms increases in individuals aged 65 years or older who are otherwise at average risk[36]. However, because the present study included patients with a mean age of 69.5 years who underwent ESD, the reason for age not being identified as a risk factor in the present study was assumed to be the inclusion of elderly patients.

The limitations of the present study include, the single-center retrospective study design, which might involve selection bias. To reduce this bias as much as possible, age-matched and sex-matched FIT-positive patients were randomly selected. Moreover, patients with a history of colorectal treatment interventions, such as polypectomy and colectomy, were excluded. Other limitations include the fact that patients with small, untreated, previously detected colorectal adenomas were included in the present study, and that factors that have been reported to affect the development of colorectal neoplasm (*e.g.*, diet, exercise, nonsteroidal anti-inflammatory drugs, and other chemopreventive agents) were not assessed.

The frequency of detecting colorectal lesions, especially advanced adenoma and carcinoma, was

higher in patients with early gastric cancer or gastric adenoma. This observation indicates that such patients are at a risk equivalent to that of FIT-positive patients, suggesting that screening colonoscopy should be performed as extensively as feasible in patients undergoing ESD. Most notably, greater caution appears to be warranted in patients with at least two of the following risk factors: hypertension, dyslipidemia, and diabetes mellitus. The frequencies of advanced adenoma and cancer are significantly increased in these patients. In the future, multicenter prospective studies need to be conducted to assess the results of our present investigation.

COMMENTS

Background

Gastric cancer mortality rate is very low after endoscopic resection of gastric neoplasms. To further improve outcomes, screening for neoplasms in other organs is assumed to be important. Colorectal neoplasms are the most commonly observed tumors outside of the stomach in patients with gastric cancer. Screening colonoscopy before surgical interventions for the stomach is now well established.

Research frontiers

There are few studies that assessed the risk of colorectal neoplasms in patients undergoing gastric endoscopic submucosal dissection (ESD). Therefore, the usefulness of screening colonoscopy in patients undergoing gastric ESD for gastric adenoma or early gastric cancer has yet to be clarified.

Innovations and breakthroughs

The frequency of detecting colorectal lesions, especially advanced adenoma and carcinoma, was higher in patients with early gastric cancer or gastric adenoma. This observation indicates that such patients are at a risk equivalent to that of fecal immunochemical test positive patients, suggesting that screening colonoscopy should be performed as extensively as possible in patients undergoing ESD.

Applications

This study will contribute to the reduction of colorectal cancer deaths in patients undergoing gastric ESD.

Terminology

ESD has been established as a common curative resection procedure for gastric neoplasms, including early gastric cancer and gastric adenoma. As the adoption of this procedure becomes ever more widespread, indications for endoscopic therapy are being expanded.

Peer-review

This is well designed and performed study with important clinical and epidemiological information.

REFERENCES

1 **Oda I**, Gotoda T, Hamanaka H, Eguchi T, Saito Y, Matsuda T, Bhandari P, Emura F, Saito D, Ono H. Endoscopic submucosal dissection for early gastric cancer: technical feasibility, operation time and complications from a large consecutive series. *Dig Endosc* 2005; **17**: 54-58 [DOI: 10.1111/j.1443-1661.2005.00459.x]

2 **Isomoto H**, Shikuwa S, Yamaguchi N, Fukuda E, Ikeda K, Nishiyama H, Ohnita K, Mizuta Y, Shiozawa J, Kohno S. Endoscopic submucosal dissection for early gastric cancer: a large-scale feasibility study. *Gut* 2009; **58**: 331-336 [PMID: 19001058 DOI: 10.1136/gut.2008.165381]

3 **Facciorusso A**, Antonino M, Di Maso M, Muscatiello N. Endoscopic submucosal dissection vs endoscopic mucosal resection for early gastric cancer: A meta-analysis. *World J Gastrointest Endosc* 2014; **6**: 555-563 [PMID: 25400870 DOI: 10.4253/wjge.v6.i11.555]

4 **Gotoda T**, Yanagisawa A, Sasako M, Ono H, Nakanishi Y, Shimoda T, Kato Y. Incidence of lymph node metastasis from early gastric cancer: estimation with a large number of cases at two large centers. *Gastric Cancer* 2000; **3**: 219-225 [PMID: 11984739]

5 **Sugimoto T**, Okamoto M, Mitsuno Y, Kondo S, Ogura K, Ohmae T, Mizuno H, Yoshida S, Isomura Y, Yamaji Y, Kawabe T, Omata M, Koike K. Endoscopic submucosal dissection is an effective and safe therapy for early gastric neoplasms: a multicenter feasible study. *J Clin Gastroenterol* 2012; **46**: 124-129 [PMID: 21959325 DOI: 10.1097/MCG.0b013e31822f3988]

6 **Emura F**, Mejía J, Donneys A, Ricaurte O, Sabbagh L, Giraldo-Cadavid L, Oda I, Saito Y, Osorio C. Therapeutic outcomes of endoscopic submucosal dissection of differentiated early gastric cancer in a Western endoscopy setting (with video). *Gastrointest Endosc* 2015; **82**: 804-811 [PMID: 25952087 DOI: 10.1016/j.gie.2015.03.1960]

7 **Tanabe S**, Ishido K, Higuchi K, Sasaki T, Katada C, Azuma M, Naruke A, Kim M, Koizumi W. Long-term outcomes of endoscopic submucosal dissection for early gastric cancer: a retrospective comparison with conventional endoscopic resection in a single center. *Gastric Cancer* 2014; **17**: 130-136 [PMID: 23576197 DOI: 10.1007/s10120-013-0241-2]

8 **Oda I**, Oyama T, Abe S, Ohnita K, Kosaka T, Hirasawa K, Ishido K, Nakagawa M, Takahashi S. Preliminary results of multicenter questionnaire study on long-term outcomes of curative endoscopic submucosal dissection for early gastric cancer. *Dig Endosc* 2014; **26**: 214-219 [PMID: 23826719 DOI: 10.1111/den.12141]

9 **Sung JJ**, Lau JY, Goh KL, Leung WK; Asia Pacific Working Group on Colorectal Cancer. Increasing incidence of colorectal cancer in Asia: implications for screening. *Lancet Oncol* 2005; **6**: 871-876 [PMID: 16257795 DOI: 10.1016/S1470-2045(05)70422-8]

10 **Tamura K**, Ishiguro S, Munakata A, Yoshida Y, Nakaji S, Sugawara K. Annual changes in colorectal carcinoma incidence in Japan. Analysis of survey data on incidence in Aomori Prefecture. *Cancer* 1996; **78**: 1187-1194 [PMID: 8826939 DOI: 10.1002/(SICI)1097-0142(19960915)78:6]

11 **Eom BW**, Lee HJ, Yoo MW, Cho JJ, Kim WH, Yang HK, Lee KU. Synchronous and metachronous cancers in patients with gastric cancer. *J Surg Oncol* 2008; **98**: 106-110 [PMID: 18452218 DOI: 10.1002/jso.21027]

12 **Lee JH**, Bae JS, Ryu KW, Lee JS, Park SR, Kim CG, Kook MC, Choi IJ, Kim YW, Park JG, Bae JM. Gastric cancer patients at high-risk of having synchronous cancer. *World J Gastroenterol* 2006; **12**: 2588-2592 [PMID: 16688807 DOI: 10.3748/wjg.v12.i16.2588]

13 **Japanese Research Society for Cancer of the Colon and Rectum**. General Rules for Clinical and Pathological Studies on Cancer of the Colon, Rectum and Anus: Histopathological Classification, 6th ed. Tokyo: Kanehara Syuppan, 1998: 60-90

14 **Kudo S**, Rubio CA, Teixeira CR, Kashida H, Kogure E. Pit pattern in colorectal neoplasia: endoscopic magnifying view. *Endoscopy* 2001; **33**: 367-373 [PMID: 11315901 DOI: 10.1055/s-2004-826104]

15 **Hewett DG**, Kaltenbach T, Sano Y, Tanaka S, Saunders BP, Ponchon T, Soetikno R, Rex DK. Validation of a simple classification system for endoscopic diagnosis of small colorectal polyps using narrow-band imaging. *Gastroenterology* 2012; **143**: 599-607.e1 [PMID: 22609383 DOI: 10.1053/j.gastro.2012.05.006]

16 **Saito S**, Hosoya Y, Togashi K, Kurashina K, Haruta H, Hyodo M, Koinuma K, Horie H, Yasuda Y, Nagai H. Prevalence of synchronous colorectal neoplasms detected by colonoscopy in patients with gastric cancer. *Surg Today* 2008; **38**: 20-25 [PMID: 18085357 DOI: 10.1007/s00595-007-3567-8]

17 **Suzuki A**, Koide N, Takeuchi D, Okumura M, Ishizone S, Suga T, Miyagawa S. Prevalence of synchronous colorectal neoplasms in surgically treated gastric cancer patients and significance of screening colonoscopy. *Dig Endosc* 2014; **26**: 396-402 [PMID: 23967873 DOI: 10.1111/den.12156]

18 **Kim SY**, Jung SW, Hyun JJ, Koo JS, Choung RS, Yim HJ, Lee SW, Choi JH. Is colonoscopic screening necessary for patients with gastric adenoma or cancer? *Dig Dis Sci* 2013; **58**: 3263-3269 [PMID: 23955386 DOI: 10.1007/s10620-013-2824-5]

19 **Lee KJ**, Kim JH, Kim SI, Jang JH, Lee HH, Hong SN, Lee SY, Sung IK, Park HS, Shim CS, Han HS. Clinical significance of colonoscopic examination in patients with early stage of gastric neoplasm undergoing endoscopic submucosal dissection. *Scand J Gastroenterol* 2011; **46**: 1349-1354 [PMID: 21905975 DOI: 10.3109/00365521.2011.613948]

20 **Joo MK**, Park JJ, Lee WW, Lee BJ, Hwang JK, Kim SH, Jung W, Kim JH, Yeon JE, Kim JS, Byun KS, Bak YT. Differences in the prevalence of colorectal polyps in patients undergoing endoscopic removal of gastric adenoma or early gastric cancer and in healthy individuals. *Endoscopy* 2010; **42**: 114-120 [PMID: 20140828 DOI: 10.1055/s-0029-1243875]

21 **Hundt S**, Haug U, Brenner H. Comparative evaluation of immunochemical fecal occult blood tests for colorectal adenoma detection. *Ann Intern Med* 2009; **150**: 162-169 [PMID: 19189905]

22 **de Wijkerslooth TR**, Stoop EM, Bossuyt PM, Meijer GA, van Ballegooijen M, van Roon AH, Stegeman I, Kraaijenhagen RA, Fockens P, van Leerdam ME, Dekker E, Kuipers EJ. Immunochemical fecal occult blood testing is equally sensitive for proximal and distal advanced neoplasia. *Am J Gastroenterol* 2012; **107**: 1570-1578 [PMID: 22850431 DOI: 10.1038/ajg.2012.249]

23 **Meucci G**, Tatarella M, Vecchi M, Ranzi ML, Biguzzi E, Beccari G, Clerici E, de Franchis R. High prevalence of Helicobacter pylori infection in patients with colonic adenomas and carcinomas. *J Clin Gastroenterol* 1997; **25**: 605-607 [PMID: 9451672]

24 **Nakatsuru S**, Yanagisawa A, Ichii S, Tahara E, Kato Y, Nakamura Y, Horii A. Somatic mutation of the APC gene in gastric cancer: frequent mutations in very well differentiated adenocarcinoma and signet-ring cell carcinoma. *Hum Mol Genet* 1992; **1**: 559-563 [PMID: 1338691]

25 **Shmuely H**, Passaro D, Figer A, Niv Y, Pitlik S, Samra Z, Koren R, Yahav J. Relationship between Helicobacter pylori CagA status and colorectal cancer. *Am J Gastroenterol* 2001; **96**: 3406-3410 [PMID: 11774957 DOI: 10.1111/j.1572-0241.2001.05342.x]

26 **Uchino S**, Noguchi M, Ochiai A, Saito T, Kobayashi M, Hirohashi S. p53 mutation in gastric cancer: a genetic model for carcinogenesis is common to gastric and colorectal cancer. *Int J Cancer* 1993; **54**: 759-764 [PMID: 8392033]

27 **Uchino S**, Tsuda H, Noguchi M, Yokota J, Terada M, Saito T, Kobayashi M, Sugimura T, Hirohashi S. Frequent loss of heterozygosity at the DCC locus in gastric cancer. *Cancer Res* 1992; **52**: 3099-3102 [PMID: 1591722]

28 **Robertson DJ**, Sandler RS, Ahnen DJ, Greenberg ER, Mott LA, Cole BF, Baron JA. Gastrin, Helicobacter pylori, and colorectal adenomas. *Clin Gastroenterol Hepatol* 2009; **7**: 163-167 [PMID: 18929688 DOI: 10.1016/j.cgh.2008.09.006]

29 **Ohtani H**, Yashiro M, Onoda N, Nishioka N, Kato Y, Yamamoto S, Fukushima S, Hirakawa-Ys Chung K. Synchronous multiple primary gastrointestinal cancer exhibits frequent microsatellite instability. *Int J Cancer* 2000; **86**: 678-683 [PMID: 10797290]

30 **Schoenfeld P**, Cash B, Flood A, Dobhan R, Eastone J, Coyle W, Kikendall JW, Kim HM, Weiss DG, Emory T, Schatzkin A, Lieberman D. Colonoscopic screening of average-risk women for colorectal neoplasia. *N Engl J Med* 2005; **352**: 2061-2068 [PMID: 15901859 DOI: 10.1056/NEJMoa042990]

31 **Rex DK**. Colonoscopy: a review of its yield for cancers and adenomas by indication. *Am J Gastroenterol* 1995; **90**: 353-365 [PMID: 7872270]

32 **Imperiale TF**, Wagner DR, Lin CY, Larkin GN, Rogge JD, Ransohoff DF. Risk of advanced proximal neoplasms in asymptomatic adults according to the distal colorectal findings. *N Engl J Med* 2000; **343**: 169-174 [PMID: 10900275 DOI: 10.1056/NEJM200007203430302]

33 **Regula J**, Rupinski M, Kraszewska E, Polkowski M, Pachlewski J, Orlowska J, Nowacki MP, Butruk E. Colonoscopy in colorectal-cancer screening for detection of advanced neoplasia. *N Engl J Med* 2006; **355**: 1863-1872 [PMID: 17079760 DOI: 10.1056/NEJMoa054967]

34 **Jinjuvadia R**, Lohia P, Jinjuvadia C, Montoya S, Liangpunsakul S. The association between metabolic syndrome and colorectal neoplasm: systemic review and meta-analysis. *J Clin Gastroenterol* 2013; **47**: 33-44 [PMID: 23090040 DOI: 10.1097/MCG.0b013e3182688c15]

35 **Park W**, Lee H, Kim EH, Yoon JY, Park JC, Shin SK, Lee SK, Lee YC, Kim WH, Noh SH. Metabolic syndrome is an independent risk factor for synchronous colorectal neoplasm in patients with gastric neoplasm. *J Gastroenterol Hepatol* 2012; **27**: 1490-1497 [PMID: 22432868 DOI: 10.1111/j.1440-1746.2012.07128.x]

36 **Heitman SJ**, Ronksley PE, Hilsden RJ, Manns BJ, Rostom A, Hemmelgarn BR. Prevalence of adenomas and colorectal cancer in average risk individuals: a systematic review and meta-analysis. *Clin Gastroenterol Hepatol* 2009; **7**: 1272-1278 [PMID: 19523536 DOI: 10.1016/j.cgh.2009.05.032]

P- Reviewer: Facciorusso A, Seow-Choen F, Vujasinovic M
S- Editor: Gong ZM **L- Editor**: A **E- Editor**: Wang CH

World Journal of Gastroenterology

Submit a Manuscript: http://www.f6publishing.com

World J Gastroenterol 2017 June 21; 23(23): 4270-4277

DOI: 10.3748/wjg.v23.i23.4270

ISSN 1007-9327 (print) ISSN 2219-2840 (online)

ORIGINAL ARTICLE

Retrospective Study

Outcomes of right-lobe and left-lobe living-donor liver transplantations using small-for-size grafts

Wong Hoi She, Kenneth SH Chok, James YY Fung, Albert CY Chan, Chung Mau Lo

Wong Hoi She, Department of Surgery, the University of Hong Kong, Hong Kong, China

Kenneth SH Chok, Albert CY Chan, Chung Mau Lo, Department of Surgery and State Key Laboratory for Liver Research, The University of Hong Kong, Hong Kong, China

James YY Fung, Department of Medicine and State Key Laboratory for Liver Research, The University of Hong Kong, Hong Kong, China

Author contributions: She WH and Chok KSH contributed to study conception and design, and drafted the manuscript; She WH contributed to data acquisition, analysis and interpretation; Fung JYY, Chan ACY and Lo CM revised the article critically for important content; Lo CM gave final approval of the revised version; all authors approved the submitted version of the paper.

Conflict-of-interest statement: We have no financial relationships to disclose.

Data sharing statement: No additional data are available.

Manuscript source: Invited manuscript

Correspondence to: Kenneth SH Chok, MS, Associate Professor, Department of Surgery, the University of Hong Kong, 102 Pok Fu Lam Road, Hong Kong, China. kennethchok@gmail.com
Telephone: +852-22553025
Fax: +852-28165284

Received: January 24, 2017
Peer-review started: February 1, 2017
First decision: February 23, 2017
Revised: March 9, 2017
Accepted: May 19, 2017
Article in press: May 19, 2017
Published online: June 21, 2017

Abstract

AIM

To analyze the outcomes of living-donor liver transplantation (LDLT) using left-lobe (LL) or right-lobe (RL) small-for-size (SFS) grafts.

METHODS

Prospectively collected data of adult patients who underwent LDLT at our hospital in the period from January 2003 to December 2013 were reviewed. The patients were divided into the RL-LDLT group and the LL-LDLT group. The two groups were compared in terms of short- and long-term outcomes, including incidence of postoperative complication, graft function, graft survival, and patient survival. A SFS graft was defined as a graft with a ratio of graft weight (GW) to recipient standard liver volume (RSLV) (GW/RSLV) of < 50%. The Urata formula was used to estimate RSLV.

RESULTS

Totally 218 patients were included for analysis, with 199 patients in the RL-LDLT group and 19 patients in the LL-LDLT group. The two groups were similar in terms of age (median, 53 years in the RL-LDLT group and 52 years in the LL-LDLT group, $P = 0.997$) but had significantly different ratios of men to women (165:34 in the RL-LDLT group and 8:11 in the LL-LDLT group, $P < 0.0001$). The two groups were also significantly different in GW ($P < 0.0001$), GW/RSLV ($P < 0.0001$), and graft cold ischemic time ($P = 0.007$). When it comes to postoperative complication, the groups were comparable ($P = 0.105$). Five patients died in hospital,

4 (2%) in the RL-LDLT group and 1 (5.3%) in the LL-LDLT group (P = 0.918). There were 38 graft losses, 33 (16.6%) in the RL-LDLT group and 5 (26.3%) in the LL-LDLT group (P = 0.452). The 5-year graft survival rate was significantly better in the RL-LDLT group (95.2% *vs* 89.5%, P = 0.049). The two groups had similar 5-year patient survival rates (RL-LDLT: 86.8%, LL-LDLT: 89.5%, P = 0.476).

CONCLUSION

The use of SFS graft in LDLT requires careful tailor-made surgical planning and meticulous operation. LL-LDLT can be a good alternative to RL-LDLT with similar recipient outcomes but a lower donor risk. Further research into different patient conditions is needed in order to validate the use of LL graft.

Key words: Small for size liver graft; Right lobe graft; Left lobe graft; Living donor liver transplantation

Core tip: Liver transplant has become an established treatment for liver failure. The use of living-donor liver graft is one important strategy to expand the donor pool. The use of left lobe graft remains controversial due to the potential problem of small-for-size syndrome. This study illustrates that the use of left lobe graft can produce outcomes similar to right lobe graft. However, the study contains selection bias since most of the recipients of left lobe grafts had relatively lower Model for End-stage Liver Disease scores and were women, who are lighter in weight. Therefore, further study should focus on the establishment of criteria for the use of left lobe graft to allow safe transplant.

She WH, Chok KSH, Fung JYY, Chan ACY, Lo CM. Outcomes of right-lobe and left-lobe living-donor liver transplantations using small-for-size grafts. *World J Gastroenterol* 2017; 23(23): 4270-4277 Available from: URL: http://www.wjgnet.com/1007-9327/full/v23/i23/4270.htm DOI: http://dx.doi.org/10.3748/wjg.v23.i23.4270

INTRODUCTION

Living-donor liver transplantation (LDLT) was first established as an excellent treatment method for children with end-stage liver disease[1-3]. The lack of cadaveric liver grafts in Asian countries has led to the development of LDLT using the left liver lobe (LL)[4] and the right liver lobe (RL)[5], which has increased the donor pool[6], allowing more patients to be transplanted. The LL is only approximately one-third of the whole liver[7] and thus is generally not adequate for a recipient whose body size is similar to or bigger than that of the donor. Hence the RL is more preferable. Nonetheless, donor right hepatectomy carries a mortality risk of 0.5% whereas it is only 0.1% in donor left hepatectomy[8]. The use of LL was once considered near abandonment because oftentimes it was insufficient for the metabolic demand of recipients, leading to small-for-size (SFS) syndrome. SFS syndrome is caused by a SFS graft, which is defined as a graft with a ratio of graft weight (GW) to recipient standard liver volume (RSLV) (GW/RSLV) of < 50%[9-11]. SFS syndrome describes the constellation of cholestasis, coagulopathy and ascites; it can progress to gastrointestinal bleeding and renal failure. Portal hypertension and sinusoidal injury may lead to graft failure[12,13]. With SFS syndrome, patient survival and graft survival after LDLT would be poor[9,14-16]. However, some studies of LL-LDLT did show promising results[17-21]. Although lowering graft size requirement increases recipient risks, it can improve the applicability of LL-LDLT and, mostly importantly, reduce donor risks[6]. This retrospective study aimed to analyze the outcomes of LDLTs using SFS grafts, be them LLs or RLs.

MATERIALS AND METHODS

Data of adult patients who underwent LDLT at our hospital in the period from January 2003 to December 2013 were reviewed. Donor and recipient operations were performed as described elsewhere[22]. The decision of using LL or RL was multifactorial - with donor and recipient factors all considered - but principally depended on Model for End-stage Liver Disease (MELD) score, GW/RSLV, the ratio of GW to recipient body weight, and donor liver anatomy. In general, if the estimated volume of a LL exceeded 35% of the RSLV, LL would be used. However, graft selection was still decided on a case-by-case basis, with consideration of various factors including anatomical variation and recipient condition (MELD score). The bottom line was that the estimated volume of the future liver remnant of the donor must not be < 35% of the donor's total liver volume. Standard liver volume was calculated using the Urata formula [liver volume (mL) = body surface area (m^2) × 706.2 + 2.4][7]. If a RL graft contained the native middle hepatic vein, a single venous cuff would be constructed with a venoplasty of the middle and right hepatic veins[23] to enhance outflow capacity.

LL graft implantation was similar to RL graft implantation. The procedure was done without bypass. The common trunk of the left and middle hepatic veins was first anastomosed to the recipient inferior vena cava. The portal vein was then anastomosed to the recipient portal vein. Clamps were removed to allow revascularization. Hepatic arteries were always reconstructed under the microscope. As to the method of biliary reconstruction, hepaticojejunostomy was preferred in LL-LDLT whereas duct-to-duct anastomosis was preferred in RL-LDLT unless multiple ductal openings were encountered.

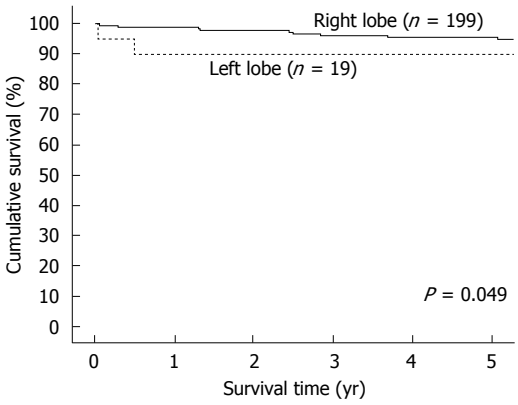

Figure 1 Comparison of graft survival.

Portal flow measurement and flow modulation

A venous cannula was inserted into the inferior mesenteric vein to measure the portal pressure, especially if the GW/RSLV was ⩽ 35%. The portal flow was to be maintained at 100-250 mL/min/100 g to prevent SFS syndrome. The use of splenic artery ligation and the use of ligation of spontaneous splenic renal shunt were determined intraoperatively.

Immunosuppression and prophylaxis regimens

Starting from January 2001, 20 mg of basiliximab was given intravenously within 6 h of graft reperfusion and on postoperative day 4. Steroid injection was given intraoperatively with 1 g of hydrocortisone and on postoperative day 1 with 500 mg of hydrocortisone. Immunosuppression was maintained with oral tacrolimus given within 12 h of transplant at a dosage of 0.15 mg/kg body weight/D, and the dose was titrated to achieve a trough level of 5-10 ng/mL. Mycophenolate mofetil at a dosage of 1-1.5 g/d was started within 48 h of transplant and was tapered off within 3 mo. Maintenance steroid was not given routinely. All recipients also orally took 200 mg of fluconazole and 480 mg of cotrimoxazole daily and 400 mg of acyclovir thrice a day for 3 mo for prophylaxis. For patients with renal dysfunction (a creatinine level before administration of tacrolimus twice the normal level), the tacrolimus trough level was kept at 3-5 ng/mL, and prednisolone at 20 mg/d was added. Pentamidine (300 mg) inhalation was given monthly for 3 mo to patients with renal impairment or glucose-6-phosphate dehydrogenase deficiency because the use of acyclovir or cotrimoxazole was prohibited[24]. For hepatitis B virus carriers and recipients of grafts donated by donors who had hepatitis core antibodies, nucleoside analogue monoprophylaxis (entecavir) was administered.

Statistical analysis

Patient data used in the study were prospectively collected. The patients were divided into the RL-LDLT group and the LL-LDLT group. For further analysis, they were divided into three groups according to GW/RSLV: ⩽ 35%, > 35%-40%, and > 40%-< 50%. The RL-LDLT and LL-LDLT groups were compared in terms of short- and long-term outcomes, including incidence of postoperative complication, graft function, graft survival, and patient survival. Recipient conditions were compared on postoperative day 7 and then yearly. Continuous variables were expressed as medians and interquartile ranges and compared by the Kruskal-Wallis test. Categorical variables were compared by Spearman's test. Survival rates were plotted as Kaplan-Meier curves and compared by log-rank analysis. Statistical significance was defined as $P < 0.05$. All statistical calculations were performed with SPSS, version 20.0 (SPSS, Chicago, IL, United States), by the statistician at the Department of Surgery, The University of Hong Kong.

RESULTS

From January 2003 to December 2013, 218 adults underwent LDLT with a GW/RSLV < 50%. Nineteen of them had LL-LDLT and 199 had RL-LDLT. The two groups of patients were similar in terms of age (median, 53 years in the RL-LDLT group and 52 years in the LL-LDLT group, $P = 0.997$) but had significantly different ratios of men to women (165:34 in the RL-LDLT group and 8:11 in the LL-LDLT group, $P < 0.0001$). The patients' diagnoses are shown in Table 1 and their perioperative details are shown in Table 2. The two groups of patients were significantly different in GW ($P < 0.0001$), GW/RSLV ($P < 0.0001$), and graft cold ischemic time ($P = 0.007$). Table 3 shows the patients' survival outcomes and postoperative complications, as well as the reasons for graft losses and the causes of deaths. The only one significant difference between the groups was graft survival ($P = 0.049$), which can also be viewed in Figure 1. Figure 2 is a Kaplan-Meier plot for patient survival of the series ($P = 0.476$).

Donor details can be found in Table 4. Like the patients, the two groups of donors were similar in terms of age (median, 34 years in the RL-LDLT group and 32 years in the LL-LDLT group, $P = 0.847$) but had significantly different ratios of men to women (39:160 in the RL-LDLT group and 16:3 in the LL-LDLT group, $P < 0.001$). When it comes to postoperative complication, the two groups of donors were comparable (16.6% in the RL-LDLT group and 5.3% in the LL-LDLT group, $P = 0.905$). One donor death occurred and it was in the RL-LDLT group (0.5% *vs* 0%, $P = 1$). The death was due to severe peptic ulcer disease resulting in aortoduodenal fistula.

On further analysis, patients with different GW/RSLV (⩽ 35% *vs* > 35%-40% *vs* > 40%- < 50%) were comparable in terms of graft survival and patient survival. No significant result was shown on multivariate analysis.

Table 1 Patients' demographic characteristics and diagnoses

	RL-LDLT (n = 199)	LL-LDLT (n = 19)	P value
Median age (yr) (range)	53 (17-72)	52 (17-67)	0.997
Male:Female	165:34	8:11	0.000
Diagnosis			
Liver cirrhosis			
Cryptogenic	3	1	
Hepatitis B virus infection	85	0	
Hepatitis C virus infection	15	5	
Alcohol	4	0	
Infection of hepatitis B and C viruses	2	0	
Alcohol + hepatitis C virus infection	3	0	
Alcohol + hepatitis B virus infection	1	0	
Chronic active hepatitis B	1	1	
Fulminant hepatic failure			
Cryptogenic	1	1	
Hepatitis B	2	0	
Autoimmune	1	0	
Drug-induced	3	1	
Biliary atresia	2	0	
Primary sclerosing cholangitis	0	1	
Primary biliary cirrhosis	2	1	
Graft failure	4	0	
Liver cirrhosis with acute deterioration			
Cryptogenic	2	0	
Hepatitis B	30	3	
Alcohol	1	0	
Autoimmune	1	0	
Wilson's disease	2	0	
Chronic active hepatitis with acute flare			
Hepatitis B	32	1	
Autoimmune	1	0	
Osler-Weber-Rendu syndrome	1	0	
Neuroendocrine syndrome	0	1	
Familial amyloid polyneuropathy	0	1	
Caroli disease	0	1	
Recurrent pyogenic cholangitis	0	1	
Hepatocellular carcinoma	83 (41.7%)	5 (26.3%)	0.191

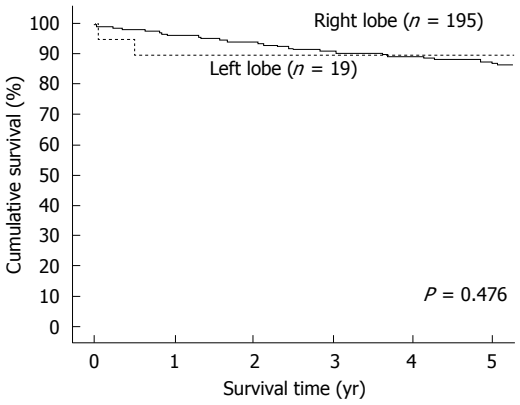

Figure 2 Comparison of patient survival.

DISCUSSION

Liver transplant has been documented as a life-saving treatment for liver failure and the result is remarkable[25]. However, the scarcity of liver grafts from deceased donors remains a major issue while the number of patients waiting for a liver transplant is rising[26,27]. The problem has led to not only the employment of LDLT but also the use of suboptimal liver grafts - grafts with mild steatosis and grafts from older donors, obese donors, and donors with a borderline small potential residual liver volume[28-31]. At our center, the use of RL for LDLT has been well established with satisfactory long-term graft survival and patient survival[32].

This study reviewed the outcomes of LDLT in patients who received a SFS graft. These patients were prone to SFS syndrome. SFS syndrome is defined by the presence of prolonged cholestasis, coagulopathy and ascites in the absence of ischemia within the first week of liver transplant caused by a partial liver graft that is inadequate to sustain metabolic demand in the recipient. The underlying reason for this is the presence of portal hypertension and graft size mismatch. This condition leads to a reduction in intrahepatic vascular bed with higher portal flow per gram of liver tissue, which leads to a rise in portal pressure and sinusoidal shear stress. Such stress may cause sinusoidal endothelial cell injury and provoke a sequence of hepatocellular damage and cell death[14,33,34], which is manifested by hepatocyte ballooning, steatosis, centrilobular necrosis and parenchymal cholestasis in the histology of the engrafted liver[35-37].

The current study found that SFS RL graft and SFS LL graft did not have much difference when patient survival is concerned - which echoes the results in the literature[38,39] - but the SFS RL grafts had better survival than the SFS LL grafts (P = 0.049). This study is a single-center retrospective study. At our center, RL-LDLT has been the standard for years whereas LL-LDLT, despite the technical similarity, is a relatively unfamiliar procedure, which is also reflected in the small number of patients in the LL-LDLT group. Probably we were still at the learning-curve phase in LL-LDLT. Furthermore, this group of patients underwent transplant for liver failure. In an acute condition (such as acute liver failure or fulminant liver failure), the patient would be very sick with a high MELD score. In the past, patients with high MELD scores were denied LDLT because it would be unwise to put donors in risk for recipient outcomes that would be inferior. However, studies have shown that LDLT can provide patients who have high MELD scores with excellent graft function and patient survival[24,40,41]. The preference for RL graft is due to the shorter cold ischemic time and, in general, greater liver mass. Furthermore, almost all RL grafts we used contained the middle hepatic vein. The inclusion of the middle hepatic vein in a graft allows better venous drainage of the graft and hence ensure good liver function to meet the metabolic demand even if the patient is in critical condition[42]. Therefore, the use of LL graft needs justification, especially in the face of acute liver failure. Having said that, LL graft

Table 2 Patients' perioperative details

	RL-LDLT (*n* = 199)	LL-LDLT (*n* = 19)	*P* value
Waiting time (d)	11 (1-1354)	16 (1-381)	0.190
Preoperative MELD score	20 (6-50)	14 (6-40)	0.184
GW (g)	530 (320-715)	410 (310-585)	0.000
GW/RSLV (%)	42.8 (28.4-46.998)	36.3 (27.3-46.96)	0.000
GW/RBW (%)	0.77 (0.46-1.03)	0.72 (0.49-1.04)	0.236
Graft cold ischemic time (min)	105 (53-243)	85 (69-134)	0.007
Recipient warm ischemic time (min)	51 (25-89)	45 (27-63)	0.088
Splenic artery ligation	0	0	-
Portosystemic shunt	0	0	-
Ligation of shunt	2 (1.0%)	0	1.000
Blood transfusion (units)	4 (0-39)	2 (0-14)	0.099
Fresh frozen plasma transfusion (units)	9 (0-38)	6 (0-23)	0.145
Platelet transfusion (units)	6 (0-32)	3 (0-22)	0.341
Operation time (min)	685 (400-1203)	670 (485-1273)	0.738
Intensive care unit stay (d)	4 (1-124)	6 (2-16)	0.055
Hospital stay (d)	17 (2-128)	23 (10-68)	0.072
Follow-up period (d)	86.9 (0.07-162.9)	133.7 (0.53-159.2)	0.054

Data are presented as median (range). MELD: Model for End-stage Liver Disease; GW: Graft weight; RSLV: Recipient standard liver volume; RBW: Recipient body weight; LDLT: Living-donor liver transplantation; LL: Left-lobe; RL: Right-lobe.

Table 3 Survival outcomes and postoperative complications in recipients *n* (%)

	RL-LDLT (*n* = 199)	LL-LDLT (*n* = 19)	*P* value
In-hospital death	4 (2)	1 (5.3)	0.918
Graft loss	33 (16.6)	5 (26.3)	0.452
Patient status - Alive:Dead	169:30	15:4	0.722
Graft survival			0.049
1-yr	98.50%	89.50%	
3-yr	95.80%	89.50%	
5-yr	95.20%	89.50%	
Patient survival			0.476
1-yr	95.90%	89.50%	
3-yr	90.80%	89.50%	
5-yr	86.80%	89.50%	
Postoperative complication[1]			0.105
No complication	92 (46.2)	7 (36.8)	
Grade 1	42 (21.1)	3 (15.8)	
Grade 2	21 (10.6)	0	
Grade 3a	19 (9.5)	5 (26.3)	
Grade 3b	14 (7.0)	3 (15.8)	
Grade 4a	7 (3.5)	0	
Grade 4b	2 (1.0)	0	
Grade 5	2 (1.0)	1 (5.3)	
Reason for graft loss			
Patient death	28	3	
Hepatic artery thrombosis	1	0	
Portal vein thrombosis	1	0	
PV/IVC thrombosis	1	0	
Recurrent Wilson's disease	1	0	
Biliary complication	0	1	
Reactivation of hepatitis C	0	1	
Rejection	1	0	
Cause of death			
Acute myocardial infarction	2	0	
Chronic rejection	1	0	
Unknown	2	0	
Invasive aspergillosis	1	0	
Malignant cachexia	16	0	
Sepsis/multiorgan failure	3	2	
Subarachnoid hemorrhage	1	0	
Graft failure from PV/IVC thrombosis	1	0	
Lymphoproliferative disease	1	0	
Pulmonary hypertension	1	0	
Respiratory failure	1	0	
Chronic heart failure	0	1	
Reactivation of hepatitis C	0	1	

[1]Clavien grading. PV: Portal vein; IVC: Inferior vena cava; LDLT: Living-donor liver transplantation; LL: Left-lobe; RL: Right-lobe.

can still provide reasonable recipient survival. Most importantly, a LL living donor risks much less than a RL living donor. Further comparison between LL and RL grafts can be made when more LL-LDLTs have been performed for different types of patients with different conditions.

In this study, most of the patients in the LL-LDLT group were women. In general, women have a smaller body size. So, although the grafts were lighter and had a smaller GW/RSLV, they fitted well in the patients, who were mostly women. Women with a lower body mass index and a low-to-medium MELD score have been found to be disadvantaged in the "MELD score era" because of the heavy influence of creatinine level on MELD score; they tend to have a lower priority on the liver transplant waitlist and a higher waitlist mortality[43-45]. Balancing donor risks and recipient outcomes, even if there is graft size mismatch, the use of LL graft for LDLT can potentially expand the donor pool to shorten the waiting time and, at the same time, lower the donor risk.

The mortality risk for donors is 0.1% for LL-LDLT and 0.5% for RL-LDLT[8]. The figures are small and at first sight there seems to be not much difference. However, in the long run if a large number of living

Table 4 Donor details

	RL-LDLT (n = 199)	LL-LDLT (n = 19)	P value
Male:Female	39:160	16:3	0.000
Median age (yr) (range)	34 (18-58)	32 (18-55)	0.847
Death	1 (0.5%)	0	1.000
Postoperative complication[1]			0.905
No complication	166	18	
Grade 1	14	1	
Grade 2	8	0	
Grade 3a	4	0	
Grade 3b	5	0	
Grade 4a	1	0	
Grade 4b	0	0	
Grade 5	1	0	

[1]Clavien grading. LDLT: Living-donor liver transplantation; LL: Left-lobe; RL: Right-lobe.

donors are donating their RLs, the mortality of RL living donors will be significant. In this study, the donor mortality rates - 0.5% in RL-LDLT and 0% in LL-LDLT - were similar to the rates recorded in the literature.

The first successful LL-LDLT was reported in 1994[46]. Generally, a LL graft is 30%-40% of the SLV in adults[7]; as such, SFS syndrome tends to develop. SFS syndrome often results in poor graft survival and patient survival[9,14-16]. However, it has been shown that LL-LDLT can achieve excellent graft survival and patient survival[4] and the results of LL-LDLT can be comparable to those of RL-LDLT[17-21]. The primary goal of LDLT is to minimize donor risks (morbidity and mortality) while maximizing recipient benefits.

Using LL graft instead of RL graft has the advantage of lower donor morbidity[47] and mortality[8], but sometimes a LL graft would not suffice. If the prognosis for a patient is poorer because of a high MELD score or an old donor age, using the larger RL would improve the transplant outcome[19]. In the current study, all the grafts were small for size, and LL-LDLT and RL-LDLT had little difference when long-term patient survival is concerned. In view of this, maybe we can opt for the LL more often. For patients with a low MELD score and relatively stable condition, if a deceased-donor graft is unavailable, the use of LL graft can be advocated after balancing donor risks and potential recipient outcomes.

At our center, if SFS syndrome is expected, flow modulation will be performed. In the operation, portal flow and portal pressure are measured. Additional portal inflow modulations, such as splenic artery ligation[23] and portocaval shunt[48] may be employed[49]. In the current study, although all grafts were small for size, not many patients needed flow modulation. Some patients even required ligation of the spontaneous portosystemic shunt due to inadequate portal flow. All patients had good outcomes.

We wanted to find out the risk for complication and mortality in using SFS LL graft. Unfortunately, due to the small number of cases that used SFS LL graft, it was difficult to run a statistic on it. A multivariate analysis on the relevant data was performed but the result was negative; it was a nonsignificant finding.

The findings of this study may not be universally applicable. Our center is experienced in LDLT, especially RL-LDLT, which might have contributed to the favorable outcomes in the study[32]. Moreover, there were only 19 patients in the LL-LDLT group. The study has a relatively high risk of type-2 error. Furthermore, this is a retrospective cohort study with inevitable selection bias. Although every LDLT center has its LDLT protocol, every LDLT should be individualized, and the selection criteria adopted by a center cannot be universally applied.

The use of SFS graft in LDLT requires careful tailor-made surgical planning and meticulous operation. LL-LDLT can be a good alternative to RL-LDLT with similar recipient outcomes but a lower donor risk. Further research into different patient conditions is needed in order to validate the use of LL graft.

COMMENTS

Background

The use of the right lobe graft in living donor liver transplantation has been well established. However the use of the left lobe graft remained cautious, as a lot of patients suffered from complication or mortality due to the small for size graft. This study reviewed the results of the use of small for size grafts (left lobe or right lobe) and analyzed the outcomes of transplantation using left lobe small for size graft.

Research frontiers

Donor safety is of paramount importance in living donor liver transplantation. In the past, the mortality rate for right lobe graft donation was around 0.5%, whereas the mortality rate for left lobe graft donation was around 0.1%. The result of using right lobe small for size graft has been well established. However comparison between right lobe small for size graft and left lobe small for size graft is scarce.

Innovations and breakthroughs

This paper focused on the graft outcome and patient outcome of using small for size graft. Although the use of the right lobe and the use of the left lobe achieved similar patient survival, we should analyze the results cautiously, as most of the time recipients using a left lobe graft were relatively less risky.

Applications

This study has delivered an important message that allows further enlargement of the donor pool. Left lobe small for size graft can achieve results similar to right lobe small for size graft while reducing donor risk. Further studies can be conducted to find out which subgroup of patients would benefit from left lobe graft the most and to decide the safety limit of using left lobe small for size grafts.

Terminology

Right lobe graft: A graft that is the right liver lobe, usually containing the middle hepatic vein; Left lobe graft: A graft that is the left liver lobe; Small for size graft: A graft with a ratio of graft weight to recipient standard liver volume of < 40%-50%, or with a ratio of graft to recipient weight of 0.8%-1.0%; Small for size syndrome: Constellation of cholestasis, coagulopathy and ascites. It can progress to gastrointestinal bleeding and renal failure.

Peer-review

Interesting and well written manuscript. Useful for surgeons facing with liver living donor transplantation.

REFERENCES

1 **Tanaka K**, Uemoto S, Tokunaga Y, Fujita S, Sano K, Nishizawa T, Sawada H, Shirahase I, Kim HJ, Yamaoka Y. Surgical techniques and innovations in living related liver transplantation. *Ann Surg* 1993; **217**: 82-91 [PMID: 8424706 DOI: 10.1097/00000658-199301000-00014]

2 **Emond JC**, Heffron TG, Kortz EO, Gonzalez-Vallina R, Contis JC, Black DD, Whitington PF. Improved results of living-related liver transplantation with routine application in a pediatric program. *Transplantation* 1993; **55**: 835-840 [PMID: 7682738 DOI: 10.1097/00007890-199304000-00029]

3 **Broelsch CE**, Burdelski M, Rogiers X, Gundlach M, Knoefel WT, Langwieler T, Fischer L, Latta A, Hellwege H, Schulte FJ. Living donor for liver transplantation. *Hepatology* 1994; **20**: 49S-55S [PMID: 8005580 DOI: 10.1002/hep.1840200712]

4 **Soejima Y**, Shimada M, Suehiro T, Hiroshige S, Ninomiya M, Shiotani S, Harada N, Hideki I, Yonemura Y, Maehara Y. Outcome analysis in adult-to-adult living donor liver transplantation using the left lobe. *Liver Transpl* 2003; **9**: 581-586 [PMID: 12783399 DOI: 10.1053/jlts.2003.50114]

5 **Liu CL**, Fan ST, Lo CM, Wei WI, Chan SC, Yong BH, Wong J. Operative outcomes of adult-to-adult right lobe live donor liver transplantation: a comparative study with cadaveric whole-graft liver transplantation in a single center. *Ann Surg* 2006; **243**: 404-410 [PMID: 16495707 DOI: 10.1097/01.sla.0000201544.36473.a2]

6 **Chan SC**, Fan ST, Chok KS, Sharr WW, Dai WC, Fung JY, Chan KY, Balsarkar DJ, Lo CM. Increasing the recipient benefit/donor risk ratio by lowering the graft size requirement for living donor liver transplantation. *Liver Transpl* 2012; **18**: 1078-1082 [PMID: 22927142 DOI: 10.1002/lt.23433]

7 **Urata K**, Kawasaki S, Matsunami H, Hashikura Y, Ikegami T, Ishizone S, Momose Y, Komiyama A, Makuuchi M. Calculation of child and adult standard liver volume for liver transplantation. *Hepatology* 1995; **21**: 1317-1321 [PMID: 7737637 DOI: 10.1002/hep.1840210515]

8 **Barr ML**, Belghiti J, Villamil FG, Pomfret EA, Sutherland DS, Gruessner RW, Langnas AN, Delmonico FL. A report of the Vancouver Forum on the care of the live organ donor: lung, liver, pancreas, and intestine data and medical guidelines. *Transplantation* 2006; **81**: 1373-1385 [PMID: 16732172 DOI: 10.1097/01.tp.0000216825.56841.cd]

9 **Emond JC**, Renz JF, Ferrell LD, Rosenthal P, Lim RC, Roberts JP, Lake JR, Ascher NL. Functional analysis of grafts from living donors. Implications for the treatment of older recipients. *Ann Surg* 1996; **224**: 544-552; discussion 552-554 [PMID: 8857858 DOI: 10.1097/00000658-199610000-00012]

10 **Park KM**, Lee SG, Lee YJ, Hwang S, Nam CW, Choi KM, Nam CH, Choi DN, Kim KH, Choi KT, Ko KS, Min PC. Adult-to-adult living donor liver transplantation at Asian Medical Center, Seoul, Korea. *Transplant Proc* 1999; **31**: 456-458 [PMID: 10083188 DOI: 10.1016/S0041-1345(98)01706-0]

11 **Kiuchi T**, Tanaka K, Ito T, Oike F, Ogura Y, Fujimoto Y, Ogawa K. Small-for-size graft in living donor liver transplantation: how far should we go? *Liver Transpl* 2003; **9**: S29-S35 [PMID: 12942476 DOI: 10.1053/jlts.2003.50198]

12 **Kiuchi T**, Oike F, Yamamoto H. Small-for-size graft in liver transplantation. *Nagoya J Med Sci* 2003; **66**: 95-102 [PMID: 14727686]

13 **Troisi R**, de Hemptinne B. Clinical relevance of adapting portal vein flow in living donor liver transplantation in adult patients. *Liver Transpl* 2003; **9**: S36-S41 [PMID: 12942477 DOI: 10.1053/jlts.2003.50200]

14 **Kiuchi T**, Kasahara M, Uryuhara K, Inomata Y, Uemoto S, Asonuma K, Egawa H, Fujita S, Hayashi M, Tanaka K. Impact of graft size mismatching on graft prognosis in liver transplantation from living donors. *Transplantation* 1999; **67**: 321-327 [PMID: 10075602 DOI: 10.1097/00007890-199901270-00024]

15 **Ben-Haim M**, Emre S, Fishbein TM, Sheiner PA, Bodian CA, Kim-Schluger L, Schwartz ME, Miller CM. Critical graft size in adult-to-adult living donor liver transplantation: impact of the recipient's disease. *Liver Transpl* 2001; **7**: 948-953 [PMID: 11699030 DOI: 10.1053/jlts.2001.29033]

16 **Tanaka K**, Ogura Y. "Small-for-size graft" and "small-for-size syndrome" in living donor liver transplantation. *Yonsei Med J* 2004; **45**: 1089-1094 [PMID: 15627301 DOI: 10.3349/ymj.2004.45.6.1089]

17 **Soejima Y**, Shirabe K, Taketomi A, Yoshizumi T, Uchiyama H, Ikegami T, Ninomiya M, Harada N, Ijichi H, Maehara Y. Left lobe living donor liver transplantation in adults. *Am J Transplant* 2012; **12**: 1877-1885 [PMID: 22429497 DOI: 10.1111/j.1600-6143.2012.04022.x]

18 **Taketomi A**, Kayashima H, Soejima Y, Yoshizumi T, Uchiyama H, Ikegami T, Yamashita Y, Harada N, Shimada M, Maehara Y. Donor risk in adult-to-adult living donor liver transplantation: impact of left lobe graft. *Transplantation* 2009; **87**: 445-450 [PMID: 19202452 DOI: 10.1097/TP.0b013e3181943d46]

19 **Kurihara T**, Yoshizumi T, Yoshida Y, Ikegami T, Itoh S, Harimoto N, Ninomiya M, Uchiyama H, Okabe H, Kimura K, Kawanaka H, Shirabe K, Maehara Y. Graft selection strategy in adult-to-adult living donor liver transplantation: When both hemiliver grafts meet volumetric criteria. *Liver Transpl* 2016; **22**: 914-922 [PMID: 26953726 DOI: 10.1002/lt.24431]

20 **Shimada M**, Shiotani S, Ninomiya M, Terashi T, Hiroshige S, Minagawa R, Soejima Y, Suehiro T, Sugimachi K. Characteristics of liver grafts in living-donor adult liver transplantation: comparison between right- and left-lobe grafts. *Arch Surg* 2002; **137**: 1174-1179 [PMID: 12361430 DOI: 10.1001/archsurg.137.10.1174]

21 **Ikegami T**, Masuda Y, Ohno Y, Mita A, Kobayashi A, Urata K, Nakazawa Y, Miwa S, Hashikura Y, Miyagawa S. Prognosis of adult patients transplanted with liver grafts & lt; 35% of their standard liver volume. *Liver Transpl* 2009; **15**: 1622-1630 [PMID: 19877227 DOI: 10.1002/lt.21716]

22 **Fan ST**, Lo CM, Liu CL. Technical refinement in adult-to-adult living donor liver transplantation using right lobe graft. *Ann Surg* 2000; **231**: 126-131 [PMID: 10636112 DOI: 10.1097/00000658-200001000-00018]

23 **Lo CM**, Fan ST, Liu CL, Wong J. Hepatic venoplasty in living-donor liver transplantation using right lobe graft with middle hepatic vein. *Transplantation* 2003; **75**: 358-360 [PMID: 12589159 DOI: 10.1097/01.TP.0000046527.19422.3E]

24 **Chok KS**, Fung JY, Chan AC, Dai WC, Sharr WW, Cheung TT, Chan SC, Lo CM. Comparable Short- and Long-term Outcomes in Living Donor and Deceased Donor Liver Transplantations for Patients With Model for End-stage Liver Disease Scores ≥35 in a Hepatitis-B Endemic Area. *Ann Surg* 2016; Epub ahead of print [PMID: 26910204 DOI: 10.1097/SLA.0000000000001671]

25 **Au KP**, Chan SC, Chok KS, Chan AC, Wong TC, Sharr WW, Lo CM. Durability of small-for-size living donor allografts. *Liver Transpl* 2015; **21**: 1374-1382 [PMID: 26123155 DOI: 10.1002/lt.24205]

26 **Punch JD**, Hayes DH, LaPorte FB, McBride V, Seely MS. Organ donation and utilization in the United States, 1996-2005. *Am J Transplant* 2007; **7**: 1327-1338 [PMID: 17428283 DOI: 10.1111/j.1600-6143.2007.01779.x]

27 Eurotransplant. Eurotransplant Annual Reports: Eurotransplant International Foundation. Available from: URL: http://www.eurotransplant.org/cms/index.php?page=annual_reports

28 **Lo CM**, Fan ST, Liu CL, Yong BH, Wong Y, Lau GK, Lai CL, Ng IO, Wong J. Lessons learned from one hundred right lobe living donor liver transplants. *Ann Surg* 2004; **240**: 151-158 [PMID: 15213631 DOI: 10.1097/01.sla.0000129340.05238.a0]

29 **Soejima Y**, Taketomi A, Yoshizumi T, Uchiyama H, Harada N, Ijichi H, Yonemura Y, Shimada M, Maehara Y. Feasibility of left

lobe living donor liver transplantation between adults: an 8-year, single-center experience of 107 cases. *Am J Transplant* 2006; **6**: 1004-1011 [PMID: 16611337 DOI: 10.1111/j.1600-6143.2006.01284.x]
30 **Tanemura A**, Mizuno S, Wada H, Yamada T, Nobori T, Isaji S. Donor age affects liver regeneration during early period in the graft liver and late period in the remnant liver after living donor liver transplantation. *World J Surg* 2012; **36**: 1102-1111 [PMID: 22374540 DOI: 10.1007/s00268-012-1496-1]
31 **Kim SJ**, Na GH, Choi HJ, Yoo YK, Kim DG. Surgical outcome of right liver donors in living donor liver transplantation: single-center experience with 500 cases. *J Gastrointest Surg* 2012; **16**: 1160-1170 [PMID: 22426687 DOI: 10.1007/s11605-012-1865-y]
32 **Chan SC**, Lo CM, Ng KK, Fan ST. Alleviating the burden of small-for-size graft in right liver living donor liver transplantation through accumulation of experience. *Am J Transplant* 2010; **10**: 859-867 [PMID: 20148811 DOI: 10.1111/j.1600-6143.2010.03017.x]
33 **Dahm F**, Georgiev P, Clavien PA. Small-for-size syndrome after partial liver transplantation: definition, mechanisms of disease and clinical implications. *Am J Transplant* 2005; **5**: 2605-2610 [PMID: 16212618 DOI: 10.1111/j.1600-6143.2005.01081.x]
34 **Tucker ON**, Heaton N. The 'small for size' liver syndrome. *Curr Opin Crit Care* 2005; **11**: 150-155 [PMID: 15758596 DOI: 10.1097/01.ccx.0000157080.11117.45]
35 **Hammond JS**, Guha IN, Beckingham IJ, Lobo DN. Prediction, prevention and management of postresection liver failure. *Br J Surg* 2011; **98**: 1188-1200 [PMID: 21725970 DOI: 10.1002/bjs.7630]
36 **Rahbari NN**, Garden OJ, Padbury R, Brooke-Smith M, Crawford M, Adam R, Koch M, Makuuchi M, Dematteo RP, Christophi C, Banting S, Usatoff V, Nagino M, Maddern G, Hugh TJ, Vauthey JN, Greig P, Rees M, Yokoyama Y, Fan ST, Nimura Y, Figueras J, Capussotti L, Büchler MW, Weitz J. Posthepatectomy liver failure: a definition and grading by the International Study Group of Liver Surgery (ISGLS). *Surgery* 2011; **149**: 713-724 [PMID: 21236455 DOI: 10.1016/j.surg.2010.10.001]
37 **Guglielmi A**, Ruzzenente A, Conci S, Valdegamberi A, Iacono C. How much remnant is enough in liver resection? *Dig Surg* 2012; **29**: 6-17 [PMID: 22441614 DOI: 10.1159/000335713]
38 **Ikegami T**, Yoshizumi T, Sakata K, Uchiyama H, Harimoto N, Harada N, Itoh S, Nagatsu A, Soejima Y, Maehara Y. Left lobe living donor liver transplantation in adults: What is the safety limit? *Liver Transpl* 2016; **22**: 1666-1675 [PMID: 27540888 DOI: 10.1002/lt.24611]
39 **Braun HJ**, Dodge JL, Roll GR, Freise CE, Ascher NL, Roberts JP. Impact of Graft Selection on Donor and Recipient Outcomes After Living Donor Liver Transplantation. *Transplantation* 2016; **100**: 1244-1250 [PMID: 27123878 DOI: 10.1097/TP.0000000000001101]
40 **Selzner M**, Kashfi A, Cattral MS, Selzner N, McGilvray ID, Greig PD, Levy GA, Renner EL, Grant DR. Live donor liver transplantation in high MELD score recipients. *Ann Surg* 2010; **251**: 153-157 [PMID: 19858705 DOI: 10.1097/SLA.0b013e3181bc9c6a]
41 **Chok KSh**, Chan SC, Fung JY, Cheung TT, Chan AC, Fan ST, Lo CM. Survival outcomes of right-lobe living donor liver transplantation for patients with high Model for End-stage Liver Disease scores. *Hepatobiliary Pancreat Dis Int* 2013; **12**: 256-262 [PMID: 23742770 DOI: 10.1016/S1499-3872(13)60042-9]
42 **Liu CL**, Fan ST, Lo CM, Yong BH, Fung AS, Wong J. Right-lobe live donor liver transplantation improves survival of patients with acute liver failure. *Br J Surg* 2002; **89**: 317-322 [PMID: 11872056 DOI: 10.1046/j.0007-1323.2001.02035.x]
43 **Fink MA**, Berry SR, Gow PJ, Angus PW, Wang BZ, Muralidharan V, Christophi C, Jones RM. Risk factors for liver transplantation waiting list mortality. *J Gastroenterol Hepatol* 2007; **22**: 119-124 [PMID: 17201891 DOI: 10.1111/j.1440-1746.2006.04422.x]
44 **Axelrod DA**, Pomfret EA. Race and sex disparities in liver transplantation: progress toward achieving equal access? *JAMA* 2008; **300**: 2425-2426 [PMID: 19033595 DOI: 10.1001/jama.2008.732]
45 **Mathur AK**, Schaubel DE, Gong Q, Guidinger MK, Merion RM. Sex-based disparities in liver transplant rates in the United States. *Am J Transplant* 2011; **11**: 1435-1443 [PMID: 21718440 DOI: 10.1111/j.1600-6143.2011.03498.x]
46 **Hashikura Y**, Makuuchi M, Kawasaki S, Matsunami H, Ikegami T, Nakazawa Y, Kiyosawa K, Ichida T. Successful living-related partial liver transplantation to an adult patient. *Lancet* 1994; **343**: 1233-1234 [PMID: 7909905 DOI: 10.1016/S0140-6736(94)92450-3]
47 **Umeshita K**, Fujiwara K, Kiyosawa K, Makuuchi M, Satomi S, Sugimachi K, Tanaka K, Monden M; Japanese Liver Transplantation Society. Operative morbidity of living liver donors in Japan. *Lancet* 2003; **362**: 687-690 [PMID: 12957090 DOI: 10.1016/S0140-6736(03)14230-4]
48 **Troisi R**, Ricciardi S, Smeets P, Petrovic M, Van Maele G, Colle I, Van Vlierberghe H, de Hemptinne B. Effects of hemiportocaval shunts for inflow modulation on the outcome of small-for-size grafts in living donor liver transplantation. *Am J Transplant* 2005; **5**: 1397-1404 [PMID: 15888047 DOI: 10.1111/j.1600-6143.2005.00850.x]
49 **Chan SC**, Lo CM, Chok KS, Sharr WW, Cheung TT, Tsang SH, Chan AC, Fan ST. Modulation of graft vascular inflow guided by flowmetry and manometry in liver transplantation. *Hepatobiliary Pancreat Dis Int* 2011; **10**: 649-656 [PMID: 22146631 DOI: 10.1016/S1499-3872(11)60110-0]

P- Reviewer: Fujino Y, Salvadori M **S- Editor**: Qi Y **L- Editor**: A
E- Editor: Wang CH

World Journal of Gastroenterology

Submit a Manuscript: http://www.f6publishing.com

World J Gastroenterol 2017 June 21; 23(23): 4278-4284

DOI: 10.3748/wjg.v23.i23.4278

ISSN 1007-9327 (print) ISSN 2219-2840 (online)

ORIGINAL ARTICLE

Clinical Trials Study

Potential application of neogalactosylalbumin in positron emission tomography evaluation of liver function

Shun-Da Du, Shao-Hua Li, Bao Jin, Zhao-Hui Zhu, Yong-Hong Dang, Hai-Qun Xing, Fang Li, Xue-Bing Wang, Xin Lu, Xin-Ting Sang, Hua-Yu Yang, Shou-Xian Zhong, Yi-Lei Mao

Shun-Da Du, Shao-Hua Li, Bao Jin, Xin Lu, Xin-Ting Sang, Hua-Yu Yang, Shou-Xian Zhong, Yi-Lei Mao, Department of Liver Surgery, Peking Union Medical College Hospital, Chinese Academy of Medical Sciences and Peking Union Medical College, Beijing 100730, China

Shao-Hua Li, Department of Hepatobiliary Surgery, Sun Yat-sen University Cancer Center, Guangzhou 510060, Guangdong Province, China

Zhao-Hui Zhu, Yong-Hong Dang, Hai-Qun Xing, Fang Li, Department of Nuclear Medicine, Peking Union Medical College Hospital, Chinese Academy of Medical Sciences and Peking Union Medical College, Beijing 100730, China

Xue-Bing Wang, Key Laboratory of Radiopharmaceuticals, Ministry of Education, College of Chemistry, Beijing Normal University, Beijing 100875, China

Author contributions: Du SD, Zhu ZH, Li F, Wang XB, Sang XT, Zhong SX and Mao YL designed the research; Du SD, Li SH, Jin B, Zhu ZH, Dang YH, Xing HQ, Lu X and Yang HY performed the research; Dang YH, Xing HQ, Wang XB and Yang HY contributed new reagents/analytic tools; Du SD, Li SH, Zhu ZH, Li F, Lu X, Sang XT, Yang HY and Mao YL analyzed the data; Du SD, Li SH, Jin B, Zhu ZH, Yang HY and Mao YL wrote the paper.

Supported by National Natural Science Foundation of China, No. 30901453 and No. 81201566; National Key Technology Research and Development Program of China, No. BAI06B01; and Youth Grant of Peking Union Medical College Hospital.

Institutional review board statement: Animal Care and Use Committee of Peking Union Medical College Hospital.

Conflict-of-interest statement: All authors state that no conflicts of interest exist.

Data sharing statement: Technical appendix, statistical code, and dataset available from the corresponding author at yileimao@126.com.

Manuscript source: Unsolicited manuscript

Correspondence to: Yi-Lei Mao, MD, PhD, Department of Liver Surgery, Peking Union Medical College Hospital, Chinese Academy of Medical Sciences and Peking Union Medical College, No. 1 Shuai-Fu-Yuan, Wangfujing, Beijing 100730, China. yileimao@126.com
Telephone: +86-10-69156042
Fax: +86-10-69156043

Received: August 27, 2016
Peer-review started: August 28, 2016
First decision: February 27, 2017
Revised: March 12, 2017
Accepted: April 12, 2017
Article in press: April 12, 2017
Published online: June 21, 2017

Abstract

AIM

To investigate the evaluation of neogalactosylalbumin (NGA) for liver function assessment based on positron emission tomography technology.

METHODS

Female Kunming mice were assigned randomly to two groups: fibrosis group and normal control group. A murine hepatic fibrosis model was generated by intraperitoneal injection of 10% carbon tetrachloride

(CCl_4) at 0.4 mL every 48 h for 42 d. ^{18}F-labeled NGA ([^{18}F]FNGA) was synthesized and administered at a dosage of 3.7 MBq/mouse to both fibrosis mice and normal control mice. Distribution of [^{18}F]FNGA amongst organs was examined, and dynamic scanning was performed. Parameters were set up to compare the uptake of tracers by fibrotic liver and healthy liver. Serologic tests for liver function were also performed.

RESULTS

The liver function of the fibrosis model mice was significantly impaired by the use of CCl_4. In the fibrosis model mice, hepatic fibrosis was verified by naked eye assessment and pathological analysis. [^{18}F]FNGA was found to predominantly accumulate in liver and kidneys in both control group (n = 21) and fibrosis group (n = 23). The liver uptake ability (LUA), peak time (T_p), and uptake rate (LUR) of [^{18}F]FNGA between healthy liver (n = 8) and fibrosis liver (n = 10) were significantly different (P < 0.05, < 0.01, and < 0.05, respectively). LUA was significantly correlated with total serum protein level (TP) (P < 0.05). T_p was significantly correlated with both TP and glucose (Glu) concentration (P < 0.05 both), and LUR was significantly correlated with both total bile acid and Glu concentration (P < 0.01 and < 0.05, respectively).

CONCLUSION

[^{18}F]FNGA mainly accumulated in liver and remained for sufficient time. Functionally-impaired liver showed a significant different uptake pattern of [^{18}F]FNGA compared to the controls.

Key words: Neogalactosylalbumin; Positron emission tomography; Liver function; Liver fibrosis; Mouse model

Core tip: Neogalactosylalbumin (NGA) is a specific ligand for asialoglycoprotein receptor that is exclusively expressed on the surface of hepatic parenchymal cells. This study showed [^{18}F]FNGA mainly accumulated in liver and remained for sufficient time. Functionally-impaired liver showed a significant different uptake pattern of [^{18}F]FNGA compared to controls.

Du SD, Li SH, Jin B, Zhu ZH, Dang YH, Xing HQ, Li F, Wang XB, Lu X, Sang XT, Yang HY, Zhong SX, Mao YL. Potential application of neogalactosylalbumin in positron emission tomography evaluation of liver function. *World J Gastroenterol* 2017; 23(23): 4278-4284 Available from: URL: http://www.wjgnet.com/1007-9327/full/v23/i23/4278.htm DOI: http://dx.doi.org/10.3748/wjg.v23.i23.4278

INTRODUCTION

Asialoglycoprotein receptor (ASGPR) is expressed abundantly on the surfaces of mammalian hepatic parenchymal cells but rarely on extra-hepatic cells[1-3]. It is believed that the amount of ASGPR represents the number and density of functional hepatocytes in the liver[4,5]. Studies revealed that expression of ASGPR on hepatic cell surface decreases in both cirrhosis and obstructive jaundice patients, with more significant reduction in cirrhosis patients. Sawamura *et al*[6] found that cell surface expression of ASGPR is very low on hepatocyte carcinoma cells. No ASGRP expression has been found in any metastatic cancer in liver. Tomiguchi *et al*[7] noted that among patients with chronic active hepatitis, the decrease of ASGPR level is highly correlated with liver fibrosis and necrosis. Therefore, quantitative assessment of the ASGPR expression in liver could directly reflect liver function with a desired accuracy[8].

Technetium-99-labeled neogalactosylalbumin (^{99m}Tc-NGA), a ligand with high affinity to ASGPR, was developed[9,10] and is being applied for differential diagnosis of focal nodular hyperplasia and hepatic cancer with single photon emission computed tomography (SPECT)[11]. However, it is the analogue of NGA, technetium-labeled galactosyl human serum albumin (^{99m}Tc-GSA), that became widely used in many studies due to the non-specific binding between ^{99m}Tc and NGA. ^{99m}Tc-GSA became the first approved receptor binding reagent for scintigraphy in Japan[12]. However, the sensitivity, spatial resolution, and quantitative capacity of SPECT limited its application, whereas positron emission tomography (PET) exhibited significant advantages over SPECT[13-15]. Currently, there is no study using NGA PET scan for liver function evaluation.

^{18}F is the most popular positron-emitting isotope for PET imaging. It has a low positron energy and proper physical half-life (110 min), which makes it suitable for *in vivo* study. ^{18}F-labeled deoxyglucose (FDG) has been applied widely in clinical diagnosis and evaluation of neoplasms. In this study, we successfully synthesized ^{18}F-labeled NGA, and performed a preliminary investigation on a liver fibrosis mouse model for quantitative live function analysis.

MATERIALS AND METHODS

Establishment of murine liver fibrosis model

All animal experiment protocols were approved by the Institutional Animal Care and Use Committee and carried out in accordance with guidelines of the Laboratory Animal Center of Peking Union Medical College. Female Kunming mice, 6-7 wk and 19-25 g, were obtained from Beijing Weitonglihua Experimental Animal Corporation (Beijing, China). Liver fibrosis was induced by intraperitoneal (ip) injection of 10% carbon tetrachloride oil solution (CCl_4) (National Chemical Reagent Group, Beijing, China) at 0.4 mL every 48 h for 42 d[16].

Table 1 Serological tests of various items for liver function in both fibrosis and control mice

	Control, n = 29	Fibrosis, n = 31
TP as g/L	52.83 ± 0.94[a]	49.71 ± 0.90
ALB as g/L	27.01 ± 0.39[a]	25.23 ± 0.51
ALP as U/L	96.70 ± 11.48[b]	53.44 ± 5.41
ChE as kU/L	5.63 ± 0.23[b]	4.51 ± 0.32
Glu as mmol/L	10.89 ± 0.88[a]	13.91 ± 1.44

[a]$P < 0.05$, [b]$P < 0.01$ *vs* fibrosis. TP: Total protein; ALB: Albumin; ALP: Alkaline phosphatase; ChE: Cholinesterase; Glu: Glucose.

Radiolabeling of NGA

^{18}F-labeled neogalactosylalbumin ([^{18}F]FNGA) was synthesized in Beijing Normal University Chemistry College using a protocol published earlier[17]. The radioactive purity was > 99%. The administration dose was 3.7 MBq for each mouse.

Distribution assay of [^{18}F]FNGA

[^{18}F]FNGA (3.7 MBq in 100 μL solution containing about 40 μg NGA) was injected through the tail vein. Blood samples were collected through orbital bleeding at 5, 30 or 60 min after injection, immediately followed by sacrifice of the animal by cervical dislocation and collection of organ samples. Radioactivity of each organ was measured using a radioactive detector (RM-905a; China) and expressed as relative radioactive dosage per gram (%ID/g), with the accumulated radioactivity in the organ divided by the total injected dose per gram of body weight.

Serological examination

Blood samples were collected through orbital bleeding from all animals at different periods after injection of [^{18}F]FNGA. Testing items included total protein (TP), albumin (ALB), alanine aminotransferase (ALT), aspartate aminotransferase (AST), alkaline phosphatase (ALP), total bile acid (TBA), lactate dehydrogenase (LD), cholinesterase (ChE), urea nitrogen (BUN), serum creatinine (Cr), blood glucose (Glu), total cholesterol (Tc), triglycerides (Tg), calcium ions (Ca), adenosine dehydrogenase (ADA), sodium ions (Na), potassium ions (K), prothrombin time (PT), and international normalized ratio (INR).

MicroPET scan

Mice were anaesthetized by chloral hydrate. Immediately after [^{18}F]FNGA injection at 7.4 MBq/kg, a mouse was laid on a microPET scanner (Siemens, Germany) and serial static emission scanning was performed at 120 kV, 100 mA/s and with a 5 mm section cranial thickness. A whole-body PET emission scan was performed with 2-min acquisition per bed position using a 3-dimensional acquisition mode with 1 min interval in a total of 30 min. A second phase scanning was also performed immediately after the 30-min scan at 5 min per scan with 1 min interval for a total of 30 min. Region of interest (ROI) was drawn and the standardized uptake values (SUV) in each ROI was measured.

PET image analysis

The images were semi-quantitatively analyzed by ImageJ software of the microPET for the average SUV within the ROI. Total body radioactivity (R_{Total}) was measured by the entire body scan, excluding the injection spot on the tail. Parameters were set up specifically as follows, to reflect the liver capacity for tracer uptake: Liver uptake ability (LUA) was calculated as the peak radioactive value (R_p) in liver ROI divided by the R_{Total}; Peak time (T_p) was the time when radioactivity in ROI reaches to the R_p; Clearance index (CI) was the radioactivity in the heart ROI at the time of liver T_p divided by the radioactivity of the first scanning in the heart ROI; Liver uptake rate (LUR) was defined as $LUR = [(R_p-R_{t1})/R_{Total}]/(T_p-T_1)$, where T_1 was the point time of the first scan and R_{t1} was the liver radioactivity of the first scan.

Statistical analysis

Statistical analysis was performed with SPSS 13.0 software (IBM, Chicago, IL, United States). Data were expressed as mean ± SD. Shapiro-Wilk test was employed for normal distribution data. Independent *t*-test was used for comparison between the groups with normal distribution, and Mann-Whitney method was used for those with abnormal distribution. Pearson or Spearman examination was applied for correlation test for normal or non-normal distribution samples, respectively.

RESULTS

Liver function in fibrosis model mice

The number of blood samples was 31 from the fibrosis mice and 29 from the control mice, with the exception of 2 fibrosis mice having failed sampling. As shown in Table 1, liver function of the fibrosis model mice was significantly impaired by the use of CCl_4 for 42 d. Laboratory tests for liver function demonstrated significant differences between the fibrosis model mice and the controls in TP, ALB, and Glu with $P < 0.05$, and in ALP and ChE with $P < 0.01$. Obvious pinkish fiber cords were observed, even with the naked eye, in the fibrosis model mice. Hepatic fibrosis was also verified by pathological analysis (data not shown)[16].

Biological distribution of [^{18}F]FNGA in mice

Animals were sacrificed after injection of [^{18}F]FNGA according to the following order: 5 min (8 fibrosis and 6 control mice), 30 min (8 fibrosis and 8 control mice), and 60 min (7 fibrosis and 7 control mice). Organs were removed for radioactivity measurement. Figure 1 demonstrates the distribution of [^{18}F]FNGA in both control mice (Figure 1A) and fibrosis model mice (Figure

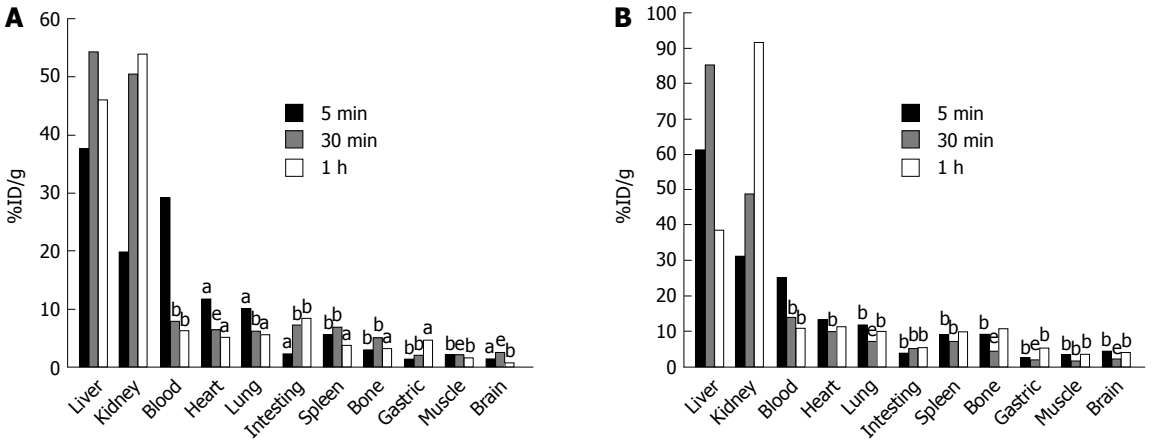

Figure 1 [^{18}F]FNGA distribution in both control and fibrosis mice at various time points. Relative radioactivity levels are shown at various time points from organs of control mice (n = 21) (A) and CCl_4-induced fibrosis mice (n = 23) (B). $^{b}P < 0.01$ *vs* Liver, $^{a}P < 0.05$ *vs* Liver, $^{e}P < 0.001$ *vs* Liver. [^{18}F]FNGA: ^{18}F-labeled neogalactosylalbumin.

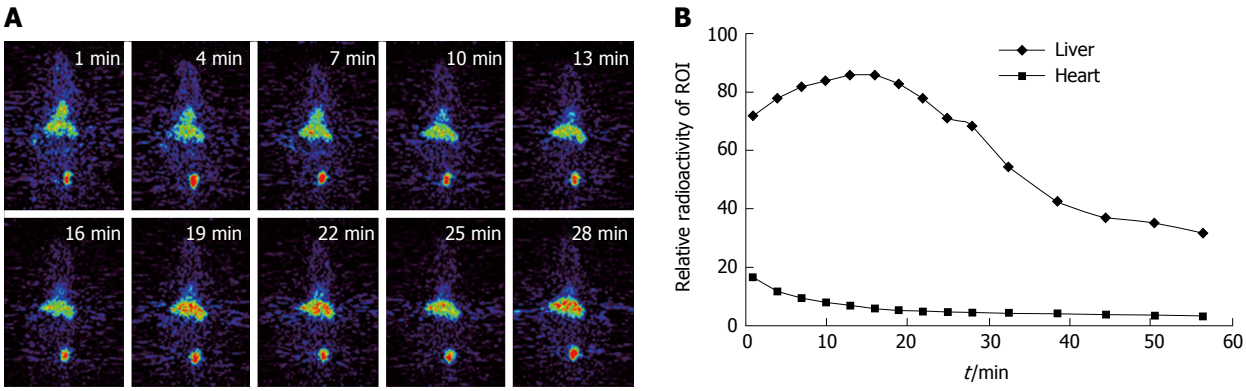

Figure 2 Positron emission tomography images from a scanning of control mouse in a 30-min period. A: Each scan took 2 min followed by 1 min break; B: Dynamic radioactivity curves from region of interest for liver and heart from positron emission tomography scanning.

1B). [^{18}F]FNGA was found to accumulate mainly in liver and kidney over the time of observation in both control and fibrosis model mice, except for the initial high level in blood detected at 5 min after injection.

PET scanning

Whole body scan was performed on 10 fibrosis and 8 control mice. Clear liver images were acquired without obvious interference from other abdominal organs. Figure 2A exhibits the serial images of a control mouse over a period of 30 min. The liver outline can be clearly observed at 4 min after tracer injection. The liver radioactivity reached the peak level in the control mouse at about 19 min. However, radioactivity in the fibrosis liver reached the peak much later than that in the control group. The tracer remained in the liver at a high level throughout the scanning period. In addition, a clear heart outline was presented in the early phase. In the later phase of the scanning, high tracer accumulation was found in the bladder. Very low radioactivity was detected in the brain, lung, and limbs.

The typical dynamic curves of [^{18}F]FNGA in liver and heart of a control mouse are shown in Figure 2B. High radioactivity was observed in both organs immediately after [^{18}F]FNGA administration. Liver exhibited a continuous accumulation till reaching a peak level, whereas heart showed a quick clearance after [^{18}F]FNGA injection.

Effect of NGA as a PET tracer for evaluation of liver function

Parameters based on the PET images are shown in Figure 3. The LUA was significantly lower in fibrotic liver than that in the normal liver ($P < 0.05$; Figure 3A). The T_p took significantly longer in fibrotic liver to reach a peak than in the normal liver ($P < 0.01$; Figure 3B). The [^{18}F]FNGA accumulating rate (LUR) of fibrotic liver was significantly slower than that of the controls ($P < 0.05$; Figure 3C). No significant differences were found in CI between the two groups.

Correlation of PET parameters with the lab tests

Correlation was found between the PET parameters and serological tests including TP, TBA, and Glu (Table 2). LUA was significantly correlated with TP, T_p was significantly correlated with both TP and Glu, and LUR was significantly correlated with both TBA and Glu,

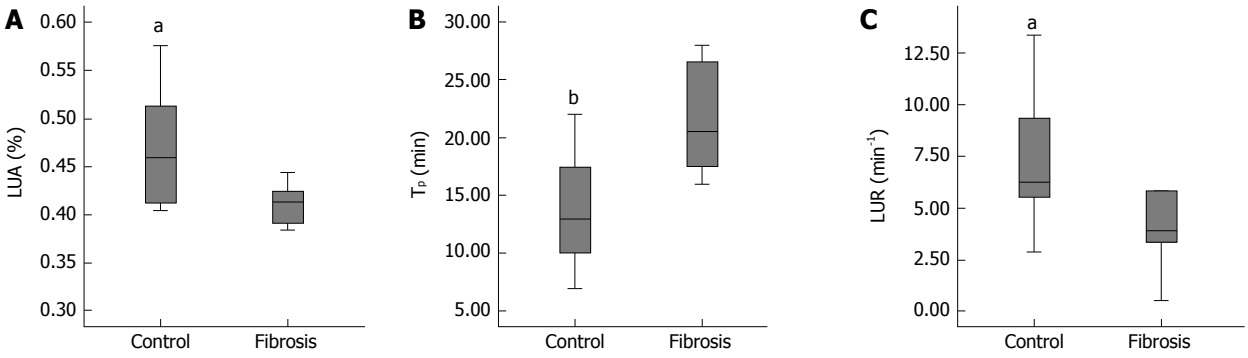

Figure 3 Comparison of the [^{18}F]FNGA positron emission tomography scan parameters between fibrosis mice (n = 10) and control mice (n = 8). A: The LUA was significantly lower in fibrosis liver than that in normal liver; B: The T_p took significantly longer in fibrosis liver to reach a peak than in the normal liver; C: The LUR of fibrosis liver was significantly slower than that of the controls. [a]P < 0.05, [b]P < 0.01 *vs* fibrosis. [^{18}F]FNGA: ^{18}F-labeled neogalactosylalbumin; LUA: Liver uptake capacity; T_p: Peak time; LUR: Liver uptake rate.

Table 2 Correlation of positron emission tomography scan parameters with serological test results, n = 18

	LUA		Tp		LUR	
	r	*P* value	*r*	*P* value	*r*	*P* value
TP	0.559	0.038	-0.632	0.015	0.286	0.321
TBA	-0.225	0.438	0.303	0.292	-0.690	0.006
Glu	-0.631	0.068	0.719	0.029[a]	-0.730	0.025

[a]P < 0.05. LUA: Liver uptake capacity; Tp: Peak time; LUR: Liver uptake rate; TP: Total protein; TBA: Total bile acid; Glu: Glucose.

with P < 0.05 in the above conditions.

DISCUSSION

Multiple methods have been applied in clinical assessment for liver function, including serological tests[18], Child-Pugh and model for end-stage liver disease (commonly known as MELD) scoring systems, indocyanine green clearance, and medical imaging modalities like computed tomography, magnetic resonance imaging, and SPECT[19,20]. The above-mentioned methods provide data on certain types of liver function to meet the clinical purposes for diagnosis and treatment. However, they have prominent limitations for accurate evaluation. PET has become increasingly important as a functional diagnostic tool with various applications, especially in the diagnosis and evaluation of malignant tumors. Recently, effort has been made in using PET for liver function evaluation through sophisticated calculation of ^{18}F-FD-Galactose clearance[21]. It requires extra invasive arterial sampling, the procedure is far from practical, and the result is not visually observational.

To the best of our knowledge, this is the first study applying [^{18}F]FNGA in the evaluation of liver function in a fibrotic liver animal model. We demonstrated the significant differences between the fibrotic liver and the normal control liver in their [^{18}F]FNGA LUA, PT, and LUR. In addition, the tracer retained in liver for sufficient long time (> 60 min) and generated a clear image of liver, which is a critical tracer for PET scanning.

Several advantages of [^{18}F]FNGA were observed for this application to liver function assessment. The rapid clearance from the cardiovascular system, as well as the extended retention in the liver, minimizes the influence to liver imaging and parameter calculation. The tracer was mainly excreted through kidneys, which was an obvious difference from the ^{99m}Tc-GSA, which is mainly excreted from the gallbladder-gastrointestinal (GGI) tract. Therefore, the imaging result would be less likely to be influenced by obstruction of the GGI tract, which could lead to more accurate liver function evaluation. However, concern has existed about the possible influence of renal function on scanning result. In this study, all animals were normal healthy, except for the induction of liver fibrosis. And, there is no known effect of CCl_4 on renal function. Nevertheless, further study will be needed in animals with kidney defect.

The receptor index (LHL15 and HH15) in the ^{99m}Tc-GSA study was widely accepted and has been taken as reference because both NGA and GSA bind to the same receptor on hepatocytes[20]. In this study, therefore, we generated CI and LUA that played similar functional roles as HH15 and LHL15, respectively. In addition, LUR, which evaluated the liver uptake rate for [^{18}F]FNGA, also showed significant differences between the control and fibrotic livers, with the fibrotic liver showing a much slower rate. In addition, these parameters were found to be highly correlated with traditional liver function indicators, such as TP and TBA, suggesting that these parameters are appropriate for liver function evaluation.

When liver function was impaired, blood glucose cannot be quickly converted into glycogen, thus leading to an elevated blood glucose level. In fact, some have proposed the use of an oral glucose tolerance test curve to determine the degree of liver dysfunction, tolerance for surgery, and prognosis[22]. We found that both LUR and T_p were significantly correlated with blood glucose level, suggesting that the blood glucose level indeed may indicate one of the aspects of the liver function.

This is a preliminary study investigating the use of [^{18}F]FNGA as a PET tracer, with limitations existing in many regards. First, this study did not demonstrate the correlation of the severity of fibrosis and tracer uptake by the liver. Second, the mechanism of biological metabolism of the [^{18}F]FNGA needs to be further investigated. Though the animal model employed in this study was well-established, the liver damage in the model could not be quantitatively defined. A progressive liver function loss would be more appropriate to evaluate the role the [^{18}F]FNGA PET scan images in reflection of the liver function damage.

Functionally-impaired liver showed a significantly different uptake pattern of [^{18}F]FNGA compared to control liver in PET examination. [^{18}F]FNGA was mainly accumulated and retained in the liver, and for sufficient time for PET imaging. Excretion from the kidney could be another advantage for [^{18}F]FNGA to avoid gastro-intestinal side effect.

COMMENTS

Background

There are several liver function evaluation methods routinely using in the clinic, such as serological tests, Child-Pugh and model for end-stage liver disease (commonly known as MELD) scoring systems, *etc*. But, none of these can assess the function of any particular anatomical fraction of the liver. Asialoglycoprotein receptor (ASGPR) is expressed abundantly on the surfaces of mammalian hepatic parenchymal cells. It is believed that the amount of ASGPR represents the number and density of functional hepatocytes in the liver. A ligand with high affinity to ASGPR, neogalactosyl albumin (NGA) was developed. To date, however, there has been no study using NGA positron emission tomography (PET) scan for liver function evaluation.

Research frontiers

This is the first study applying ^{18}F-labeled neogalactosylalbumin ([^{18}F]FNGA) in the evaluation of liver function in a fibrotic liver animal model. Functionally-impaired liver showed a significant different uptake pattern of [^{18}F]FNGA compared to control liver in PET examination.

Innovations and breakthroughs

This is the first study to show [^{18}F]FNGA mainly accumulated and retained in the liver, and for sufficient time for PET. Our data demonstrated that the parameters from the pharmacokinetics curve of NGA were significantly different between control and fibrosis mice. More importantly, the data was significantly correlated with the major traditional serological tests.

Applications

In the present manuscript, we have reported, for the first time, application of [^{18}F]FNGA in the evaluation of liver function in a fibrotic and normal liver animal model. Under PET/computed tomography (CT) scan, it could primarily achieve the goals that present the liver function with computerized 3-D imagining techniques. Thus, this can be an intuitive tool to design operations and may predict the risk of hepatectomy. Finally, it can also be used in other medical fields for assessing liver function.

Terminology

Neogalactosylalbumin, positron emission tomography, liver function, liver fibrosis, mouse model.

Peer-review

This is a very interesting application of the PET/CT technique to the analysis of liver pathophysiology. The data are convincing and the specificity of the labeling is adequate.

REFERENCES

1 **Akaki S**, Mitsumori A, Kanazawa S, Togami I, Takeda Y, Joja I, Hiraki Y. Technetium-99m-DTPA-galactosyl human serum albumin liver scintigraphy evaluation of regional CT/MRI attenuation/signal intensity differences. *J Nucl Med* 1998; **39**: 529-532 [PMID: 9529304]

2 **Burgess JB**, Baenziger JU, Brown WR. Abnormal surface distribution of the human asialoglycoprotein receptor in cirrhosis. *Hepatology* 1992; **15**: 702-706 [PMID: 1372583]

3 **Morell AG**, Irvine RA, Sternlieb I, Scheinberg IH, Ashwell G. Physical and chemical studies on ceruloplasmin. V. Metabolic studies on sialic acid-free ceruloplasmin in vivo. *J Biol Chem* 1968; **243**: 155-159 [PMID: 5635941]

4 **Gärtner U**, Stockert RJ, Morell AG, Wolkoff AW. Modulation of the transport of bilirubin and asialoorosomucoid during liver regeneration. *Hepatology* 1981; **1**: 99-106 [PMID: 7026402]

5 **Meyer B**, Luo HS, Bargetzi M, Renner EL, Stalder GA. Quantitation of intrinsic drug-metabolizing capacity in human liver biopsy specimens: support for the intact-hepatocyte theory. *Hepatology* 1991; **13**: 475-481 [PMID: 1671846]

6 **Sawamura T**, Nakada H, Hazama H, Shiozaki Y, Sameshima Y, Tashiro Y. Hyperasialoglycoproteinemia in patients with chronic liver diseases and/or liver cell carcinoma. Asialoglycoprotein receptor in cirrhosis and liver cell carcinoma. *Gastroenterology* 1984; **87**: 1217-1221 [PMID: 6092193]

7 **Tomiguchi S**, Kira T, Oyama Y, Nabeshima M, Nakashima R, Tsuji A, Kojima A, Takahashi M, Yoshimatsu S, Sagara K. Correlation of Tc-99m GSA hepatic studies with biopsies in patients with chronic active hepatitis. *Clin Nucl Med* 1995; **20**: 717-720 [PMID: 7586877]

8 **Kaibori M**, Ha-Kawa SK, Uchida Y, Ishizaki M, Saito T, Matsui K, Hirohara J, Tanaka K, Kamiyama Y. Liver regeneration in donors evaluated by Tc-99m-GSA scintigraphy after living donor liver transplantation. *Dig Dis Sci* 2008; **53**: 850-855 [PMID: 17676394 DOI: 10.1007/s10620-007-9902-5]

9 **Vera DR**, Krohn KA, Scheibe PO, Stadalnik RC. Identifiability analysis of an in vivo receptor-binding radiopharmacokinetic system. *IEEE Trans Biomed Eng* 1985; **32**: 312-322 [PMID: 3997184 DOI: 10.1109/TBME.1985.325544]

10 **Vera DR**, Krohn KA, Stadalnik RC, Scheibe PO. Tc-99m galactosyl-neoglycoalbumin: in vitro characterization of receptor-mediated binding. *J Nucl Med* 1984; **25**: 779-787 [PMID: 6737077]

11 **Kurtaran A**, Müller C, Novacek G, Kaserer K, Mentes M, Raderer M, Pidlich J, Eibenberger K, Angelberger P, Virgolini I. Distinction between hepatic focal nodular hyperplasia and malignant liver lesions using technetium-99m-galactosyl-neoglycoalbumin. *J Nucl Med* 1997; **38**: 1912-1915 [PMID: 9430468]

12 **Stadalnik RC**, Vera DR. The evolution of (99m)Tc-NGA as a clinically useful receptor-binding radiopharmaceutical. *Nucl Med Biol* 2001; **28**: 499-503 [PMID: 11516694]

13 **Hayakawa N**, Nakamoto Y, Kurihara K, Yasoda A, Kanamoto N, Miura M, Inagaki N, Togashi K. A comparison between 11C-methionine PET/CT and MIBI SPECT/CT for localization of

parathyroid adenomas/hyperplasia. *Nucl Med Commun* 2015; **36**: 53-59 [PMID: 25244350 DOI: 10.1097/MNM.0000000000000216]
14 **Erritzoe D**, Talbot P, Frankle WG, Abi-Dargham A. Positron emission tomography and single photon emission CT molecular imaging in schizophrenia. *Neuroimaging Clin N Am* 2003; **13**: 817-832 [PMID: 15024964]
15 **Parker MW**, Iskandar A, Limone B, Perugini A, Kim H, Jones C, Calamari B, Coleman CI, Heller GV. Diagnostic accuracy of cardiac positron emission tomography versus single photon emission computed tomography for coronary artery disease: a bivariate meta-analysis. *Circ Cardiovasc Imaging* 2012; **5**: 700-707 [PMID: 23051888 DOI: 10.1161/CIRCIMAGING.112.978270]
16 **Li SH**, Qiu L, Cheng XQ, Li J, Du SD, Mao YL. The establishment of hepatic fibrosis model in mice through intraperitoneal injection with low concentrationcarbon tetrachloride. *Basic Clinical Med* 2014; **34**: 1694-1695
17 **Yang W**, Mou T, Peng C, Wu Z, Zhang X, Li F, Ma Y. Fluorine-18 labeled galactosyl-neoglycoalbumin for imaging the hepatic asialoglycoprotein receptor. *Bioorg Med Chem* 2009; **17**: 7510-7516 [PMID: 19796957 DOI: 10.1016/j.bmc.2009.09.017]
18 **Limdi JK**, Hyde GM. Evaluation of abnormal liver function tests. *Postgrad Med J* 2003; **79**: 307-312 [PMID: 12840117]
19 **Ribero D**, Curley SA, Imamura H, Madoff DC, Nagorney DM, Ng KK, Donadon M, Vilgrain V, Torzilli G, Roh M, Vauthey JN. Selection for resection of hepatocellular carcinoma and surgical strategy: indications for resection, evaluation of liver function, portal vein embolization, and resection. *Ann Surg Oncol* 2008; **15**: 986-992 [PMID: 18236112 DOI: 10.1245/s10434-007-9731-y]
20 **Taniguchi M**, Okizaki A, Watanabe K, Imai K, Uchida K, Einama T, Shuke N, Miyokawa N, Furukawa H. Hepatic clearance measured with (99m)Tc-GSA single-photon emission computed tomography to estimate liver fibrosis. *World J Gastroenterol* 2014; **20**: 16714-16720 [PMID: 25469042 DOI: 10.3748/wjg.v20.i44.16714]
21 **Sørensen M**, Mikkelsen KS, Frisch K, Villadsen GE, Keiding S. Regional metabolic liver function measured in patients with cirrhosis by 2-[^{18}F]fluoro-2-deoxy-D-galactose PET/CT. *J Hepatol* 2013; **58**: 1119-1124 [PMID: 23339954 DOI: 10.1016/j.jhep.2013.01.012]
22 **Mao YL**, Du SD. [Improvement of the methods of liver function assessment for primary hepatocellular carcinoma]. *Zhonghua Waike Zazhi* 2010; **48**: 1530-1533 [PMID: 21176664]

P- Reviewer: Aurello P, Boscá L, Mura VL **S- Editor**: Ma YJ
L- Editor: Filipodia **E- Editor**: Zhang FF

World Journal of Gastroenterology

Submit a Manuscript: http://www.f6publishing.com

World J Gastroenterol 2017 June 21; 23(23): 4285-4292

DOI: 10.3748/wjg.v23.i23.4285

ISSN 1007-9327 (print) ISSN 2219-2840 (online)

ORIGINAL ARTICLE

Observational Study

Magnetic resonance imaging may predict deep remission in patients with perianal fistulizing Crohn's disease

Lucie Thomassin, Laura Armengol-Debeir, Cloé Charpentier, Valerie Bridoux, Edith Koning, Guillaume Savoye, Céline Savoye-Collet

Lucie Thomassin, Laura Armengol-Debeir, Cloé Charpentier, Guillaume Savoye, Department of Gastroenterology, Rouen University Hospital, University of Rouen, F-76031 Rouen, France

Cloé Charpentier, Edith Koning, Céline Savoye-Collet, Department of Radiology, Rouen University Hospital, University of Rouen, F-76031 Rouen, France

Valerie Bridoux, Department of Digestive Surgery, Rouen University Hospital, University of Rouen, F-76031 Rouen, France

Author contributions: Thomassin L, Armengol-Debeir L, Savoye G and Savoye-Collet C contributed to study conception and design; Thomassin L, Armengol-Debeir L, Charpentier C, Bridoux V, Koning E, Savoye G and Savoye-Collet C contributed to data acquisition; Thomassin L, Koning E, Savoye G and Savoye-Collet C contributed to data analysis and interpretation; Thomassin L and Savoye-Collet C wrote the paper; Thomassin L, Savoye G and Savoye-Collet C contributed to manuscript editing.

Conflict-of-interest statement: There are no conflict of interest to report.

Data sharing statement: No additional data are available.

Manuscript source: Invited manuscript

Correspondence to: Celine Savoye-Collet, MD, PhD, Department of Radiology, Rouen University Hospital, University of Rouen, QUANTIF LITIS EA 4108, 1 rue de Germont, F-76031 Rouen, France. celine.savoye-collet@chu-rouen.fr
Telephone: +33-232-886496
Fax: +33-232-888235

Received: January 11, 2017
Peer-review started: January 12, 2017
First decision: March 16, 2017
Revised: April 3, 2017
Accepted: May 9, 2017
Article in press: May 9, 2017
Published online: June 21, 2017

Abstract

AIM

To evaluate the imaging course of Crohn's disease (CD) patients with perianal fistulas on long-term maintenance anti-tumor necrosis factor (TNF)-α therapy and identify predictors of deep remission.

METHODS

All patients with perianal CD treated with anti-TNF-α therapy at our tertiary care center were evaluated by magnetic resonance imaging (MRI) and clinical assessment. Two MR examinations were performed: at initiation of anti-TNF-α treatment and then at least 2 years after. Clinical assessment (remission, response and non-response) was based on Present' s criteria. Rectoscopic patterns, MRI Van Assche score, and MRI fistula activity signs (T2 signal and contrast enhancement) were collected for the two MR examinations. Fistula healing was defined as the absence of T2 hyperintensity and contrast enhancement on MRI. Deep remission was defined as the association of both clinical remission, absence of anal canal ulcers and healing on MRI. Characteristics and imaging patterns of patients with and without deep remission were compared by univariate and multivariate analyses.

RESULTS

Forty-nine consecutive patients (31 females and 18 males) were included. They ranged in age from 14-70 years (mean, 33 years). MRI and clinical assessment were performed after a mean period of exposure to anti-TNF-α therapy of 40 ± 3.7 mo. Clinical remission, response and non-response were observed in 53.1%, 20.4%, and 26.5% of patients, respectively. Deep remission was observed in 32.7% of patients. Among the 26 patients in clinical remission, 10 had persisting inflammation of fistulas on MRI (T2 hyperintensity, *n* = 7; contrast enhancement, *n* = 10). Univariate analysis showed that deep remission was associated with the absence of rectal involvement and the absence of switch of anti-TNF-α treatment or surgery requirement. Multivariate analysis demonstrated that only the absence of rectal involvement (OR = 4.6; 95%CI: 1.03-20.5) was associated with deep remission.

CONCLUSION

Deep remission is achieved in approximately one third of patients on maintenance anti-TNF-α therapy. Absence of rectal involvement is predictive of deep remission.

Key words: Crohn's disease; Anal fistula; Magnetic resonance imaging; Anus disease/diagnosis; Biotherapy

Core tip: Assessment of perianal fistulas is essential to guide management in Crohn's disease (CD). Magnetic resonance imaging (MRI) allows assessment of morphological and disease activity. Achieving both clinical remission and healing on MRI is a target in the management of perianal CD. In this study, we describe the clinical and radiological evolution of perianal CD in patients on long-term anti-tumor necrosis factor-α treatment. The period of follow-up was two times longer than those in previous studies. Deep remission is possible in one third of patients. Absence of rectal involvement is predictive of deep remission.

Thomassin L, Armengol-Debeir L, Charpentier C, Bridoux V, Koning E, Savoye G, Savoye-Collet C. Magnetic resonance imaging may predict deep remission in patients with perianal fistulizing Crohn's disease. *World J Gastroenterol* 2017; 23(23): 4285-4292 Available from: URL: http://www.wjgnet.com/1007-9327/full/v23/i23/4285.htm DOI: http://dx.doi.org/10.3748/wjg.v23.i23.4285

INTRODUCTION

Crohn's disease (CD) is a chronic inflammatory bowel disease, often associated with perianal complications such as fistulas or abscesses[1,2]. Perianal fistulas affect about one-third of patients during the evolution of CD and contribute to impaired quality of life[3]. This disease remains a challenging clinical condition, which is often refractory to conventional therapy. Management is based on combined therapies including antibiotics, drainage surgery, immunosuppressants and anti-tumor necrosis factor (TNF)-α therapy[4-11]. Induction therapy with anti-TNF-α drugs allows a complete response after 12 wk in 50% of patients but appears to be of short duration and maintenance therapy is required[8]. Recently, expanded allogeneic adipose-derived mesenchymal stem cells have been proved to be effective as reported by Panés *et al*[12] in the Lancet.

Magnetic resonance imaging (MRI) is a highly accurate non-invasive modality for the diagnosis and classification of perianal fistulas; as such it is considered to be the gold standard imaging technique for perianal CD[13-16]. It allows accurate morphological assessment to obtain information on perianal disease activity that can be used for follow-up[17-19]. Improvement in MRI techniques including 3 Tesla imaging and serial MRI examination have emerged as a standard to prepare, to guide and finally to gauge the success of treatment[20]. An MRI-based score (Van Assche) is available and uses different criteria to describe the anatomy (extension) and complexity (active inflammation, abscess) of the fistula[19,21]. Clinically, perianal disease activity in CD is assessed according to fistula drainage[7]. This simple clinical test is effective in defining treatment failure but not in assessing the degree of response, especially when fistula drainage is intermittent. It has been demonstrated that stopping drainage from cutaneous orifices does not necessarily mean that perianal disease has decreased or healed[22,23]. Clinical response often contrasts with the persistence of fistulas on MRI[21,24]. Assessment of fistula activity is challenging and is commonly performed based on T2 hyperintensity[25-27]. T2 weighted sequence with fat suppression is the optimal technique for MRI of fistulas[15]. A gadolinium enhanced T1 weighted sequence is useful for differentiating fluid/pus and granulation tissue[5,26-29]. The definition of fistula healing on MRI is usually based on the disappearance of T2 hyperintense signal and more recently on the absence of gadolinium contrast enhancement[18]. Achieving both clinical remission and healing on MRI is probably the most ambitious target in the management of perianal CD. Healing of lesions can be monitored in luminal CD[30,31].

The aims of this study were to describe the clinical and imaging courses of patients with perianal fistulas on long-term maintenance anti-TNF-α therapy and to identify clinical, endoscopic or imaging features associated with deep remission.

MATERIALS AND METHODS

Patients

Between 2003 and 2013, all consecutive patients

with fistulizing perianal CD treated with maintenance anti-TNF-α therapy at our tertiary care center were evaluated by clinical assessment and two MRI examinations. Patients treated with fibrin glue and plug were excluded. MRI was performed at the initiation of anti-TNF-α treatment and then at least 2 years after. This study was approved by the Institutional Review Board and informed consent was waived. Patients were diagnosed with CD by either endoscopy and/or histology and had at least one draining perianal fistula. Patients with an abscess had surgical drainage with seton placement, when appropriate, accompanied by a short course of antibiotics (fluoroquinolones and metronidazole). Seton removal was scheduled after completion of anti-TNF-α induction treatment. Immunosuppressant drugs were maintained or started (azathioprine, methotrexate or purinethol). All patients received anti-TNF-α induction treatment either with infliximab (5 mg/kg at weeks 0, 2 and 6) or with adalimumab (160, 80, 40 mg at week 0, 2 and 4, respectively). This induction treatment was followed by maintenance therapy based on infliximab 5 mg/kg every 8 wk or adalimumab 40 mg every other week. Each treatment could be optimized by increasing the dose or by decreasing the interval between injections. Certozilumab was used in three patients after infliximab or adalimumab failure with an induction treatment of 400 mg at weeks 0, 2 and 4 followed by maintenance therapy (400 mg every 4 wk).

Patients' characteristics [age, sex, smoking status, family history of inflammatory bowel diseases (IBD), CD history and activity, duration of disease, localizations of disease according to Montreal criteria, C-reactive protein (CRP) level, albumin rate, and surgical treatment] and rectal involvement at endoscopy were assessed.

MRI

All patients were evaluated by MRI before starting anti-TNF-α therapy and at least 2 years after treatment induction.

MRI examination was performed on a Philips Achieva 1.5 Tesla (Philips Medical Systems, Best, the Netherlands) using a torso phased-array coil. Patients did not receive any bowel preparation. All patients were placed in a supine position, with the pelvis centered on the coil. T2-weighted two-dimensional (2D) turbo spin-echo (TSE) sequences (TR = 6000 ms, TE = 500 ms, scan time = 5 min, matrix of 312 × 512, field of view 250 mm) and T2-weighted 2D TSE sequences with spectral presaturation inversion recovery (SPIR) (TR = 2000 ms, TE = 50 ms, scan time = 5 min, matrix of 312 × 512, field of view 250 mm) were obtained. T1-weighted 2D TSE sequences with and without fat suppression with SPIR (TR = 500 ms, TE = 10 ms, scan time = 5 min, matrix of 285 × 384, field of view = 250 mm) sequences were performed after gadolinium enhancement after checking for normal renal function. The intravenous injection was a mean dose of 15-20 mL gadolinium-DTPA (Magnevist, Schering, Germany) and the scan delay was 60 s. T2-weighted imaging was performed in transverse, sagittal and coronal planes. T1-weighted imaging was performed in transverse and coronal planes. Coronal and transverse planes were angled exactly parallel and perpendicular to the long axis of the anal canal.

The MRI images were assessed by two experienced gastrointestinal radiologists blinded to information on clinical outcome (CSC, EK). The same standardized report was used for initial and follow-up MR examinations. The items studied and their attributed values according to Van Assche were as follows: complexity of the fistula tracks (single unbranched = 1, single branched = 2, multiple = 3); location regarding the sphincters (inter/extra-sphincteric = 1, transsphincteric = 2, suprasphincteric = 3); extension (infralevatoric = 1, supralevatoric = 2); hyperintense appearance in T2-weighted sequences (absent = 0, mild = 4, pronounced = 8); presence of abscesses (hyperintense fluid collections > 3 mm in T2-weighted sequences = 4); and rectal wall involvement (thickened rectal wall = 2). In addition to Van Assche scoring, fistula enhancement after gadolinium-DTPA injection was analyzed and recorded as present or absent.

Clinical and MRI evaluations

Clinical evaluation: Clinical assessment was performed by senior gastroenterologists specialized in IBD (GS, LAD). All clinical examinations were performed by the same physician dedicated to one patient according to Present's criteria[7]. A second clinical evaluation was performed to assess the clinical response under treatment. Drainage of fistula openings was studied under gentle finger compression and identified as open and actively draining or closed. Clinical remission was defined as the absence of any draining fistulas and the absence of self-reported drainage episodes by the patient at two successive evaluations. Clinical response was defined as a reduction of 50% or more from baseline in the number of draining fistulas at the clinical evaluation, or in case of non-attendance at the clinical evaluation, as any persisting draining fistulas self-reported by the patient. Patients were considered non-responders in all other circumstances. Anal and rectoscopic patterns were collected to assess the presence of ulcers.

MR evaluation: The two MR examinations were compared to determine changes in items of Van Assche's score. Fistula enhancement was also compared in order to determine whether or not there was persistence of enhancement. Healing on MRI was defined as the disappearance of T2 hyperintensity and contrast enhancement after gadolinium injection.

Deep remission: Deep remission was defined as the association of clinical remission and the absence of

Table 1 Patients' characteristics *n* (%)

	Patients (*n* = 49)
Age yr (mean; extreme)	33; 14-70
Sex ratio (men/women)	0.58
Familial history of IBD	4 (8.2)
Smoking	21 (42.9)
Mean duration of CD (mo)	72 (0-300)
Location	
L1 ileal	4 (8.2)
L2 colonic	15 (30.6)
L3 ileocolonic	22 (44.9)
L2 or L3 + L4 upper disease	8 (16.3)
Disease behavior	
Inflammatory	34 (69.4)
Structuring	8 (16.3)
Penetrating	7 (14.3)
Extraintestinal manifestations	11 (22.4)
Ileocolonic resection	11 (22.4)
Previous perianal surgery	40 (81.6)
CRP (mg/L)	11.5 (1.6-167)
Albumin rate (g/L)	35.2 (20-49.2)

IBD: Inflammatory bowel disease; CD: Crohn's disease; L: Location; CRP: C-reactive protein.

anal canal ulcers and healing on MRI.

Statistical analysis

Qualitative data are presented as numbers and percentages and quantitative data as mean and maximal range values. Comparison of patients according to clinical response or MRI response was made by χ^2 test for qualitative and by Student's *t* test for quantitative variables. A multivariate analysis was carried out using a model of logistic regression for variables with $P < 0.15$. Results were considered significant when the *P*-value was < 0.05. BiostaTGV software was used for statistical analyses.

RESULTS

Patients' characteristics and baseline clinical assessment

Forty-nine patients (31 females and 18 males) were enrolled in this study. They ranged in age from 14-70 years, with a mean age of 33 years. Initial clinical characteristics of patients are presented in Table 1. Perineal involvement was present at diagnosis of CD in 6 (12%) patients. An ileocolonic location was observed in 22 (44.9%) patients, pure colonic disease in 15 (30.6%) and an isolated ileal location in 4 (8.2%). Extraintestinal manifestations were present in 11 (22.4%) patients. Disease behavior at diagnosis was considered as inflammatory in 34 (69.4%), stricturing in 8 (16.3%) and penetrating in 7 (14.3%). Eleven (22.4%) patients had ileocolonic resection.

At baseline all patients complained of spontaneous drainage episodes. Active drainage of the fistula opening was confirmed by gentle finger compression in all patients. Rectal involvement at endoscopy was observed in 27 patients.

Table 2 Baseline magnetic resonance imaging evaluation *n* (%)

	Patients (*n* = 49)
Van Assche score (mean)	13
Ramified fistula	13 (26.5)
Multiple fistula	10 (20.4)
Inter/extrasphincteric fistula	31 (63.3)
Transsphincteric fistula	15 (30.6)
Suprasphincteric fistula	3 (6.1)
Infralevatoric extension	43 (87.8)
Supralevatoric extension	6 (12.2)
Abscess	19 (38.8)
Rectal involvement	21 (42.9)
T2 hyperintensity	
Absent	3 (6.1)
Mild	11 (22.4)
Pronounced	35 (71.4)
Enhancement	49 (100)
Anorecto-vaginal fistula	7 (14.3)

Baseline MRI evaluation

MRI characteristics at inclusion are summarized in Table 2. The average Van Assche score was 13 ± 4. The most common fistula location was inter- or extra-sphincteric (63.3%) and an infralevatoric extension was observed in 87.8% of patients. Nineteen (38.8%) patients (38.8%) had an abscess. Pronounced T2 hyperintensity of fistula tracks was found in 35 (71.4%) patients. All fistulas were enhanced by gadolinium injection.

Treatment

Forty-three (87.8%) patients received infliximab with a mean treatment duration of 23 ± 20 mo and a mean number of 13 treatments. Six (12.2%) patients received adalimumab with a mean duration of 21 ± 14 mo. Thirty-one (63.3%) patients had an associated immunosuppressant drug. During the study period, eleven (22.4%) patients had a switch of anti-TNF-α treatment. Twenty-one (42.8%) patients required surgical drainage of their perianal lesions. The average follow-up period was 40 ± 27 mo.

Clinical and imaging evaluations

Among the 49 patients, 26 (53.1%) were in clinical remission, 10 (20.4%) in clinical response and 13 (26.5%) were non-responders at the end of follow-up.

Deep remission (clinical remission, absence of anal canal ulcers and healing on MRI) was observed in 16 (32.7%) patients (Figure 1).

Van Assche score increased in 30 (61.2%) patients and decreased in 11 (22.4%) patients. Average Van Assche score was 8 ± 6. T2 hyperintensity disappeared but contrast enhancement persisted after gadolinium injection in 4 patients. Van Assche score was significantly lower in patients in clinical remission than in non-responders (0 *vs* 14, $P < 0.05$).

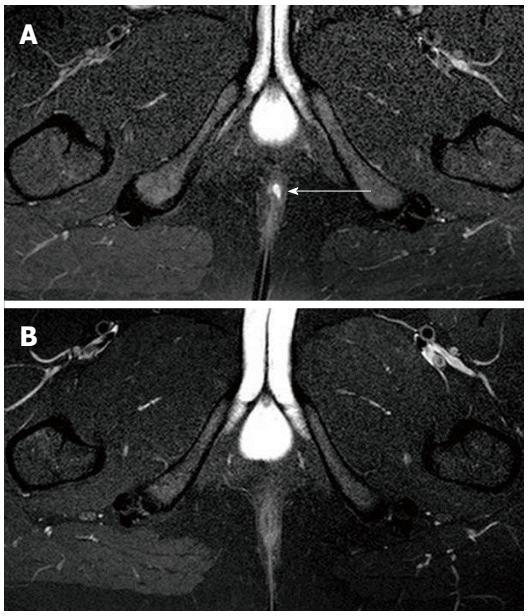

Figure 1 Comparison of initial magnetic resonance imaging (A) and follow-up magnetic resonance imaging (B). Axial spectral presaturation inversion recovery T2-weighted sequence at the same anatomical level. Presence of an initial active fistula (A, arrow) and disappearance of the hyperintensity at follow-up (B): this patient was in clinical response.

Moreover, the disappearance of both T2 hyperintensity and gadolinium contrast enhancement, between the baseline and final MRI, was significantly more frequent in patients in clinical remission (92.3% *vs* 26.9% and 100% *vs* 38.5%, respectively, $P < 0.05$). No significant change in these patterns was observed in non-responders.

Predictive factors of clinical remission

In univariate analysis, clinical remission was significantly associated with male gender (52% *vs* 20%, $P = 0.04$), low initial CRP (6 mg/L *vs* 13 mg/L, $P = 0.04$), absence of rectal involvement (42.3% *vs* 69.6%, $P = 0.05$), absence of ramified fistula at initial MRI (11.5% *vs* 43.5%, $P = 0.02$), absence of antibiotics at diagnosis (53.8% *vs* 87%, $P = 0.02$), longer duration of treatment with infliximab (32 mo *vs* 16 mo, $P = 0.0004$), absence of perianal lesion with infliximab (8.3% *vs* 63.2%, $P = 0.001$), and absence of switch of anti-TNF-α treatment (3.8% *vs* 43.5%, $P = 0.001$).

In multivariate analysis, two factors were significantly associated with clinical remission: absence of rectal involvement (42.3% *vs* 69.6%, OR = 4.7, 95%CI: 1.21-49) and absence of switch of anti-TNF-α (3.8% *vs* 43.5%, OR = 7.7).

Predictive factors of deep remission

In univariate analysis, deep remission was significantly associated with absence of rectal involvement (37.5% *vs* 63.6%, $P = 0.12$), absence of surgical drainage at diagnosis (68.8% *vs* 87.9%, $P = 0.011$), absence of antibiotics at diagnosis (50% *vs* 78.8%, $P = 0.04$), longer duration of treatment with infliximab (27 mo *vs* 18 mo, $P = 0.039$), absence of perianal lesion with infliximab (7.1% *vs* 30.6%, $P = 0.008$) and absence of switch of anti-TNF-α treatment (0% *vs* 33.3%, $P = 0.009$).

In multivariate analysis one factor was significantly associated with deep remission: absence of rectal involvement (37.5% *vs* 63.6%, OR = 4.6, 95%CI: 1.03-20.5).

DISCUSSION

In this study, we describe the clinical and radiological evolution of fistulizing perianal CD in a cohort of 49 patients on anti-TNF-α treatment with a mean follow-up period of 40 mo. Of note, the period of follow-up in our study was two times longer than those in previous studies. At the end of follow-up, not only were 53% of our patients in clinical remission but one third was in deep remission, corresponding to clinical remission associated with healing on MRI. One third of patients in clinical remission had a persisting pathology on MRI. In multivariate analysis, there were two predictive factors of clinical remission: absence of rectal involvement at diagnosis and absence of switch of anti-TNF-α during follow-up. Only the absence of rectal involvement remained predictive of deep remission.

The demographic characteristics and clinical remission rates of our patients are comparable to those of other studies[32,33]. The percentage of anorecto-vaginal fistulas in our study (20.4%) was higher than that described in the first study but similar to the most recent ones[34-36]. Our clinical remission rate was slightly higher than those in other studies, probably due to our longer follow-up period and longer duration of anti-TNF-α treatment[8,18,22,23,37]. Additionally, it might also be related to longer seton drainage time as setons were removed after completion of induction treatment. Moreover, 40% of our patients required surgical seton drainage, which is higher than those in previous studies but allowed us to achieve earlier and more efficient drainage before introducing anti-TNF-α treatment[18,21,22]. The treatment regimen we used was comparable to those of previous studies[10].

In our study, deep remission was found in 32.7% of patients. Bell, who reported follow-up in only seven patients, defined improvement as disappearance or reduction of fistulas but there was no analysis of contrast enhancement in MRI[23]. Van Assche, in a series of six patients, reported disappearance of T2 hyperintensity in three patients and absence of fistula in two patients on MRI[21]. Ng found complete healing, defined as absence of T2 hyperintensity of fistula, in 30% of 25 patients at 18 mo[22]. In a previous study from our center, including 20 patients with 1-year follow-up, we reported an improvement in Van Assche score as well as disappearance of T2 hyperintensity and contrast enhancement in 30% of patients[21]. The current study follows this approach

with a higher number of patients and longer follow-up and the same MR parameters: T2 hyperintensity used in the Van Assche score and analysis of contrast enhancement. Analysis of contrast enhancement has now clearly proven its interest in follow-up and characterization between inflammatory or fibrotic ileocolonic lesions[31,38]. Recent MRI sequences like diffusion or magnetization transfer could be used in the future for evaluation of patients under treatment[20,39,40]. Compared to our previous study, we found a higher (one third) rate of deep remission at 40 mo than at 12 mo (one quarter)[18]. In univariate analysis, longer duration of treatment and increased rate of healing were significantly associated with deep remission.

Identifying predictive factors for deep remission remains challenging[41]. Tougeron, in a study on 26 patients with infliximab induction therapy, reported that predictive factors significantly associated with clinical remission were low albumin and CD activity index, absence of active luminal disease and absence of endoscopic rectal involvement in univariate analysis; endoscopic rectal involvement was the only factor in multivariate analysis[36]. We confirm the data related to rectal involvement in endoscopy. The presence of proctitis is highly relevant for fistula management and prognosis[15]. In our study, assessment of proctitis by MRI was performed with rectal wall thickness according to Van Assche criteria. Other interesting patterns such as contrast enhancement and MRI features involving the mesorectal tissue like presence of creeping fat have been suggested more recently[42].

The role of MRI in the monitoring of patients on long-term anti-TNF therapy is not well defined. Regular perineal MRI could be useful to assess response to treatment. If unfavorable, optimization or modification of treatment could be proposed. We could consider decreasing or discontinuing treatment in patients in deep remission, but with regular monitoring to detect potential recurrences. Recent data on trough level suggest that monitoring drugs may be useful in making appropriate decisions in this setting[43].

Nonetheless, our study has limitations like absence of perineal disease activity index and trough level monitoring. We did not include patients participating in other therapeutic trials using local therapies like fibrin glue or plug[44-46].

In conclusion, our findings show that deep remission is possible in one third of patients on maintenance anti-TNF-α therapy. Concerning predictive patterns, only absence of rectal involvement is predictive of deep remission. Our results may serve as a basis for future management of anti-TNF-α treatment once deep remission is acquired.

ACKNOWLEDGMENTS

The authors are grateful to Nikki Sabourin-Gibbs, Rouen University Hospital, for her help in editing the manuscript.

COMMENTS

Background

Perianal fistulas remain a challenging clinical condition and their management is based on combined therapies. Anti-tumor necrosis factor (TNF)-α maintenance therapy is often required. Magnetic resonance imaging (MRI) allows accurate morphological assessment to obtain information on perianal disease activity that can be used for follow-up.

Research frontiers

Anti-TNF-α maintenance therapy is usually required to treat perineal fistulas. MRI examination has emerged to gauge the success of treatment as achieving both clinical remission and healing on MRI is probably the most ambitious target.

Innovations and breakthroughs

In this study, the authors describe the clinical and radiological evolution of perianal Crohn's disease (CD) in patients on long-term anti-TNF-α treatment. The period of follow-up was two times longer than those in previous studies.

Applications

Regular perineal MRI could be useful to assess response to treatment. In case of unfavourable outcome, optimization or modification of treatment could be proposed and in patients in deep remission de-escalation could be considered.

Peer-review

This study described the clinical and radiological evolution of fistulizing perianal CD in a cohort of 49 patients who were treated with anti-TNF-α agents for 40 mo. Authors concluded that deep remission was achieved in approximately one third of patients who were administered with anti-TNF-α therapy and the absence of rectal involvement was predictive of deep remission. However, one third of clinical remission patients had a persisting pathology on MRI. This study is of clinical value to patients with perianal CD.

REFERENCES

1 **Chouraki V**, Savoye G, Dauchet L, Vernier-Massouille G, Dupas JL, Merle V, Laberenne JE, Salomez JL, Lerebours E, Turck D, Cortot A, Gower-Rousseau C, Colombel JF. The changing pattern of Crohn's disease incidence in northern France: a continuing increase in the 10- to 19-year-old age bracket (1988-2007). *Aliment Pharmacol Ther* 2011; **33**: 1133-1142 [PMID: 21488915 DOI: 10.1111/j.1365-2036.2011.04628.x]

2 **Cosnes J**, Gower-Rousseau C, Seksik P, Cortot A. Epidemiology and natural history of inflammatory bowel diseases. *Gastroenterology* 2011; **140**: 1785-1794 [PMID: 21530745 DOI: 10.1053/j.gastro.2011.01.055]

3 **Schwartz DA**, Pemberton JH, Sandborn WJ. Diagnosis and treatment of perianal fistulas in Crohn disease. *Ann Intern Med* 2001; **135**: 906-918 [PMID: 11712881]

4 **Van Assche G**, Dignass A, Reinisch W, van der Woude CJ, Sturm A, De Vos M, Guslandi M, Oldenburg B, Dotan I, Marteau P, Ardizzone A, Baumgart DC, D'Haens G, Gionchetti P, Portela F, Vucelic B, Söderholm J, Escher J, Koletzko S, Kolho KL, Lukas M, Mottet C, Tilg H, Vermeire S, Carbonnel F, Cole A, Novacek G, Reinshagen M, Tsianos E, Herrlinger K, Oldenburg B, Bouhnik Y, Kiesslich R, Stange E, Travis S, Lindsay J. The second European evidence-based Consensus on the diagnosis and management of Crohn's disease: Special situations. *J Crohns Colitis* 2010; **4**: 63-101 [PMID: 21122490 DOI: 10.1016/j.crohns.2009.09.009]

5 **Rutgeerts P**. Review article: treatment of perianal fistulizing Crohn's disease. *Aliment Pharmacol Ther* 2004; **20** Suppl 4: 106-110 [PMID: 15352905 DOI: 10.1111/j.1365-2036.2004.02060.x]

6 **Schwartz DA**, Herdman CR. Review article: The medical treatment

of Crohn's perianal fistulas. *Aliment Pharmacol Ther* 2004; **19**: 953-967 [PMID: 15113362 DOI: 10.1111/j.1365-2036.2004.01917.x]

7 **Present DH**, Rutgeerts P, Targan S, Hanauer SB, Mayer L, van Hogezand RA, Podolsky DK, Sands BE, Braakman T, DeWoody KL, Schaible TF, van Deventer SJ. Infliximab for the treatment of fistulas in patients with Crohn's disease. *N Engl J Med* 1999; **340**: 1398-1405 [PMID: 10228190 DOI: 10.1056/NEJM199905063401804]

8 **Sands BE**, Anderson FH, Bernstein CN, Chey WY, Feagan BG, Fedorak RN, Kamm MA, Korzenik JR, Lashner BA, Onken JE, Rachmilewitz D, Rutgeerts P, Wild G, Wolf DC, Marsters PA, Travers SB, Blank MA, van Deventer SJ. Infliximab maintenance therapy for fistulizing Crohn's disease. *N Engl J Med* 2004; **350**: 876-885 [PMID: 14985485 DOI: 10.1056/NEJMoa030815]

9 **Colombel JF**, Sandborn WJ, Rutgeerts P, Enns R, Hanauer SB, Panaccione R, Schreiber S, Byczkowski D, Li J, Kent JD, Pollack PF. Adalimumab for maintenance of clinical response and remission in patients with Crohn's disease: the CHARM trial. *Gastroenterology* 2007; **132**: 52-65 [PMID: 17241859 DOI: 10.1053/j.gastro.2006.11.041]

10 **Colombel JF**, Schwartz DA, Sandborn WJ, Kamm MA, D'Haens G, Rutgeerts P, Enns R, Panaccione R, Schreiber S, Li J, Kent JD, Lomax KG, Pollack PF. Adalimumab for the treatment of fistulas in patients with Crohn's disease. *Gut* 2009; **58**: 940-948 [PMID: 19201775 DOI: 10.1136/gut.2008.159251]

11 **Lichtenstein GR**, Yan S, Bala M, Blank M, Sands BE. Infliximab maintenance treatment reduces hospitalizations, surgeries, and procedures in fistulizing Crohn's disease. *Gastroenterology* 2005; **128**: 862-869 [PMID: 15825070]

12 **Panés J**, García-Olmo D, Van Assche G, Colombel JF, Reinisch W, Baumgart DC, Dignass A, Nachury M, Ferrante M, Kazemi-Shirazi L, Grimaud JC, de la Portilla F, Goldin E, Richard MP, Leselbaum A, Danese S. Expanded allogeneic adipose-derived mesenchymal stem cells (Cx601) for complex perianal fistulas in Crohn's disease: a phase 3 randomised, double-blind controlled trial. *Lancet* 2016; **388**: 1281-1290 [PMID: 27477896 DOI: 10.1016/S0140-6736(16)31203-X]

13 **Buchanan G**, Halligan S, Williams A, Cohen CR, Tarroni D, Phillips RK, Bartram CI. Effect of MRI on clinical outcome of recurrent fistula-in-ano. *Lancet* 2002; **360**: 1661-1662 [PMID: 12457791 DOI: 10.1016/S0140-6736(02)11605-9]

14 **Panes J**, Bouhnik Y, Reinisch W, Stoker J, Taylor SA, Baumgart DC, Danese S, Halligan S, Marincek B, Matos C, Peyrin-Biroulet L, Rimola J, Rogler G, van Assche G, Ardizzone S, Ba-Ssalamah A, Bali MA, Bellini D, Biancone L, Castiglione F, Ehehalt R, Grassi R, Kucharzik T, Maccioni F, Maconi G, Magro F, Martín-Comín J, Morana G, Pendsé D, Sebastian S, Signore A, Tolan D, Tielbeek JA, Weishaupt D, Wiarda B, Laghi A. Imaging techniques for assessment of inflammatory bowel disease: joint ECCO and ESGAR evidence-based consensus guidelines. *J Crohns Colitis* 2013; **7**: 556-585 [PMID: 23583097 DOI: 10.1016/j.crohns.2013.02.020]

15 **Gecse KB**, Bemelman W, Kamm MA, Stoker J, Khanna R, Ng SC, Panés J, van Assche G, Liu Z, Hart A, Levesque BG, D' Haens G. A global consensus on the classification, diagnosis and multidisciplinary treatment of perianal fistulising Crohn's disease. *Gut* 2014; **63**: 1381-1392 [PMID: 24951257 DOI: 10.1136/gutjnl-2013-306709]

16 **Gionchetti P**, Dignass A, Danese S, Magro Dias FJ, Rogler G, Lakatos PL, Adamina M, Ardizzone S, Buskens CJ, Sebastian S, Laureti S, Sampietro GM, Vucelic B, van der Woude CJ, Barreiro-de Acosta M, Maaser C, Portela F, Vavricka SR, Gomollón F. 3rd European Evidence-based Consensus on the Diagnosis and Management of Crohn's Disease 2016: Part 2: Surgical Management and Special Situations. *J Crohns Colitis* 2017; **11**: 135-149 [PMID: 27660342 DOI: 10.1093/ecco-jcc/jjw169]

17 **Savoye G**, Savoye-Collet C. How deep is remission in perianal Crohn's disease and do imaging modalities matter? *Am J Gastroenterol* 2010; **105**: 1445-1446; author reply 1446 [PMID: 20523317 DOI: 10.1038/ajg.2010.35]

18 **Savoye-Collet C**, Savoye G, Koning E, Dacher JN, Lerebours E. Fistulizing perianal Crohn's disease: contrast-enhanced magnetic resonance imaging assessment at 1 year on maintenance anti-TNF-alpha therapy. *Inflamm Bowel Dis* 2011; **17**: 1751-1758 [PMID: 21744430 DOI: 10.1002/ibd.21568]

19 **Tozer P**, Ng SC, Siddiqui MR, Plamondon S, Burling D, Gupta A, Swatton A, Tripoli S, Vaizey CJ, Kamm MA, Phillips R, Hart A. Long-term MRI-guided combined anti-TNF-α and thiopurine therapy for Crohn's perianal fistulas. *Inflamm Bowel Dis* 2012; **18**: 1825-1834 [PMID: 22223472 DOI: 10.1002/ibd.21940]

20 **Sheedy SP**, Bruining DH, Dozois EJ, Faubion WA, Fletcher JG. MR Imaging of Perianal Crohn Disease. *Radiology* 2017; **282**: 628-645

21 **Van Assche G**, Vanbeckevoort D, Bielen D, Coremans G, Aerden I, Noman M, D'Hoore A, Penninckx F, Marchal G, Cornillie F, Rutgeerts P. Magnetic resonance imaging of the effects of infliximab on perianal fistulizing Crohn's disease. *Am J Gastroenterol* 2003; **98**: 332-339 [PMID: 12591051 DOI: 10.1111/j.1572-0241.2003.07241.x]

22 **Ng SC**, Plamondon S, Gupta A, Burling D, Swatton A, Vaizey CJ, Kamm MA. Prospective evaluation of anti-tumor necrosis factor therapy guided by magnetic resonance imaging for Crohn's perineal fistulas. *Am J Gastroenterol* 2009; **104**: 2973-2986 [PMID: 19755971 DOI: 10.1038/ajg.2009.509]

23 **Bell SJ**, Halligan S, Windsor AC, Williams AB, Wiesel P, Kamm MA. Response of fistulating Crohn's disease to infliximab treatment assessed by magnetic resonance imaging. *Aliment Pharmacol Ther* 2003; **17**: 387-393 [PMID: 12562451]

24 **Ardizzone S**, Maconi G, Colombo E, Manzionna G, Bollani S, Bianchi Porro G. Perianal fistulae following infliximab treatment: clinical and endosonographic outcome. *Inflamm Bowel Dis* 2004; **10**: 91-96 [PMID: 15168807]

25 **Tissot O**, Bodnar D, Henry L, Dubreuil A, Valette PJ. [Ano-perineal fistula in MRI. Contribution of T2 weighted sequences]. *J Radiol* 1996; **77**: 253-260 [PMID: 8734205]

26 **Szurowska E**, Wypych J, Izycka-Swieszewska E. Perianal fistulas in Crohn's disease: MRI diagnosis and surgical planning: MRI in fistulazing perianal Crohn's disease. *Abdom Imaging* 2007; **32**: 705-718 [PMID: 17334876 DOI: 10.1007/s00261-007-9188-2]

27 **Halligan S**, Stoker J. Imaging of fistula in ano. *Radiology* 2006; **239**: 18-33 [PMID: 16567481 DOI: 10.1148/radiol.2391041043]

28 **Horsthuis K**, Lavini C, Bipat S, Stokkers PC, Stoker J. Perianal Crohn disease: evaluation of dynamic contrast-enhanced MR imaging as an indicator of disease activity. *Radiology* 2009; **251**: 380-387 [PMID: 19401571 DOI: 10.1148/radiol.2512072128]

29 **Horsthuis K**, Ziech ML, Bipat S, Spijkerboer AM, de Bruine-Dobben AC, Hommes DW, Stoker J. Evaluation of an MRI-based score of disease activity in perianal fistulizing Crohn's disease. *Clin Imaging* 2011; **35**: 360-365 [PMID: 21872125 DOI: 10.1016/j.clinimag.2010.09.003]

30 **Ordás I**, Rimola J, Rodríguez S, Paredes JM, Martínez-Pérez MJ, Blanc E, Arévalo JA, Aduna M, Andreu M, Radosevic A, Ramírez-Morros AM, Pinó S, Gallego M, Jauregui-Amezaga A, Ricart E, Panés J. Accuracy of magnetic resonance enterography in assessing response to therapy and mucosal healing in patients with Crohn's disease. *Gastroenterology* 2014; **146**: 374-382.e1 [PMID: 24177375 DOI: 10.1053/j.gastro.2013.10.055]

31 **Rimola J**, Planell N, Rodríguez S, Delgado S, Ordás I, Ramírez-Morros A, Ayuso C, Aceituno M, Ricart E, Jauregui-Amezaga A, Panés J, Cuatrecasas M. Characterization of inflammation and fibrosis in Crohn's disease lesions by magnetic resonance imaging. *Am J Gastroenterol* 2015; **110**: 432-440 [PMID: 25623654 DOI: 10.1038/ajg.2014.424]

32 **Sandborn WJ**, Fazio VW, Feagan BG, Hanauer SB. AGA technical review on perianal Crohn's disease. *Gastroenterology* 2003; **125**: 1508-1530 [PMID: 14598268]

33 **Bouguen G**, Siproudhis L, Bretagne JF, Bigard MA, Peyrin-Biroulet L. Nonfistulizing perianal Crohn's disease: clinical features, epidemiology, and treatment. *Inflamm Bowel Dis* 2010; **16**: 1431-1442 [PMID: 20310013 DOI: 10.1002/ibd.21261]

34 **Singh B**, McC Mortensen NJ, Jewell DP, George B. Perianal Crohn's disease. *Br J Surg* 2004; **91**: 801-814 [PMID: 15227686 DOI: 10.1002/bjs.4613]

35 **Radcliffe AG**, Ritchie JK, Hawley PR, Lennard-Jones JE, Northover JM. Anovaginal and rectovaginal fistulas in Crohn's disease. *Dis Colon Rectum* 1988; **31**: 94-99 [PMID: 3338350]

36 **Tougeron D**, Savoye G, Savoye-Collet C, Koning E, Michot F, Lerebours E. Predicting factors of fistula healing and clinical remission after infliximab-based combined therapy for perianal fistulizing Crohn's disease. *Dig Dis Sci* 2009; **54**: 1746-1752 [PMID: 19003531 DOI: 10.1007/s10620-008-0545-y]

37 **Roumeguère P**, Bouchard D, Pigot F, Castinel A, Juguet F, Gaye D, Capdepont M, Zerbib F, Laharie D. Combined approach with infliximab, surgery, and methotrexate in severe fistulizing anoperineal Crohn's disease: results from a prospective study. *Inflamm Bowel Dis* 2011; **17**: 69-76 [PMID: 20623697 DOI: 10.1002/ibd.21405]

38 **Rimola J**, Rodriguez S, García-Bosch O, Ordás I, Ayala E, Aceituno M, Pellisé M, Ayuso C, Ricart E, Donoso L, Panés J. Magnetic resonance for assessment of disease activity and severity in ileocolonic Crohn's disease. *Gut* 2009; **58**: 1113-1120 [PMID: 19136510 DOI: 10.1136/gut.2008.167957]

39 **Dohan A**, Taylor S, Hoeffel C, Barret M, Allez M, Dautry R, Zappa M, Savoye-Collet C, Dray X, Boudiaf M, Reinhold C, Soyer P. Diffusion-weighted MRI in Crohn's disease: Current status and recommendations. *J Magn Reson Imaging* 2016; **44**: 1381-1396 [PMID: 27249184 DOI: 10.1002/jmri.25325]

40 **Pinson C**, Dolores M, Cruypeninck Y, Koning E, Dacher JN, Savoye G, Savoye-Collet C. Magnetization transfer ratio for the assessment of perianal fistula activity in Crohn's disease. *Eur Radiol* 2017; **27**: 80-87 [PMID: 27085695 DOI: 10.1007/s00330-016-4350-2]

41 **Louis E**, Vernier-Massouille G, Grimaud JC, Bouhnik Y, Laharie D, Dupas JL, Pillant H, Picon L, Veyrac M, Flamant M, Savoye G, Jian R, De Vos M, Paintaud G, Piver E, Colombel JF, Mary JY, Lemann M. 961 Infliximab Discontinuation in Crohn's Disease Patients in Stable Remission On Combined Therapy with Immunosuppressors: A Prospective Ongoing Cohort Study. *Gastroenterology* 2009; **136**: A146 [DOI: 10.1016/S0016-5085(09)60659-4]

42 **Tutein Nolthenius CJ**, Bipat S, Mearadji B, Spijkerboer AM, Ponsioen CY, Montauban van Swijndregt AD, Stoker J. MRI characteristics of proctitis in Crohn's disease on perianal MRI. *Abdom Radiol* (NY) 2016; **41**: 1918-1930 [PMID: 27315072 DOI: 10.1007/s00261-016-0802-z]

43 **Ungar B**, Levy I, Yavne Y, Yavzori M, Picard O, Fudim E, Loebstein R, Chowers Y, Eliakim R, Kopylov U, Ben-Horin S. Optimizing Anti-TNF-α Therapy: Serum Levels of Infliximab and Adalimumab Are Associated With Mucosal Healing in Patients With Inflammatory Bowel Diseases. *Clin Gastroenterol Hepatol* 2016; **14**: 550-557.e2 [PMID: 26538204 DOI: 10.1016/j.cgh.2015.10.025]

44 **Senéjoux A**, Siproudhis L, Abramowitz L, Munoz-Bongrand N, Desseaux K, Bouguen G, Bourreille A, Dewit O, Stefanescu C, Vernier G, Louis E, Grimaud JC, Godart B, Savoye G, Hebuterne X, Bauer P, Nachury M, Laharie D, Chevret S, Bouhnik Y. Fistula Plug in Fistulising Ano-Perineal Crohn's Disease: a Randomised Controlled Trial. *J Crohns Colitis* 2016; **10**: 141-148 [PMID: 26351393 DOI: 10.1093/ecco-jcc/jjv162]

45 **Grimaud JC**, Munoz-Bongrand N, Siproudhis L, Abramowitz L, Sénéjoux A, Vitton V, Gambiez L, Flourié B, Hébuterne X, Louis E, Coffin B, De Parades V, Savoye G, Soulé JC, Bouhnik Y, Colombel JF, Contou JF, François Y, Mary JY, Lémann M. Fibrin glue is effective healing perianal fistulas in patients with Crohn's disease. *Gastroenterology* 2010; **138**: 2275-2281, 2281.e1 [PMID: 20178792 DOI: 10.1053/j.gastro.2010.02.013]

46 **Silverberg MS**, Satsangi J, Ahmad T, Arnott ID, Bernstein CN, Brant SR, Caprilli R, Colombel JF, Gasche C, Geboes K, Jewell DP, Karban A, Loftus EV, Peña AS, Riddell RH, Sachar DB, Schreiber S, Steinhart AH, Targan SR, Vermeire S, Warren BF. Toward an integrated clinical, molecular and serological classification of inflammatory bowel disease: report of a Working Party of the 2005 Montreal World Congress of Gastroenterology. *Can J Gastroenterol* 2005; **19** Suppl A: 5A-36A [PMID: 16151544]

P- Reviewer: Cao GW, Kaimakliotis P, Wasserberg N
S- Editor: Ma YJ **L- Editor**: Wang TQ **E- Editor**: Wang CH

World Journal of Gastroenterology

Submit a Manuscript: http://www.f6publishing.com

World J Gastroenterol 2017 June 21; 23(23): 4293-4302

DOI: 10.3748/wjg.v23.i23.4293

ISSN 1007-9327 (print) ISSN 2219-2840 (online)

ORIGINAL ARTICLE

Observational Study

New totally intracorporeal reconstructive approach after robotic total gastrectomy: Technical details and short-term outcomes

Amilcare Parisi, Francesco Ricci, Alessandro Gemini, Stefano Trastulli, Roberto Cirocchi, Giorgio Palazzini, Vito D'Andrea, Jacopo Desiderio

Amilcare Parisi, Francesco Ricci, Alessandro Gemini, Stefano Trastulli, Roberto Cirocchi, Jacopo Desiderio, Department of Digestive Surgery, St. Mary's Hospital of Terni, University of Perugia, 05100 Terni, Italy

Roberto Cirocchi, Department of General Surgery, St. Mary's Hospital of Terni, University of Perugia, 05100 Terni, Italy

Giorgio Palazzini, Vito D'Andrea, Department of Surgical Science, "La Sapienza" University, 00185 Rome, Italy

Author contributions: Parisi A and Desiderio J were involved in study conception and design; Parisi A, Ricci F, Gemini A, Trastulli S, Cirocchi R, Palazzini G, D'Andrea V and Desiderio J collected data and were involved in critical revision and drafting of the final manuscript.

Institutional review board statement: The study was approved by the region ethics committee (CEAS Umbria).

Informed consent statement: Not required for the present study.

Conflict-of-interest statement: No benefits in any form have been received or will be received from a commercial party related directly or indirectly to the subject of this article.

Data sharing statement: Technical appendix available from the corresponding author at djdesi85@hotmail.it.

Manuscript source: Invited manuscript

Correspondence to: Jacopo Desiderio, MD, Department of Digestive Surgery, St. Mary's Hospital of Terni, University of Perugia, Via Tristano di Joannuccio 1, 05100 Terni, Italy. jacopo.desiderio@studenti.unipg.it
Telephone: +39-349-7531121
Fax: +39-744-205078

Received: January 25, 2017
Peer-review started: February 1, 2017
First decision: March 3, 2017
Revised: March 31, 2017
Accepted: May 9, 2017
Article in press: May 9, 2017
Published online: June 21, 2017

Abstract

AIM

To show outcomes of our series of patients that underwent a total gastrectomy with a robotic approach and highlight the technical details of a proposed solution for the reconstruction phase.

METHODS

Data of gastrectomies performed from May 2014 to October 2016, were extracted and analyzed. Basic characteristics of patients, surgical and clinical outcomes were reported. The technique for reconstruction (Parisi Technique) consists on a loop of bowel shifted up antecolic to directly perform the esophago-enteric anastomosis followed by a second loop, measured up to 40 cm starting from the esojejunostomy, fixed to the biliary limb to create an enteroenteric anastomosis. The continuity between the two anastomoses is interrupted

just firing a linear stapler, so obtaining the Roux-en-Y by avoiding to interrupt the mesentery.

RESULTS

Fifty-five patients were considered in the present analysis. Estimated blood loss was 126.55 ± 73 mL, no conversions to open surgery occurred, R0 resections were obtained in all cases. Hospital stay was 5 (3-17) d, no anastomotic leakage occurred. Overall, a fast functional recovery was shown with a median of 3 (3-6) d in starting a solid diet.

CONCLUSION

Robotic surgery and the adoption of a tailored reconstruction technique have increased the feasibility and safety of a minimally invasive approach for total gastrectomy. The present series of patients shows its implementation in a western center with satisfying short-term outcomes.

Key words: Esophagojejunal anastomosis; Gastric cancer; Total gastrectomy; Robotic surgery; Minimally invasive surgery

Core tip: Minimally invasive surgery is growing interest for gastric cancer. Technology has allowed to increase the safety and feasibility of this approach, even in demanding procedures. Total gastrectomy represents a challenge in this context due to the need to ensure a safe esophagojejunal anastomosis. Leakages can strongly influence the postoperative course of the patient until lead to serious consequences.

Parisi A, Ricci F, Gemini A, Trastulli S, Cirocchi R, Palazzini G, D'Andrea V, Desiderio J. New totally intracorporeal reconstructive approach after robotic total gastrectomy: Technical details and short-term outcomes. *World J Gastroenterol* 2017; 23(23): 4293-4302 Available from: URL: http://www.wjgnet.com/1007-9327/full/v23/i23/4293.htm DOI: http://dx.doi.org/10.3748/wjg.v23.i23.4293

INTRODUCTION

Minimally invasive surgery for gastric cancer is growing attention due to its potential advantages in enhancing the postoperative recovery of patients and quality of life[1]. The main limitations are the proper execution of an extended lymphadenectomy, when required, and a safe approach for reconstruction.

The latter is still the object of controversy and most surgeons are concerned about the possibility to perform a totally intracorporeal procedure after a total gastrectomy.

Recent spread of the robotic systems has modified the way we perform minimally invasive surgery and has led to the evolution of traditional laparoscopy. This progress allows surgeons to overcome the limits of laparoscopy through a 3D vision, articulated instruments, filtering of physiological tremor and absence of fulcrum effects, thus increasing dexterity and precision in dissection and suturing movements. These are key factors required for complex and technical demanding reconstructions to restore the digestive continuity.

However, nowadays, few studies[2] have discussed about reconstruction techniques for minimally invasive gastric surgery even if this issue is the most impacted factor on postoperative outcomes.

Hybrid procedures are common described in the literature, in most of cases an extracorporeal reconstruction approach has been adopted because allows to easily overcome the difficulties of an intracorporeal Roux-en-y procedure.

The main limitations surgeons have in minimally invasive reconstruction after total gastrectomy are: reduced freedom of movements in the pneumoperitoneum space, properly identification of the segment of small bowel for the E-J anastomosis and then the level where perform the Jejunojejunal anastomosis. Moreover, traditional laparoscopic instruments cannot enable a hand-sewn anastomosis, thus surgeons have adopted techniques based on the use of mechanical staplers. However, intrinsic limitations of these methods should be considered when approaching an intracorporeal anastomosis involving the esophagus.

This study aims to show outcomes after adopting a new robot-sewn intracorporeal reconstruction technique after total gastrectomy, conceived at our Institution, that can simplify and make friendly this challenging phase.

MATERIALS AND METHODS

Type of study

This is a single-institution observational study, evaluating a new reconstruction approach after total gastrectomy. The study was registered at clinical trials.gov with the registration number: NCT02325453.

Eligibility

Patients with the following characteristics were included: preoperative staging assessment in accordance to international guidelines[3,4], Early Gastric Cancer, Advanced Gastric Cancer, curative surgery, robotic surgical approach. Exclusion criteria were: metastatic disease, palliative resection, synchronous malignancy in other organs, synchronous other major abdominal surgery, high operative risk (ASA > 4).

Data collection

Data of gastrectomies performed from May 2014 to

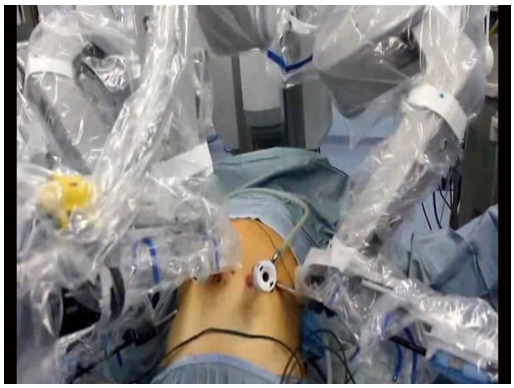

Figure 1 Robotic docking.

October 2016, at St. Mary's Hospital of Terni (Italy), were extracted and analyzed.

Data were collected by reviewing medical records and surgeries performed[5]. A tailored web-based protected system was used (https://imigastric.logix-software.it/).

The present study was planned and developed in accordance with the STROBE guidelines and statement[6].

Reported outcomes

Descriptive information on characteristics of patients, details of procedures and tumor findings were reported.

Operative results, data on the postoperative course and assessment of complications were based on the following primary outcomes: Estimated blood loss (EBL, mL), retrieved lymphnodes (No.), hospital stay (d), resumption of a liquid and solid diet (POD), in-hospital complications (No., Type), 30 d readmission (No.).

Secondary outcomes included: the operative time (min), margin status (No. negative/total) and R assessment (No. R0 resections), intraoperative complications and death (No.), resumption of peristalsis (POD).

Statistical analysis

IBM SPSS Statistics V.23 was used in this study and an intention to treat analysis was performed. Continuous variables were reported as mean ± SD or median and range. Numbers and percentages were used to express dichotomous variables.

Surgical technique

A 4-arm Da Vinci SI Robotic Surgical System is used during the procedure (Figure 1). The surgical technique can be divided into six phases: (1) coloepiploic mobilization; (2) ligation of the right gastroepiploic artery; (3) ligation of the right gastric artery and section of the duodenum; (4) lymphadenectomy of major vessels; (5) section of the esophagus; and (6) double-loop reconstruction method (Parisi Technique).

The pneumoperitoneum is created with a Veress needle in the peri-umbilical region. The intra-abdominal pressure is set to 12 mmHg.

The mobilization of the stomach can be performed by either traditional laparoscopy or robotic surgery, depending on patient characteristics and surgeon preferences.

First, a complete coloepiploic mobilization is achieved using the harmonic scalpel from right to left and the epiploon retrocavity is opened. During this phase lymph stations no. 4d, 4sa and 4sb are isolated and removed.

During the second phase the superior right colic vein is identified and the trunk of Henle is found. After this step, the gastroepiploic vein is sectioned at its origin. The right gastroepiploic artery is tied between hem-o-locks at its origin and the lymph nodes in station no. 6 are removed.

The first portion of the duodenum is released and the assistant introduces an articulated linear stapler for its section.

The lymphadenectomy of major vessels begins at the level of the proper hepatic artery.

The right gastric artery is identified and sectioned between hem-o-locks, at its origin, thus removing station no. 5. The lesser omentum is also dissected releasing station no. 3.

All the soft tissue along up to hepatic pedicle is removed including station no. 12a. Station no.8 is removed from the common hepatic artery. The dissection continues to the left of side of the celiac trunk to remove the station no. 9. Station no. 7 is dissected and the left gastric artery is sectioned. The splenic artery is followed and station no. 11p is removed, while the tissue on the proximal part of the artery (11p) is cleared based on the tumor and patient characteristics. Station no. 10 is not routinely dissected, because the high risk of major injuries due to anatomical characteristics of western patients that almost always does not allow a safety dissection of that area.

Finally, the soft tissue representing station no. 1 and no. 2 is dissected, thus releasing the esophagus and the anterior and posterior branches of the Vagus nerve which are sectioned.

In the last phase, the digestive continuity is restored with the Parisi Technique (Figure 2). Two stitches are placed to secure the esophagus to the diaphragm pillars (Figure 3). Then, the assistant temporarily removes the robotic arm no. 2 and changes the robotic trocar (8 mm) with a 12 mm trocar in order to introduce the stapler with the correct angle of section.

The esophagus is thereby sectioned and closed (Figure 3), through the mechanical linear stapler, considering the right distance from the tumor and avoiding tensions.

At the beginning the surgeon at the console detects the angle of Treitz to move the bowel loops above the

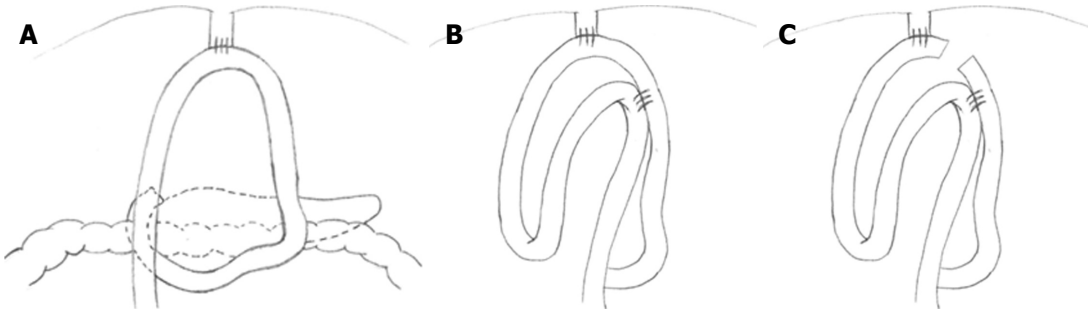

Figure 2 Double loop reconstruction method. A: 1 step: E-J anastomosis; B: 2 step: J-J anastomosis using the second loop; C: 3 step: interruption of continuity between the two anastomoses.

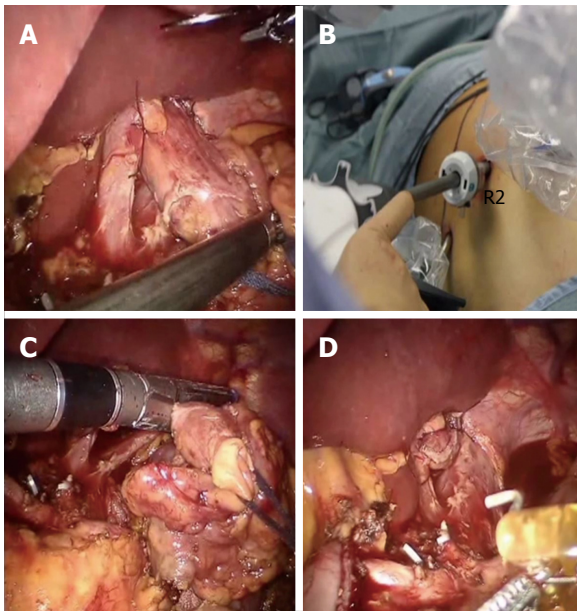

Figure 3 Division of the esophagus. A: After fixing the esophagus to the diaphragm pillars; B: An articulated mechanical linear stapler is introduced by the assistant through a 12 mm trocar; C and D: The esophagus is sectioned and closed.

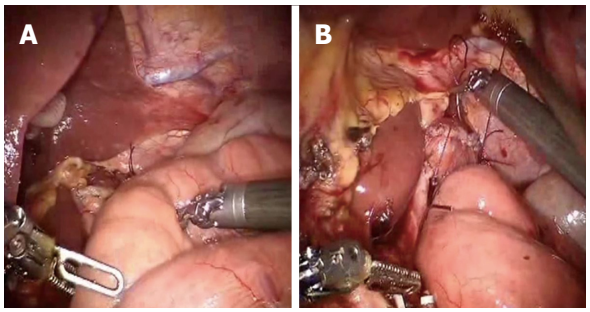

Figure 4 A first loop of small bowel is identified and brought antecolic (A), two stiches are placed to pair it with the esophagus (B).

transverse colon close to the sectioned esophagus. The selected portion of jejunum must be free from stretching and twisting, to ensure a successful anastomosis. The selected loop is fixed with two stitches to the posterior wall of the esophagus (Figure 4), placing the biliary

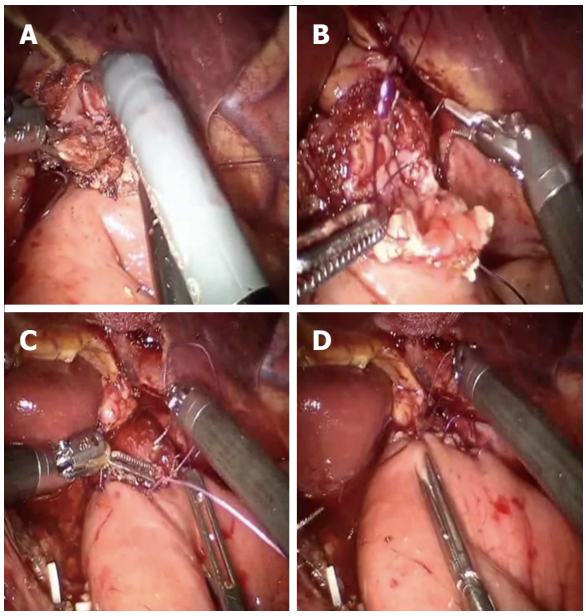

Figure 5 Esophagus and jejunum are opened (A), the posterior layer (B) is first performed followed by the anterior layer (C and D).

side on the esophagus left and the alimentary side on the right. The first loop is prepared. The surgeon performs an end-to-side esophago-jejunal robot-sewn anastomosis (Figure 5). The operator starts performing a first posterior layer with interrupted stitches using a Vicryl 2/0 for each point, joining the jejunal serosal and the muscle layer of the esophagus. Then, both the small intestine and the esophagus are opened. The surgeon performs the internal layer with a running suture, using a 3/0 PDS wire. During each step of the suture both the small intestine wall and the esophageal wall are full-thickness crossed. After this step, the anterior plane is approached. A second running suture joins the posterior one at the anastomosis angles. The anterior plane is completed with interrupted stitches covering the internal layer. The second loop is identified at a distance of about 30 to 40 cm from the E-J anastomosis. This loop is located close to the first anastomosis, on the left side, and it is used to perform the jejunojejunal anastomosis. At this point, the

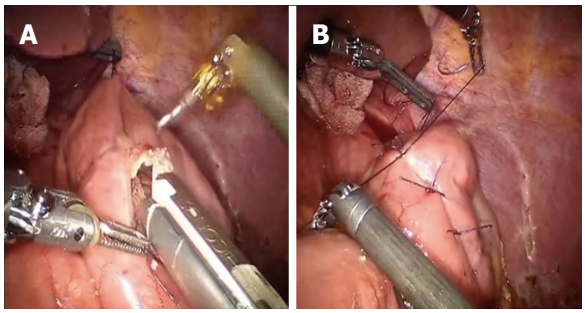

Figure 6 Second loop is identified at 40 cm from the E-J anastomosis, along the alimentary limb, and brought up to the first anastomosis on its left side through a mechanical stapler (A), a side to side jejunojejunal anastomosis is created between the second loop and the biliary limb of the first loop (B).

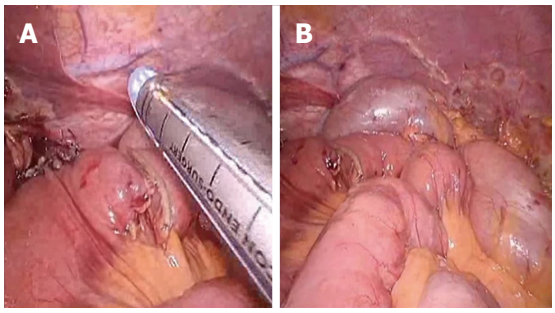

Figure 7 Two anastomoses are easily interrupted by firing the stapler (A and B).

Table 1 Characteristics of patients

Characteristics	
Sex (male/female), no.	31/24
Age (yr)	72.56 ± 10.67
BMI (kg/m^2)	24.42 ± 72.56
Comorbidity, *n* (%)	35 (66.04)
ASA score, *n*	
I	8
II	19
III	28
IV	0
Tumor location, *n*	
Lower third	12
Middle third	30
Upper third	13

surgeon fixes the chosen intestinal segment (second loop) to the biliary limb of the first loop with two sero-serosal stitches. The assistant fires the stapler (Figure 6) and then the surgeon at the console closes the entry holes of the stapler with two layers of sutures (the first is a running suture and the second layer is made with interrupted stitches). The operation ends with the interruption of the digestive continuity between the two anastomoses (Figure 7) by firing a linear stapler and thus creating a modified Roux-en-Y.

Table 2 Operative results

Outcomes	
Overall operative time, min	354.21 ± 68.8
Incision for specimen extraction, *n*	
Right McBurney incision	55
length of minilaparotomy, cm	5 (4-6)
Intraoperative blood loss, Ml	126.55 ± 73
Intraoperative morbidity, *n*	0
Intraoperative Mortality, *n*	0
Conversion, *n*	0
Extent of lymphadenectomy, *n*	
D1	0
D1+	5
D2	50

A suction drain is positioned close to the E-J anastomosis, while the naso-enteric tube is not placed. The specimen is removed through a 5 cm Mc Burney incision, in the right iliac fossa.

RESULTS

Data of 55 consecutive patients underwent the robotic double-loop reconstruction method (called Parisi technique) after performing a robotic total gastrectomy for gastric cancer were considered in the present study. Table 1 reported patients' characteristics. Mean age was 72.56 ± 10.67, 66.04% of patients had one or more comorbidities and the mean BMI was 24.42 ± 72.56. Most tumors were in the middle third of the stomach (54.54%).

If the tumor is localized at the lower third of the stomach, usually we perform a BII subtotal gastrectomy, with a robotic intracorporeal anastomosis. However, in some selected cases we prefer to perform a total gastrectomy.

In 12 of the reported cases, where the tumor was located in between the lower and the middle third of the stomach, we decided, after discussion with the patient, to perform a total than a subtotal gastrectomy for the following reasons: (1) some patients were less than 65 years old and we wanted to reduce the risk of recurrence on the residual limb (5 patients); (2) the lesion appeared to extensively involve the lower two thirds of the stomach (5 patients); and (3) in two cases with diffuse type, there was not only a main pre-pyloric lesion but also a biopsy proven adenocarcinoma at the upper third.

Total operative time was 354.21 ± 68.8 (Table 2). Intraoperative blood loss was 126.55 ± 73. No conversion to open surgery or major intraoperative complications occurred. The median number of retrieved lymph nodes was 35 (95%CI: 15-47). All specimens were evaluated as R0 resections. Histopathological characteristics are shown in Table 3.

Table 4 summarizes the postoperative findings.

Table 3 Clinical outcomes during hospitalization and complications

Outcomes	
Time to peristalsis, d	1 (1-3)[1]
Time to resume liquid diet, d	2 (2-5)[1]
Time to resume solid intake, d	3 (3-6)[1]
Length of hospital stay, d	5 (3-17)[1]
Postoperative 30-d complications, *n*	0
Reoperations, *n*	0
30-d mortality, *n*	0

[1]Values are expressed as median (range).

Table 4 Histopathological data

Outcomes	
Diameter of the tumor, cm	4.25 (1-8)[1]
Proximal margin, cm	6 (2-11)[1]
Number of harvested lymph nodes, *n*	35 (15-47)[1]
TNM staging, *n* (%)	
Stage 0	0
Stage ⅠA	8 (14.55)
Stage ⅠB	9 (16.37)
Stage ⅡA	12 (21.82)
Stage ⅡB	11 (20.00)
Stage ⅢA	7 (12.72)
Stage ⅢB	6 (10.91)
Stage ⅢC	2 (3.63)
Stage Ⅳ	0
Residual tumor, *n*	
R0	55
R1	0
R2	0

[1]Values are expressed as median (range).

The median hospital stay was 5 d. We observed a fast recovery of different levels of food intake after gastrectomy, enabling patients to go through a liquid diet (Median = 2; 95%CI: 2-5) until starting a solid diet (Median = 3; 95%CI: 3-6). No major complications or death occurred. None of the 55 patients experienced anastomotic leakage.

DISCUSSION

The restoration of the digestive tract after total gastrectomy is a technically demanding phase.

Minimally invasive surgery has been developed in recent years even for complex oncological procedures thanks to new available devices and increased surgeons experience[2].

In the literature (Table 5), only 22 studies[5,7-27] from 16 institutions have reported the use of robotic surgery in gastric cancer including total gastrectomy. Eleven studies are comparative[9,11-15,17,18,21-23], others are case series and personal experiences[5,7,8,10,16,19,20,24,27]. Limitations of studies are to provide outcomes including in their analysis different types of gastric resection. In fact, only 5 studies[5,17,22,24,27] reported information on total gastrectomy alone. Others reported data on surgical interventions within a more general analysis including different types of gastric resections as subtotal or proximal gastrectomy. Overall, 466 procedures on total gastrectomy can be detected in the literature. This makes difficult to better understand the real effect of robotic surgery on total gastrectomy that is a different and more complex surgery.

Moreover, Table 6 shows that most of studies reported limited information. Only eight studies showed data on patient and tumor characteristics or operative and clinical results[2,17,20-24,26].

Regarding the technique used, all studies reported the assistance of the robot in the mobilization of the stomach and in lymphadenectomy. Ten authors reported an extracorporeal reconstruction and only eleven studies[2,8-10,13,16,18,19,23,24,26] reported a robotic assistance in this phase and an intracorporeal approach.

There are two main issues to consider: the way to perform the Roux-en-y reconstruction and how to perform it.

In the intracorporeal approach, a circular stapler is generally used but other solutions include the Orvil[16] or the Overlap technique[16,23]. Some authors[10,25] described the use of the robot to perform a manual purse-string around the anvil, but only few reports[5,13,19,24] in the literature reported its use for a complete hand-sewn anastomosis.

Surgeons are generally afraid to perform the latter, because the high surgical skills required in conventional surgery and the risk for leakage if not well performed.

By the other hand and regardless of the approach, using mechanical staplers has standardize the way to perform the reconstruction after total gastrectomy and apparently give more safety. If this is true in open surgery, this is more challenging when adopting an intracorporeal approach. A mechanical trouble when firing the stapler or a leakage for incomplete closing at the E-J level can lead the patient to serious complications until death.

We decided to develop a new technique to overcome the reported limitations of the intracoproreal approach. Particularly we found a feasible and safe way to perform a complete robotic reconstruction without the need to convert the procedure to open or laparoscopic surgery or using others potentially dangerous techniques.

The accuracy of the robotic system, the micro-surgical instruments and particularly the endowrist allow the surgeon to perform movements that are even difficult to reproduce in open surgery.

We believe that this technology should be exploited in complex digestive procedures, as in a total gastrectomy and our study demonstrates the usefulness of the robotic system in performing a safe hand-sewn E-J anastomosis.

Table 5 Literature review on robotic total gastrectomy, overall number of reported cases

	Year	Type	Subject	Country	Institution	Period	No.
Present study	2017	Prospective CS	RTG	Italy	St. Mary's Hospital of Terni	2014-2016	55
Jiang *et al*[24]	2015	Retrospective CS	RAG	China	Nanjing University Medical College	2010-2012	65
Kim *et al*[14]	2012	nonRCT	RAG *vs* LG *vs* OG	South Korea	Yonsei University College of Medicine	2005-2010	109
Son *et al*[15]	2014	nonRCT	RTG *vs* LTG			2005-2010	51
Woo *et al*[11]	2011	nonRCT	RAG *vs* LG			2005-2009	62
Song *et al*[7]	2009	Prospective CS	RAG			2005-2007	33
Park *et al*[20]	2013	Retrospective CS	RAG	South Korea	National Cancer Center	2009-2012	46
Yoon *et al*[17]	2012	nonRCT	RTG *vs* LTG			2009-2011	36
Kang *et al*[13]	2012	nonRCT	RAG *vs* LG	South Korea	Ajou University School of Medicine	2008-2011	16
Hur *et al*[8]	2010	Retrospective CS	RAG			2010	2
Hyun *et al*[18]	2013	nonRCT	RAG *vs* LG	South Korea	Korea University Anam Hospital	2009-2010	9
Son *et al*[15]	2012	nonRCT	RAG *vs* LG	South Korea	Seoul University Bundang Hospital	2007-2011	1
Junfeng *et al*[21]	2014	nonRCT	RAG *vs* LG	China	Third Military Medical University	2010-2013	26
Liu *et al*[19]	2013	Prospective CS	RAG	China	Subei People's Hospital of Jiangsu	2011-2013	54
Giulianotti *et al*[25]	2003	Retrospective CS	RAG	Italy	Misericordia Hospital of Grosseto	2000-2002	10
Coratti *et al*[26]	2015	Retrospective CS	RAG	Italy		2000-2014	38
D'Annibale *et al*[10]	2011	Retrospective CS	RAG	Italy	S. Giovanni Addolorata Hospital	2004-2009	11
Caruso *et al*[9]	2011	nonRCT	RAG *vs* OG	Italy	Hospital of Spoleto	2006-2010	12
Suda *et al*[23]	2014	nonRCT	RAG *vs* LG	Japan	Fujita Health University	2009-2012	30
Huang *et al*[12]	2012	nonRCT	RAG *vs* LG *vs* OG	Taiwan	Taipei Veterans General Hospital	2010-2012	7
Vasilescu *et al*[16]	2012	Retrospective CS	RAG	Romania	Fundeni Clinical Institute	2008-2012	19
Zawadzki *et al*[27]	2014	CR	RAG	Poland	Wroclaw Medical University	2014	1
Parisi *et al*[5]	2015	Prospective CS	RTG	Italy	St. Mary's Hospital of Terni	2014-2015	22
Total[1]							466

[1]Excluding the present study.

Although it may appear more complex than other techniques, during our experience, we have gained some tricks: (1) the esophagus should be fixed to both sides at the diaphragmatic pillars to avoid retraction in the chest; (2) a jejunal loop which can be easily approached to the esophagus is essential; (3) two interrupted stiches can help in pairing the esophagus and the jejunum, delimiting the two ends of the E-J anastomosis. Then other two central stitches are placed to complete the posterior external layer. Vicryl is preferable; (4) only at this point the esophagus and the jejunum wall should be opened, we suggest using monopolar curved scissors; (5) two running sutures for the internal layer, the first posterior and the second one anterior are preferable than an interrupted suturing. At the beginning of our experience we performed this step with interrupted stiches but after few cases we decided to move to a running suture because faster and it gives a feeling of safety and high adherence between the visceral walls; and (6) PDS sutures for the internal layer is best, because the combination of an absorbable suture and an extended anastomotic support. This suture gives fluidity and at the same time tightness, when the thread is pulled in tension.

The double loop approach is the other innovative element we reported. This technique can speed up the reconstruction and have several relevant advantages: (1) the loop of bowel can be chosen without tension; (2) there is no confusion between biliary and alimentary tract; and (3) it is not necessary to interrupt the mesentery, reducing the risk of bleeding and internal hernias.

In conclusion, the present study is one of the largest series focused on robotic total gastrectomy in the literature and has shown satisfactory outcomes. The innovative technique adopted has demonstrated feasibility and safety when performing both the E-J and the J-J anastomoses with an intracorporeal robotic approach.

Every method for reconstruction has to tackle the functional problems of blind loop syndrome, or of inadequate transition (*e.g.*, weight loss) through the substitute stomach.

The short-term follow-up didn't highlight any functional problems until now, while the evaluation on long term results of our approach is ongoing.

Table 6 Literature review on robotic total gastrectomy, details of the reported data

	Robot - Assistance			Type	E-J anastomosis	Anastomosis performance	Site of minilaparotomy	Operative and clinical data	Patients and tumor details
	Lymphadenectomy	Stomach mobilization	Reconstruction						
Jiang *et al*[24]	Performed	Performed		Roux-en-Y	EXTRA	Circular stapler	Not provided	Provided	Provided
			Performed	Roux-en-Y	INTRA	Robot-sewn	Not provided		
Kim *et al*[14]	Not provided	Not provided	Not provided	Roux-en-Y	Not provided	Not provided	Not provided	Lack	Lack
Son *et al*[15]	Performed	Performed		Roux-en-Y	EXTRA	Circular stapler	Upper midline	Provided	Provided
				Roux-en-Y	INTRA LAP	Circular stapler	Left lower port		
Woo *et al*[11]	Performed	Performed		Roux-en-Y	EXTRA	Not provided	Not provided	Lack	Lack
				Roux-en-Y	INTRA LAP	Not provided	Not provided		
Song *et al*[7]	Performed	Performed		Roux-en-Y	EXTRA	Circular stapler	Upper midline	Lack	Lack
				Roux-en-Y	INTRA LAP	Circular stapler	Not provided		
Park *et al*[20]	Performed	Performed		Roux-en-Y	EXTRA	Not provided	Upper midline	Provided	Lack
Yoon *et al*[17]	Performed	Performed		Roux-en-Y	EXTRA	Circular stapler	Not provided	Provided	Provided
Kang *et al*[13]	Performed	Performed		Roux-en-Y	EXTRA	Circular stapler	Upper midline	Lack	Lack
			Performed	Roux-en-Y	INTRA	Robot-sewn	Not provided		
Hur *et al*[8]	Performed	Performed	Performed	Roux-en-Y	INTRA	Robot-sewn	Not provided	Lack	Lack
Hyun *et al*[18]	Performed	Performed		Roux-en-Y	EXTRA	Circular stapler	Upper midline	Lack	Lack
			Not provided	Roux-en-Y	INTRA	Not provided	Umbilical port		
Son *et al*[15]	Performed	Performed		Roux-en-Y	EXTRA	Not provided	Not provided	Lack	Lack
Junfeng *et al*[21]	Performed	Performed		Roux-en-Y	EXTRA	Circular stapler	Upper midline	Provided	Provided
Liu *et al*[19]	Performed	Performed	Performed	Roux-en-Y	INTRA	Robot-sewn	Camera port	Lack	Lack
Giulianotti *et al*[25]	Performed	Performed	Performed	Roux-en-Y	INTRA	Circular stapler	Not provided	Lack	Lack
Coratti *et al*[26]	Performed	Performed	Performed	Roux-en-Y	INTRA	Robot-sewn	Not provided	Provided	Provided
D'Annibale *et al*[10]	Performed	Performed	Performed	Roux-en-Y	INTRA	Circular stapler	Suprapubic	Lack	Lack
Caruso *et al*[9]	Performed	Performed	Performed	Roux-en-Y	INTRA	Circular stapler	Upper midline	Lack	Lack
Suda *et al*[23]	Performed	Performed	Performed	Roux-en-Y	INTRA	Linear stapler	Not provided	Provided	Provided
Huang *et al*[12]	Performed	Performed		Roux-en-Y	INTRA LAP	Circular stapler	Periumbilical	Lack	Lack
Vasilescu *et al*[16]	Performed	Performed	Performed	Roux-en-Y	INTRA	Circular stapler	Not provided	Lack	Lack
Parisi *et al*[5]	Performed	Performed	Performed	Roux-en-Y	INTRA	Robot-sewn	McBurney	Provided	Provided

COMMENTS

Background

The development of surgical technology during last decades has allowed surgeons to offer patients new approaches and treatment strategies. Several studies have shown the usefulness of robotic systems when performing a gastrectomy for cancer and its potential advantages when compared with traditional laparoscopic devices. However, if it has been well evaluated the role of both laparoscopic and robotic surgery for distal or subtotal gastrectomy, particularly in the eastern population, there is a big debate on safety and feasibility of intracorporeal procedures for reconstruction of the alimentary tract after a total gastrectomy. The present study has addressed this issue in a western center.

Research frontiers

Despite the spread of minimally invasive procedures for complex major abdominal surgeries, few studies have been performed on the totally robotic approach for gastric cancer. Current indications are still object of debate. Moreover, only few centers have tried to find solutions for the reconstruction phase after total gastrectomy.

Innovations and breakthroughs

Robotic systems have revolutionized minimally invasive surgery. Surgeons can overcome the limits of traditional laparoscopy through a three-dimensional vision and articulated instruments. This technological progress should be exploited

particularly when performing a demanding phase of a procedure, as in suturing movements. The present study shows a new robotic technique for a reconstructive approach. The double loop method can simplify the way to perform the reconstruction phase after a total gastrectomy and can allow surgeons to overcome the current limitations.

Applications

This study shows the possibility to safely perform a completely intracorporeal anastomosis after a total gastrectomy, considered one of the biggest obstacles in minimally invasive surgery.

Terminology

Robotic systems are used in minimally invasive surgery and allow the primary surgeon to perform the procedure through a remote console.

Peer-review

It is a good observational study who reported the outcome of robotic total gastrectomy in one Institution. Total gastrectomy with minimally invasive technique is quite challenging with either laparoscopic technique or robotic technique. With a series of 55 patients who successfully recovered, they can be convinced by the authors and draw such a conclusion that it can be safe.

REFERENCES

1 **Marano A**, Choi YY, Hyung WJ, Kim YM, Kim J, Noh SH. Robotic versus Laparoscopic versus Open Gastrectomy: A Meta-Analysis. *J Gastric Cancer* 2013; **13**: 136-148 [PMID: 24156033 DOI: 10.5230/jgc.2013.13.3.136]

2 **Parisi A**, Nguyen NT, Reim D, Zhang S, Jiang ZW, Brower ST, Azagra JS, Facy O, Alimoglu O, Jackson PG, Tsujimoto H, Kurokawa Y, Zang L, Coburn NG, Yu PW, Zhang B, Qi F, Coratti A, Annecchiarico M, Novotny A, Goergen M, Lequeu JB, Eren T, Leblebici M, Al-Refaie W, Takiguchi S, Ma J, Zhao YL, Liu T, Desiderio J. Current status of minimally invasive surgery for gastric cancer: A literature review to highlight studies limits. *Int J Surg* 2015; **17**: 34-40 [PMID: 25758348]

3 **Japanese Gastric Cancer Association**. Japanese gastric cancer treatment guidelines 2010 (ver. 3). *Gastric Cancer* 2011; **14**: 113-123 [PMID: 21573742 DOI: 10.1007/s10120-011-0042-4]

4 **NCCN**. Clinical Practice Guidelines in Oncology: Gastric Cancer. Version I.2014, 2014 Available from: URL: http://wwwnccnorg/professionals/physician_gls/pdf/gastricpdf

5 **Parisi A**, Ricci F, Trastulli S, Cirocchi R, Gemini A, Grassi V, Corsi A, Renzi C, De Santis F, Petrina A, Pironi D, D'Andrea V, Santoro A, Desiderio J. Robotic Total Gastrectomy With Intracorporeal Robot-Sewn Anastomosis: A Novel Approach Adopting the Double-Loop Reconstruction Method. *Medicine* (Baltimore) 2015; **94**: e1922 [PMID: 26656323 DOI: 10.1097/MD.0000000000001922]

6 **von Elm E**, Altman DG, Egger M, Pocock SJ, Gøtzsche PC, Vandenbroucke JP. The Strengthening the Reporting of Observational Studies in Epidemiology (STROBE) Statement: guidelines for reporting observational studies. *Int J Surg* 2014; **12**: 1495-1499 [PMID: 25046131 DOI: 10.1016/j.ijsu.2014.07.013]

7 **Song J**, Oh SJ, Kang WH, Hyung WJ, Choi SH, Noh SH. Robot-assisted gastrectomy with lymph node dissection for gastric cancer: lessons learned from an initial 100 consecutive procedures. *Ann Surg* 2009; **249**: 927-932 [PMID: 19474671 DOI: 10.1097/01.sla.0000351688.64999.73]

8 **Hur H**, Kim JY, Cho YK, Han SU. Technical feasibility of robot-sewn anastomosis in robotic surgery for gastric cancer. *J Laparoendosc Adv Surg Tech A* 2010; **20**: 693-697 [PMID: 20809816 DOI: 10.1089/lap.2010.0246]

9 **Caruso S**, Patriti A, Marrelli D, Ceccarelli G, Ceribelli C, Roviello F, Casciola L. Open vs robot-assisted laparoscopic gastric resection with D2 lymph node dissection for adenocarcinoma: a case-control study. *Int J Med Robot* 2011; **7**: 452-458 [PMID: 21984205 DOI: 10.1002/rcs.416]

10 **D'Annibale A**, Pende V, Pernazza G, Monsellato I, Mazzocchi P, Lucandri G, Morpurgo E, Contardo T, Sovernigo G. Full robotic gastrectomy with extended (D2) lymphadenectomy for gastric cancer: surgical technique and preliminary results. *J Surg Res* 2011; **166**: e113-e120 [PMID: 21227455 DOI: 10.1016/j.jss.2010.11.881]

11 **Woo Y**, Hyung WJ, Pak KH, Inaba K, Obama K, Choi SH, Noh SH. Robotic gastrectomy as an oncologically sound alternative to laparoscopic resections for the treatment of early-stage gastric cancers. *Arch Surg* 2011; **146**: 1086-1092 [PMID: 21576595 DOI: 10.1001/archsurg.2011.114]

12 **Huang KH**, Lan YT, Fang WL, Chen JH, Lo SS, Hsieh MC, Li AF, Chiou SH, Wu CW. Initial experience of robotic gastrectomy and comparison with open and laparoscopic gastrectomy for gastric cancer. *J Gastrointest Surg* 2012; **16**: 1303-1310 [PMID: 22450954 DOI: 10.1007/s11605-012-1874-x]

13 **Kang BH**, Xuan Y, Hur H, Ahn CW, Cho YK, Han SU. Comparison of Surgical Outcomes between Robotic and Laparoscopic Gastrectomy for Gastric Cancer: The Learning Curve of Robotic Surgery. *J Gastric Cancer* 2012; **12**: 156-163 [PMID: 23094227 DOI: 10.5230/jgc.2012.12.3.156]

14 **Kim KM**, An JY, Kim HI, Cheong JH, Hyung WJ, Noh SH. Major early complications following open, laparoscopic and robotic gastrectomy. *Br J Surg* 2012; **99**: 1681-1687 [PMID: 23034831 DOI: 10.1002/bjs.8924]

15 **Son SY**, Lee CM, Ahn SH, Lee JH, Park DJ, Kim HH. Clinical Outcome of Robotic Gastrectomy in Gastric Cancer in Comparison with Laparoscopic Gastrectomy: A Case-Control Study. *J Minim Invas Surg* 2012; **15**: 27-31

16 **Vasilescu C**, Procopiuc L. Robotic surgery of locally advanced gastric cancer: a single-surgeon experience of 41 cases. *Chirurgia* (Bucur) 2012; **107**: 510-517 [PMID: 23025119]

17 **Yoon HM**, Kim YW, Lee JH, Ryu KW, Eom BW, Park JY, Choi IJ, Kim CG, Lee JY, Cho SJ, Rho JY. Robot-assisted total gastrectomy is comparable with laparoscopically assisted total gastrectomy for early gastric cancer. *Surg Endosc* 2012; **26**: 1377-1381 [PMID: 22083338 DOI: 10.1007/s00464-011-2043-0]

18 **Hyun MH**, Lee CH, Kwon YJ, Cho SI, Jang YJ, Kim DH, Kim JH, Park SH, Mok YJ, Park SS. Robot versus laparoscopic gastrectomy for cancer by an experienced surgeon: comparisons of surgery, complications, and surgical stress. *Ann Surg Oncol* 2013; **20**: 1258-1265 [PMID: 23080320 DOI: 10.1245/s10434-012-2679-6]

19 **Liu XX**, Jiang ZW, Chen P, Zhao Y, Pan HF, Li JS. Full robot-assisted gastrectomy with intracorporeal robot-sewn anastomosis produces satisfying outcomes. *World J Gastroenterol* 2013; **19**: 6427-6437 [PMID: 24151361 DOI: 10.3748/wjg.v19.i38.6427]

20 **Park JY**, Kim YW, Ryu KW, Eom BW, Yoon HM, Reim D. Emerging Role of Robot-assisted Gastrectomy: Analysis of Consecutive 200 Cases. *J Gastric Cancer* 2013; **13**: 255-262 [PMID: 24511422 DOI: 10.5230/jgc.2013.13.4.255]

21 **Junfeng Z**, Yan S, Bo T, Yingxue H, Dongzhu Z, Yongliang Z, Feng Q, Peiwu Y. Robotic gastrectomy versus laparoscopic gastrectomy for gastric cancer: comparison of surgical performance and short-term outcomes. *Surg Endosc* 2014; **28**: 1779-1787 [PMID: 24385251 DOI: 10.1007/s00464-013-3385-6]

22 **Son T**, Lee JH, Kim YM, Kim HI, Noh SH, Hyung WJ. Robotic spleen-preserving total gastrectomy for gastric cancer: comparison with conventional laparoscopic procedure. *Surg Endosc* 2014; **28**: 2606-2615 [PMID: 24695982 DOI: 10.1007/s00464-014-3511-0]

23 **Suda K**, Man-I M, Ishida Y, Kawamura Y, Satoh S, Uyama I. Potential advantages of robotic radical gastrectomy for gastric adenocarcinoma in comparison with conventional laparoscopic approach: a single institutional retrospective comparative cohort study. *Surg Endosc* 2015; **29**: 673-685 [PMID: 25030478 DOI: 10.1007/s00464-014-3718-0]

24 **Jiang ZW**, Liu J, Wang G, Zhao K, Zhang S, Li N, Li JS. Esophagojejunostomy reconstruction using a robot-sewing technique during totally robotic total gastrectomy for gastric cancer. *Hepatogastroenterology* 2015; **62**: 323-326 [PMID: 25916057]

25 **Giulianotti PC**, Coratti A, Angelini M, Sbrana F, Cecconi S,

Balestracci T, Caravaglios G. Robotics in general surgery: personal experience in a large community hospital. *Arch Surg* 2003; **138**: 777-784 [PMID: 12860761 DOI: 10.1001/archsurg.138.7.777]

26 **Coratti A**, Fernandes E, Lombardi A, Di Marino M, Annecchiarico M, Felicioni L, Giulianotti PC. Robot-assisted surgery for gastric carcinoma: Five years follow-up and beyond: A single western center experience and long-term oncological outcomes. *Eur J Surg Oncol* 2015; **41**: 1106-1113 [PMID: 25796984 DOI: 10.1016/j.ejso.2015.01.014]

27 **Zawadzki M**, Witkiewicz W. Laparoscopic robotic total gastrectomy. *Wideochir Inne Tech Maloinwazyjne* 2014; **9**: 650-654 [PMID: 25562009 DOI: 10.5114/wiitm.2014.45128]

P- Reviewer: Garcia-Olmo D, Klinge U, Wu AW **S- Editor**: Qi Y
L- Editor: A **E- Editor**: Zhang FF

World Journal of Gastroenterology

Submit a Manuscript: http://www.f6publishing.com

World J Gastroenterol 2017 June 21; 23(23): 4303-4310

DOI: 10.3748/wjg.v23.i23.4303

ISSN 1007-9327 (print) ISSN 2219-2840 (online)

EVIDENCE-BASED MEDICINE

Substantial hepatic necrosis is prognostic in fulminant liver failure

Paul Ndekwe, Marwan S Ghabril, Yong Zang, Steven A Mann, Oscar W Cummings, Jingmei Lin

Paul Ndekwe, Steven A Mann, Oscar W Cummings, Jingmei Lin, Department of Pathology and Laboratory Medicine, Indiana University School of Medicine, Indianapolis, IN 46202, United States

Marwan S Ghabril, Department of Internal Medicine, Division of Gastroenterology and Hepatology, Indiana University School of Medicine, Indianapolis, IN 46202, United States

Yong Zang, Department of Biostatistics, Indiana University School of Medicine, Indianapolis, IN 46202, United States

Author contributions: Ndekwe P and Lin J designed research/study; Ndekwe P, Ghabril MS, Mann SA and Lin J performed research/study and collected data; Ndekwe P, Ghabril MS, Zang Y, Mann SA, Cummings OW and Lin J analyzed data; Ndekwe P, Ghabril MS, Mann SA, Cummings OW and Lin J wrote paper.

Institutional review board statement: This study was reviewed and approved by the Institutional Review Board of Indiana University School of Medicine.

Conflict-of-interest statement: The authors have no conflicts of interest to disclose.

Data sharing statement: No additional data are available.

Manuscript source: Invited manuscript

Correspondence to: Jingmei Lin, MD, PhD, Department of Pathology and Laboratory Medicine, Indiana University School of Medicine, 350 West 11th Street, Indianapolis, IN 46202, United States. jinglin@iupui.edu
Telephone: +1-317-4916159
Fax: +1-317-4916419

Received: October 6, 2016
Peer-review started: October 10, 2016
First decision: December 19, 2016
Revised: March 21, 2017
Accepted: May 19, 2017
Article in press: May 19, 2017
Published online: June 21, 2017

Abstract

AIM

To evaluate if any association existed between the extent of hepatic necrosis in initial liver biopsies and patient survival.

METHODS

Thirty-seven patients with fulminant liver failure, whose liver biopsy exhibited substantial necrosis, were identified and included in the study. The histological and clinical data was then analyzed in order to assess the relationship between the extent of necrosis and patient survival, with and without liver transplantation. The patients were grouped based on the etiology of hepatic necrosis. Each of the etiology groups were then further stratified according to whether or not they had received a liver transplant post-index biopsy, and whether or not the patient survived.

RESULTS

The core tissue length ranged from 5 to 44 mm with an average of 23 mm. Causes of necrosis included 14 autoimmune hepatitis, 10 drug induced liver injury (DILI), 9 hepatitis virus infection, and 4 unknown origin. Among them, 11 showed submassive (26%-75% of the parenchymal volume) and 26 massive (76%-100%) necrosis. Transplant-free survival was worse in patients with a higher extent of necrosis (40%, 71.4% and 100% in groups with necrosis of 76%-100%, 51%-75%

and 26%-50%, respectively). Additionally, transplant-free survival rates were 66.7%, 57.1%, and 25.0% in groups of autoimmune hepatitis, DILI, and viral hepatitis, respectively. Even after liver transplantation, the survival rate in patients as a result of viral hepatitis remained the lowest (80%, 100%, and 40% in groups of autoimmune hepatitis, DILI, and viral hepatitis, respectively).

CONCLUSION

Adequate liver biopsy with more than 75% necrosis is associated with significant transplant-free mortality that is critical in predicting survival.

Key words: Submassive necrosis; Massive necrosis; Fulminant liver failure; Liver transplantation; Biopsy; Histopathology

Core tip: Fulminant liver failure is clinically characterized by an abrupt onset of jaundice and liver dysfunction with subsequent development of encephalopathy and coagulopathy in patients with or without preexisting liver disease. Liver biopsy may play a role in predicting patient survival, and may also potentially play a role in optimizing the utilization of resources in the setting of fulminant liver failure.

Ndekwe P, Ghabril MS, Zang Y, Mann SA, Cummings OW, Lin J. Substantial hepatic necrosis is prognostic in fulminant liver failure. *World J Gastroenterol* 2017; 23(23): 4303-4310 Available from: URL: http://www.wjgnet.com/1007-9327/full/v23/i23/4303.htm DOI: http://dx.doi.org/10.3748/wjg.v23.i23.4303

INTRODUCTION

Fulminant liver failure is clinically characterized by an abrupt onset of jaundice and liver dysfunction with subsequent development of encephalopathy and coagulopathy in patients with or without preexisting liver disease[1-6]. Common etiologies for fulminant liver failure include viral hepatitis, autoimmune hepatitis, and drug induced liver injury (DILI)[7,8]. Other precipitating events comprise alcoholic liver disease, ischemia, portal vein thrombosis, and infection[9-11]. In some cases, a precipitating factor is never identified[9-11]. Regardless of the etiology, fulminant liver failure is typically associated with high morbidity and mortality[1]. In the clinical setting, the grade of encephalopathy has a strong association with prognosis[12]. Other prognostic indicators encompass coagulation factors (INR or Factor V levels), serum bilirubin, transaminases, creatinine, arterial pH, and serum lactate[12]. Additionally, computed tomographic assessment of liver atrophy is said to be of prognostic value[13]. As such, multiple prognostic models (*e.g.*, Clichy, King's College), based mainly on laboratory values and clinical findings, have been used to rapidly assess the need for transplantation[4,9-12].

Liver biopsy is the gold standard for evaluating hepatic diseases. However, these fulminant liver failure models do not directly taken into account the histopathological findings obtained *via* liver biopsy. Submassive or massive liver necrosis is the worst histological finding that is seen in association with fulminant liver failure, although it is not seen in every biopsy. In fulminant liver failure, the prognosis for those with significant hepatic necrosis is generally thought to be poor. And yet, the extent of necrosis in a biopsy, and its importance in predicting patient outcomes, is less well defined in the literature[7,14]. One study even casts doubt on the value of hepatic necrosis as a prognostic indicator[7].

In this study, we aimed to evaluate if there is any association between the degree of hepatocellular necrosis and patient survival. Additionally, we attempted to identify any relationship between the underlying etiology of necrosis and survival. Lastly, we evaluated the outcomes of liver transplantation following a histopathological diagnosis of significant hepatic necrosis.

MATERIALS AND METHODS

Patients and histology

A search of our institution's pathology database was performed in order to retrospectively identify native liver biopsies with a diagnosis of either submassive or massive hepatic necrosis. Thirty-seven liver biopsies, originally performed from 2004 to 2013, were identified. The biopsies were distributed among 37 individual patients who were clinically diagnosed with fulminant liver failure. Hepatic necrosis is defined as death of hepatocytes, which maybe single cell, multiple cells in piecemeal, focal, multifocal, submassive or massive (Figure 1). Submassive hepatic necrosis is defined as necrosis involving 26%-75% of the parenchymal volume, while massive necrosis involves more than 75%. The percentage of hepatic necrosis is determined based on the total amount of necrotic hepatic tissue present *vs* the amount of total parenchyma. Hematoxylin and eosin (H&E) slides for each of the individual biopsies were reviewed by an experienced pathologist (Lin J) to assess the percentage of necrosis and other pathologic features.

A review of each individual patient's electronic medical chart was performed and relevant clinical data was obtained. Collected data included age, gender, etiology of hepatic necrosis, presence of hepatic encephalopathy, whether or not the patient received treatment related to the underlying disease, whether or not liver transplantation was performed after the index liver biopsy, and survival time. Additional clinical

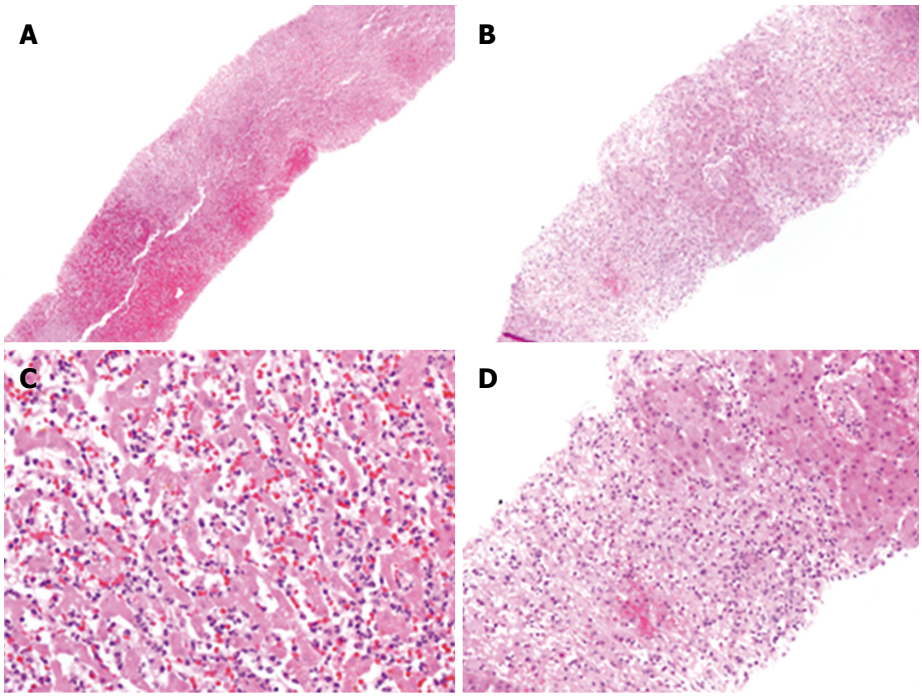

Figure 1 Mass and submassive liver necrosis. A: Low power magnification showing complete hepatocellular necrosis in a core biopsy (× 40); B: Medium power magnification showing a liver biopsy with perivenular predominant hepatocellular necrosis and intermixed viable hepatocytes located around the portal tract (× 40); C: High magnification of image A showing hepatocellular necrosis and profound inflammatory infiltrate in which the architecture of hepatocyte is preserved (× 200); D: High magnification of image B reveals the collapse of parenchyma that is replaced by necroinflammatory infiltrate in comparison to the adjacent viable hepatocytes in the right upper corner (× 200).

information included patient INR values, presence of a bacterial infection, and whether or not ascites was present.

The histological and clinical data was then analyzed in order to assess the relationship between the extent of necrosis and patient survival, with or without liver transplantation. Patients were sorted into three groups based on the percentage of necrosis present within the biopsy (26%-50%, 51%-75%, and 76%-100%). Each of the three percentage groups was then further stratified according to whether or not they had subsequently received a liver transplant.

A separate analysis of all data was then performed in order to assess the relationship between the etiology of hepatic necrosis and patient prognosis, with or without liver transplantation. The patients were grouped based on etiology of hepatic necrosis. Etiologies included autoimmune hepatitis, DILI, viral hepatitis, and unknown. An unknown etiology was defined as any case in which there was no clearly identified cause following an extensive clinical workup. Each of the etiology groups were then further stratified according to whether or not they had received a liver transplant post-index biopsy, and whether or not the patient survived.

Statistical analysis

Statistical analysis methodologies included Fisher's exact test and χ^2 test. P values of < 0.05 were considered statistically significant. All statistics were performed by an experienced statistician (Zang Y).

RESULTS

Patients and liver biopsies

The patients within the study ranged in age from 18 to 75 years old with a mean age of 41 years. Two patients were less than 20 years old; 10 were in the 21-30 year old age group, 4 in the 31-40 age group, 7 in the 41-50 age group, 6 in the 51-60 age group, 5 in the 61-70 age group, and 3 patients were older than 70. Fourteen (37.8%) were male and 23 (62.2%) were female.

Tissue adequacy for pathologic assessment was evaluated. Of 37 liver biopsies, the core tissue length ranged from 5 mm to 44 mm with an average of 23 mm. Twenty-three biopsies (62%) were in the length of > 20 mm, 11 (30%) in the range of 10-20 mm , and 3 (8%) < 10 mm.

Causes of submassive or massive liver necrosis included autoimmune hepatitis in 14 patients, DILI in 10 (9 due to acetaminophen and 1 due to clopidogrel), hepatitis virus infection in 9 patients (1 hepatitis A, 5 hepatitis B, 2 hepatitis C, and 1 with both hepatitis B and C), and unknown origin in 4. All patients within the study underwent biopsy with a clinical diagnosis of fulminant liver failure. Survival times for all 37 patients ranged from less than 1 mo to 127 mo according to

Table 1 Clinical features of the patients who had submassive or massive hepatic necrosis *n* (%)

Extent of necrosis	Patients (*n* = 37)	Ascites	Bacterial infection	INR mean and range
26%-50%	1	0 (0)	0 (0)	1.34 (1.34)
51%-75%	10	1 (10)	0 (0)	2.19 (0.95-4.52)
76%-100%	26	5 (19.2)	3 (11.5)	2.64 (1.10-5.91)

The INR data were not available for one patient in the 51%-75% and 76%-100% groups, respectively.

the last visit record for each patient. The mean survival time was 41 mo.

Ascites, INR, bacterial infection, and hepatic necrosis

As shown in Table 1, the single patient with 26-50% necrosis had an INR of 1.34, and no clinical evidence of bacterial infection or ascites. Only 1 of the 10 patients with 51%-75% necrosis had ascites. The mean INR for the patients within this group was 2.19, with individual values ranging from 0.95 to 4.52. None of the patients within this group had evidence of a bacterial infection. Three of the 26 patients with 76%-100% hepatic necrosis had a bacterial infection. The mean INR for patients in this group was 2.64, with individual values ranging from 1.10-5.91. Five of these patients had ascites.

Statistical analysis using Fisher exact test demonstrated that there was no significant association between the presence of ascites and extent of necrosis (P = 0.71). Additionally, Fisher's exact test showed no significant association between the presence of bacterial infection and extent of necrosis (P = 0.58). Analysis of variance showed that there was no significant association between mean INR level and extent of necrosis (P = 0.45).

Outcome of percentage of hepatic necrosis with respect to survival

As shown in Table 2, one patient had 26%-50% hepatic necrosis at the time of biopsy. Ten patients had 51%-75% and 26 patients had 76%-100% necrosis. No bridging fibrosis or cirrhosis was appreciated in any of them. The patient within the 26%-50% group did not receive a transplant and is currently still living well with a followup of 86 mo. Out of the 10 patients with 51%-75% necrosis, 3 received a liver transplant and are still alive (100%) with a mean followup of 86 mo (range, 66-103 mo). Within this group, 5 of the 7 who did not receive a transplant are currently still living (71.4%) with a mean followup of 72 mo (range, 21-127 mo) and 2 died (both < 1 mo after the index liver biopsy). Within the 76%-100% necrosis group, 11 underwent liver transplantation; of these, 7 are still alive (63.6%) and 4 died. Of the 15 transplant-free patients within this group, 6 survived (40%) with a mean followup of 65 mo (range, 28-122 mo) and 9 died (mean, 3 mo; range, 1-14 mo after the index biopsy).

In summary, transplant-free survival appeared worse in patients with a higher extent of necrosis (40%, 71.4% and 100% in groups with necrosis of 76%-100%, 51%-75% and 26%-50%, respectively). Although higher-extent hepatic necrosis appeared to be associated with worse prognosis, statistically there was no significance between the submassive and the massive necrosis groups (P > 0.05).

Liver transplantation improved patient survival. The patients who received liver transplantation appeared to have somewhat better survival rates compared with non-transplanted patients (100% *vs* 71.4% and 63.6% *vs* 40.0% in 51%-75% and 76%-100% necrosis groups, respectively). However, statistical analysis using Fisher's exact test showed no significant difference in the survival rates of patients within the transplanted and non-transplanted groups, probably due to a small sample size.

Outcome of etiologies causing substantial necrosis respective to survival

Further analysis based upon the etiology of substantial hepatic necrosis, transplantation status, and survival was shown in Table 3. For the 10 cases of drug induced hepatic necrosis, only 3 were transplanted and all of them survived (100%). Four of the 7 who did not receive a transplant survived (57.1%). Overall survival rates for DILI group were not statistically different, depending on transplantation status (P = 0.475).

Of the 14 cases due to autoimmune hepatitis, 5 underwent liver transplantation and 4 patients survived (80.0%). Six of the 9 patients with autoimmune hepatitis who did not receive transplant survived (66.7%).Overall survival rates were not significantly different, depending on transplantation status (P = 1).

Five patients within the viral hepatitis group underwent transplantation and only 2 survived (40.0%). In comparison, only 1 of the 4 viral hepatitis patients survived without transplantation (25.0%). Although the overall survival rate was higher in the transplant group, there was no statistical significance (P = 1).

For the 4 cases of unknown hepatic necrosis, only 1 patient was transplanted. This patient survived. One of the 3 who did not receive a transplant survived. Overall survival rates for the unknown group with or without transplantation were 100% and 33.3%, respectively. Although transplant group had higher survival rate, there was no statistical significance (P = 1).

In summary, transplant-free survival rates were 66.7%, 57.1%, and 25.0% in groups of autoimmune hepatitis, DILI, and viral hepatitis, respectively. Although the survival rates appeared different among the various etiology groups, a statistically significant difference only existed between autoimmune hepatitis and viral hepatitis groups (P = 0.048). Even after

Table 2 Prognosis of the patients who had submassive or massive hepatic necrosis with respect to liver transplantation *n* (%)

Extent of necrosis	Patients (*n* = 37)	Received transplant (*n* = 14)		Transplant free (*n* = 23)	
		Died	Survived	Died	Survived
26%-50%	1	NA	NA	NA	1 (100)
51%-75%	10	NA	3 (100)	2 (28.6)	5 (71.4)
76%-100%	26	4 (36.4)	7 (63.6)	9 (60.0)	6 (40.0)

NA: Not applicable.

Table 3 Prognosis of the patients who had submassive or massive hepatic necrosis with respect to the etiology *n* (%)

Etiology	Patients (*n* = 37)	Received transplant (*n* = 14)		Transplant free (*n* = 23)	
		Died	Survived	Died	Survived
DILI	10	NA	3 (100)	3 (42.9)	4 (57.1)
AIH	14	1 (20.0)	4 (80.0)	3 (33.3)	6 (66.7)
Viral hepatitis	9	3 (60.0)	2 (40.0)	3 (75.0)	1 (25.0)
Unknown	4	NA	1 (100)	2 (66.7)	1 (33.3)

NA: Not applicable; AIH: Autoimmune hepatitis; DILI: Drug induced liver injury.

Table 4 Hepatic encephalopathy with respect to the extent of hepatic necrosis *n* (%)

Extent of necrosis	Patient number (*n* = 37)	Encephalopathy	
		Present (*n* = 5)	Absent (*n* = 32)
26%-50%	1	0	1 (100)
51%-75%	10	0	10 (100)
76%-100%	26	5 (19.2)	21 (80.8)

liver transplantation, the survival rate in patients as a result of viral hepatitis remained the lowest when compared with the other groups, although no statistical significance has been reached between DILI and viral hepatitis (P = 0.058 or 0.090), or between DILI and autoimmune hepatitis (P = 0.116 or 0.408) in the setting of transplant or transplant-free, respectively.

Correlation between hepatic encephalopathy, extent of necrosis, transplant and survival

As demonstrated in Table 4, the patient within 26%-50% necrosis group did not have encephalopathy; nor did any of the patients within 51%-75% group. Five patients within 76%-100% group had encephalopathy (19.2%). Thus, it appears that a higher extent of liver necrosis is possibly associated with encephalopathy. Further analysis of the patients who had encephalopathy revealed that the sole surviving patient (10%) within this group underwent liver transplantation, with a followup time of 92 mo. This finding was statistically significant when compared to the transplant-free group (57.1%, $P < 0.05$).

Of the 21 patients in 76%-100% necrosis group without encephalopathy, 10 underwent transplantation, and the survival rate was statistically significant (60.0%) when compared to the survival rate of 54.5% in those who did not undergo transplantation ($P < 0.05$). Encephalopathy is an important prognostic predictor. The survival rate for transplant-free patients with encephalopathy was much lower compared with the group without encephalopathy (0% *vs* 54.5%; $P < 0.05$).

DISCUSSION

Studies addressing the prognostic value of liver biopsies with substantial necrosis are rare, and the conclusions are not well defined in the literature[14,15]. Hanau and colleagues questioned the value of hepatic necrosis in predicting clinical outcome, because about 50% of the biopsies in their study showed minimal bridging necrosis[7]. In their 1995 study, patients were selected based solely on their clinical characteristics (*e.g.*, signs and symptoms of fulminant liver failure with elevated liver function tests).In contrast, we selected and stratified our study cohorts based on the extent of necrosis in the liver biopsies. Although Hanau's study included 38 cases, only 12 liver biopsies demonstrated either > 90% (3) or 10%-90% (9) necrosis. Additionally, Hanau and colleagues found that only one of seven (14.3%) patients whose liver biopsy demonstrated ⩾ 70% necrosis survived without transplantation, keeping in line with our finding. In another study in 1993, Donaldson and colleagues found that only 2 of 19 patients (10.5%) with > 70% necrosis survived without transplantation[14]. These findings indicate that the percentage of hepatic necrosis may be an important prognosticator for patient survival. As noted, our transplant-free survival rates are much higher with 71.4% and 40% for 51%-75% and > 75% necrosis, respectively. A possible explanation for the difference in transplant-free survival might be related to the different therapeutic options utilized in the respective study cohorts. It seems likely that some more effective non-transplant related treatments

were available for the patients in our study; as the two aforementioned studies took place more than two decades ago. Since then, it appears that no report has been added in the literature in the regard of prognostic value of liver biopsy in an advantaged era of liver transplantation for the past 20 years. To the best of our knowledge, our study is the largest ever to address whether or not there is an association between substantial hepatic necrosis and prognosis (11 with 26%-75% and 26 with > 75% necrosis)[7,14]. Despite a difference in approaches between our study, the Donaldson study, and the Hanau study, a similar trend seems to be present; as the degree of hepatic necrosis increases, the transplant-free survival rate declines. However, the statistical significance of this trend is still not readily apparent, and more studies are certainly warranted.

Adequacy is an important matter to consider, given the well-known fact that necrosis is often heterogeneously distributed throughout the liver[7]. The mean core tissue length of 23 mm in our study and 21 mm in Donaldson's[14] study are both adequate. Specimen adequacy is not mentioned in Hanau's study[7]. Inadequate biopsy specimens, localized liver necrosis[7], and a prolonged interval between the time of symptoms and biopsy, are the most common causes of a discrepancy between the extent of necrosis in a liver biopsy when compared to hepatectomy specimens from the same patient (our unpublished data). Therefore, if a liver biopsy is going to be obtained, it is best obtained from a patient where diffuse hepatic necrosis is suspected; provided that the biopsy will be adequate and is taken as soon as possible following the onset of symptoms. Localized liver necrosis due to ischemia or other injury can be feasibly monitored by CT/MRI imaging, and the interpretation of the biopsy should be considered as a local event.

Importantly, our study has indicated that there may be association between etiology and patient survival in the setting of submassive or massive necrosis, which has not been discussed in the prior reports[7,14,15]. In our study, survival was the worst in those with hepatotropic viral hepatitis as the underlying etiology, regardless of the status of liver transplantation. Patients with autoimmune hepatitis induced hepatic necrosis had the best transplant-free survival and those with DILI had the best survival after transplantation. It is not entirely clear why different causes may lead to different survival from our study. One might speculate that differences in patient age, availability of effective therapeutic options, or preexisting co-morbidities might play a role in prognosis. In our study, the median age for those with massive hepatic necrosis was 49, 43, 48, and 44 years in autoimmune hepatitis, DILI, viral hepatitis, and unknown groups, respectively (Supplement 1). This finding demonstrates a lack of correlation between age and prognosis in the setting of substantial hepatic necrosis, although age has been suggested as playing a role in Hanau's study[7]. In our study, the autoimmune hepatitis group had the greatest median age, and yet had the best overall survival . It is likely that effective therapeutic agents in autoimmune hepatitis might play a role in explaining why transplant-free survival is better when compared with other etiologies. However, due to the small number of cases in each of the substratified groups, no definitive conclusions can be drawn and further investigation seems warranted.

Bacterial infections and ascites were present more frequently in patients with a higher extent of hepatic necrosis. Mean INR for the patients with higher percentages of hepatic necrosis were also higher than in patients with a smaller percentage of necrosis. However none of these trends were found to be statistically significant. It is likely that a larger study may be able to identify a statistically significant association between these individual parameters.

Hepatic encephalopathy is present more frequently in the patients with massive necrosis. However, the incidence seems low in our study (19.2%). The relatively low incidence of encephalopathy might reflect the characteristics of the study cohort in our institution. The lack of a clear statistically significant association between extent of necrosis and encephalopathy is likely due to the relatively low number of patients in our study. In patients with hepatic encephalopathy and massive necrosis, the prognosis is extremely miserable. The only patient with encephalopathy who survived received a liver transplant. This finding suggests that encephalopathy due to hepatic necrosis may be associated with increased mortality. It also suggests that liver transplantation may be useful in this setting[16-20].

In conclusion, accurate histopathological evaluation in patients with fulminant liver failure is useful. However, more research with a larger number of patients is required to truly identify any significant associations between the extent of hepatic necrosis and prognosis. The significance of liver biopsy is not limited to identifying or confirming the etiology; it is also a valuable tool in the assessment of prognosis and management decisions in regard to liver transplantation. As demonstrated, the percentage of liver necrosis in an adequate liver biopsy is a prognostic indicator of survival. More than 75% hepatic necrosis is associated with substantial transplant-free mortality, thus massive hepatic necrosis is worth considering as an indicator for liver transplantation. Importantly, survival is associated with etiology with the worst in those with hepatotropic viral hepatitis even after liver transplantation. Taken together, assessing the extent of hepatic necrosis and its underlying etiology can aid in screening candidates who may benefit most from liver transplantation, a lifesaving but expensive and high risk procedure. Early identification of transplant candidates is critical in optimizing the utilization of

resources.

COMMENTS

Background

Patients with fulminant hepatic failure often receive liver biopsies as part of the clinical work-up. In many instances, extensive hepatic necrosis is identified. The significance of extensive hepatic necrosis within a liver biopsy, as it relates to patient prognosis or treatment decisions, has not been well described.

Research frontiers

To our knowledge, no new studies addressing the significance of biopsy proven hepatic necrosis as it relates to patient prognosis have been published for over twenty years. The objective of our study was to identify what associations if any exist between hepatic necrosis, patient clinical characteristics, and survival.

Innovations and breakthroughs

This study shows trends suggesting that the extent of hepatic necrosis is associated with poorer patient survival. Further, we noticed a trend that patients who undergo liver transplantation tend to have a longer survival time. Additionally, higher extents of hepatic necrosis typically showed trends with clinical factors such as higher mean INR, and increased frequency of ascites or bacterial infections. While these trends all seemed to be present within our study, no statistical significance was identified, likely due to the small size of our study (in spite of us having the largest number of cases to date).

Applications

The trends evident within our study may provide future investigators with a starting point for their inquiries into how hepatic necrosis may play a role in patient management.

Terminology

Fulminant liver failure is clinically characterized by an abrupt onset of jaundice and liver dysfunction with subsequent development of encephalopathy and coagulopathy in patients with or without preexisting liver disease. Hepatic necrosis is defined as death of hepatocytes, which maybe single cell, multiple cells in piecemeal, focal, multifocal, submassive or massive. Submassive hepatic necrosis is defined as necrosis involving 26%-75% of the parenchymal volume, while massive necrosis involves more than 75%.

Peer-review

This paper evaluated if any association existed between the extent of hepatic necrosis and patient survival through observing the data resulted from 37 patients with fulminant liver failure, whose liver biopsy exhibited substantial necrosis. It was found that transplant-free survival was worse in patients with a higher extent of necrosis (40%, 71.4% and 100% in groups with necrosis of 76%-100%, 51%-75% and 26%-50%, respectively). So, the author concluded that adequate liver biopsy with more than 75% necrosis is associated with significant transplant-free mortality that is critical in predicting survival. This study has some scientific and clinic significances.

REFERENCES

1 **Shakil AO**, Kramer D, Mazariegos GV, Fung JJ, Rakela J. Acute liver failure: clinical features, outcome analysis, and applicability of prognostic criteria. *Liver Transpl* 2000; **6**: 163-169 [PMID: 10719014 DOI: 10.1002/lt.500060218]

2 **Singhal A**, Vadlamudi S, Stokes K, Cassidy FP, Corn A, Shrago SS, Wright HI, Kohli V. Liver histology as predictor of outcome in patients with acute liver failure. *Transpl Int* 2012; **25**: 658-662 [PMID: 22487361 DOI: 10.1111/j.1432-2277.2012.01470.x]

3 **Sugawara K**, Nakayama N, Mochida S. Acute liver failure in Japan: definition, classification, and prediction of the outcome. *J Gastroenterol* 2012; **47**: 849-861 [PMID: 22825549 DOI: 10.1007/s00535-012-0624-x]

4 **Arroyo V**, Moreau R, Jalan R, Ginès P; EASL-CLIF Consortium CANONIC Study. Acute-on-chronic liver failure: A new syndrome that will re-classify cirrhosis. *J Hepatol* 2015; **62**: S131-S143 [PMID: 25920082 DOI: 10.1016/j.jhep.2014.11.045]

5 **Wlodzimirow K**, Abu-Hanna A, Chamuleau RA. Acute-on-chronic liver failure - its definition remains unclear. *J Hepatol* 2013; **59**: 190-191 [PMID: 23462694 DOI: 10.1016/j.jhep.2013.02.011]

6 **Wlodzimirow KA**, Eslami S, Abu-Hanna A, Nieuwoudt M, Chamuleau RA. A systematic review on prognostic indicators of acute on chronic liver failure and their predictive value for mortality. *Liver Int* 2013; **33**: 40-52 [PMID: 22429562 DOI: 10.1111/j.1478-3231.2012.02790.x]

7 **Hanau C**, Munoz SJ, Rubin R. Histopathological heterogeneity in fulminant hepatic failure. *Hepatology* 1995; **21**: 345-351 [PMID: 7843704]

8 **Kessler WR**, Cummings OW, Eckert G, Chalasani N, Lumeng L, Kwo PY. Fulminant hepatic failure as the initial presentation of acute autoimmune hepatitis. *Clin Gastroenterol Hepatol* 2004; **2**: 625-631 [PMID: 15224287]

9 **Jalan R**, Gines P, Olson JC, Mookerjee RP, Moreau R, Garcia-Tsao G, Arroyo V, Kamath PS. Acute-on chronic liver failure. *J Hepatol* 2012; **57**: 1336-1348 [PMID: 22750750 DOI: 10.1016/j.jhep.2012.06.026]

10 **Jalan R**, Gines P, Olson JC, Mookerjee RP, Moreau R, Garcia-Tsao G, Arroyo V, Kamath PS. Reply to: "Acute-on-chronic liver failure - its definition remains unclear". *J Hepatol* 2013; **59**: 191 [PMID: 23485518 DOI: 10.1016/j.jhep.2013.02.017]

11 **Jalan R**, Mookerjee RP. Acute-on-chronic liver failure: an early biopsy is essential? *Gut* 2010; **59**: 1455-1456 [PMID: 20947880 DOI: 10.1136/gut.2010.214627]

12 **O'Grady J**. Modern management of acute liver failure. *Clin Liver Dis* 2007; **11**: 291-303 [PMID: 17606208 DOI: 10.1016/j.cld.2007.04.011]

13 **Yamagishi Y**, Saito H, Tada S, Horie Y, Kato S, Ishii H, Shimojima N, Haga J, Shimazu M, Kitajima M, Hibi T. Value of computed tomography-derived estimated liver volume/standard liver volume ratio for predicting the prognosis of adult fulminant hepatic failure in Japan. *J Gastroenterol Hepatol* 2005; **20**: 1843-1849 [PMID: 16336442 DOI: 10.1111/j.1440-1746.2005.03949.x]

14 **Donaldson BW**, Gopinath R, Wanless IR, Phillips MJ, Cameron R, Roberts EA, Greig PD, Levy G, Blendis LM. The role of transjugular liver biopsy in fulminant liver failure: relation to other prognostic indicators. *Hepatology* 1993; **18**: 1370-1376 [PMID: 8244261]

15 **Kirsch R**, Yap J, Roberts EA, Cutz E. Clinicopathologic spectrum of massive and submassive hepatic necrosis in infants and children. *Hum Pathol* 2009; **40**: 516-526 [PMID: 19121848 DOI: 10.1016/j.humpath.2008.07.018]

16 **Chan AC**, Fan ST, Lo CM, Liu CL, Chan SC, Ng KK, Yong BH, Chiu A, Lam BK. Liver transplantation for acute-on-chronic liver failure. *Hepatol Int* 2009; **3**: 571-581 [PMID: 19680733 DOI: 10.1007/s12072-009-9148-8]

17 **Duan BW**, Lu SC, Wang ML, Liu JN, Chi P, Lai W, Wu JS, Guo QL, Lin DD, Liu Y, Zeng DB, Li CY, Meng QH, Ding HG, Chen XY, Liao HY, Ma LQ, Chen Y, Zhang J, Xiang HP, Duan ZP, Li N. Liver transplantation in acute-on-chronic liver failure patients with high model for end-stage liver disease (MELD) scores: a single center experience of 100 consecutive cases. *J Surg Res* 2013; **183**: 936-943 [PMID: 23558257 DOI: 10.1016/j.jss.2013.03.008]

18 **Farmer DG**, Anselmo DM, Ghobrial RM, Yersiz H, McDiarmid SV, Cao C, Weaver M, Figueroa J, Khan K, Vargas J, Saab S, Han S, Durazo F, Goldstein L, Holt C, Busuttil RW. Liver transplantation for fulminant hepatic failure: experience with more than 200 patients over a 17-year period. *Ann Surg* 2003; **237**: 666-675; discussion 675-676 [PMID: 12724633 DOI: 10.1097/01.SLA.0000064365.54197.9E]

19 **Gotthardt D**, Riediger C, Weiss KH, Encke J, Schemmer P, Schmidt J, Sauer P. Fulminant hepatic failure: etiology and indications for liver transplantation. *Nephrol Dial Transplant* 2007; **22** Suppl 8: viii5-viii8 [PMID: 17890263 DOI: 10.1093/ndt/

gfm650]
20 **Ostapowicz G**, Fontana RJ, Schiødt FV, Larson A, Davern TJ, Han SH, McCashland TM, Shakil AO, Hay JE, Hynan L, Crippin JS, Blei AT, Samuel G, Reisch J, Lee WM. Results of a prospective study of acute liver failure at 17 tertiary care centers in the United States. *Ann Intern Med* 2002; **137**: 947-954 [PMID: 12484709]

P- Reviewer: Gong ZJ **S- Editor**: Gong ZM **L- Editor**: A
E- Editor: Zhang FF

World Journal of Gastroenterology

Submit a Manuscript: http://www.f6publishing.com

World J Gastroenterol 2017 June 21; 23(23): 4311-4316

DOI: 10.3748/wjg.v23.i23.4311

ISSN 1007-9327 (print) ISSN 2219-2840 (online)

CASE REPORT

Benefit of everolimus in treatment of an intrahepatic cholangiocarcinoma patient with a *PIK3CA* mutation

Ji-Lai Bian, Mei-Mei Wang, En-Juan Tong, Jing Sun, Ming Li, Zhi-Bo Miao, Yan-Lin Li, Bai-Hong Zhu, Jia-Jia Xu

Ji-Lai Bian, Mei-Mei Wang, En-Juan Tong, Jing Sun, Ming Li, Department of Medical Oncology, The Fifth People's Hospital of Dalian, Dalian 116021, Liaoning Province, China

Zhi-Bo Miao, Yan-Lin Li, Bai-Hong Zhu, Origimed Inc, Shanghai 201114, China

Jia-Jia Xu, Institute of Precision Medicine, 3D Medicines Inc, Shanghai 201114, China

Author contributions: Bian JL and Wang MM followed the patient; Miao ZB, Li YL, Zhu BH and Xu JJ provided genetic analysis for the variants tested in the patient; Tong EJ, Sun J and Li M searched related articles; Bian JL and Li YL wrote the paper; all authors have read and approved the final manuscript.

Conflict-of-interest statement: There are no potential conflicts of interest relevant to this article.

Manuscript source: Unsolicited manuscript

Correspondence to: Dr. Ji-Lai Bian, Department of Medical Oncology, The Fifth People's Hospital of Dalian, Dalian 116021, Liaoning Province, China. bianjilai123@126.com
Telephone: +86-411-842112244
Fax: +86-411-842112244

Received: February 26, 2017
Peer-review started: February 27, 2017
First decision: April 10, 2017
Revised: April 22, 2017
Accepted: May 19, 2017
Article in press: May 19, 2017
Published online: June 21, 2017

Abstract

Intrahepatic cholangiocarcinoma (ICC) is a relatively rare form of liver cancer with a poor prognosis. The therapeutic options for patients with advanced ICC are limited and usually ineffective. There is currently no approved targeted therapy for ICC, although accumulating evidence supports inhibition of the PI3K/Akt/mTOR signaling pathway as a promising therapeutic strategy in the treatment of ICC. Here, we report a patient with stage IV ICC harboring a *PIK3CA* mutation who responded well to the mTOR inhibitor everolimus. Computed tomography and magnetic resonance imaging demonstrated shrinkage of the tumor and maintenance of a partial response for 6.5 mo after everolimus treatment as the best response. To the best of our knowledge, this is the first clinical case report in the literature of clinical benefit from everolimus treatment in an ICC patient with *PIK3CA* mutation.

Key words: Everolimus; Next generation sequencing; *PIK3CA*; Intrahepatic cholangiocarcinoma

Core tip: We report a stage IV intrahepatic cholangiocarcinoma (ICC) patient harboring a *PIK3CA* mutation who responded well to the mTOR inhibitor everolimus. Computed tomography and magnetic resonance imaging demonstrated shrinkage of the tumor and the maintenance of partial response for 6.5 mo after everolimus treatment as the best response. To the best of our knowledge, this is the first clinical case report in the literature of an ICC patient with *PIK3CA* mutation deriving benefit from everolimus treatment.

Bian JL, Wang MM, Tong EJ, Sun J, Li M, Miao ZB, Li YL, Zhu BH, Xu JJ. Benefit of everolimus in treatment of an intrahepatic

cholangiocarcinoma patient with a *PIK3CA* mutation. *World J Gastroenterol* 2017; 23(23): 4311-4316 Available from: URL: http://www.wjgnet.com/1007-9327/full/v23/i23/4311.htm DOI: http://dx.doi.org/10.3748/wjg.v23.i23.4311

INTRODUCTION

Cholangiocarcinoma, the second most common primary malignancy of the liver, is divided into four categories based on the anatomic location of origin within the biliary system as follows: intrahepatic, hilar, distal biliary, and ampullary[1,2]. Complete surgical resection remains the only potentially curative option for patients with intrahepatic cholangiocarcinoma (ICC). However, because most cases are diagnosed at advanced stages, only one-third of ICC tumors are amenable for surgical resection with a 5-year survival rate of 20%-40%[3,4], and unresectable ICC carries a dismal prognosis. Systemic chemotherapy, conventional external beam radiation, and brachytherapy are established standard treatments but show limited success and are associated with toxicity[2].

Doublet gemcitabine and cisplatin therapy is currently proposed as the standard first-line therapy for patients with an advanced disease; however, the efficiency is limited[5]. Locoregional therapy appears to have a better effect against ICC[6], but more data are needed to define its role. To date there has been no approved targeted molecular therapy for ICC and identification of a definitive treatment remains an unmet need. Recently, the use of next-generation sequencing (NGS) technologies has enabled the identification of frequently observed actionable molecular alterations that hold the promise of improving the management of advanced ICC patients.

The phosphatidylinositol 3-kinase (PI3K)/Akt/mammalian target of rapamycin (mTOR) signaling pathway plays an essential role in regulating cell survival and proliferation[6]. Mutation in *PIK3CA* has been reported in 8% of ICC patients according to The Cancer Genome Atlas (TCGA) database, and activating mutations of *PIK3CA* that are related to tumorigenesis and cancer progression have been identified in a broad spectrum of malignant tumors[7,8]. Therefore, inhibition of the mTOR pathway represents a promising therapeutic strategy in the treatment of ICC. Everolimus is a novel macrolide derivative of rapamycin that inhibits mTOR and was approved by the Food and Drug Administration (FDA) for the treatment of advanced renal cell carcinoma[9] and other cancer types[10]. However, whether everolimus is effective against ICC is unknown. In studies of ICC-related cancers, *in vitro* and *in vivo* results demonstrated that everolimus exhibits cytotoxic and antimetastatic effects in a cholangiocarcinoma cell line[11]. These results suggest that everolimus may be a potential therapeutic agent for the treatment of patients with ICC possessing an aberrant PI3K/Akt/mTOR signaling pathway.

Here, we report a patient with stage IV ICC harboring a *PIK3CA* mutation who responded well to the mTOR inhibitor everolimus, demonstrating that inhibition of the PI3K/Akt/mTOR signaling pathway is a promising therapeutic avenue for ICC. To the best of our knowledge, this is the first clinical case report in the literature of an ICC patient with *PIK3CA* mutation deriving benefit from everolimus treatment.

CASE REPORT

A 31-year-old Chinese man presented with 1-mo history of progressive abdominal distension and was admitted to hospital. A computed tomography (CT) scan revealed a space-occupying mass in the liver with massive peritoneal effusion and some pleural effusion in both sides of the chest. The patient had no history of alcohol abuse, hepatitis, or cirrhosis, and denied any family history of cancers and other hereditary diseases. He was transferred to our hospital in December 2015. Physical examination revealed a distended abdomen with tenderness and muscle guarding, and his abdominal girth was measured at 105 cm. No icteric sclera or xanthochromia was detected, and the Murphy's sign was negative. Liver function test indicated that the levels of total protein and albumin were 57.6 g/L and 32.4 g/L, respectively, which were below normal and indicated malnutrition and hypoalbuminemia, whereas bilirubin and aminotransferase were within the normal range. The tumor markers carcinoembryonic antigen (CEA), alpha-fetoprotein (AFP), cancer antigen 19-9 (CA19-9), and carbohydrate antigen 72-4 (CA72-4) were all within the normal range. Further magnetic resonance imaging (MRI) of the liver showed a 9.9 cm × 7.4 cm mass at the posterior right lobe of the liver with multiple swollen retroperitoneal lymph nodes and massive peritoneal effusion (Figure 1A and E). The Eastern Cooperative Oncology Group (ECOG) performance score was 2-3. Abdominal paracentesis was performed repeatedly to relieve abdominal distension, which was also used to collect exfoliated tumor cells from the ascites for cytological diagnosis; however, no tumor cells were detected. Consequently, core needle biopsy of the liver mass was performed and the specimens were sent for pathological evaluation, which indicated a poorly differentiated adenocarcinoma. Immunohistochemical staining showed that the cells were positive for CK7, CK19, CK8, and CEA and negative for glypican-3, hepatocyte marker, and vimentin. These results suggested a diagnosis of stage IV ICC (cT3N1M1).

There is currently no standard treatment for ICC, and chemotherapy is generally ineffective. This patient was not suitable for chemotherapy due to his poor physical condition, therefore he was recommended for NGS to identify possible therapeutic targets. His liver

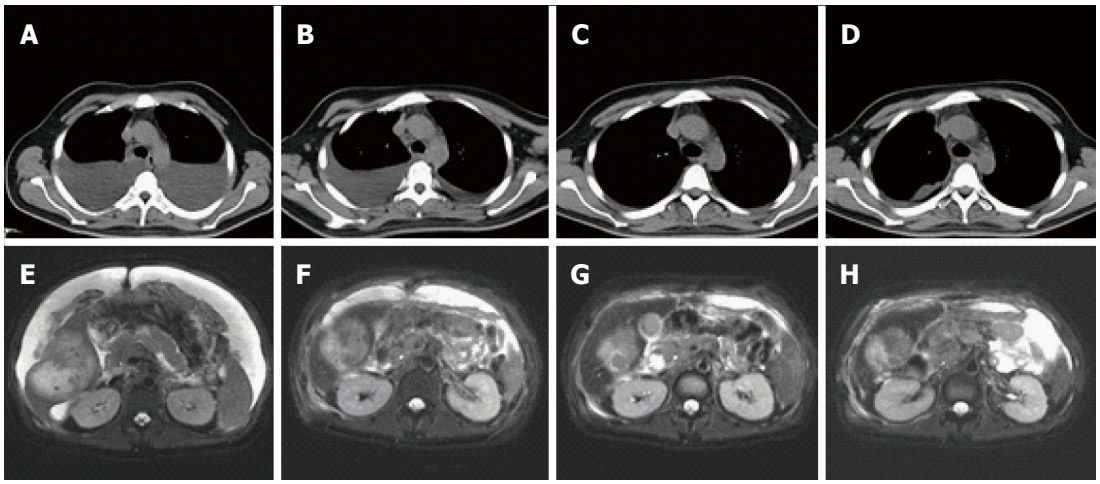

Figure 1 Computed tomography and magnetic resonance imaging scans show that, compared to the baseline (A and E), the patient's peritoneal effusion decreased after 3 cycles of chemotherapy treatment (B and F), tumor shrank after everlimus treatment for 2 mo (C and G), and stable disease was achieved after everlimus treatment for 4 mo (D and H).

biopsy specimen and matched blood sample were sent for NGS panel analysis after consent was obtained from the patient himself and his family. We detected all genomic alteration types, including base substitutions, insertions and deletions, copy number alterations, and rearrangements, for more than 390 genes commonly associated with cancers. While we were waiting for the NGS results, intraperitoneal chemotherapy with cisplatin plus Endostar was initiated for the control of ascites. The patient was perfused with three cycles of cisplatin 30 mg in 250 mL of normal saline (NS) and Endostar 60 mg in 250 mL of NS every 5 d. Amino acids, fat emulsion, and albumin were added during the treatment for nutritional support. Before the first intraperitoneal chemotherapy the patient felt aggravated chest stuffiness and a CT scan demonstrated increased pleural effusion. After three cycles of treatment, the patient's abdominal girth decreased from 105 cm to 85 cm and the CT scan indicated decreased peritoneal effusion (Figure 1B and F).

In January 2016, the genomic profile of the patient revealed three somatic mutations, including E545G mutation of the *PIK3CA* gene (NM_006218), R132C mutation of the *IDH1* gene (NM_005896) and c.714+1G>T mutation of the *PBRM1* gene (NM_018313). As preclinical data suggest that activating mutations in *PIK3CA* may predict a sensitivity to inhibitors of the PI3K/AKT/mTOR pathway[11], the patient received everolimus (10 mg orally daily), provided off-label with insurance approval. CT scans showed a notable decrease in pleural effusion and tumor shrinkage after everolimus treatment for 2 mo (Figure 1C and G). One month after everolimus treatment, the levels of total protein and albumin increased to 76.2 g/L (normal range, 63-82 g/L) and 42.9 g/L (normal range, 35-50 g/L), respectively, and the ECOG performance score was evaluated as 1. MRI showed shrinkage of the tumor from 9.9 cm × 7.4 cm to 6.4 cm × 4.3 cm, which was considered a partial response (PR) according to Response Evaluation Criteria in Solid Tumors criteria.

In May 2016, the patient suddenly displayed icterus, icteric sclera, and xanthochromia. On May 8, the levels of total bilirubin, direct bilirubin, indirect bilirubin, and ammonia increased to 145, 122, 23, and 64 μmol/L, respectively. Serum levels of alanine transaminase (ALT) and aspartate aminotransferase (AST) levels were 404 and 321 U/L and those of total protein and albumin were 76 and 42 g/L, respectively. His abdominal girth increased from 85 cm to 87 cm, and color Doppler ultrasound demonstrated a slight increase in pleural and peritoneal effusion (Figure 1D and H). The Child-Pugh score of the patient was classified as Class B, therefore the everolimus dosage was decreased to 5 mg orally once daily (half the standard dose) from May 10 with consideration of his liver dysfunction. Magnetic resonance cholangiopancreatography showed a high-position biliary obstruction, and local three-dimensional conformal radiotherapy (3DCRT) was started on May 16. However, the 3DCRT was ineffective because the icteric index and liver function showed continued aggravation with no improvement in biliary obstruction. On May 30, surgical biliary drainage was performed to reduce icterus. The patient continued to receive everolimus (5 mg once daily) to the present time. At the latest follow-up on July 16, the tumor response remained as stable disease and the progression-free survival (PFS) had lasted for more than 6.5 mo from the initial treatment with everolimus.

DISCUSSION

Genomic profiling of the patient revealed three somatic mutations: E545G mutation of *PIK3CA* and mutations of *IDH1* and *PBRM1* genes. Activating mutations in the region encoding the p110α subunit of PI3K (PIK3CA) have been identified in a broad spectrum of

malignant tumors. Codon 545 is a hotspot for PIK3CA mutations that are known to activate the PI3K/Akt/mTOR signaling pathway[12,13]. However, the E545K substitution is much more common in cancers than the E545G mutation; E545K represents 25% of all PIK3CA mutations[14] whereas E545G has only been reported in a few carcinomas[15]. *In vitro* research studies comparing the activity of mutant PIK3CA proteins have shown that the E545G substitution displays strong transforming activity in chicken embryo fibroblasts, although its effect is lower than that of the more common E542K and E545K substitutions[16].

Both the *IDH1* and *PBRM1* genes are recurrently mutated in ICC with frequencies of 4.9% and 18%, respectively[17]. Mutations in *IDH1* and *IDH2* are confined to the active site and result in the production of a neomorphic metabolite 2-hydroxyglutarate (2HG), which is normally found in scarce amounts, through NADPH-dependent reduction of 2-OG to the R enantiomer of 2HG. Frequent somatic hotspot mutations in *IDH1* have been identified in gliomas, chondrosarcomas, myeloid leukemias, and other cancers. Suppression of endogenous mutant *IDH1* expression was recently reported in HT180, a fibrosarcoma cell line with a native *IDH1* R132C heterozygous mutation[18]. PBRM1 is associated with chromatin remodeling and is crucial for the suppression of aggressive clear cell renal cell carcinoma (ccRCC) tumors[19]. However, there are no preclinical or early clinical data implicating *IDH1* and *PBRM1* as biomarkers for targeted cancer therapy in ICC.

The mTOR inhibitor everolimus has been approved by the FDA for the treatment of advanced RCC, subependymal giant cell astrocytoma (SEGA), and progressive neuroendocrine tumors (PNET) of pancreatic origin as monotherapy, and of advanced hormone receptor-positive, HER2-negative breast cancer in combination with exemestane. The effect of everolimus is clearly proven in many cancers, especially those with *PIK3CA* mutations. Phase III clinical trials suggested that patients with HER2-positive advanced breast cancer with *PIK3CA* mutations could derive a PFS benefit from everolimus[20]. Recent research demonstrated that mTOR pathway activating mutations confer sensitivity to everolimus regardless of cancer type[21]. A case report supported the use of everolimus monotherapy in a patient with refractory metastatic gastric cancer harboring PIK3CA and pS6 aberrations[22]. In our case study, everolimus exhibited good efficacy in an ICC patient. The adverse effects of everolimus on liver dysfunction may be a cause for concern. In May 2011 the FDA approved everolimus for the treatment of PNET of pancreatic origin. The approval was based on a randomized controlled trial of everolimus 10 mg/d (n = 207) *vs* placebo (n = 203) in patients with unresectable, locally advanced, or metastatic pancreatic neuroendocrine tumors. The median PFS for patients treated with everolimus was 11.0 mo *vs* 4.6 mo for patients treated with placebo. However, deaths occurred in seven patients treated with everolimus and one patient treated with placebo[23]. The causes of death in patients treated with everolimus included one case with hepatic failure. Although there is no direct evidence that everolimus is related to hepatic failure, hepatobiliary patients should be kept under strict surveillance when taking everolimus.

Generally speaking, ICC is a relatively rare cancer, accounting for 3% of gastrointestinal malignancies, and has a poor prognosis. The limited number of patients leads to a lack of clinical trials conducted specifically in ICC patients, which precludes the generation of clinical practice guidelines establishing a "standard of care" for these patients. At present, the prognosis for patients diagnosed with unresectable ICC is poor, with a life expectancy of approximately 1 year and actuarial probability of survival of 5% at 5 years with traditional chemotherapy[2,24]. To date, no molecular targeted therapy has been proven effective for ICC. To the best of our knowledge, this is the first clinical case report in the literature of benefit from everolimus treatment in an ICC patient with a *PIK3CA* mutation. This patient is still considered progression-free with good quality of life at the latest follow-up, highlighting the potential of the PI3K/Akt/mTOR signaling pathway as a therapeutic target in ICC.

To our knowledge, this case represents the first report of an ICC patient with a *PIK3CA* mutation who derived benefit from everolimus treatment. However, whether the presence of mutation of *IDH1* and *PBRM1* contributed to the patient's response to targeted therapy is unclear, and the reason for the patient's response to everolimus and prolonged survival has yet to be elucidated.

COMMENTS

Case characteristics

A 31-year-old Chinese man presented with 1-mo history of progressive abdominal distension and was admitted to hospital.

Clinical diagnosis

Physical examination revealed a distended abdomen with tenderness and muscle guarding, and his abdominal girth was measured at 105 cm.

Differential diagnosis

Hepatocellular carcinoma, intrahepatic cholangiocarcinoma, stage IV intrahepatic cholangiocarcinoma (cT3N1M1).

Laboratory diagnosis

Liver function test indicated that the levels of total protein and albumin were 57.6 g/L and 32.4 g/L, respectively, which were below normal and indicated malnutrition and hypoalbuminemia, whereas bilirubin and aminotransferase were within the normal range. The tumor markers carcinoembryonic antigen, alpha-fetoprotein, cancer antigen 19-9, and carbohydrate antigen 72-4 were all within the normal range.

Imaging diagnosis

A computed tomography (CT) scan revealed a space-occupying mass in the liver with massive peritoneal effusion and some pleural effusion in both sides of

the chest.

Pathological diagnosis

Pathological examination revealed intrahepatic cholangiocarcinoma (ICC).

Treatment

The genomic profile of the patient revealed three somatic mutations, including E545G mutation of the *PIK3CA* gene, R132C mutation of the *IDH1* gene and c.714+1G>T mutation of the *PBRM1* gene. Based on the gene alteration testing report and the clinical trial studies, the patient received everolimus (10 mg orally daily), provided off-label with insurance approval.

Term explanation

The mTOR inhibitor everolimus has been approved by the FDA for the treatment of advanced RCC, subependymal giant cell astrocytoma, and progressive neuroendocrine tumors of pancreatic origin as monotherapy, and of advanced hormone receptor-positive, HER2-negative breast cancer in combination with exemestane. To the best of our knowledge, this is the first clinical case report in the literature of an ICC patient with a *PIK3CA* mutation deriving benefit from everolimus treatment.

Experiences and lessons

Results observed in this case encourage further research on the activity of everolimus in ICC, based on the presence of PIK3CA mutation. This could lead to a selection of ICC patients to be treated with this drug, and could help identify a novel treatment strategy for PIK3CA-mutated ICC patients.

Peer-review

Very interesting case report. In this study, the authors report a stage IV ICC patient harboring a PIK3CA mutation who responded well to the mTOR inhibitor everolimus.

REFERENCES

1 **Blechacz B**, Komuta M, Roskams T, Gores GJ. Clinical diagnosis and staging of cholangiocarcinoma. *Nat Rev Gastroenterol Hepatol* 2011; **8**: 512-522 [PMID: 21808282 DOI: 10.1038/nrgastro.2011.131]

2 **Mahadevan A**, Dagoglu N, Mancias J, Raven K, Khwaja K, Tseng JF, Ng K, Enzinger P, Miksad R, Bullock A, Evenson A. Stereotactic Body Radiotherapy (SBRT) for Intrahepatic and Hilar Cholangiocarcinoma. *J Cancer* 2015; **6**: 1099-1104 [PMID: 26516357 DOI: 10.7150/jca.13032]

3 **Bridgewater J**, Galle PR, Khan SA, Llovet JM, Park JW, Patel T, Pawlik TM, Gores GJ. Guidelines for the diagnosis and management of intrahepatic cholangiocarcinoma. *J Hepatol* 2014; **60**: 1268-1289 [PMID: 24681130 DOI: 10.1016/j.jhep.2014.01.021]

4 **de Jong MC**, Nathan H, Sotiropoulos GC, Paul A, Alexandrescu S, Marques H, Pulitano C, Barroso E, Clary BM, Aldrighetti L, Ferrone CR, Zhu AX, Bauer TW, Walters DM, Gamblin TC, Nguyen KT, Turley R, Popescu I, Hubert C, Meyer S, Schulick RD, Choti MA, Gigot JF, Mentha G, Pawlik TM. Intrahepatic cholangiocarcinoma: an international multi-institutional analysis of prognostic factors and lymph node assessment. *J Clin Oncol* 2011; **29**: 3140-3145 [PMID: 21730269 DOI: 10.1200/JCO.2011.35.6519]

5 **Valle J**, Wasan H, Palmer DH, Cunningham D, Anthoney A, Maraveyas A, Madhusudan S, Iveson T, Hughes S, Pereira SP, Roughton M, Bridgewater J. Cisplatin plus gemcitabine versus gemcitabine for biliary tract cancer. *N Engl J Med* 2010; **362**: 1273-1281 [PMID: 20375404 DOI: 10.1056/NEJMoa0908721]

6 **Vogl TJ**, Schwarz W, Eichler K, Hochmuth K, Hammerstingl R, Jacob U, Scheller A, Zangos S, Heller M. Hepatic intraarterial chemotherapy with gemcitabine in patients with unresectable cholangiocarcinomas and liver metastases of pancreatic cancer: a clinical study on maximum tolerable dose and treatment efficacy. *J Cancer Res Clin Oncol* 2006; **132**: 745-755 [PMID: 16858591 DOI: 10.1007/s00432-006-0138-0]

7 **Schneck H**, Blassl C, Meier-Stiegen F, Neves RP, Janni W, Fehm T, Neubauer H. Analysing the mutational status of PIK3CA in circulating tumor cells from metastatic breast cancer patients. *Mol Oncol* 2013; **7**: 976-986 [PMID: 23895914 DOI: 10.1016/j.molonc.2013.07.007]

8 **Dunlap J**, Le C, Shukla A, Patterson J, Presnell A, Heinrich MC, Corless CL, Troxell ML. Phosphatidylinositol-3-kinase and AKT1 mutations occur early in breast carcinoma. *Breast Cancer Res Treat* 2010; **120**: 409-418 [PMID: 19418217 DOI: 10.1007/s10549-009-0406-1]

9 **Motzer RJ**, Escudier B, Oudard S, Hutson TE, Porta C, Bracarda S, Grünwald V, Thompson JA, Figlin RA, Hollaender N, Urbanowitz G, Berg WJ, Kay A, Lebwohl D, Ravaud A. Efficacy of everolimus in advanced renal cell carcinoma: a double-blind, randomised, placebo-controlled phase III trial. *Lancet* 2008; **372**: 449-456 [PMID: 18653228 DOI: 10.1016/S0140-6736(08)61039-9]

10 **Krueger DA**, Care MM, Holland K, Agricola K, Tudor C, Mangeshkar P, Wilson KA, Byars A, Sahmoud T, Franz DN. Everolimus for subependymal giant-cell astrocytomas in tuberous sclerosis. *N Engl J Med* 2010; **363**: 1801-1811 [PMID: 21047224 DOI: 10.1056/NEJMoa1001671]

11 **Moolthiya P**, Tohtong R, Keeratichamroen S, Leelawat K. Role of mTOR inhibitor in cholangiocarcinoma cell progression. *Oncol Lett* 2014; **7**: 854-860 [PMID: 24527093 DOI: 10.3892/ol.2014.1799]

12 **Karakas B**, Bachman KE, Park BH. Mutation of the PIK3CA oncogene in human cancers. *Br J Cancer* 2006; **94**: 455-459 [PMID: 16449998 DOI: 10.1038/sj.bjc.6602970]

13 **Hafner C**, López-Knowles E, Luis NM, Toll A, Baselga E, Fernández-Casado A, Hernández S, Ribé A, Mentzel T, Stoehr R, Hofstaedter F, Landthaler M, Vogt T, Pujol RM, Hartmann A, Real FX. Oncogenic PIK3CA mutations occur in epidermal nevi and seborrheic keratoses with a characteristic mutation pattern. *Proc Natl Acad Sci USA* 2007; **104**: 13450-13454 [PMID: 17673550 DOI: 10.1073/pnas.0705218104]

14 **Samuels Y**, Wang Z, Bardelli A, Silliman N, Ptak J, Szabo S, Yan H, Gazdar A, Powell SM, Riggins GJ, Willson JK, Markowitz S, Kinzler KW, Vogelstein B, Velculescu VE. High frequency of mutations of the PIK3CA gene in human cancers. *Science* 2004; **304**: 554 [PMID: 15016963 DOI: 10.1126/science.1096502]

15 **López-Knowles E**, Hernández S, Malats N, Kogevinas M, Lloreta J, Carrato A, Tardón A, Serra C, Real FX. PIK3CA mutations are an early genetic alteration associated with FGFR3 mutations in superficial papillary bladder tumors. *Cancer Res* 2006; **66**: 7401-7404 [PMID: 16885334 DOI: 10.1158/0008-5472.CAN-06-1182]

16 **Gymnopoulos M**, Elsliger MA, Vogt PK. Rare cancer-specific mutations in PIK3CA show gain of function. *Proc Natl Acad Sci USA* 2007; **104**: 5569-5574 [PMID: 17376864 DOI: 10.1073/pnas.0701005104]

17 **Prensner JR**, Chinnaiyan AM. Metabolism unhinged: IDH mutations in cancer. *Nat Med* 2011; **17**: 291-293 [PMID: 21383741 DOI: 10.1038/nm0311-291]

18 **Jin G**, Pirozzi CJ, Chen LH, Lopez GY, Duncan CG, Feng J, Spasojevic I, Bigner DD, He Y, Yan H. Mutant IDH1 is required for IDH1 mutated tumor cell growth. *Oncotarget* 2012; **3**: 774-782 [PMID: 22885298 DOI: 10.18632/oncotarget.577]

19 **Pawłowski R**, Mühl SM, Sulser T, Krek W, Moch H, Schraml P. Loss of PBRM1 expression is associated with renal cell carcinoma progression. *Int J Cancer* 2013; **132**: E11-E17 [PMID: 22949125 DOI: 10.1002/ijc.27822]

20 **André F**, Hurvitz S, Fasolo A, Tseng LM, Jerusalem G, Wilks S, O'Regan R, Isaacs C, Toi M, Burris H, He W, Robinson D, Riester M, Taran T, Chen D, Slamon D. Molecular Alterations and Everolimus Efficacy in Human Epidermal Growth Factor Receptor 2-Overexpressing Metastatic Breast Cancers: Combined Exploratory Biomarker Analysis From BOLERO-1 and BOLERO-3. *J Clin Oncol* 2016; **34**: 2115-2124 [PMID: 27091708

DOI: 10.1200/JCO.2015.63.9161]
21 **Lim SM**, Park HS, Kim S, Kim S, Ali SM, Greenbowe JR, Yang IS, Kwon NJ, Lee JL, Ryu MH, Ahn JH, Lee J, Lee MG, Kim HS, Kim H, Kim HR, Moon YW, Chung HC, Kim JH, Kang YK, Cho BC. Next-generation sequencing reveals somatic mutations that confer exceptional response to everolimus. *Oncotarget* 2016; **7**: 10547-10556 [PMID: 26859683 DOI: 10.18632/oncotarget.7234]
22 **Park JH**, Ryu MH, Park YS, Park SR, Na YS, Rhoo BY, Kang YK. Successful control of heavily pretreated metastatic gastric cancer with the mTOR inhibitor everolimus (RAD001) in a patient with PIK3CA mutation and pS6 overexpression. *BMC Cancer* 2015; **15**: 119 [PMID: 25886409 DOI: 10.1186/s12885-015-1139-7]
23 **Yao JC**, Shah MH, Ito T, Bohas CL, Wolin EM, Van Cutsem E, Hobday TJ, Okusaka T, Capdevila J, de Vries EG, Tomassetti P, Pavel ME, Hoosen S, Haas T, Lincy J, Lebwohl D, Öberg K. Everolimus for advanced pancreatic neuroendocrine tumors. *N Engl J Med* 2011; **364**: 514-523 [PMID: 21306238 DOI: 10.1056/NEJMoa1009290]
24 **Sia D**, Tovar V, Moeini A, Llovet JM. Intrahepatic cholangiocarcinoma: pathogenesis and rationale for molecular therapies. *Oncogene* 2013; **32**: 4861-4870 [PMID: 23318457 DOI: 10.1038/onc.2012.617]

P- Reviewer: Imai K, McHenry L, Shimizu Y **S- Editor**: Qi Y
L- Editor: Wang TQ **E- Editor**: Wang CH

Published by **Baishideng Publishing Group Inc**
7901 Stoneridge Drive, Suite 501, Pleasanton, CA 94588, USA
Telephone: +1-925-223-8242
Fax: +1-925-223-8243
E-mail: bpgoffice@wjgnet.com
Help Desk: http://www.f6publishing.com/helpdesk
http://www.wjgnet.com

ISSN 1007-9327